Reactor Physics

Waclaw Gudowski

Preface

This interactive text book is intended to engineering students as a basic course in the physics of nuclear reactors. It is designed to be appropriate as a course for nuclear energy engineering master students as well as for a stand-alone course that can be taken by undergraduates in mechanical, electrical, or other fields of engineering who have not had a previous background in nuclear energy. This interactive text book should equally well be useful to practicing engineers from a variety of disciplines which require familiarity with the physics of nuclear reactors.

This text book can be read as a paper copy, however its full value can be appreciated at a computer monitor with visible animations, video materials and thousands of link to original publications of relevance for physics underlying the reactor physics. Whereever in the text you see an animation icon/button or a hyperlink in ***an italic blue font*** - just do not hesitate to click-on!

Many books and diferent written materials have been used in forming up this interactive text book. Acknowledgement and references to used in the text books:

D.J. Bennet & J.R. Thomson	"The Elements of Nuclear Power" Longman Scientific & Technical, 1989
Nicholas Tsoulfanidis	"Measurements and Detection of Radiation" Hemisphere Publishing Corporation, 1983.
Henry A. Boorse, Lloyd Motz,	"The Atomic Scientists" Jefferson H. Waever Wiley Sci ence Edi tion, 1989
David Bodansky	"Nuclear Energy. Principles, Practices and Prospects" American Institute of Physics, 1996
Elemer E. Lewis	"Fundamentals of Nuclear Reactor Physics"
P.F. Zweifel	"Reactor Physics" McGraw- Hill, 1973.
S. Garg, F. Ahmed,	"Physics of Nuclear Reactors" L.S. Kothari Tata McGraw- Hill, 1986
Electronic Nobel Museum	http://www.nobel.se

Different materials and numerous figures found on the internet together with Swedish technical reports are also presented in the text book and lectures. All Nobel lectures have been collected from the http://www.nobelprize.org .
Some multimedia material was kindly delivered by the SKB - Swedish Nuclear Fuel and Waste Management Co.

Contents

12. 2 Group Diffusion

13. Reactor Kinteics

14. Reactor Dynamics

15. Monte Carlo

Chapter 1

Introduction: Milestones of Physics leading to Nuclear Power - 1895-1954

1.1 Situation before 1895

The turn of the century marked a profound revolution in the development of science and our understanding of the fundamental principles of the natural world. During the nineteenth century classical physics - **the laws of motion** formulated initially by I. Newton in 1687, **electromagnetic field theory** developed to maturity by J.C. Maxwell , and thermodynamics with important contribution of of S. Carnot, W.Rankine, R. Clausius, William Thomson (Lord Kelvin) and L. Boltzman - had reached an advanced state of development. The physical world seemed to be well understood based on the laws of motion, electromagnetism and thermodynamics. To some it seemed that physics was reaching such a state of maturity that few fundamental principles remained to be discovered. Also chemistry had reached a considerable degree of sophistication but on a largely empirical basis, the fundamental basis of chemistry remained mysterious. Much had been learned about the Earth and solar system as well. Estimates of the age of the Earth had risen from about 6000 years in the late eighteenth century to tens or hundreds of millions of years; and the view that life, the Earth, and the rest of the solar system had arisen in a single great upheaval in recent times had been replaced by the idea of gradual change over years. An influence of revolutionary Ch. Darwin's theory of evolution had its impact on physics and other natural sciences.

Physicists of the end of 19th century believed that atoms - if they really existed - consisted of hydrogen atoms (approximately) and they expected only minor refinements to get ``an extra decimal place" of accuracy.

But there were visible problems. Essentially nothing was known about the fundamental structure of matter that gave rise to the Periodic Law and other chemical behaviors - the very existence of atoms was largely conjectural. Geology and astronomy seemed in serious conflict since the apparent age of the geologic record could not be reconciled with the only power source for the Sun then conceivable, gravitational contraction, which would exhaust itself in mere millions of years. An important part of classical thermodynamics was stubbornly resisting resolution - the properties of blackbody radiation with ist ultaviolet "catastrophy". In fact by the end of 1900s it had become clear that within the existing framework of physics no solution of the blackbody problem was possible (the untenable prediction made by existing physics was termed the "ultraviolet catastrophe"). Something important was missing. And soon the inadequacy of classical physics was proofed. **The era of modern physics began with an unexpected discovery of x-rays.**

1.2 Discovery of x-rays

W.C. Röntgen 1895
Nobel Prize 1901, ***(click here to read more about X-rays discovery)***

Late in the evening of Friday, November 8, 1895, Roentgen was working alone in his darkened laboratory with a Crooks tube in a black box which was closely covered. During these experiments, he observed that a few crystals of barium platinocyanide, which accidentally lay on the table , gave off a fluorescent glow. Roentgen examined this observation, deducing that the fluorescence could only have been caused by a hitherto unknown radiation stemming from the Crooks tube. He discovered that this radiation could penetrate solid substances and that it has the same effect on a photographic plate as light. The first "Roentgen exposures" that were made were of metal objects locked in a wooden case, and of the skeleton of his wife's hand.

Once the news was made public, it produced a sensation throughout the civilized world. Popular interest was greatly heightened by report that X-ray pictures could be taken through walls and opaque screens. This caused a widespread apprehension that all privacy might be destroyed. While this penetrating property of the rays was correctly described, privacy was certainly not endangered owing to the cumbersome equipment necessary and the fact that the pictures are not taken by reflected radiation. The medical uses of the rays for photographing through the flesh and in detailing the bony structure of the body were immediately recognized.

Röntgen's discovery of X-rays was in fact a lucky accident. Röntgen described these circumstances as follows:

"I was working with a Crookes tube covered by a shield of black cardboard. A piece of barium platino-cyanide paper lay on the bench there. I had been passing a current through the tube and I noticed a peculiar black line across the paper.... The effect was one which could only be produced, in ordinary parlance, by the passage of light. No light could come from the tube, because the shield which covered it was impervious to any light known.....I assumed that the effect must have come from the tube, since its character indicated that it could come from nowhere else. I tested it. In a few minutes there was no doubt about it."

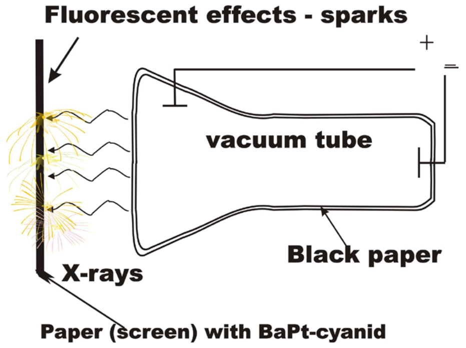

Figure 1.1 Schematic sketch of Röntgen's experiment

Röntgen's first two communications about the rays, which had appeared in the Würzburg Sitzungsberichte, described the circumstances of the discovery and then several salient properties of the rays. First, he noted that all substances are more or less transparent to the rays but the denser substances, especially the heavy metals such as platinum and lead, are less so, although density is not the only factor to be considered. Next, detectors of X-rays were considered; besides fluorescence, the sensitivity of both photographic plates and films were noted. Röntgen described that X-rays are not ultraviolet rays because they cannot be refracted by prisms or lenses made of variety of materials. (Later experiments were to show that a slight refraction can be observed, and that X rays exhibit the properties of light waves of very short wavelenghts.) Also X rays cannot be cathode rays because they cannot be deflected by a magnet, but they originate where cathode rays strike. Shadow pictures and pinhole photographs confirm the ray nature of the X rays but interference phenomena cannot be produced. The first communication closed with the suggestion that X-rays are propagated as longitudinal vibrations in the ether, a guess that proved to be erroneous.

Figure 1.2 X-ray picture of Roentgen's wife hand.

W.C. Roentgen had now become a scientist who was renowned all over the world. His fame was reflected, in the course of his life, by the eighty (80) or so awards and memberships conferred on or offered to him by scientific associations in Germany and abroad. In a few cities, as in Wuerzburg, streets were named after him. The most prominent honor conferred was the Nobel Prize for physics which he accepted personally in Stockholm on December 10, 1901. The money, 50000 kroner, he left by will to Wuerzburg University; unfortunately, after World War I, it was totally devalued by inflation. Beginning with the summer term in 1900, he taught physics at Munich University; he had declined two honorable calls from Berlin University as well as the nobility offered to him by the Prinzregent Luitpold.
Read the article about:
Roentgen´s communication about the X-ray discovery
List of Nobel prize winners related to use of X-ray technique.

1.3 Discovery of radioactivity - 1896

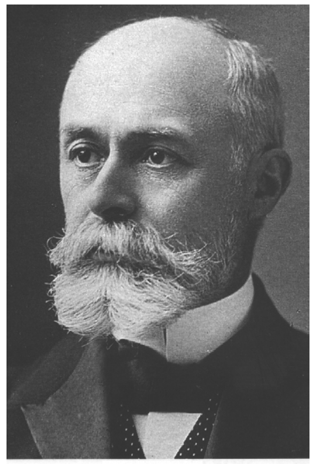

Becquerel

Antoine Henri Becquerel (1852-1908) ***(click here for his Nobel lecture)***

Maria Sklodowska-Curie (1867-1934) & Pierre Curie (1859-1906) ***(click here for Curies Nobel lecture)***

Nobel Prize 1903

Maria Sklodowska-Curie was awarded the second Nobel Prize 1911 in chemistry ***(click here for her Nobel lecture)***

The discovery of natural radioactivity is credited to Henri Becquerel in 1896. As with many discoveries, this one was by accident. Becquerel had placed a uranium salt compound on top of a photographic plate. The plate was covered with dark paper and stored in a light tight area. When that plate was later developed a mysterious fogging of the plate was observed. The uranium salt compound had caused an image (fogging) to be recorded through the protective paper wrapping.

It was not until 1898 that Marie Curie recognized the new phenomenon of radiation. While working with uranium ores, curie coined the term “radiation” and isolated two new radioactive materials from the ore, radium and polonium.

Marie Curie

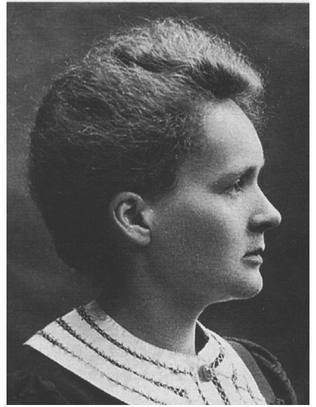

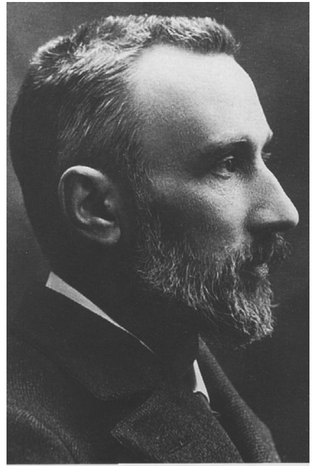

Pierre Curie

As it will be shown the use of radiation helped scientists to explore the structure of the atom and the structure of the atom helped explain the origin and characteristics of the radiation itself.

H. Becquerel was born into a family of scientists. His grandfather had made important contributions in the field of electrochemistry while his father had investigated the phenomena of fluorescence and phosphorescence. Becquerel not only inherited their interest in science, he also inherited the minerals and compounds studied by his father. And so, upon learning how Wilhelm Roentgen discovered X rays from the fluorescence they produced, Becquerel had a ready source of fluorescent materials with which to pursue his own investigations of these mysterious rays.

The material Becquerel chose to work with was potassium uranyl sulfate, $K_2UO_2(SO_4)_2\ 2H_2O$, which he exposed to sunlight and placed on photographic plates wrapped in black paper. When developed, the plates revealed an image of the uranium crystals. Becquerel concluded ***(click here to read his article)*** “that the phosphorescent substance in question emits radiation which penetrates paper opaque to light.” Initially he believed that the sun’s energy was being absorbed by the uranium which then emitted X rays.

Further investigation was delayed because the skies over Paris were overcast and the uranium - covered plates Becquerel intended to expose to the sun were returned to a drawer for about a week. After this week he developed the photographic plates expecting only faint images to appear. To his surprise, the images were clear and strong. This meant that the uranium emitted radiation without an external source of energy such as the sun. Becquerel had discovered radioactivity, the spontaneous emission of radiation by a material. Later, Becquerel demonstrated that the radiation emitted by uranium shared certain characteristics with X rays but, unlike X rays, could be deflected by a magnetic field and therefore must consist of charged particles. For his discovery of radioactivity, Becquerel was awarded the 1903 Nobel Prize for physics together with Marie and Pierre Curies.

Marie Sklodowska-Curie was born in 1867 in Warsaw, Poland. After 1891, when she moved to France, she became famous for her work in radioactivity and was twice a winner of the Nobel Prize. In 1903 she and her husband, Pierre Curie, shared with Henri Becquerel the Nobel Prize for Physics, for their investigation of radioactivity, which Becquerel discovered. Later in 1911 she was the sole winner of the Nobel Prize for Chemistry, for the isolation of pure radium. Not only was Marie Sklodowska-Curie the first woman to receive a Nobel Prize, but she was also the first person to be awarded two Nobel Prizes.

By the time Pierre Curie met Marie Sklodowska, he had already established an impressive reputation. In 1880, he and his brother Jacques had discovered piezoelectricity whereby physical pressure applied to a crystal resulted in the creation of an electric potential. He also had made important investigations into the phenomenon of magnetism including the identification of a temperature, the Curie point, above which a material’s magnetic properties disappear. However, shortly after his marriage to Marie in 1895, Pierre subjugated his research to her interests.

Together, they began investigating the phenomenon of radioactivity recently discovered in uranium ore. Although the phenomenon was discovered by Henri Becquerel, the term radioactivity was coined by Marie. After chemical extraction of uranium from the ore, Marie noted the residual

material to be more “active” than the pure uranium. She concluded that the ore contained, in addition to uranium, new elements that were also radioactive. This led to their discoveries of the elements of polonium and radium, but it took four more years of processing tons of ore under oppressive conditions to isolate enough of each element to determine its chemical properties.

For their work on radioactivity, the Curies were awarded the 1903 Nobel Prize in physics. Tragically, Pierre was killed three years later in an accident while crossing street in a rainstorm. Pierre’s teaching position at the Sorbonne was given to Marie. Never before had a woman taught there in its 650 year history! Her first lecture began with the very sentence her husband had used to finish his last. In his honor, the 1910 Radiology Congress chose the *curie* as the basic unit of radioactivity: the quantity of radon in equilibrium with one gram of radium (current definition: 1 Ci = $3.7\text{x}10^{10}$ dps - disintegrations per second). A year later, Marie was awarded the Nobel Prize in chemistry for her discoveries of radium and polonium, thus becoming the first person to receive two Nobel Prizes. For the remainder of her life she tirelessly investigated and promoted the use if radium as a treatment for cancer. Marie Curie died July 4, 1934, overtaken by pernicious anemia no doubt caused by years of overwork and radiation exposure.

Click here to read more about discovery of radioactivity

1.4 Discovery of electron, its charge and mass

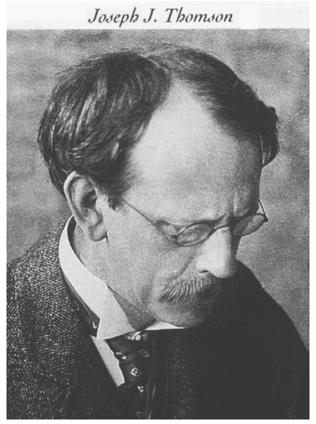

Sir J.J. Thomson 1897

Nobel Prize 1906 ***(click here to read his Nobel lecture)***

Joseph John Thomson was born on December 18, 1856 in Cheetham, a suburb of Manchester. His father was a bookseller and publisher. It was originally intended that he should be an engineer, and, at the age of fourteen, he was sent to Owens College - later Manchester University - until there was a vacancy for an apprentice at the engineering firm selected.

After two years his father died, and his mother could not afford the large premium required for the apprenticeship. He therefore gave up engineering and in 1876 came to Trinity College, Cambridge to read Mathematics. In those days the Wranglers (undergraduates with First Class in the Mathematics Tripos) were placed in order of merit, and there was great competition to come top of the list. Thomson took the Tripos in 1880 and was placed second. The Senior Wrangler that year was Joseph Larmor, who became famous later for his contributions to theoretical physics.

He began work in the Cavendish Laboratory in 1880 under Lord Rayleigh, the second Cavendish Professor, and, when Rayleigh resigned the Cavendish chair in 1884, Thomson was elected to it, despite the fact that he was only 28 at the time, and was known more for his mathematical ability than for his skill in experimental physics.

The appointment of Thomson to the Cavendish chair proved to be an inspired choice. He started experiments on the discharge of electricity through gases at low pressure, a subject which he pursued for the rest of his working life. It led to the discovery of the electron in 1897, one of the most significant events in science. The experiments leading to the discovery are described below.

Under Thomson’s leadership the Cavendish Laboratory continued to make fundamental discoveries. Thomson’s further work on gas discharges led to Aston’s mass spectrometer, and the discovery of isotopes. Thomson received the Nobel Prize in 1906 for `his theoretical and experimental researches on the discharge of electricity through gases’. He was knighted in 1908 and received the Order of Merit in 1912. He was the President of the Royal Society from 1915 until 1920, and the Master of Trinity from 1918 until his death on August 30, 1940.

After his death Lawrence Bragg said `He, more than any other man, was responsible for the fundamental change in outlook which distinguishes the physics of this century from that of the last.’

The discovery of the electron ***(click to read original article)***

The electron plays a fundamental role in every branch of pure and applied science, and its discovery by Thomson marked a major advance in our understanding of nature. Here is a brief description of Thomson’s work leading to the electron discovery:

Under normal conditions a gas is a poor conductor of electricity. However, if the gas in a glass container is at a reduced pressure, and a voltage is applied across two electrodes inside the container, a discharge occurs and the gas becomes conducting. Streams of bright lines are observed to come from the cathode, the negative electrode; they are known as cathode rays. From the time of their discovery by the German physicist Plücker in 1858 there was much controversy over the nature of the cathode rays. Most of the German physicists thought they were some form of radiation, whereas the majority of British physicists thought they were streams of negatively charged particles. In 1897 Thomson carried out a series of experiments which demonstrated conclusively that the second view is correct.

A key observation made by Thomson was that the cathode rays are deflected by an electric field. Hertz had previously tried and failed to observe such a deflection, which gave support to the view that the cathode rays are not electric particles. Thomson realised that the reason for Hertz’s failure was that the gas in his container was not at a sufficiently low pressure. Consequently, positive and negative ions in the gas neutralised the electric field that Hertz was applying. Thomson reduced the pressure and observed a deflection.

The basic features of Thomson’s apparatus are shown in the Figure 1.3. The cathode C is at a negative potential of several hundred volts, and the anode S_1 is earthed. The cathode rays travel towards the anode and pass through a slit in it. They continue through a second slit in the plug S_2, and traveling in a straight line (shown black in the diagram) strike the end of the tube at the point O, where they produce a narrow well--defined phosphorescent patch. P_1 and P_2 are a pair of parallel metal plates across which a potential difference may be applied. This gives rise to an electric field in the space between them along which the cathode rays are traveling. If the plate P_1 is positive the cathode rays are deflected upwards.

They follow the path shown in red and produce a phosphorescent patch at the point A. A scale is pasted on the outside of the tube to measure the amount of the deflection.

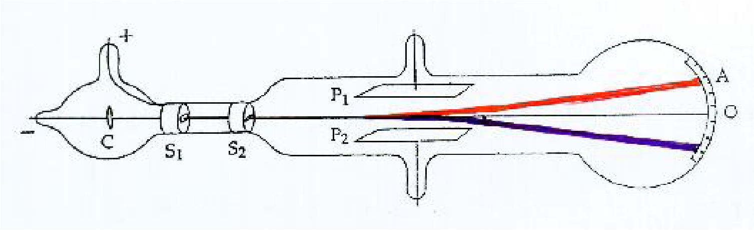

Figure 1.3 Thomson's original diagram of his apparatus used for determining the specific charge e/m0 of the electron.

Instead of an electric field, a magnetic field may be used to deflect the particles. This is done by placing two coils (not shown in the diagram) on either side of the discharge tube in the region of P_1 and P_2. When a current flows through the coils a magnetic field is produced perpendicular to the previous electric field and to the direction of the cathode rays. Its direction is such that the cathode rays are deflected downwards and follow the blue path in the diagram.

Thomson determined the velocity of the cathode rays by applying the electric and magnetic fields simultaneously and adjusting their relative magnitudes so that the deflections they produced were equal and opposite. The cathode rays were then undeflected and traveled along the black line to reach the point O. The force on a charge e in an electric field E is Ee, while the force due to a magnetic field B, when the charge is moving with velocity v, is Bev. The electric and magnetic fields were made to act over the same path length d of the rays. Since the two deflections are equal, so are the two forces, i.e. Ee = Bev, and the velocity of the particles is given by the simple relation v = E/B. Thomson then measured the deflection produced by the electric field alone. This, combined with the values of E, v and d, gave the value of the ratio of the charge e to the mass m of the particles.

*I*f magnetic field applied at P_1-P_2 positions so force on particle :
Ee = Bev
in a case of getting spot back on position P_1 (i.e. electric and magnetic fields reduce each others force so that electrons hit the point P_1 as without any field applied)

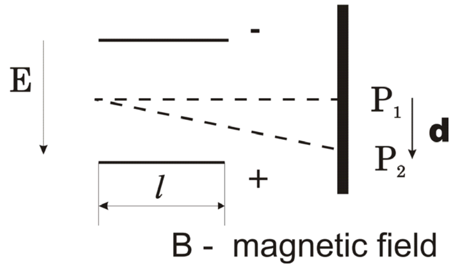

For $P_1 \neq P_2$
Distance P_1-P_2 = d can be measured:

$$d = \frac{1}{2}at^2 = \frac{1}{2}E\frac{e}{m}\left(\frac{l}{v}\right)^2$$

and e/m can be derived:

$$\frac{e}{m} = \frac{2d}{E}\frac{v^2}{l^2}$$

Thomson's claim to be the discoverer of the electron rests on two key observations. First, he found that the value of e/m was of the order of 1000 times larger than its value for the lightest particle then known, which was the hydrogen ion in electrolysis. On the assumption that the charge was the same for both particles, this meant that the mass of the new particle was of the order of 1000 times less than that of the hydrogen atom. (We now know that it is 1837 times less.) Secondly, he repeated the measurements for different gases and for different materials for the electrodes, and found that the value of e/m was independent of both the nature of the gas and the material of the electrode. In other words the particle he had discovered was a universal constituent of matter.

Thomson made the first announcement of the existence of the electron - or `corpuscle' as he called it - at the Royal Institution on April 30, 1897. The word electron, coined originally by Johnstone Stoney in 1891 and used in another context, was applied almost immediately by other scientists to Thomson's corpuscle, but Thomson himself did not adopt the universal usage until almost twenty years later.

Determination of a fundamental electron charge

Millikan, Robert (1868-1953)

Nobel Prize ***(click here to read his Nobel lecture)***, 1923; for his work on the elementary charge of electricity and on the photoelectric effect.

Robert Millikan was one of the first American scientists to be well recognized in Europe. He graduated from Columbia University in 1893 and journeyed to Germany where he studied with Planck and others. When offered a position at the University of Chicago he returned to America.

In 1909 he performed the first of a series of experiments to measure the fundamental charge of an electron, the Millikan Oil Drop Experiment. The value determined by this experiment was used in Bohr's formula for the energy of the Hydrogen line spectrum as a first confirmation of the quantized atom. In 1915, his group of collaborators confirmed Einstein's Photoelectric Effect by verifying that the energy of the emitted electrons was directly dependent on the frequency of the incident light. From this research and the methods that he had to develop he became the first to study of spectroscopy in the vacuum ultraviolet. He named and studied "cosmic rays" as well.

A scrutiny of his notebook, however, shows that he only selected ``good" oil drops to publish, making notes such as ``Beauty-- Publish" and ``One of the best I've ever had--- Publish." In 1916, Millikan experimentally verified Einstein's predictions on the photoelectric effect, measuring the value of Planck's constant (h) in the process.
Click here to read Millikan's article.

1.5 Energy QUANTA - The birth of quantum physics

Max Planck, 1900

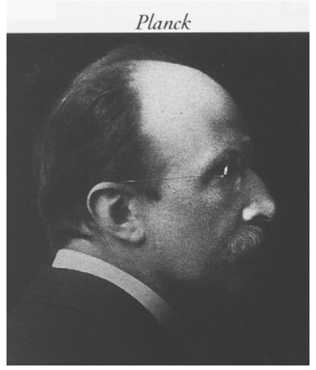

Nobel Prize 1918 ***(click here to read his Nobel lecture)***

Max Planck initiated the study of quantum mechanics when he announced in 1900 his theoretical research into radiation and absorption of a black body.

Planck came from an academic family, his father being professor of law at Kiel and both his grandfather and great-grandfather had been professors of theology at Göttingen. In 1867 Planck's family moved to Munich and he attended school there. He did well at school, but not brilliantly, usually coming somewhere between third and eighth in his class.

In 1874, at the age of 16, he entered the University of Munich. Before he began his studies he discussed the prospects of research in physics with Philipp von Jolly, the professor of physics there, and was told that physics was essentially a complete science with little prospect of further developments. Fortunately Planck decided to study physics despite the bleak future for research that was presented to him.

Planck describes why he chose physics:

"The outside world is something independent from man, something absolute, and the quest for the laws which apply to this absolute appeared to me as the most sublime scientific pursuit in life. "

Planck then studied at Berlin where his teachers included Helmholtz and Kirchhoff. He later wrote that he admired Kirchhoff greatly but found him dry and monotonous as a teacher. Planck returned to Munich and received his doctorate at the age of 21 with a thesis on the second law of thermodynamics. He was then appointed to a teaching post at the University of Munich in 1880 and he taught there until 1885.

In 1885 Planck was appointed to a chair in Kiel and held this chair for four years. After the death of Kirchhoff in 1887, Planck succeeded him in the chair of theoretical physics at the University of Berlin in 1889. He was to hold the Berlin chair for 38 years until he retired in 1927.

While in Berlin Planck did his most brilliant work and delivered outstanding lectures. He studied thermodynamics in particular examining the distribution of energy according to wavelength. By combining the formulas of Wien and Rayleigh, Planck announced in 1900 a formula now known as Planck's radiation formula. In a letter written a year later Planck described proposing the formula saying:

" ... the whole procedure was an act of despair because a theoretical interpretation had to be found at any price, no matter how high that might be. "

Within two months Planck made a complete theoretical deduction of his formula renouncing classical physics and introducing the quanta of energy (see picture below). At first the theory met resistance but due to the successful work of Niels Bohr in 1913, calculating positions of spectral lines using the theory, it became generally accepted. Planck received the Nobel Prize for Physics in 1918. ***Click here to read his article.***

Planck took little part in the further development of quantum theory, this being left to Paul Dirac and others. Planck took on administrative duties such as Secretary of the Mathematics and Natural Science Section of the Prussian Academy of Sciences, a post he held from 1912 until 1943. He had been elected to the Academy in 1894.

Planck was president of the Kaiser Wilhelm Gesellschaft, the main German research organisation, from 1930 until 1937. He remained in Germany during World War II through what must have been times of the deepest difficulty since his son Erwin was executed for plotting to assassinate Hitler.

After World War II he again became president of the Kaiser Wilhelm Gesellschaft in 1945-1946 for the second time defending German science through another period of exceptional difficulty.

BEGINNING OF QUANTUM PHYSICS

In 1859 Gustav Kirchhoff proved a theorem about blackbody radiation. A blackbody is an object that absorbs all the energy that falls upon it and, because it reflects no light, it would appear black to an observer. A blackbody is also a perfect emitter and Kirchhoff proved that the energy emitted E depends only on the temperature T and the frequency *v* of the emitted energy, i.e.

E = J(T,*v*) or E=e(λ,T)

Kirchhoff challenged physicists to find the function J.

In 1879 Josef Stefan, a Slovene physicist, mathematician, and poet of Slovenia proposed, on experimental grounds, that the total energy emitted by a hot body was proportional to the fourth power of the temperature. In the generality stated by Stefan this is false. The same conclusion was reached in 1884 by Ludwig Boltzmann for blackbody radiation, this time from theoretical considerations using thermodynamics and Maxwell's electromagnetic theory. The result, now known as the Stefan-Boltzmann law, does not fully answer Kirchhoff challenge since it does not answer the question for specific wavelengths.

In 1896 Wilhelm Wien proposed a solution to the Kirchhoff challenge. However although his solution matches experimental observations closely for small values of the wavelength, it was shown to break down in the far infrared by Rubens and Kurlbaum. Kirchhoff, who had been at Heidelberg, moved to Berlin. Boltzmann was offered his chair in Heidelberg but turned it down. The chair was then offered to Hertz who also declined the offer, so it was offered again, this time to Planck and he accepted.

Rubens visited Planck in October 1900 and explained his results to him. Within a few hours of Rubens leaving Planck's house Planck had guessed the correct formula for Kirchhoff's J function. This guess fitted experimental evidence at all wavelengths very well but Planck was not satisfied with this and tried to give a theoretical derivation of the formula. To do this he made the unprecedented step of assuming that the total energy is made up of indistinguishable energy elements - **quanta of energy**. Its smallest partion has been called a Planck constant - h.

Table I shows evolution of the equation of black body emission spectrum from 1887 until its final form formulated by Planck in 1900. Pay attention to fact that Plank formula in contrary to earlier formulations has only *universal constants*: c - speed of light, k - Boltzman constant and h - Planck constant.

Table I. **Evolution of the equation of black body emission spectrum**

Year	Author	Formula
1887	Wladimir Michelson	$e(\lambda,T)=aT^{3/2}\lambda^{-6}\exp(-b/\lambda^{2}T)$
1888	Heinrich Weber	$e(\lambda,T)=a\lambda^{-2}\exp(cT-b/\lambda^{2}T^{2})$
1896	Wilhelm Wien	$e(\lambda,T)=a\lambda^{-5}\exp(-b/\lambda T)$
1896	Friedrich Paschen	$e(\lambda,T)=a\lambda^{-5.6}\exp(-b/\lambda T)$
1900	Lord Rayleigh	$e(\lambda,T)=aT\lambda^{-4}\exp(-b/\lambda T)$
1900	Otto Lumer and Ernst Pringsheim	$e(\lambda,T)=aT\lambda^{-4}\exp(-b/(\lambda T)^{1.25})$
1900	Otto Lumer and Eugen Jahnke	$e(\lambda,T)=aT\lambda^{-5}\exp(-b/(\lambda T)^{0.9})$
1900	Max Thiesen	$e(\lambda,T)=aT^{0.5}\lambda^{-4.5}\exp(-b/\lambda T)$

Table I. Evolution of the equation of black body emission spectrum

Year	Author	Formula
1900	Max Planck	$e(\lambda,T)=8\pi hc\lambda^{-5}\left(\frac{1}{\exp(hc/k\lambda T)-1}\right)$

Planck himself gave credit to Boltzmann for his statistical method but Planck's approach was fundamentally different. However in 1900 theory had deviated from experiment and was based on a hypothesis with no experimental basis. But very soon this revolutionary approach has been confirmed experimentally.

1.6 Equivalence of Energy and Mass

A. Einstein 1905

Nobel Prize 1921***(click here to read his Nobel lecture)***

(click here to read the article on the photelectric effect)

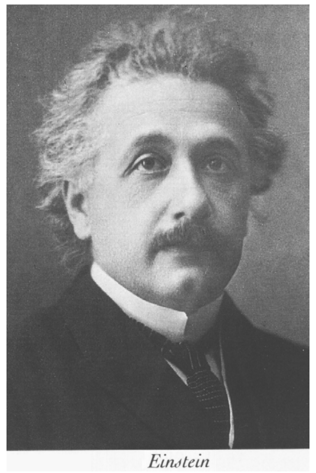

Einstein

Albert Einstein (1879-1955) contributed more than any other scientist to the modern vision of physical reality. His theory of relativity is held as human thought of the highest quality.

Albert Einsein was born 14 of March 1879 in Ulm, Germany. Around 1886 Einstein began his school in Munich. As well as his violin lessons, which he had from age six to age thirteen, he also had religious education at home where he was taught Judaism. Two years later he entered the Luitpold Gymnasium and after this his religious education was given at school.

He studied mathematics, in particular the calculus, beginning around 1891. In 1894 Einstein's family moved to Milan but Einstein remained in Munich. In 1895 Einstein failed an examination that would have allowed him to study for a diploma as an electrical engineer at the Eidgenössische Technische Hochschule (ETH) in Zurich. Einstein renounced German citizenship in 1896 (to avoid military service) and was to be stateless for a number of years. He did not even apply for Swiss citizenship until 1899, citizenship being granted in 1901.

Following the failing of the entrance exam to the ETH, Einstein attended secondary school at Aarau planning to use this route to enter the ETH in Zurich. While at Aarau he wrote an essay (for which was only given a little above half marks!) in which he wrote of his plans for the future:

> *If I were to have the good fortune to pass my examinations, I would go to Zurich. I would stay there for four years in order to study mathematics and physics. I imagine myself becoming a teacher in those branches of the natural sciences, choosing the theoretical part of them. Here are the reasons which lead me to this plan. Above all, it is my disposition for abstract and mathematical thought, and my lack of imagination and practical ability.*

Einstein succeeded with his plan graduating in 1900 as a teacher of mathematics and physics. One of his friends at ETH was Marcel Grossmann who was in the same class as Einstein. Einstein tried to obtain a post, writing to Hurwitz who held out some hope of a position but nothing came of it. Three of Einstein's fellow students, including Grossmann, were appointed assistants at ETH in Zurich but clearly Einstein had not impressed enough and still in 1901 he was writing round universities in the hope of obtaining a job, but without success.

He did manage to avoid Swiss military service on the grounds that he had flat feet and varicose veins. By mid 1901 he had a temporary job as a teacher, teaching mathematics at the Technical High School in Winterthur. Then Grossmann's father tried to help Einstein get a job by recommending him to the director of the patent office in Bern. Einstein was appointed as a technical expert third class.

Einstein worked in this patent office from 1902 to 1909, holding a temporary post when he was first appointed, but by 1904 the position was made permanent and in 1906 he was promoted to technical expert second class. While in the Bern patent office he completed an astonishing range of theoretical physics publications, written in his spare time without the benefit of close contact with scientific literature or colleagues.

Einstein earned a doctorate from the University of Zurich in 1905 for a thesis *On a new determination of molecular dimensions*. He dedicated the thesis to Grossmann.

In the first of three papers, all written in 1905, Einstein examined the phenomenon discovered by Max Planck, according to which electromagnetic energy seemed to be emitted from radiating objects in discrete quantities. The energy of these quanta was directly proportional to the frequency of the radiation. This seemed to contradict classical electromagnetic theory, based on Maxwell's equations and the laws of thermodynamics which assumed that electromagnetic energy consisted of waves which could contain any small amount of energy. Einstein used Planck's quantum hypothesis to describe the electromagnetic radiation of light.

Einstein's second 1905 paper proposed what is today called the special theory of relativity. He based his new theory on a reinterpretation of the classical principle of relativity, namely that the laws of physics had to have the same form in any frame of reference. As a second fundamental hypothesis, Einstein assumed that the speed of light remained constant in all frames of reference, as required by Maxwell's theory.

Later in 1905 Einstein showed how mass and energy were equivalent. Einstein was not the first to propose all the components of special theory of relativity. His contribution is unifying important parts of classical mechanics and Maxwell's electrodynamics.

The third of Einstein's papers of 1905 concerned statistical mechanics, a field of that had been studied by Ludwig Boltzmann and Josiah Gibbs.

After 1905 Einstein continued working in the areas described above. He made important contributions to quantum theory, but he sought to extend the special theory of relativity to phenomena involving acceleration. The key appeared in 1907 with the principle of equivalence, in which gravitational acceleration was held to be indistinguishable from acceleration caused by mechanical forces. Gravitational mass was therefore identical with inertial mass.

In 1908 Einstein became a lecturer at the University of Bern after submitting his Habilitation thesis *Consequences for the constitution of radiation following from the energy distribution law of black bodies*. The following year he become professor of physics at the University of Zurich, having resigned his lectureship at Bern and his job in the patent office in Bern.

By 1909 Einstein was recognised as a leading scientific thinker and in that year he resigned from the patent office. He was appointed a full professor at the Karl-Ferdinand University in Prague in 1911. In fact 1911 was a very significant year for Einstein since he was able to make preliminary predictions about how a ray of light from a distant star, passing near the Sun, would appear to be bent slightly, in the direction of the Sun. This would be highly significant as it would lead to the first experimental evidence in favour of Einstein's theory.

Figure 1.4 Memorial of Einstein's stay in Prague

About 1912, Einstein began a new phase of his gravitational research, with the help of his mathematician friend Marcel Grossmann, by expressing his work in terms of the tensor calculus of Tullio Levi-Civita and Gregorio Ricci-Curbastro. Einstein called his new work the general theory of relativity. He moved from Prague to Zurich in 1912 to take up a chair at the Eidgenössische Technische Hochschule in Zurich.

Einstein returned to Germany in 1914 but did not reapply for German citizenship. What he accepted was an impressive offer. It was a research position in the Prussian Academy of Sciences together with a chair (but no teaching duties) at the University of Berlin. He was also offered the directorship of the Kaiser Wilhelm Institute of Physics in Berlin which was about to be established.

Einstein published, late in 1915, the definitive version of general theory.

When British eclipse expeditions in 1919 confirmed his predictions of interaction of light with gravity resulting in "bending" of starlight by the gravitational field of the sun , Einstein was idolised by the popular press. The London Times ran the headline on 7 November 1919:-

> *Revolution in science - New theory of the Universe - Newtonian ideas overthrown.*

During 1921 Einstein made his first visit to the United States. His main reason was to raise funds for the planned Hebrew University of Jerusalem. However he received the Barnard Medal during his visit and lectured several times on relativity.

Einstein received the Nobel Prize in 1921 but not for relativity rather for his 1905 work on the photoelectric effect. In fact he was not present in December 1922 to receive the prize being on a voyage to Japan. Around this time he made many international visits. He had visited Paris earlier in 1922 and during 1923 he visited Palestine. After making his last major scientific discovery on the association of waves with matter in 1924 he made further visits in 1925, this time to South America.

Bohr and Einstein were to carry on a debate on quantum theory which began at the Solvay Conference in 1927. Planck, Bohr, de Broglie, Heisenberg, Schrödinger and Dirac were at this conference, in addition to Einstein. Einstein had declined to give a paper at the conference and:-

> *... said hardly anything beyond presenting a very simple objection to the probability interpretation .... Then he fell back into silence ...*

Indeed Einstein's life had been hectic and he was to pay the price in 1928 with a physical collapse brought on through overwork. However he made a full recovery despite having to take things easy throughout 1928.

By 1930 he was making international visits again, back to the United States. A third visit to the United States in 1932 was followed by the offer of a post at Princeton. The idea was that Einstein would spend seven months a year in Berlin, five months at Princeton. Einstein accepted and left Germany in December 1932 for the United States. The following month the Nazis came to power in Germany and Einstein was never to return there.

Click here to read Einstein's artivle on electromagnetics of moving particles.

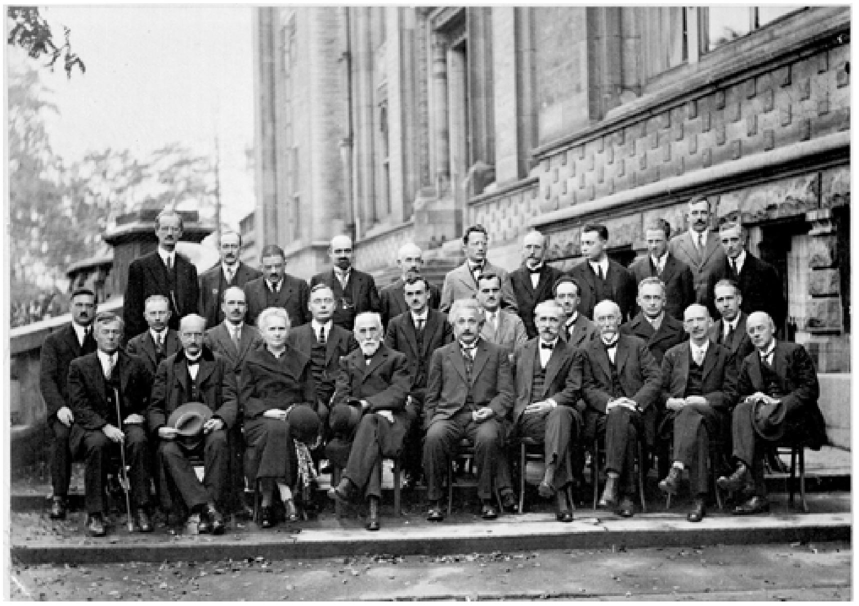

Figure 1.5 The 5th Solvay Conference was held in Brussels from 23-29 October 1927. The group photo contains just about everyone who was anyone during the golden age (except Rutherford and W H Bragg).
In the photo:
Back row: A Piccard, E Henriot, P Ehrenfest, Ed Herzen, Th De Donder, E Schroedinger, E Verschaffelt, W Pauli, W Heisenberg, R H Fowler, L Brillouin.
Middle row: P Debye, M Knudsen, W L Bragg, H A Kramers, P A M Dirac, A H Compton, L de Broglie, M Born, N Bohr.
Front row: I Langmuir, M Planck, Mme Curie, H A Lorentz, A Einstein, P Langevin, Ch E Guye, C T R Wilson, O W Richardson

EQUIVALENCE OF MASS AND ENERGY

$$m = \frac{m_0}{\sqrt{1 - \left(\frac{V}{c}\right)^2}}$$

$$m = total\ \ mass\ = rest\, mass\,(m_0) + kinetic\ \ mass$$

$$m = m_0\left(1 + \frac{1}{2}\left(\frac{V}{c}\right)^2 - \ldots\ldots\right)$$

$$mc^2 = m_0 c^2 + \frac{1}{2} m_0 V^2 - \ldots\ldots$$

$$E_{tot} = E_0 + E_{kin}$$

$$E = mc^2$$

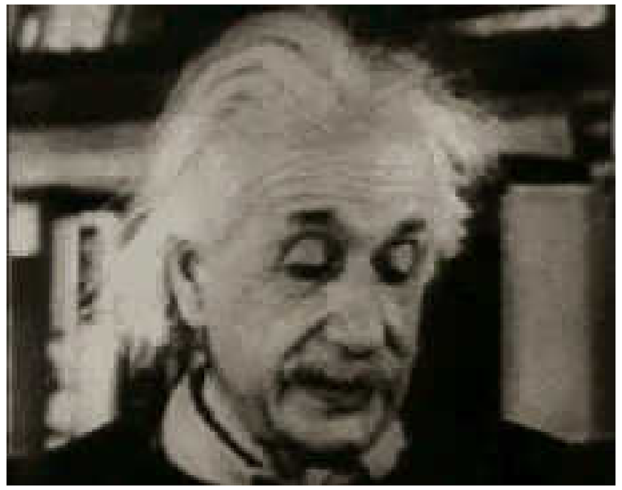

1.7 Number of electrons/atom

Ch. G. Barkla 1911
Nobel Prize, 1917 ***(click here to read his Nobel lecture)***

Barkla

Charles Glover Barkla was born on June 7, 1877 at Widnes Lancashire, England, where his father, J.M. Barkla, was Secretary to the Atlas Chemical Company. He was educated at the Liverpool Institute and entered University College, Liverpool, in 1894 to study mathematics and physics, the latter under Oliver Lodge. He graduated with First Class Honours in Physics in 1898 and in the following year he obtained his master's degree. Also in 1899 he was awarded a research scholarship by the Royal Commissioners for the Exhibition of 1851 and he proceeded to Trinity College, Cambridge, to work in the Cavendish Laboratory with J.J.Thomson. He migrated to King's College during 1900 and in 1902 returned to Liverpool as Oliver Lodge Fellow.

From I905 to I909 he was successively demonstrator, assistant lecturer in physics and special lecturer in advanced electricity at the University, and in I909 he succeeded H.A. Wilson as Wheatstone Professor of Physics in the University of London. In I9I3, Barkla accepted the Chair in Natural Philosophy in the University of Edinburgh and he held this position until his death.

Barkla's first researches concerned the velocity of electric waves along wires but in 1902 he commenced his investigations on Roentgen radiation which were to occupy almost his whole life. His discovery of homogeneous radiations characteristic of the elements showed that these elements had their characteristic line spectra in X-ray and he was the first to show that secondary emission is of two kinds, one consisting of X-rays scattered unchanged, and the other a fluorescent radiation peculiar to the particular substance.

He discovered the polarisation of X-rays, an experimental result of considerable importance for it meant that X-radiation could be regarded as similar to ordinary light. Barkla made valuable contributions to present knowledge on the absorption and photographic action of X-rays and his later work demonstrated the relation between the characteristic X-radiation and the corpuscular radiation accompanying it. He has also shown both the applicability and the limitation of the quantum theory in relation to Roentgen radiation. The results of his findings are recorded in various papers which have appeared mainly in the Transactions and Proceedings o f the Royal Society.

He had a considerable reputation as an examiner in physics. Barkla, a Fellow of the Royal Society, had several honorary degrees. He was appointed Bakerian Lecturer (Royal Society) in 1916 and he was award.- ed the Hughes Medal in the following year. Charles Glover Barkla married Mary Esther, the eldest daughter of John T. Cowell of Douglas, Receiver-General of the Isle of Man, in 1907 They had two sons and one daughter.

Barkla died at Braidwood, Edinburgh on October 23, I944.

Click here to read Barkla's article.

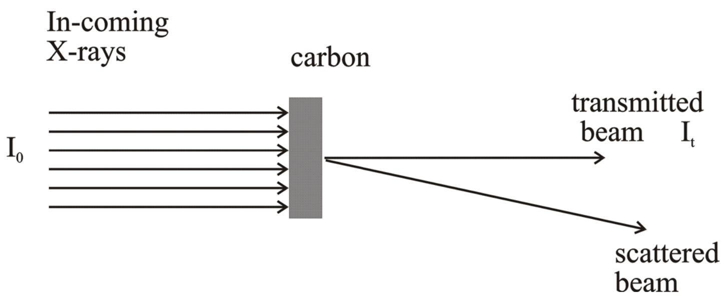

$$\frac{\Delta I}{I} = -\sigma_e \, n \, \Delta x$$

$$I = I_0 \, e^{-n\sigma_e x}$$

Figure 1.6 Barkla's simple scattering experiment of X-rays on a carbon sample.

where:

n — Number of electrons per unit volume

σ_e — scattering cross-section

σ_e obtained from measurements of ratio between scattered and incoming energy.
$n=3.00\text{x}10^{23}\times\rho$ (ρ density of absorber)
Number of electrons in 1 $\text{cm}^3 = N_0$ /A
$N_0=6.01\text{x}10^{23}$ A=12

$$\frac{number\ of\ electrons}{number\ of\ carbon\ atoms} = \frac{3\times10^{23}\times12}{6.02\times10^{23}} = 6$$

1.8 Discovery of atom nucleus

Ernest Rutherford (1871-1937)

Sir E. Rutherford discovery of atom nucleus in 1911 ***(Click here to read his article)***

Nobel Prize 1908 (chemistry) ***(Click here to read his Nobel Lecture)***

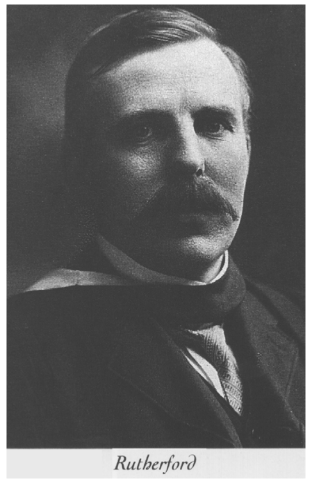

Ernest Rutherford is considered the father of nuclear physics. Indeed, it could be said that Rutherford invented the very language to describe the theoretical concepts of the atom and the phenomenon of radioactivity. Particles named and characterized by him include the alpha particle, beta particle and proton.

Even the neutron, discovered by James Chadwick, owes its name to Rutherford. The exponential equation used to calculate the decay of radioactive substances was first employed for that purpose by Rutherford and he was the first to elucidate the related concepts of the half--life and decay constant. With Frederick Soddy at McGill University, Rutherford showed that elements such as uranium and thorium became different elements (i.e., transmuted) through the process of radioactive decay. At the time, such an incredible idea was not to be mentioned in polite company: it belonged to the realm of alchemy, not science.

For this work, Rutherford won the 1908 Nobel Prize in chemistry. In 1909, now at the University of Manchester, Rutherford was bombarding a thin gold foil with alpha particles when he noticed that although almost all of them went through the gold, one in eight thousand would "bounce" (i.e., scatter) back. The amazed Rutherford commented that it was "as if you fired a 15--inch naval shell at a piece of tissue paper and the shell came right back and hit you."

From this simple observation, Rutherford concluded that the atom's mass must be concentrated in a small positively--charged nucleus while the electrons inhabit the farthest reaches of the atom. Although this planetary model of the atom has been greatly refined over the years, it remains as valid today as when it was originally formulated by Rutherford. In 1919, Rutherford returned to Cambridge to become director of the Cavendish laboratory where he had previously done his graduate work under J.J. Thomson. It was here that he made his final major achievement, the artificial alteration of nuclear and atomic structure. By bombarding nitrogen with alpha particles, Rutherford demonstrated the production of a different element, oxygen. "Playing with marbles" is what he called; the newspapers reported that Rutherford had "split the atom." After his death in 1937, Rutherford's remains were buried in Westminster Abbey near those of Sir Isaac Newton.

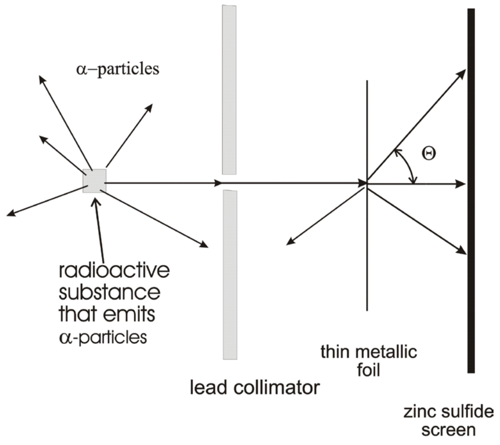

Assuming Thomson model of atom
Θ – can be large only through
multiple scattering or ...?

Geiger-Marsden ***(click to read article)*** showed that intensity at 90o angle $I(90^0)/I(0^0) \sim 1/8000$, i.e. much larger than expected assuming Thomson-model.

Rutherford assumed that the whole mass of the atom is concentrated in the center, in the nucleus which is much smaller than atom itself!

Due to Rutherford $I(\theta)/I(0) \sim 1/\sin^4(\theta/2)$

Hans Geiger

Hans Geiger was born in 1883 in Germany. Working in Manchester England with Ernest Rutherford, he built the first successful detector (the Geiger counter) for individual alpha particles (helium nuclei) and other ionizing radiations.

Geiger used his counter in early experiments which led to the identification of alpha particles as the nucleus of the helium atom. He moved to Berlin in 1912 where he continued his work on the structure of the atom. In the 1920's, at the University of Kiel, he perfected, along with Walther Müller, his particle counter. The Geiger--Müller counter detects alpha particles (helium nuclei), beta particles (electrons), and gamma particles (photons).

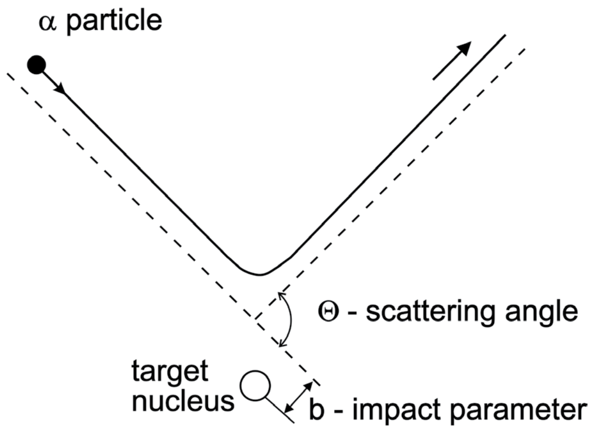

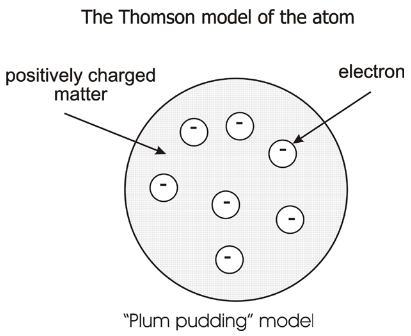

Figure 1.7 The Thomson model of atom - “jelly” cake model of the atom

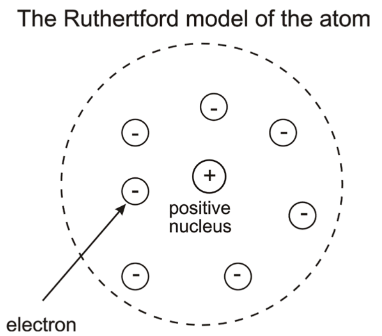

Figure 1.8 The Rutherford model of atom. Bohr put the electrons on the orbits

1.9 New Model of an Atom and Quantum Mechanics

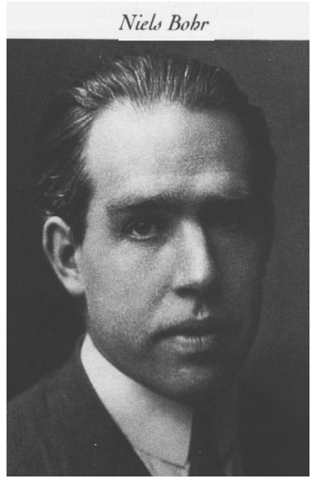

Niels Bohr 1913 - 1925

Nobel Prize 1922 ***(click here to read his Nobel lecture)***

Click here to read the article on atom model.

Niels Henrik David Bohr

Born: 7 Oct 1885 in Copenhagen, Denmark

Died: 18 Nov 1962 in Copenhagen, Denmark

Niels Bohr studied at the University of Copenhagen which he entered in 1903. He won a gold medal from the Royal Danish Academy of Sciences for his theoretical analysis of vibrations of water jets as a means of determining surface tension. He received his Master's degree from the University of Copenhagen in 1909 and his doctorate in 1911 with a thesis Studies on the electron theory of metals.

Bohr went to England to study with Sir J.J. Thomson at Cambridge. He had intended to spend his entire study period in Cambridge but he did not get on well with Thomson so, after a meeting with Ernest Rutherford in Cambridge in December 1911, Bohr moved to Manchester in 1912. There he worked with Rutherford's group on the structure of the atom. Rutherford became Bohr's role model both for his personal and scientific qualities. Using quantum ideas due to Planck and Einstein, Bohr conjectured that ***an atom could exist only in a discrete set of stable energy states.***

Bohr returned to Copenhagen during 1912 and continued to develop his new theory of the atom completing the work in 1913. The same year he published three papers of fundamental importance on the theory of the atom that influenced Einstein and other scientists. The first paper was on the hydrogen atom, the next two on the structure of atoms heavier than hydrogen.

After being a lecturer in Copenhagen, then in Manchester, Bohr was appointed to a chair of theoretical physics at the University of Copenhagen in 1916. An Institute of Theoretical Physics was created for him there and, from its opening in 1921, he was its director for the rest of his life.

Bohr is best known for the investigations of atomic structure referred to above and also for work on radiation, which won him the 1922 Nobel Prize for physics. He said in 1923:

> *“Notwithstanding the fundamental departure from the ideas of the classical theories of mechanics and electrodynamics involved in these postulates, it has been possible to trace a connection between the radiation emitted by the atom and the motion of the particles which exhibits a far--reaching analogy to that claimed by the classical ideas of the origin of radiation. “*

It was Bohr's view of quantum theory which was eventually to become accepted. Einstein expressed grave doubts about Bohr's interpretation and Bohr, Einstein and Ehrenfest spent many hours in deep discussion, but Bohr's view prevailed.

Bohr's other major contributions, in addition to quantum theory, include his theoretical description of the periodic table of elements around 1920, his theory of the atomic nucleus being a compound structure in 1936, and his understanding of uranium fission in terms of the isotope 235 in 1939.

Bohr was of Jewish origins and, when the Nazis occupied Denmark his life became exceeding difficult. He had to escape in 1943 by being taken to Sweden by fishing boat. From there he was flown to England where he began to work on the project to make a nuclear fission bomb. After a few months he went with the British research team to Los Alamos in the USA where they continued work on the project.

However Bohr was deeply concerned about the control of nuclear weapons and from 1944 he tried to persuade Churchill and Roosevelt for the need to have international cooperation. He wrote a public letter to the United Nations in 1950 arguing for rational, peaceful atomic policies. Bohr received the first U.S. Atoms for Peace Award in 1957.

Derivation of The Bohr Early Quantum Theory

Here is the essence of Bohr's 1913 paper which appeared in Volume 26 of the Philosophical Magazine and was entitled “On the Constitution of Atoms and Molecules”. He started by assuming a circular orbit for electrons around the nucleus. The electron charge is “e” and the nucleus has “Z” positive charges, each of magnitude “e”. “m” is the electron mass, “v” is its velocity, and “r” is the radius of its orbit.

The total energy “E” of such a system is the sum of its kinetic and potential energy. This sum must be a constant for the atom to be stable. The kinetic energy comes simply from its elementary definition and the potential energy is just Coulomb's Law.

$$E = \frac{1}{2}mv^2 - \frac{eZe}{r}$$

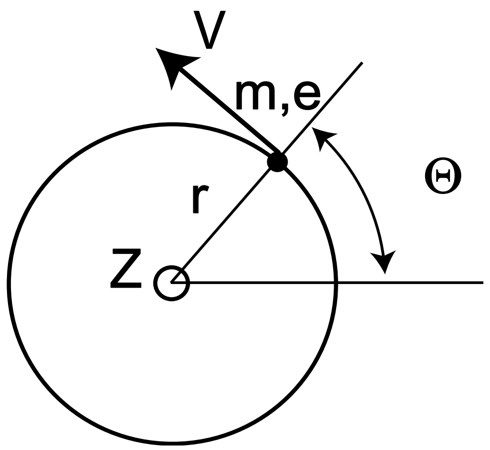

Figure 1.9 Simple model of Bohr's atom

Furthermore, for this system to be stable, it is assumed that the attractive Coulomb force of the charged particles is balanced by the centripetal force of the rotating electron. These basic definitions give us this relation.

$$Centripetal\ Force = \frac{mv^2}{r} = \frac{eZe}{r^2} = Coulomb\ Force$$

By combining these two expressions, we arrive at the following expression for the energy of the bound system. The bound system energy is negative while if the electron is freed from the nucleus, r=∞ ; the energy is 0.

$$mv^2 = \frac{eZe}{r}$$

$$E = \frac{1}{2}mv^2 - mv^2 = -\frac{1}{2}v^2 = -\frac{1}{2}\frac{eZe}{r}$$

The circumference of the orbit is, of course, 2πr, and when traveling at velocity v, the frequency of the orbit is simply

$$f = \frac{v}{2\pi r}\ so\ that\ v = 2\pi rf$$

We can use the above relations to eliminate r and v and obtain an expression for the frequency as

$$E = -\frac{1}{2}mv^2 = -\frac{1}{2}m\left(4\pi^2 r^2 f^2\right)$$

$$f = \frac{\sqrt{2}(-E)^{\frac{3}{2}}}{2\pi r\sqrt{m}}\ and\ since\ E = -\frac{1}{2}\frac{eZe}{r}\ and\ r = -\frac{eZe}{2E}$$

$$f = \frac{\sqrt{2}(-E)^{\frac{3}{2}}}{\pi\, eZe\sqrt{m}}$$

Now here is another big assumption. Scientists liked to associate the radiation from an orbiting particle with its mechanical orbital frequency. Here is an electron orbiting with the frequency given above. Bohr assumed that it was stable but that energy would be given up when it was taken out of its orbit to infinity. There its frequency would be zero. He suggested that the frequency of the emitted light would be the average of the mechanical frequency before and after the transition, which is obviously just f/2.

1.10 Discovery of nuclear reactions

Rutherford 1919 ***(click here to read his article)***

Nobel Prize 1908 (chemistry)

Before 1919 no one had succeeded in disturbing the stability of ordinary nuclei or affecting the disintegration rates of those that were naturally radioactive. In 1919 Rutherford showed that high-energy alpha particles could cause an alteration in the nucleus of an ordinary element. Specifically he succeeded in changing a few atoms of nitrogen into atoms of oxygen by bombarding them with alpha particles. The process involved may be written

$$^{4}_{2}He(\alpha) + ^{14}_{7}N \rightarrow ^{17}_{8}O + ^{1}_{1}H(p)$$

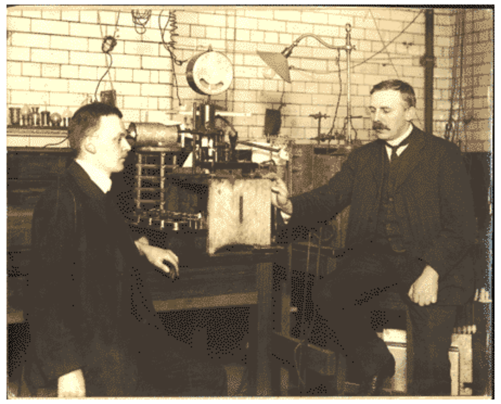

Figure 1.10 E. Rutherford (right) and H. Geiger at Cavendish Laboratory

Rutherford measured the range of α-particles (from RaC α-source) using a scintillation detector.

Range of a particles should be about ~ 7cm in CO_2 and N_2 of atmospheric pressure.

He observed that:

In CO_2 no scintillations if $l_1 > 7$ cm

In N_2 scintillations up to $l_2 \sim 40$ cm.

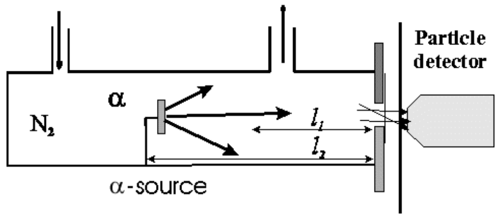

Figure 1.11 Scheme of the Rutherford experiment. α-source mounted on the moveable arm, particle detected in the right-hand side detector.

Rutherford suggested that nuclear reactions are taking place with kinetic energy release:

$$^{4}_{2}He(\alpha) + ^{14}_{7}N \rightarrow ^{17}_{8}O + ^{1}_{1}H(p)$$

In all reactions was $(E_{kin})_{proton} > (E_{kin})_{\alpha}$

Energy came from nuclear reaction.

HOW?

Description of nuclear reactions:

a + b ——> c + d

a(b,c)d

4 laws:

1) Number of nucleons equal before and after reactions

2) Number of charges equal before and after reactions

3) Energy conserves

4) Momentum conserves

Basic mass-energy conservation equation:
$E_a + E_b + M_a c^2 + M_b c^2 = E_c + E_d + M_c c^2 + M_d c^2$

Energy of nuclear reactions, Q, comes from a mass-defect:

$$Q = \left[\left(M_a + M_b \right) - \left(M_c + M_d \right) \right] \times c^2$$

$$if$$

$$Q > 0 \rightarrow exothermic\ reactions$$

$$Q < 0 \rightarrow endothermic\ reactions$$

Example:

^3H (d,n) ^4He

M(^3H) : 3.0160	M(^4He) : 4.0026
M(^2H) : 2.0141	M(n) : 1.0087
5.0301	5.0113

Q = 0.0188 * 931 = 17.6 Mev

NUCLEAR REACTION CHANNELS

1) Emission of a -particle:

$$^{238}_{92}U \rightarrow ^{234}_{90}Th + ^{4}_{2}He(\alpha) + \gamma$$

2) Emission of ß-particles:

$$^{60}_{27}Co \rightarrow ^{60}_{28}Ni + ^{0}_{-1}\beta + \overline{\nu} + \gamma$$

3) Emission of positron:

$$^{57}_{26}Fe \rightarrow ^{57}_{25}Mn + ^{0}_{1}\beta(\overline{\beta}) + \nu + \gamma$$

4) K-capture:

$$^{7}_{4}Be + ^{0}_{-1}\beta \rightarrow ^{7}_{3}Li + \nu + \gamma$$

1.11 Particle-wave dualism

Prince L.V. de Broglie (f. 1892), 1924

Nobel Prize 1929 ***(click here to read Nobel lecture)***

Figure 1.12 Louis de Broglie

Louis Victor Pierre Raymond duc de Broglie ***(click here to read his article)***

Born: 15 Aug 1892 in Dieppe, France
Died: 19 March 1987 in Paris, France

Louis de Broglie studied history at the Sorbonne in Paris, a career in the diplomatic service. At the age of 18 he began to study physics and after being assigned a research topic in history he chose, after worrying greatly about the decision, to undertake research in physics.

De Broglie was best known for his particle--wave duality theory that matter has the properties of both particles and waves. His doctoral thesis of 1924 put forward this theory of electron waves, based on the work of Einstein and Planck. The wave nature of the electron was experimentally confirmed in 1927 by C J Davisson, C H Kunsman and L H Germer in the U.S.A. and by G P Thomson in Scotland. De Broglie, during an interview in 1963, described how his discoveries came about:

> *"As in my conversations with my brother we always arrived at the conclusion that in the case of x--rays one had both waves and corpuscles, thus suddenly -- ... it was certain in the course of summer 1923 -- I got the idea that one had to extend this duality to material particles, especially to electrons. And I realised that, on the one hand, the Hamilton--Jacobi theory pointed somewhat in that direction, for it can be applied to particles and, in addition, it represents a geometrical optics; on the other hand, in quantum phenomena one obtains quantum numbers, which are rarely found in mechanics but occur very frequently in wave phenomena and in all problems dealing with wave motion. "*

After his doctorate, de Broglie remained at the Sorbonne, becoming professor of theoretical physics at the Henri Poincaré Institute in 1928. De Broglie taught there until he retired in 1962. In 1945 he became an adviser to the French Atomic Energy Commissariat.

De Broglie's theory of electron matter waves was later used by Schrödinger to develop wave mechanics. De Broglie received the Nobel Prize in 1929.

He wrote many popular works which demonstrate his interest in the philosophical implications of modern physics, including Matter and Light: The New Physics (1939); The Revolution in Physics (1953); Physics and Microphysics (1960); and New Perspectives in Physics (1962).

The central question in de Broglie's life was whether the statistical nature of atomic physics reflects an ignorance of the underlying theory or whether statistics is all that can be known. For most of his life he believed the former although as a young researcher he had at first believed that the statistics hide our ignorance. Perhaps surprisingly, he returned to this view late in his life stating that the statistical theories hide a completely determined and ascertainable reality behind variables which elude our experimental techniques.

Wave-particle duality

a wave can exhibit particle-like characteristics

- ***light waves like photons***
- ***Blackbody radiation***
- ***Photo-electric effect***

a particle can exhibit wave-like characteristics

- ***electrons showing diffraction and interference***
- ***particles with momentum → de Broglie wavelength***

This type of behaviour only shows up when we look on the atomic or sub-atomic scale

Wave Behaviour of Particles

de Broglie showed that a particle of momentum p has, associated with it, a wave of wavelength λ= h/p, called the de Broglie wavelength.

The wave which is associated with the particle has the property that the square of its amplitude at a particular point gives the probability of finding the particle at that point. The mathematical expression which describes the wave is called the wave function

$$\lambda = \frac{h}{mv}$$

$$for\ neutrons:$$

$$\lambda_{\mathring{A}} = \frac{3956}{v\left[\frac{m}{s}\right]} = \frac{0.286}{\sqrt{E[eV]}}$$

1.12 Exclusion principles for electrons in atom (1925) and prediction of neutrino (1930)

Wolfgang Pauli (1900-1958)

Nobel Prize 1945 ***(click here to read his Nobel lecture)***

Born: 25 April 1900 in Vienna, Austria

Died: 15 Dec 1958 in Zurich, Switzerland

Wolfgang Pauli was the son of a medical doctor who was himself to become a university professor. Wolfgang attended school in Vienna where he began a deep study of mathematics and physics. He entered the University of Munich in 1918 and, while still an undergraduate at Munich, wrote an article on the theory of relativity which became the standard text.

At Munich, Pauli was taught by Sommerfeld who soon recognised his genius. This genius was also recognised by Einstein who, after reading Pauli's article on relativity, wrote:

"Whoever studies this mature and grandly conceived work might not believe that its author is a twenty--one year old man. "

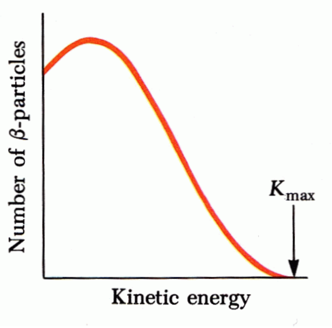

Figure 1.13 Neutrino could explain why beta-particles have a continu- ous energy spectrum.

Pauli received his doctorate, supervised by Sommerfeld, for a thesis on the quantum theory of ionised molecular hydrogen in 1920. He was then appointed to Göttingen as Born's assistant. Pauli spent the year 1922--23 at Bohr's Institute. In 1923, he was appointed a lecturer at Hamburg, then in 1924 he proposed a quantum spin number for electrons.

Pauli is best known for the Pauli exclusion principle, proposed in 1928, which states that no two electrons in an atom can have the same four quantum numbers.

In 1928 Pauli was appointed professor at Zurich. He predicted mathematically, in 1930, that conservation laws in beta-decay required the existence of a new particle which he proposed to call the neutron but it was named the *neutrino* by Fermi. It was later found experimentally by Reins and Cowan. (Click here to read about neutrino communique) .

In 1940 Pauli was appointed to the chair of theoretical physics at Princeton then he returned to Zurich after World War II. He was awarded the Nobel Prize in 1945 ***(click here to read his Nobel lecture)***.

Neutrino experiment

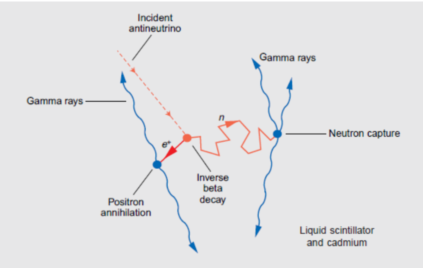

Figure 1.14 Principle of neutrino detection in the Reins and Cowan experiment

In 1951 Fred Reines at Los Alamos thought about doing some real challenging physics problem. In a conversation with Clyde Cowan they decided to work on detecting the neutrino. Their first plans were to detect neutrinos emitted from a nuclear explosion. Realizing that nuclear reactors could provide a neutrino flux of 1013 neutrinos per square centimeter per second, they instead mounted an experiment at the Hanford nuclear reactor in 1953. The Hanford experiment had a large background due to cosmic rays even when the reactor was off. The detector was then moved to the new Savannah River nuclear reactor in 1955. This had a well shielded location for the experiment, 11 meters from the reactor center and 12 meters underground.

The detection of the neutrino was as the initiator of the inverse-beta decay reaction of:

anti-neutrino + proton -> neutron + positron.

The target was water with $CdCl_2$ dissolved in it. The positron was detected by its slowing down and annihilating with an electron producing two 0.5 MeV gamma rays in opposite directions. The pair of gamma rays was detected in time coincidence in liquid scintillator above and below the water by photomultiplier tubes detecting the scintillation light. The neutron was also slowed by the water and captured by the cadmium microseconds after the positron capture. In the capture several gamma rays were emitted which were also detected in the scintillator as a delayed coincidence after the positron's annihilation gamma ray detection. The detector contained 200 liters of water in two tanks with up to 40 kg of dissolved $CdCl_2$.

The water tanks were sandwiched between three scintillator layers which contained 110 5" photomultipliers each, and the whole experiment measured only about 2 meters in each direction.

At Savannah River, Reines and Cowan carried out a series of measurements to show that (see Reines' personal accounts below):

(a) the reactor-associated delayed coincidence was consistent with theoretical expectation;
(b) the first pulse of the delayed coincidence signal was due to positron annihilation;
(c) the second pulse was due to neutron capture;
(d) the signal was a function of the number of target protons; and
(e) the reactor-associated signal was not caused by gamma rays or neutrons from the reactor.

The rarity of neutrino capture is shown in their signal rate, which was about three events per hour in the entire detector. The signal to background ratio was about four to one. Thus in 1956 was born the rich and continually exciting field of experimental neutrino physics, as discussed in other articles in this newsletter. This discovery was recognized by honoring Frederick Reines with the Nobel Prize in 1995. ***Click here to read more about the first neutrino experiment - source: Los Alamos Science.***

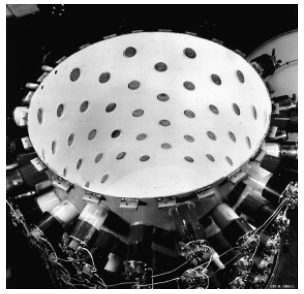

Figure 1.15 The scintillation detector for the 1953 neutrino detection experiment at Hanford

Neutrinos, they are very small.
They have no charge and have no mass
And do not interact at all.
The earth is just a silly ball
To them, through which they simply pass,
Like dustmaids down a drafty hall
Or photons through a sheet of glass.
They snub the most exquisite gas,
Ignore the most substantial wall,
Cold-shoulder steel and sounding brass,
Insult the stallion in his stall,
And, scorning barriers of class,
Infiltrate you and me! Like tall
And painless guillotines, they fall
Down through our heads into the grass.
At night, they enter at Nepal
And pierce the lover and his lass
From underneath the bed—you call
It wonderful; I call it crass

1.13 Development of wave mechanics

Erwin Schrödinger, 1926

Nobel Prize 1933 together with PAM Dirac ***(click here to read Schrödinger's Nobel lecture)***

Born: 12 Aug 1887 in Vienna, Austria

Died: 4 Jan 1961 in Alpbach, Austria

Schrödinger was a student at Vienna from 1906 and taught there for ten years from 1910 to 1920 with a break for military service in World War I. While at Vienna he worked on radioactivity, proving the statistical nature of radioactive decay. He also made important contributions to the kinetic theory of solids, studying the dynamics of crystal lattices.

After leaving Vienna in 1920 he was appointed to a professorship in Jena. After only a short time there he moved to a chair in Stuttgart, then to a chair in Wroclaw before accepting the chair of theoretical physics at Zurich in late 1921. During these years of changing from one place to another, Schrödinger studied physiological optics, in particular the theory of colour vision.

Zurich was to be the place where Schrödinger made his most important contributions. From 1921 he studied atomic structure. Then in 1924 he began to study quantum statistics, soon after this reading de Broglie's thesis which was to have a major influence on his thinking.

Schrödinger published very important work relating to wave mechanics and the general theory of relativity in a series of papers in 1926. Wave mechanics, proposed by Schrödinger in these papers, was the second formulation of quantum theory, the first being matrix mechanics due to Heisenberg. The relation between the two formulations of wave mechanics and matrix mechanics was understood by Schrödinger immediately as this quotation from one of his 1926 papers shows:--

> *"To each function of the position-- and momentum-- coordinates in wave mechanics there may be related a matrix in such a way that these matrices, in every case satisfy the formal calculation rules of Born and Heisenberg. ... The solution of the natural boundary value problem of this differential equation in wave mechanics is completely equivalent to the solution of Heisenberg's algebraic problem."*

For this work Schrödinger was awarded the Nobel prize in 1933.

Schrödinger went to Berlin in 1927 where he succeeded Planck in the chair of theoretical physics and he became a colleague of Einstein's.

Although he was a Catholic, Schrödinger decided in 1933 that he couldn't live in a country in which persecution of Jews had become a national policy. He left, spending time in Britain where he was at the University of Oxford from 1933 until 1936. In 1936 he went to Austria and spent the years 1936--1938 in Graz. However the advancing Nazi threat caught up with him again in Austria and he fled again, this time settling in Dublin, Ireland in 1939.

His study of Greek science and philosophy is summarised in Nature and the Greeks (1954) which he wrote while in Dublin. Another important book written during this period was What is life (1944) which led to progress in biology. He remained in Dublin until he retired in 1956 when he returned to Vienna and wrote his last book Meine Weltansicht (1961) expressing his own metaphysical outlook.

During his last few years Schrödinger remained interested in mathematical physics and continued to work on general relativity, unified field theory and meson physics.

1.14 Formulation of uncertainty principle

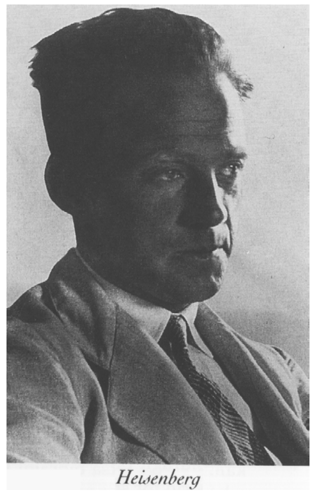

Werner Karl Heisenberg, 1927

Nobel Prize 1932, ***(click here to read his Nobel lecture)***

Born: 5 Dec 1901 in Würzburg, Germany

Died: 1 Feb 1976 in Munich, Germany

Werner Heisenberg attended school in Munich and the entered the University of Munich. There he, and his fellow student Pauli, studied physics under Sommerfeld. After completing his undergraduate course he continued study for his doctorate presenting his doctoral dissertation in 1923 on turbulence in fluid streams.

Heisenberg, as Pauli had done shortly before, went from Munich to the University of Göttingen where he studied there under Max Born. In 1924 he went to the Institute for Theoretical Physics in Copenhagen where he studied under Niels Bohr. A lecture series by Niels Bohr convinced him to work on quantum theory.

In 1927 Heisenberg was appointed to a chair at the University of Leipzig. He was to hold this post until, in 1941, he was made director of the Kaiser Wilhelm Institute for Physics in Berlin.

Heisenberg did important work in nuclear and particle physics, but his most important work was in quantum mechanics.

Heisenberg invented matrix mechanics, the first version of quantum mechanics, in 1925. He did not invent these concepts as a matrix algebra, however, rather he focused attention on a set of quantised probability amplitudes. These amplitudes formed a non-commutative algebra. It was Max Born and Pascual Jordan in Göttingen who recognised this non-commutative algebra to be a matrix algebra.

Matrix mechanics was further developed in a three author paper by Heisenberg, Born and Jordan published in 1926. Heisenberg published The Physical Principles of Quantum Theory in 1928. In 1932 he was awarded the Nobel Prize in physics for this work.

Heisenberg is best known for the Uncertainty Principle which he discovered in 1927. It was in 1927 that Heisenberg attended the Solvay Conference in Brussels. He wrote in 1969:

> *"To those of us who participated in the development of atomic theory, the five years following the Solvay Conference in Brussels in 1927 looked so wonderful that we often spoke of them as the golden age of atomic physics. The great obstacles that had occupied all our efforts in the preceding years had been cleared out of the way; the gate to an entirely new field, the quantum mechanics of the atomic shells stood wide open, and fresh fruits seemed ready for the picking. "*

"The more precisely the POSITION is determined,the less precisely the MOMENTUM is known" sounds the uncerainty principle.

In the 1930s Heisenberg and Pauli used a quantised realisation of space in their lattice calculations.

Heisenberg hoped this mathematical property would lead to a fundamental property of nature with a 'fundamental length' as one of the constants of nature.

In 1932 Heisenberg wrote a three part paper which describes the modern picture of the nucleus of an atom. He treated the structure of the various nuclear components discussing their binding energies and their stability. These papers opened the way for others to apply quantum theory to the atomic nucleus.

During the Second World War he headed the unsuccessful German nuclear weapons project. He worked with Otto Hahn, one of the discoverers of nuclear fission, on the development of a nuclear reactor but failed to develop an effective program for nuclear weapons. Whether this was because of lack of resources or a lack of a desire to put nuclear weapons in the hands of the Nazis, it is unclear. After the war he was interned in Britain with other leading German scientists. However he returned to Germany in 1946 when he was appointed director of the Max Planck Institute for Physics and Astrophysics at Göttingen. In 1958 the Institute moved to Munich and Heisenberg continued as its director.

He was also interested in the philosophy of physics and wrote Physics and Philosophy (1962) and Physics and Beyond (1971).

Click here to read more about Heisenberg.

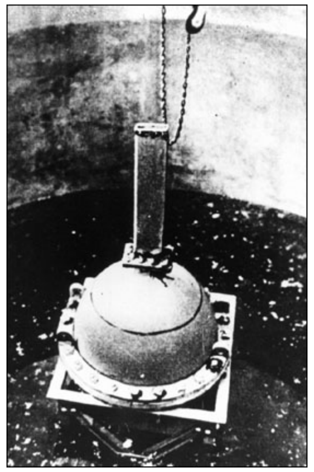
*Figure 1.16 **E**arly german experiments with a critical mass*

THE HEISENBERG UNCERTAINTY PRINCIPLE

The Heisenberg Uncertainty Relations are of the form:

$$\Delta p \Delta q \geq \frac{h}{4\pi}$$

$$\Delta E \Delta t \geq \frac{h}{4\pi}$$

They express the limitations imposed by nature on the precision with which we can simultaneously know certain pairs of quantities, like Energy and time, or momentum p and position q.

1.15 Combination of quantum mechanics and special relativity theory - theoretical description of electron (1928).

Prediction of POSITRONS (1931).

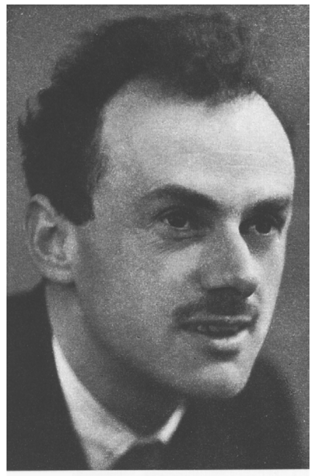
Dirac

Paul Adrien Maurice Dirac (1902-1984)

Nobel Prize 1933 ***(click here to read his Nobel lecture)***

Born: 8 Aug 1902 in Bristol, Gloucestershire, England

Died: 20 Oct 1984 in Tallahassee, Florida, USA

PA M Dirac is famous as the creator of the complete theoretical formulation of quantum mechanics. He studied electrical engineering at the University of Bristol before doing research in mathematics at St John's College Cambridge. His first major contribution to quantum theory was a paper written in 1925. He published The principles of Quantum Mechanics in 1930 and for this work he was awarded the Nobel Prize for Physics in 1933.

Dirac was one of the founders of quantum mechanics. He was also among the first to attempt to integrate Einstein's special theory of relativity into the formalism of quantum mechanics. This led to his prediction of the existence of antimatter, in particular the positron and the phenomenon of electron-positron pair production. Dirac was appointed Lucasian professor of mathematics at the University of Cambridge in 1932, a post he held for 37 years.

He was made a fellow of the Royal Society in 1930, was awarded the Royal Society's Royal Medal in 1939 and the Society awarded him the Copley Medal in 1952.

In 1971 Dirac was appointed professor of physics at Florida State University and was appointed to the Order of Merit in 1973.

1.16 Discovery of deuterium

Harold Clayton Urey (1893-1981), 1931

Nobel prize in chemistry, 1934 ***(Click here to read his Nobel lecture)***

The son of a country clergyman, Harold Clayton Urey was born in Walkerton, Indiana, on April 25, 1893. His father died when he was six years old and his mother remarried, again to a clergyman. He obtained his early education in the Indiana public schools and graduated from high school in 1911. Being unable to go directly to college, Urey taught for several years in rural schools before entering the University of Montanain 1914. Three years later he obtained his B.S. In chemistry. Because of the World War I, Urey took position in Philadelphia in a chemical plant engaged in war production. He later described this experience as most fortunate because it convinced him that academic work, not industrial chemistry, was his major interest. The direction of this academic work was to the University of Montana, where he became an instructor in chemistry. Five years later, in 1921, he went to the University of California at

Berkeley to study for doctorate in chemistry under Prof. Gilbert N. Lewis. Lewis was an inspiring teacher and leader in chemistry and undoubtly greatly influenced Urey's career.

Following the receipt of the Ph.D. Degree Urey received a fellowship from the American-Scandinavian Foundation which he used for a year´s postdoctoral study at Bohr's Institute for Theoretical Physics in Copenhagen. Returning to the United States in 1924, he served for 5 years as associate in chemistry at the Johns Hopkins University in Baltimore. It was during this time that he wrote with Arthur E. Ruark his widely used book Atoms, Molecules and Quanta, published 1930.

In 1929 Urey accepted a position as associate professor of chemistry at Columbia University. Very shortly thereafter he began the investigation for which he received the Nobel Prize in 1934 - the isolation of the hydrogen isotope of mass two, heavy hydrogen - deuterium. This research was carried out with the assistance of dr. Ferdinand G. Brickwedde, then head of the cryogenic section of the U.S. National Bureau of Standards, and Dr. George M. Murphy at Columbia University.

Research with heavy hydrogen and methods of concentrating stable isotopes occupied Urey during the following years until United States´s entry into World War II. As a consequence of his experience in isotope separation he was appointed to head the group designated as the SAM (Substitute Alloy Materials) Laboratory established at Columbia University to investigate the separation of uranium isotopes 235 and 238 for the purposes of making an atomic bomb. This laboratory was a part of the Army´s Manhattan District Project and subsequently became the research laboratory that provided the fundamental data necessary for the construction of the large-scale diffusion separation plant built by the Kellex Corporation at Oak Ridge, Tennessee.

At the end of the war, Urey joined the Institute for Nuclear Studies at the University of Chicago and became distinguished service professor of chemistry. His scientific interest now took a new direction. He began research on the origin of the earth and the planetary system, the evolution of life on earth and the temperatures of the oceans in past geological ages. His book, Planets, Their Origin and Development, was published by Yale University Press in 1952. In 1958 he left Chicago to assume the chair of professor of chemistry-at-large in the University of California at La Jolla. He remained a resident of La Jolla until his death on January 5, 1981.

In a 1932 paper in Physical Review, (click here to read this article) Urey, Brickwedde and Murphy outlined and analyzed the techniques employed to isolate deuterium. They conclude that fractional distillation offered the best chance for success, since the mass ratios of the different hydrogen isotopes are much larger than for heavier elements, for which fractional distillation did not work well.

Urey and his fellow authors found that the calculated vapour pressure for the H^1H^2 molecule should be about one third of that of the ordinary hydrogen molecule H^1H^1 when the gas is in equilibrium with the solid phase at the triple point temperature of ordinary hydrogen.

1.17 Discovery of a Neutron

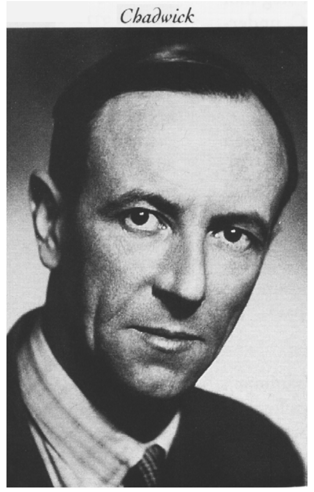

James Chadwick (1891-1974), 1932

Nobel Prize - 1935 ***(click here to read his Nobel lecture)***

In 1907, while enrolling at the University of Manchester, James Chadwick accidentally found himself in the line for those hoping to major in physics. Chadwick, who had intended to be a mathematician, was too shy to admit he was mistaken and stayed in line. Thus began the career of one of this century's most distinguished physicists. In 1913 he received his master's degree and left for Germany to work with Hans Geiger. There, Chadwick was the first to show that beta particles possess a range of energies up to some maximum value. Trapped in Germany when WW I broke out, Chadwick was imprisoned in a horse stall at a racetrack that served as an internment camp. As soon as the war ended and he gained his freedom, Chadwick returned to England and joined forces with Ernest Rutherford. Intrigued by Rutherford's speculation about a subatomic particle with no charge, Chadwick began a series of experiments to demonstrate the existence of such a particle. Initially, none of the experiments succeeded. Then, in 1930, Walther Bothe and Herbert Becker described an unusual type of gamma ray produced by bombarding the metal beryllium with alpha particles. Chadwick recognized that the properties of this radiation were more consistent with what would be expected from Rutherford's neutral particle. When Frédéric and Irène Joliot-Curie subsequently claimed that Bothe and Becker's "gamma rays" could eject high energy protons from paraffin, Chadwick knew these were not gamma rays. The subsequent experiments by which Chadwick proved the existence of the neutron earned him the 1935 Nobel Prize in physics. Not only did this singular particle provide physicists with a superlative tool for investigating the atom, it was also used to produce a wide variety of new radioisotopes and permitted the initiation of nuclear chain reactions.

Hans Bethe has referred to Chadwick's discovery as the historical beginning of nuclear physics ***(click here to read Chadwick's article)***.

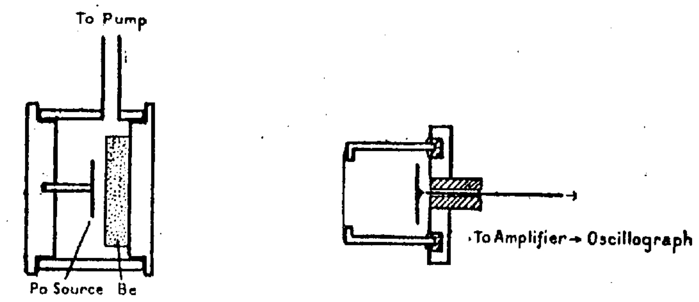

Figure 1.17 A sketch of Chadwick's experiment with neutrons

James Chadwick showed that beryllium (Be), when exposed to an alpha particles, gave off a particle which was not deflected (accelerated) by electric or magnetic forces. The particle was thus uncharged, yet it was massive enough to knock protons out of a sample of paraffin (which is rich in hydrogen).

To explain "strange" radiation from beryllium, I. Curie and F. Joliot had proposed a reaction:

$$ {}^{9}_{4}Be + {}^{4}_{2}He \to {}^{13}_{6}C + \gamma + Energy $$

experiments, however, contradicted this explanation

Chadwick guessed:

$$ {}^{9}_{4}Be + {}^{4}_{2}He \to {}^{12}_{6}C + {}^{1}_{0}n + Energy $$

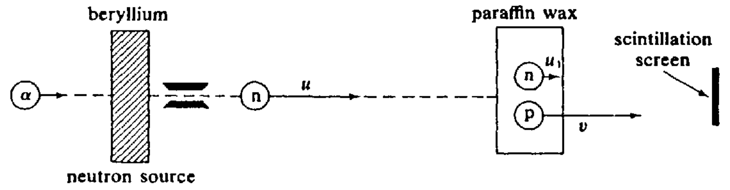

How Chadwick calculated the neutron mass?

Using the scheme of the experiment as above and its calculational model like below

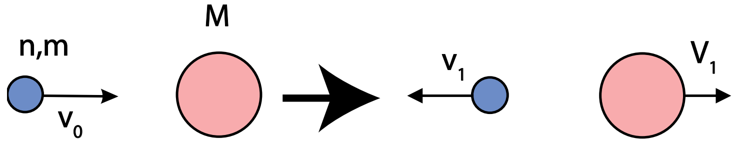

and by applying the mechanical collision laws Chadwick found:

$$ \left. \begin{cases} m(v_0 + v_1) = MV_1 \\ \dfrac{1}{2}MV_1^2 = \dfrac{1}{2}m v_0^2 + v_1^2) \end{cases} \right\} \to V_1 = \frac{2m}{M+m} v_0 $$

M - nucleus mass
m - neutron mass

v_0 - neutron velocity before collision
v_1 - neutron velocity after collision
V_1 - velocity of nucleus after collision

V_1 had been derived for two types of recoil nuclei, namely the proton and Nitrogen. Mass of ${}^{11}_{5}B$ and ${}^{14}_{7}N$ were known, so

$$ {}^{11}_{5}B + {}^{4}_{2}He \to {}^{14}_{7}N + {}^{1}_{0}n $$

Chadwick estimated neutron mass m=1.2 compared to mass of the proton M=1.

Click here to read more about Chadwick's discovery.

The Neutron has come to be.
Loaded with Mass is he.
Of Charge, forever free.
Pauli, do you agree?

Now a reality,
Once but a vision.
What classicallity,
Grace and precision!
Hailed with cordiality,
Honored with song,
Eternal Neutrality
Pulls us along!

R. Rhodes, "The Making of the Atomic Bomb"

THE STRUCTURE OF THE NUCLEUS IN PRINCIPLE SOLVED:
M —->$^{N+Z}$ A

Nucleus:
Protons - Z
Neutrons - N
Mass Number - A=Z+N

ISOTOPES : Z - constant, different N and A

ISOBARS : A - constant, different Z and N

ISOTONES : N -constant, different A and Z

1.18 Mass Spectrometry invented.

Francis W. Aston, Arthur J. Dempster, Kenneth T. Bainbridge 1918-1933

1922 Nobel prize in chemistry for F. W. Aston. ***Click here to read his Nobel lecture***

Click here to read more about mass spectroscopy.

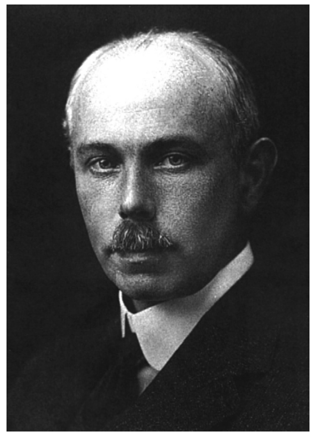

F.W. Aston

Frederick Soddy's discovery of isotopes through research in the radiochemical elements about the year 1910, and their exploration in the next three years, must have suggested to more than one investigator that such atoms should be sought in the stable elements. However, the way such a search might be started was by no means clear. It remained for J. J. Thomson with his positive ray apparatus to open the doors for such investigations in 1912. As we have already seen, Thomson analyzed a sample of very pure neon, and his apparatus showed that atoms of mass 20 and 22 were present in the gas. The possibility that the atoms of mass 22 found in the positive rays might be NeH_2 prompted Thomson to put F. W. Aston, his assistant, to work on the diffusion separation of the gas. After the most laborious efforts, Aston achieved what appeared to be a significant separation of fractions of differing mass, but the advent of World War I prevented further researches on the problem.

During the war F. Aston conceived the idea of extending the isotope study by developing a mass spectrograph as an improvement of Thomson's parabola method. The spectrograph that he designed was built at Cambridge in 1919. The details were presented in his 1920 letter to Nature, entitled "Positive Rays and Isotopes," together with photographs of the mass spectra obtained with its use. Neon was the first element examined and its isotope was immediately revealed; atomic masses of 20 and 22 (on the scale oxygen = 16) were clearly present, the precision of the mass numbers being estimated at 1/10th percent.

This spectrograph was used to analyze some 50 elements in the following six years, revealing the almost universal existence of isotopes. Exceptions appeared in the elements of odd atomic number, the great majority of these having no isotopes; that is, atoms of one mass only were present. Aston assumed that the most important result of the research was the discovery that the measured mass of all the atoms, except hydrogen, was integral on the basis oxygen = 16. This is called the whole number rule. But a second and, subsequently, a third mass spectrograph of increasing precision showed that this was not substantiated by more precise measurements. Aston's research thus showed that Prout's hypothesis, made more than a hundred years previously and intermittently revived, was untenable. The addition of masses, equal to that of hydrogen, did not give the masses of the succeeding elements in the periodic table. It was also clear that the elements were not built up, as the whole number rule suggested, of mass units equal to 1/16th of the oxygen atom.

On the other hand, to Prout's credit, the existence of the nuclear atom made it appear that all the elements were made up of protons and electrons, the elemental building material of hydrogen atoms. But even from this point of view it was evident that the masses of the elements were not arrived at by the simple addition of the masses of the protons and electrons of which they were apparently composed. The elemental masses as measured by the spectrograph showed a mass defect as compared to the sum of the masses of their free constituent particles. This defect in mass was explained, on the basis of Einstein's mass-energy equation $E = mc^2$ as representing the energy that was radiated away in the formation of the nucleus. It was therefore the binding energy of the particles in the nucleus; the greater the mass defect, the more stable the nucleus. The further clarification of this point of view had to await the advent of experimental nuclear physics in the 1930s and the discovery of the neutron.

It is convenient at this point to summarize the nomenclature brought into physics by these advances in the measurement of atomic masses. The atomic number was defined as the number of (integral) elementary nuclear positive charges; the mass number was taken as the nearest whole number to the mass of the isotope considered (later it was taken to be the number of protons and neutrons in the nucleus). The mass of the isotope was its mass on the scale oxygen = 16, although this subsequently had to be changed owing to the discovery that oxygen itself had isotopes. The reference atom was then changed to a comparison of masses on the basis that the most prevalent isotope of oxygen was of mass 16. In order to convey an idea of the stability of nuclei, Aston later introduced a quantity called the packing fraction, defined as the ratio of the mass defect to the mass number. It must be pointed out that the importance of determining the isotopic constitution of the elements and the individual isotopic masses drew many able investigators to this field and resulted in the invention of several different mass spectrometers. For details regarding the outstanding investigators and their instruments the reader should consult the indexes of the various physical journals.

Until he came to Cambridge, Aston had a rather varied career. The son of a metal merchant, he was born in a suburb of Birmingham, England, and as a youth displayed a strong bent for experimenting with mechanical devices and with chemicals. He graduated from secondary school with highest honors in mathematics and science and entered Mason College, later the University of Birmingham, in 1893. His chemistry teachers at Birmingham were Tilden and Frankland and he studied physics under J. H. Poynting. With Frankland he worked on problems in organic chemistry, publishing his first paper in 1901. By no means was all of his work done in university laboratories because in 1896 he fitted up a loft in his home as a private laboratory and workshop. Here he carried on private research for many years. In 1900 he entered the employ of a brewing company and continued in industrial work until 1905 when he returned to university work on a scholarship. In 1908, on the death of his father, he took a year off to make a trip around the world. On his return he continued working on glass discharge tubes and on vacuum apparatus to exhaust them, including an automatic Toepler-type pump of his own construction. His outstanding skill in this field led in 1910 to his association with J. J. Thomson at Cambridge as a research assistant. He was soon engaged with Thomson on the development of the latter's positive-ray apparatus and on the diffusion separation of neon in 1913.

After service in World War I, he returned to Cambridge to work independently on his mass spectrograph. He was made a fellow of Trinity College, Cambridge, in 1919 and maintained his residence in the college for the remainder of his life. By 1922 his isotope work was deemed to be so outstanding that he was awarded the Nobel Prize in chemistry. As time went on, other able investigators entered this field, but Aston continued his investigations, increasing the precision of his work.

In his mature years Aston was a quiet, reserved man; above average height, he had an erect carriage. He was a strong individualist and maintained from his youth the conservative views characteristic of a middle-class upbringing in the late Victorian period. He was fond of travel and sports, and his interest in and knowledge of music was so extensive that he served for many years as the music critic of the Cambridge Review. In finance, he was also unusually able, so that toward the end of his life he had amassed considerable means. His biographer for the Royal Society summed up his life, perhaps most aptly, with the phrase: "Aston's life was a chain of uninterrupted success."

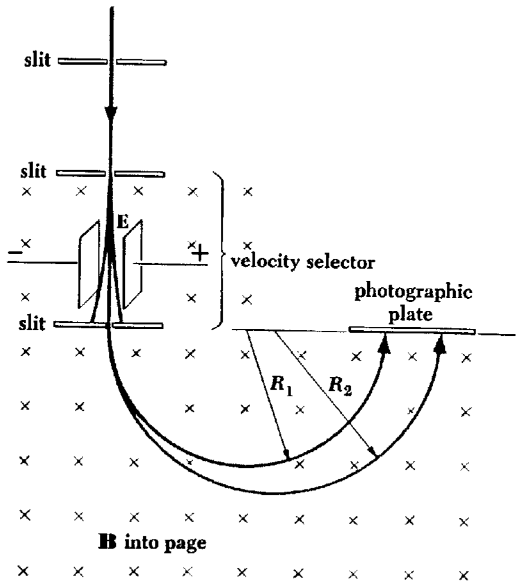

The principle of mass spectrometry

Balance between electric field (E) and magnetic field (B):

$EQ = Q\vec{B} \otimes \vec{v}$ Q= charge of ion

v=E/B v= ion velocity

In a uniform magnetic field ions are deflected:

$Q\vec{B} \otimes \vec{v} = \frac{Mv^2}{R}$ $M = ion\ mass$

$R = \frac{v}{B}\frac{M}{Q}$ $R = radii\ of\ the\ orbit$

$M = \frac{RBQ}{v}$

Balance of energy in nuclear reactions could be controlled:

$M_1c^2 + M_2\,c^2 = M_3\,c^2 + M_4\,c^2$ + Energy

1.19 Invention of Accelerators


John Cockroft

John D. Cockroft, Ernest T. Walton 1932, Nobel Prize 1951 for principles of a linear accelerator (Linac) ***(click here to read the Nobel lectures)***

Robert van de Graaff - 1931-1933

Ernest Lawrence 1934-36, Nobel Prize 1939 for invention of a circular accelerator (Cyclotron) ***(click here to read his Nobel lecture)***

Since Rutherford experiments with alpha parfticle bombardment of gold foils scientists began intensive work with particle collisions. These investigators had primarily used alpha particles from radioactive sources to bombard nuclei of various kinds, and some nuclear transformations had been produced. However, natural radioactive sources of particles were much too limited to be very useful for a systematic study of nuclei. Since the neutron had not yet been discovered when particle accelerators were first produced, charged particles had to be used to probe nuclei. It was therefore necessary to devise various schemes to accelerate such particles to energies that would penetrate the nucleus. Transformations induced by particle bombardment of the nucleus involve two conditions. The nucleus and the bombarding projectile (alpha particle, proton, and so on) are electrically charged. The colliding particles have a wave character. Consequently one must apply quantum mechanics (the Schrödinger wave equation) to the interaction of charged particles. Since the nucleus and the alpha particles are both positively charged and *repel each other, the problem is essentially that of the penetration of potential barriers by particles.*

The quantum-mechanical theory of the penetration of potential barriers shows that for a given nucleus the depth of penetration of the bombarding particle increases with increasing **energy** but decreases with increasing **mass** and **charge** of the projectile. In other words, for a given energy it is advantageous to use as bullets the lightest particles with the smallest charge, all other things being equal. This fact immediately points to electrons or protons. However, electrons cannot form even quasi-stable systems within nuclei and therefore cannot excite them. In a sense, trying to excite nuclei with electrons (unless the electrons have enormously high energies and hence very short de Broglie wavelengths) is like trying to excite atomic electrons with radio waves. **This predicament left the choice between protons and alpha particles**. Since the theory of the penetration of potential barriers indicates that a million-volt proton has as much penetrating power as a 16-million-volt alpha particle, the proton was finally chosen as the projectile to use in probing the nucleus.

The production of particles of sufficient energy to excite nuclear reactions was attempted almost simultaneously by John Cockcroft and Ernest Walton in England, and by Robert Van de Graaff, and Ernest Lawrence and Milton Livingstone in the United States. The methods adopted by these investigators for attaining the necessary accelerating voltages differed. Cockcroft and Walton decided that the most promising method was to rectify high-voltage, low-temperature frequency alternating current; Van de Graaff believed that the development of a high-voltage electrostatic generator offered the most advantages; Lawrence and Livingstone favored the application of a series of incremental pulsed voltages applied to ions confined in a spiral path by a magnetic field. This device, the cyclotron, has proved to be the most useful for producing the highest energy particles.

The first system that successfully produced artificial nuclear reactions was that of Cockcroft and Walton. Of the three accelerators it was the least novel. The necessary high voltage was obtained by means of a conventional a.c.. transformer. One of its secondary terminals was connected to the plate of a kenetron and the other to one plate of a suitable capacitor. The kenetron is a two element (filament and plate) electron tube capable of rectifying alternating current at high potential. In the simplest arrangement the circuit was completed by connecting the filament of the kenetron to the other plate of the capacitor. The two electrodes of the accelerating tube were then connected in parallel with the capacitor. One transformer supplied the high voltage a.c. rectified by the kenetron; two other transformers were used in connection with the hydrogen discharge tube.

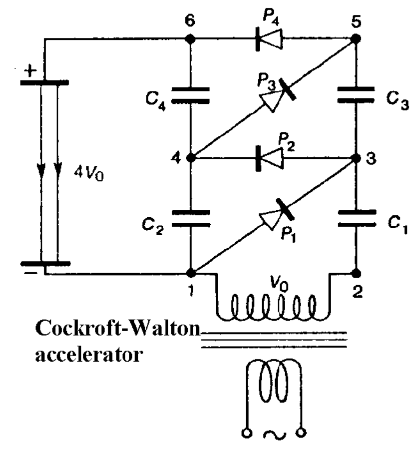

Figure 1.18 A simplified scheme of the Cockroft-Walton accelerator

The current required for the operation of the accelerator is only a few microamperes so that the potential supplied to the accelerating tube is kept sensibly constant by a small capacitor. The protons from the discharge are used as projectiles to induce nuclear reactions. These protons enter the target chamber where they are incident on the material whose nucleus is to be studied.

The first substance studied with this apparatus was lithium. A round target of the element, 5 cm in diameter, was placed at an angle of 450 to the beam of the accelerated protons. When 125 kilovolt protons were incident on the target, scintillations began to appear. Several tests proved that the scintillations were produced by alpha particles. Cockcroft and Walton therefore concluded that the bombardment had resulted in the formation of unstable beryllium 8 which then split into two parts. The reaction may be written as follows:

$$ {}^1_1H + {}^7_3Li \rightarrow {}^8_4Be \rightarrow {}^4_2He(\alpha) + {}^4_2He(\alpha) $$

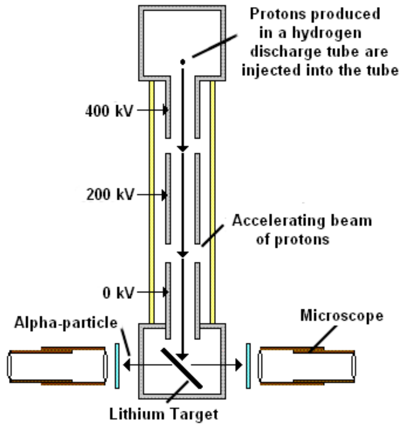

The evidence for the pair production of alpha particles was investigated with results supporting the above conclusions. A series of heavier elements up to uranium was then subjected to proton bombardment, in some instances up to 600 kV. The preliminary results suggested that, in most instances, the ejected particles were alpha particles. Next, the evidence for the pair production of alpha particles was investigated with results supporting the above conclusions. A series of heavier elements up to uranium was then subjected to proton bombardment, in some instances up to 600 kV. The preliminary results suggested that, in most instances, the ejected particles were alpha particles.

The significance of this experiment must be emphasized. Cockcroft and Walton were the first to construct an ion accelerator of sufficient energy to produce nuclear disintegrations. The way was thus opened to study one of the most important but previously almost inaccessible fields of physics. The results showed that nuclei could be disrupted by particles of lower energy than previously supposed. From the balancing of the disintegration equation for Li, **Einstein's mass-energy equivalence was proved without doubt**. For this pioneering work Cockcroft and Walton received the Nobel Prize in physics in 1951.

Sir John Douglas Cockcroft was born in Todmorden, England, on May 27, 1897. His father was a cotton manufacturer, but Cockcroft was strongly attracted to science and mathematics. After a traditional British education, he matriculated at Manchester University and studied mathematics under Horace Lamb. At the end of the war he returned to Manchester to study electrical engineering at the College of Technology, after which he worked as an engineer for the Metropolitan-Vickers Electrical Company. Soon his deep interest in mathematics and the physical sciences drew him back to the university. Like Dirac, he left engineering to study mathematics at St. John's College, Cambridge. There he took the mathematical tripos in 1924 and embarked upon physics as a career. Like many brilliant young experimentalists of the period, he went to the Cavendish Laboratory and worked under Lord Rutherford.

Cockcroft did not go at once into experimental nuclear physics. At that time it appeared that the only way of penetrating the nucleus was with the alpha particles emitted by such radioactive nuclei as uranium and radium; this procedure was not too promising for large-scale investigations. Only a few nuclei could be transmuted. Moreover, Rutherford himself had already done the basic work in this field, so that little more could be done along these lines. Cockcroft therefore chose another research field and began working with the great Russian physicist P. Kapitza on the production of intense magnetic fields and the generation of low temperatures.

In 1928 Cockcroft turned to nuclear physics with an entirely new idea for penetrating nuclei with artificially accelerated protons rather than natural alpha particles. Experimental studies had shown that the energies of alpha particles emitted by radioactive nuclei were, in general, much smaller than one would expect if these particles were propelled from the nucleus by the full Coulomb repulsion This puzzling fact was not understood until the theoretical investigations of Gamow, and of Condon and Gurney, showed that alpha particles, because of their wave nature, do indeed penetrate the Coulomb potential barrier at relatively low energies.

In 1928 when Cockcroft was still formulating his ideas, Gamow visited the Cavendish Laboratory and Cockcroft outlined his plan to him. Supported by Gamow, he sent a memorandum to Rutherford proposing that boron and lithium be bombarded by accelerated protons. In this memorandum he showed that boron could be penetrated by a proton of only 300 kilovolts of energy and that the conditions for lithium were even more favorable. Rutherford agreed to the proposal, and Cockcroft was joined in his project by Ernest Walton, who was then developing one of the first linear accelerators, as well as one of the earliest betatrons. Their collaboration in 1932 resulted in the first proton-induced artificial nuclear disintegrations.

Cockcroft continued his experimental work on the artificial transmutation of elements and in 1933 produced a wide variety of such phenomena, using both protons and deuterons as his projectiles. At the same time he produced artificial radioactivity of various nuclei by proton bombardment. His experimental abilities were quickly recognized and he was appointed director of the Royal Society Mond Laboratory in Cambridge. At that time he was already a fellow of St. John's College, having been elected in 1929; he then became, in turn, university demonstrator and lecturer. In 1939 he was appointed Jacksonian professor of natural philosophy.

When World War II broke out, Cockcroft accepted the post of assistant director of scientific research in the Ministry of Supply and devoted his skills to the development of a coast-to-coast radar defense system. In the autumn of 1940 he came to the United States as a member of the Tizard Mission and then returned to England to become head of the Air Defense Research and Development Establishment. In 1944 Cockcroft went to Canada as head of the Canadian Atomic Energy Project and became director of the Montreal and Chalk River Laboratories. He remained in Canada for two years and then, in 1946, returned to England as director of the Atomic Energy Research Establishment at Harwell. In 1954 Cockcroft was appointed a research member of the United Kingdom Atomic Energy Authority and remained with this agency as a full-time member until 1959, when he was elected master of Churchill College, Cambridge. He then continued with the Atomic Energy Authority on a part-time basis. He was later appointed chancellor of the Australian National University at Canberra. He received many honors for his scientific work and was president of the Institute of Physics, of the British Physical Society, and of the British Association for the Advancement of Science. He was a fellow of the Royal Society and received honorary doctorates from many universities. He died on September 18, 1967, at Cambridge.

Ernest Walton

Ernest Thomas Sinton Walton, Cockcroft's partner, followed a direct path from his early schooling to a career in science. He was born on October 3, 1903, in Dungarvan, Waterford County, on the south coast of Ireland, the son of a Methodist minister from County Tipperary, who, because of his calling, had to move every few years. As a consequence Ernest attended various schools. His aptitude in mathematics and science was evident at a very early age and he was encouraged to continue these studies. He was therefore sent as a boarder in 1915 to the Methodist College in Belfast, where he did brilliant work in mathematics and physics. In 1922 he was awarded a scholarship and entered Trinity College, Dublin, where he read honors courses in mathematics and experimental physics. He graduated with highest honors in these subjects in 1926 and received his M.S. degree in 1927.

On receiving a research scholarship in 1927 from the Royal Commissioner for the Exhibition of 1851, he went to Cambridge University to work at the Cavendish Laboratory under Lord Rutherford. Although Walton's first research papers dealt with hydrodynamics, he shifted to particle accelerators when he began working with Rutherford. A senior research award from the Department of Scientific and Industrial Research in 1930 permitted him to continue with his graduate studies and research. In 1931 he received his Ph.D. degree.

During this period Walton met Cockcroft, who was already working on using relatively low-energy protons to penetrate nuclei by taking advantage of the wave character of the proton, which permits it to pass through the Coulomb barrier. Realizing that protons of only a few hundred kilovolts, rather than millions of volts, would do the job and that this was well within the technological capabilities of that time, Walton worked on improving the high-voltage X-ray and cathode-ray tubes that were then available. Finally, in collaboration with Cockcroft, he constructed a linear accelerator that produced protons of the right energy, which were then used to disintegrate lithium and to transmute boron. Walton shared the Nobel Prize with Cockcroft in 1951 for this pioneer work.

From 1932 to 1934 Walton was Clerk Maxwell scholar at Cambridge. He then returned to Trinity College, Dublin, as fellow. In 1946 he was appointed the Erasmus Smith professor of natural and experimental philosophy, and in 1960 he was elected senior fellow. In addition to his academic work, Walton participated in other educational, civic, and religious activities. He was connected with the Dublin Institute for Advanced Studies, the Institute for Industrial Research and Standards, the Royal City of Dublin Hospital, the Royal Irish Academy, the Royal Dublin Society, and other institutions. In addition to the Nobel Prize, he received the Hughes medal in 1938, jointly with Cockcroft. In 1959 the Queen's University in Belfast awarded him an honorary Doctor of Science degree. Walton published numerous papers on hydrodynamics, nuclear physics, and microwaves in the journals of various scientific societies.

The cyclotron

Ernest Orlando Lawrence (1901 - 1958)

(Click here to read Lawrence article)

Linear accelerators (as well as Van de Graaff accelerator) suffered at the beginning of the serious technical difficulties related to the generation of high voltages. Lawrence introduced a new procedure to accelerate ions to very high speeds in a series of steps, each of which would involve only a relatively small voltage. He proposed a spiral path for the ion, which would cause it to move back and forth across a voltage in'rement in the plane of the spiral. To arrange this so that electric field always accelerates the ion, one must first have a magnetic field at right angles to the plane of the ion's path and then alternating electric field that changes direction periodically in phase with the motion of the ion. Such device is called a cyclotron.

The ion starts moving at right angles to a region across which there is a voltage (see next figure). Initially, the motion of the ion is parallel to the electric field. If a constant magnetic field is now introduced at right angles to the electric field, the ion will move in a circular orbit of fixed radius (Lorentz force will keep the ion on the orbit) If the speed of the ion were constant, the radius of its circular orbit would alwyas be the same. But if the speed of the ion is increased, and the magnetic field remains the same, it then moves in a larger orbit. Now one has to change the electric field periodically in such a way that every time an ion passes through the region where the voltage jumps

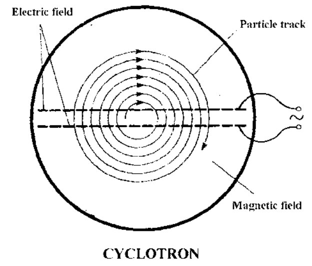

Figure 1.19 Principle scheme of Cyclotron

the field accelerates the ion.

If the ion were always moving with the same speed, the radius of its orbit would always be the same, and the ion would always cross the voltage region at equal time intervals. But the speed of the ion is constantly increasing so that its orbit gets larger and larger. It is not at once apparent that the time intervals between passages cross this region remain the same. But this is the case because the circumference of the orbit and the speed of the ion increase proportionately so that the ion traverses the larger orbit in the same time. This means that, if the direction of the electric field is reversed at intervals equal to the time it take the ion to go halfway around, all the ions will be acted upon by the field in exactly the same way at all the times. The electric field can be regularly alternated in such a way as always to give the ion additional push when it crosses the voltage region. This the basic principle of the cyclotron as it was developed by Lawrence.

It is easy to see that with this device protons or other light ions can be accelerated to high speeds by having them cross the electric field frequently. The cyclotron is important because it performs this operation in relatively small space. As Lawrence pointed out, one needs only have a potential of 4 000 volts across the accelerating gap to obtain speeds corresponding to 1 200 000 volts for protons, if each proton is sent across the gap 150 times. By then, it is moving in so large an orbit that it is near the edge of the apparatus.

Although the principle of the cyclotron is fairly simple, the actual construction and operation presented many problems. Factors such as arrangement of the ion source, the constancy and uniformity of the magnetic field, and the focusing action of the magnetic and electric fields required care to achieve optimum results.

Three years after Ernest Orlando Lawrence had received his doctorate in physics from Yale University and just after he had joined the faculty at the University of California, he carefully took an inventory of what research work he had already done and laid out a plan of action for the future. At that time, although atomic physics seemed to offer the most exciting opportunities for a young physicist., Lawrence was strongly attracted by nuclear physics, which he correctly evaluated as "the next great frontier of the experimental physics."

The neutron had not yet been discovered, consequently the only charged particles (protons or alpha particles) could be used to probe the nucleus and had to he speeded up to very high energies to overcome the repulsion of the nucleus. Keeping this point in mind, Lawrence decided that the greatest promise lay in constructing ion accelerators, and he began to investigate the machines that were then available. Discarding the idea of improving such devices, since he felt that they were already in the hands of very competent people, he searched for new methods of producing high voltages. By chance, in 1929, he ran across an article by a German engineer, Wideröe, that contained the germ of the idea for the cyclotron Although Lawrence could not read German, the diagrams in the article were enough to start him off in the right direction, and so the era of large, nuclear-smashing machines was born. Although the first cyclotron was a small device, about one foot across, there appeared to be no limit, in principle, to the ultimate size of such an instrument. Since that time, accelerators have steadily increased in size.

Lawrence, himself, was well equipped intellectually, and by training, to do the kind of imaginative experimental work that the cyclotron project required. He was born on August 8, 1901, at Canton, South Dakota, of Norwegian immigrants. Lawrence attended elementary and high school in Canton and then went on to St. Olaf College. In 1919 he entered the University of South Dakota and received his B.A. degree in chemistry in 1922. From there he went to the University of Minnesota, receiving his M.A. in chemistry, to the University of Chicago, where he studied physics, and then to Yale University, where he received his Ph.D. in physics in 1925. This was a remarkable achievement in those days since few students were able to complete their doctorate in less than six years after graduating from college.

Figure 1.21 Start-up of Lawrence proton cyclotron called "Atom crusher". From the left : Lawrence, CVompton, Seaborg and Oppenheimer. Click for a video clip.

Figure 1.20 One of the first electron-cyclotrons. Museum of Industry and Technology, Chicago, USA.

Receiving a National Research Fellowship, he spent the next two years at Yale and was then appointed an assistant professor – again achieving something of a record since he was only 26 years old. He remained on the Yale faculty for one year and then accepted an appointment as associate professor of physics at the University of California at Berkeley. Two years later he was promoted to full professor, the youngest at Berkeley, and in 1936, at the age of 35, was named director of the university's radiation laboratory. He had already invented a cyclotron in 1929 so that his reputation as a top physicist was well established.

Lawrence was deeply involved in nuclear physics when World War II began. It was natural for him to be assigned one of the major roles in the development of the atomic bomb, to which he made important contributions. Like most of those working on this project, he was firmly convinced of the need to bring about international control of the bomb or, at least, international agreement on the suspension of testing. He worked hard toward this end and was a member of the 1958 Geneva Conference.

Lawrence's interests in and contributions to physics were extremely broad, as indicated by his published papers, which averaged three and one half a year from 1924 to 1940 – an almost unbelievable productivity. During this time he made better and larger models of the cyclotron, discovered many radioactive isotopes of known elements, applied the cyclotron the medical and biological problems, became consultant to the Institute of Cancer Research at Columbia University, invented a method of obtaining time intervals as short as three billionths of a second, and devised very precise methods for measuring the values of atomic constants.

He received numerous awards and honors such as the Elliott Cresson medal of the Franklin Institute, the Comstock Prize of the National Academy of Science, the Hughes Medal of the Royal Society, the 1939 Nobel Prize, the Duddell medal of the Physical Society of Great Britain, the Faraday medal, the Enrico Fermi Award, and the Medal for Merit. He was an officer of the Legion of Honor and held honorary doctorates from one British and 13 American universities.

Lawrence was a very vigorous man, interested in many intellectual and physical activities including literature, music, boating, tennis, and ice-skating. He died on August 27, 1958, at Palo Alto, California.

The Electrostatic Generator:

Robert J. Van de Graaff

Robert Jemison Van de Graaff (1901-1967)

To produce extremely high, steady voltage over the necessary range raised inherent difficulties not easily overcome for linear accelerators. The limitations of the high -voltage -rectifier method were realized by Robert Van de Graaff, who set about solving the problem of high voltage by a path that differed from that of Cockcroft and Walton. Realizing the advantages of a steady high potential for ion acceleration, Van de Graaff tried to find a simple means of achieving it.

The simplest solution seemed to demand a return to the earliest methods for generating high potentials, an electrostatic method in which charges were continuously carried to a hollow sphere to raise its potential. The sphere could be charged to voltages limited only by the corona breakdown at the surface of the sphere. To carry the charge, Van de Graaff hit on the idea of using a continuous belt on which charge could be sprayed by the brush discharge between a metal surface and a group of charged points. A belt moving over a pulley near the ground and another inside the sphere carried the charge from the charging position into the interior of the sphere where it was drawn off by a second series of sharp points and conveyed to the surface of the sphere.

Robert Jemison Van de Graaff was born in Tuscaloosa, Alabama, on December 20, 1901. He obtained his B.S. degree in 1922 from the University of Alabama and his M.S. degree in 1923. From 1924 to 1925 he was a student at the Sorbonne in Paris. In 1925, he won a Rhodes Scholarship and, for the next three years, continued his study of physics at Oxford, where he was awarded the Doctor of Philosophy degree in 1928. It was during this time that he conceived the idea of developing high-voltages by means of the continuous charging of a high potential spherical electrode. In 1929 a small model of what we now call the Van de Graaff Generator was built *"to demonstrate the soundness of the principles involved."* It performed as expected, generating a maximum potential of 80,000 volts.

From 1929 to 1951, Van de Graaff held a National Research Council Fellowship at Princeton University. This period was devoted to the further development of his electrostatic method for generating high voltages. A larger generator was constructed and its operation tested in vacuum to determine the value of vacuum insulation. To test the usefulness of the generator as a particle accelerator and for scientific research in general, a 1.5 million-volt generator was completed in 1931. Thereafter, larger, higher-voltage generators were made at the Massachusetts Institute of Technology, where Van de Graaff was appointed research associate during the years 1931 to 1934. In 1934, he was appointed Associate Professor of Physics, an appointment he held until 1967. During World War II, he served as director of a project sponsored by the government's Office of Scientific Research and Development to develop radiographic equipment for surveying the internal mechanical structure of metals and welded seams. In 1926 he became a director of the High Voltage Engineering Company of Cambridge, Massachusetts, and, the following year, a member of its executive committee, positions which he held for many years. Before his death on January 16, 1967, Van de Graaff was honored by the award of the Elliot Cresson medal of the Franklin Institute and the Duddell medal of the Physical Society of Great Britain.

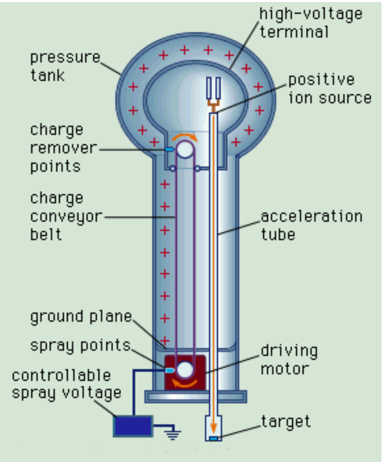

Figure 1.22 A layout of the Van der Graaff electrostatic accelerator

The Van de Graaff generator was used throughout the world, not only as an accelerator for studies in low-energy nuclear physics but also for such purposes as X-ray radiography, radiation therapy, food sterilization, and, on a limited scale, as an ion injector for the very high-energy particle accelerators. Accelerators.

Click here to read de Graaff notice about his accelerator.

1.20 Discovery of a POSITRON

C. Anderson (1905- 1991), 1932

Nobel Prize 1936 ***(click here to read his Nobel lecture)***

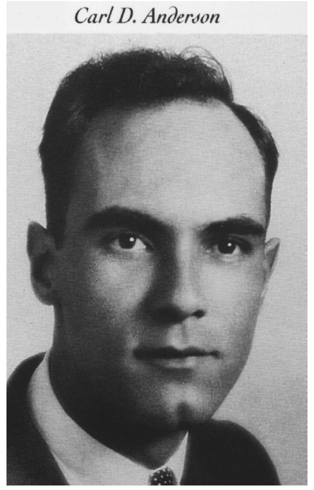

Carl David Anderson was born in New York City of Swedish parents on September 3, 1905. After the typical American boyhood, with its grammar and high-school education, Anderson entered the California Institute of Technology at Pasadena and in 1927 received his B.Sc, degree in physics and engineering. After his graduation, he devoted all his time to physics and in 1930 received his Ph.D. degree in physics from the same institution, where he remained as a research fellow until 1933. He was then appointed assistant professor of physics and, in 1939, full professor, a position which he held for the remainder of his professional career. Anderson's early career was his most productive. In 1932 he discovered the positron, for which he received the Nobel Prize in 1956; two years later, working with S. Neddermeyer, he discovered the mu-meson (called muon today).

One of the most remarkable features of Dirac's theory of the electron was the concept of an infinite sea of negative-energy electrons at all points of the vacuum. Although this idea followed directly from the mathematics of the theory, it was very difficult to accept it when the theory was first announced. The very idea of a negative energy particle is "unphysical" – contrary to our feeling that the laws of physics must describe a real observable world.

Because of this difficulty, Dirac himself at first proposed that the negative- energy electron states inherent in his theory be regarded as mathematical fictions and that they be disregarded in the application of his theory to physical phenomena. However, the theory gives a correct description of the behavior of an electron only if the negative-energy states are actually taken into account. To do so is to impart a physical reality to the negative-energy states; one must assign to each of them one electron (thus introducing an infinite number of negative-energy electrons in the vacuum). Otherwise all the positive-energy electrons in the universe would jump down to the negative-energy states and the material universe would disappear instantaneously in a vast burst of energy. The presence of negative-energy electrons in all the negative-energy states prevents such a catastrophe, owing to the Pauli exclusion principle.

When Dirac proposed this infinite sea of negative-energy electrons, he indicated that it would not conflict with observation, since such a sea of negative-energy electrons can never be observed. All that is observable is some departure from the uniform distribution of negative-energy electrons in the vacuum. Dirac showed that such a departure could occur if one of the negative-energy electrons absorbed enough energy (in the form of a photon or by means of some sort of collision) to lift it into a state of positive energy. If this were to occur, the negative state occupied by the negative-energy electron would be empty and the negative-energy electron itself would appear as a real electron with positive energy. The hole thus created in the sea of negative- energy electrons would now be observable as a positively charged particle with positive energy. In this way a pair of particles would be created, one an ordinary electron, and the other a positively charged particle with the same mass as the electron. Dirac suggested that the chance of creating this pair in some laboratory on earth would be small because it would require energy equivalent to at least twice the mass of the electron. However, enough energy is present in cosmic radiation to create such a pair as it passes through a sheet of matter. Therefore, one should look at the photographs of cosmic ray tracks to detect them; this procedure is how the positrons were first discerned.

Production and properties of positrons

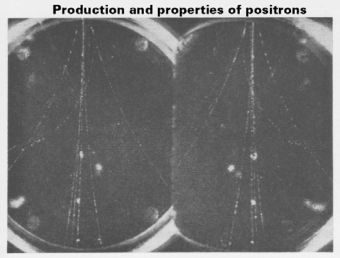

Fig. 5. A small cosmic-ray shower of positive and negative electrons. (Magnetic field 7,900 gauss.)

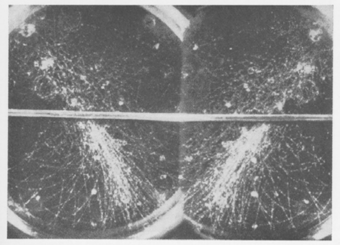

Fig. 6. A cosmic-ray shower of more than one hundred positive and negative electrons. (Magnetic field 7,900 gauss.)

On August 2, 1932, Carl Anderson found tracks of positively charged particles on his cosmic ray photographs. He knew that they were not tracks of protons, the only positively charged particles recognized at the time. To study the energy and the charge on cosmic ray particles one introduces a magnetic field in the cloud chamber through which the particles pass. The magnetic field turns the negatively charged particles in one direction and the positively charged particles in the other. If one knows the mass of the particle, one can then calculate its energy from the curvature of its path in the magnetic field. If the path is only slightly curved, the energy is large; if the path is highly curved, the energy is small. For a particle of given charge and mass, the radius of curvature of the path varies as the square root of the kinetic energy of the particle.

The paths of the particles Anderson observed had large curvatures. He knew that if these particles were protons, they would have had rather low energies. In fact, they would have had hardly enough kinetic energy to go more than a few millimeters in air. The lengths of the actual paths in air were found to be ten or more times greater than would be expected for a proton of such energy. The particles were also discovered to have enough energy to penetrate 6 mm of lead. From this analysis Anderson concluded that these positive particles must have masses of the electron's order of magnitude and must have a unit positive charge.

At first, Anderson did not identify these positive electrons, or positrons, with the Dirac holes in the sea of negative-energy states. The early photographs did not show a pair being created, as

demanded by the Dirac theory. However, this oversight was due to faulty observation. Soon afterwards it was found that whenever the track of a positron appeared on a photographic plate, it was accompanied by the track of an electron of opposite curvature. Moreover, the positron tracks ended abruptly, whereas the electron tracks twisted around and died out gradually.

It is easy to see the reason for this on the basis of the Dirac theory. Since a positron is a hole in a sea of negative-energy states, any electron it meets will be annihilated with the emission of energy. The positron thus disappears abruptly at the end of a short path because there are always many free electrons about in the cloud chamber. The electron that is created, on the other hand, is an ordinary particle that loses its kinetic energy slowly through collisions with other ordinary particles in the cloud chamber. Its track is therefore an intricate one. As the electron loses kinetic energy and slows down, the magnetic field in the cloud chamber curves it more and more sharply so that the path may end in a series of small loops.

Anderson's discovery, for which he won the Nobel Prize, established the Dirac theory as one of the most reliable in physics and, for the first time, showed that the complexities of elementary-particle physics were far greater than had been imagined. It also opened up a vast new domain of research, suggesting the existence of negative-energy protons and neutrons. These particles were discovered many years later. We now know that for every type of fundamental particle in the universe there is an antiparticle; the members of any pair are related to one another in the same way the electron is related to the positron. This finding has led to the concept of antimatter and to the speculation that there are parts of our universe (perhaps half of it) that consist of antimatter. When matter and antimatter meet, they destroy one another and give rise to pure energy.

Click here to read article about positron discovery

1.21 Discovery of artificial (induced) radioactivity

The Joliot-Curies, Nobel Laureates for their discovery of the synthesis of radioactive isotopes.

F. Joliot and I. Curie

I. Curie& F. Joliot 1934,

Nobel Prize in chemistry, 1935 ***(click here to read Nobel lecture)***

In 1925, Frédéric Joliot accepted the position of special assistant to Marie Curie. The next year, he married Marie's daughter, Irène, forming one of the most remarkable scientific partnerships of all time: Frédéric served the role of chemist, Irène that of physicist. Unfortunately, the early stage of their careers was defined by failure rather than success. Not only did they fail to discover the neutron, misidentifying it as a gamma ray, they also just missed discovering the positron. Later on, however,it was their observations of these very particles that led to their discovery of artificial radioactivity, which is considered to be their greatest triumph. Irène and Frédéric had noted that the bombardment of aluminum with alpha particles resulted in the emission of neutrons and positrons. As expected, the neutrons were emitted only as long as the aluminum was being bombarded by alpha particles. What astonished Frédéric and Irène was the continued emission of positrons long after the alpha source had been removed from the target. Immediately, Frédéric and Irène performed careful analyses which showed that the alpha bombardment had produced a positron-emitting radionuclide of phosphorous from the aluminum. Not only had they produced the first artificial radionuclide, they were the first to experimentally confirm transmutation, the conversion of one element into another element! Up to this point, the only radioactive materials available for medical and scientific research were those that occurred naturally. Now a method was available for creating a wide new variety of radioisotopes. The impact was immense, and for this discovery the Joliot-Curies won the 1935 Nobel Prize for chemistry.

$$^{27}_{13}Al + ^{4}_{2}He \rightarrow ^{30}_{15}P + ^{1}_{0}n$$

Half-life: 3 min 15 sincerely.

$$^{30}_{15}P \rightarrow ^{30}_{14}Si + ^{+}\beta$$

The goal of the experiment was to show that radioactivity comes from Phosphorus.

Later, during WW II, they helped hamper German efforts to develop an atomic bomb by ensuring that the entire stock of heavy water from the Norsk Hydro Plant was secured and shipped to Britain before France and Norway came under German control. After the war, they made major contributions to the construction of France's first nuclear reactor.

Click here to read discovery of artificial radioactivity

1.22 Activation of nuclei with neutrons

Fermi

Fermi, Amaldi, Rasetti 1932-1936 *(click here to read their article)*

Enrico Fermi - Nobel Prize 1938 *(click here to read his Nobel lecture)*

The Italian physicist Enrico Fermi, b. Sept. 29, 1901, d. Nov. 28, 1954, is best known as a central figure in the MANHATTAN PROJECT to build the first ATOMIC BOMB. Fermi received his doctorate from the University of Pisa in 1922. After working under Max BORN at Göttingen and Paul Ehrenfest at Leiden, he returned to Italy in 1926 and became professor of theoretical physics at the University of Rome. In 1938, on the eve of World War II, he escaped to the United States directly from Stockholm after receiving his Nobel Prize..

Fermi's early work on the statistical distribution of elementary particles led him to divide these atomic constituents into two groups, known as fermions and bosons, depending on their spin characteristics. This division is now accepted as standard. His subsequent work on radioactivity and atomic structure involved experiments on the production of artificial radioactivity by bombarding matter with neutrons. He discovered that slow moving neutrons were especially effective in producing radioactive atoms. Not realizing he had split the atom, Fermi announced what he thought were elements beyond uranium. He won the 1938 Nobel Prize for physics for his work on nuclear processes.

In 1938 Fermi was forced to flee Italy to escape the Fascist regime of Benito Mussolini. He was one of a large group of intellectuals who fled other countries of Europe due to the rise of National Socialism (the Nazi Party) in Germany and Fascism in Italy. Fermi settled in the United States, and became professor of physics at Columbia University in 1939. He moved to the University of Chicago in 1942 where he developed the first atomic pile, and produced the first nuclear chain reaction. During World War II he became part of the team that developed the atomic bomb at Los Alamos, New Mexico. After the war he pioneered research on high energy particles.

Fermi had an early start in the academic arena of physics. At the young age of 21, he had gotten his doctorate from the University of Pisa in Italy, and by the age of 24 was working out a new type of statistics applicable to particles obeying the famous Pauli exclusion principle. Unfortunately, Bose--Einstein statistics did not work in this case. The importance of Fermi statistics was immediately appreciated by physicists and established Fermi as a leader in the international community of theoreticians.

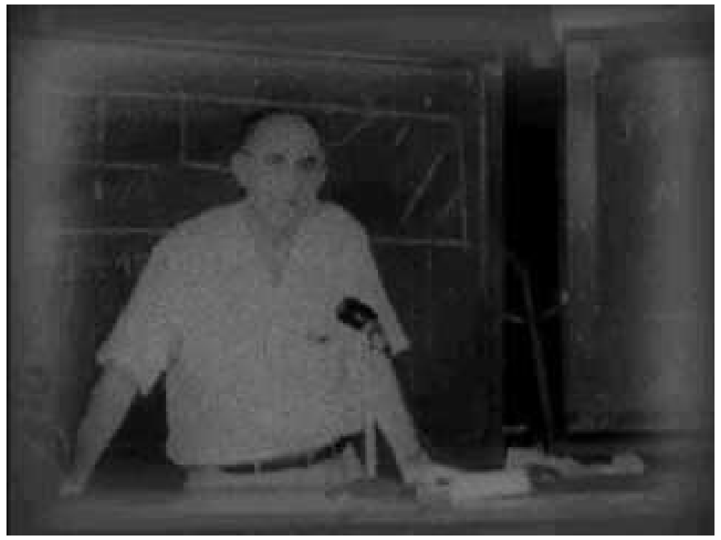

Several years later, quantum mechanics had reached its full development; nonrelativistic problems, at least in principle, were solvable except for some small mathematical difficulties. In this sense atomic physics was showing signs of exhaustion and one could expect the next really important advances to be in the study of the nucleus. Realizing this, Fermi decided to switch to nuclear physics. Fermi began to collaborate with such men as Hans Bethe, Edward Teller, Rudolf Peierls, Fritz London, Felix Bloch, George Blazek, among others.

After winning the Nobel Prize in 1938, he decided to leave Italy for good. He barely settled himself in Columbia University in New York, when Niels Bohr brought news of the discovery of fission. This discovery made a tremendous impression on all physicists, because they saw the possibility of the emission of secondary neutrons as the start of a chain reaction. At once, Fermi started experimenting in this direction.

Enrico Fermi was the mastermind of the crucial experiment on December 2, 1942 that produced the chain reaction needed to make an atomic bomb. He conducted this experiment on a bitterly cold day at an unused squash court at the University of Chicago.

He spent most of the period from September

he served as a general consultant. He collab

enriched uranium in ^{235}U and heavy water. He also actively participated in the first test of the atomic bomb in the desert near Alamogordo, New Mexico, on July 16, 1945. Following the successful test of the bomb, he was appointed by President Truman to the interim committee charged with advising the president on the use of the bomb and on many fundamental policies concerning atomic energy.

In 1946, The University of Chicago created the Institute for Nuclear Studies and offered a professorship to Fermi. The offer proved attractive to Fermi, and early in 1946 he and his family left Los Alamos for Chicago. He remained at the University of Chicago for the rest of his life.

For more information on Enrico Fermi:

Laura Fermi, Atoms in the Family, Chicago, 1954

This is a biography by his wife emphasizing the non scientific aspect of his life.

On May 10, 1934 Fermi's research group published a report on experiments with neutron bombardment of uranium. This was the first such investigation to be reported on. Several radioactive products are detected, but positive identifications were not made. Interpreting the results of neutron bombardment of uranium became known as the "Uranium Problem" since the large number of different radioactivities produced defied rational explanation. The dominant theory was that a number of transuranic elements never before seen were being produced, but the chemical behavior as well as the nuclear behavior of these substances were unexpected and confusing.

The first statement of the correct resolution of the Uranium Problem was published by German chemist Ida Noddack in September. Her letter in Zeitshrift für Angewandte Chemie argued that **the anomalous radioactivities produced by neutron bombardment of uranium may be due to the atom splitting into smaller pieces**. No notice of this suggestion was taken.

Fermi discovered the extremely important principle of neutron behavior called "moderation" on October 22, 1934. Moderation is the phenomenon of enhanced capture of low energy neutrons, as when they are slowed down by repeated collisions with light atoms.

Here are examples of neutron induced nuclear reactions studied by Fermi:

$$ {}^{6}_{3}Li + {}^{1}_{0}n \rightarrow {}^{3}_{1}H + {}^{4}_{2}He + Q $$
$$ {}^{1}_{1}H + {}^{1}_{0}n \rightarrow {}^{2}_{1}H + Q $$
$$ {}^{197}_{79}Au + {}^{1}_{0}n \rightarrow {}^{198}_{79}Au \rightarrow {}^{198}_{80}Hg + \beta^{-} $$

Fermi defined probability of the neutron interactions with nuclei expresses as cross-section, σ .

Fermi believed that transuranic elements are created by irradiation of Uranium.

1.23 Discovery and explanation of fission

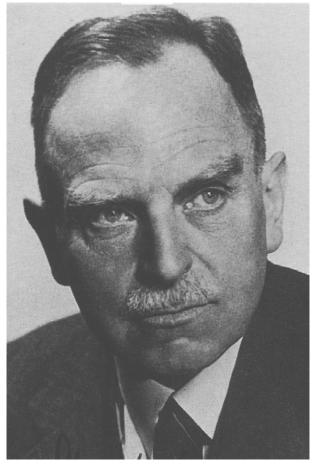

Otto Hahn

O. Hahn, L. Meitner, Frisch 1938-1939

O. Hahn, Nobel Prize (Chemistry) 1944, ***(click here to read his Nobel lecture)***

Otto Hahn was the chemist whose discovery of nuclear fission ultimately led to the ending of WW II. The story of Hahn's discovery began in 1938 with a report by Irène Joliot-Curie that bombarding uranium with neutrons had resulted in the production of a radionuclide of thorium, which they later speculated was a transuranium element similar to lanthanum. The astounded Hahn told Irène's husband, Frédéric, that such a thing was nonsense and that he would perform an experiment to prove as much. In the process of duplicating her work, Hahn and co-worker Fritz Strassmann discovered that, among other things, three isotopes of barium had been produced. This was incredible because the mass of barium is about half that of uranium. No known reaction could explain such a huge change. When they published their results (Jan. 6, 1939) Hahn and Strassmann noted that such a thing was "in opposition to all the phenomena observed up to the present in nuclear physics." Hahn, conscious of the fact that as a chemist he was treading in the domain of physics,

did not offer an explanation. Instead, he left it up to Lise Meitner, his longtime collaborator, to whom he had sent a letter (December 19, 1938) describing his findings and asking "Perhaps you can suggest some fantastic explanation," which she explained as nuclear fission. Nevertheless, despite the contributions of Strassmann and Meitner, it was Hahn who was awarded the 1944 Nobel Prize in chemistry for the discovery. Unfortunately, Hahn was not at the awards ceremony to receive his prize. At the time he learned of the award, he was being held by the British who were seeking information from him about the failed German effort to develop an atomic bomb. As the Chairman of the Nobel Committee for Chemistry reported "Professor Hahn . . . Has informed us that he is regrettably unable to attend this ceremony." ***Click here to read about discovery of fission***.

O. Hahn and L. Meitner

Simplified animations of fission

Lise Meitner

Born in Vienna in 1878, Meitner was one of eight children; her father was among the first group of Jewish men to practice law in Austria. As with Marie Sklodowska-Curie (but rare for a woman at the turn of the century), the intellectual atmosphere that surrounded Meitner as a child nurtured her scientific proclivity. Only the second woman to obtain a doctoral degree in physics at the University of Vienna, she was soon drawn into the novel study of radioactivity.

In 1907 she moved to Berlin, the Mecca of theoretical physics, where she was introduced to Einstein and Max Plank, the father of the quantum. More important, she met Otto Hahn, who became her closest collaborator and a valued friend. They were an interdisciplinary yin and yang: Hahn, the chemist, Meitner, the physicist. While he was methodical, she was bold. Together, in 1917, they discovered a new element, protactinium. Lise Meitner, forever linked in people's minds with the monumental discovery of nuclear fission, made many significant contributions to science throughout a long and productive career.

Lise Meitner

Figure 1.23 Lise Meitner in Sweden 1955 together with H. Brynielsson and S. Eklund - Swedish pioneers of nuclear technology

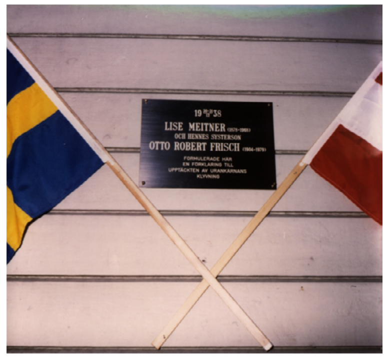

Figure 1.24 In memory of L. Meitner and O. Frisch stay in Kungälven in Sweden

The first significant result of this collaboration was an important technique for purifying radioactive material that took advantage of the recoil energy of atoms produced in alpha decay. Later, at the Kaiser Wilhelm Institute in Austria, she was the first to explain how conversion electrons were produced when gamma ray energy was used to eject orbital electrons. She also provided the first description of the origin of auger electrons, i.e., outer-shell orbital electrons ejected from the atom when they absorbed the energy released by other electrons falling to lower energies. When Nazi Germany annexed Austria in 1938, Meitner, a Jew, fled to Sweden. In her absence, Hahn and Fritz Strassmann continued experiments they had begun earlier with Meitner and demonstrated that barium was produced when a uranium nucleus was struck by neutrons. This was absolutely startling because barium is so much smaller than uranium! Hahn wrote to Meitner, "*it [uranium] can't really break up into barium . . . try to think of some other possible explanation.*" While visiting her nephew Otto Frisch for the Christmas holidays in Denmark, she and Frisch proved that a splitting of the uranium atom was energetically feasible. They employed Niels Bohr's model of the nucleus to envision the neutron inducing oscillations in the uranium nucleus. Occasionally the oscillating nucleus would stretch out into the shape of a dumbbell. Sometimes, the repulsive forces between the protons in the two bulbous ends would cause the narrow waist joining them to pinch off and leave two nuclei where before there had been one. Meitner and Frisch described the process in a landmark letter to the journal Nature with a term borrowed from biology: fission.

Typical fission reactions:

$$ {}^{235}_{92}U + n \rightarrow \left({}^{235}_{92}U\right)^{*} \rightarrow X + Y + neutrons $$

$$ {}^{235}_{92}U + n \rightarrow \left({}^{235}_{92}U\right)^{*} \rightarrow {}^{144}_{56}Ba + {}^{89}_{36}Kr + 3\,{}^{1}_{0}n $$

$$ {}^{235}_{92}U + n \rightarrow \left({}^{235}_{92}U\right)^{*} \rightarrow {}^{140}_{54}Xe + {}^{94}_{38}Sr + 2\,{}^{1}_{0}n $$

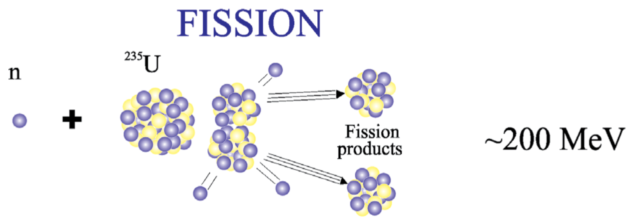

1.24 Liberation of c:a 3 neutrons per fission proven

Lev Kowarski and von Halban 1939

Kowarski showed, that c:a 3- 3.5 neutrons are liberated in fission (1939).

April 22, Nature, "Number of neutrons liberated in the nuclear fission of uranium" (click here to read)

F. Joliot and I. Curie-Joliot presented a theory of nuclear chain-reaction. (Click here to read their article)

Lew Kowarski was born in Saint Petersburg in 1907 in polish-russian family. Following the Bolshevik Revolution his family fled west under adventurous circumstances and settled in Vilnius (then in Poland). During his youth, Lew, talanted musician, became a naturalized French physicist.

He received a Chemical Engineering degree from the University of Lyon and an Sc.B. and Ph.D. from the University of Paris where he carried out research on neutron counting.

He joined Frédéric Joliot-Curie's group in 1934, where Hans von Halban came in 1937. They established in 1939 the possibility of nuclear chain reactions and nuclear energy production. While doing their research, the events of World War II forced them to eventually move to England, bringing with them the world's entire stock of heavy water, given on loan by Norway to France so that it would not fall into German hands. They continued their research at the Cavendish laboratory in Cambridge for the MAUD Committee, part of the wartime Tube Alloys project.

After war Kowarski worked in the Montreal Laboratory in Canada and supervised the construction of Canada's first nuclear reactor (ZEEP) at the Chalk River Laboratories in 1945.

Hans von Halban (Leipzig, 24 January 1908 - Paris, 28 November 1964) was a French physicist, of Austrian-Jewish descent. Hans Halban was educated in Leipzig, where his father, Hans von Halban Sr. was a professor of physical chemistry. The family moved to Zürich in 1928. Halban finished his doctoral studies in physics at the Swiss Federal Institute of Technology, Zurich in 1936.

He then worked for a year with the nuclear physicist Niels Bohr at the Institute of Physics, University of Copenhagen. In collaboration with Otto Frisch he discovered that heavy water had very low neutron absorption compared with ordinary water.

In 1937 Halban was invited to join the team of Frédéric Joliot-Curie at the Collège de France in Paris. The team also included Francis Perrin and Lew Kowarski. In 1939 the group measured the mean number of neutrons emitted during nuclear fission, and established the possibility of nuclear chain reactions and nuclear energy production. In August the group showed that the rate of fission in Uranium Oxide was increased by immersion in ordinary water.

During the Second World War he was invited by Churchill's government to continue his research at Cambridge University. In 1942, along with British and other European "refugee scientists", Halban was sent to Montreal as head of the research laboratories at the Montreal Laboratory, part of the nascent Manhattan Project.

CHAIN REACTION possible, click below for the model

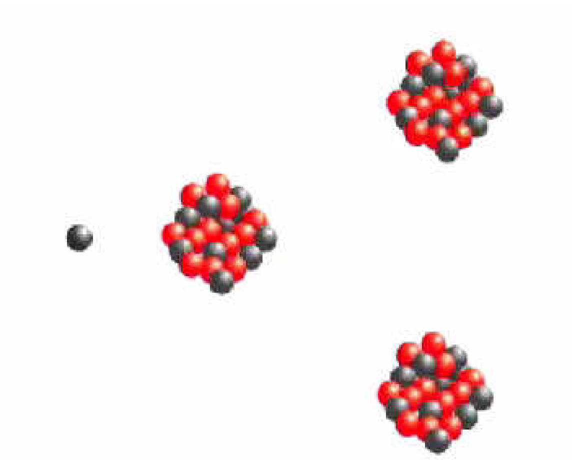

1.25 Theory of nuclear fission. ONLY ^{235}U useful for fission

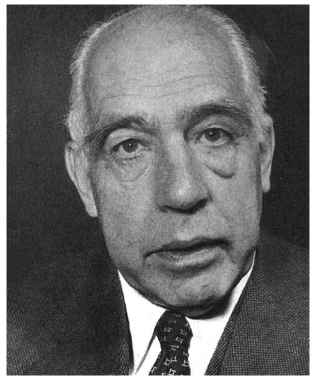

Nils Bohr

N. Bohr & J.Wheeler, 1939

February 5, 1939 - Niels Bohr realizes that ^{235}U and ^{238}U-must have different fission properties, that 238U could be fissioned by fast neutrons but not slow ones, and that 235U accounted for observed slow fission in uranium.

At this point there were too many uncertainties about fission to see clearly whether or how self-sustaining chain reactions could arise. Key uncertainties were :

1) the number of neutrons emitted per fission, and

2) the cross sections for fission and absorption at different energies for the uranium isotopes.

For a chain reaction there would need to be both a sufficient excess of neutrons produced, and the ratio between fission to absorption averaged over the neutron energies present would need to be sufficiently large.

The different properties of ^{235}U and ^{238}U were essential to understand in determining the feasibility of an atomic bomb, or of any atomic power at all. The only uranium available for study was the isotope mixture of natural uranium, in which ^{235}U comprised only 0.71%.

August 31, 1939 - Bohr and John A. Wheeler publish a theoretical analysis of fission. This theory implies ^{235}U is more fissile than ^{238}U, and that the undiscovered element 94-239 is also very fissile. These implications are not immediately recognized.

Look: Physical Review, ***"The mechanism of nuclear fission" (click here)*** and ***Fermi's notice about fission of Uranium***

As far as the making of the first atomic bomb goes, Bohr's "droplet model" theory was the interpretation of nuclear fission. This is a type of reaction that may be initiated by the impact of a neutron on a very heavy nucleus. The compound nucleus formed by the capture of the neutron has so little stability, that it can split into two fragments of about the same mass and charge. It was Otto Hahn's and Fritz Strassman's chemical identification of such fragments as decay products that led Bohr's colleagues O. R. Frisch and Lise Meitner to recognize that the fission mechanism was the only conceivable interpretation.

The first experiments actually showing the emission of the fragments were performed at Bohr's lab in Copenhagen by Frisch in January, 1939. By then Bohr had left for the United States. It was on his departure that he heard of Frisch's idea and project. During the voyage and shortly after his arrival in the States, he outlined the whole theory of the process. In the following months, this theory was refined and elaborated in great detail, with A. J. Wheeler's collaboration.

By one of his most brilliant feats of rigorous induction from an experiment, he unraveled the complex case of uranium, concluding that only the rare isotope of mass number 235 was fissionable by slow neutrons, while the abundant isotope of mass 238 was no t. He showed by a very simple argument that this difference was due solely to the fact that the number of neutrons in the two isotopes were odd and even, receptively.

The discovery that the highly unstable fission fragments emitted neutrons immediately raised the question of the possibility of a chain reaction leading to the liberation of huge amounts of energy. The answer to this question was found soon enough through the work of the Manhattan Project in Los Alamos, New Mexico.

In 1943, Bohr had decided to leave Copenhagen for England to work on some of the problems on the making of the atomic bomb. Although he did take part, both in England and in the United States, in discussions of the physical problems related to the development of nuclear weapons, his main concern was to make the statesmen, as well as the physicists, aware of the political and human implications of the new source of power.

After the war, Niels Bohr continued to work towards peace. In 1950, he published an "open letter" to the United Nations in which he made a plea for an "open world" without nuclear weapons. When the European Center for Nuclear Research was formed in 1952, the theoretical division was installed in Bohr's Institute in Copenhagen. In 1955, he took a leading part in the foundation and organization of a Danish establishment of the constructive application of nuclear energy. He continued for the rest of his life to speak out against the negative uses of nuclear research.

1940 John Ray Dunning, Eugene Theodore Boothe and Aristid Grosse, displayed that it was ^{235}U which fissioned rather than ^{238}U.

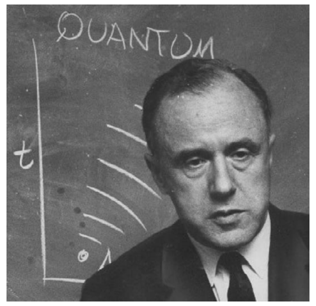

John A. Wheeler

John Archibald Wheeler (July 9, 1911 – April 13, 2008) was an American theoretical physicist who was largely responsible for reviving interest in general relativity in the United States after World War II. As mentioned above Wheeler worked with Niels Bohr in explaining the basic principles behind nuclear fission. As one of the later collaborators of Albert Einstein, he tried to achieve Einstein's vision of a unified field theory. He is also known for having coined the terms black hole, quantum foam and wormhole and the phrase "it from bit". For most of his career, Wheeler was a professor at Princeton University and was influential in mentoring a generation of physicists who made notable contributions to quantum mechanics and gravitation.

Together with many other leading physicists, during World War II, Wheeler interrupted his academic career to participate in the development of the atomic bomb during the Manhattan Project, working at the Hanford Site in Washington, where several large nuclear reactors were constructed to produce the element plutonium for atomic bombs. Even before the Hanford Site started up the "B-Pile" (the first of its three reactors), Wheeler had anticipated that the accumulation of "fission product poisons" would eventually impede the ongoing nuclear chain reaction by absorbing many of the thermal neutrons that were needed to continue a chain reaction. Wheeler deduced that an isotope of the noble gas xenon (^{135}Xe), by calculating its half-life in radioactive decay, would be one most responsible.

Some years later, Wheeler went on to work on the development of the more powerful hydrogen bomb under the Project Matterhorn nuclear weapons program.

After concluding his Manhattan Project work, Wheeler returned to Princeton University to resume his academic career. In 1957, while working on mathematical extensions to the Theory of General Relativity, Wheeler introduced the concept and the word wormhole to describe hypothetical "tunnels" in space-time. His work became an inspiration of many science-fiction authors.

1.26 L. Szilard& E. Wigner convinced Einstein to sign the letter to USA:s president F.D. Roosevelt - 1939.

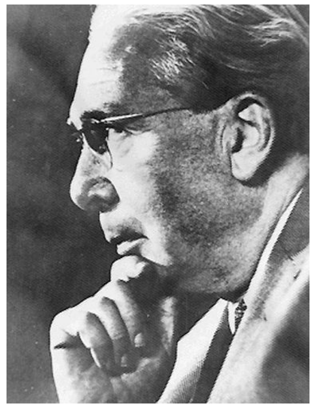

Leo Szilard

Leo Szilard: Physicist, Molecular Biologist a "WUNDERKIND" of nuclear physics and enginnering.

Born Budapest, Hungary, February 11, 1898.

Died La Jolla, California, U.S.A. May 30, 1964.

Szilárd was born in 1898 to middle class parents in Budapest, Hungary as the son of a civil engineer. From 1908–1916 Leó attended Reáliskola high school in his home town. Showing an early interest in physics and a proficiency in mathematics, in 1916 took the Eötvös Prize, a national prize for mathematics.

He enrolled as an engineering student at Budapest Technical University during 1916. The following year, he was drafted into the Austro-Hungarian Army as an officer-candidate. Prior to his regiment being sent to the front lines, Szilárd fell ill with Spanish Influenza and he was returned home for hospitalization. Later he was informed that his regiment had been nearly annihilated in battle, so the sickness probably saved his life. He was discharged honorably at the end of the war.

During 1919 he resumed engineering studies at Budapest Technical University but soon decided to leave Hungary. Szilárd continued engineering studies at Technische Hochschule (Institute of Technology) in Berlin-Charlottenburg. He soon changed to physics there and took physics classes from Einstein, Planck, and Max von Laue. His dissertation on thermodynamics *On The Manifestation of Thermodynamic Fluctuations* during 1922 was praised by Einstein and awarded top honors. In 1923 he was awarded a doctorate in physics from Humboldt University of Berlin.

He was appointed as assistant to von Laue at the University of Berlin's Institute for Theoretical Physics during 1924. During 1927 he finished his habilitation and became a Privatdozent (private lecturer) in physics at University of Berlin. During his time in Berlin he was working on numerous technical inventions. For example, in 1928 he submitted a patent application for the linear accelerator and, in 1929, he applied for a patent for the cyclotron. During the 1926-1930 period, he worked with Einstein to develop a refrigerator, notable because it had no moving parts. Szilárd's

1929 paper, On the reduction of entropy in a thermodynamic system by the interference of an intelligent being Z. Physik 53, 840-856, introduced the thought experiment now called Szilárd's engine and was important in the history of attempts to understand Maxwell's demon.

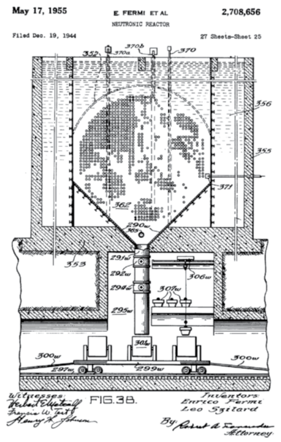

Figure 1.25 Fermi-Szilard's reactor

Although the atom had been split and energy released, nuclear fission had not yet been discovered. Szilárd conceived of the idea of nuclear chain reaction (analogous to a chemical chain reaction), using recently-discovered neutrons. The idea did not use the mechanism of nuclear fission, which was not then known, but Szilárd realized that if neutrons could initiate any sort of energy-producting nuclear reaction, such as the one that had occurred in lithium, and could be produced themselves by the same reaction, energy might be obtained with little input, since the reaction would be self-sustaining. The following year he filed for a patent on the concept of the neutron-induced nuclear chain reaction.Szilárd first attempted to create a nuclear chain reaction using beryllium and indium, but these elements did not produce a chain reaction. During 1936, he assigned the chain-reaction patent to the British Admiralty to ensure its secrecy (GB 630726). Szilárd also was the co-holder, with Nobel Laureate Enrico Fermi, of the patent on the nuclear reactor (U.S. Patent 2,708,656).

During 1938 Szilárd accepted an offer to conduct research at Columbia University in Manhattan, and moved to New York, and was soon joined by Fermi. After learning about the successful nuclear fission experiment conducted during 1939 in Germany by Otto Hahn, Fritz Strassmann, Lise Meitner, and Otto Robert Frisch, Szilárd and Fermi concluded that uranium would be the element capable of sustaining a chain reaction. Szilárd and Fermi conducted a simple experiment at Columbia and discovered significant neutron multiplication in uranium, proving that the chain reaction was possible and enabling nuclear weapons. Szilárd later described the event: *"We turned the switch and saw the flashes. We watched them for a little while and then we switched everything off and went home." He understood the implications and consequences of this discovery, though. "That night, there was very little doubt in my mind that the world was headed for grief."*[6]

At around that time the Germans and others were in a race to produce a nuclear chain reaction. German attempts to control the chain reaction sought to do so using graphite, but these attempts proved unsuccessful. Szilárd realized graphite was indeed perfect for controlling chain reactions, just as the Germans had determined, but that the German method of producing graphite used boron carbide rods, and the minute amount of boron impurities in the manufactured graphite was enough to stop the chain reaction. Szilárd had graphite manufacturers produce boron-free graphite. As a result, the first human-controlled chain reaction occurred on December 2, 1942.

Szilárd was directly responsible for the creation of the Manhattan Project. He drafted a confidential letter to Franklin D. Roosevelt explaining the possibility of nuclear weapons, warning of Nazi work on such weapons and encouraging the development of a program which could result in their creation. During August 1939 he approached his old friend and collaborator Albert Einstein and convinced him to sign the letter, lending his fame to the proposal. The Einstein–Szilárd letter resulted in the establishment of research into nuclear fission by the U.S. government and ultimately to the creation of the Manhattan Project. Later, Szilárd relocated to the University of Chicago to continue work on the project. There, along with Fermi, he helped to construct the first "neutronic reactor", a uranium and graphite "atomic pile" in which the first self-sustaining nuclear chain reaction was achieved, during 1942.

As the war continued, Szilárd became increasingly dismayed that scientists were losing control over their research to the military, and argued many times with General Leslie Groves, military director of the project. His resentment towards the U.S. government was exacerbated by his failure to prevent the destructive use of the atomic bomb through having a test explosion that could be witnessed by Japanese observers who would then have the opportunity to surrender and spare lives.

Szilárd became a naturalized citizen of the United States during 1943.

As mentioned before, Szilárd was the first person to conceive of a device that, using a nuclear chain reaction as fuel, could be used as a bomb.

As a survivor of the political and economic devastation in Hungary following World War I, Szilárd developed an enduring passion for the preservation of human life and freedom, especially freedom to communicate ideas.

He hoped that the U.S. government would not use nuclear weapons because of their potential for use against civilian populations. Szilárd hoped that the mere threat of such weapons would force Germany and/or Japan to surrender. He drafted the Szilárd petition advocating demonstration of the atomic bomb. However with the European war concluded and the U.S. suffering many casualties in the Pacific Ocean region, the new U.S. President Harry Truman agreed with advisers and chose to use atomic bombs against Hiroshima and Nagasaki over the protestations of Szilárd and other scientists.

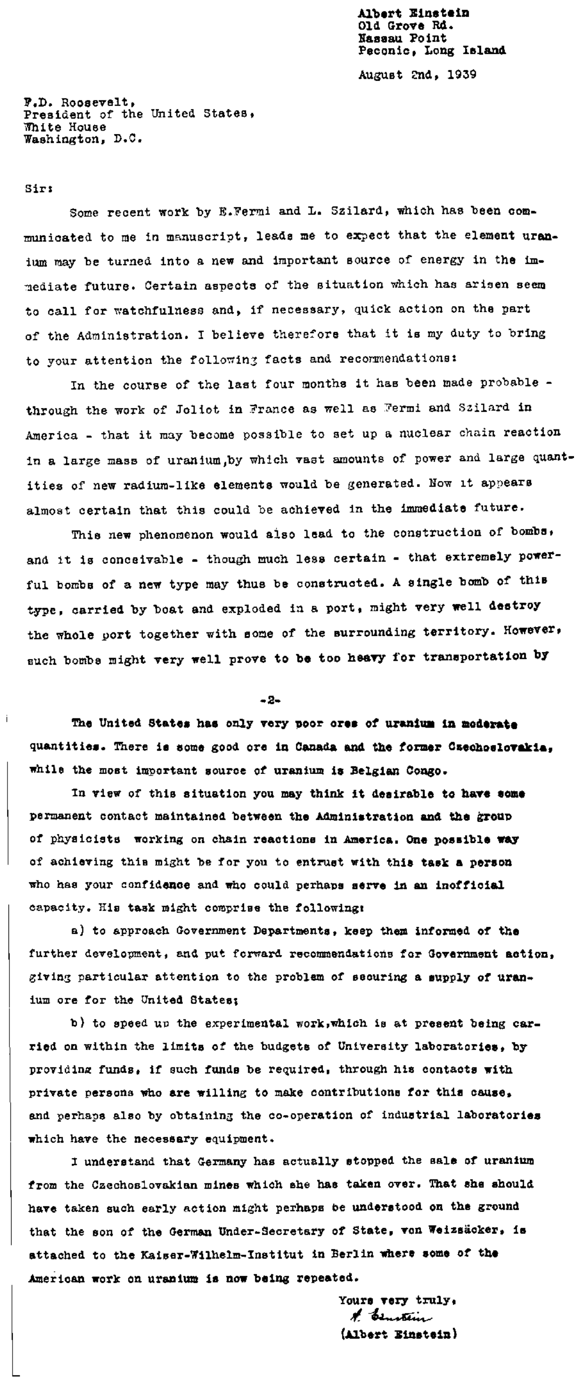

Albert Einstein
Old Grove Rd.
Nassau Point
Peconic, Long Island

August 2nd, 1939

F.D. Roosevelt,
President of the United States,
White House
Washington, D.C.

Sir:

Some recent work by E.Fermi and L. Szilard, which has been communicated to me in manuscript, leads me to expect that the element uranium may be turned into a new and important source of energy in the immediate future. Certain aspects of the situation which has arisen seem to call for watchfulness and, if necessary, quick action on the part of the Administration. I believe therefore that it is my duty to bring to your attention the following facts and recommendations:

In the course of the last four months it has been made probable - through the work of Joliot in France as well as Fermi and Szilard in America - that it may become possible to set up a nuclear chain reaction in a large mass of uranium,by which vast amounts of power and large quantities of new radium-like elements would be generated. Now it appears almost certain that this could be achieved in the immediate future.

This new phenomenon would also lead to the construction of bombs, and it is conceivable - though much less certain - that extremely powerful bombs of a new type may thus be constructed. A single bomb of this type, carried by boat and exploded in a port, might very well destroy the whole port together with some of the surrounding territory. However, such bombs might very well prove to be too heavy for transportation by

-2-

The United States has only very poor ores of uranium in moderate quantities. There is some good ore in Canada and the former Czechoslovakia, while the most important source of uranium is Belgian Congo.

In view of this situation you may think it desirable to have some permanent contact maintained between the Administration and the group of physicists working on chain reactions in America. One possible way of achieving this might be for you to entrust with this task a person who has your confidence and who could perhaps serve in an inofficial capacity. His task might comprise the following:

a) to approach Government Departments, keep them informed of the further development, and put forward recommendations for Government action, giving particular attention to the problem of securing a supply of uranium ore for the United States;

b) to speed up the experimental work,which is at present being carried on within the limits of the budgets of University laboratories, by providing funds, if such funds be required, through his contacts with private persons who are willing to make contributions for this cause, and perhaps also by obtaining the co-operation of industrial laboratories which have the necessary equipment.

I understand that Germany has actually stopped the sale of uranium from the Czechoslovakian mines which she has taken over. That she should have taken such early action might perhaps be understood on the ground that the son of the German Under-Secretary of State, von Weizsäcker, is attached to the Kaiser-Wilhelm-Institut in Berlin where some of the American work on uranium is now being repeated.

Yours very truly,
A. Einstein
(Albert Einstein)

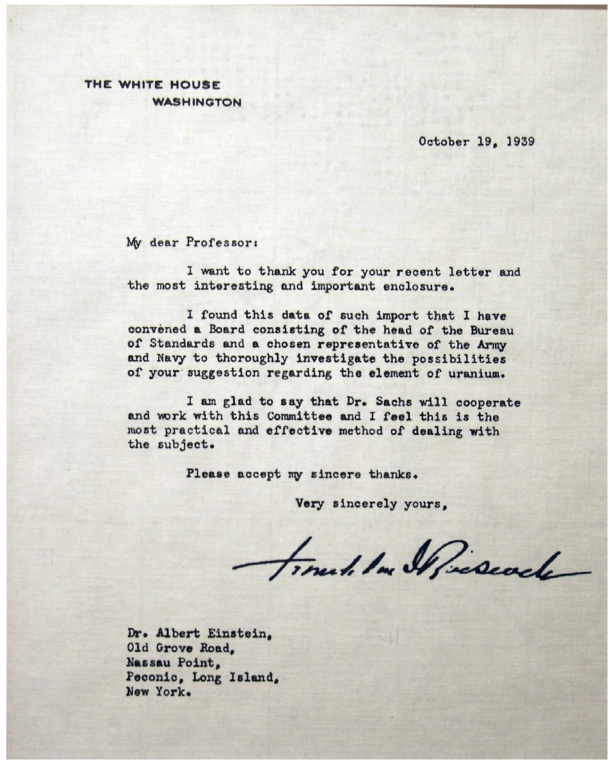

THE WHITE HOUSE
WASHINGTON

October 19, 1939

My dear Professor:

I want to thank you for your recent letter and the most interesting and important enclosure.

I found this data of such import that I have convened a Board consisting of the head of the Bureau of Standards and a chosen representative of the Army and Navy to thoroughly investigate the possibilities of your suggestion regarding the element of uranium.

I am glad to say that Dr. Sachs will cooperate and work with this Committee and I feel this is the most practical and effective method of dealing with the subject.

Please accept my sincere thanks.

Very sincerely yours,
Franklin D Roosevelt

Dr. Albert Einstein,
Old Grove Road,
Nassau Point,
Peconic, Long Island,
New York.

Figure 1.26 President Roosevelt's answer to Einstein's letter

Figure 1.27 Reconstruction of the event of Einstein-Szilárd's letter to Pres. Roosevelt

During 1947, Szilárd switched topics of study because of his horror of atomic weapons, changing from physics to molecular biology, working extensively with Aaron Novick. In February 1950 Szilárd proposed a cobalt bomb, a new kind of nuclear weapon using cobalt as a tamper, which he said might destroy all life on the planet.

During 1961 Szilárd published a book of short stories, The Voice of the Dolphins, in which he dealt with the moral and ethical issues raised by the Cold War and his own role in the development of atomic weapons.

During 1960, Szilárd was diagnosed with bladder cancer. He underwent radiation therapy at New York's Memorial Hospital using a treatment regimen that he designed himself. A second round of treatment followed during 1962; Szilárd's cancer remained in remission thereafter. During May 1964, Szilárd died in his sleep of a heart attack at the age of sixty-six.

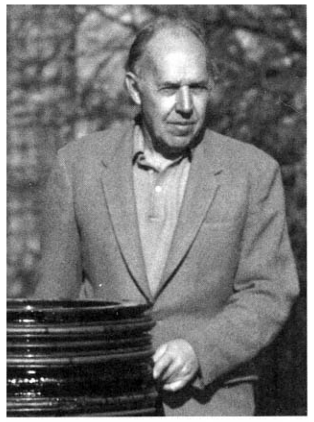

Richard Brooke Roberts

1.27 All research on fission classified (top secret!)

1939 - Discovery of delayed neutrons , Richard Brook Roberts

1940-42 - Discovery of Neptunium and Plutonium

McMillan & Abelson, Radioactive element 93, Phys. Rev. May 27, 1940

Glenn T. Seaborg, Kennedy and Segré, discover ^{239}Pu, 1940; published 1942 and 1946

Glenn Seaborg and Edwin McMillan - Nobel Prize in Chemistry 1951 ***(click to read this article and the Nobel lecture of G. Seaborg and McMillan)***

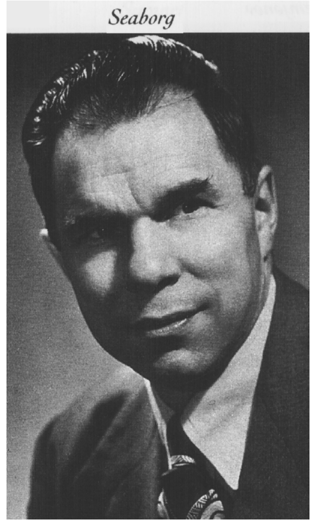

Richard Brooke Roberts (1910-1980) spent most of his career in the biophysics group at the Department of Terrestrial Magnetism of the Carnegie Institution of Washington. He contributed importantly to many scientific advances in this period in microbiology, the beginnings of molecular biology, and study of the brain. One high point was the proof (with Kenneth McQuillen and me) that in Escherichia coli, protein synthesis occurred on ribosomes. He also named the ribosome. R. Roberts started out as a nuclear physicist and among several discoveries showed that delayed neutrons were emitted in uranium fission. This discovery was of great practical consequence because delayed neutrons slow the responses in a nuclear reactor enough to permit power control by mechanical movement of control rods. This made fission process practical for power. generation R. Roberts was involved in early planning of what became the Manhattan Project.

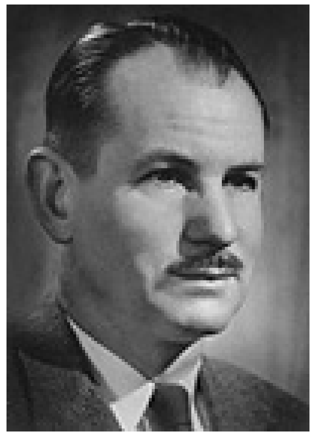

Edwin M. McMillan

Glenn T. Seaborg was born in 1912 on Michigan's Upper Peninsula. During the first eighty-four years of his life, he has made many important contributions to the science of nuclear chemistry and to science education. Glenn T. Seaborg discovered ten elements including plutonium, the element that has had the largest impact on the twentieth century of any element. Seaborg also discovered several radioisotopes of existing elements. One of these radioisotopes, technetium - ^{99m}Tc revolutionized medical imaging and is now used in a majority of nuclear medicine procedures. Seaborg's contributions to education have been equally impressive. He served as the second chancellor of the Berkeley campus of the University of California and as an advisor to several presidents on matters of education and arms control. Dr. Seaborg continues to serve on the faculty of UC-Berkeley and as a researcher at the Lawrence Berkeley National Lab.

In 1939, Seaborg and the other Berkeley faculty became exhilarated by the news of the experiments of Otto Hahn and Fritz Strassman. These experiments, which were being carried out in Germany, were providing the first evidence of a nuclear fission reaction.

In 1940, Edwin M. McMillian and Philip Abelson were attempting to replicate Hahn and Strassman's results in Berkeley's cyclotron, in an effort to understand the fission process. McMillian and Abelson measured the energies of the fission fragments by measuring the distances that they traveled after the nucleus fissioned. However, McMillian noticed another source of radioactivity. This source of radioactivity did not have the energy to recoil away from the uranium's surface like the fission fragments did. McMillian found the substance to have a half-life of 2.3 days. McMillian hypothesized that the new product had been formed by the uranium nucleus capturing the neutron but not splitting. McMillian and Abelson ran chemical tests and discovered that they had produced an isotope of element 93. The new element was to be named neptunium because Neptune was the planet after Uranus, and Uranus was the basis of the name of uranium. The process they discovered consisted of two reactions:

$$^{1}_{0}n + {}^{238}_{92}U \rightarrow {}^{239}_{92}U + \gamma$$

$$^{239}_{92}U \rightarrow {}^{239}_{93}Np + \beta^{-} + \overline{\nu}$$

They found that the uranium nucleus had captured a neutron and then decayed by beta decay to form ^{239}Np.

McMillian postulated that other elements could be formed by this process. By this time, Seaborg had begun work on the chemical properties of neptunium. McMillian continued work on the transuranium elements with Seaborg and other members of the Department of Chemistry at Berkeley. However, World War II started on 1 September 1939, and war projects were demanding greater attention than the discovery of new elements. In November of 1940, McMillian was called away from Berkeley to work at the Massachusetts Institute of Technology on sonar and radar.

While the loss of McMillian was a setback, McMillian gave his consent to Seaborg working on the search for element 94. On 14 December 1940, the Seaborg group at Berkeley began their work on the discovery of element 94. They began by placing samples of uranium oxide in the sixty-inch cyclotron at Berkeley. They bombarded their samples of uranium oxide with deuterium nuclei. They produced and separated neptunium by the following reaction:

$$^{238}_{92}U + {}^{2}_{1}H\,(D) \rightarrow {}^{238}_{93}Np + 2\,{}^{1}_{0}n$$

However, as the weeks passed, the alpha radioactivity coming from their sample of ^{238}Np increased. They separated the alpha emitter from the other elements in the mixture. On the 23 and 24 of February 1941, they discovered element 94. Like neptunium, element was given a name that was analogous with the solar system. They named element 94 plutonium after the last planet in the solar system, Pluto. They discovered that element 94 was produced by the beta decay of ^{238}Np:

$$^{238}_{93}Np \rightarrow {}^{238}_{94}Pu + \beta^{-} + \overline{\nu}$$

Seaborg and his group showed a humorous side when choosing the symbol for plutonium. They were discussing a symbol of Pm, but someone suggested the element have the symbol of Pu for the obvious humor value: Pu - a stylized abbreviation that stands for the sound of disgust in reaction to a bad smell.

However, the group had imposed a code of silence on itself because World War II was raging in Europe. Therefore, neptunium and plutonium were referred to as "element 93" and "element 94" or by their code names. Plutonium's code name was "copper." The scientists had no problems with this until real copper was introduced into their experiments. The scientists began referring to plutonium as "copper" and copper as "honest-to-God copper. "Seaborg's group submitted their work on plutonium to the journal Physical Review, but scientific journals had voluntarily agreed not to publish any work in nuclear chemistry and physics during World War II.

While the group was looking for plutonium in their deuterium-bombarded uranium, Segrè worked on looking for the 239 isotope of plutonium. Segrè knew that ^{239}Np decayed by beta decay, and believed that he could find plutonium by that route. However, ^{239}Pu was not identified until later in the spring of 1941. On 28 March 1941, the Seaborg group found something exciting about the new isotope of plutonium. By bombarding small samples of ^{239}Pu in the old thirty-seven inch cyclotron, the scientists found that ^{239}Pu fissions more readily than ^{235}U.

The fissionability of ^{239}Pu turned out to be important. Originally, the Manhattan Project sought to build a fission bomb based on ^{235}U. However, the news that ^{239}Pu was fissionable gave the project an alternate route to their goal. Work on the plutonium bomb began at the University of Chicago under Enrico Fermi. Fermi's Lab was known as the Metallurgical Lab. The scientists at the Metallurgical Lab built the world's first functioning nuclear reactor. The reactor was originally located in the abandoned squash courts under the bleachers at Stagg Field. The reactor produced plutonium, but the scientists knew very little of the properties of plutonium. Glenn Seaborg was the chemist who knew the most about the properties of plutonium. Therefore, Seaborg joined the Metallurgical Lab on April 19, 1942, his thirtieth birthday.

Seaborg's work at the Metallurgical Lab or the Met Lab as it was sometimes called, yielded two new elements. In the summer of 1944, Seaborg and his co-workers isolated curium from material produced in the sixty inch cyclotron at Berkeley. Curium was produced by the following reaction:

$$^{239}_{94}Pu + {}^{4}_{2}He(\alpha) \rightarrow {}^{242}_{96}Cm + n$$

Later in 1944, Seaborg and his colleagues isolated americium from material in the nuclear reactor. Americium was produced by the following reactions:

$$^{239}_{94}Pu + n \rightarrow ^{240}_{94}Pu + \gamma$$

$$^{240}_{94}Pu + n \rightarrow ^{241}_{94}Pu + \gamma$$

$$^{241}_{94}Pu \rightarrow ^{241}_{95}Am + \beta^{-} + \overline{\nu}$$

Seaborg holds patents on both these elements, which makes him the only person to hold a patent on a chemical element

Seaborg returned to Berkeley in 1946 with his wife Helen whom he had married on a short trip to Berkeley in 1942. At Berkeley, he became involved in two efforts. The first effort was the establishment the research group to work on the transuranium elements at Berkeley. The other goal was starting his family with his wife, Helen. He was very successful in both goals. The team he established at Berkeley would discover **six** elements. He and his wife Helen had **six** children.

Five years after returning to Berkeley, he and Edward McMillan, traveled to Stockholm, Sweden to be presented with the Nobel Prize for their work on actinide chemistry ***(click here to read the nobel lectures)***.

Figure 1.28 "Mike" - the first thermonuclear weapon test

Seaborg and his colleagues discovered element 97 in December of 1949. They named the element Berkelium after the city of Berkeley where the University of California campus that they worked at is located. Berkelium was first produced in the sixty inch cyclotron from americium by the following reaction:

$$^{241}_{95}Am + ^{4}_{2}He(\alpha) \rightarrow ^{243}_{97}Be + 2n$$

Very shortly after discovering berkelium, the Berkeley team discovered element 98. They named this element californium after the state and the University of California. Californium was produced in the sixty inch cyclotron from curium by the following reaction:

$$^{242}_{96}Am + ^{4}_{2}He(\alpha) \rightarrow ^{245}_{98}Cf + n$$

Shortly after the discovery of berkelium and californium, the New Yorker magazine said that the university had showed a lack of foresight and planning in naming these elements. The magazine said that the they should have given the names universitium, ofium, californium, and berkelium to elements 97, 98, 99, and100 respectively. Seaborg quickly replied that he and his group showed good foresight because if he had done that some scientist from New York might discover elements 99 and 100, and name them newium and yorkium.

The discoveries of elements 99 and 100 would have to wait for about two years after the discoveries of berkelium and californium. These elements were discovered in a method unlike any of the other transuranium elements. These elements were first discovered in the fallout of the "Mike" thermonuclear detonation (see picture). Drone aircraft flew through the fallout cloud and collected fallout on pieces of filter paper. These pieces of filter paper were sent to several labs around the United

States. Seaborg and his group discovered elements 99 and 100. The elements were named after Albert Einstein and Enrico Fermi respectively, and came to be called einsteinium and fermium. When the labs required more material to study the chemical properties of these elements, Operation Paydirt was initiated to retrieve coral contaminated by fallout from the explosion.

Element 101 was discovered by Seaborg and his colleagues in February of 1955. They named the element mendelevium after the inventor of the periodic table, Dmitri Mendelev. The element was first produced in the sixty inch cyclotron from einsteinium by the following reaction:

$$^{253}_{99}Es + ^{4}_{2}He(\alpha) \rightarrow ^{256}_{101}Md + n$$

Seaborg discovered the next element he discovered in April of 1958. Element 102 was first produced in the Heavy Ion Linear Accelerator. They named the element nobelium after Alfred Nobel and the Nobelprize, which Seaborg shared with McMillian in 1951. Nobelium was first produced from curium by the following reaction:

$$^{246}_{96}Cm + ^{12}_{6}C \rightarrow ^{254}_{102}No + 4n$$

1.28 Start of the World's first nuclear reactor - the first objective of the Manhattan Project

2 December 1942.

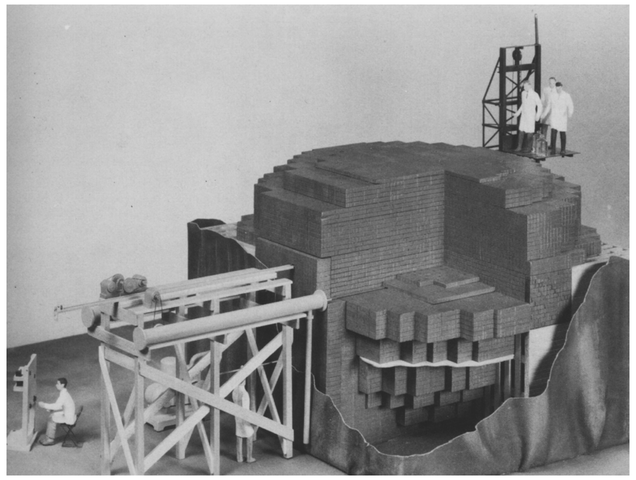

Figure 1.29 A model of Chicago Pile 1 (CP1)

The Manhattan Project was the code name for the US effort during World War II to produce the atomic bomb. It was named for the Manhattan Engineer District of the US Army Corps of Engineers, because much of the early research was done in New York City.

Sparked by refugee physicists in the United States, the program was slowly organized after nuclear fission was discovered by German scientists in 1938, and many US scientists expressed the fear that Hitler would attempt to build a fission bomb. In 1942 General Leslie Groves was chosen to lead the project, and he immediately purchased a site at Oak Ridge, Tenn., for facilities to separate the necessary ^{235}U from the much more common ^{238}U. He also appointed theoretical physicist J. Robert Oppenheimer as director of the weapons laboratory, built on an isolated mesa (flat land area) at Los Alamos, New Mexico.

Although Los Alamos had been selected as the site of the laboratory that would design nuclear weapons for the Manhattan Engineer District (MED), it was not until Dec. 2, 1942, that Enrico Fermi and his group at the metallurgical laboratory at the University of Chicago achieved an experimental demonstration of a chain reaction. This was a result of a program begun in 1939 in response to Albert Einstein's letter to President Franklin Delano Roosevelt warning of the German program to exploit fission for military purposes. Three years were required to achieve results that demonstrated the danger, although, unknown to American physicists, the Germans had not succeeded in achieving a chain reaction in their experiments.

The achievement of a chain reaction was important, not only because it would prove the principle of the atomic bomb, but also because a chain-reacting pile could be used to produce plutonium, one of the nuclear explosives American scientists hoped to use in their weapons. Indeed, MED Commander Leslie Groves had already asked the DuPont Corp. to build production reactors in Hanford, Wash., for that purpose.

Fermi was the champion of the American effort in the secret race to achieve a chain reaction in uranium. His antagonist was German physicist Werner Heisenberg one of the creators of quantum mechanics and among the most distinguished theoretical physicists in the world. Fermi had left Italy to escape fascist persecution in 1938, collecting his Nobel Prize in Stockholm, Sweden, en route to Columbia University, where he began his experiments to build a chain-reacting pile in 1939 after the discovery of fission. Heisenberg was recruited to work on a chain-reacting pile in September 1939 by Nazi physicist Kurt Diebner.

While Fermi chose graphite to slow down, or “moderate,” the neutrons produced in the fission of ^{235}U so that they could cause further fissions in a chain reaction, Heisenberg chose heavy water, in part because experiments conducted by Walter Bothe at the University of Heidelberg indicated that pure graphite was inadequate as a moderator.

These results were based upon mistaken calculations and gave Fermi an advantage. Heavy water was also chosen because Heisenberg’s early experiments with paraffin as a moderator failed to produce any chain reaction. Fermi’s early experiments at Columbia, in contrast, used highly purified graphite, paid for by the federal government in response to Einstein’s letter.

The price was $6,000 for 40 tons purified of boron and other neutron-absorbing elements that might inhibit a chain reaction. This was increased by $40,000 when the National Defense Research Committee was created in 1940. None of the piles built at Columbia with these funds succeeded in producing a neutron multiplication greater than one, which would indicate the presence of a chain reaction.

Heisenberg’s first experiments with heavy water at the Kaiser-Wilhelm Institute in Berlin-Dahlem and in Leipzig, Germany, were encouraging enough for him to promote nuclear energy to the German government. He warned its representatives in the fall of 1941 that the Americans were pursuing a nuclear explosive (plutonium) that could be made in a chain-reacting pile. The warning resulted in receiving the highest priority for his work from Albert Speer, Hitler’s minister of munitions. The Leipzig pile, however, had burned in a fire caused by a pyrophoric reaction of its powdered uranium with air, and Allied bombing of Berlin forced Heisenberg to move his materials there to Haigerloch in Württemberg, Germany.

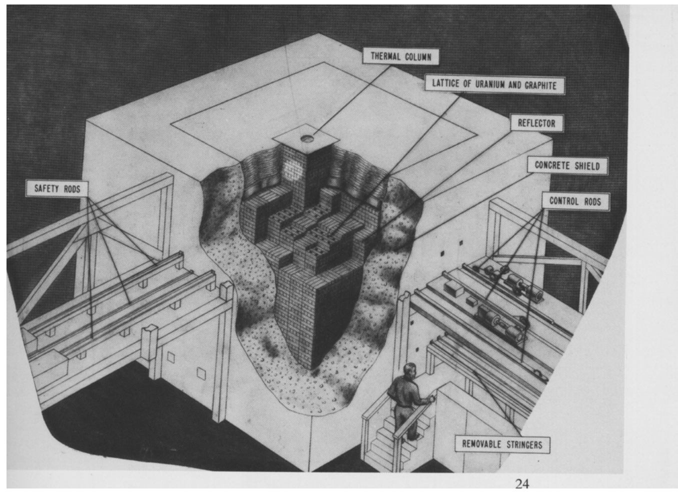

Figure 1.30 Layout of Chicago Pile - 1

After FDR’s decision to commit the United States government to a full-scale atomic bomb program in October 1941, Fermi’s pile had been moved to the University of Chicago, where it was rebuilt in a squash court under the west stands of Stagg Field, which were no longer in use. There, he used uranium metal, rather than the pyrophoric powder Heisenberg had used or the uranium oxide used in his earlier experiments at Columbia, to build a larger pile.

Figure 1.31 An artistic vision of CP1 experiment

The Chicago pile included 400 tons of graphite and 22,000 “pseudospheres”of uranium stacked in 57 layers with cadmium sheets nailed to flat wooden strips as control and safety rods. on Dec. 2, Fermi supervised the final steps of his experiment. He calculated the number of fission neutrons to be expected as the control rod was pulled from the pile. In addition to safety rods controlled electronically so that they would be pushed into the pile if neutron detectors indicated a runaway reaction, another, weighted with lead, would fall into the pile if physicist Norman Hilberry cut a rope with a hatchet. If all else failed, a three-man “suicide squad” of physicists stood ready to drench the pile with cadmium sulfate. That morning, Fermi ordered the control rod raised foot by foot from the pile until one of the safety rods,triggered at a preset point that he had forgotten, was released and slid into the pile, with weights crashing to the floor. He ordered it removed again, saw the counters indicate the previous flux and then broke the tension by ordering the crew to lunch. After lunch, the control rod was pulled out 13 feet again, then another six inches, then, after the safety rod was reinserted, another foot. The safety rod was withdrawn, and the counters rattled as the trace indicating neutron multiplication climbed straight up, indicating a self-sustaining chain reaction.

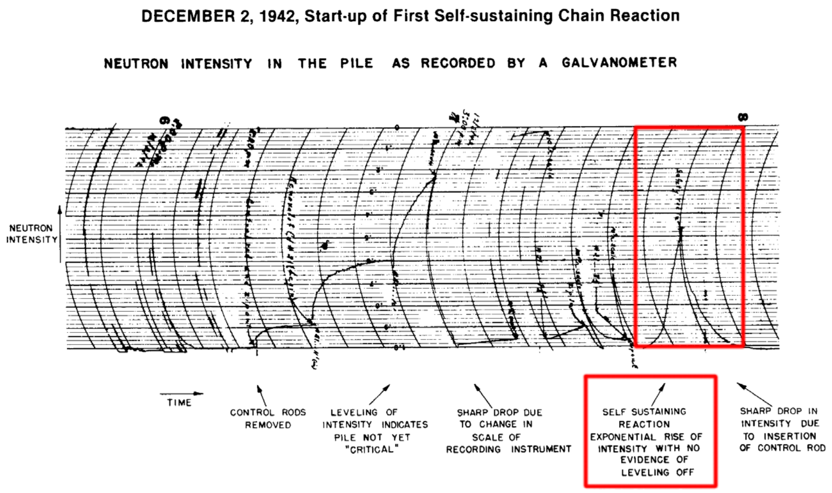

After operating for 28 minutes, producing about 200 watts of power, the pile was shut down. Eugene Wigner (a Hungarian physicist who helped to write the Einstein letter to FDR) handed Fermi a bottle of Bertolli Chianti and passed around paper cups to the crew. Leona Woods Marshall, the only woman present, broke the silence with the comment: “Let’s hope that we are the first to succeed.”

Arthur Compton called the head of the NDRC, James Conant, and told him cryptically, **“the Italian navigator has just landed in the New World,”** the secret phrase agreed to, to signal success.

First nuclear reactor video - click the frame

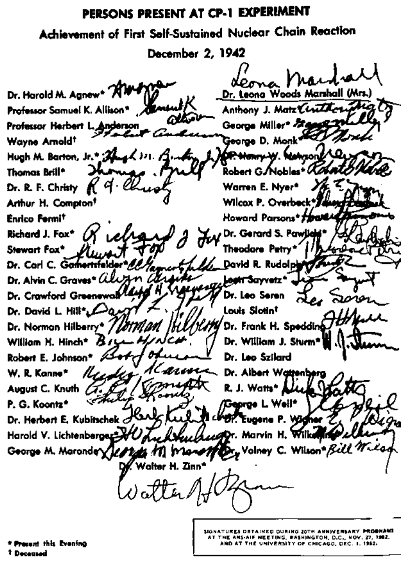

PERSONS PRESENT AT CP-1 EXPERIMENT

Achievement of First Self-Sustained Nuclear Chain Reaction

December 2, 1942

Dr. Harold M. Agnew*
Professor Samuel K. Allison*
Professor Herbert L. Anderson
Wayne Arnold†
Hugh M. Barton, Jr.*
Thomas Brill*
Dr. R. F. Christy
Arthur H. Compton†
Enrico Fermi†
Richard J. Fox*
Stewart Fox*
Dr. Carl C. Gamertsfelder*
Dr. Alvin C. Graves*
Dr. Crawford Greenewalt
Dr. David L. Hill*
Dr. Norman Hilberry*
William H. Hinch*
Robert E. Johnson*
W. R. Kanne*
August C. Knuth
P. G. Koontz*
Dr. Herbert E. Kubitschek
Harold V. Lichtenberger*
George M. Maronde

Dr. Leona Woods Marshall (Mrs.)
Anthony J. Matz
George Miller*
George D. Monk*
Dr. Henry W. Newson
Robert G. Nobles*
Warren E. Nyer*
Wilcox P. Overbeck*
Howard Parsons*
Dr. Gerard S. Pawlicki*
Theodore Petry*
David R. Rudolph*
Leon Sayvetz*
Dr. Leo Seren
Louis Slotin†
Dr. Frank H. Spedding
Dr. William J. Sturm*
Dr. Leo Szilard
Dr. Albert Wattenberg
R. J. Watts*
George L. Weil*
Dr. Eugene P. Wigner
Dr. Marvin H. Wilkening
Dr. Volney C. Wilson*

Dr. Walter H. Zinn*

Leona Marshall
Harold Agnew
Samuel K. Allison
Herbert Anderson
Hugh M. Barton Jr.
Thomas Brill
R. F. Christy
Robert G. Nobles
Richard J. Fox
Stewart Fox
Leo Seren
Norman Hilberry
Bill Hinch
Bob Johnson
Kanne
W. J. Sturm
Dick Watts
Bill Wilson
Walter H. Zinn

* Present this Evening
† Deceased

SIGNATURES OBTAINED DURING 20TH ANNIVERSARY PROGRAM AT THE ANS-AIF MEETING, WASHINGTON, D.C., NOV. 27, 1962, AND AT THE UNIVERSITY OF CHICAGO, DEC. 1, 1962.

Figure 1.32 The scientists who worked on the project were back row, from left, Norman Hilberry, Samuel Allison, Thomas Brill, Robert Nobles, Warren Nyer, and Marvin Wilkening. Middle row, Harold Agnew, William Sturm, Harold Lichtenberger, Leona Marshall and Leo Szilard,. Front row, Enrico Fermi, Walter Zinn, Albert Wattenber and Herbert Anderson.

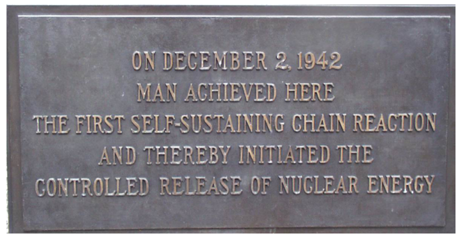

ON DECEMBER 2, 1942
MAN ACHIEVED HERE
THE FIRST SELF-SUSTAINING CHAIN REACTION
AND THEREBY INITIATED THE
CONTROLLED RELEASE OF NUCLEAR ENERGY

1.29 Test of the First Atomic Bomb

16 July 1945

HISTORICAL BACKGROUND OF PROJECT TRINITY

The development of a nuclear weapon was a low priority for the United States before the outbreak of World War II. However, scientists exiled from Germany had expressed concern that the Germans were developing a nuclear weapon. Confirming these fears, in 1939 the Germans stopped all sales of uranium ore from the mines of occupied Czechoslovakia. In a letter sponsored by group of concerned scientists, Albert Einstein informed President Roosevelt that German experiments had shown that an induced nuclear chain reaction was possible and could be used to construct extremely powerful bombs.

In response to the potential threat of a German nuclear weapon, the United States sought a source of uranium to use in determining the feasibility of a nuclear chain reaction. After Germany occupied Belgium in May 1940, the Belgians turned over uranium ore from their holdings in the Belgian Congo to the United States. Then, in March 1941, the element plutonium was isolated, and the ^{239}Pu isotope was found to fission as readily as the scarce uranium isotope, ^{235}U. The plutonium, produced in a uranium-fueled nuclear reactor, provided the United States with an additional source of material for nuclear weapons.

In the summer of 1941, the British Government published a report written by the Committee for Military Application of Uranium Detonation (MAUD). This report stated that a nuclear weapon was possible and concluded that its construction should begin immediately. The MAUD report, and to a lesser degree the discovery of plutonium, encouraged American leaders to think more seriously about developing a nuclear weapon. ***Click here to read MAUD Report***. On 6 December 1941, President Roosevelt appointed the S-1 Committee to determine if the United States could construct a nuclear weapon. Six months later, the S-1 Committee gave the President its report, recommending a fast-paced program that would cost up to $100 million and that might produce the weapon by July 1944.

Robert Oppenheimer

The President accepted the S-1 Committee's recommendations. The effort to construct the weapon was turned over to the War Department, which assigned the task to the Army Corps of Engineers. In September 1942, the Corps of Engineers established the Manhattan Engineer District (MED) to oversee the development of a nuclear weapon. This effort was code-named the **"Manhattan Project".**

Within the next two years, the MED built laboratories and production plants throughout the United States. The three principal centers of the Manhattan Project were the Hanford, Washington, Plutonium Production Plant; the Oak Ridge, Tennessee, ^{235}UProduction Plant; and the Los Alamos Scientific Laboratory in northern New Mexico. At LASL, Manhattan Project scientists and technicians, directed by Dr. Gentlemen - Robert Oppenheimer, investigated the theoretical problems that had to be solved before a nuclear weapon could be developed.

Click here to read so called "Los Alamos Primer", the first written manual for Los Alamos sci-

entists about the principles of nuclear fission and its application for the atomic bomb research.

During the first two years of the Manhattan Project, work proceeded at a slow but steady pace. Significant technical problems had to be solved, and difficulties in the production of plutonium, particularly the inability to process large amounts, often frustrated the scientists. Nonetheless, by 1944 sufficient progress had been made to persuade the scientists that their efforts might succeed. A test of the plutonium implosion device was necessary to determine if it would work and what its effects would be. In addition, the scientists were concerned about the possible effects if the conventional explosives in a nuclear device, particularly the more complex implosion-type device, failed to trigger the nuclear reaction when detonated over enemy territory. Not only would the psychological impact of the weapon be lost, but the enemy might recover large amounts of fissionable material..

In March 1944, planning began to test-fire a plutonium-fueled implosion device. At LASL, an organization designated the X-2 Group was formed within the Explosives Division. Its duties were "to make preparations for a field test in which blast, earth shock, neutron and gamma radiation would be studied and complete photographic records made of the explosion and any atmospheric phenomena connected with the explosion". Dr. Oppenheimer chose the name **TRINITY** for the project in September 1944.

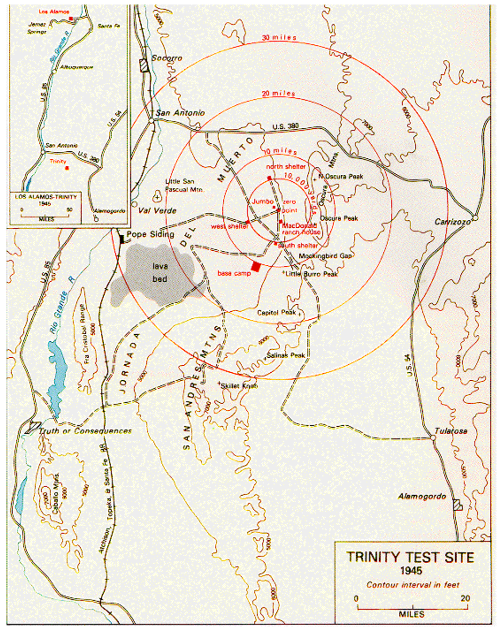

Figure 1.33 Trinity Test Site - 1945

THE PROJECT TRINITY SITE

The TRINITY site was chosen by Manhattan Project scientists after thorough study of eight different sites. The site selected was an area measuring 29 by 39 kilometers* in the northwest corner of the Alamogordo Bombing Range. The Alamogordo Bombing Range was located in a desert in south-central New Mexico called the Jornada del Muerto ("Journey of Death"). The site was chosen for its remote location and good weather and because it was already owned by the Government. MED obtained permission to use the site from the Commanding General of the Second Air Force (Army Air Forces) on 7 September 1944 .

Vertical distances are given in feet; altitudes are measured from mean sea level, while heights are measured from surface level, unless otherwise noted.

Ground zero for the TRINITY detonation was at UTM coordinates 630266. Three shelters, located approximately 9,150 meters north, west, and south of ground zero, were built for the protection of test personnel and instruments. The shelters had walls of reinforced concrete and were buried under a few feet of earth. The south shelter was the Control Point for the test (12). The Base Camp, which was the headquarters for Project TRINITY, was located approximately 16 kilometers southwest of ground zero. The principal buildings of the abandoned McDonald Ranch, where the active parts of the TRINITY device were assembled, stood 3,660 meters southeast of ground zero.

THE PROJECT TRINITY ORGANIZATION

The organization that planned and conducted Project TRINITY grew out of the X-2 Group. LASL, though administered by the University of California, was part of the Manhattan Project, supervised by the Army Corps of Engineers Manhattan Engineer District. The chief of MED was Maj. **Gen. Leslie Groves** (see picture) of the Army Corps of Engineers. Major General Groves reported to both the Chief of Engineers and the Army Chief of Staff The Army Chief of Staff reported to the Secretary of War, a Cabinet officer directly responsible to the President.

The director of the Project TRINITY organization was Dr. Kenneth Bainbridge. Dr. Bainbridge reported to Dr. J. Robert Oppenheimer, the director of LASL. A team of nine research consultants advised Dr. Bainbridge on scientific and technical matters.

From March 1944 until the beginning of 1946, several thousand people participated in Project TRINITY. These included not only the LASL scientists, but also scientists, technicians, and workmen employed at MED installations throughout the United States. According to entrance logs, film badge data, and other records, about 1,000 people either worked at or visited the TRINITY site from 16 July 1945 through 1946 .

Figure 1.34 Gen. Leslie Groves

THE ACTIVITIES AT PROJECT TRINITY

The TRINITY nuclear device called Gadget - see Figure 1.36 - was detonated on a 100-foot tower (shown in the figure below) on the Alamogordo Bombing Range, New Mexico, at 05:30 Mountain War Time, on 16 July 1945. The detonation had a yield of 19 kilotons and left an impression 2.9 meters deep and 335 meters wide. The cloud resulting from the detonation rose to an altitude of over 10 000 m.

At shot-time, the temperature was 21.8 degrees Celsius, and the surface air pressure was 850 millibars. Winds at shot-time were nearly calm at the surface but attained a speed of 10 knots from the southwest at 10,300 feet. At 34,600 feet, the wind speed was 23 knots from the southwest. The winds blew the cloud to the northeast.

Figure 1.35 The base camp of the Trinity site

The planned firing date for the TRINITY device was 4 July 1945. On 14 June 1945, Dr. Oppenheimer changed the test date to no earlier than 13 July and no later than 23 July. On 30 June, the earliest firing date was moved to 16 July, even though better weather was forecast for 18 and 19 July. Because the Allied conference in Potsdam, Germany, was about to begin and the President needed the results of the test as soon as possible, the TRINITY test organization adjusted its schedules accordingly and set shot-time at 0400 hours on 16 July.

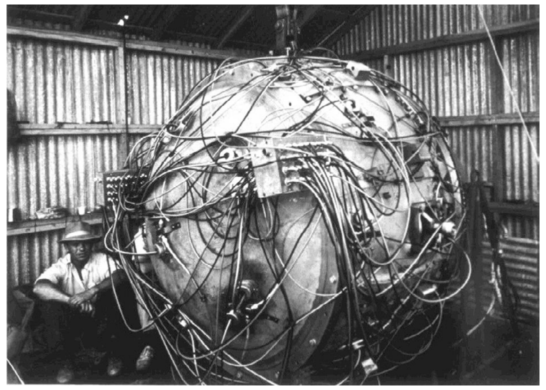

Figure 1.36 The Gadget - the first atomic, plutonium bomb detoneted on 16 July 1945

The final preparations for the detonation started at 22:00 on 15 July. To prevent unnecessary danger, all personnel not essential to the firing activities were ordered to leave the test site. During the night of 15 July, these people left for viewing positions on Compania Hill, 32 kilometers northwest of ground zero. They were joined by several spectators from LASL.

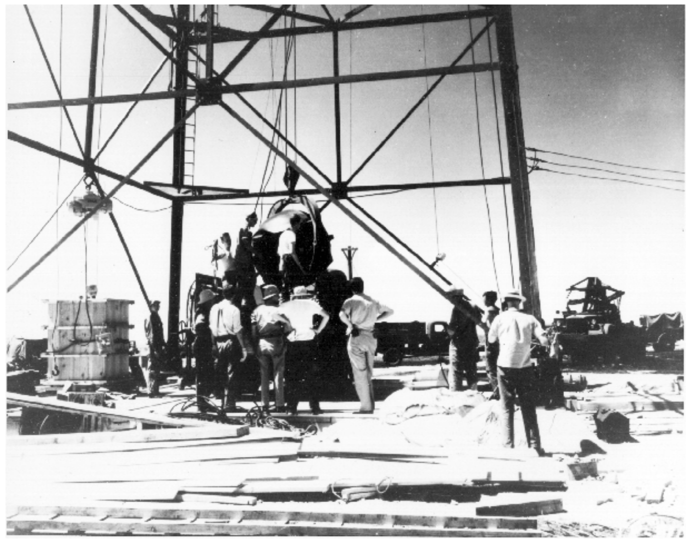

Figure 1.37 Lifting up the GADGET on the tower.

At the time of detonation, 99 project personnel were in the three shelters: 29 in the north shelter, 37 in the west shelter, and 33 in the south shelter. Dr. Oppenheimer, Dr. Bainbridge, and other key personnel awaited the firing at the south shelter, which served as the Control Point.

The remainder of the test site personnel were positioned at the Base Camp 16 kilometers south-southwest of ground zero, or on Compania Hill, or at the guard posts. Important Government officials, such as General Groves and Dr. Vannevar Bush, Director of the U.S. Office of Scientific Research and Development, viewed the detonation from a trench at the Base Camp.

DETONATION AND POSTSHOT ACTIVITIES

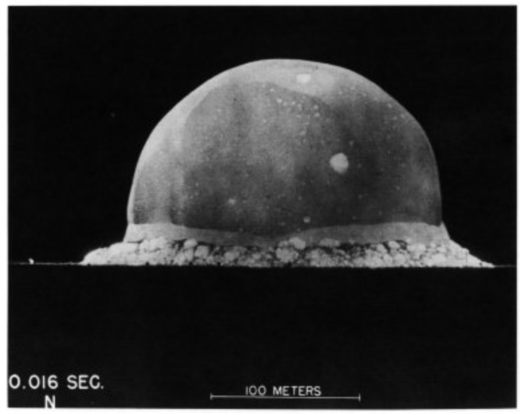

Figure 1.38 Trinity Explosion - 0.016 sec. after detonation

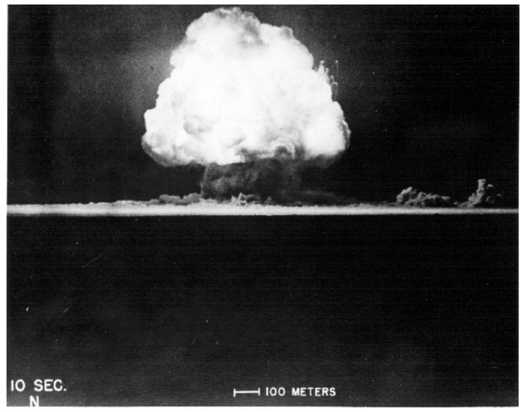

Figure 1.39 Trinity explosion - 10 seconds after time 0.

Because of bad weather, the Project TRINITY director (Dr. Bainbridge) delayed the detonation, which had been scheduled for 04:00 hours. By 04:45, however, the forecast was better, and shot-time was set for 05:30. This gave the scientists 45 minutes to arm the device and prepare the instruments in the shelters. The final countdown began at 0510, and the device was detonated at 05:29:45 Mountain War Time from the Control Point in the south shelter.

CLICK HERE TO READ GEN. GROVES REPORT TO WAR DEPARTMENT

No one was closer than 9,150 meters to ground zero at the time of the detonation. With the exception of a few men holding the ropes of barrage balloons or guiding cameras to follow the fireball as it ascended, all shelter personnel were in or behind the shelters. Some left the shelters after the initial flash to view the fireball. As a precautionary measure, they had been advised to lie on the ground before the blast wave arrived. Project personnel located beyond the shelters, such as at the Base Camp and on Compania Hill, were also instructed to lie on the ground or in a depression until the blast wave had passed. However, the blast wave at these locations was not as strong as had been expected.

In order to prevent eye damage, Dr. Bainbridge ordered the distribution of welder's filter glass. Because it was not known exactly how the flash might affect eyesight, it was suggested that direct viewing of the fireball not be attempted even with this protection. The recommended procedure was to face away from ground zero and watch the hills or sky until the fireball illuminated the area. Then, after the initial flash had passed, one could turn around and view the fireball through the filter glass. Despite these well-publicized instructions, two participants did not take precautions. They were temporarily blinded by the intense flash but experienced no permanent vision impairment.

People as far away as Santa Fe and El Paso saw the brilliant light of the detonation. Windows rattled in the areas immediately surrounding the test site,

Figure 1.40 Gadget explosion video

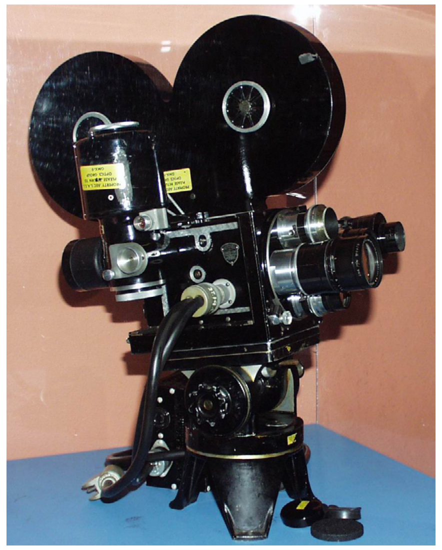

Figure 1.42 A specially constructed high-speed, high-quality movie camera to film nuclear explosions (Bradbury Museum, Los Alamos)

Figure 1.41 Evaporated tower and crater after explosion

Figure 1.43 The monument at Trinity site - ground ZERO - point

waking sleeping ranchers and townspeople. To dispel any rumors that might compromise the security of Project TRINITY, the Government announced that an Army munitions dump had exploded. However, immediately after the destruction of Hiroshima, the Government revealed to the public what had actually occurred in the New Mexico desert.

Two B-29 aircraft from Kirtland Field, Albuquerque, New Mexico, participated in post-shot events. Their planned mission was to pass over the test area shortly before the explosion to simulate a bomb drop. After the TRINITY device had been detonated, the aircraft would circle near ground zero, while the men onboard would measure the atmospheric effects of the nuclear explosion. This would enable them to determine whether a delivery aircraft would be endangered. However, because of bad weather on shot-day, Dr. Oppenheimer canceled the aircraft's flight in the ground zero area. Instead, the two B-29s, each with 12 men on board, flew along the perimeter of the bombing range and observed the shot from a distance of 19 to 29 kilometers.

1.30 First atom bombs dropped over Hiroshima and Nagasaki

Figure 1.44 A model of Little Boy at Bradbury Museum at Los Alamos.

On August 6 and 9, 1945, the cities of Hiroshima and Nagasaki were destroyed by the first atomic bombs used in warfare. The Enola Gay plane took off on August 6, 1945 with an atomic bomb, called Little Boy and dropped it at 8:16 over a city of Hiroshima. The bomb exploded on target about 600 m above the ground.

Over 70 000 people were instantly killed in Hiroshima and at least as many very seriously injured. By the end of 1945 number of casulties raised to above 140 000. In one single blast equivalent to about 13 kilotons of TNT Hiroshima ceased to exist as a functioning society.

Figure 1.45 Video of Hiroshima atomic bomb attack

August 9, 1945, the B-29 plane nicknamed Bock's Car dropped over Nagasaki city a plutonium bomb, called a Fat Man. About 75000 people were killed in this single blast and about the same amount was seriously injured. The damage was less extensive compared to Hiroshima in spite of a higher yield of 22 kilotons of TNT, due to the geography of the Nagasaki area and partially to the fact that bomb was exploded 2 miles out off the target.

Figure 1.46 A model of a Fat Man atomic bomb (implosion type) at the Bradbury Museum, Los Alamos.

Figure 1.47 Video of Nagasaki explosion

1.31 USA publishes so called Smyth Report: "Atomic Energy for Military Purposes", 1945

Click here to read the whole report (A good repetition of principles of fission physics!!)

The Smyth Report was the common name given to an administrative history written by physicist Henry DeWolf Smyth about the Allied World War II effort to develop the atomic bomb, the Manhattan Project. The full title of the report was "A General Account of the Development of Methods of Using Atomic Energy for Military Purposes." It was released to the public on August 12, 1945, after the atomic bombings of Hiroshima and Nagasaki on August 6 and 9.

The Report was to serve two functions. First, it was to be the official U.S. government history and statement about the development of the atomic bombs, outlining the development of the then-secret laboratories and production sites at Los Alamos, New Mexico, Oak Ridge, Tennessee, and Hanford, Washington, and the basic physical processes responsible for the functioning of nuclear weapons, in particular nuclear fission and the nuclear chain reaction. Secondly, it serves as a barometer for other scientists as to what information was declassified—anything said in the Smyth Report could be said freely in open literature. For this reason, the Smyth Report focused heavily on information already available in declassified literature, such as much of the basic nuclear physics used in weapons, which was either already widely known in the scientific community or could have been easily deduced by a competent scientist.

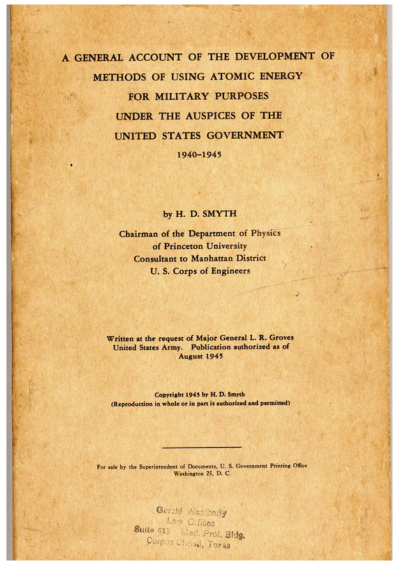

A GENERAL ACCOUNT OF THE DEVELOPMENT OF
METHODS OF USING ATOMIC ENERGY
FOR MILITARY PURPOSES
UNDER THE AUSPICES OF THE
UNITED STATES GOVERNMENT
1940–1945

by H. D. SMYTH
Chairman of the Department of Physics
of Princeton University
Consultant to Manhattan District
U. S. Corps of Engineers

Written at the request of Major General L. R. Groves
United States Army. Publication authorized as of
August 1945

Copyright 1945 by H. D. Smyth
(Reproduction in whole or in part is authorized and permitted)

For sale by the Superintendent of Documents, U. S. Government Printing Office
Washington 25, D. C.

Gerald Weatherly
Law Offices
Suite 413 Med. Prof. Bldg.
Corpus Christi, Texas

Figure 1.48 Cover page of the Smyth Report

1.32 First "nuclear" electricity: Experimental Breeder Reactor - I

Idaho, December 20, 1951

On Dec. 20, 1951, Experimental Breeder Reactor-I lit four lightbulbs to demonstrate the first usuable amount of electricity from nuclear energy. EBR-I was designed, built and operated by Argonne in Idaho. It was barely enough to power a simple string of four, 100-watt light bulbs, but the 16 scientists and engineers - all staff members of Argonne National Laboratory, which designed and built the reactor - recorded their historic achievement by chalking their names on the wall beside the generator.

The design purpose of EBR-I was not to produce electricity but instead to validate nuclear physics theory which suggested that a breeder reactor should be possible. In 1953, experiments revealed the reactor was producing additional fuel during fission, thus confirming the hypothesis. However, on November 29, 1955, the reactor at EBR-I suffered a partial meltdown during a coolant flow test. The flow test was trying to determine the cause of unexpected reactor responses to changes in coolant flow. It was subsequently repaired for further experiments, which determined that thermal expansion of the fuel rods and the thick plates supporting the fuel rods was the cause of the unexpected reactor response

Figure 1.49 Experimental Breeder Reactor - 1 (EBR-1) site at Idaho National Laboratory

Figure 1.50 The control panel of the EBR-1

1.33 First commercial nuclear reactor started.

Obninsk, Soviet Union (Russia today), 1954

The reactor in Obninsk (called APS-1 Obninsk), about 120 km south of Moscow is considered to be the first "commercial" nuclear power station delivering energy to the local community until today. This reactor is one of the prototypes of the Chernobyl-type reactors with graphite moderator and water coolant (see figure below).

June 26, 1954 reactor started its operation at thermal power of 30 MW producing 5 MW of elelctrical power. After 5 years of commercial operation reactor was turned into research and test reactor. Experiments conducted on this reactor was mainly focused on fuel and constructional material irradiations, water chemistry and isotope production. First graphite moderated and water cooled reactors of high power - reactors at Beloyarsk nuclear power plant at Ural mountain - were designed based on experiences from this reactor. The first reactor of Beloyarsk power plant was of 100 MW_{el} , second one - 200 MW_{el}. Reactor at Obninsk and Beloyarsk reactors were also used to investigate the concept of steam overheating in the reactor core. Unfortunately, steam overheating leads to unacceptable safety behavior of the reactor - strong positive temperature reactivity coefficient - and this concept was soon abandoned in nuclear technology.

Figure 1.51 Information board at the Obninsk reactor site saying: The First Atomic Power Station

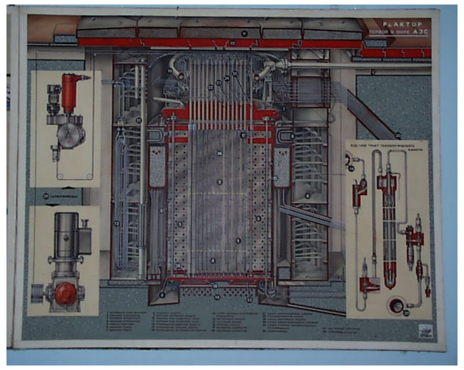

Figure 1.52 The cross-section of the Obninsk reactor core - pay attention to the graphite-water type design.

Figure 1.53 An "unqualified" operator (the author) running reactor - just for a moment.

Figure 1.54 The control room of the Obninsk reactor.

The power plant remained active until April 29, 2002 when it was finally shut down.

List of Milestones in Development of Modern Physics

Chronological History of Modern Physics
(Click on blue text to go to the relevant publication or info-article)

1895 ***Wilhelm Conrad Roentgen***

Discovered X--rays, somewhat accidentally. ***Nobel prize winner 1901.***

1896 ***Antoine Henri Becquerel***

Discovered the radioactivity of uranium salts. ***Joint Nobel prize winner with the Curies in 1903.***

1896 ***Pieter Zeeman***

Discovered the splitting of spectral lines by atoms in strong magnetic fields. Jointly awarded Nobel prize with H A Lorentz in 1902.

1897 ***Joseph John Thomson***

Experimentally calculated q/m for cathode rays (electrons). ***Awarded the Nobel prize in 1906***.

1897 ***Ernest Rutherford (Lord Rutherford of Nelson)***

Showed that the radioactive decay of Uranium consisted of hard and soft emissions, that is alpha and beta decays. ***Awarded Nobel prize in 1906 (Chemistry).***

1898 ***Marie Sklodowska Curie and Pierre Curie***

Isolated polonium and radium. ***They, together with Becquerel, were awarded the Nobel prize in 1903.***

1900 ***Lord (John William Strutt) Rayleigh*** and later James Hopwood Jeans

Produced a blackbody radiation law and was later revised and published as the Rayleigh--Jeans law. ***The Nobel prize awarded to Lord Rayleigh in 1904.***

1900 ***Max Carl Ernst Ludwig Planck***

Released his revolutionary theory of the quantisation of electromagnetic radiation -- the beginning of Quantum Mechanics.

1900 Henri Becquerel

displayed that cathode rays were in fact electrons.

1900 ***Paul Villiard***

Discovered a new radiation -- gamma rays.

1903 ***Ernest Rutherford and Frederic Soddy***

Found that in radioactive decay the radioactive element transmutes into another element.

1905 ***Albert Einstein***

Publishes his theory of relativity amongst other papers on brownian motion and ***the photoelectric effect.***

1905 Egon von Schweildler

Derived from the theory of probability, the radioactive decay law.

1906 ***Charles Barkla***

Discovers that each element has a characteristic X-ray and that the degree of penetration of these X-rays is related to the atomic weight of the element

1909--1911 ***Robert Andrews Millikan***

Carried out his oil drop experiments to reveal that electric charge is multiple proportions of the electron charge. In the process he carried the most precise measurement of the electronic charge and Avogadro's number. He was awarded the Nobel prize in 1923.

1911--1913 ***Ernest Rutherford, Hans Geiger and Ernest Marsden***

Conducted their famous experiments which concluded with the nuclear model having to be applied in order to explain the results of alpha particle scattering by thin metal foils.

1911 ***Charles Thomson Rees Wilson***

Constructed the first cloud chamber, which became one of the most important tools in nuclear physics.

1912 ***Hans Geiger***

Produced an empirical law which related the energy of emitted alpha particles to the disintegration constant of the parent nucleus.

1913 ***Frederick Soddy***

Introduced the term "isotopes."

1913 ***Niels Henrik David Bohr***

Developed his atomic theory of the atom.

1915 ***Albert Einstein***

Publishes his General Theory of relativity.

1919 ***Ernest Rutherford***

Produced the first transmutation of an element in the laboratory by alpha particle bombardment of nitrogen to produce hydrogen and oxygen.

1919

Observations of a solar eclipse confirmed the deviation of starlight as predicted by the general theory of relativity. Einstein is made famous!

1923 ***Arthur Holly Compton***

Discovered the Compton effect which displayed that the photon has momentum.

1924 ***Louis Victor, Duc de Broglie***

The idea of matter waves -- de Broglie waves. ***Was awarded the Nobel prize in 1929.***

1925 ***George Eugene Uhlenbeck*** and ***Samuel Abraham Goudsmit***

Brought spin and magnetic moment of the electron into atomic theory.

1925 ***Wolfgang Pauli***

Introduces the Pauli exclusion principle. ***He was awarded the Nobel prize in 1945.***

1925 - 1926 ***Werner Heisenberg***

Invention of matrix formalism for the Heisenberg quantum mechanics. Systems with one degree of freedom. Development of matrix formalism for the Heisenberg quantum mechanics.

1925 ***Max Born, Werner Karl Heisenberg and Pascual Jordan***

Developed quantum mechanics. ***Born with W. Bothe were awarded the Nobel prize in 1954.***

1926 ***Erwin Schroedinger***

Introduced wave mechanics for the hydrogen atom. Was awarded the Nobel prize in conjunction with ***P A M Dirac in 1933***.

1926 ***Enrico Fermi*** and ***Paul Adrien Maurice Dirac***

Both introduced the statistics of fermions.

1927 ***Werner Heisenberg***

Introduced the uncertainty principle.

1928 Hans Geiger and W Müller

Produced the Geiger-Müller tube (detector of radiation).

1931 ***Harold Urey***

Discovers deuterium using evaporation concentration techniques and spectroscopy

1931 Robert Jemison Van De Graaff

Made the first high voltage particle accelerator for nuclear physics research.

1931 ***Wolfgang Pauli***

Introduces the idea of the neutrino which is emitted simultaneously with the electron in ß--decay.

1932 ***Ernest Orlando Lawrence and Milton Stanley Livingston***

Constructed the first cyclotron.

1932 ***John Douglas Cockcroft and Ernest Thomas Sinton Livingston***

Produced the first nuclear reaction with a high voltage accelerator by bombarding lithium with high--energy protons causing it to transmute. This also confirmed Einstein mass--energy equivalence.

1932 ***James Chadwick***

Discovers the neutron and was ***awarded the Nobel prize in 1935***.

1932 ***Carl Anderson***

Discovers the positron

1934 ***Pavel Aleksejevic Cherenkov***

Discovers Cherenkov radiation. A bluish glow in substances when bombarded with high--energy ß particles.

1934 ***Irene and Frédéric Joliot--Curie***

Discovered artificial radioactivity through bombardment of aluminum atoms with alpha particles. They created artificially radioactive phosphorus-30

1934 Leo Szilard

Realizes that nuclear chain reactions may be possible (patented nuclear reactor)

1934 ***Enrico Fermi***

Formulates his theory of beta decay

1934 ***Enrico Fermi***

Suggests bombarding uranium atoms with neutrons to make a 93 proton element. With Amaldi and Rasetti performed activation of elements with neutrons.

1935 ***Hideki Yukawa***

Released his theory of nuclear binding forces by particle exchange. With the particle being later named the meson.

1936 ***Eugene Wigner***

Develops the theory of neutron absorption by atomic nuclei.

1937 ***Niels Bohr***

announced the theory of the nucleus resembling that of a liquid drop.

1939 ***Otto Hahn and Fritz Strassman***

Bombard uranium salts with thermal neutrons and discover barium among the reaction products.

1939 Lise Meitner and Otto Frisch

Determine that nuclear fission is taking place in the Hahn-Strassman experiments

1939 ***Lev Kowarski and von Halban***

Determined that about 3 neutrons are released in fission (possibility for chain reaction)

1939 ***Niels Bohr and John Archibald Wheeler***

Produced the theory of nuclear fission.

1940 John Ray Dunning, Eugene Theodore Boothe and Aristid Grosse

Proved that it was uranium 235 which fissioned rather than uranium 238.

1942 Enrico Fermi and his team in the Manhattan project

Constructed the first nuclear fission reactor. It possessed a power level of half a watt.

1945, July 16

First nuclear bomb tested at Trinity-site (New Mexico, USA)

Chapter 2

Nuclear Structure, Nuclear Stability and Radioactivity

2.1 Nuclear structure

The modern concept of the atom is that it can be subdivided into “sub-atomic” parts. This was not always the case. Before Thomson’s discovery of the electron, the atom was thought to be the smallest individual particle of matter. The concept of the atom is still correct but now we know there are many sub-atomic particles of which the atoms are composed.

There are two fundamental definitions that are necessary before we explore the structure of an individual atom. These are the definitions of a chemical element and an atom.

A **chemical element** is a basic form of matter composed of atoms of one distinct type that can not be decomposed into smaller units by chemical processes. An element is a category of atoms of all the same atomic number.

An **atom** is the smallest particle of an element that can enter into a chemical reaction.

Obviously, these definitions are closely linked. Today we know of 90 naturally occurring elements (types of atoms) and 28 more have been produced artificially by different nuclear reactions.

The structure of the atom is based on the Bohr model of the atom. The Bohr model is essentially an adaptation of the earlier work of Rutherford. The atom is now known to consist of a small, dense, positively charged core, called the nucleus, surrounded by one or more negatively charge electrons in distinct orbitals. The electrons balance the charge of the nucleus in the neutral atom. Electrons are very much smaller than the whole atom. For comparison, if the atom was the size of a room, the electron would be less than this dot “.”. Consequently, there is relatively large distances between electrons and an atom has a large amount of empty space within its volume. This space allows radiation to travel through mostly empty space and large distances may be need before an interaction can occur.

The nucleus itself is composed of protons and neutrons, which are now also known to have more fundamental parts. The constituents of the nucleus are called nucleons. By far the majority of the mass of the atom is located in the nucleus.

The experiment leading to the conclusion that the atom contained a dense, positively charged nucleus was conducted by Ernest Rutherford in 1911. ***(Click here to read about Rutherford´s discovery).***

The electrical properties of the composite atom were known to be neutral. The charge on an individual electron is -1, as previously proved by Thomson’s cathode ray tube studies. Therefore, there must be equal number of positive charges in the nucleus to account for the neutral atom. The dimensions of an atom are hard to imagine. The diameter of an atom is on the order of 10^{-8} cm with the nucleus being four orders of magnitude smaller, i.e. 10^{-12} cm. The radius of the nucleus can be approximated by the equation :

$$R = 1.25 \times 10^{-13} A^{1/3}$$

where :

R = the radius in cm

A = the atomic mass number.

The nucleus is an incredibly dense form of matter comprising the majority of the mass of an atom. The approximate density of the nucleus is 10^{14} g/cm^3.

The different atoms are distinguished from each other by the number of protons in their nucleus. The number of protons in a nucleus is now referred to as the atomic number.

We now know that isotopes are species of one particular kind of atom (element) with the same number of protons but different number of neutrons. This is not exactly the same meaning as the word “nuclide”, which is often confused with “isotope”. All isotopes are nuclides but all nuclides are not isotopes of the same element. The existence of isotopes was first postulated in 1913. Their existence was proved in 1919 by Aston after the creation of the first mass-spectrograph. Although they were proved to exist, there was no satisfactory explanations for isotopes since this was before the discovery of the neutron in 1932.

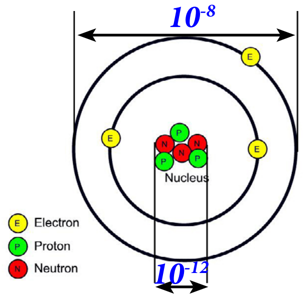

Figure 2.1 Lithium-7 structure

The structure of a lithium-7 - $^{7}_{3}Li$ - atom (an isotope of lithium) is illustrated in Figure 2.1. Lithium always contains 3 protons but can contain either 2, 3, 4, 5 or 6 neutrons.

Since isotopes of a given chemical compound all have the same chemical properties their existence was discovered by detecting small minute differences in their mass. To distinguish various nuclides and isotopes a common ZNA notation is used. Z represents the number of protons in an atoms nucleus and is called the atomic number. The number of neutrons in the nucleus is given by N and is simply termed the neutron number. The sum of Z + N is the atomic mass number or just the mass number, and is given the symbol A. Obviously, Z + N = A. Since the mass of both the proton and the neutron is nearly one amu, the atomic mass number is rounded off to a whole number. The atomic mass number approximates the mass of the entire atom since the electrons contribute very little mass to the whole atom.

Any nuclide can be represented by a conventional notation that lists the atomic number (Z) and atomic mass number (A) with the appropriate chemical symbol. An example of this is $^{235}_{92}U$. In this example, A = 235, Z = 92 and N can be calculated by A - Z = N. In this example, the number of neutrons in can be determined by 235 - 92 = 143. Often the atomic number is omitted since the chemical symbol implies the same meaning.

The scale for the mass of the atomic constituents is the Atomic Mass Unit or amu. The standard for the atomic mass unit is defined as 1/12 of the mass of the Carbon-12 nuclide. The mass of the Carbon-12 isotope is defined as exactly 12.00000 amu. One amu is approximately 1.66 x10^{-27} kg. Because the entire atom is defined as 12.00000 the individual constituents must have a total mass of greater than this due to binding energy. Using this scale, the rest mass of the atomic constituents and their relative charge are listed in Table I.

Table I. Properties od subatomic particles

Particle Rest Mass	Rest Mass amu	Rest Mass Mev	Electric charge
Proton	1.00727	938.2723	+1
Neutron	1.00866	939.5656	0
Electron	0.000548	0.510999	-1

2.2 Nuclear forces *(based on materials from e-Nobel museum)*

Since there were only two basic forces known in the beginning of the 20th century, gravitation and electromagnetism, and it was seen that electromagnetism is responsible for the forces in the atom, it was natural to believe that it was also responsible for the forces keeping the nucleus together. In the 1920's it was known that the nuclei contain protons, in fact the hydrogen nucleus is just a proton, and somehow it was believed that electrons could be involved in keeping the protons together. However, an idea like this has immediate problems. What is the difference between the electrons in the nucleus and the ones in orbit around the nucleus? What is the consequence of Heisenberg's uncertainty relation if electrons are squeezed into the small nucleus? The only support for the idea, apart from there being no other known elementary particles, was that in certain radioactive decays electrons were seen to come from the nucleus. However, in 1932 discovered a new type of radiation that could emanate from the nuclei, a neutral one and his experiment showed that there are indeed electrically neutral particles inside the nuclei, which came to be called neutrons. Soon after explained the nuclei as a consequence of two different nuclear forces. The Strong Nuclear Force is an attractive force between protons and neutrons that keep the nucleus together and the Weak Nuclear Force is responsible for the radioactive decay of certain nuclei. It was realized that the strength of the two forces differed a lot. The typical ratio is of the order of 10^{14} at ordinary energies.

2.2.1 Strong Interactions

A natural idea now was to search for a mechanism like the one in electromagnetism to mediate the strong force. Already in 1935 ***Hideki Yukawa (click here to read his Nobel lecture)*** proposed a field theory for the strong interaction where the mediating field particle was to be called a meson.

However, there is a significant difference between the strong force and the electromagnetic one in that the strong force has a very short range (typically the nuclear radius). This is the reason why it has no classical counterpart and hence had not been discovered in classical physics. Yukawa solved this problem by letting the meson have a mass. Such a particle was also subsequently seemingly found from cosmic rays by . The discovery of nuclear fission in the late 1930's led to an enormous interest in nuclear physics and in the war years most physicists worked on problems with fission so it was not until after the war that Yukawa's ideas were taken up again. It was then realized that the particle found by Anderson could not be the meson of strong interactions, since it interacted far too little with matter, and it was then shown that this particle, now called the muon, is a heavy cousin of the electron. However, the meson, now called pion, was finally discovered in cosmic rays by in 1947 and its properties were measured. A new dilemma now appeared. When the big accelerators started to operate in the 1950's, the pions were produced vindicating Yukawa's theory, but when his field theory was scrutinised according to the rules set up by Feynman, it was shown that indeed the theory is renormalisable but the coupling constant is huge, larger than one. This means that a diagram with several interactions will give a larger contribution than the naive one with the exchange of only one pion, which is the one though that does gives a rough picture of the scattering of two protons. The perturbation expansion does not make sense. Also the scattering of protons produced new strongly interacting particles beside the pion, which were named hadrons. Indeed a huge menagerie of elementary particles were discovered, some of them with a life time of some 10^{-8} to 10^{-10} s and some with a lifetime of 10^{-23} s. This problem was solved by Murray Gell-Mann when he proposed that all the strongly interacting particles are indeed bound states of even more fundamental states, the quarks. This idea was eventually experimentally verified in the Stanford experiments in the years around 1970 led by J. Friedman, H. Kendall and R. taylor. To understand the forces inside the nucleus one really had to understand the field theory for quarks. Before describing the forces between quarks one has to discuss the other nuclear force, the weak one.

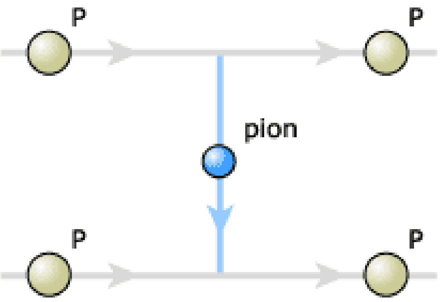

Figure 2.2 Yukawa's model of strong interactions

2.2.2 Weak interactions

With the discovery of the neutron it was found that the neutron decays into a proton and an electron and a then hypothetical particle proposed by Wolfgang Pauli, which came to be called the neutrino (really the antineutrino). Since in the nucleus the mass of the nucleons are virtual the process can also go the other way in which a proton decays into a neutron, a positron and a neutrino. The first to set up a model for this interaction was in which it was supposed that the interaction was instantaneous among the matter particles. In the late 1950's Fermi's theory was modified to account for parity violation by Marshak and Sudarshan and by Feynman and Gell-Mann. Parity violation of the weak interactions had been postulated and in 1956 and experimentally verified by Wu and collaborators the year after. (The weak interactions can distinguish between left and right.)

However, the model introduced had severe problems. It is not renormalisable so it cannot really make sense as a general theory. On the other hand the model worked extremely well for many processes. How could one reconcile these two facts? During the 1960's new field theoretic descriptions were proposed and to reconcile the facts above one introduced mediating particles that were extremely heavy. For low energy processes such a particle can only propagate a very short distance and in practice it will look as if the interaction takes place in one point giving the model above for the energies that at the time could be probed. The scheme used, the so-called 'Non-Abelian Gauge Theories' were used by S. Glashow, S. Weinberg and A. Salam in independent works to suggest a model that would generalise the model above. Such a field theory is a generalisation of

QED in which there are several mediating particles which also can have self interactions. In the beginning of the 1970's this scheme of models were proven to be renormalisable and hence good quantum theories by Gerardus 't Hooft and Martinus J.G. Veltman. Overwhelming experimental evidence for the model was gathered in the 1970's and finally in 1983 the mediating particles were discovered at CERN in an experiment led by C. Rubbia and S. van der Meer. Indeed the mediating particles are very heavy, almost 100 times the mass of the proton.

2.2.3 The Standard Model

The success of non-abelian gauge theories led physicists to suggest that such models should also be used to describe the interactions among the quarks. This led to the so-called Standard Model in which all the matter particles are treated together, i.e. the electron and its heavier partners the muon and the tau-particle and the corresponding neutrinos, which all have only weak interactions, together with the quarks which can have both strong and weak interactions. The force particles, i.e. the mediators are then the photon for electromagnetism, the W and Z particles for the weak force and the gluons for the strong force. Even though the Standard Model unifies the interactions there are differences in the details. The photon and the gluons are massless particles while the W and Z particles have a mass. The photon leads to Coulomb's law for large distances while the gluons lead to a confining force between the quarks. In fact the force increases with distance like the one for a spring, such that the quarks are permanently bound in the hadrons. Even so the properties of the gluons have been firmly established by experimenters and there is ample evidence that this model is indeed the correct model at the energies that present day accelerators can probe.

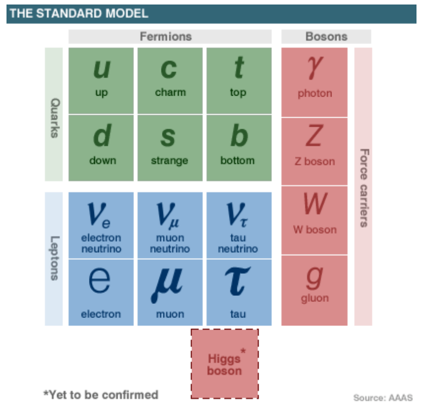

Figure 2.3 Constituents of matter due to the Standard Model

2.2.4 Unification of all Interactions

In the standard model above there is no mentioning of the gravitational force. It has been said that it is so tremendously weak that we do not need to take it into account at particle experiments. However, on general grounds there must be a quantum version of the gravity force that acts at small enough distances. If we try to just copy the quantisation of the electromagnetic field in terms of photons we should quantize the gravity field into so-called gravitons. However, the procedure of Feynman, Tomonaga and Schwinger does not work here. Einstein's gravity is non-renormalisable. Where is the problem? Is it Einstein's theory or quantum mechanics that is not complete? The two great conceptual milestones of the 20th century, Quantum Mechanics and Einstein's General Relativity are simply not consistent with each other. Einstein thought for his whole life that quantum mechanics is indeed incomplete, but so many tests of it have by now been made that physicists are instead trying to generalise Einstein's theory. The remarkable success with the Standard Model has also shown that the idea of unification of the forces is a valid one. Why are there four different forces or are they really different? They do indeed, show up as different forces in the experiments we do, but the Standard Model shows that the electromagnetic and the weak forces are unified for energies above 100 GeV. Similarly the model shows that also the strong force seemingly so different unifies with the other one at energies above 10^{15}GeV. Can the gravitational one be fit into this scheme?

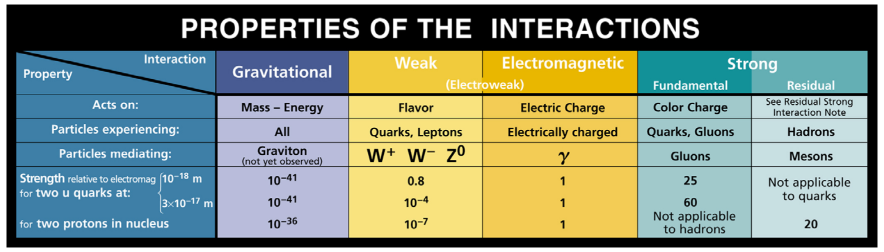

PROPERTIES OF THE INTERACTIONS

Interaction / Property	Gravitational	Weak	Electromagnetic	Strong	
		(Electroweak)		Fundamental	Residual
Acts on:	Mass – Energy	Flavor	Electric Charge	Color Charge	See Residual Strong Interaction Note
Particles experiencing:	All	Quarks, Leptons	Electrically charged	Quarks, Gluons	Hadrons
Particles mediating:	Graviton (not yet observed)	W^+ W^- Z^0	γ	Gluons	Mesons
Strength relative to electromag for two u quarks at: 10^{-18} m	10^{-41}	0.8	1	25	Not applicable to quarks
3×10^{-17} m	10^{-41}	10^{-4}	1	60	
for two protons in nucleus	10^{-36}	10^{-7}	1	Not applicable to hadrons	20

Figure 2.4 Properties of interaction in unification approach

It can be shown that at energies of the order of 10^{19} GeV the gravity force will be as strong as the other ones, so there should be a unification of all the forces at least at that energy, which is an energy so unbelievably high that it has only occurred in our universe at a time 10-42 s after the Big Bang. However, physics should also be able to describe phenomena that occurred then, so there should be a unified picture which also includes gravity. Such a scheme has now been proposed, The Superstring Model in which particles are described by one-dimensional objects, strings. This model indeed gives Einstein's theory for low energies and can be made compatible with the Standard Model at the energies where it has been probed. It is also a finite quantum theory so a perturbation theory for gravity based on the Superstring Model is indeed consistent. It is still too early to say if this is the final 'theory of everything', but there is no paradox or inconsistency in the model as far as has been understood. Finally the model makes one more unification, namely of the matter particles and the force particles, having just one sort of particles. This is also the ultimate goal of physicists, to have one unified force and one unified kind of particles.

For the general knowledge needed in the Reactor Physics one can specify several important properties of the nuclear forces:

1. The nuclear forces are attractive. This must be so or the nucleus of an atom would fly apart due to the electrostatic repulsion of the positively charged protons.
2. The nuclear forces are strong. This force must obviously be strong enough to overcome the Coulomb repulsion of the positively charged protons. The nuclear force is often referred to as simply the "strong force".
3. The nuclear forces are short-ranged. Particles must come very close to the nucleus before they are influenced by the nuclear force.
4. The nuclear forces appear to be charge independent. The force between two neutrons is identical to the force between two protons, when corrected for the electrostatic repulsion that exists between two positive charges.
5. The nuclear forces are saturable. This means that the force effects only nearly adjacent nucleons. As the nucleus increases its dimensions the force weakens. There are no stable nuclei above an atomic number of 90.

2.3 Stability of Nuclei

2.3.1 Binding energy and mass - energy equivalency

One of the most amazing concepts of the modern theory of atomic structure is that the mass of the atom is always less than for the sum of the masses which make up the nucleus. This has been proved by direct measurement of nuclear masses by use of the mass spectrograph and other methods. This can readily be shown by the following example :

The mass of the Carbon-12 atom is defined as exactly 12.000 amu. The neutral C-12 atom contains 6 protons, 6 neutrons and 6 electrons. The exact mass of a neutral C-12 atom, based on its constituents, should therefore be :

6 protons x 1.00727 amu/proton	= 6.04362 amu
6 neutrons x 1.00866 amu/neutron	= 6.05196 amu
6 electrons x 0.000548 amu/electron	= 0.003288 amu
Total	= 12.098868 amu

This is not the mass of Carbon-12 though, since the mass is actually 12.000 amu. The difference in the mass of the constituent parts of an atom and the atom itself is known as the mass defect. For this example, the mass defect of the C-12 atom is 12.098868 - 12.0000 = 0.098868 amu.

The difference in the mass of the constituents of the atom and the atom itself is converted to energy and is used to hold the atom together. This is known as the Binding Energy. The mass is converted to energy in accordance with Einstein's famous equation :

$$E = mc^2$$

Based on this equation, the energy equivalency of 1 amu of mass is approximately 931.3 MeV. The binding energy of the Carbon-12 atom is therefore :

0.098868 amu x 931.3 MeV/amu = 92.076 MeV

The more nucleons that an atom contains, the higher the total binding energy. It is therefore more common to calculate the average binding energy per nucleon. This is nothing more than the total binding energy divided by the total number of nucleons. The B.E./nucleon for ^{12}C is :

92.076 MeV / 12 nucleons = 7.67 MeV/nucleon

Similar calculations for all nuclides can be performed. The results of these calculations can be displayed on a graph as shown in Figure 2.5. This figure displays the B.E./nucleon versus the mass number of the nuclides. The higher the B.E./nucleon, the more stable the nuclide.

Using this curve, it becomes possible to explain why energy is produced from the fusion of light nuclei and the fissioning of heavy nuclides. In both cases the resultant products have more energy per nucleon than the reactants.

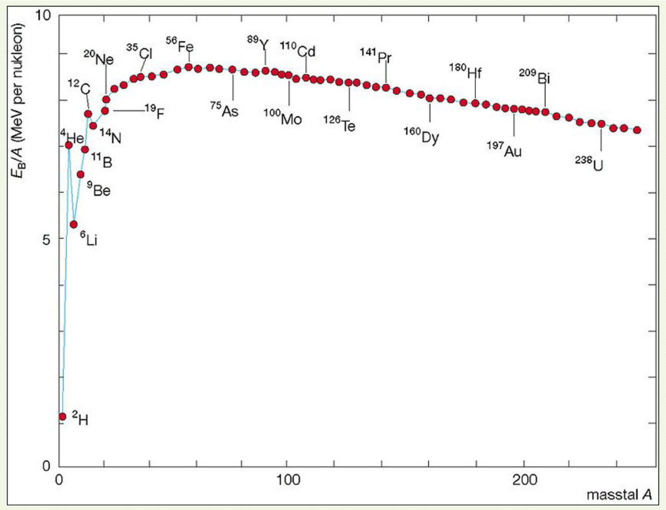

Figure 2.5 Binding energy per nucleon as a function of atomic mass

2.3.2 Neutron--Proton Ratio

The second factor is the neutron to proton ratio of the atoms nucleus. If a plot of the number

of neutrons versus the number of protons is drawn,Figure 2.6 is obtained with black color indicating stable isotopes. This figure illustrates only a few of the stable isotopes. The graph plots the number of neutrons and the number of protons contained in each stable nuclei.

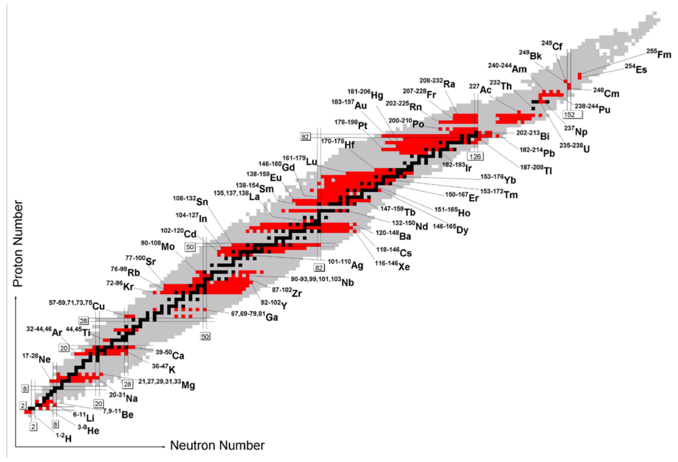

Figure 2.6 Number of protons versus number of neutron for known isotopes. The black color indicates stable isotopes.

The neutron to proton ratios for the smallest stable mass materials is 1 to 1. However, the nuclei of the larger atoms begin to have more neutrons than protons. This indicates the existence of a preferred neutron to proton ratio which is more stable. Larger atoms must increase their nuclear mass without increasing the electrostatic repulsion of the protons to remain stable. This is accomplished by the addition of neutrons. If the required neutron to proton ratio is not found in an atom's nucleus, the atom will be unstable and therefore be radioactive and emit radiation. The heaviest stable nuclide is lead-208 (^{208}Pb). ^{208}Pb has 82 protons and 146 neutrons (208-82 - double magic nucleus). The neutron to proton ratio is therefore :

146/82=1.54

2.4 Neutron--Proton Pairing

A third factor affecting the stability of a nucleus is related to the pairing of the nucleons. About 85% of the materials in the earth's crust are composed of nuclides which have even numbers of protons and even numbers of neutrons. It would appear that this even pairing leads to stability. The number of nuclides with an even number of protons and neutrons far outweighs the number of nuclides with an odd number of protons and neutrons. This is summarized in Table II.

Table II. Distribution of the Nuclear Constituents in Stable Nuclides

A Number	Z Number	N Number	Number of Stable Nuclides
Even	Even	Even	161
Odd	Even	Odd	55
Odd	Odd	Even	60
Even	Odd	Odd	4
Total			270

Also, elements with an even number of protons tend to have more stable isotopes than elements with an odd number of protons. Several examples are given below in Table III. Obviously, certain configurations tend to be more stable than other configurations. If the nuclide has the even--even combination of neutrons and protons and also meets the neutron to proton ratio requirements, then that nuclide is likely stable.

Table III. N-P (Neutron-Proton) Pairing

Element	Stable Isotopes
Cobalt (27 protons)	^{59}Co
Nickel (28 protons)	^{58}Ni, ^{60}Ni, ^{61}Ni, ^{62}Ni, ^{64}Ni
Xenon (54 protons)	^{124}Xe, ^{126}Xe, ^{128}Xe, ^{129}Xe, ^{130}Xe, ^{131}Xe, ^{132}Xe, ^{134}Xe, ^{136}Xe
Cesium (55 protons)	^{133}Cs

2.4.1 "Magic" Numbers

Finally, the last observable effect leading to nuclear stability are the so called "magic numbers". These numbers are 2, 8, 20, 28, 50, 82 & 126. Nuclides, which have either the number of protons or the number of neutrons equal to one of these magic numbers, are more likely to be stable. This can be seen in the Chart of the Nuclides.

When either the number of protons or the number of neutrons has one of the values 2, 8, 20, 28, 50, 82 or 126, the binding energy is higher than when other numbers of protons or neutrons are present. This relationship gives rise to the theory that energy shells exist in the nucleus in a manner similar to electron shells. The magic numbers may represent filled nuclear shells and the atoms with filled shells tend to be more stable.

The answer to why are things radioactive has not been answered directly. The answer lies in a complex relationship between the nucleus' size, the ratio of neutrons to protons for the given nuclear size, any pairing which exists in the nucleus and whether or not a magic number is exhibited.

2.5 Radiation

All of the known nuclides can be classified as either stable or radioactive. If a given nuclide is not stable it will be radioactive with its own unique half-life and decay products. A radionuclide is any unstable nuclide which emits radiation in the process of seeking stability. We define radiation as:

The emission and propagation of energy through space or through a material medium in the form of particulate emissions or electromagnetic waves.

Radioactive decay on the atomic level is a stochastic process, meaning Radioactive decay on the atomic level is a stochastic process, meaning that if you could examine a single radioactive atom, no certainty as to when that atom would spontaneous decay could be determined. Therefore, radioactive decay is governed by the laws of Poisson statistics.

Radiation consists of two general types of phenomena:

1. Particulate emissions (α, β^-, β^+, proton, neutron, etc.)
    - Charged particles
    - Uncharged particles

2. Electromagnetic emissions (X-ray, gamma rays, i.e. photons).

Radiation does not require a transporting medium to traverse space or material. Radiation energy has the ability to do work on biological and physical systems. Unfortunately, this work is usually destructive.

2.5.1 Energy Measurement of Radiation

One of the principle characteristics of radiation is its energy. A radiation's energy is a measure of its kinetic energy or energy due to motion. The non--relativistic kinetic energy of a particle is proportional to the mass of the particle and the square of its velocity. Since a proton has a rest mass of approximately 2000 times that of an electron, for the same kinetic energy, the electron will be moving much faster. In general, the higher the energy of a particular radiation the more penetrating it is and the more potential risk will be associated with it.. Particulate forms of radiation also have a mass - energy equivalency.

The SI unit of work and energy is the joule (J). A joule is equal to one newton expended along a distance of one meter. (1 J = 1 N x 1 m). A newton is that force required to accelerate a 1 kilogram mass 1 m/s^2. This unit of energy is typically too large to be useful when discussing the normal range of a radiation's energy.

A more useful unit is the electron-volt (eV). The electron volt is the energy acquired by an electron during its acceleration across a one volt potential. This is diagrammed in Figure 2.7. There are 1.602x10^{-19} joules per electron volt or 6.24x10^{18} eV in 1 joule. Radiation energy is typically measured in the multiples of the electron volt, kiloelectron volts (1 keV= 1.000 eV) and the million electron volts (1 MeV = 1,000,000eV).

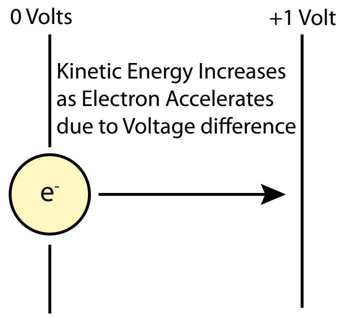

Figure 2.7 Illustration of 1 eV energy unit

2.5.2 Ionization

Radiation can be further classified as either ionizing or non--ionizing radiations. Ionization is any process which results in the formation ions. Ions are formed when the normal electrical neutrality of atoms are disrupted by either the addition or removal of electrons. An ion is a group of atoms, a single atom or a subatomic particle which carries a net electrical charge, either positive or negative.

Ions are produced when:

Electrons are captured by a neutral atom----only possible at low energies
Radiation interacts with orbital electrons causing the removal of one or more of the electrons
Nuclear collision and interactions at high energies

What determines whether radiation is ionizing or non-ionizing in a given material is the energy of the radiation and the properties of the absorber. Gross generalities as to what is ionizing and what in non-ionizing is all that is normally encountered since a given radiation may be ionizing in some material and non-ionizing in another material.

Ionizing radiations are emitted naturally by radioactive nuclei, can be produced through the acceleration of charged particles, and in nuclear reactions. Ionizing radiation can be directly or indirectly ionizing. If the radiation of interest is energetic enough to cause the ionization of the material it passes through, then that radiation is ionizing radiation. For a given absorber, ionizing radiation is always more energetic than non-ionizing radiation.

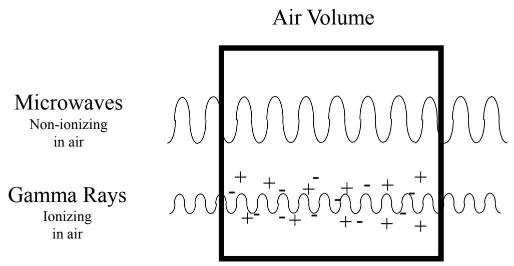

Figure 2.8 Ionizing versus non-ionizing radiation

This concept is most easily applied to gases as it can be seen at Figure 2.8. The amount of energy required to cause ionization in a material is known as the ionization energy. The approximate value for air is 33 electron volts per ion pair. The individual photons of the microwave radiation are not energetic enough to cause ionization in the air but the gamma photons are. Therefore, in air, gamma radiation is ionizing and microwave radiation is not. Since the energy of the gamma photons are much greater than 33 eV, many ion pairs can be formed in the air.

The number of ion pairs formed by the radiation's interactions with the absorber per unit length of travel is the "specific ionization". The average specific ionization is the number of ion pairs formed divided by the distance in which those ion pairs are found. Radiation can be highly ionizing (have a high specific ionization value) or weakly ionizing. It is still considered ionizing radiation if any ionization occurs. Table IV lists the specific ionization in air for various types and energies of radiation.

Table IV. Specific Ionization In Air

Radiation	Energy (MeV)	Ion Pairs/cm
Alpha	3	55000
	6	40000
Beta	0.5	110
	1	92
	3	77
Gamma	0.5	0.6
	1	1.1
	3	2.5

The transfer of energy to air by ionizing radiation is the basis for the definition of exposure. On the average, the amount of energy necessary to produce one ion pair in air is 33 eV. The production of each ion pair results in the liberation of two basic units of charge, one positive and one negative. The basic unit of charge is equal to 1.66 x 10^{-19} coulombs. If we recall that a roentgen is defined as the production of charges equal to 2.58 x 10^{-4} C/kg in air, we can make the following conversions:

$$1R=\frac{2.58\times10^{4}C}{kg_{air}}\times\frac{unit\,charge}{1.66\times10^{-19}C}\times\frac{ion\;pair}{2\,unit\;charges}=7.77\times10^{14}\frac{ion\;pairs}{kg_{air}}$$

$$1R=\frac{7.77\times10^{14}\,i.p.}{kg_{air}}\times\frac{33\,eV}{i.p.}=\frac{2.56\times10^{16}\,eV}{kg_{air}}=\frac{2.56\times10^{10}\,MeV}{kg_{air}}$$

Most radiations encountered in a nuclear power plant environment and in nuclear medicine are ionizing radiations. Ionizing radiation can cause damage to any absorber (including you) by causing the formation of ions in that absorber. The exact mechanism by which radiation causes ionization is discussed in greater detail in a later lectures.

2.6 Radioactive Decay Modes

The radioactive decay of a parent radionuclide is defined by the type of radiation(s) given off and the energy of the radiation(s). Radiation includes particulate emissions as well as electromagnetic emissions. The radiation given off can be further defined as to whether it is nuclear or atomic in origin. Nuclear radiations emanate from the nucleus of a radioactive atom and result in a change of identity and/or energy level of the atom.

The principle modes of radioactive decay from nuclear transitions include:

1. Alpha - α - emission
2. Beta - β^- minus emission
3. Positron or beta positive - β^+ - emission
4. Electron Capture
5. Spontaneous Fission
6. Isomeric Transition or gamma - γ - emission

All of the nuclear transitions may be accompanied with either gamma radiation or internal conversion electrons.

Atomic radiations may be associated with these nuclear emissions. Atomic radiations are emitted from the electron shells of the radioactive atoms and result in the change of energy of these orbital electrons. These associated radiations include:

1. Auger electrons
2. X-ray photons

2.6.1 Alpha - α - decay mode

Alpha particles are stable entities identical to a helium nucleus. They consist of two protons and two neutrons. Their rest mass is 4.0026 amu and their charge is +2 units. Because of their mass and charge, alpha particles are an intensely ionizing form of radiation. Alpha particles are emitted with discrete values of energy normally between 4 and 8 MeV. Alpha energies are characteristic of the nuclide which emits them.

Approximately 175 radionuclides have been identified which decay by alpha emission. Some common alpha emitters include ^{222}Rn, ^{226}Ra, ^{238}U, ^{239}Pu, and ^{241}Am. Generally, atoms with large mass (Z>>82) are capable of ejecting an alpha particle. In alpha decay, an atom with atomic number Z and mass number A produces a daughter product with an atomic number Z-2 and a mass number of A-4. In general form, this can be expressed as :

$$^{A}_{Z}\mathrm{X}\rightarrow\,^{A-4}_{Z-2}\mathrm{Y}+\,^{4}_{2}\mathrm{He}(\alpha)+\mathrm{Q}+2\,\mathrm{e}^{-}$$

where :
X = the chemical symbol for the parent radionuclide
Y = the chemical symbol for the daughter nuclide.

All alpha emissions follow this general form. A specific example is :

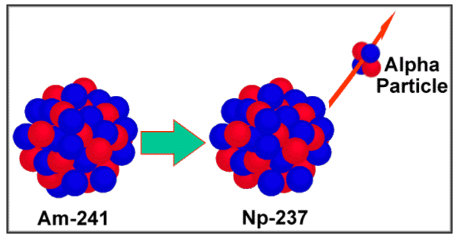

Figure 2.9 An example of α decay of Americium-241

$$^{222}_{88}\mathrm{Ra} \rightarrow {}^{218}_{86}\mathrm{Rn} + {}^{4}_{2}\mathrm{He}$$

The alpha particle may carry all of the decay energy between the parent and the daughter or the daughter may be left in an excited state. If an excited state remains it subsequently will de- excitate, normally by gamma emission. Because alpha radiation comes from massive nuclei, the source of alphas in a nuclear power plant are either from the uranium fuel or from the natural thorium or uranium decay series

2.6.2 Beta Minus Decay

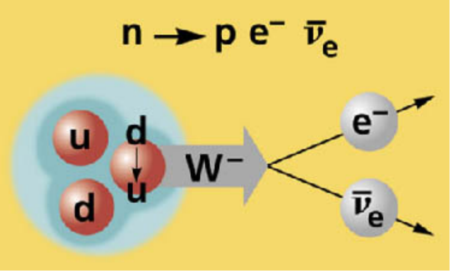

Figure 2.10 Beta decay of neutrons

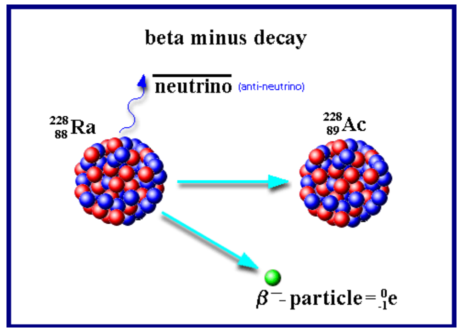

Figure 2.11 An example of β decay of Radon-228

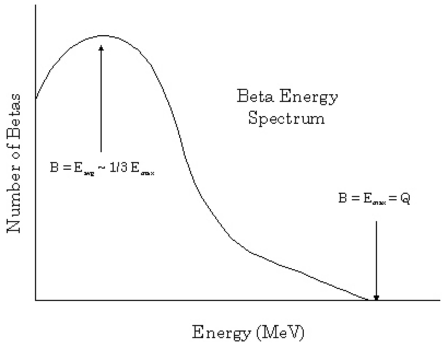

Figure 2.12 Hypothetical beta spectrum

Most beta minus emitters are located below and to the right of the stability line on the Chart of the Nuclides.

Some - emitters exist above Z=82. These materials can all be classified as neutron rich materials. In other words, they have more neutrons in their nucleus than is required to maintain stability.

β minus emission is characterized by the conversion of an excess neutron into a proton by the ejection of a beta minus particle and an anti-neutrino. This reduces the neutron excess in these materials and consequently stability for this new combination of nucleons is greater. Once the beta particle is emitted, it has all the characteristics of an electron. It has a rest mass of approximately 1/1800 amu and a charge of -1 unit.. Some common beta emitters include ^{3}H, ^{14}C, ^{32}P, and ^{35}S.

The general form, a beta minus emission is described by:

$$^{A}_{Z}X \rightarrow {}^{A}_{Z+1}Y + {}_{-1}\beta + \overline{\nu} + Q$$

A specific example of this general form is :

$$^{1}_{0}n \rightarrow {}^{1}_{1}p + {}_{-1}\beta + \overline{\nu} + Q$$

$$^{16}_{7}N \rightarrow {}^{16}_{8}O + {}_{-1}\beta + \overline{\nu} + Q$$

As with all radioactive decay processes, the energy difference between the parent and the daughter nuclide is a constant. However, during the beta emission process that total energy is shared between the beta particle and the anti-neutrino in a random fashion. The daughter product also receives some of the decay energy. The total energy, Q, is shared with these decay products in accordance with the following :

$$Q = KE_{\beta} + KE_{\overline{\nu}}$$

The results of this sharing of the decay energy between the beta and the anti-neutrino produces an energy distribution curve as shown in Figure 2.12 and Figure 2.13. This figure shows the energy of the beta particle vs the number of times that energy is given off. The maximum energy the beta can have is equal to Q, the total energy difference between the parent and daughter nuclides. This is known as the E_{max} endpoint energy.

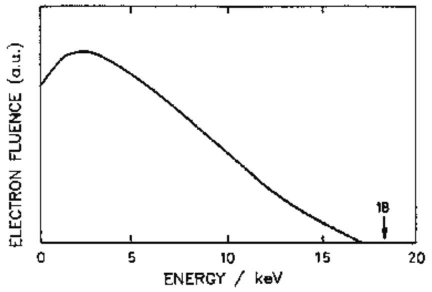

Figure 2.13 Beta spectrum of Tritium decay

2.6.3 Beta Positive Decay (Positron Emission)

A beta positive or positron emission is essentially the opposite of the beta minus emission. It occurs in material above and to the left of the stability line in the Chart of the Nuclides which are all proton rich materials. Since the fission of ^{235}U results in fission products which are neutron rich, positron emitters are not encountered in the nuclear energy environment.

A beta positive emission is characterized by the conversion of a proton to a neutron with the accompanying ejection of a positron and a neutrino. The result is the proton excess in these materials is reduced and the daughter product approaches the stability line. A positron emission can not occur unless the energy difference between the parent and the daughter product is at least 1.022 MeV.

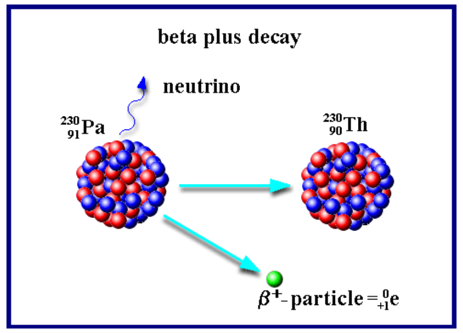

Figure 2.14 An example of β⁺ decay of Protactinium-230

The proton to neutron conversion is described by :

$$^{1}_{1}p \rightarrow {}^{1}_{0}n + {}_{+1}\beta + \nu + Q$$

Using the atomic number and mass of the parent and daughter product this becomes :

$$^{A}_{Z}X \rightarrow {}^{A}_{Z-1}Y + {}_{+1}\beta + \nu + Q$$

Specific examples of this decay type are :

$$^{18}_{9}F \rightarrow {}^{18}_{8}O + {}_{+1}\beta + \nu + Q$$

$$^{11}_{6}C \rightarrow {}^{11}_{5}B + {}_{+1}\beta + \nu + Q$$

The positron has the same mass a beta minus particle. The charge is +1 unit. Its decay energy is shared with the neutrino similar to that already discussed for the beta minus emission. The distribution of energy for the beta positive particle is similar to β_{-} as presented at Figure 2.12.

2.6.4 Electron Capture

Electron capture is a competing mode of decay for proton rich materials. This decay mode is characterized by an orbital electron being captured by the nucleus where a proton is converted into a neutron and a neutrino is emitted. The electron which is captured is most likely from the inner

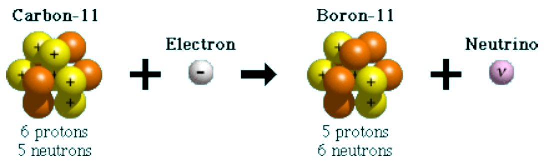

Figure 2.15 Model of electron capture in Carbon-11

shell (K shell) of the atom but may also be from the L shell or the M shell. The electron capture decay is abbreviated EC.

If the energy difference between the parent and the daughter is greater than 1.022 MeV, then electron capture and positron emission are both possible. If the energy difference between the parent and the daughter is less than 1.022 MeV, then electron capture is the only mode for decay. In this mode of decay the neutrino carries away all of the decay energy.

The general form for the electron capture decay mode is:

$$ {}_{1}^{1}p + {}_{-1}e \rightarrow {}_{0}^{1}n + {}_{+1}\beta + \nu + Q $$

Using the atomic number and the atomic mass of the parent and daughter nuclides, this general equation becomes :

$$ {}_{Z}^{A}X + {}_{-1}e \rightarrow {}_{Z-1}^{A}Y + \nu + Q $$

After an inner orbital electron is captured, the other electrons in the atom will reorient themselves to fill the vacancy and emit X-rays or Auger electrons in the process.

A specific example of an electron capture decay is the decay of ^{57}Co. The equation describing this decay is:

$$ {}_{27}^{57}Co + {}_{-1}e \rightarrow {}_{26}^{57}Fe + \nu + Q $$

2.6.5 Spontaneous Fission

Extremely heavy nuclei may spontaneously split into two large fragments. On the average one fragment is approximately 1/3 the mass of the parent and the other fragment is approximately 2/3 the mass of the parent. This process is known as spontaneous fission (SF). This is thought to be a spontaneous event and no external neutron is required for it to occur.

The spontaneous fission rate for over 35 radionuclides have been determined. The fission rate for these nuclides varies from about 6 x 10^{-8} fissions/gram-second for thorium-232 to about 1 x 10^{17} fissions/gram-second for fermium 256.

Due to the large fission rate from the normal operation of the reactor, additional fission products from spontaneous fission can not be identified separately.

2.6.6 Isomeric Transition or gamma - γ - emission

Ground States and Excited States

For any specific combination of nucleons (a nuclide), there exists a minimum energy value for the combination. This is also true for the orbital electrons. Normally, an atom or nucleus will exist at this minimum energy level. A nucleus or atom existing at an energy level which is the minimum for that combination is said to be in the "ground state".

The results of radioactive decay and other nuclear reactions often create nuclei which have more energy than the ground state for the particular nuclei. A nucleus or atom existing in an energy state above the minimum is said to be in an "excited state".

A. Internal Conversion

The radioactive decay modes mentioned above, all result in the change of identity for the nucleus. The number and/or type of nucleons in the nucleus changes following these radioactive emissions. However, the radioactive emission often leaves the daughter product in an excited state. An atom will not exist in an excited state indefinitely and will de-excitate by emitting additional energy. This energy is normally in the form of ***gamma photons*** but also includes ***internal conversion electrons***.

In the internal conversion process, the excitation energy of the nucleus is transferred into kinetic energy of one of the ***innermost electrons.*** This electron is then ejected from the atom with an energy equal to the transition energy of the excited state minus the ionization energy of the electron affected. These values are characteristic of the material emitting them.

B. Isomeric Transition

The process of de-excitation by gamma emission is normally immediately following the emission of the appropriate radioactive particle, α, β– or β+. However, some nuclei exist in an excited state long enough to be independently identified as a unique energy level. The state of the atoms which can be independently identified in this way is called a "metastable state". The Chart of the Nuclides uses a one second cutoff to define a metastable state. The nuclide must exist in the excited state for at least 1 second before it is considered metastable.

The metastable state of a ground state nuclide is called an isomer of that nuclide. The de-excitation of an isomer by gamma emission is called an "isomeric transition". Isomeric transition is often abbreviated IT in nuclear data references.

A specific example of a radioactive decay process involving isomeric transition is:

$$ {}_{42}^{99}Mo \rightarrow {}_{43}^{99}Tc^{m} + {}_{-1}\beta + \overline{\nu} $$
$$ {}_{43}^{99}Tc^{m} \rightarrow {}_{43}^{99}Tc + \gamma $$

Because of this de-excitation process, most materials which emit either alpha or beta particles also emit gamma radiation. Gamma energies are discrete quantities.

Photon Emission and the Electromagnetic Spectrum

Gamma photons are part of the electromagnetic spectrum as are X-rays, visible light, radiowaves and microwaves. The difference between these is the energy and the frequency of the radiation. Two different representations of the entire electromagnetic spectrum is shown in Figure 2.17.

Electromagnetic waves are perio- dic changes in electric and magnetic fields which travel out- ward through space at the speed of light, c, in a vacuum. An electromagnetic wave consists of both an electric field component and a magnetic field component at right

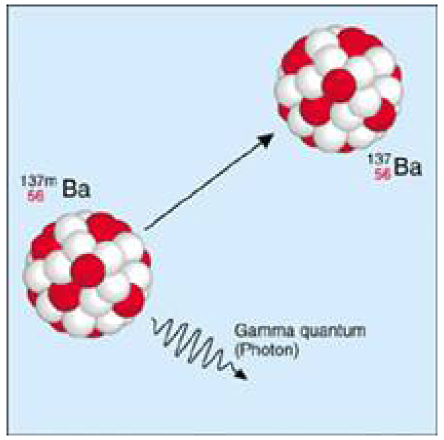

Figure 2.16 A model of gamma de-excitation of Ba-137

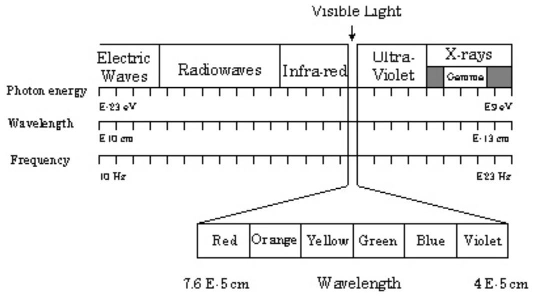

Figure 2.17 Spectrum of electromagnetic radiation

angles to each other. This is illustrated in Figure 8. The concept of a photon as a particle of light was first proposed by Max Planck in 1901. All electromagnetic phenomena are now considered to consist of these particles called photons. Photons are considered to be independent, quantized units of all electromagnetic phenomena.

A photon has no charge and a rest mass of zero. The difference between a gamma photon and a visible light photon, or any other photon in the electromagnetic spectrum, is the energy of that photon. The energy of a photon is directly proportional to the frequency of that photon. The constant of proportionality is known as Planck's constant. Mathematically : $E = h\nu$

where :

E = the energy of the photon

h = Planck's constant = 4.1357 x 10^{-15} eV-sec

ν = the frequency of the electromagnetic vibration.

Since h is a constant, the higher the frequency of vibration, the higher the energy. The energy and other physical relationships for photons are summarized in Table V :

Table V. Properties of Electromagnetic Waves

Property	Relationship
Energy	$E = h\nu$
Wavelength	$\lambda = \frac{c}{\nu}$
Mass Equivalence	$m = \frac{h\nu}{c^2}$
Momentum	$p = \frac{h\nu}{c}$

Optical radiation is a narrow portion the electromagnetic spectrum. However, within their narrow portion of the spectrum, optical radiation sources usually emit a broad range of wavelengths. This is apparent in Figure 2.17.

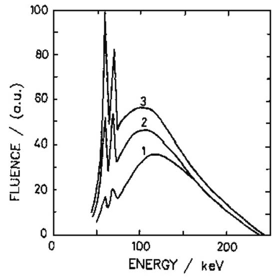

Figure 2.18 Sample X-ray spectrum

X-rays are created when accelerated electrons collide with high Z materials such as tungsten. Most of these X-rays are created by the bremsstrahlung process and consequently have a continuous spectrum with energies up to the maximum energy of the electrons. In addition, there are characteristic X-rays which are indicative of the atoms electron structure. When electrons in the atomic orbitals of a target material are excited or ejected, by high velocity/high energy electrons impacting it, for example, the subsequent vacancies are filled from outer higher energy electrons. The excess energy of these higher energy electrons is emitted as X-rays. These X-rays are characteristic of the material's atomic structure and have lower energy than gamma photons. Characteristic X-ray lines are superimposed over the bremsstrahlung spectrum as shown in Figure 2.18. This figure also illustrates the effects of filtering or shielding the X-ray source. Filtering reduces the lower energy X-rays more than it reduces higher energies emissions.

X-rays were the first and most extensively studied of the radiations and continue to have the greatest application to the population as a whole.

Gamma radiation accompanies other radioactive modes or is emitted during isomeric transition. These gamma rays are monoenergetic and characteristic of the nuclide which emits them. Some important gamma emitters include ^{60}Co, ^{137}Cs, ^{125}I, ^{131}I, ^{99m}Tc, and ^{198}Au.

Atomic Radiations

Any event, such as electron capture, which knocks an electron out of an orbital or raises a low energy electron to a higher energy level, will result in the de-excitation of the atom's electron shells. This de-excitation causes the emission of radiations known as atomic radiations. This includes X-ray and **Auger electrons**.

An X-ray photon is an electromagnetic phenomena of atomic origin. They generally possess lesser energy than a gamma photon.

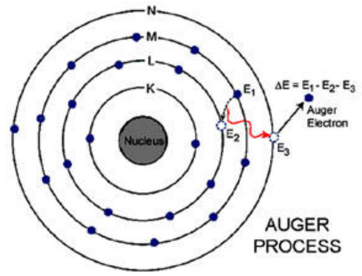

Figure 2.19 A model of Auger-electron emission

A competing process with X-ray emission is the emission of Auger electrons. Atoms have been observed to occasionally de-excitate by emitting an additional electron. These electrons are termed Auger electrons. A complete decay scheme will list any Auger electrons associated with a particular radioactive decay. They are similar to the internal conversion electrons which compete with gamma emission for de-excitation of a nucleus.

Chapter 3

Radiation Interaction with Matter

3.1 Introduction

The purpose of this lecture is to describe the mechanisms by which ionizing radiation transfers energy to matter. The process of the energy transfer and the resulting effects on the absorber are both important. This information is essential in the understanding of radiation detection theory, radiation shielding, biological effects, etc.

Ionizing radiation has been previously defined, but can now be explained in more detail. Any radiation that is capable are producing a separation of electrons from an atom or molecule is considered to be ionizing radiation. The separation of an electron from its atom can occur if the transfer of energy from the radiation is sufficient to overcome the electron-binding energy in the atom or molecule.

The lower limit for when a particular type and energy of radiation can cause ionization depends on the medium. In general, the lower limit establishes that approximately 10 eV of energy needs to be transferred in a single event to cause ionization. However, this is only a lower limit and it may require hundreds of eV in some materials.

Radiation interactions can be divided into two broad categories:

3.1.1 Directly interactions

These interactions occur for all charged particles due the Coulomb force. The magnitude of this force is related to the charges on both particle and the distance between them. This force is proportional to the charges between the particles and inversely proportional to the square of the distance. Consequently, a charged particle traveling through a given medium does not have to "collide" to transfer sufficient energy to cause ionization. The Coulomb force acts over limited distances.

Any event which results in the transfer of energy due to the Coulomb forces is loosely termed as charged particle interactions. Charged particle interactions occur with direct collision with orbital electrons and with atomic nuclei. The directly ionizing types of radiation which interact by this method include: alpha particles, beta particles, electrons and protons.

3.1.2 Indirectly interactions

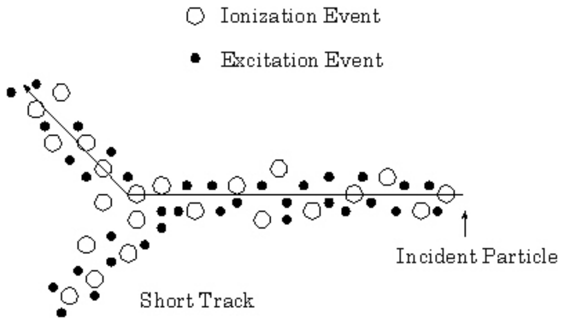

Figure 3.1 Ionization and excitation tracks in matter

Indirectly interactions occur with uncharged radiations, either particulate or electromagnetic. This includes neutrons and gamma and x-ray photons. These radiations undergo interactions which result in the release of charged particles. The released charged particles can cause additional direct ionization.

These interactions are not subject to charged particle forces and instead must "collide" with an another particle to transfer energy.

Ionizing radiations can also cause excitation. Excitation occurs when sufficient energy is transferred to an atom to change an electron's orbital configuration or state of motion. However, the electrons due not gain sufficient energy to be released and no charge separation occurs in excitation. The ultimate de-excitation of the altered atom will emit the excess energy which may be ionizing or non-ionizing. Ionization and excitation normally occur simultaneously when original radiation is considered to be ionizing. The resultant track of the radiation's passage through matter may appear as in Figure 3.1.

3.2 Total Absorption Versus Scattering Reactions

A collision between a given type of radiation and a target may be a direct physical impact. Indeed, for the uncharged radiations this is required before energy transfer takes place. For the charged particle interactions, direct physical impact is not essential since the Coulomb forces act over limited distances. A "collision" is considered to be any event where there is an exchange of momentum, kinetic energy and possibly charge between the colliding particles or photons.

A given collision may result in the total absorption of the incident radiation by the absorbing medium. When this occurs, the incident radiation is completely absorbed and its energy is transferred to the absorber. The incident radiation ceases to exist following total absorption. The incident radiation may also transfer only a portion of its energy into the absorber, with remaining energy scattered from the "collision" site. Radioactive scattering reactions may be classified as either elastic or inelastic scattering.

An elastic scattering collision is one in which energy is scattered from the collision site but the total kinetic energy between the colliding materials remains the same. The kinetic energy of the particles or photons may be transferred, but the total for the system remains the same.

An inelastic scattering collision is one in which the total kinetic energy of the initially colliding materials is not conserved. This is usually due to the emission of additional electromagnetic energy following the collision or due to the atomic excitation of one of the colliding particles. This does not mean that inelastic collision violate the physical laws of conservation of energy. It only means that the kinetic energy of the particles reappears in a different form.

3.3 Alpha Interactions with Matter

An alpha particle is a heavy combination of two protons and two neutrons. The net charge on the particle is +2. As a result of this size and charge, alpha particles are highly ionizing. However, because of alpha particles mass and the rapid transfer of energy during its interactions, alpha particles have a very low penetrating ability and their range in material is quite small.

The rate at which energy is lost is proportional to the square of the charge, i.e. the more highly charged the more interactive electric field is produced and the higher the probability of an ionization and interaction along the path of energy dissipation.

Alpha particles interact by charged-particle interactions. These interactions may result in total absorption of the alpha particle, elastic or inelastic scattering reactions.

The interactions of an alpha particle with matter is a random process, dependent on the density of the absorber and the trajectory of the alpha particle. In gases, the trajectory is nearly a straight line, due to the high mass of the alpha. Monoenergetic alpha particles will travel very nearly the same total distance in a medium before losing all their energy. The average distance of travel in a given material is considered to be the "range" of that particle in the particular medium. The higher the energy of the particle the higher the range.

The range of an alpha particle in air is approximated by one of the following expressions. Since most alpha particles are emitted with an energy between 4 and 8 MeV the second equation is usually applicable.

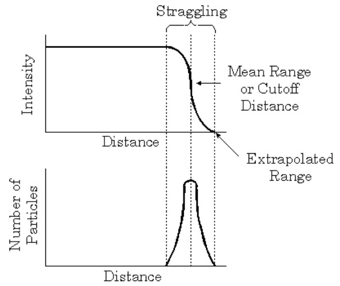

Figure 3.2 Range concept for charged particles.

$$R_\alpha = 0.56\,E \ \ (E < 4\,MeV)$$

$$R_\alpha = 1.24\,E - 2.62\,(4\,MeV < E < 8\,MeV)$$

where:

R_α = the range of the alpha particle in cm

E = the alpha particle energy in MeV

An illustration of the range concept is given in Figure 3.2. Note that the number of particles reaching the given range is statistically distributed around the mean range shown in this figure.

A graph of the range of alpha particles in air for various energy alpha radiation is presented in Figure 3.3.

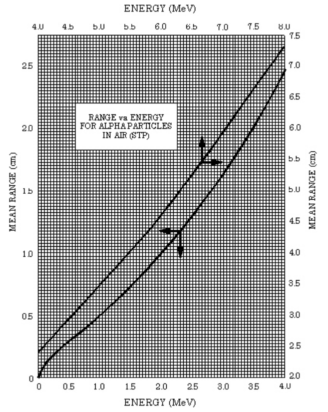

Figure 3.3 Alpha particle range in air

As radiation penetrates matter, it transfers its kinetic energy to the surroundings. The average amount of energy required to cause the production of one ion pair in a given absorber is nearly constant and is known as the W-value. In air, this value is approximately 33 eV. Since the energy of a particular alpha is monoenergetic, the number of ion pairs which will be produced by the total transfer of the alpha's kinetic energy is therefore :

$$\#i.p. = \frac{E_\alpha}{33eV}$$

For a 3.3 MeV alpha particle, this results in the production of 100,000 ion pairs over a range of about 1.8 cm in air (from Figure 3.3. The specific ionization is the number of ion pairs averaged over the distance traveled. In this case, the specific ionization is:

$$\frac{100000\,i.p.}{1.8\,cm}=5.5\times10^{4}\,i.p./cm$$

This is an average value, since the alpha is losing energy continuously the actual specific ionization changes continuously. As the alpha loses kinetic energy, its velocity is reduced and the length of time that the electric force field is exerted in any specific plane increases. The peak ionization occurs just before the alpha loses all of its energy. When the kinetic energy of the alpha equals zero, it will attract two electrons and become an inert, helium gas atom. A graph of the specific ionization versus the energy that the alpha particle has remaining is shown in Figure 3.4. This graph is known as the Bragg Curve. It shows the maximum ionization does occur when the alpha energy is nearly zero. Similar affects are exhibited for all charged particles.

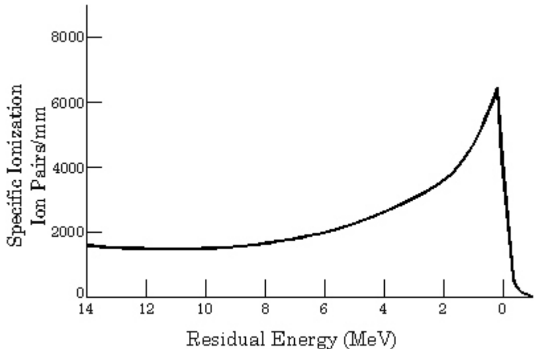

Figure 3.4 Bragg curve for alpha particles.

The predominant interaction mechanism for alpha particles with matter are inelastic in nature and result in the ionization and excitation of an absorber.

Alphas may also be totally absorbed, as in the following reaction :

$${}^{9}_{4}Be+{}^{4}_{2}He\rightarrow{}^{12}_{6}C+{}^{1}_{0}n$$

When attempting to measure alpha emitters, consideration must be given to their low penetrating ability. These considerations include: small separation distances between the source and the detector, drawing a vacuum between the source and the detector to minimize absorption in air, and thin entrance windows on the detectors to minimize absorption.

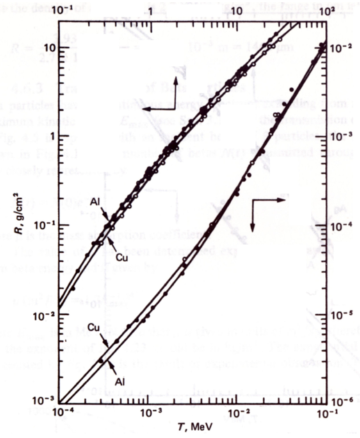

Figure 3.5 Beta particle range in matter

3.4 Beta Interactions with Matter

Beta particles also interact by the charged-particle interactions. There are however, several distinct differences between the alpha particle interactions and the beta particle interactions. These differences result from the fact that the beta particle's charge is +/- 1 (half that of the alpha particle) and its mass is 1/1836 amu (over 7000 times less than the alpha particle).

A 4 MeV beta particle will have a much greater initial velocity through a given absorber than an 4 MeV alpha particle will. Neglecting relativistic effects, the kinetic energy of a particle is given by KE = 1/2 mv2. For particles of the same energy , the smaller particle has greater velocity. Since the mass of the beta particle is so low, compared to that of the alpha particle, the velocity is much greater.

Because of the higher velocity, the beta particle is less likely to interact by the Coulomb forces due to the brief time the beta is near an electron. The beta interacts less frequently as it penetrates matter and as a result, the range of the beta particle is higher than that for an equal energy alpha particle. The range of beta particles in various forms of matter is shown in Figure 3.5

If we continue to use air as the absorbing medium and 3.3 MeV for the initial energy of the beta particle, comparisons with the alpha interactions can be established. From Figure 3.5, the maximum range of the beta particle in air is about 1300 cm. Compare this to the equivalent 1.8 cm range for the alpha particle.

The ionization constant for air is still about 33 eV.

The maximum number of ion pairs possible is still 100,000. The specific ionization for the 3.3 MeV beta particle in air is therefore :

$$\frac{100000\,i.p.}{1300\,cm}=76.3\,i.p./cm$$

The specific ionization for beta particles is much less than for the alpha particle, however, the range is much greater. Throughout the given range, ionization and excitation of the absorber's atoms occur. The Bragg principle still applies. There are some other distinct differences between beta and alpha radiations which must be addressed. The first of these is the trajectory of the beta particle.

Simple phenomenological equation estimates a range of β radiation using an approximation for mass density thickness dependence on b energy. Mass density thickness, R_{el}, is the range of the radiation in an absorber (in cm) times the density of the absorber (in g/cm^3). For electrons mass density thinkness as a function of energy is described in a very simple equation:

$R_{el}(g/cm^2)=0.546xE\ (MeV) - 0.108$

And consequently the range of electrons is

$R_{el}(cm)=R_{el}(g/cm^2)/\rho$

Since the beta particle has much lower mass than the alpha particle does, it is more likely to be deflected from a straight line path as it penetrates matter. Some of the beta particles entering a dense absorber will be deflected back against the original path of entry. This is possibly from a single deflection or from multiple scattering events. The deflection of a beta particle back against the original direction , whether due to a single or multiple scattering events, is known as backscattering. This situation is illustrated in Figure 3.6.

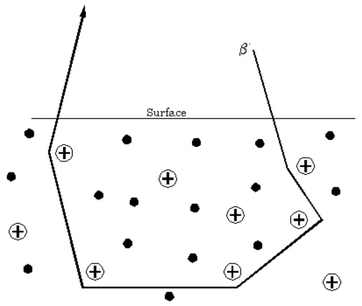

Figure 3.6 Possible deflection of beta particle from initial trajectory.

The degree of backscattering is dependent on many factors. Some of these factors are :

1. The atomic number of the absorbing material.
2. The thickness of the absorbing material.
3. The beta particle energy.
4. Distances between the source and the absorber.

Two other specific beta interactions with matter have been identified. These are the Cerenkov and the Bremsstrahlung interactions.

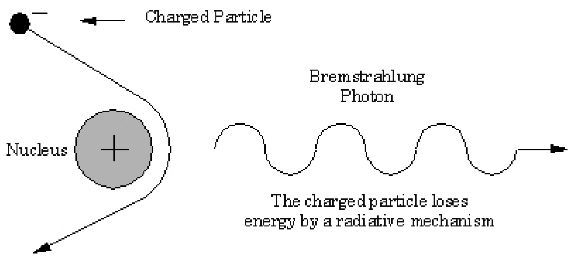

Figure 3.7 Illustration of bremsstrahlung production

A. Bremsstrahlung

When a beta particle passes near the nucleus of a high Z material, (i.e. tungsten, Z=74) it can be substantially slowed and deflected through large angles. The change in the kinetic energy of the beta particle due to the deceleration is emitted as photon energy. A continuous spectrum of photons is emitted up to the maximum energy of the beta. The word “Bremsstrahlung” is German for “braking radiation” and was derived from the slowing down of the incident beta particle. The Bremsstrahlung process is illustrated in Figure 3.7.

This interaction is an inelastic collision process, since the total kinetic energy of the particles in the system changes. This change is the emission of electromagnetic photons. Bremsstrahlung radiation is more prevalent with high energy betas transversing high Z absorbers. Consequently, pure beta emitters should not be shielded by lead, or other high Z absorbers, as highly penetrating electromagnetic radiation will be produced - see Figure 3.8.

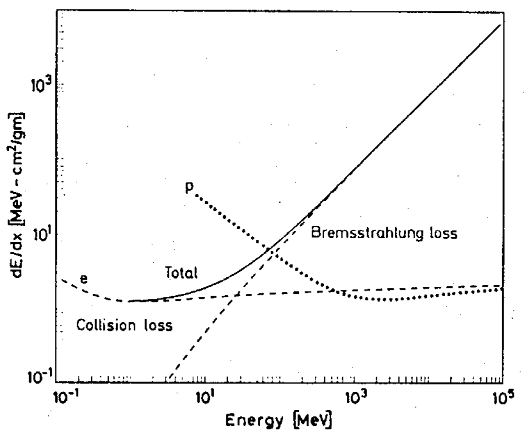

Figure 3.8 Bremsstrahlung energy losses for electrons-e and protons-p

B. Cerenkov radiation emission

Beta particles are also responsible for the production of the blue light emission near highly radioactive fuel rods and swimming pool type of reactors. The blue light emission is known as Cerenkov radiation and results when high speed beta particles are emitted from radionuclides into a medium at speeds greater than the speed of light for that medium. For example, the speed of light in water is about 75% of the speed of light in a vacuum. When a high energy beta particle is first emitted by a radionuclide, its velocity in water may exceed that of light.

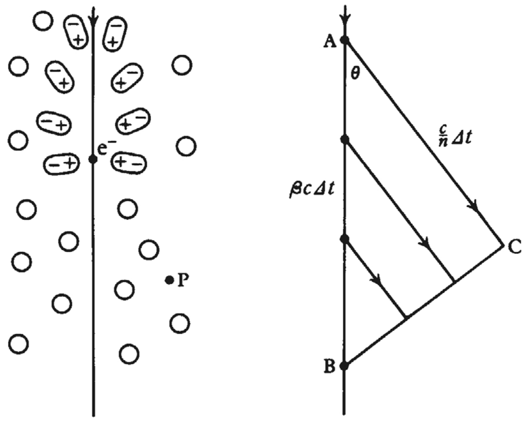

Figure 3.9 Cerenkov radiation. Polarization of atoms of transparent medium by passage of charged particles (left) and formation of cohertent wave front (right)

During the time that the velocity of the beta is greater than that of the light in the same medium, Cerenkov radiation is emitted - see Figure 3.9 and Figure 3.10. This is an electromagnetic emission that is predominantly in the blue regions of the visible portion of the spectrum. This emission represents an energy loss of the original beta particle and a reduction in the speed of that beta particle. The light is seen only near the surface of the fuel rod, for example, because within a few inches the speed of the beta is less than that of light.

3.5 Photon Interactions with Matter

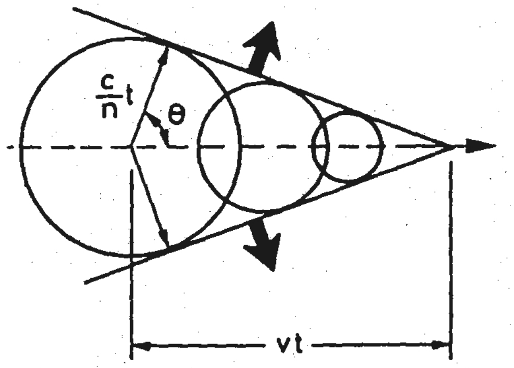

Figure 3.10 Cerenkov radiation: an electromagnetic shockwave is formed when the charged particle travels faster than the speed of light in the same medium

Photons are indirectly ionizing forms of radiation. They cause limited ionization by themselves, but also cause the release of charged particles which are directly ionizing. The secondary ionization products formed from the initial photon interaction events cause additional ionizations.

For charged particles, the range of the particle in matter can be determined relatively easily and is approximately constant for a given energy in a given material. This is not the case for electromagnetic radiations and the range concept is not used. Instead, a tenth thickness concept is applied. This concept states that following the passage of an electromagnetic radiation beam through a tenth thickness of material, only 1/10th of the original beam intensity exists. The actual tenth thickness of a material depends on the material. This results in the fact that the range of electromagnetic radiations in matter is not constant for equal energy radiations.

Photons, irregardless of the type or source (gamma, x-ray, Bremsstrahlung, and annihilation radiations), have higher penetrating abilities and lower specific ionization values than any of the charged particles. For example, the tenth-thickness of air for 3 MeV gamma photons is about 5400 meters (5.4x105 cm) and the specific ionization is only about 2.5 i.p./cm.

Electromagnetic photons in the energy ranges of our interest, interact with matter by three primary mechanisms, photoelectric effect, Compton scattering and pair production. Photoelectric and pair production interactions result in the total absorption of the incident gamma energy. Compton scattering is an inelastic scattering reaction which reduces the energy of the incident photon but does not eliminate it. The method of interaction depends on the actual photon energy and the composition of the absorber.

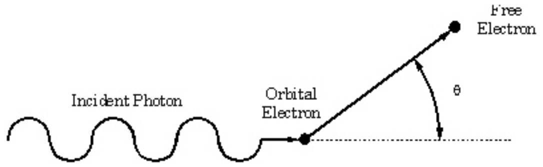

Figure 3.11 Photoelectric effect interaction.

A. Photoelectric Effect

Low energy photons are likely to transfer their energy to an absorber by the photoelectric effect. The photoelectric effect causes the total absorption of the incident photon energy.

The photoelectric effect was first described in 1905 by Einstein. It is the transfer of energy from a photon to an orbital electron of a given atom in the absorber . The results of the interaction are that an electron gains sufficient energy to be ejected from the atom. The ejected electron is known as a photoelectron. The atom is left with an excess + charge. The incident photon energy must exceed the particular electron’s binding energy for this to occur.

The conservation of energy law applies. The energy balance is :

$$E_\gamma = E_{e^-} + \phi$$

$$\phi - \text{energy needed to break the electron free (so called `exit labour`)}$$

The photoelectric interaction occurs principally with K-shell electrons but also occurs in the L and M shells. The interaction always leaves an atom with a vacancy in the atomic orbitals. When this orbital is filled by the rearrangement of the atomic electrons, the atom will emit characteristic X-rays or possibly Auger electrons.

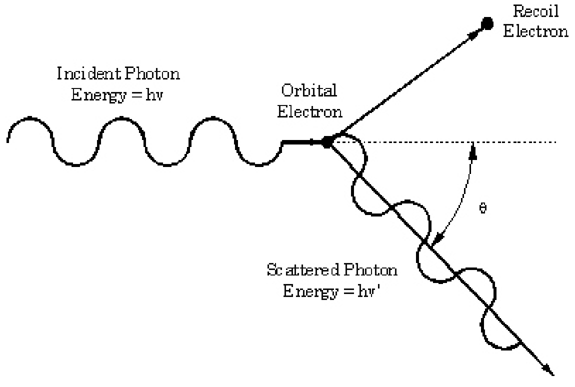

Figure 3.12 Illustration of Compton scattering interaction

The probability of this interaction increases with the Z number of the absorber and decreases rapidly as the energy of the photon increases.

B. Compton Scattering

As the energy of the incident photon increases, photon scattering reactions begin to predominate over the photoelectric effect absorptions. The scattering of an incident photon off of an orbital electron is called Compton scattering after its discoverer, Arthur Compton. This interaction is an inelastic scattering reaction. The probability of Compton scattering reactions also decreases with increasing energy.

The incident photon transfers some of its energy to the electron following a collision. However, a photon emerges from the collision at a reduced wavelength (less energy) and a new direction of travel. The energy of the incident photon is divided between the kinetic energy of the electron, the binding energy of the electron, and the energy remaining with the scattered photon.

The Compton scattering interaction is illustrated in Figure 3.12.

How much energy is transferred to the electron and how much energy the scattered gamma retains is a function of the incident photon's energy and the scattering angle. The energies and scattering angles may be calculated using a series of related equations based on conservation of energy and momentum.

The energy of the scattered photon in the Compton scattering reaction is determined by:

$$h\nu' = \frac{h\nu\, m_e c^2}{m_e c^2 + h\nu(1-\cos\theta)}$$

where

hν' = the energy of the scattered photon

hν = the energy of the incident photon

m_ec^2= the energy equivalent of the electron at rest

θ= the Compton scattering angle

The kinetic energy of the electron is the difference between the incident photon and the scattered photon.

$$E_{kin,e} = h\nu - h\nu'$$

where hν' and hν are as above. The scattering angle of the electron is determined by:

$$\cos\theta = 1 - \frac{m_e c^2}{h}\left(\frac{1}{\nu'} - \frac{1}{\nu}\right)$$

Where θ is the scattering angle of the electron and the other symbols are as above.

A "head-on collision" (scattering angle = 180 degrees) will transfer the maximum energy to the electron which is projected in a forward direction. At this scattering angle the scattered photon will have the minimum energy possible, which is never zero.

If the incident photon misses an electron, the scattering angle equals 0. The scattered photon and the original photon have the same energy (and are therefore indistinguishable). No energy is transferred to the electron in this case. All scattering angles between 0 and 180o are possible but the distribution of scattering angles changes with photon energy.

The very useful form of Compton equation is relation between incident photon wavelength and scattered photon wavelength as a function of angle:

$$\lambda' - \lambda = \frac{h}{m_e c}(1-\cos\theta),$$

$$\Delta\lambda = \lambda_c(1-\cos\theta)$$

Where $\lambda_c = \frac{h}{m_e c} = 2.426\times10^{-12}\, m$ is called as a Compton wavelength

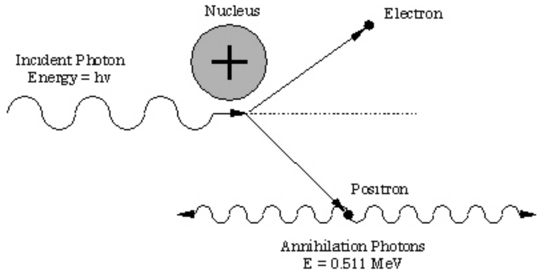

Figure 3.13 Pair-production interaction.

C. Pair Production

The last predominant gamma interaction with matter is known as pair production. The pair production interaction results in the total absorption of the incident gamma photon. The pair production interaction is depicted in Figure 3.13.

Unlike the other gamma interactions which occur with orbital electrons, the pair production interaction occurs near the nucleus of heavy elements. If the energy of the photon exceeds the energy equivalence of two electrons this interaction is possible and increases in probability as the energy increases. In pair production the energy of the photon is converted into two particles, an electron and a positron. The rest mass energy equivalent of these two particles is 0.511 MeV each. Therefore, this interaction is impossible if the original incident photon has an energy less than 1.022 MeV.

Any energy greater than this minimum appears as kinetic energy of the electron and positron pair. Both particles lose their energy as they penetrate the absorber by the charged particle interactions already discussed. The positron will annihilate with an electron once its kinetic energy is zero. This annihilation results in the reconversion of mass into energy. Two gammas of exactly 0.511 MeV are liberated from the annihilation and they propagate through the absorber in opposite directions. These photons may then undergo additional photoelectric or Compton interactions.

D. Other Photon Interactions

There are other less significant photon interaction mechanisms. They are listed for the reader but not discussed. These interactions include :

Rayleigh Scattering

Thomson Scattering

Nuclear Resonance Scattering (Mössbauer)

Bragg Scattering

Photodisintegration - Photonuclear Effect

3.6 Probability of Interaction and Attenuation of gamma Radiation

Either the photoelectric effect or Compton scattering may occur if the photon energy is less than 1.02 MeV. If the energy is great enough to cause pair production, then that interaction may occur also. Which of these reactions is most likely, depends on the photon energy and the absorber.

The first attenuation coefficient of importance is the "linear attenuation coefficient". This can be defined as a reaction probability per unit thickness of absorber and has units of reciprocal distance. The linear attenuation coefficient is given the symbol μ.

Mathematically,

$$\mu = \frac{\left(-\frac{dN}{N}\right)}{dx}$$

where:

$\frac{dN}{N}$ = the fraction of the number of particles N which experience a reaction,

and;

dx = the distance penetrated.

The total linear attenuation coefficient of a given absorber is the sum of all individual linear attenuation coefficients for the reactions possible in that absorber. In the case of gamma radiation, there is a certain probability that a gamma photon will interact by the photoelectric effect, another probability it will interact by Compton scattering or pair production. In this case, the total linear attenuation coefficient is the sum of these three interaction probabilities. Mathematically,

$$\mu_{total} = \mu_{photoelectric} + \mu_{Compton} + \mu_{pair}$$

Similar to the mass stopping power, it is often more practical to relate the linear attenuation coefficient to the density of the absorber by dividing through by the density. This leads to what is known as the "mass attenuation coefficient". The mass attenuation coefficient has units of cm^2/g or m^2/kg and is given by :

$$\chi = \frac{\mu}{\rho}$$

where:

μ = the linear attenuation coefficient, and;

ρ = the density of the absorber.

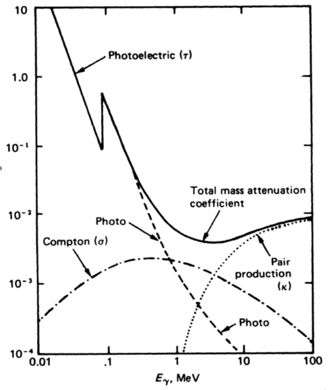

Figure 3.14 Mass attenuation coefficients for lead

The mass attenuation coefficient is a measure of the probability of interaction. A common graph of this for a lead absorber is shown in Fig. 12. At low energies, photoelectric effect has the greatest values. At medium energies, Compton scattering predominates. Once pair production is energetically possible, it contributes to the absorption of gamma energy. A well known curve of the linear attenuation coefficients for gamma radiation in aluminum and lead is illustrated in Figure 3.15 .

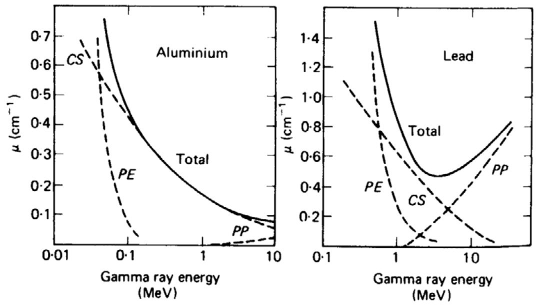

Figure 3.15 Gamma radiation absorption coefficient for aluminum and lead

3.6.1 Exponential Attenuation

Figure 3.16 illustrates the impingement of a narrow beam of gamma photons on the face of a slab with thickness x. The intensity of the radiation before striking the slab is given by I_o. When the linear attenuation coefficient is known, the attenuated intensity, I, after passage through the slab is given by :

$$I = I_0 e^{-\mu x}$$

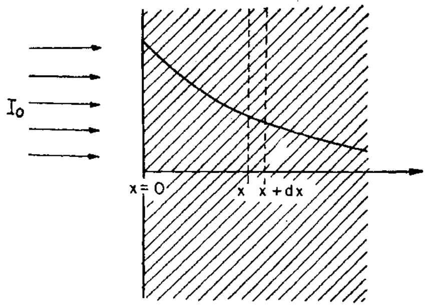

Figure 3.16 Radiation beam incident of a slabs shield

When the mass attenuation coefficient is known this equation becomes :

$$I = I_0 e^{-\chi x \rho}$$

The reduction of wide-beam radiation by penetration through a slab shield is not as great as for narrow-beam geometries. This is attributed to buildup. Many interaction events do not completely remove an incident photon from the beam. It may be scattered instead and exit the slab. In wide-beam geometries, this scattered photon may be scattered towards a detector on the other side of the slab. Additional photons may liberated by the pair production interaction or the Bremmstrahlung effects produced by the secondary radiations. The effects of buildup on the reduction of radiation is shown in Figure 3.17. The dotted line represents the predicted decrease without buildup. The solid line represents the actual reduction taking into account scattering and other reactions.

Buildup modifies above equations as follows :

$$I = I_0\, B(E)\, e^{-\mu x}$$

$$I = I_0\, B(E) e^{-\mu_m x \rho}$$

where B (E) is the "buildup factor". Tables of buildup factors are available and they can be looked up in the tables to be used. An example of buildup factors is presented on Figure 3.18 . Since buildup factors increase the intensity of radiation, they always have values greater than 1.

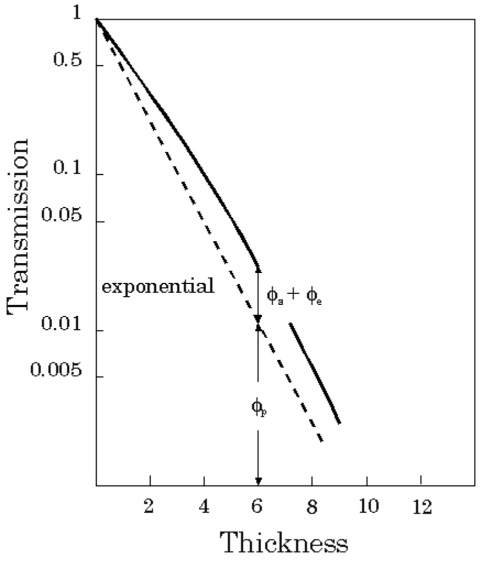

Figure 3.17 Effects of buildup. The dotted line represents the predicted decrease without buildup, the solid line represents the actual reduction taking into account scattering and other reactions

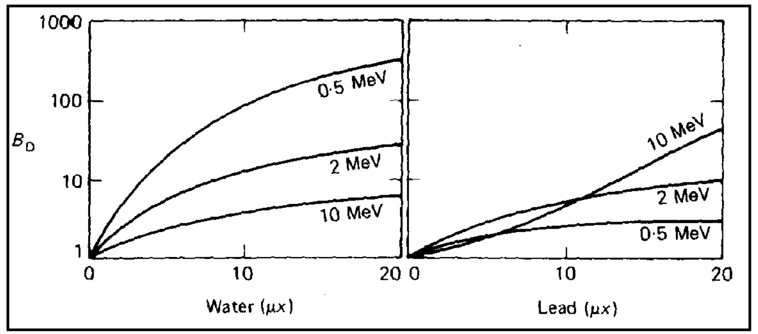

Figure 3.18 Build-up factors for a point source of radiation in water and lead.

3.7 Stopping power of shielding materials

A fundamental quantity of interest for the absorption of this radiation energy is the amount of energy transferred per unit length of travel of the radiation in a given absorber. This is called the *"stopping power"*. The stopping power depends on the type and energy of the radiation as well as the absorber material. The stopping power is an instantaneous value and changes as the energy of the radiation changes. As the energy of the radiation becomes less the stopping power of the absorber increases. The stopping power of an absorber for a charged particle is given by :

$$S = \left(\frac{dT}{dx}\right) = \left(\frac{dT}{dx}\right)_c + \left(\frac{dT}{dx}\right)_r$$

where:

S = energy lost per unit length of travel. For example, MeV/cm.

-dT = the average kinetic energy lost while traversing a distance, dx. The negative sign indicates that energy is lost by the radiation as it traverses the absorber.

dx = the distance traversed by the radiation.

The stopping power is made up of two components. The energy loss by charged particle collisions (subscript c) and the energy lost as radiative losses (subscript r). Unless specifically stated, the stopping power is considered to be the total of these two mechanisms. The collisional energy loss mechanism predominates with heavy charged particles. The radiative energy losses predominate with high energy β or electrons.

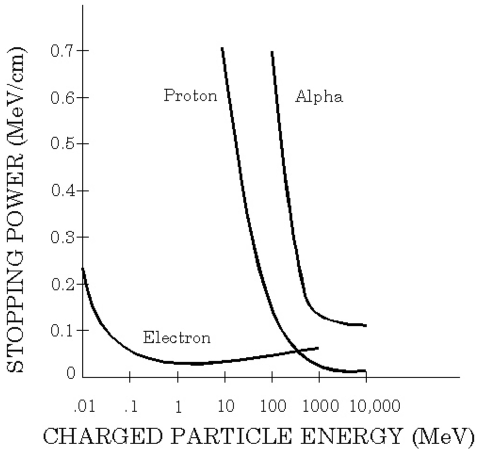

Figure 3.19 Stopping power of different chasrged particles as a function of incident energy

3.7.1 Mass Stopping Power

Since the stopping power is affected by the electron density of the absorber, it is more common to discuss the Mass Stopping Power. This is simply the stopping power of the medium divided by the density of the medium.

$$\frac{S}{\rho} = \left(\frac{\frac{dT}{dx}}{\rho}\right)$$

where ρ – the density of the absorber.

The mass stopping power for any absorber is nearly independent of the actual absorber material. Since the stopping power is dependent on the electron density of the absorber, when the stopping power is corrected for density, this is taken into account. The number of electrons in a given neutral atom is equal to Z, the atomic number. The mass of a given atom is defined by A, the atomic mass. The electron density is given by the ratio of Z/A. In all atoms, except for hydrogen, the ratio of Z/A is between 0.4 and 0.5. So the mass stopping power can be considered to be independent of the absorber and only depends on the properties of the radiation. See Figure 3.20 for an example of mass stopping power of electrons of different energy.

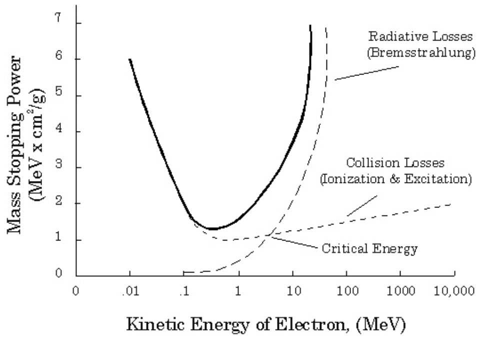

Figure 3.20 Mass stopping power of electrons as a function of incident energy

3.8 Neutron Interactions with Matter

Neutron interactions is discussed in details in a dedicated lecture ***(click here to open the lecture)***.

Chapter 4

Radioactive Decay

4.1 Introduction

By the spontaneous emission of charged particles and/or photons. Radioactive decay is a general term for any nuclear transition where a radioactive parent atom spontaneously emits radiation and turns into a new material, known as the daughter product. The daughter product may be stable but it also may be radioactive and decay into another daughter product (granddaughter to the original parent). All radioactive material is in the constant process of changing into different materials that are more stable. For example, ^{60}Co spontaneously decays into ^{60}Ni, which is stable. In this example the parent radionuclide is ^{60}Co and the daughter nuclide is ^{60}Ni, which is not radioactive.

As a radioactive parent decays a new radioactive material may be produced. This is called "ingrowth" and it can not be disregarded.

All radioactive decay processes are characterized by the type of radiation given off and the energy of the emitted radiation. The energy level difference between the parent and the daughter in a radioactive decay process is a constant. This is the amount of energy carried off by the radiation as the parent atom decays.

Radioactive decay is governed by the physical conservation laws. The following quantities are conserved during the radioactive decay process :

1. The total energy of the system.
2. The net electrical charge.
3. Total mass number (i.e. the number of nucleons)
4. The total momentum for the system.

4.2 Rate of Radioactive Decay

Radioactive decay is a spontaneous process and it is impossible to predict when a single radioactive atom will decay. However, when a large quantity of atoms are observed, it can be shown that the amount of radioactivity in a sample, due to a parent nuclide, does decrease over time. Obviously, the number of atoms decaying at the start of a given time period will be greater than the number of atoms decaying at the end of that time period because there were more atoms to start with. The standard method of identifying the quantity of a radioactive material is to state the average number of nuclear disintegrations occurring per unit of time. The number of disintegrations per second or per minute, for example. This is known as the "activity" of the source.

There are two basic units used to express the activity of a source. One unit is thecurie (Ci) which has been used more frequently in the past. The other unit is based on the SI system of measurement and is called the becquerel (Bq). The curie was originally based on the activity of one gram of pure radium but has since been standardized to be a known disintegration rate from any radioactive material. The curie is the quantity of radioactive nuclide disintegrating at the rate of 3.7×10^{10} atoms per second (abbreviated Ci). Several fractions of the curie are in common usage.

The becquerel is the special name for the SI unit of activity. One becquerel is one reciprocal second or 1 s^{-1}. 3.7×10^{10} Bq = 1 Ci. Obviously, then there are 3.7×10^{10} Bq per curie.

The law of radioactivity was experimentally discovered 1899 by Julius Elster and Hans Geitel:

$$
\begin{aligned}
&dN = -\lambda\, Ndt \\
&\frac{dN}{dt} = -\lambda\ N \rightarrow activity, or\ \ radioactivity \qquad (4.1) \\
&(units: Curie, Becquerel) \\
&N = N_0 e^{-\lambda t}
\end{aligned}
$$

:

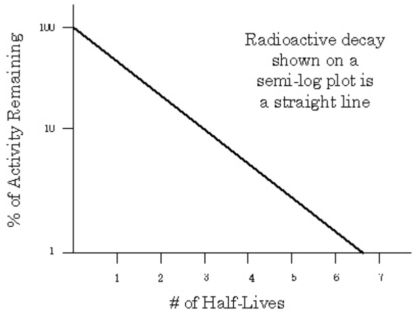

Figure 4.1 Radioactive Decay on Semi-Log Graph

where

N = the number of atoms remaining after time t,

N_o = the number of atoms at to.

λ= the decay constant.

e = the base of the natural logarithms.

t = the time between the N and N_o and must be in the same units as λ.

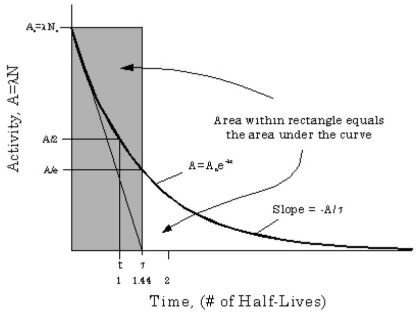

Figure 4.2 Concept of mean life time

Some useful relations:

$$Mean\ life\ time \rightarrow \tau = \frac{1}{N_0}\int_0^\infty tdN = \frac{1}{\lambda}$$

$$Half\ life\ time \rightarrow T_{1/2} = \frac{\ln 2}{\lambda} = \frac{0.693}{\lambda} = 0.693\,\tau$$

A relation of different activity units in the standard multiples and the associated decay rate is given in Table VI.

Table VI. (Radio-)Activity units

Unit of Activity	Disintegration Rate (disintegrations /second - dps)	Disintegration Rate (disintegrations / min - dpm)	SI Equivalent (becquerels, Bq)
Ci	3.7×10^{10} dps	2.2×10^{12} dpm	3.7×10^{10} Bq
mCi	3.7×10^{7} dps	2.2×10^{9} dpm	3.7×10^{7} Bq
mCi	3.7×10^{4} dps	2.2×10^{6} dpm	3.7×10^{4} Bq
nCi	3.7×10^{1} dps	2.2×10^{3} dpm	3.7×10^{1} Bq
pCi	3.7×10^{-2} dps	2.2 dpm	3.7×10^{-2} Bq

Although the curie is a measure of the activity, it does not give information about the number of atoms or the mass of the radioactive material which would equal a curie. The amount of activity per unit mass of material is known as the "specific activity". This can vary widely because of different masses of the atoms and different half-lives involved. Table VII lists some examples of the specific activity for various materials.

Table VII. Specific Activity of Selected Materials

Radionuclide	Specific activity (curies/gram)
^{3}H	9.63×10^{3}
^{16}N	9.79×10^{10}
^{36}Cl	3.21×10^{-2}
^{60}Co	0.13×10^{3}
^{90}Sr	1.41×10^{2}
^{238}U	3.34×10^{-7}

The instantaneous rate of change in the number of atoms decaying over time is directly proportional to the number of atoms present in the sample. The constant of proportionality is known as the decay constant.

The decay equations (4.1) only apply to the radioactive decay of a parent radionuclide. Since the parent nuclide forms a daughter product, the rate of the decay of the parent is also the rate of production of the daughter. Assuming that the daughter product is stable, no further considerations need to be given to the daughter product. However, when a daughter product (or granddaughter, etc.) is also radioactive, then the amount of daughter product material present at any time depends on the rate at which it is being formed from the parent and at the rate at which it is decaying.

When both the parent and the daughter are radioactive and depending on the relative half-lives of them, a condition of radioactive equilibrium may be established. Radioactive equilibrium is defined when the rate of change of the activity of the daughter radionuclide is equal to the rate of change of the activity of the parent radionuclide, even though their half-lives are different.

This is not to be misunderstood to say the amount of activity. It is instead the rate at which the amount that is present changes with time.

Whether the equilibrium condition is established depends on the relative difference between the half-lives of the parent and the daughter radionuclides If the conditions are such that equilibrium is established, it can be further classified as either transient equilibrium or secular equilibrium.

4.3 Radioactive series

Equation describing concentration (number) of nuclei of isotope B produced from radioactive decay of isotope A and in its turn decaying into the stable isotope C, has a form:

$$
\begin{aligned}
&A \xrightarrow{\lambda_a} B \xrightarrow{\lambda_b} C \\
&\left(\frac{dN_b}{dt}\right)_{netto} = \left(\frac{dN_a}{dt}\right)_{a\to b} - \left(\frac{dN_b}{dt}\right)_{b\to c} = \lambda_a N_a - \lambda_b N_b \\
&N_a = N_{a0} e^{-\lambda_a t} \\
&\frac{dN_b}{dt} = \lambda_a N_{a0} e^{-\lambda_a t} - \lambda_b N_b
\end{aligned}
\tag{4.2}
$$

where :

A = the parent radionuclide,

B = the daughter (1st progeny) radionuclide,

C = the granddaughter (2nd progeny) radionuclide, which is stable,

λ_a, = the decay constant of the parent radionuclide,

λ_b = the decay constant for the daughter radionuclide.

Solution of equation (4.2) is:

$$
N_b = N_{b0} e^{-\lambda_b t} + N_{a0} \frac{\lambda_a}{\lambda_b - \lambda_a} \left(e^{-\lambda_a t} - e^{-\lambda_b t} \right) \tag{4.3}
$$

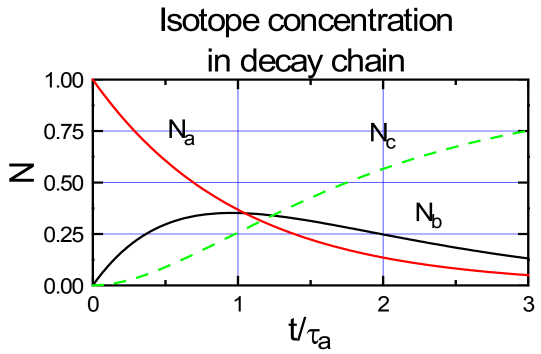

Figure 4.3 Graphical illustration of a solution of equation (4.2)

Assuming $N_{b0}=0$ we get a solution shown at Figure 4.3.

4.3.1 No Equilibrium (called sometimes also Radioactive Equilibrium

$$
\begin{aligned}
&if\ \lambda_a >> \lambda_b \\
&N_b \sim N_{a0} e^{-\lambda_b t} (1 - e^{-(\lambda_a - \lambda_b) t})
\end{aligned}
\tag{4.4}
$$

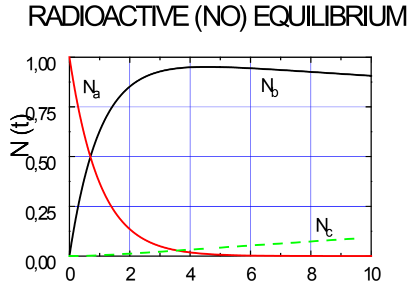

Figure 4.4 Radioactive equilibrium

No equilibrium is established if the half-life of the parent is less than the half-life of the daughter. There is no time at which the rate of change of the number of atoms of the parent is the same as the rate of change for the daughter. For example, the radioactive parent ^{131m}Te (half-life = 30.0 hours) decays into the radioactive daughter ^{131}I, which has a longer half-life (8.04 days).

A graph of this "no equilibrium" condition is shown in Figure 4.5 for the ^{131m}Te -> ^{131}I parent - daughter pair. Given an initial parent population the number of parent atoms at any time can be calculated using equation (4.4). The activity of the parent can then be determined by equation (4.2).

Under these conditions, the activity of the daughter product builds up to exceed the activity of the parent. The total activity in the sample does not decrease at the rate of the parent due to the ingrowth of the daughter. After the parent has decayed away, the total activity equals the daughter activity and the rate of decrease is equal to that of the daughter. Nowhere in this graph are the slope of the lines representing the parent activity and the daughter activity equal. Therefore, no equilibrium value is established.

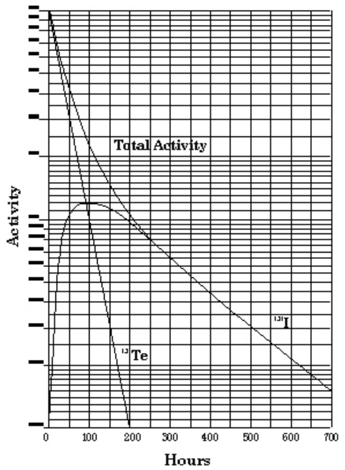

Figure 4.5 Decay of ^{131}I and ^{131m}Te in radioactive no-equilibrium case

4.3.2 Secular Equilibrium

Secular equilibrium is established when the half-life of the parent exceeds the half-life of the daughter by approximately 1000.

In the case of secular equilibrium, there is very little decay of the parent, due to its very long half-life, while the ingrowth of the daughter is quite rapid (relative to the half-life of the parent). This results in the daughter activity building up to that of the parent very quickly. The total activity therefore initially increases over time. The parent, the daughter and the total activity then decreases at a rate equal to that of the parent. This is defined as secular equilibrium.

$$
\begin{aligned}
&\lambda_b >> \lambda_a \\
&N_b \approx N_{a0} \frac{\lambda_a}{\lambda_b} e^{-\lambda_a t} \left(1 - e^{-(\lambda_b - \lambda_a) t}\right)
\end{aligned}
\tag{4.5}
$$

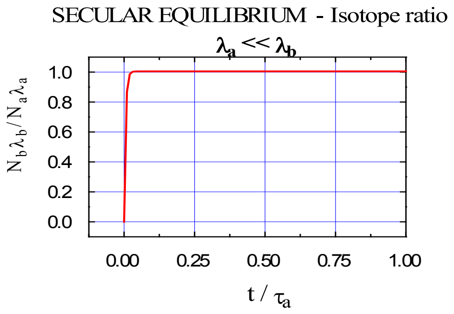

Figure 4.6 Parent-to-daughter isotope ration in secular equilibrium of decay

The decay of ^{90}Sr ($t_{1/2}$ = 29.0 years) yields ^{90}Y as a daughter product ($t_{1/2}$ = 64.0 hours). In this case the half-life of the parent is 3972 times longer than the daughters. The decay of ^{137}Cs into ^{137m}Ba also establishes secular equilibrium. In this case the ^{137}Cs half-life is 6.2x10^6 times longer than the daughter's. Another example is the decay of ^{144}Ce into ^{144}Pr. Here the parent half-life is 2.3x10^4 times longer than the daughter's half-life.

There are several secular equilibrium examples in the natural decay chains. For example, ^{222}Rn has a half-life of 3.8 days and its radioactive daughters all have short half-lives and will develop equilibrium with it in a few hours.Figure 4.7 illustrates the buildup of several of it daughters over time.

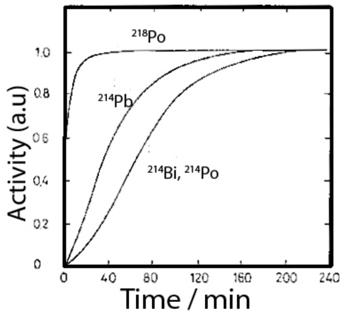

Figure 4.7 Secular equilibrium of some of the ^{222}Rn daughters

4.3.3 Transient Equilibrium

Transient equilibrium is a situation in which equilibrium is reached by a parent-daughter radioactive isotope pair where the half-life of the daughter is shorter than the half-life of the parent. Contrary to Secular equilibrium, the half-life of the daughter is not negligible compare to parent's half-life.

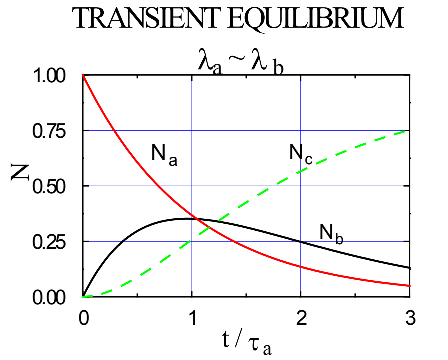

Figure 4.8 An example of transient equilibrium between isotopes N_a *and* N_b

Transient equilibrium is established when the parent radionuclide has a half-life of approximately 10 to 10^3 times longer than the daughter product. These times are not exact and there is no clear cutoff which defines the conditions of no equilibrium, transient equilibrium and secular equilibrium.

$$\lambda_a \sim \lambda_b$$

$$N_b = N_{a0} \frac{\lambda_a}{\lambda_a - \lambda_b} e^{-\lambda_b t} \left(1 - e^{-(\lambda_b - \lambda_a)t}\right) \tag{4.6}$$

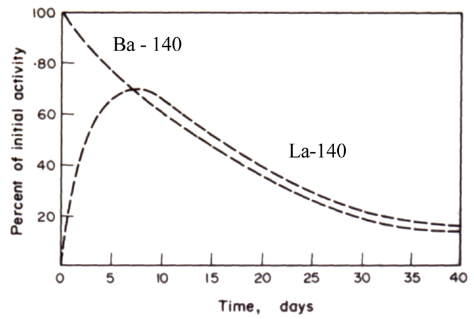

Figure 4.9 Transient equilibrium of ^{140}*Ba (*$t_{1/2}$*=12.7 d)/*^{140}*La (*$t_{1/2}$ *=40.27 h*

For example, the parent radionuclide ^{88}Kr decays into the radioactive daughter product ^{88}Rb. The parent half-life is 2.8 hours (168 minutes) and the daughter half-life is 17.7 minutes. The relative difference between the two half-lives is therefore, 168/17.7 = 9.5. Given a pure parent, radioactive transient equilibrium will be established between the ^{88}Kr and the ^{88}Rb.

Under the conditions of transient equilibrium, the daughter product activity builds up to a level greater than the parent and then decays at the same rate. The total activity increases until the daughter activity peaks and then it also decreases at a rate equal to the original decay rate of the parent. The slope of the line for the parent activity, the daughter activity and the total activity become equal. Equilibrium is established when this occurs.

Figure 4.9 illustrates this phenomenon for the ^{140}Ba/^{140}La parent-daughter pair. An initially pure parent sample (^{140}Ba)was at t=0.

Another example of transient equilibrium is the Molybdenum-99 generator producing Technetium-99 for nuclear medicine diagnostic procedures. Such a generator is sometimes called cow because the daughter product, in this case Technetium 99 is milked at regular intervals.

EXAMPLE:

Estimate atomic ratio and activity ratio between ^{235}U and its decay daughter ^{231}Pa.

Pay attention to extremely small atomic ratio and equal activity ratio, a nice feature giving large spectroscopic possibilities.

$$\alpha \to T_{1/2} = 7.04 \times 10^8 y \qquad \beta \to T_{1/2} = 25.5h$$

$$^{235}U ------------> {}^{231}Th -----------> {}^{231}Pa$$

Estimate atomic ratio (~mass ratio) $\frac{N_{Th}}{N_U}$ after 50h-

$$N_B = \frac{\lambda_a N_{A0}}{\lambda_B - \lambda_A}\left(e^{-\lambda_A t} - e^{-\lambda_B t}\right)$$

$$\lambda_A = \frac{0.693}{7.04 \times 10^8 \times 365 \times 24} = 1.12 \times 10^{-13} h^{-1}$$

$$\lambda_B = \frac{0.693}{25.5} = 2.72 \times 10^{-2} h^{-1}$$

$$\frac{N_B}{N_A} = \frac{1.12 \times 10^{-13}}{2.72 \times 10^{-2}}\left(1 - e^{-2.72 \cdot 10^{-2} \cdot 50}\right) = 3.06 \times 10^{-12}$$

Relative activity after 50 h is

$$\frac{\lambda_A \cdot N_A + \lambda_b \cdot N_B}{\lambda_A \cdot N_{A0}} = \left[N_A \approx N_{A0}\right] = 1.74$$

Chapter 5

Nuclear Data References

5.1 Introduction

There are several sources of information available about radioactive decay modes, energies of the radioactive decay products, half-lives, abundances, etc. A few of these sources have become well accepted standards which are kept current as new information is available. These available references:

- Chart of the Nuclides
- Atomic Data and Nuclear Data Tables;
- Radioactive Decay Data Tables
- Table of the Isotopes; and the
- Radiological Health Handbook.

5.2 Chart of the Nuclides

Perhaps the most widely used, general reference for this information is the Chart of the Nuclides. The term nuclide has come to mean a species of atom characterized by the number of protons and neutrons that the atom contains. This includes both stable and radioactive species. There are about 2500 known nuclides.

The Chart of the Nuclides is based on arranging all known nuclides, both stable and radioactive, on a grid system. This graphs the number of protons contained within the nuclide against the number of neutrons within the nuclide. This general arrangement is shown in Figure 5.1. The numbers along the left hand side identifying the horizontal rows represent the number of protons (the atomic number Z). Each successive vertical column indicates the number of neutrons, N. The intersection of a row with a column is the nuclide which has that given combination of protons and neutrons. Information about that specific nuclide is placed in the box form by this intersection. Heavier lines are used to outline the magic number values of 2, 8, 20, 28, 50, 82, & 126.

Each horizontal row includes all nuclides of a single chemical element. All nuclides of the same

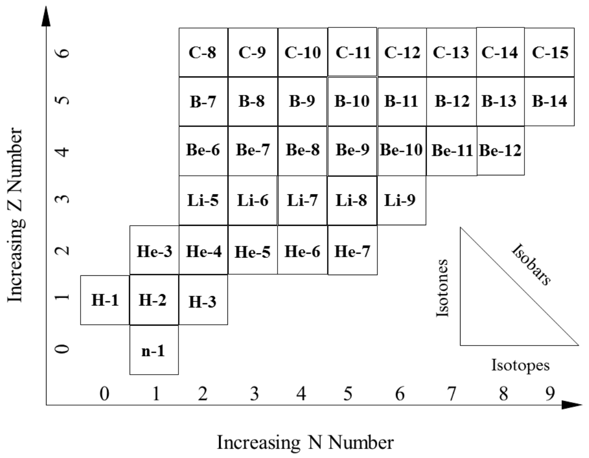

Figure 5.1 General arrangement of the Chart of the Nuclides

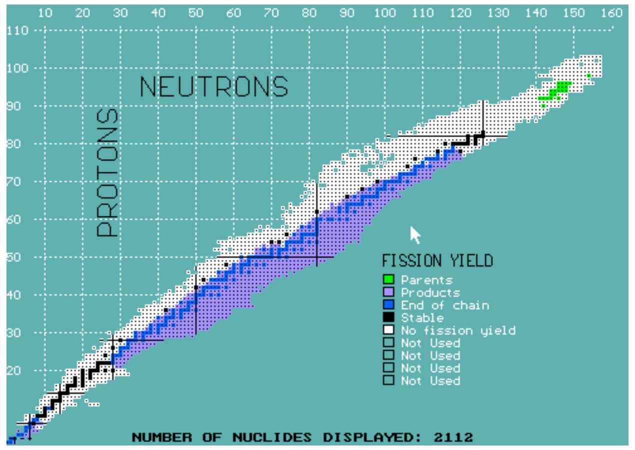

Figure 5.2 Chart of the Nuclides

chemical elements have the same chemical symbol and are known as isotopes of that element. Nuclides contained in a vertical column all have the same number of neutrons. Nuclides with the same N number are referred to as isotones. Diagonally in one direction, all nuclides have the same A number (Z+N=A). Nuclides with different combinations of protons and neutrons which total to a constant A number are known as isobars.

By illustrating the known nuclides in this manner, it is easy to establish general trends for the nuclides. This can be seen in Figure 5.2. Close observation of this figure will show that the stable nuclides run through the center of the Chart up through an A number of about 200. Above this point are the majority of the radionuclides which emit alpha particles.

Below and to the right of the stable nuclides are the β^- emitters. These materials have too large of a neutron to proton ratio to remain stable. All these materials emit β^- particles, which lowers the neutron to proton ratio.

Above and to the left of the stability line are the β^+ emitters or materials which undergo electron capture. These materials have too low of a neutron to proton ratio compared to the stable nuclides. These decay modes convert proton into neutron, thereby raising the neutron to proton ratio.

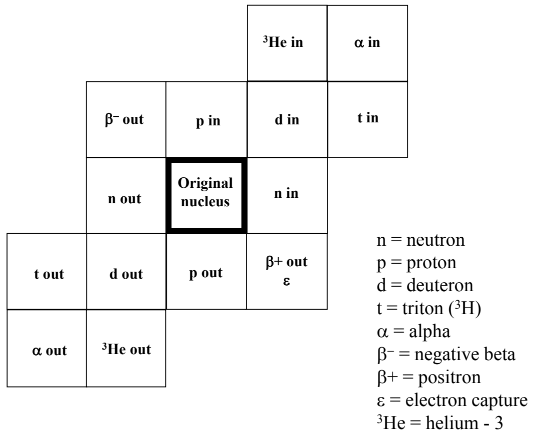

Figure 5.3 Relative locations of nuclides resulting from radioactive decay

Since radioactive decay changes the constituents of the nucleus, the Chart of the Nuclides can act as a roadmap to determine the decay chain associated with a given radionuclide. As a general guide to this approach, refer to Figure 5.3. If a parent radionuclide is located at the grid space labeled "Original Nucleus", the daughter product will be at the relative location shown in the figure, each possible location corresponds to a type of radiation emitted or absorbed. For example, consider the radioactive decay of Uranium-238 which emits an alpha particle. The relative location of the daughter product on the Chart of the Nuclides is down two and to the left two spaces from the original location. This location is Thorium-234 in our example.

Additional daughter products can be identified in this manner.

A similar approach can be taken for some of the more common nuclear bombardment reactions other than fission. The relative location of the product formed from a given reaction can be located relative to the original nucleus by referring to Figure 5.4. For example, the product of a nuclear reaction which absorbs a proton and emits a neutron (designated (p,n)) would be located to the left one position and up one position.

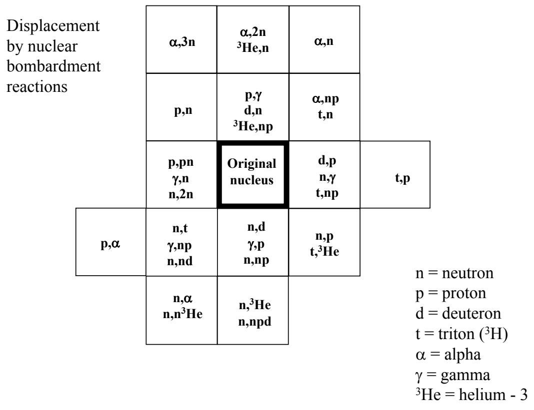

Figure 5.4 Relative locations of the products of nuclear reactions

Corresponding changes in the Z and N numbers are readily determined.

The specific data contained in each grid of the Chart of the Nuclides varies depending on the general classification of nuclide. The Chart of the Nuclides displays data slightly differently for the following general classifications :

1. The chemical element box, first entry in each row.
2. Stable nuclides.
3. Long-lived, naturally occurring radioactive nuclides.
4. Other radioactive nuclides.

An example of the data contained in the grids for each of these classifications is included in this handout. From these examples, and the instructions on the actual Chart, the student should be able to identify any entry in the Chart.

5.3 Chemical Element Box

The first square in every row contains a chemical element summary. In this square, the first line lists the chemical symbol for the element corresponding to the Z number given. The second line lists the atomic weight of the element based on the Carbon-12 scale. The atomic weight of the element is the weighted average for all stable nuclides of the element, weighted in accordance with their individual isotopic abundances. If no stable isotopes of the nuclide exist, there is no atomic weight listed. The third line in these squares is the element name. The last line of information in these squares is the thermal neutron absorption cross-section for the element in barns, followed by the resonance integral. This is also given in units of barns or a sub-multiple.

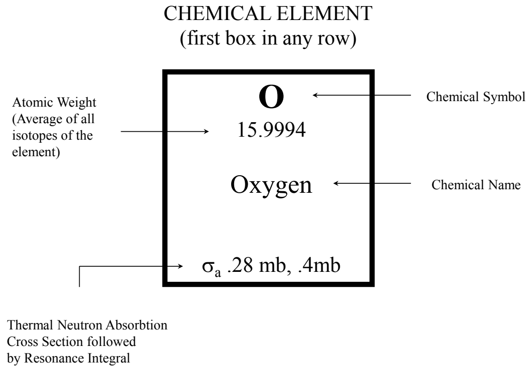

Figure 5.5 Chemical element box for O-16

The chemical element box for the row with 8 protons is shown in Figure 5.5. The chemical symbol is O. The elemental atomic weight is 15.9994 atomic mass units. This element is oxygen which has a low thermal neutron absorption cross-section of 0.28 millibarns (mb). The resonance integral is 0.4 mb.

5.4 Stable Nuclides

There are several factors which determine whether a nuclide will be stable. Among these factors are the atomic mass, the neutron/proton ratio of the nucleus, and pairing of nucleons. On the Chart of the Nuclides, spaces shaded in gray indicate naturally occurring nuclides. This includes naturally occurring radioactive nuclides. The 270 stable nuclides are shown as all gray. A study of the Chart will indicate that the first of the stable nuclides are low in mass and near a neutron/proton ration of 1. As the mass of the stable nuclides increases up through lead-208, the neutron to proton ratio changes to about 1.54.

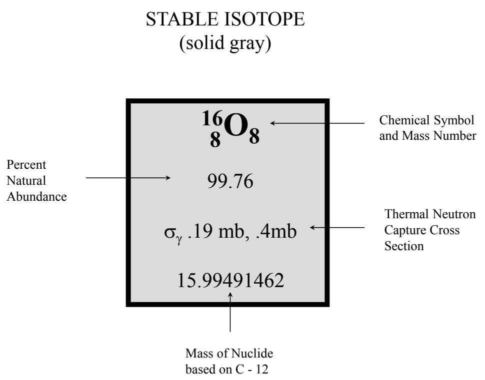

Figure 5.6 Stable nuclide box

An example of the information contained in a stable nuclide grid is given in Figure 5.6. The first line contains the chemical symbol and mass number. The second line indicates the percent abundance of that isotope, as found in nature. Subsequent lines list the thermal neutron cross-section and resonance integral in barns. This value indicates how well this nuclide reacts with thermal neutrons.

The last line is always the atomic mass of the nuclide based on the Carbon-12 scale. This is the mass of the specific nuclide which differs from the average mass of the element shown in the chemical element square.

5.5 Naturally Occurring Radioactive Nuclides

Naturally occurring radioactive nuclides fall into three categories. Nuclides with half-lives long enough to prevent their loss from the time they were first formed, nuclides which are decay daughters of such long-lived nuclides, and nuclides formed in the atmosphere by cosmogenic interactions. An example of this last category is Carbon-14 which is produced in the atmosphere by cosmic ray interactions with nitrogen.

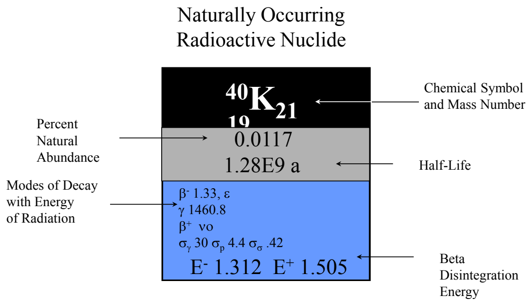

Figure 5.7 Naturally occurring radioactive material box

A naturally occurring radioactive material is identified in the Chart of the Nuclides by a heavy black band across the top of the grid. Only the parent of the long-lived naturally occurring decay chains are treated with a heavy black band across their grid square. The daughter products are treated separately.

Figure 5.7 illustrates the box of a naturally occurring radioactive nuclide, 40K. The first data line contains the element symbol and mass number. The second line is the isotopic abundance as found in nature. Since these materials are also radioactive, additional information is listed. The next line shows the half-life of the nuclide which is followed by the types and energies of the radiations emitted. 40 K is a somewhat unique nuclide in the sense that it can decay to stability either by beta minus or beta positive emission. The next line specifies the neutron absorption cross-section. Some squares also list the atomic mass depending on the available space remaining in the square. The last line indicates the beta disintegration energy.

5.6 Member of Naturally Occurring Decay Chain

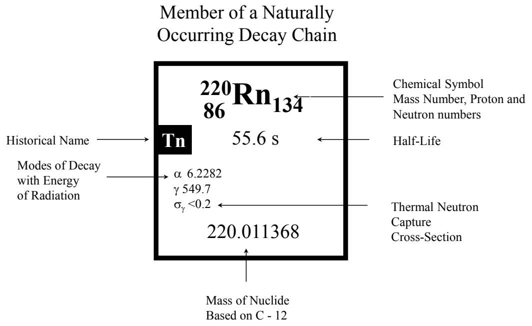

Figure 5.8 Member of a naturally occurring decay chain

The daughter products of the naturally occurring decay chains are indicated by a smaller black band below the chemical symbol and mass number. This band extends halfway across the grid square and contains the historical abbreviation for the nuclide. Figure 5.8 contains an example of this type of nuclide, ^{220}Rn. ^{220}Rn was historically called Thoron (Tn).

To the right of the small black section is the radionuclide's half-life, except for the stable daughter of the chain where the isotopic abundance is listed. The remaining information is basically the same as in the other type grids. Included are the type and energies of the principle radiations emitted as well as the total beta disintegration energy. The atomic mass of the nuclide is listed at the bottom of the block.

5.7 Artificially Produced Radioactive Nuclides

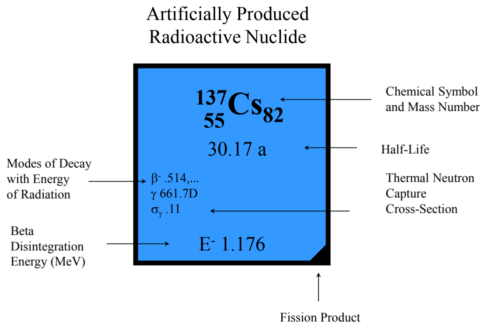

Figure 5.9 Artificially produced radioactive material

Artificially produced radioactive materials makeup the majority of the known nuclides. These nuclides have been produced by man made events such as nuclear fission and particle accelerator collisions.

Figure 5.9 contains the information for ^{137}Cs, an artificially produced radioactive nuclide. The small black triangle in the lower right hand corner indicates that ^{137}Cs is a fission product of slow neutron fission of either ^{233}U, ^{235}U or ^{239}Pu. Some fission products are stable.

Also contained in this grid are the half-life, type and energy of radiation emitted, neutron cross-section information and beta disintegration energy.

An interesting fact of the ^{137}Cs data is the "D" following the gamma energy emission. This indicates that this gamma associated with Cs is really a delayed emission of the Barium 137m daughter product. Any sample of ^{137}Cs will emit this gamma although the gamma is not actually from the nuclear transition of ^{137}Cs. The ^{137m}Ba block contains the same gamma energy information.

5.8 Nuclide with Two Isomeric States

Many squares in the Chart of the Nuclides are divided; for example the square for cobalt 60. These squares illustrate that the nuclide has one or more isomeric states (excited states). Isomers possess the same mass number and atomic number but different radioactive properties and energy levels. ^{60}Co and ^{60m}Co are examples and the grid square for this nuclide is illustrated in Figure 5.10

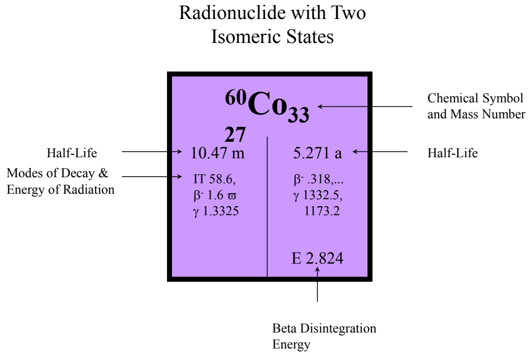

Figure 5.10 Nuclide with two isomeric states

The Chart of the Nuclides lists isomeric states when the nuclide has a half-life greater than 1 second. The grid square for a nuclide having metastable states is split down the middle with the higher energy isomer to the left and the lower energy isomer or ground state to the right. The ground state may be stable (gray color), as is ^{107}Ag, or radioactive, as is ^{60}Co.

Figure 5.10 shows that ^{60}Co has a single high energy isomer with a half-life of 10.48 minutes. The high energy state can relieve its excess energy by gamma emission. When this occurs it is known as isomeric transition (IT). The high energy isomer may also decay by particle emission before the excess energy is relieved by gamma emission.

5.9 Fission Yields

One other general feature of the Chart of the Nuclides is important to note. This is the information presented along a line which runs diagonally through the grids. These lines mark nuclides of constant mass (isobars).

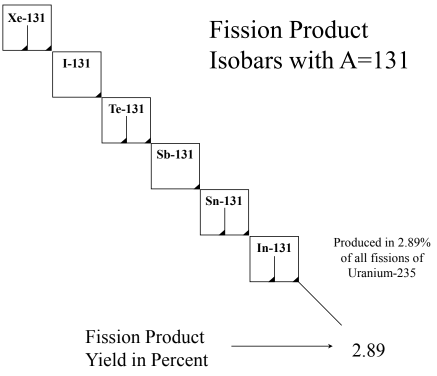

Figure 5.11 Fission Product Isobars with A=131

The numbers printed below this diagonal line indicate the fission yield for the given mass in percent. A graphical representation of these values produces the fission yield distribution curve.

Different materials of the same mass have an equal probability of being formed when fission occurs. For example, ^{131}I is formed from fission as often as is ^{131}Te, ^{131}Sb, ^{131}Sn or ^{131}In . This fission yield is 2.89 %. This means that a fission product of mass 131 will be formed from 2.89 percent of all fission events when ^{235}U is the fuel. Due to the Beta minus decay of the ^{131}In to ^{131}Sn to ^{131}Sb etc. and the different half-lives, the amount of each nuclide in a fission product sample will change with time.

Figure 5.11 is an example of how this information is presented.

5.10 Atomic Data and Nuclear Data Tables

There are many other references available which contain nuclear decay data. Two of these references are the Atomic Data and Nuclear Data Tables and the Radioactive Decay Data Tables. These references present basically the same information, although it is organized in a different fashion. The Atomic Data and Nuclear Data Tables however only list gamma ray emissions whereas the Radioactive Decay Data Tables list all emissions.

The Atomic Data and Nuclear Data Tables published by Academic Press referenced here is broken into three sections. The first section lists gamma rays in order of increasing energy for nuclides with half-lives less than 1 day. The second section lists gamma rays in order of increasing energy for nuclides with half-lives greater than 1 day. The third section lists the predominant gamma emissions from major nuclides ordered by increasing mass. Listing gamma energies in order of increasing energy is a very useful way to look up the nuclide causing the production of a measured gamma energy, if the source is not identified.

It is unlikely that an energy measurement will exactly match the value in the tables. Therefore, the reader should scan the list above and below the referenced energy to rule out other possibilities.

5.11 IV. Radioactive Decay Data Tables

The Radioactive Decay Data Tables published by the Technical Information Center of the US Department of Energy (DOE) as DOE/TIC-11026 is an example of many compilations of this sort. This document lists the major nuclides in order of mass and then lists the associated radiations and their energies. To use this type of table, the nuclide must be known. The user can then determine the types and abundances of the radiations associated with the nuclide. One example of. where this might be particularly useful is in trying to identify a low abundance gamma energy which might be showing up in a high activity sample.

5.12 V. Internet and Computer Program Resources.

Some good visualisation programs and internet data basis are avaiable:

1. Neutron cross section data library graphical interface: JANIS program distributed by NEA/OECD. Look at http://www.nea.fr/janis/welcome.html. Also JANIS-on-line service is avaiable: http://www.nea.fr/janis/webstart/janis.jnlp

2. Internet data basis:

http://ie.lbl.gov/toi.htm - Table of Isotopes, also exist as a stand alone program TOI

http://www-nds.iaea.org/ - data basis at IAEA

http://www.nndc.bnl.gov/index.jsp at Brookhaven National Lab. USA

http://t2.lanl.gov/data/data.html at Los Alamos National Laboratory

http://wwwndc.tokai.jaeri.go.jp/nucldata/ at JAERI in Japan

http://atom.kaeri.re.kr/ - at KAERI in Korea.

Chapter 6

Radiation Protection and Environment

6.1 Introduction

The human senses cannot detect radiation or discern whether a material is radioactive. That is why experiences with the dangers of radioactive materials preceded by many years the discovery of radioactivity. The atmospheres of mines in Central Europe that had been exploited for their heavy metals since mefieval times were unknowingly so radioactive that the miners developed a fatal lung disease which was later diagnosed as lung cancer. There were serious intuitive reasons that people calle uranium ore a "pechblende" - "bad luck ore".

Some radioactivesubstances were used well before it was known that they were radioactive. The Welscach gas mantle , developed in 1885, utilized incandescent properties of thorium-cerium oxide to greatly increase the luminosity of gaslight in many parts of the world, and uranium oxide has long be used to provide a vivid orange color in ceramic glazes.

In some parts of the world natural radioactivity has been exploited for its supposed benefit to health. There is no fully satisfactory explanation for how this custom originated, but it is known that the popularity of mineral waters in spas around the world led to their establishment as health resorts as long ago as Roman times. When the phenomenon of radioactivity has been discovered, test of these mineral waters showed some of them to contain abnormally high concentration of natural radioelements.

Today a variety of instruments can detect and measure radiation reliably and accurately, we also understand much better both positive and negative effects of radiation on living organisms.

Radiation protection of the population in most of the countries is managed by state authorities, like the Swedish Radiation Safety Authority in Sweden. Moreover there is an international body - the International Commission on Radiological Protection (ICRP) - formulating well thought through recommendations for national authorities. The International Commission on Radiological Protection is an advisory body providing recommendations and guidance on radiation protection; It was founded in 1928 by the International Society of Radiology (ISR) and was then called the 'International X-ray and Radium Protection Committee'. Then it was restructured to better take account of uses of radiation outside the medical area, and given its present name, in 1950. ICRP is a not-for-profit organisation in the United Kingdom and currently has its scientific secretariat in Ottawa, Canada.

6.2 Measuring and monitoring of radiation

Ionising radiation is measured in the international units, the gray (Gy) and the Sievert (Sv).

The amount of radiation, or 'dose', received by a person is measured in terms of the energy absorbed in the body tissue, and is expressed in Grays. In order to understand a conception of dose one need first to define a unit of radio-activity corresponding to radioactive decay of nuclei:

1 Bq (bequerel) = 1 disintegration/s

An older unit was called Curie - Ci - and 1 Ci = $3.7x10^{10}$ Bq and it corresponds to (radio-)activity of 1 g ^{226}Ra.

What is important for interactions of radiation with living organisms is an energy absorption in (energy intake) in living cells. This energy aborpion - energy intake - is called a ***DOSE:***

The unit of DOSE is 1 Gy (Gray) = 1 Joule of energy absorbed in 1 of tissue.

Previous unit, which is still in use:

1 rad = an energy absorption of 0.01 joule/kg which implies that 1 rad=0.01 Gy

It is important to note that the unit of Gy (or rad) is valid for all sort of radiation and this is a physical unit measuring energy absorption in tissue. However, it does not quantify an effect of this energy absorption on living cells. It was shown already in early 20th that equal exposure to different types of radiation do not necessarily produce equal biological effects. One gray of alpha radiation, for example, will have a greater effect than one gray of beta radiation. When we talk about radiation effects, we therefore express the radiation in units called **Sieverts. One Sievert of radiation produces a constant biological effect regardless of the type of radiation.** To get the biological effect - so called DOSE EQUIVALENT - of given DOSE (energy intake) one has to multiply this DOSE with a **Quality Factor** - **QF** . QF has a simplified definition:

QF is the (biologcal) effect of a given energy intake (DOSE) of a given sort of radiation normalized (compared) to energy intake (DOSE) of röntgen (gamma) radiation.

Consequently, Sievert describes biological effects of absorbed radiation. More strict definition of QF will be given later.

Quality factors - QF - are determined based on the degree of ionization produced in water by the passage of radiation through it. Water is the major constituent of soft body tissue and ionization is responsible for harmful effects in living cells. The currently accepted quality factors are presented in Figure 6.1 and listed in Table I.

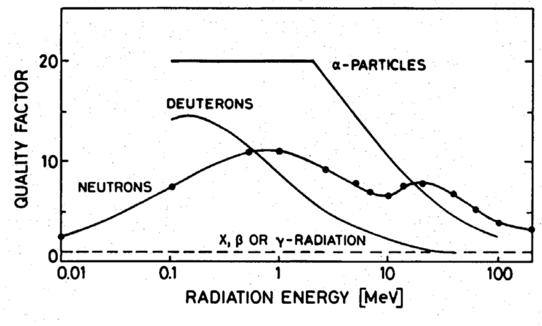

Figure 6.1 Quality factor for different radiation as a function of energy

Table I. Quality factor for various radiation type

Radiation	QF
X, γ, **β** - radiation	1
Thermal neutron	3
Recoil protons, fast neutrons, α-particles	20
Heavy ions	20

6.3 Glossary of terms and definitions of quantities in radiation protection

Absorbed Dose:

denoted as D, is the quotient of dε by dm, where dε the mean energy imparted by ionising radiation to matter of mass dm, thus:

$$D = \frac{d\bar{\varepsilon}}{dm}$$

The unit of absorbed dose is Joule per kilogram, J kg-1 and its special name is gray (Gy)

Dose Equivalent:

denoted as H, is the product of Q and D at a point in tissue, where D is the absorbed dose and Q is the quality factor at that point, thus

H=QD

The unit of dose equivalent is Joule per kilogram (J kg^{-1}) and its special name is Sievert (Sv)

Effective dose:

a summation of the equivalent doses in tissues or organs, each multiplied by the appropriate tissue weighting factor. It is given by the expression

$$E = \sum_T w_T H_T$$

where HT is the equivalent dose in tissue or organ, and w_T is the tissue weighting factor for tissue, T. The effective dose can also be expressed as the sum of the doubly weighted absorbed dose in all the tissues and organs of the body.

Effective Dose Equivalent:

denoted as HE, is the weighted average of the mean dose equivalents, each weighted by a tissue or organ weighting factor, thus:

$$H_E = \sum_T w_T H_T$$

where HT, is the mean dose equivalent in tissue, T, and w_T is the tissue weighting factor for tissue, T, as formerly recommended by the ICRP.

Energy Imparted:

denoted as e, by the ionising radiation to matter in a volume given by:

$$\varepsilon = R_{in} - R_{out} + \sum Q$$

where R_{in}, is the radiant energy incident on the volume, i.e. the sum of all the energies (excluding rest energies) of all those charged and uncharged ionising particles that enter the volume; R_{out} is the radiant energy emerging from the volume, i.e. the sum of all the energies (excluding rest energies) of all those charged and uncharged ionising particles that leave the volume; and ΣQ is the sum of all changes of the rest mass energy of nuclei and elementary particles in any interactions that occur in the volume. (In the sum, decreases are denoted by (+) and increases are denoted by (-)). The expectation value of ε, termed the mean energy imparted and denoted ε, is closely related to the definition of the absorbed dose, D.

Equivalent Dose:

denoted as $H_{T,R}$, is the absorbed dose in an organ or tissue multiplied by the relevant radiation weighting factor, thus:

$$H_{T,R} = w_R \; D_{T,R}$$

where $D_{T,R}$ is the absorbed dose averaged over the tissue or organ, T, due to radiation R, and w_R is the radiation weighting factor for radiation, R. When the radiation field is composed of radiations with different values of w_R, the absorbed dose is subdivided into blocks, each multiplied by its own value of ws and summed to determine the total equivalent dose, i.e.,

$$H_T = \sum_R w_R \; D_{T,R}$$

The unit of equivalent dose is Joule per kilogram (J kg^{-1}) and its special name is Sievert (Sv).

Fluence :

denoted as Φ, is the quotient of dN by da, where dN is the number of particles incident on a sphere of cross-sectional area da, thus:

$$\Phi = \frac{dN}{da}$$

Kerma, K:

The quotient of dE_{tr} by dm, where dE_{tr} is the sum of the initial kinetic energies of all the charged ionising particles liberated by uncharged ionizing particles in a volume element of mass dm, thus:

$$K = \frac{dE_{tr}}{dm}$$

The unit of kerma is Joule per kilogram (J kg^{-1}) and its special name is Gray (Gy).

Linear Energy Transfer :

or linear collision stopping power, L, of a material, for a charged particle, is the quotient of dE by dl, where dE is the mean energy lost by the particle, owing to collisions with electrons, in traversing a distance dl, thus:

$$L = \frac{dE}{dl}$$

Organ Dose:

for radiation protection purposes. It is the mean absorbed dose, D_T, in a specified tissue or organ of the human body, T, given by:

$$D_T = \frac{1}{m_T}\int_{m_T} D\,dm \quad or \quad \frac{\varepsilon_T}{m_T}$$

where mT is the mass of tissue or organ, D is the absorbed dose in the mass element dm, and eT is the total energy imparted in the tissue or organ.

Quality Factor:

A function, Q, of unrestricted linear energy transfer L, in water. Values of Q(L) as a function of L are in in ICRP Publication 60 (ICRP, 1991a) by the following relations:

$$Q(L) = 1 \qquad (L < 10)$$

$$Q(L) = 0.32\,L - 2.2 \quad (10 \le L \le 100)$$

$$Q(L) = \frac{300}{\sqrt{L}} \qquad (L > 100)$$

Where L is expressed in keV mm^{-1}

The mean quality factor, Q_T, in a specified tissue or organ, T, is given by

$$Q_T = \frac{1}{m_T D_T}\int_{m_T} Q D\,dm$$

where D_T is the mean absorbed dose to the tissue or organ, m_T is its mass, and Q and D are the quality factors and the absorbed dose in the mass element dm, respectively.

Relative Biological Effectiveness, RBE_M :

the ratio of the absorbed dose of a reference radiation to the absorbed dose of a given test radiation required to produce the same level1 of response, all other conditions being kept constant. The subscript M refers to a stochastic effect.

6.4 How much radiation is dangerous?

The following list and Table II give an indication of the likely effects of a range of radiation doses to the whole body:

10,000 mSv (10 Sieverts) in a short-term dose would cause immediate illness and subsequent death within a few weeks. See Figure 6.2 for comparison with even higher doses.

1,000 mSv (1 Sievert) in a short term dose would probably cause (temporary) illness such as nausea, but not death, and would probably cause cancer many years later in 5 of every 100 persons exposed to this dose.

20 mSv per year averaged over 5 years is the limit for nuclear industry employees and uranium or mineral sands miners.

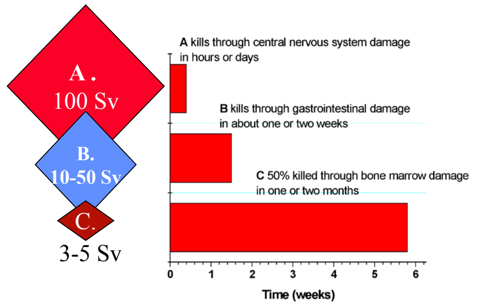

Figure 6.2 Doses cause death

10 mSv/yr is the maximum actual dose received by uranium miners, many people in Sweden living in radon-rich area are getting from 10 to 20 mSv/year.

2 mSv/yr (approx) is the normal background radiation from natural sources. This is close to the minimum dose received by all humans on earth.

0.05 mSv, a fraction of natural background radiation, is the design target for maximum annual radiation at the perimeter fence of a nuclear electricity generating station. In practice the actual dose is less

Table II. Highest allowable doses of radiation

	Maximum perimitted doses
Personal in radioactive work	50 mSv/year 100 mSv during 5 following years 700 mSv - life-dose
Highest permitted dose-rate	0.01 mSv/s
General public	5 mSv/year
Natural radiation	2.0 mSv/year
Allowable design dose-parameters for nuclear power plants	0.05 mSv/year

6.4.1 The health risks of radiation

Many things potentially of great benefit to humanity have associated risks when used. Radiation falls into this category. However, radioactive materials should only be used where the benefits significantly outweigh the risks.

Ionising radiation is only one of hundreds of things that may cause serious health effects in humans. The degree of damage caused by radiation depends in turn on many factors - dose, dose rate, type of radiation, the part of the body exposed, age and health, for example.

It has been known for many years that large doses of ionising radiation, very much larger than background levels, can cause a measurable increase in cancers, leukemias ('cancer of the blood'),and genetic mutations that affect future generations - see Table III and Table IV. But what are the chances of developing cancer from low doses of radiation? We know roughly the risk of developing cancer from radiation after dose equivalents of one gray as a result of studies of A-bomb survivors and other irradiated populations. We also know, of course, that the risk from zero radiation exposure, were such a thing possible, would be zero. But we know little of the effects of intermediate doses, and so have to try to extrapolate estimates of risks at low doses from what we know about the risks at high ones. Figure 6.3 shows various ways in which this can be done.

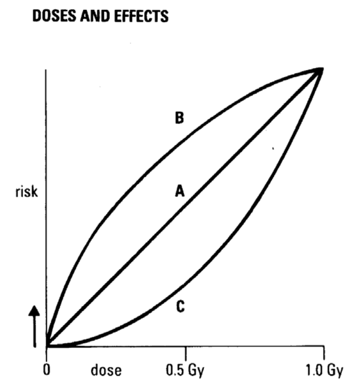

Figure 6.3 Dose to risk extarpolations to low doses

Table III. Symptoms after aquiring a dose of 4-6 Sv in short time

0-48 h	Loss of apetite, vomiting, fatique exhau
2 days - 6-8 weeks	Above syptoms disappear, patient feel b
2-3 weeks up to 6-8 weeks	Internal bleeding, diarrhoea, tremors, loss of hair, letargy, cramps, coma, death
6-8 weeks	Healing

Table IV. Threshold doses for several effects

Stage of development	Effect Threshold	dose (Sv)
Embryo	Small head circumference	0.04
Fetus	Diminished body growth Increased infant mortality	0.2
Child	Hypothyroidism	5.00
Adult	Opacity of the eye lens	2.50
Adult	Death	2.00-3.00
Adult	Aging	3.00
Adult	Erythema ((reddening of the skin)	3.00-10.00
Male adult	Temporary sterility	0.5-1.00
	Permanent sterility	>5.00
Female adult	Permanent sterility	3.00-4.00

Very generally speaking, three sorts of graphs could be drawn between the fixed points of zero and one gray (assuming that there is no **threshold,** and that therefore any increase in dose will produce an increased risk of cancer, however small). One graph (A) is a straight line. assuming that the risk increases steadily in direct proportion to the dose. The second (B) is convex, suggesting that the riskrises steeply at low doses and more slowly at high ones. The third (C) is concave. suggesting, incontrast, that the risk rises only gradually at low doses and faster at high ones. Commonly, linear dependency - graph A - is assumed. In practice one also assumes at doses below 10 millisieverts the risks are so small that the effects are not measurable.

There is also a delay of many years between a person's exposure to a potential cause of cancer and the appearance of the disease. This makes it difficult to say with any certainty which of many possible agents were the cause of a particular cancer. Cigarette smoking, dietary factors and sunlight are among the most probable causes of cancer. Radiation used improperly can increase health risks. Large doses of radiation directed at a tumour are used in radiation therapy to kill cancerous cells, while much larger doses are used to kill harmful bacteria in food, and to sterilise bandages and other medical equipment.

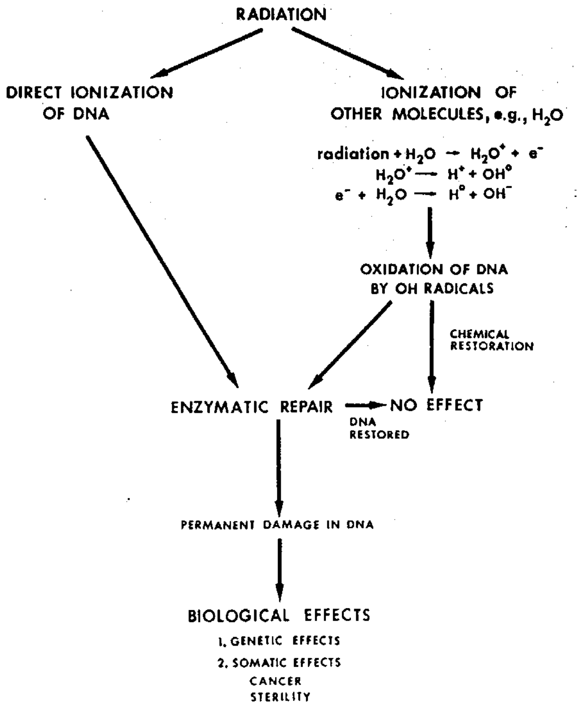

Figure 6.4 Sequence of events occuring in living matter exposed to radiation.

Figure 6.4 shows the sequence of events happening om a cell level in living materia exposed to radiation. One can see that living cells have significant capacity for self-reparation of damages originated from radiation.

6.5 Protection from radiation

Because exposure to ionising radiation carries a risk, should we avoid it entirely? Even if we wanted to, this would be impossible. We have already said that radiation has always been present in the environment and in our bodies. We can however avoid undue exposure.

We have a range of simple, sensitive instruments capable of detecting minute amounts of radiation from natural and man-made sources. In addition there are four ways in which we can protect ourselves - time, distance, shielding and containment:

Time: For people who are exposed to radiation through their work in addition to natural background radiation, the dose is reduced and the risk of illness made almost nil by limiting exposure time.

Distance: In the same way that heat from a fire is less the further away you are, so the intensity of radiation decreases the further you are from the source of the radiation.

Shielding: Barriers of lead, concrete or water give good protection from penetrating radiation such as gamma rays. Radioactive materials are therefore often stored or handled under water, or by remote control in rooms constructed of thick concrete or lined with lead (see Table V).

Containment: Radioactive materials are confined in the smallest possible space and kept out of the environment. Radioactive isotopes for medical use, for example, are dispensed in closed handling facilities, while nuclear reactors operate within closed systems with multiple barriers which keep the radioactive materials contained. Rooms have a reduced air pressure so that any leaks occur into the room and not out from the room.

Table V. Radiation shielding for various type of radiation

Radiation	Shielding
Electrons	Low-Z materials, e.g. polystyrene or lucite. High-Z materials should be avoided because of brems-strahlung production. For intense electron sources, a double layer shield consisting of an inner layer of low-Z material followed by a layer of Pb (or some other high-Z material) to absorb bremsstrahlung should be used. The inner layer should, of course, be sufficiently thick to stop the electrons while outer layer should provide sufficient attenuation of the brems-strahlung.
Positrons	High-Z material. Since the stopping of positrons is always accompanied by annihilation radiation, the shield should be designed for absorbing annihilation radiation. A double layer design, here, is usually not necessary.
Charged particles	High density materials in order to maximize dE/dx.
Neutrons	Hydrogenous materials such as water or paraffin. As for electrons, this shielding should be followed by a layer of Pb or other high-Z matrial in order to absorb γ's from neutron capture reactions.

6.6 Radiation and environment

Individuals receive radiation exposure from sources in the environment and from other manmade sources of radiation. In fact, every individual, regardless of occupation, residence, or protective measures, receives exposure from these sources of radiation. The average radiation exposure is approximately 3.5 mSv/year from all sources. Figure 6.5 represents the magnitudes of various sources of radiation. Radiation from environmental sources is often referred to as background radiation.

6.6.1 Natural Background Radiation

Natural background radiation has always been present and was in man's environment long before the invention of the atomic bomb, nuclear reactors, and other man-made sources. This radiation comes from the sun (cosmic radiation); radioactive material in the earth's surface, air, and water; and radioactive material in the human body.

The radioactive decay of a parent nuclide may result in a radioactive daughter which may in turn result in another radioactive daughter. This situation is called a radioactive decay series. There are three naturally occurring radioactive decay series which date back to the formation of the earth and still exist due to the long half-lives of the parent radionuclide. These series are termed the:

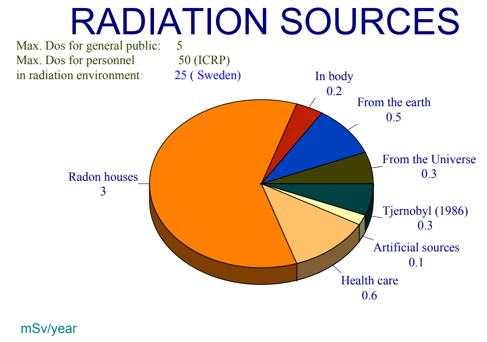

Figure 6.5 Sources of radiation and their contribution to our annual exposure in Sweden

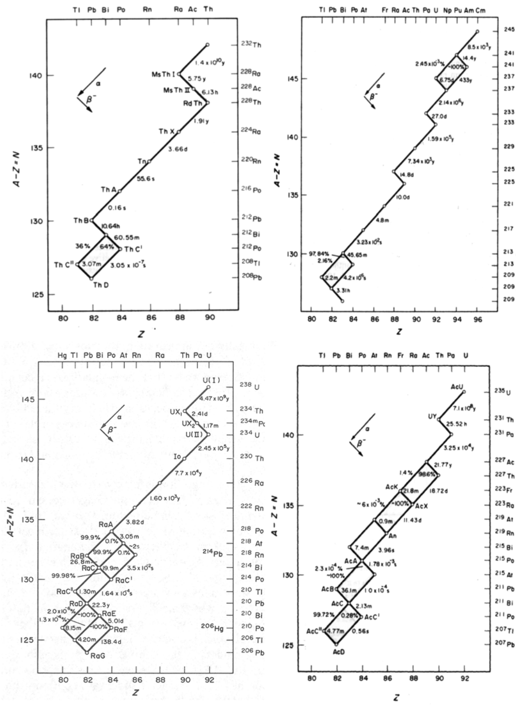

Figure 6.7 Natural radioactive series

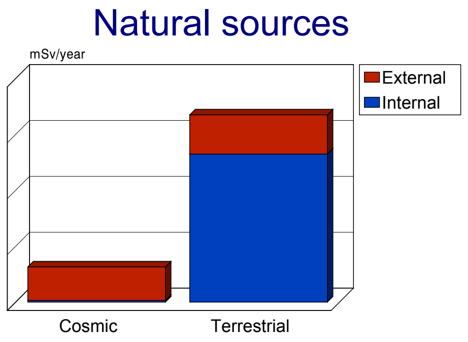

Figure 6.6 Natural sources of radiation

Thorium Series (4N)

Uranium Series (4N+2)

Actinium Series(4N+3)

A fourth long-lived series is manmade - see Figure 6.7:

Neptunium Series (4N+1)

See Figure 6.6 for diagram showing cosmic and terrestial contribution to natural radioactivity

Cosmic Radiation

Cosmic radiation, radiation coming from the sun, was discovered during attempts to reduce background radiation. Scientists had assumed that all background radiation was due to radioactive material in the air and ground. Based on this hypothesis, if a radiation detector is raised far above the earth's surface, the background should be reduced. However, detectors carried to high altitudes by balloons actually showed an increase, rather than a decrease in background radiation. These experiments and other data showed that radiation was coming from outer space.

Before entering the earth's atmosphere, cosmic radiation mainly consists of protons and alpha particles. Following interaction with atoms in the earth's atmosphere, electrons, photons, protons, and neutrons are created. These radiations, in turn, produce secondary radiations as they collide with atoms or decay on the way to the ground.

Figure 6.8 presents cosmic radiation levels at different heights. One can ask a simple question: how many transatlantic flights has to be done annually to double the annual allowable does (5 mSv/a)?

Radioactive Material in the Earth

Radioactive material in the soil such as uranium, radium, and potassium 40 (^{40}K), emit small levels of radiation. These naturally occurring radionuclides have been present in the soil since the earth was created. The amount of radioactive material in the soil is high dependent upon location. Certain areas of soil in Brazil, France, and India contain enough radioactive material to cause an average gamma dose above 10 mSv/year. Building materials such as granite, bricks or concrete contain radioactive material that also contributes to the dose received from natural radioactivity.

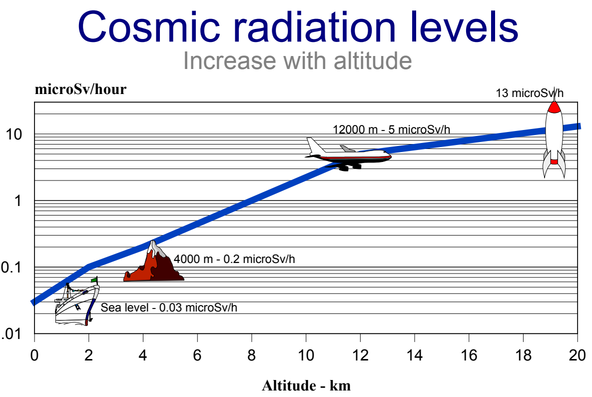

Figure 6.8 Cosmic radiation levels at different altitudes

Radioactive Material in the Air

The radioactive material in the air is primarily due to the decay of radioactive material in the soil since the earth was created. ^{238}U decays to ^{226}Ra, which decays to the gas ^{222}Rn. The decay of ^{224}Ra produces another gas ^{220}Rn, called thoron. These radioactive gases seep out of the earth or from building material and become airborne. As can be expected, the quantity of these gases present in the air depends upon the amount of the radioactive material present in the soil, the porosity of the surface, meteorological conditions and ventilation of enclosed areas. Higher levels are usually found indoors than outdoors. In addition to radon and thoron, minute amounts of ^{14}C and ^{3}H (both created by cosmic radiation) are also present in air.

Radon by far contributes the most to the annual exposure of the population in Sweden. Figure 6.9 shows in somewhat simplified way the decay chain of ^{238}U which lead to radon production.

The amount of radioactive material present in water depends upon the source of the water. Most well water contains trace amounts of uranium, thorium, and radium. Sea water contains higher concentrations of ^{40}K.

Radioactive Material in the Human Body

Radioactive material in the soil, water, and air is transferred to man by the food chain. The main radionuclides of concern in the body are ^{40}K, ^{226}Ra, ^{228}Ra, and ^{14}C of these, ^{40}K - see Figure 6.10 - is the most abundant.

Exposure Estimates from Background Radiation

Scientists estimate that the average person in Swedish. population receives a total of about 3.5 mSv per year from all of the sources of natural background radiation. This number may vary considerably based on altitude, area of the country and the type of building in which you live. Figure 6.5 presents more detailed data about the average radioactive exposure in Sweden.

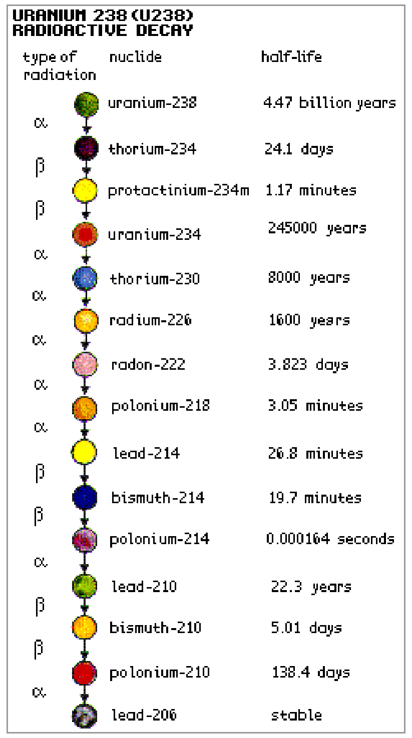

Figure 6.9 Uranium-238 decay chain leading to radon production

6.6.2 Manmade Sources of Radiation

In addition to natural background radiation, there are several sources of manmade radiation. Radiation comes from fallout as a result of atomic weapons. The medical profession uses x-rays and radiation sources to help diagnose and treat illnesses. Individuals also receive radiation exposures as a result of the operation of experimental and commercial reactors.

$$ {}^{40}_{19}K \rightarrow {}^{40}_{20}Ca + \beta^- $$

$$ T_{1/2} = 1.28 \cdot 10^9 \; år $$

$$ <\gamma> = 1461\,keV $$

$$ <\beta_-> = 1.3\,MeV $$

$$ <\beta_+> = 44\,keV $$

$$ SpA = 2.0 \cdot 10^5 \, Bq/g $$

Figure 6.10 Basic data of ^{40}K decay

A. Fallout

Fallout is the term given to debris that settles to earth as the result of an above ground atomic bomb blast. After an air burst, fission products, un-fissioned nuclear material, and weapon residues vaporized by the heat of the fireball condense into a fine suspension of small particles 10 nm to 20 µm in diameter. These particles may be quickly drawn up into the stratosphere, particularly if the explosive yield exceeds 10 kt. The amount of time it takes for fallout to reach the earth depends on the height of the cloud and meteorological conditions. It may take up to 5 years for most of the material to reach the earth. Most short half-lived radionuclides would decay before returning to earth. The radionuclides of particular concern are ^{131}I, ^{89}Sr, ^{90}Sr, and ^{137}Cs. The average dose to an individual from fallout has been about 0.02-0.08 mSv/year and today does not exceed 0.02 mSv/year.

Atmospheric nuclear weapon tests almost doubled the concentration of radioactive ^{14}C in the Northern Hemisphere, before levels slowly declined following the Partial Test Ban Treaty.

Initially little was known about the dispersion of nuclear fallout on a global scale. Ity was assumed that fallout would be dispersed evenly across the globe by atmospheric winds and gradually settle to the Earth's surface after weeks, months, and even years as worldwide fallout. Nuclear products were deposited in the Northern Hemisphere becoming however more dangerous than they had originally been estimated.

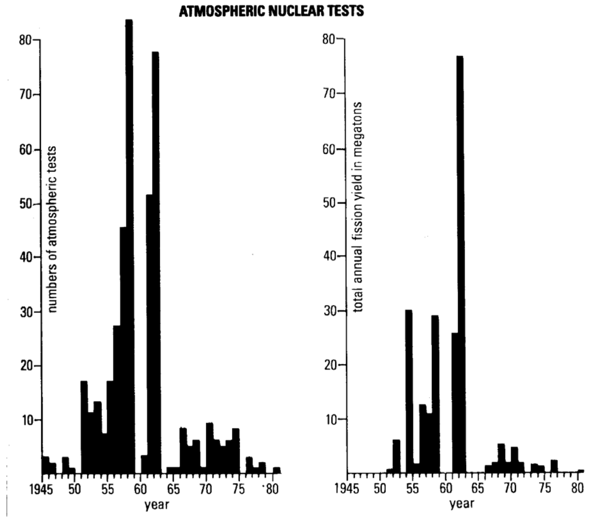

Figure 6.11 Number and yield of nuclear tests in atmosphere. In 1963 US and Soviet Union signed the atmospheric test ban treaty

The radio-biological hazard of worldwide fallout is essentially a long-term one because of the potential accumulation of long-lived radioisotopes (such as strontium-90 and caesium-137) in the body as a result of ingestion of foods containing the radioactive materials. This hazard is less pertinent than local fallout, which is of much greater immediate operational concern.

Nuclear weapon test left very large areas contaminated by radiation. The worst cases are most probably the nuclear test site Semipalatinsk, today in Kazkhstan and Novay Zemlya in Russia. The Semipalatinsk Test Site (STS or Semipalatinsk-21) was the primary testing venue for the Soviet Union's nuclear weapons. It is located on the steppe in northeast Kazakhstan (then the Kazakh SSR), south of the valley of the Irtysh River. The Soviet Union conducted 456 nuclear tests at Semipalatinsk from 1949 until 1989 with little regard for their effect on the local people or environment. The full impact of radiation exposure was hidden for many years by Soviet authorities and has only come to light since the test site closed in 1991. Area of ~18,000 km^2 was heavily contaminated and the general consensus of health studies conducted at the site since it was closed is that radioactive fallout from nuclear testing had a direct impact on the health of about 200,000 local residents.

Figure 6.12 Soviet "Superbomb" - 200 Megaton of TNT in one single bomb and one of the smalledt nuclear shell of 2 kt of TNT.

B. Medical Exposure

Sources of medical radiation exposure include x-rays used for diagnosing or treating patients, radioactive material administered to patients in liquid or gaseous form, and treatments for cancer therapy. The average direct exposure received by an individual in the general population from medical uses of radiation is about 1mSv per year

Figure 6.13 W. Gudowski at Ground-0 of Semipalatinsk Nuclear Test Site - a place for the first Soviet nuclear bomb test.

In 2008 about 84000 examinations using ^{99m}Tc were performed at Swedish hospitals together with about 7000 PET (Positron Emission Tomography) examinations using ^{15}O, ^{11}C and ^{18}F. In 2009 more than ^{2800} therapies were done. About 65% was treatment of benign thyroid diseases. Other therapies are performed with ^{153}Sm, ^{32}P, and ^{90}Y, and nearly 300 with ^{177}Lu-octreotate for treatment of neuroendocrine tumors. In total, about 106000 nuclear medicine examinations and radionuclide therapies are performed in Sweden today giving a frequency of 11.8 per 1000 people. .

The rapid pace of change in nuclear medicine makes assessment difficult, but a few trends can be identified . Of the many different radionuclides used in nuclear medicine examinations, ^{99m}Tc and ^{131}I are the most important. As a rule, the dose per procedure is less for ^{99m}Tc, which has a shorter half-life, so it is preferred and used in the majority of cases. However, the most commonly used radionuclide in developing countries is ^{131}I, and this is the main reason the average effective dose per examination is higher in these countries than in industrialized countries. The number of diagnostic nuclear medicine examinations increased in industrialized countries in the 1970s, but remained relatively constant in the 1980s. The frequency of examinations is expected to increase in developing countries,like China where more than 1000 hospitals now practice nuclear medicine.

One of the important developments is that new ^{99m}Tc-labelled compounds are replacing established compounds containing other radionuclides. Other important trends are the introduction of complex biological agents (such as radiolabelled monoclonal antibodies) for novel imaging applications and the proliferation of new compounds for studies with positron emission tomography (PET). The proliferation of single photon emission computed tomography (SPECT) and PET are expected to lead to the wider use of radioisotopes. Computed X-ray tomography and magnetic resonance tomography both provide higher resolution, however, which means that purely anatomical imaging is not an important procedure in current nuclear medicine practice. Instead, measurements of flow and biochemical reactions are important.

C. Nuclear Reactors and Nuclear Reactor Accidents

The average individual that does not work at the plant, receives an average of only 0.001 mSv/year as a result of the production of electricity by nuclear plants. This estimate includes the direct exposure from the plant itself and the dose from the release of radioactive material in air and water from the plant. Regulations have been established to limit the whole body exposure to any individual in the environment surrounding the plant during normal operation to 0.1 mSv per year.

Chernobyl reactor accident in 1986 followed by radioactive release and contamination of large areas in Europe was the most serious nuclear accident in 20th century. An explosion and fire released large quantities of radioactive contamination into the atmosphere, which spread over much of Western USSR and Europe. It is considered the worst nuclear power plant accident in history, and is one of only two classified as a level 7 event on the International Nuclear Event Scale (the other being the Fukushima Daiichi nuclear disaster). From 1986 to 2000, 350,400 people were evacuated and resettled from the most severely contaminated areas of Belarus, Russia, and Ukraine. According to official post-Soviet data, about 60% of the fallout landed in Belarus. Four hundred times more radioactive material was released than had been by the atomic bombing of Hiroshima. The disaster released 1/100 to 1/1000 of the total amount of radioactivity released by nuclear weapons testing during the 1950s and 1960s.Approximately 100,000 km^2 of land was contaminated with fallout, the worst hit regions being in Belarus, Ukraine and Russia. Slighter levels of contamination were detected over all of Europe except for the Iberian Peninsula. See Figure 6.14 for ^{137}Cs fallout over Sweden.

However, the consequences of Chernobyl radioactive fallout in Sweden are considered not to be very serious. The average annual dose to individuals did not exceed 0.03 mSv/50 years compared to about 3.5 - 4 mSv/year coming from natural radioactivity.

D. Miscellaneous Sources

Miscellaneous sources of manmade radiation include common consumer products, such as luminous dials containing tritium or radium, smoke detectors containing americium, static eliminators using polonium, porcelain dentures that contain uranium salts, and plutonium powered pace makers. The average individual is exposed to about 0.0003 mSv per year from consumer products containing radioactive material. An additional source of radiation exposure is fly ash from coal fired generating stations.

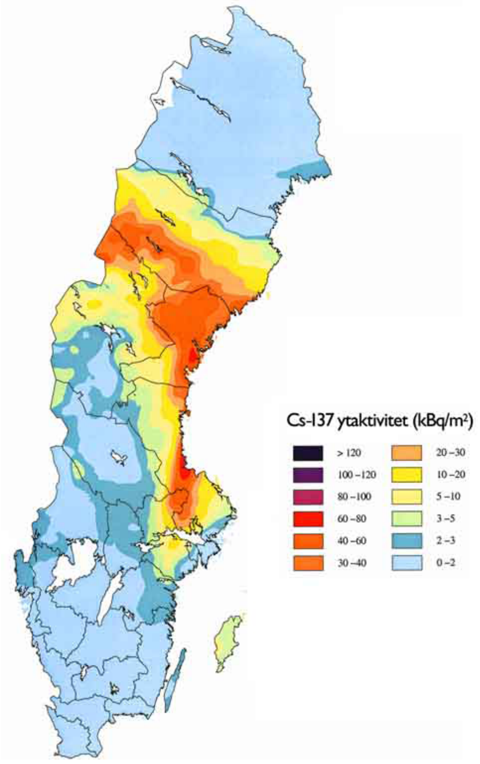

Figure 6.14 Fallout of ^{137}*Cs in Sweden after the Chernobyl accident*

Figure 6.15 W. Gudowski in front of Sarcophagus at Chernobyl

Chapter 7

Neutron Interactions with Matter

7.1 Introduction

Neutrons are uncharged particles with a mass of approximately 1 amu. They are considered as an indirectly ionizing form of radiation. Since they are not influenced by electric fields, they must collide to transfer energy. Therefore, at high energies neutrons are highly penetrating, at low energies they can be readily absorbed. A free neutron is in itself radioactive, decaying by beta emission with a half-life of 10.6 minutes. Neutrons can be produced by neutron sources, nuclear reactors and are emitted spontaneously by some heavy nuclides which spontaneously fission. Some common neutron sources are produced by combining alpha emitting nuclides with beryllium. Some such sources are Po-Be, Ra-Be, Am-Be and Pu-Be.

7.2 Neutron Discovery

In 1932, English physicist and Nobel laureate James Chadwick discovered the neutron. A few years later, Enrico Fermi and his collaborators in Rome discovered that, if various elements are bombarded by neutrons then new radioactive elements are produced. Fermi had predicted that the neutron, being uncharged, would be a useful nuclear projectile, because it is uncharged and therefore receives no electric forces from the nucleus when it approaches the nuclear surface.

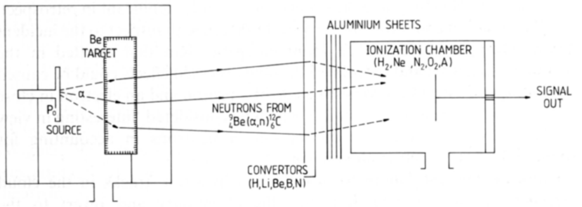

Apparatus used by Chadwick (1932) in his discovery of the neutron. Neutrons in the energy range 0–13 MeV from the reaction $^{9}Be(\alpha, n)^{12}C$ undergo elastic collisions with nuclei of H, Li, Be, B and N in convertor targets, whose energies after transmission through aluminium sheets are measured in an ionization chamber.

Figure 7.1 Schematic diagram of Chadwick neutron discovery experiment

For details of the Chadwick experiment - ***click here***.

James Chadwick showed that beryllium (Be), when exposed to an alpha particles, gave off a particle which was not deflected (accelerated) by electric or magnetic forces. The particle was thus uncharged, yet it was massive enough to knock protons out of a sample of paraffin (which is rich in hydrogens) - see Figure 7.1.

To explain "strange" radiation from beryllium, I. Curie and F. Joliot had proposed a reaction:

$$ {}_{4}^{9}Be + {}_{2}^{4}He \rightarrow {}_{6}^{13}C + Energy $$

however experiments contradicted this assumption. To resolve this experimental inadequacy Chadwick suggested another nuclear reaction explanation:

$$ {}_{4}^{9}Be + {}_{2}^{4}He \rightarrow {}_{6}^{12}C + {}_{0}^{1}n + Energy $$

which was in a good agreement with his experiment as shown on Figure 7.1. The neutron was discovered.

PARTICLE PROPERTIES OF NEUTRON

***MASS*:**

m_n = 1.008665012 u

1.6749543 x 10^{-27} kg

939.5731 MeV

***ELECTRIC CHARGE*:**

q_n = -(1.5 ± 2.2) x 10^{-20} e

ELECTRIC DIPOLE MOMENT

d < 6 x 10^{-25} e cm

***MAGNETIC DIPOLE MOMENT*:**

μ_n = -1.04187564 x 10^{-3} μ_B

1.04066884 x 10^{-3} μe

- 0.68497935 μ_p

- 1.91304308 μ_N

***NEUTRON DECAY*:**

n ---> $p + e^- + n + Q_0$

τ = 925 ± 11 s

$T_{1/2}$ = 641 ± 7.6 s

QUANTIZED PROPERTIES OF THE NEUTRON:

Spin -	J = 1/2
Intrinsic parity -	P = +1
Isospin -	I = 1/2
Component of isospin -	I_3 = -1/2
Baryon number -	B = 1
Lepton number -	$L = L_e = L_\mu = 0$
Strageness -	S = 0
Hypercharge -	Y = 1
Charm -	c = 0
Bottomness -	b = 0
Topness -	t = 0
Quark structure	udd

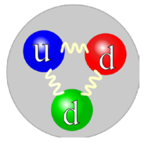

7.3 Neutron Sources

Different reactions and different processes can be used as sources of neutrons. The most common neutron sources can be classified as

- Radioisotope neutron sources
  + ^{252}Cf spontaneous fission sources
  + (α-n) sources
  + (γ- n) sources
- Nuclear reactors as neutron sources
- Accelerator-based neutron sources
  + Neutron sources based on proton and deuterium bombardment and consequent nuclear reactions
  + Electron accelerator and photonuclear reactions
  + Spallation neutron sources

7.3.1 Radioisotope neutron sources

Neutron sources that are based on the use of radioactive materials have been widely utilized in radiation laboratories for many years. In fact, the technique dates back to the described above discovery of the neutron by Chadwick in 1932, where the first observed neutrons were produced by bombarding targets of boron or beryllium by alpha particles from the radioactive decay of polonium. In addition to using reactions induced by alpha particles, practical radioisotope neutron sources have also exploited gamma ray induced photonuclear reactions and spontaneous fission. These sources share a number of relative advantages compared with other sources of neutrons. They are of small size and therefore quite portable, relatively low in cost, and are characterized by a very reliable neutron yield of predictable intensity. Their 100% duty cycle and complete freedom from maintenance considerations are in marked contrast with accelerator-based neutron sources.

These sources also have a number of significant limitation. In order to produce useful yields, relatively large activities of the various isotopes are required, necessitating careful fabrication techniques and attention to radiological safety precautions in their use. Even with relatively active sources, however, the neutron yield is often limited to several orders of magnitude below that obtainable with competing techniques. The neutrons that are produced have a fixed energy spectrum that is often quite broad. while many of the radio- isotopes used have half-lives that are very long, same short-lived isotopes require frequent replenishment or reactivation. Also, some of these neutron sources may also produce gamma rays that can interfere with some applications and, in extreme cases, nay require special handling techniques.

Despite these shortcomings, radioisotope neutron sources have been used in an impressive array of applications in nuclear science, medicine, and industrial research. They are widely employed as calibration sources for neutron instrumentation, as portable sources in neutron activation and radiography, and in other applications where a simple and portable neutron source is required.

The Calfornium-252 spontaneous fission source

The spontaneous fissioning of a heavy nucleus is the only radioactive decay process of useful half-life in which neutrons are directly emitted. All heavy nuclei are in principle unstable against spontaneous fission, and the process has been observed in both naturally occurring and artificially produced radionuclides. Virtually all these same nuclei decay predominantly by alpha emission and spontaneous fission is a substantially less probable mode of decay. Nonetheless, in some cases the fission decay probability is sufficiently high so that the prompt fission neutrons from reasonable activities of the material can provide a neutron source of practical intensity.

One nuclide, Cf, is the overwhelming favourite for the manufacture of spontaneous fission sources. This radioisotope has become widely available through its production in high flux nuclear reactors. The starting material is normally either ^{242}Pu or ^{243}Am obtained from reprocessed reactor fuel. A thermal neutron flux of at least 10^{15} n/cm^2 .s is required in the subsequent irradiation to promote multiple neutron capture and the buildup of heavier isotopes. After 10 neutron captures and 4 intervening beta decays, Pu is converted into Cf . Very high neutron fluxes are required because of the length of this chain and the fact that several isotopes (^{246}Cm and ^{248}Cm) along the way have very low capture cross sections. After the irradiation, the californium is separated through solvent extraction and purified by ion exchange chromatography. Figure 7.2 shows the decay scheme of ^{252}Cf .

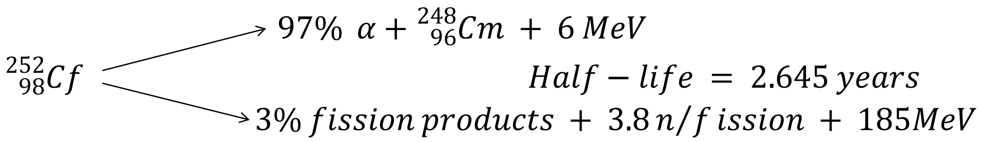

Figure 7.2 Decay scheme of ^{252}Cf

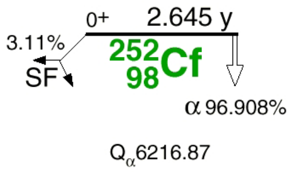

Figure 7.3 Decay scheme of ^{252}Cf in nucleaus energy level notation

The purified material can be fabricated into practical sources in a number of different ways. One common procedure is to electroplate the material from a dilute nitrate solution on a platinum-iridium wire. Alternatively, the californium can be co-precipitated with iron as a hydroxide, converted to an oxide by heating, and compressed into a small pellet. Terbiurn is sometimes used as a carrier when small sources are made. The active material is then doubly encapsulated, typically using platinum alloys for small sources, and stainless steel, aluminum, or Zircaloy-2 for those of larger size. Useful sources of only a few millimeters in dimension have been successfully produced.

Neutron Yield and Decay Properties

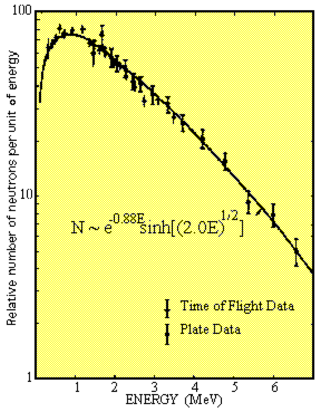

Figure 7.4 Fission neutrons energy spectrum of ^{252}Cf

About 3% of the decays are by spontaneous fission and 97% are by alpha emission The 2.65 year half- life is short enough that the fission specific activity is relatively high, but also long enough to allow neutron sources of practical lifetime. The neutron yield is 0.116 n/s per Bq, where the activity is the combined alpha and fission decay rate. Because one microgram of the material will yield 2.34 x 10^{12} n/s, very small amounts of the isotope are sufficient to make useful sources. In contrast with the other radioisotope sources described later that typically require many grams of material, californium sources involve only milligrams of the isotope. They can therefore be made physically very small, with the limits usually set by encapsulation requirements. Sealed sources are available that contain a wide range between a few micrograms to 5 milligrams of the material. Neutron output of greater than 10 n/s is therefore achievable in a single source.

Each fission event yields an average of 3.75 neutrons with a measured time-of-flight spectrum illustrated in Figure 7.4.

The fission fragments, alpha particle, and beta stopped within the source combine to produce a heat output of 39 Watts per gram of the isotope. While not important for small sources, some provision may be required for heat dissipation when very large Cf sources are used.

RADIOISOTOPE (α,n) SOURCES

Neutrons can be produced by alpha bombardment of suitable light targets. Because the alpha particles can be obtained from a number of convenient isotopes, this approach historically has been the most common means of manufacturing small portable neutron sources. Early versions were fabricated using polonium or radium, naturally occurring alpha emitters. Modern sources instead usually use one of the artificially produced transuranic isotopes because of their more favourable decay properties and/or freedom from unwanted secondary radiation.

Table I shows some properties of the more commonly used alpha active isotopes. The half-life is important from several standpoints. It must obviously be long enough to permit practical use of the source without excessive loss of yield from decay. On the other hand, the half-life should not be unnecessarily long so that the specific activity of the isotope, which is inversely proportional to half-life, remains reasonably high. Only then can a high neutron yield be achieved within a small physical volume of the source. The alpha particle energy is also of some importance. The higher the alpha energy, the greater will be the neutron yield for a specific activity.

Table I. Some characteristics of radioisotopic neutron sources

Source	Half-life	Reaction	Neutron yield(n s^{-1} g^{-1})	Neutron energy(MeV)
^{124}Sb-Be	60.9 d	(γ,n)	10^{10}	0.024
^{140}La-Be	40.2 h	(γ,n)	10^7	2.0
^{210}Po-Be	138 d	(α,n)	10^{10}	4.3
^{241}Am-Be	458 y	(α,n)	10^7	~4
^{226}Ra-Be	1620 y	(α,n)	1.3×10^5	~4
^{227}Ac-Be	21.8 y	(α,n)	1.1×10^9	~4
^{239}Pu-Be	24 400y	(α,n)	10^9	~4
^{228}Th-Be	1.91 y	(α,n)	1.7×10^{10}	4
^{252}Cf	2.65 y	fission	2.34×10^{12}	2.3

Many sources have been made using Pu as the alpha emitter. Its low specific activity has led to more recent interest in shorter-lived emitters for the fabrication of neutron sources of high yield. ^{241}Am is one such candidate, and Am-Be neutron sources are now also widely available. Still higher specific activity is possible from the curium isotopes, but their availability as a byproduct of reactor fuel reprocessing has been much more limited. Because of its convenient 18-year half-life, Cm may well become the alpha emitter of choice in future sources of this type.

The alpha particle emitters listed in Table I are seldom available in isotopically pure form. Other isotopes present with the principal emitter can have an influence on the decay behaviour of the source. Some caution should therefore be exercised in assuming that the neutron yield will decrease exactly with the half-life of the primary isotope. For example, many Pu-Be sources have been fabricated from samples of plutonium that contain a significant fraction of Pu. This isotope beta decays with a half-life of 13.2 years to form ^{241}Am, an alpha emitter. Any ^{241}Pu present in the original source will therefore gradually convert to ^{241}Am and add to the alpha particle yield. For sources in which ^{239}Pu is the principal emitter, an isotopic fraction of only 0.7% of Pu will result in an initial increase in the neutron yield of about 2% per year.

Some of the common alpha emitters (e.g., Pu) have large fission cross sections for thermal neutrons. Under some circumstances, the neutron yield from sources made with these isotopes can be slightly increased by the contribution of fission neutrons. If the source is placed in or near a moderating medium, some of the primary neutrons can become thermalized and re-enter the source. The resulting neutron-induced fission may increase the apparent neutron yield by as much as 1 to 2%.

Neutron-Producing Reactions and Energy Spectra

By far the most common target material used in (alpha,n) sources is beryllium. Neutrons are produced through the reaction:

$$ {}^{9}_{4}Be + {}^{4}_{2}He \rightarrow {}^{12}_{6}C + {}^{1}_{0}n + Energy $$

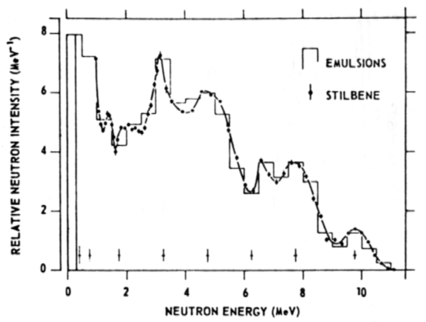

Figure 7.5 Neutron energy spectrum from a ^{239}Pu/Be source containing 90 g of the isotope

The neutron energy spectra from all alpha-Be sources are quite similar. Because the alpha particles can lose a variable amount of energy before undergoing reaction, the neutron energy spectrum is quite broad, and the relatively small differences in the initial alpha particle energy (as seen at Table I) have relatively little effect. An energy spectrum measured for a typical Pu-Be source is shown in Figure 7.5. Some success has been achieved in relating the observed structure in this spectrum to the different excited states in which the product ^{12}C nucleus can be left after the reaction.

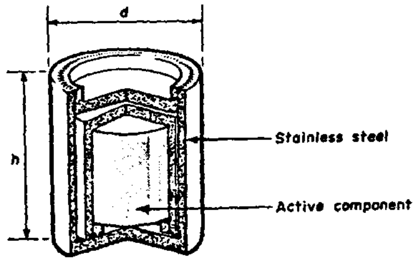

Figure 7.6 The double walled construction of Be (α,n) source

Other target materials will also produce neutrons when bombarded by alpha particles of typical energy like B, F, ^{13}C and ^{7} Li. The neutron yield is substantially less for all of these reactions than from beryllium. The reaction Q-values are also much smaller, and the resulting neutron spectra have lower average neutron energies. In some applications, the softer nature of the spectra can offset the intensity disadvantage .

A sketch of typical source construction is showed in Figure 7.6.

PHOTONEUTRON SOURCES

The combination of a high energy gamma ray emitter and a suitable target material has also been widely applied for neutron sources. These photoneutron sources are generally based on one of the following reactions:

$$ {}^{2}_{1}H + h\nu \rightarrow {}^{1}_{1}H + n + Q(= -2.226MeV) $$

$$ {}^{9}_{4}Be + h\nu \rightarrow {}^{8}_{4}Be + n + Q(= -1.66MeV) $$

In these two target nuclei, deuterium and beryllium, the binding energy of the last neutron is exceptionally low. Therefore, it is possible to liberate a neutron through the absorption of a gamma ray photon with energy low enough to be available from common radioisotope sources. All other target nuclei are of no practical interest because of their much higher binding energies.

The threshold gamma ray energy required for photoneutron production is just the absolute value of the reaction Q-value shown above.

The principal disadvantage of photoneutron sources is the inconvenience caused by the large gamma ray activities needed to produce useful intensities of neutrons . For sources of typical construction a neutron yield of 10 n/s requires a gamma ray activity of approximately 10^{10} Bq. These very high gamma ray activities generally necessitate remote handling techniques. Furthermore, the large gamma ray background may interfere with many neutron experiments.

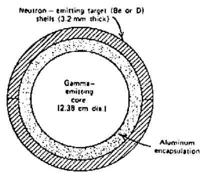

Figure 7.7 Configuration of a simple spherical photoneutron source

A sketch of typical source construction is showed in Figure 7.7.

Many of the sources have a sufficiently short half-life so that their use is practical only near a nuclear reactor facility where they can be freshly prepared. One exception is the antimony-beryllium (Sb-Be) source, with a half-life of 60 days. These sources have been used for many years in industrial applications, and have been fabricated with neutron yields as high as 1010 n/s. The energy spectra shown in Figure 7.8 were obtained by Monte Carlo calculations for the dimension shown in Figure 7.7, and already show evidence of this energy degradation caused by scattering within the source materials.

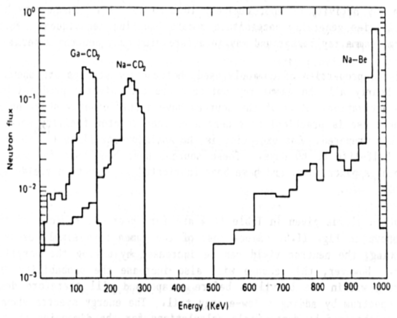

Figure 7.8 Calculated neutron spectra for three different photoneutron sources. The gamma emitters are either ^{72}Ga or ^{24}Na.

In contrast with other radioisotope neutron sources, photoneutron sources can be designed to be switched on and off. The gamma ray emitter is then separately encapsulated and is removed from the beryllium or deuterium target when neutron production is to be stopped.

7.3.2 Nuclear reactors as neutron sources

Nuclear reactors are the most "obvious" neutron sources for a reactor physicist. During our lectures we shall talk a lot about reactors - at this moment we mention only some of the most interesting reactors used as neutron sources. Two types of reactors are used for neutron based research: steady state reactor and pulsed reactors. Reactor given the highest neutron flux today is HFR (High Flux Reactor) at Institute Laue-Langevin (ILL) in Grenoble (France). Figure 7.9 shows layout of HFR reactor, and its thermal neutron spectrum at Figure 7.10.

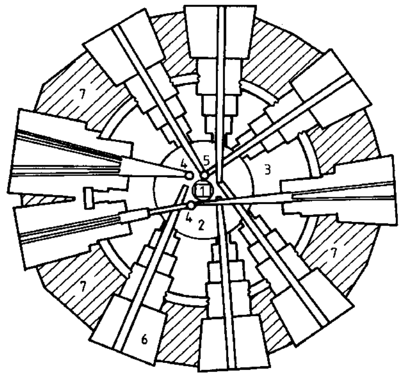

Figure 7.9 HFR reactor in Grenoble: 1. Core. 2 Heavy water reflector. 3 Light water pool. 4 Cold source. 5 Hot source. 6 Horizontal channel. 7 Concrete shield

High Flux Isotope Reactor (HFIR) - see Figure 7.11 - at Oak Ridge National Laboratory (USA) operating at 85 MW, HFIR is the highest flux reactor-based source of neutrons for research in the United States, and it provides one of the highest steady-state neutron fluxes of any research reactor in the world. HFIR is a beryllium-reflected, light-water-cooled and -moderated, flux-trap type reactor that uses highly enriched ^{235}U as the fuel. The image at Figure 6.12 is a cutaway

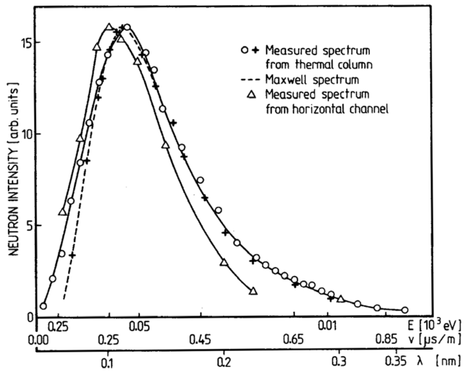

Figure 7.10 Thermal neutron spectrum of HFR reactor.

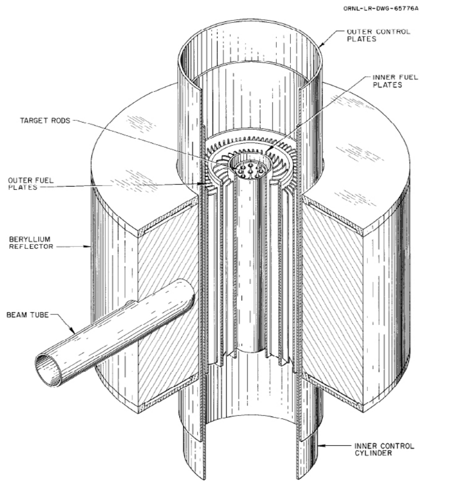

Figure 7.11 A simplified sketch of High Flux Isotope Reactor - HFIR

of the reactor which shows the pressure vessel, its location in the reactor pool, and some of the experiment facilities. The preliminary conceptual design of the reactor was based on the "flux trap" principle, in which the reactor core consists of an annular region of fuel surrounding an unfueled moderating region or "island" (see cross section view). Such a configuration permits fast neutrons leaking from the fuel to be moderated in the island and thus produces a region of very high thermal-neutron flux at the center of the island. This reservoir of thermalized neutrons is "trapped" within the reactor, making it available for isotope production. The large flux of neutrons in the reflector outside the fuel of such a reactor may be tapped by extending empty "beam" tubes into the reflector, thus allowing neutrons to be beamed into experiments outside the reactor shielding. Finally, a variety of holes in the reflector may be provided in which to irradiate materials for later retrieval.

The thermal and cold neutrons produced by HFIR are used to study physics, chemistry, materials science, engineering, and biology. The intense neutron flux, constant power density, and constant-length fuel cycles are well utilized for neutron scattering research into the fundamental properties of condensed matter.

Figure 7.13 shows a sketch of the fast-pulsed reactor IBR-2 in Dubna, Russia. Two rotating reflectors in a form of a fork , when passing close to the reactor core, put reactor into supercritical state and produce a strong neutron pulse. The peak power of this reactor is of the order of 7700 MW at the average power of only 4 MW. Figure 7.14 shows a control room of IBR-2 reactor in Dubna.

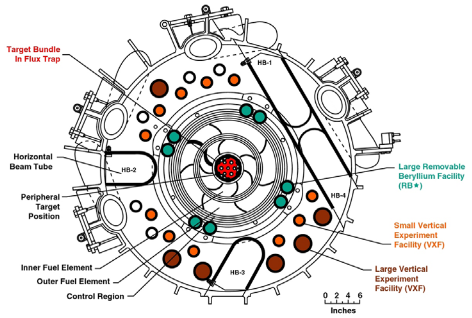

Figure 7.12 HFIR - a cutaway of the

7.3.3 Accelerator-based neutron sources

Neutron sources based on proton and deuterium bombardment and consequent nuclear reactions

These neutron sources are based on use of electrostatic generators or cyclotrons. The nuclear reactions which produce neutrons are induced by charged particle beams which are accelerated by different type of accelerators onto appropriate targets. The target material are usually the pure element or a chemical compound in the solid state, while a gas target may be used where source reactions between two hydrogen isotopes are involved. The most common neutron source reactions used for many years are the :

$^{7}Li(p,n)^{7}Be$

$^{3}H(d,n)^{3}He$

$^{2}H(d,n)^{3}He$

$^{3}H(d,n)^{4}He$

$^{1}H(t,n)^{3}He$

$^{1}H(7Li,n)^{7}Be$

where particles in the parentheses are beam and projectile particles, isotopes outside parentheses - target material and target products.

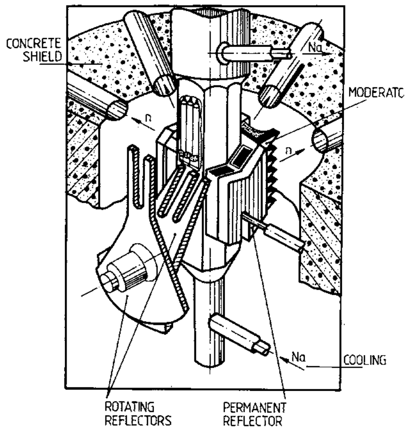

Figure 7.13 A simplified sketch of the IBR-2 reactor

Electron accelerator and photonuclear reactions

High-energy electrons incident in a thick heavy-mass target produce, in a first instance an electron-photon cascade. In a second step, Bremsstrahlung from electrons striking the target material initiates photonuclear reactions end if the target consists of fissile material, photofission reactions. This leads to the emission of neutrons with an evaporation type of spectrum. The emission of gamma rays from Bremsstrahlung is almost proportional to the Z-number of the target nucleus and to the energy of the incident electrons. The cross sections of photonuclear (gamma,n) and photofission (gamma,f) reactions exhibits a pronounced resonance in the so-called "giant" resonance region. For heavy nuclei, (gamma,n) and (gamma,f) "giant" resonances are centered around 15 MeV and have a half width of about 5 MeV. In addition, the photon spectrum from Bremsstrahlung has an energy dependence of approximately 1/E. The energy of an electron accelerator must therefore be appreciably higher than 30 MeV if a high average neutron source strength is to be obtained. Neutron yields and energy spectra from electron bombardment of heavy-element targets have been investigated experimentally and theoretically in several laboratories. Experimental studies are, however, restricted to limited electron energies and target materials, and thus need to be supplemented by suitable theoretical calculations in order to derive more general information.

Figure 7.14 Control room of IBR-2 reactor

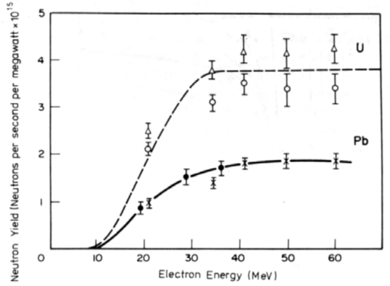

Figure 7.15 Neutron yields from electron beam interactions, yield per second and megawatt electron beam power from thick uranium and lead targets

Neutron yields from electron beam interactions can be calculated satisfactorily from electron-photon cascade models and well known photonuclear and photofission cross sections. Precise (gamma,n) cross sections have been measured. Figure 7.15 shows absolute experimental neutron yield for thick uranium and lead targets.

The characteristics of neutron production, have some important consequences for the most effective use of electron accelerators for pulsed white neutron sources:

- With low-power dissipation in the target, an accelerator with Ee = 30-40 MeV is reasonable.
- With high beam intensities, it is more advantageous to accelerate the electrons to higher energies because fast electrons are stopped over longer distance in the target, and thus cooling of

the target is facilitated

Increasing the electron energy far beyond about 100 MeV is not attractive because high energy machines are large and involve expensive buildings and shielding. The trend in design of electron linacs has in the past been towards higher peak currents, with flexibility in pulse length and repetition rate.

Spallation neutron sources

Spallation neutron sources consist basically of an accelerator providing a beam of high-energy (~1 GeV) protons or possibly heavier ions and a suitable target of heavy-element material - see Figure 7.16.

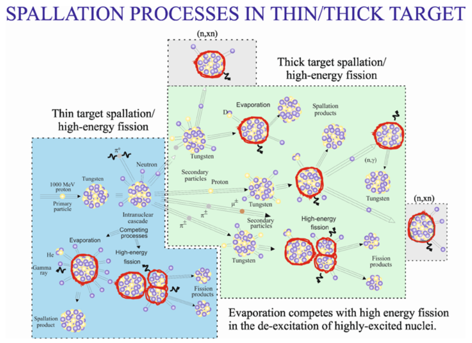

Figure 7.16 Spallation processes in thin/ thick target

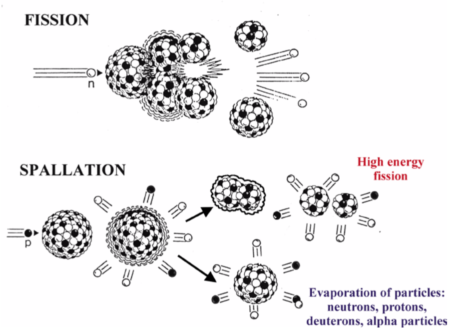

Figure 7.17 Schemtaic comparison between fission and spallation

The spallation reaction has been known for decades to cosmic-ray physicists and astrophysicists through the role it plays in determining the mass distribution of cosmic rays impinging on the earth. In masonry, spalling is the operation of breaking off splinters of stone with a chisel. In physics, the spallation reaction is the braking off of nucleons, singly and in clusters, from a nucleus by an energetic bombarding particle. Cosmic rays produce spallation reaction products in collision with interstellar natter, the products coming from both the breakup of the struck nuclei and from the projectile if the latter is a nucleus .

In the laboratory, the spallation reaction has been known since 1947 when E.O. Lawrence first observed secondary neutrons from a uranium target bombarded by 90 MeV neutrons. In 1948 it was observed that the fission of bismuth by 190 keV deuterons was preceded by the emission of 12 neutrons. Today, there is no clear-cut dividing line between spallation reactions and lower-energy nuclear reactions; when the energy of the incident particle or nucleus exceeds about 100 MeV, the reaction is said to be a spallation reaction . At lower energy the compound-nucleus model successfully accounts for many features of nuclear reactions as a large fraction of the incident particle's energy is dissipated within the target nucleus.

The copious accelerator-based neutron production from the spallation reaction began to be exploited soon after its discovery.

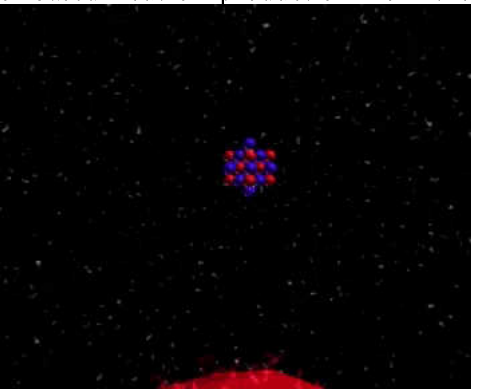

Figure 7.18 Click on for a spallation process animation

As a result of the in intense neutron sources based on the spallation reaction, neutron yields and spectra were measured for protons and deuterons of intermediate energies on thick targets at several laboratories.

How does spallation differ from fission - Figure 7.17?

- In the number of low energy neutrons produced: 2.5 (-1 for chain reaction) for fission vs up to 40-50/spallation.
- In the amount of energy deposited per neutron produced. For fission: about 120 MeV per useful neutron, for spallation (tungsten target and 1000MeV protons) - 25 MeV per neutron.
- In the amount of g-ray energy produced. 12 MeV per fission event and ~3 MeV per spallation neutron.
- In the energy spectrum of the neutrons produced. High energy tail for spallation neutrons in the forward direction.
- In the radiation damage to materials. Spallation evaporation phase produces enormous amount of hydrogen (hydrides) and helium (swelling and embrittlement).

Figure 7.19 shows the normalized neutron production per proton and GeV a function of proton energy and for different target materials. Flattening of the curves indicate that from the certain proton energy, number of neutrons is proportional to the beam power - current and proton energy are exchangeable.

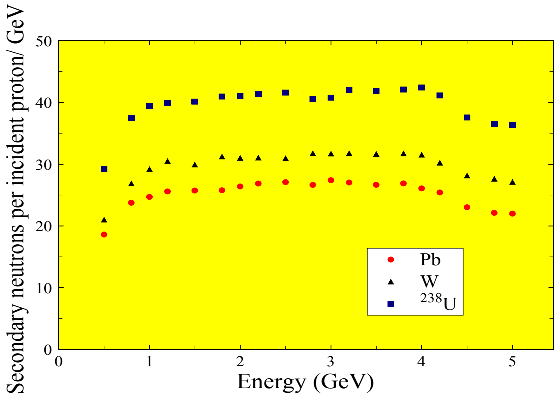

Figure 7.19 Neutron yield per incident proton and GeV for different target materials as function of the proton energy. (FLUKA-simulation code results)

Figure 7.20 shows a spectrum of spallation neutrons resulting from 1.6 GeV protons impinging at Pb/Bi spallation target. Red line shows neutron fission spectrum for comparison. One should pay attentionto double logarthmic scale of the plot.

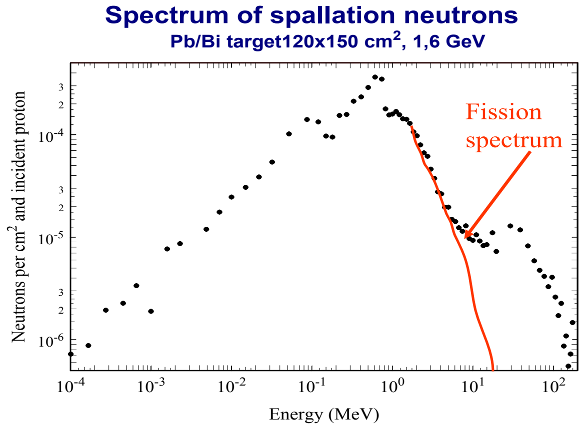

Figure 7.20 Spectrum of spallation neutrons resulting from 1.6 GeV protons impinging at Pb/Bi spallation target(FLUKA-simulation code results).

Powerful spallation neutron sources are for the time being at 3 laboratories: Oak Ridge National Laboratory (USA) hosting Spallation Neutron Source (SNS) facility, at Paul Scherer Institute (PSI) in Zürich (cyclotron-driven), and at Los Alamos National Laboratory.

The Spallation Neutron Source (SNS) is an accelerator-based neutron source designed and constructed by a unique partnership of six US national laboratories: Argonne, Lawrence Berkeley, Brookhaven, Jefferson, Los Alamos, and Oak Ridge - see Figure 7.21. As of September 1, 2007 it is the most powerful pulsed spallation neutron source in the world. At the end of 2007 SNS was recorded in the Guinness book of records.

The SNS process is, briefly:

- Negative hydrogen ions (a proton with two electrons) are first generated in pulses;
- **accelerated to 1 GeV** (almost 90 percent of the speed of light) by a linear accelerator using both standard and superconducting techniques;
- stripped of electrons and concentrated into a 2 MW proton beam of less than 1 μs pulses at 60

Hz in an accumulator ring;

- directed at a liquid mercury target (chosen for mercury's large nucleus containing many neutrons and its liquid form at ambient conditions capable of absorbing rapid temperature rise and intense bombardment shock) in the target building, which ejects 20 to 30 neutrons per mercury nucleus hit by a proton (spalling in all directions);
- which are slowed down by moderators to useful energies;
- and applied through 18 surrounding beam lines to various materials and interfaces;
- where up to 24 instruments chosen by users record the results for interpretation. Examples of the neutron scattering instruments to be used are a backscattering spectrometer for high resolution spectroscopy, and magnetism and liquid reflectometers for studies of surfaces and interfaces.

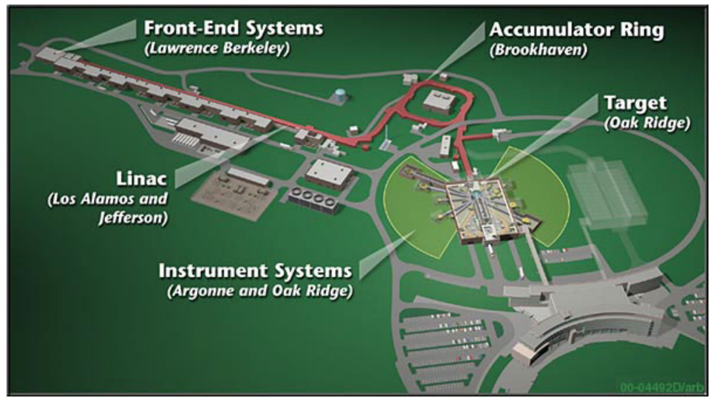

Figure 7.21 A view of an SNS-site

The European Spallation Source (ESS), is to be built **in Sweden at Lund** - see Figure 7.22. It will provide intense beams of neutrons and high-quality instruments for experiments across a wide range of research disciplines in both fundamental science and technologically important fields – from electronics and materials science to biomedicine and environmental science. The facility is expected to open in 2019 and will be fully operational in 2025. At present 17 partner countries are represented in the ESS Steering Committee.

Figure 7.22 A view of a future ESS site

The laboratory is designed around a linear accelerator in which protons are accelerated and collide with a heavy metal target. By this process, intensive pulses of neutrons are emitted and led through beamlines to experimental stations, where research on materials is done as part of the scientific front line in energy, telecommunications, manufacturing, transportation, information technology, biotechnology, and health. ESS will become 10 times more powerful than existing facilities in the US and Japan (J-Parc).

7.4 Interactions of neutrons with the matter

Neutrons are classified in accordance with their energy values. Table II lists five neutron categories and their energy values.

Neutron interactions result in the scattering or in the absorption of the neutron. Neutron scattering reaction may be elastic or inelastic in nature. All scattering reactions result in the decrease in energy of the neutron and an increase in the energy of the absorber. Neutrons released at high energies collide and lose energy to become thermalized.

Table II. Neutron Energy Ranges

Classification	Kinetic Energy
Thermal	0.025 eV
Slow	<1 keV
Intermediate	1 keV - 0.5 MeV
Fast	0.5 MeV - 10 MeV
High Energy	>>10 MeV

7.4.1 Potential Scattering: Elastic Scattering

Elastic scattering of neutrons is primarily responsible for the slowing down of neutrons released from fission. These interactions transfer kinetic energy and momentum from the neutron to the colliding medium. The energy transfer is greatest in materials rich in hydrogen content, water and hydrocarbons for example. An elastic collision with a hydrogen nucleus can cause the ejection of the proton comprising the nucleus. The proton is a charged particle and can cause addition secondary ionization.

Main feature: Kinetic energy conserved in the interaction

Potential scattering is a process in which the incident neutron is scattered or bounced off the nucleus, and it can be regarded as similar to the collision of two billiard balls of unequal mass. The nucleus re mains unchanged and at its ground state of energy during the process which involves only a transfer of kinetic energy between the neutron and the nucleus. Often the kinetic energy of the incident neutron is much greater than that of the nucleus and as a result of the interaction the neutron emerges with reduced kinetic energy. The laws of conservation of kinetic energy and conservation of momentum are both valid for this type of interaction, which for this reason is often called elastic scattering. Consider a neutron of mass m moving with velocity e, towards a nucleus of mass M. In many interactions the speed of the neutron is much greater than that of the nucleus, and the latter can be assumed to be at rest. The situation as viewed in the laboratory (L system) is shown in Figure 7.23 (L-system). We will now adopt a system of coordinates in which the centre-of-mass of the neutron-nucleus pair is at rest. In the L system the centre-of-mass is moving towards the nucleus with a velocity given by

$$\hat{v}_c = \frac{1}{M+m}\hat{v}_1$$

with velocities of neutron and nucleus in the CM-system

$$\hat{u}_1 = \frac{A}{M+m}\hat{v}_1\, ;\ \hat{U}_1 = -\frac{1}{M+m}\hat{v}_1$$

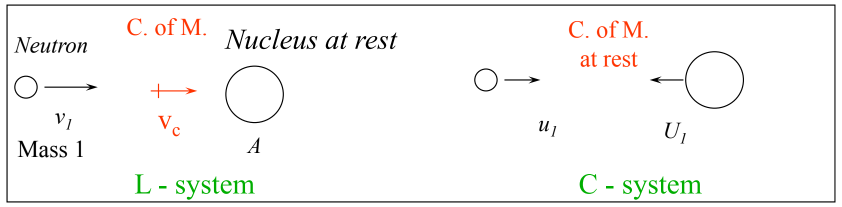

Figure 7.23 Model of a neutron collisiom in laboratory system (L-system) and in a centre of the mass (CM) system.

Consequently, momentum and kinetic energy conservations equations can be written as

$$m\hat{u}_1 + M\hat{U}_1 = 0$$

$$m\hat{u}_2 + M\hat{U}_2 = 0$$

$$\frac{1}{2}mu_1^2 + \frac{1}{2}MU_1^2 = \frac{1}{2}mu_2^2 + \frac{1}{2}MU_2^2$$

$$U_1 = U_2$$

$$u_1 = u_2$$

$$E_c = \frac{1}{2}mu_1^2 + \frac{1}{2}MU_1^2 = \frac{1}{2}\frac{mM^2}{(m+M)^2}v_1^2 + \frac{1}{2}\frac{Mm^2}{(m+M)^2}v_1^2$$

$$= \frac{1}{2}\frac{mM}{(m+M)}v_1^2$$

$$= \frac{M}{m+M}E_1$$

As mass of neutron m=1 and mass of nucleus M~A the equations above can be rewritten as:

$$\hat{v}_c = \frac{1}{A+1}\hat{v}_1 \,;\; \hat{u}_1 = \frac{A}{A+1}\hat{v}_1 \,;\; \hat{U}_1 = -\frac{1}{A+1}\hat{v}_1$$

$$E_c = \frac{A}{A+1}E_1$$

Collision in CM-system - vector analysis

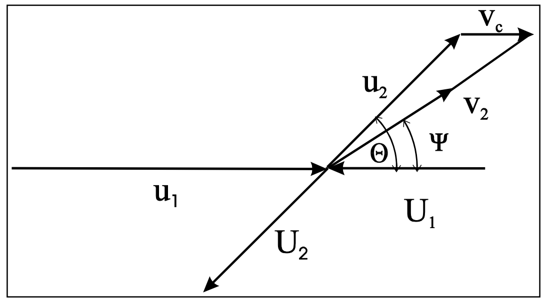

Figure 7.24 Neutron velocity after elastic scattering - vector analysis

Equation below shows that the neutron speed or energy

$$v_2^2 = u_2^2 + v_c^2 + 2u_2v_c\cos\Theta$$

$$v_2^2 = v_1^2\left\{\frac{A^2+1+2A\cos\Theta}{(A+1)^2}\right\}$$

$$E_2 = E_1\left\{\frac{A^2+1+2A\cos\Theta}{(A+1)^2}\right\}$$

after elastic scattering is a function of the energy before collision, the mass number of the scattering nucleus and the angle of scattering in the C system - see Figure 7.24. Let us consider two extreme cases. Firstly, if a glancing collision occurs in which the neutron is barely deflected, θ=0, and $E_2 = E_1$. The neutron energy is unaltered as a result of a glancing collision. Secondly, if θ = 180°, corresponding to a head-on collision as a result of which the neutron bounces back along its original path, cos θ = – l. For this case equation becomes:

$$E_2 = E_1\left(\frac{A-1}{A+1}\right)^2$$

$$\alpha = \left(\frac{A-1}{A+1}\right)^2$$

$$\frac{E_1 - E_2}{E_1} = (1-\alpha)$$

This represents the maximum fractional loss of energy that a neutron can suffer as a result of an elastic scattering collision; it is a function of the mass number of the scattering nucleus and as the mass number decreases, the maximum fractional loss of energy increases. In the limiting case for hydrogen, A = 1, a = 0 and a neutron can lose all its energy in a single head-on collision.

7.4.2 Compound Nucleus Formation

The process of compound nucleus formation involves firstly the absorption of the incident neutron into the original nucleus to form a compound nucleus:

$${}^{A}_{z}X + {}^{1}_{0}n \rightarrow \left[{}^{A+1}_{\;z}X\right] \rightarrow Y + b$$

When the compound nucleus is formed it must be at rest in the C system to conserve zero momentum, and so its kinetic energy is also zero. It follows that the kinetic energy of the neutron-nucleus pair before the reaction in the C system is transformed into excitation energy of the compound nucleus. The total excitation energy of the compound nucleus is E, + B, where B is the binding energy of a neutron in the nucleus of A+1X. For example when a low energy neutron is absorbed in boron-10 to form boron-11 the latter is formed at 11.4 MeV above its ground state. If the incident neutron had an energy of 1 MeV the boron-11 would be formed at 12.3 MeV above its ground state.

Capture

The excited compound nucleus decays immediately and emits either a particle or gamma radiation or both, and it is the product of the decay that distinguishes one type of compound nucleus interaction from another. If the compound nucleus decays to its ground state by the emission of gamma radiation only, then the complete interaction is called a capture, or sometimes radiative capture or (n, g) reaction because the effect is to capture the original neutron and emit gamma radiation. Shorthand notation for this reaction is:

$$X + n \rightarrow Y^* \rightarrow Y + \gamma$$

The Y* indicates an excited compound nucleus.Two examples of this reaction are:

$$^{23}_{11}Na+{}^{1}_{0}n\rightarrow{}^{24}_{11}Na^{*}+\gamma$$
$$or\quad{}^{23}Na(n,\gamma)\,{}^{24}Na$$

$$^{238}_{92}U+{}^{1}_{0}n\rightarrow{}^{239}_{92}U^{*}\rightarrow{}^{239}_{92}U+\gamma$$
$$or\quad{}^{238}U(n,\gamma)\,{}^{239}U$$

Radiative capture is the predominant absorption mechanism for low energy neutrons.

If the excited compound nucleus decays by the emission of an alpha particle, the reaction is known as an (n, α) reaction. If the product nucleus after the emission of the alpha particle is above its ground state of energy, it will decay to the ground state by the emission of gamma radiation.

Which decay channel "choose" the nucleus after being in excited state? Let's take example of excited Al-nucleus $\left({}^{27}_{13}Al\right)^{*}$. Al can become excited and can deexcite on different ways as shown below:

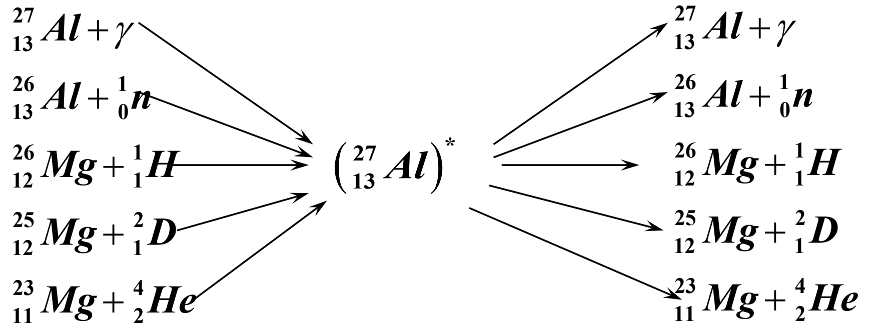

Then balance of mass determines the reaction channel:

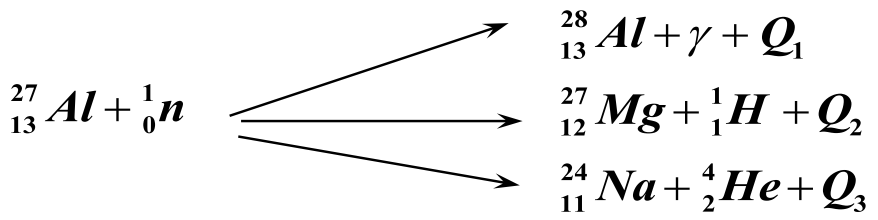

Energy and mass balance for these reactions gives:

Mass of $^{27}_{13}Al$:	26.990081
Mass neutron:	1.008986
Summa:	27.999067
Mass of $^{28}_{13}Al$:	27.990771
Difference:	+0.008296

Q1 = +0.008296 × 931 MeV = 7.72 MeV

For other reactions:

Q2 = -2.03 MeV

Q3 = -3.18 MeV

Only Q1 is positive and possible as a reaction channel, neutron absorption in Al will lead to:

$$^{27}_{13}Al+{}^{1}_{0}n\rightarrow\left({}^{28}_{13}Al\right)^{*}\rightarrow{}^{28}_{13}Al+\gamma+Q1$$

Examples of different reactions (reaction channels):

- Neutron capture (n,γ)

  $$^{23}_{11}Na+{}^{1}_{0}n\rightarrow{}^{24}_{11}Na^{*}+\gamma$$
  $$or\quad{}^{23}Na(n,\gamma)\,{}^{24}Na$$

  $$^{238}_{92}U+{}^{1}_{0}n\rightarrow{}^{239}_{92}U^{*}\rightarrow{}^{239}_{92}U+\gamma$$
  $$or\quad{}^{238}U(n,\gamma)\,{}^{239}U$$

-
- Emission of α-particle (n,α)

  $$^{10}_{5}B+{}^{1}_{0}n\rightarrow\left({}^{11}_{5}B\right)^{*}\rightarrow{}^{7}_{3}Li+{}^{4}_{2}He$$
  $$or\quad{}^{10}_{5}B(n,\alpha)\,{}^{7}Li$$

  $$^{6}_{3}Li+{}^{1}_{0}n\rightarrow{}^{4}_{2}He+{}^{3}_{1}H$$
  $$or\quad{}^{6}_{3}Li\,(n,\alpha)\;{}^{3}_{1}H$$

  $$^{3}_{2}He+{}^{1}_{0}n\rightarrow{}^{1}_{1}H+{}^{3}_{1}H$$
- $$or\quad{}^{3}_{2}He(n,p)\,{}^{3}_{1}H$$
- Emission of proton (n,p)

  $^{14}_{7}N+{}^{1}_{0}n\rightarrow{}^{14}_{6}C+{}^{1}_{1}H$ (^{14}C–production in the atmosphere)

- $^{31}_{15}P+{}^{1}_{0}n\rightarrow{}^{31}_{14}Si+{}^{1}_{1}H$
- Neutron "multiplication" through (n,2n), (n,3n)

  $^{63}_{29}Cu(n,2n)\;{}^{62}_{29}Cu$

- $^{65}_{29}Cu(n,2n)\;{}^{64}_{29}Cu$

7.4.3 Inelastic Scattering - (n,n')

If the compound nucleus decays by the emission of a neutron, the interaction is effectively a scattering process, although the emitted neutron is not necessarily the same as the incident neutron. If the nucleus resulting from the emission of the neutron (which is of course identical with the original nucleus) is still at an excited state of energy, it decays to its ground state by the emission of gamma radiation, and a process of this type is referred to as inelastic scattering (INS). The law of conservation of kinetic energy is not valid for inelastic scattering since some of the original kinetic energy is transformed to gamma radiation, and the total kinetic energy is less than it was before the reaction. An important characteristic of this reaction, which only takes place between neutrons of fairly high energy and intermediate and heavy mass nuclei, is that neutrons lose on average much more energy per collision than in the case of elastic scattering with the same nucleus. If often the emission of a neutron from the compound nucleus the original nucleus is formed at its ground state of energy, then kinetic energy is conserved in the reaction and it is called compound elastic scattering. Clearly, as far as the results of the interactions are concerned, potential scattering and compound elastic scattering can be regarded as equivalent, and the sum of these two processes is usually referred to as elastic scattering. In the case of a few of the heaviest elements the compound nucleus may be formed in such a state of excitation that it decays by splitting into two intermediate nuclei of unequal mass. This is nuclear fission and it will be considered in detail in other chapters.

Inelastic neutron scattering is a very powerful experimental technique commonly used in condensed matter research to study atomic and molecular motion as well as magnetic and crystal field excitations. Moreover inelastic neutron scattering of fast neutrons accompanied with prompt gamma - (n,n' γ) is a comonly used technique in explosive inspection systems that can detect a wide variety of substances of security importance like explosive, narcotics and nuclear materials.

Examples of inelastic neutron scattering:

$$^{14}_{7}N + ^{1}_{0}n(fast) \rightarrow ^{14}_{7}N + ^{1}_{0}n' + \gamma(1.64,\ 2.13 \text{ and } 5.11 \text{ MeV})$$

$$^{16}_{8}O + ^{1}_{0}n(fast) \rightarrow ^{16}_{8}O + ^{1}_{0}n' + \gamma(6.13 \text{ MeV})$$

7.4.4 Fission

The last neutron absorption process is nuclear fission. This results in the splitting of a nucleus into smaller components. This reaction is covered in more detail in another lecture (click here to open lecture on fission).

7.5 Neutron flux, neutron cross section for a reaction, reaction rate

It is now necessary to establish a framework for measuring neutron interaction rates quantitatively. These rates do not depend on the direction of neutron motion within the target material so we may visualize for simplicity a situation, which seldom occurs in practice, in which all neutrons are moving in the same direction in a parallel beam. The neutron flux, F, may be defined as the total number of neutrons which pass through a unit area normal to their direction per second. If all the neutrons have the same speed v, and if the neutron density is n neutrons per unit volume, then:

$$d\Phi = ndv$$

$$\Phi = \int_{all\ v} n(v)dv$$

for monoenergetic neutrons

$$\Phi = nv$$

For the case in which neutrons are moving in all directions the neutron flux can be defined as the total track length of all neutrons in a unit volume per second. This definition is consistent with the one given a few lines above for a parallel beam of neutrons, but it does not depend on that condition. Being applicable to neutrons moving randomly in all directions without reference to their direction of motion, it emphasizes the scalar (as opposed to vector nature of the neutron flux. The interaction rate between a beam of neutrons and the nuclei in a target material has been experimentally observed to be proportional:

- to the neutron flux, and
- to the number of atoms in the target, which is assumed to consist of a single isotope.

Consider a beam of neutrons, all of speed v cm/s and density n neutrons/cm^3, incident on a target of area A cm^2 and thickness dx cm containing N nuclei/cm^3, see Figure 7.25.

Interaction rate F in the target material can be expressed as:

$$F \propto \Phi\sigma NV$$

$$\sigma - \text{constant of proportionality:}$$

$$F = \sigma\Phi NV$$

Now,

σ - probability for a reaction between neutron and nucleus is called a microscopic cross-section (X-section).

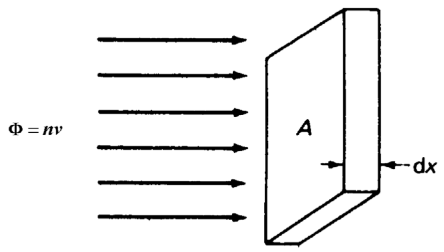

Figure 7.25 Illustration of the interaction rate of neutrons incident on the target A

Units - 1 barn = 10^{-24} cm^2

Σ- macroscopic cross section - $\Sigma = N \times \sigma$ (cm^{-1})

Reaction rate: $F = \Sigma\Phi V$

Interaction probability for a neutron in dx:

$$\frac{\text{Number of neutrons interacting per second in a target of thickness dx}}{\text{Number of neutrons per second incident on the target}} = \frac{\sigma\Phi NAdx}{\Phi A} = \sigma N\,dx = \Sigma\,dx$$

It follows that the macroscopic cross-section can be interpreted as the probability per unit track length that a neutron will interact. The attenuation of a beam of neutrons in a target material can be found by equating the rate of interaction in an element of thickness dx to the difference between the number of neutrons entering and leaving the element per second - see Figure 7.26:

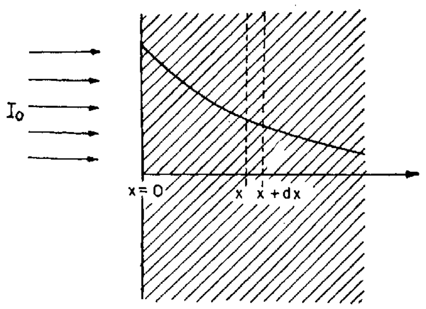

Figure 7.26 Attenuation of neutrons due to an exponential attenuation equation.

Interaction rate = (Flux in - Flux out) × A

$$\sigma\Phi N A dx = -A d\Phi$$

$$\frac{d\Phi}{\Phi} = -\sigma N dx = -\Sigma dx$$

$$\Phi(x) = \Phi_0 e^{-\Sigma x}$$

The average distance that a neutron travels without interacting is known as the mean free path, λ.

Since Σ is the probability of interaction per unit distance, the probability of a neutron interaction within a distance dx beyond x is:

$$p(x)dx = e^{-\Sigma_t x}\,\Sigma_t\,dx$$

the mean free path is then defined as

$$\lambda_t = \frac{\int_0^\infty x\,p(x)dx}{\int_0^\infty p(x)dx} = \frac{\int_0^\infty x\,\Sigma_t\,e^{-\Sigma_t x}dx}{\int_0^\infty \Sigma_t\,e^{-\Sigma_t x}dx} = \frac{1}{\Sigma_t}$$

One can also define n-statistical moments of the neutron flux

$$M_0 = \bar{\Phi}_o = \frac{\int_0^\infty \Phi dx}{\int_0^\infty dx}$$

$$M_1 = \lambda = \frac{\int_0^\infty x\Phi dx}{\int_0^\infty \Phi dx} = \frac{\int_0^\infty x\Phi_0 e^{-\Sigma x}dx}{\int_0^\infty \Phi_0 e^{-\Sigma x}dx} = \frac{1}{\Sigma}$$

and consequently:

$$Scattering - free\,mean\;free\;path:$$

$$\lambda_s = \frac{1}{\Sigma_s}$$

$$Absorption - free\,mean\;free\;path:$$

$$\lambda_a = \frac{1}{\Sigma_a}$$

$$Mean\;free\;path:$$

$$\frac{1}{\lambda_t} = \frac{1}{\lambda_s} + \frac{1}{\lambda_a}$$

Examples of the mean free path;

	1 MeV	**0.025 eV**
H_2O	$\sigma_s^H \sim 10$ b	$\sigma_s^{H2O} \sim 100$ b
$\Sigma_s = N\sigma_s$	$(6\times10^{23}\times2\times10\times10^{-24})/18 = 2/3$	$(6\times10^{23}\times100\times10^{-24})/18 = 10/3$
	λ_s = 1.5 cm	**λ_s= 0.3 cm**
D_2O	$\sigma_s^D \sim 3$ b	$\sigma_s^{D2O} \sim 15$ b
$\Sigma_s = N\sigma_s$	$(6\times10^{23}\times2\times3\times10^{-24})/20 = 0.18$	$(6\times10^{23}\times15\times10^{-24})/20 = 0.45$
	λ_s = 5.5 cm	**λ_s= 2.2cm**

Example:

Calculate the total macroscopic cross-section for H_2O for thermal neutrons (superposition approximation).

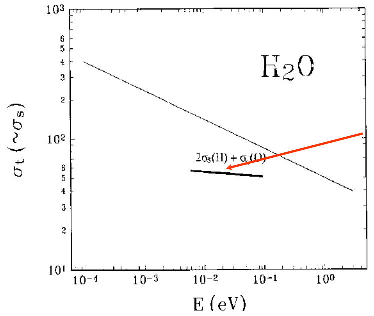

Figure 7.27 Total thermal neutron cross section for water

Data:

ρ_{H2O} = 1 g/cm³

Molecular weight, M = 2×1.008+16 = 18.016

Avogadro's number = 6.023×1023 molecules/mol

$\sigma_{tH} = \sigma_s + \sigma_a = 30.6 + 0.33 = 30.93$ barn

$\sigma_{tO} = \sigma_s + \sigma_a = 4.2 + 0.0002 = 4.2002$ barn

$$\Sigma_t^{H_2O} = \frac{\rho \times A_v}{M}\left(2\times\sigma_t^H + \sigma_t^O\right) = \frac{1.0\times6.023\times10^{23}}{18.016}(2\times30.93+4.2002)\times10^{-24} =$$

$$= 2.201 cm^{-1}$$

$$\sigma_t = 2\times\sigma_t^H + \sigma_t^O = 66\,barns$$

Attention: This is not true - thermal neutrons "see" water molecules and ONE CAN NOT assume that water is a "mixture" of hydrogen and oxygen nuclei (atoms).

7.5.1 Partial Cross-Sections

One defines partial microscopic cross-sections corresponding to the type of neutron interactions with matter:

- **Scattering X-section, σ_s.** Probability that neutron re-emitts from the compound nucleus or that neutron potentially scatters on the nucleus surface: $\sigma_s = \sigma_{n,n} + \sigma_{n,n'} = \sigma_s + \sigma_i$
- **Absorption X-section, σ_a.** Probability that neutron is captured by the nucelus. Absorption can lead to fission, pure capture and other reactions like (n,p), (n,α) etc. $\sigma_a = \sigma_f + \sigma_c$
- **Fission X- section,σ_f** . Probablity that nucleus fission in result of neutron absorption.
- **Capture X-section, σ_c.** Probability that neutron is captured and remains in the excited absorbing nucleus. The nucleus can de-excite thruogh e.g. emission of γ-quanta ($\sigma_{n,\gamma}$)
- **Total X-section, σ_t** $= \sigma_s + \sigma_i + \sigma_f + \sigma_c$

7.5.2 σ(E) - **Energy Variation of Neutron Cross Section**

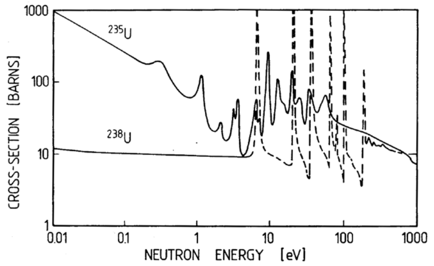

Figure 7.28 Total microscopic neutron neutron cross section for ^{235}U and ^{238}U vs neutron energy

Cross-sections for neutron interactions are in many cases not constant, but vary with neutron energy - see Figure 7.28. A complete description of the variation of cross-sections is beyond the scope our lectures, and we will restrict ourselves to a general view, with a more detailed look at some examples of particular interest in nuclear engineering. In general the variation of cross-section depends on the type of interaction involved, whether scattering or absorption, and the mass number of the element involved. For reasons that will be clear later we will restrict ourselves to neutron energies between 0 01 eV and 10 MeV. Elastic scattering cross-sections for light elements are more or less independent of neutron energy up to about 1 MeV. For intermediate and heavy elements the elastic scattering cross-section is constant at low energy and exhibits some variation at higher energy. However, we are usually more interested in light elements as far as elastic scattering is concerned so as a generalization we may regard ss , as being constant at all energies for all elements of interest. Furthermore, there is not a great deal of variation from one element to another, and nearly all elements have scattering cross-sections in the range 2 to 20 barns. The important exceptions to this concern water and heavy water in which the molecular structure affects the scattering of low energy neutrons what was mentioned above.

Inelastic scattering occurs principally between high energy neutrons and intermediate and heavy elements, and is of importance in nuclear engineering because high energy neutrons can lose a large fraction of their energy as a result of inelastic scattering with heavy elements such as uranium. Inelastic scattering with light nuclei is not of much importance because the threshold energy below which $\sigma_i = 0$ is very high. The threshold energies for inelastic scattering for oxygen, sodium and uranium are about 6.5 MeV, 0.4 MeV and 0.05 MeV respectively, and above these thresholds the inelastic scattering cross-section rises to a more or less constant and rather small value, generally a few barns. Absorption cross-sections exhibit much more variation than elastic scattering cross-sections, not only from one isotope to another but also with varying neutron energy. The cross-section for many light isotopes is inversely proportional to the neutron speed over a wide range of energies, i.e.

$$\sigma_a = c_1 \left(\frac{1}{E_n} \right)^{0.5}$$

$$E_n = \frac{mv^2}{2} \sigma_a \sim \frac{1}{v}$$

$$\sigma_f \sim \frac{1}{v}$$

$$\sigma_c \sim \frac{1}{v}$$

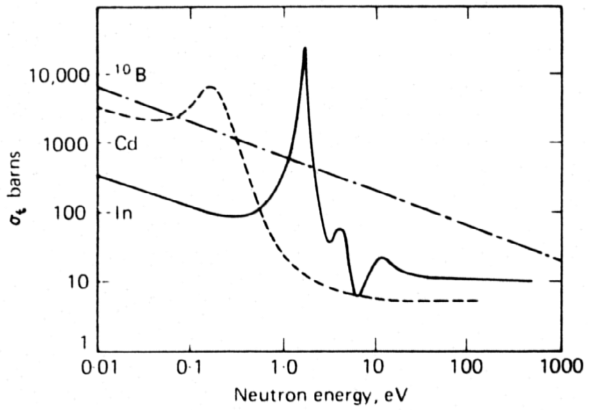

Figure 7.29 The total neutron cross section for Boron -10, Cadmium and Indium

The variation for Boron-10 is shown in Figure 7.29. For heavy isotopes the 1/v variation is exhibited at low energies up to about 10 eV. In the intermediate energy range from about 10 eV to 1000 eV the cross-section displays a very erratic behaviour and rises to a number of peaks known as resonances at which the cross-section values may be very large. At high energies above 1000 eV the resonances cannot be resolved and the cross-section assumes a fairly constant value of a few barns. The variation of σ_t, for ^{238}U is shown in Figure 7.28.

Isotopes of intermediate mass exhibit a behaviour between that of the light and heavy isotopes, thus a typical variation would be $\sigma_a \propto \frac{1}{v}$ at low energies, then a few resonances at intermediate energies, and finally a rather low and slightly varying value at high energies. The cross-sections of cadmium and indium are shown in Figure 7.29. It is possible to explain qualitatively some of the reasons for the characteristic variations of absorption cross-sections. At energies be low the resonance energy region the probability of interaction is governed by the time during which the neutron is in the neighbourhood of the nucleus, and this time varies inversely as the neutron speed. Thus we have the variation expressed by $\sigma_a \propto \frac{1}{v}$. To explain the resonance peaks it should be borne in mind that we are dealing with interactions involving compound nucleus formation. The compound nucleus is formed with an excitation energy of B + Ec where B is the binding energy of a neutron in the compound nucleus and Ec is the neutron energy multiplied by A/(A + 1). If the energy of the neutron is such as to produce the compound nucleus at or very near one of its excited states as shown on Figure 7.30 the probability of the interaction taking place is very high, corresponding to a high value of the cross-section. If, on the other hand, the energy of the incident neutron is such as to produce the compound nucleus at some energy midway between two excited levels, the probability of the interaction is very low, corresponding to a low value of the cross-section. Heavy nuclei such as ^{238}U have a large number of closely spaced excited levels which accounts for the large number of resonances in the absorption cross-section of ^{238}U. The fission cross-sections of ^{235}U, ^{238}U and ^{239}Pu vary in much the

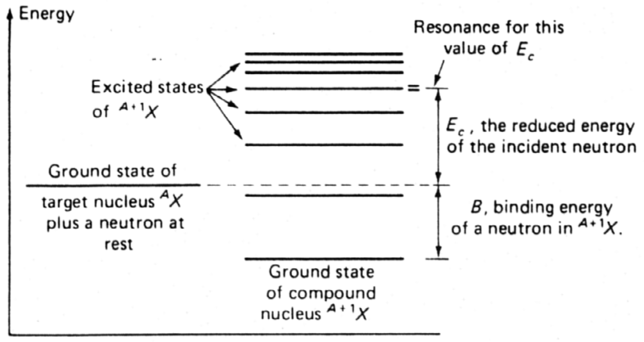

Figure 7.30 Energy levels and resonance absorption.

same way as capture cross-sections of heavy isotopes described above. Figure 7.28 shows the variation of st , for ^{238}U which exhibits the characteristic 1/v portion at low energy, resonances at intermediate energy, and the smooth curve a high energy where individual reso- nances overlap. The fission cross-sections of ^{238}U and ^{232}Th show the existence of a threshold neutron energy below which fission does not take place - Figure 7.32. Above the threshold a, rises to a more or less constant and rather small value, see Figure 7.31 for the fission cross-section of ^{238}U.

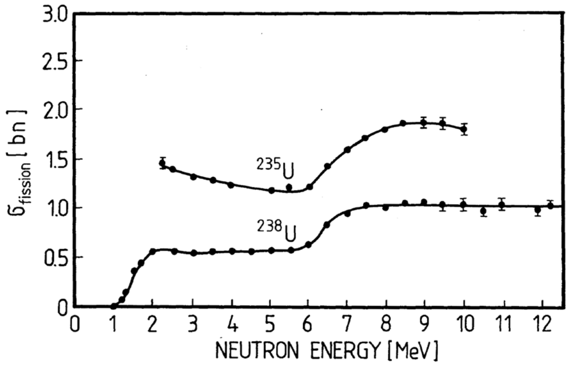

Figure 7.31 Fission cross section of uranium isotopes at higher energies. Treshold character of ^{238}U cross section visible at about 1 MeV.

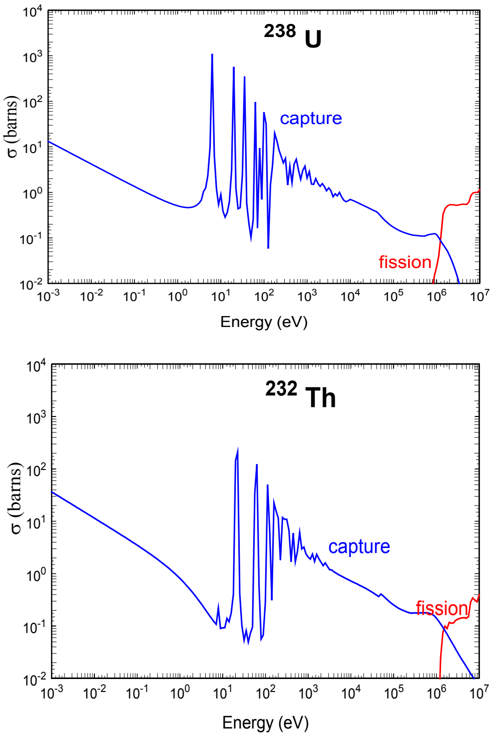

Figure 7.32 Capture and fission cross section of ^{238}U and ^{232}Th. Treshold character of fission cross section visible clearly at about 1 MeV.

Chapter 8

Nuclear Fission

8.1 Introduction

Fission occurs within a very short time - < 10^{-17} after absorption of neutron and the most of the fission neutrons are ejected almost instantaneously, within abut 10^{-14} sincerely of the fission event. These are referred to as "prompt" neutrons. However, a small fraction - < 1 % - of the neutrons emitted in fission arises from the decay of fission products and may be delayed by as much as a minute after the fission event. These neutrons are referred to as "delayed" neutrons. As we shall see later, the presence of these delayed neutrons is very important for reactor control.

Heavy nuclei have also been observed to split into three parts of comparable size, rather than 2 parts. Such events are referred as "ternary" fissions. However, this occurs very rarely; the probability of occurrence being about 1 in 400. Ternary fission is almost always accompanied by the emission of an alpha particle. Sometimes a triton, rather than alpha particle may be emitted.

Bohr and Wheeler developed the theory of fission using the analogy between nuclear forces and the forces which bind molecules together in a liquid. Using this model, proposed by Weizsacker in 1935 they successfully explained the existence of spontaneous fission and predicted the less abundant (~0.7%) isotope,^{235}U, to undergo fission more readily than the more abundant isotope (~99.3%) 238U. They also showed that if the energy of neutrons produced in fission could be reduced to thermal energy, their effectivness in causing fission of ^{235}U would increase by almost factor of 100.

8.2 Liquid drop model of fission

The model based on the idea of liquid-drop model (also referred to as ***a collective model***), contains no reference to the behavior of individual nucleons (and in this sense is complementary to the shell model). We note two similarities between nuclear data and the behavior of incompressible fluids. First, the density of all nuclear matter is roughly constant, just as for an incompressible fluid. Second, just as the binding energy per nucleon, E_b/A, is roughly constant from nucleus to nucleus, the heat of vaporization per unit mass is constant for different size drops of an incompressible fluid. (The heat of vaporization is the energy required to separate a drop of fluid into its component molecules, and the total mass of a nucleus is proportional to A. Thus, Eb/A is analogous to the heat of vaporization per unit mass.) Following this analogy, we can write an empirical formula for the mass of a nu- cleus, M(A,Z), by including terms of the type that would be included in computing the energy of a liquid drop, as follows:

1. A zeroth-order term that is just the sum of the rest masses of the nucleons:

ZMp + NMN = ZMp + (A-Z)MN

2. A term proportional to the volume of the nucleus (or μ A), which takes into account the nearly constant binding energy per nucleon:

$-\alpha A$

where α_V is positive because a binding energy reduces the mass of the nucleus.

3. A term proportional to $A^{2/3}$ or, equivalently, to the surface area of the nucleus:

$+\beta A^{2/3}$

A nucleon near the surface is not bound as strongly as one in the interior, so b takes into account a reduced binding energy and is positive. This term is the analogue of a surface-tension term in a liquid drop.

The remaining three terms take into account some simple observations specific to the nucleus:

4. A term for the Coulomb repulsion between all the protons in the nucleus. This term tends to increase the mass of the nucleus. If we suppose that the protons are distributed uniformly throughout a sphere of radius $R_A = r_0 A^{1/3}$, then the energy required to assemble that charge is

$$\frac{3}{5}\frac{Z(Z-1)e^2}{4\pi\varepsilon_0 r_0 A^{1/3}} = 0.72\frac{Z(Z-1)}{A^{1/3}}MeV$$

The contribution of the energy to the mass is this quantity divided by c^2.

5. A term that has a minimum for N = Z accounts for the tendency for the number of neutrons to equal the number of protons. If terms 1 through 4 were the only terms present, then the energy could be lowered by taking Z to zero; that is, nuclei would consist exclusively of neutrons. In fact, there are no nuclei with many more neutrons than protons, and nuclei are particularly stable when N = Z. This term is written as

$$\gamma\frac{(A-2Z)^2}{A}$$

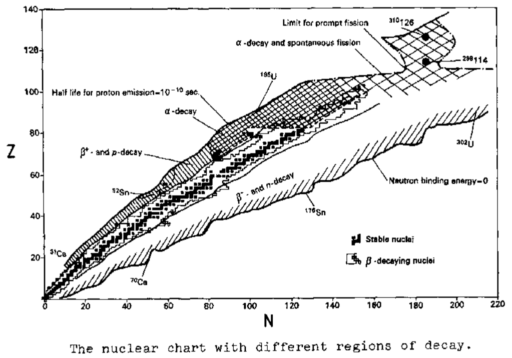

Figure 8.1 The nuclear chart with a stability chain and different regions of decay.

Where γ is positive. This term describes well existence of stability chain shown on the Figure 8.1.

6. Several terms that describe the tendency for nuclei with even numbers of protons and/or neutrons to be more deeply bound than nuclei with odd numbers of protons and/or neutrons. This tendency occurs because the spins of two nucleons in each "shell" are antiparallel. Such terms have the empirical form

For Z, N even: $\Delta = -\frac{\delta}{A^{1/2}}$

The sum of all these terms is **the semiempirical mass formula:**

$$M_A = ZM_p + (A-Z)M_n - \alpha A + \beta A^{\frac{2}{3}} + \varepsilon Z(Z-1)A^{-\frac{1}{3}} + \frac{\gamma(A-2Z)^2}{A} - \delta A^{-\frac{1}{2}}$$

$$\Delta M = M_A - ZM_p - (A-Z)M_n = -\alpha A + \beta A^{\frac{2}{3}} + \varepsilon Z(Z-1)A^{-\frac{1}{3}} + \frac{\gamma(A-2Z)^2}{A} - \delta A^{-\frac{1}{2}}$$

The parameters are determined empirically by fitting this relation with many different nuclear masses to the binding energy curve - see Figure 8.2. The result of this fitting is:

$$-\Delta M = 15.8\,A - 17.8\,A^{\frac{2}{3}} - 0.71\,Z(Z-1)A^{-\frac{1}{3}} - \frac{23.7(A-2Z)^2}{A} + \delta\,A^{-\frac{1}{2}}$$

α, β, ε, γ, δ are given in MeV units and

δ → **- 34** for Odd-Odd nuclei
δ → **+ 34** for Even-Even nuclei
δ → **0** for O-E, E-O nuclei

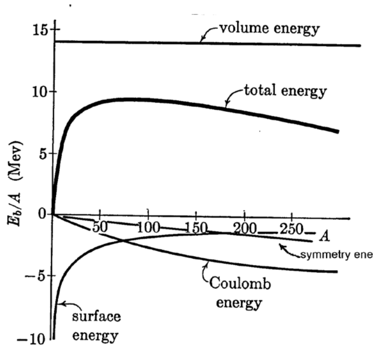

Figure 8.2 Contributions of the volume energy, surface, symmetry energy, and Coulomb energy to the average bindning energy per nucleon as a as function of mass number.

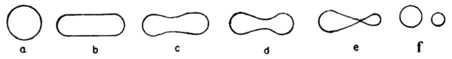

Figure 8.3 Various stages of a nucleus undergoing fission according to the liquid drop model.

Figure 8.4 Click here to see fission process as a liquid drop split (courtesy National Encyclopedia)

In a large nucleus containing many nucleons there are two main forces which are operative: (i) Coulomb repulsion, and (ii) nuclear forces between the nucleons. Nuclear forces are short range and charge independent. Therefore, if a nucleon lies deep inside the nucleus where it is surrounded by other nucleons on all sides, the average force acting on it will be zero. However, a nucleon on the surface will be attracted only by those nucleons which are inside the nucleus (within the range of nuclear forces) and there will be a net unbalanced force directed towards the centre of nucleus. This is similar to the force of surface tension in a liquid. Hence, if we treat the nucleus as a charged liquid drop then in its lowest state it will be spherically symmetric (the forces of surface tension being weaker than Coulomb force). However, when a nucleus captures a neutron (a charged particle or gamma-quant), a compound nucleus if formed in an excited state with an energy equal to the kinetic energy of the incident neutron and the energy liberating in re-pairing of nucleons inside the nucleus. The energetic compound nucleus will undergo strong surface oscillations which tend to distort the spherical shape. The force of surface tension will tend to restore the original shape while the Coulomb force tends to further distort it. If the energy of excitation is small, the distortions produced in the nucleus would be small and the nucleus would return to ground state by the emission of γ-rays. However, if the energy gained by the nucleus is large, the distortion of the nucleus would be also large and the whole system could be pushed into a bump-bell shape. Once the separation between the two charged centres exceeds some critical value, the electrostatic repulsion between the two halves may push the apart. The nucleus then splits into two separate nuclei - a process called fission. This sequence of events is shown on Figure 8.3. It may be pointed out here that the state e, when the two nuclei are just in contact, is referred to as scission state. The energy of the Coulomb field at e transforms into the kinetic energy of fission products, which fly away with very high speed.

8.2.1 Critical energy for fission

The difference in energy between the system in the scission state and the nucleus in ground state is called the 'critical' energy of fission and is denoted by E_c. To calculate E_c we assume that

- the original nucleus in its ground state is spherical,
- in going from one state to another, the total volume of the system does not change,
- the oscillations of the compound nucleus in the excited state deform the surface only.

For simplicity, we consider the case of symmetric fission in which the two fragments are exactly alike in charge and mass. (In actual practice this happens very rarely). Thus, if the charge and mass of the original nucleus are Z and A, respectively, then both fragments will be of charge Z/2 and mass A/2 (we assume both Z and A to be even). Then, the surface energy of the initial spherical drop will be

$$E_{si} = TS = 4\pi R^2 T$$

where T, S and R are the surface tension, the surface area and the nuclear radius, respectively. i - stands for initial. The Coulomb energy of the original undeformed nucleus is

$$E_{Ci} = \frac{3}{5}\frac{Z(Z-1)e^2}{R} \approx \frac{3}{5}\frac{(Ze)^2}{R}$$

If we use the relation , the energy of the undistorted nucleus in its ground state, obtained by adding the above two contributions, will be

$$E_{si} + E_{Ci} = E_i = 4\pi T r_0^2 A^{2/3} + \frac{3}{5}\frac{(Ze)^2}{r_0 A^{1/3}}$$

The surface energy of the two fragments when they are just in contact (state e in.Figure 8.3) is

$$E_s = 2 \times 4\pi \left(\frac{R}{2^{1/3}}\right) T = 8\pi r_0^2 \left(\frac{A}{2}\right)^{2/3} T$$

Where $R/2^{1/3}$ is the radius of each fragment. (This is a direct consequence of the symmetric fission and invariant volume assumptions). The Coulomb energy of these fragments at e will be a sum of two terms: one representing the (Coulomb) energy of the two (undistorted) fragments and the other arising from the repulsion between them:

$$E_c = 2 \times \frac{3}{5}\frac{(Ze/2)^2}{(R/2^{1/3})} + \frac{(Ze/2)^2}{2 \times (R/2^{1/3})} = \frac{3}{5}\frac{Z^2 e^2}{2r_0 (A/2)^{1/3}} + \frac{(Ze/2)^2}{8r_0 (A/2)^{1/3}}$$

Hence, the energy of fission fragments is given by

$$E_s + E_C = E_f = 8\pi T r_0 (A/2)^{2/3} + \frac{3}{5}\frac{Z^2 e^2}{2r_0 (A/2)^{1/3}} + \frac{(Ze/2)^2}{8r_0 (A/2)^{1/3}}$$

The difference in energy between that of the original nucleus and the two equal fragments in contact is by definition, the critical energy - Figure 8.5 for fission:

$$E_{critic} = E_f - E_i = 4\pi T r_0 (A/2)^{2/3}\left(2^{1/3} - 1 - \frac{3}{40\pi}\frac{Z^2 e^2}{r_0^3 AT}\left(2 - 2^{1/3} - \frac{5}{12}\times 2^{1/3}\right)\right) =$$

$$= 4\pi T r_0^2 A^{2/3} a\left(1 - \frac{3}{40\pi} b \frac{Z^2 e^2}{r_0^3 AT}\right) \tag{8.1}$$

Where

$$a = (2^{1/3} - 1) = 0.260 \ and \ b = \left(2 - 2^{1/3} - \frac{5}{12}\times 2^{1/3}\right) a^{-1} \approx 1$$

Having derived an expression for E_{critic} we will now discuss the condition for the stability of a nucleus against spontaneous fission. For spontaneous fission to occur, E, must be zero. Taking b=1, Eq. (8.1) gives

$$1 = \frac{3}{40\pi}\frac{Z^2 e^2}{r_0^3 AT} \ or \tag{8.2}$$

$$\left(\frac{Z^2}{A}\right)_{SF} = \frac{40\pi r_0^3 T}{3e^2} = 2\times \frac{4\pi r_0^2 T}{\frac{3}{5}\frac{e^2}{r_0}}$$

This equation defines the limiting value of Z^2/A for stability of nuclei against spontaneous fission. From for binding energy per nucleon we note that $4\pi r_0^2 T = \beta = 17.8$ and $(3/5)e^2/r_o = e = 0.71$. Using these values in Eq. (8.2) we get

$$\left(\frac{Z^2}{A}\right)_{SF} = 50.1$$

A more generally accepted value of $(Z^2/A)_{SP}$, based on fission data, is 47.8. We note that for ^{238}U the value of Z^2/A = 35.56 and for ^{239}Pu it is 36.97. From this we may conclude that within the frame work of this theory, even the heaviest naturally occurring element is stable against spontaneous fission.

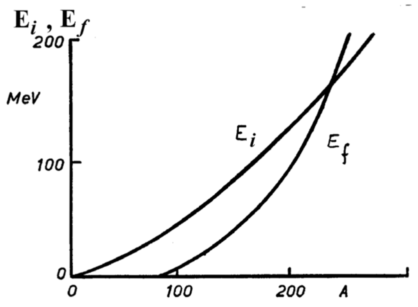

Figure 8.5 Critical energy for spontaneous fission, $E_{crit}=E_f-E_i$

For convenience we introduce a quantity Δ called the fissionability parameter, by the relation

$$\Delta \equiv \frac{(Z^2/A)}{(Z^2/A)_{SF}}$$

From this it is clear that a nucleus will be stable against spontaneous fission provided Δ < 1. If Δ> 1, it will disintegrate spontaneously. In terms of Δ and β, we may rewrite Eq. (8.1) as

$$E_{critic} = \beta A^{2/3} a(1 - b\Delta) = 17.8A^{2/3}(0.260 - 0.215\Delta)$$

For some nuclei of interest, the calculated as well as observed values of critical energy are given in Table I. The corresponding values of the energy of excitation E_{ex} defined as the difference of binding energies of the compound nucleus and the target nucleus in their ground states, are also given. (This is also the binding energy of the last neutron in the compound nucleus.) It is important to note that in cases where the energy of excitation is greater than the critical energy for fission ($E_{ex} - E_{crit} > 0$), the nuclei will undergo fission by thermal neutron capture. However, when Eex is less than E_{crit} ($E_{crit} - E_{ex} > 0$), there will exist a threshold on neutron energy for fission. We note from table that for (even-odd) nuclei like ^{233}U, ^{235}U and ^{239}Pu, $E_{ex} > E_{crit}$ whereas for (even-even) nuclei like ^{232}Th and ^{238}U, $E_{ex} < E_{crit}$. This difference arises because of the spin term in the Weiszacker formula .

Table I. Critical and Excitation Energy for Heavy Nuclei

Target nucleus	Z^2	E_{crit}(MeV)		E_{ex}(MeV)
		Liquid drop	Observed	
^{232}Th	34.91	6.5	5.95	5.1
^{233}U	36.33	4.6	5.49	6.6
^{235}U	36.02	5.3	5.75	6.4
^{238}U	35.56	5.5	5.80	4.9
^{239}Pu	36.97	4.0	5.48	6.4

Nuclei such as ^{233}U, ^{235}U, ^{239}Pu which can readily be fissioned by thermal neutrons are referred to as **'fissile'** isotopes. On the other hand, ^{232}Th and ^{238}U, which fission only by fast neutrons are referred to as **'fissionable'** isotopes. It may be mentioned here that by suitable neutron reactions, some fissionable isotopes can be transformed into fissile isotopes and the former are also referred to as 'fertile' isotopes.

For isotopes of: $^{233}_{92}U,\ ^{235}_{92}U,\ ^{239}_{94}Pu,\ ^{241}_{94}Pu$ we have a case that binding energy of neutrons are bigger than E_{crit} even if incident neutron energy is equal to 0.

For isotopes of $^{232}_{90}Th,\ ^{238}_{92}U,\ ^{240}_{94}Pu,\ ^{242}_{94}Pu$ fission is possible only if energy of incident neutrons is > 1 MeV

In the above discussion of the liquid drop model of fission, we have made some simplifying assumptions. All of them are not always justifiable. Using this theory one cannot, therefore, account for all the observed properties of fission. This has led to modifications of this theory and we now understand the mechanism of fission far better, but a complete and consistent description of this process is still lacking. *"The fission process has occupied a unique place in the development of nuclear physics, but should be recognized as part of a wider range of phenomena involving large scale nuclear deformations and collective flow that are now becoming accessible in the study of reactions produced* *by accelerated heavy ions*." These words of Bohr and Mottleson truely reflect the current status of our understanding of fission.

Recently, pions and muons have also been used to probe dynamics of fission but this theory goes beyond the scope of our lectures.

Figure 8.5 shows the variation of E_f as a function of mass. It can be seen that fission reactions can be exothermic from the mass about 83. However spontaneous penetration of the Coulomb barrier begins to be probably only at mass about 250.

$$E_f > 0\, if\, \frac{E_{Coulomb}}{E_{surface}} = \frac{\gamma}{\beta}\frac{Z^2}{A} > 0.7 \rightarrow \frac{Z^2}{A} > 17 \rightarrow A > 83$$

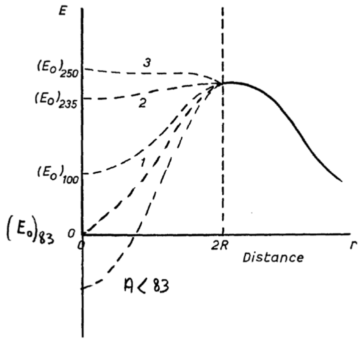

Figure 8.6 Schematic picture of Coulomb barrier and energy of fission for different atomic masses

8.3 Fission Products

We will now consider some basic characteristics of nuclear fission. As a typical example, we consider the fission of ^{235}U induced by thermal neutrons. It proceeds as follows:

$$^{235}_{92}U + n \rightarrow (^{236}_{92}U)^* \rightarrow 2\ fissions\ products + n\ neutrons + \gamma + Q$$

The primary reaction products are: two middle weight nuclei called fission fragments, n neutrons (the value of n is usually 2 or 3), a few γ-rays and energy Q (whose average value is nearly 200 MeV). The fission fragments are highly unstable and attain stability by emitting β-particles, neutrinos - ν, γ-rays and sometimes **even neutrons (an important process as we'll see).** We will now discuss these fission products in turn.

8.3.1 Primary Fission Fragments

Mass Distribution

In a fission reaction caused by thermal neutrons, the fission fragments are usually of unequal mass; one being much heavier than the other. Such a fission is said to be asymmetric. Investigations have shown that ^{235}U can fission in more than 40 different ways which means that about 80 different nuclei are directly produced in fission. These are referred to as 'primary' fission fragments. The heavier fission fragments normally lie in the mass range 125-150 with a well defined maximum around mass number 140, whereas the lighter fragments lie in the mass range 80-110 with the maximum around mass number 95. Of the heavier nuclei that have been observed as primary fission fragments in ^{235}U fission, one may mention $^{147}_{57}La, ^{140}_{54}Xe, ^{135}_{52}Te, ^{149}_{60}Nd$ while the corresponding light fragments are $^{87}_{35}Br, ^{94}_{38}Sr, ^{99}_{40}Zr, ^{85}_{32}Gd$, respectively.

The mass distribution of fission fragments is shown most conveniently in the form of fission yield curve. For thermal fission of ^{235}U, the yield curve is shown in Figure 8.5. The curve has a saddle back shape and shows two peaks corresponding to the two groups of fragments mentioned earlier. To understand this curve, let us consider a particular light fragment. The curve shows the percentage yield of this isotope produced amongst the light fragments. Similarly, if we consider a heavier fragment, the curve will give its percentage yield amongst the heavier group. Therefore, the total fission yield is 200% (because the yield for the light and heavy group of fragments is 100% separately). A maximum yield of about 6.3% is obtained for nuclei with mass numbers 95 and 140. **Attention: observe the logarithmic scale of Y-axis**.

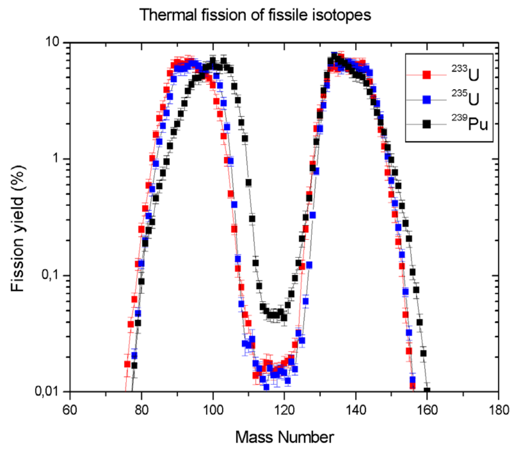

Figure 8.7 Mass-yield curve for thermal fission of ^{233}U, ^{235}U and ^{239}Pu

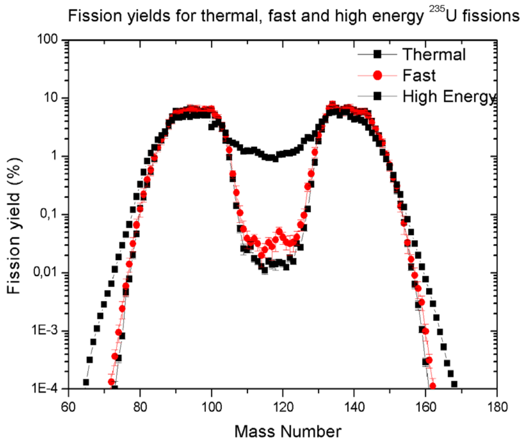

Figure 8.8 Mass-yield curve for thermal, fast and high energy fission of ^{235}U

It is important to note that when thermal neutrons are used to produce fission in ^{235}U symmetric fission is very rare; its probability being about 600 times less than its fission into most probable fragments (with A = 95 and 140). However, the probability of symmetric fission increases with increase in the energy of incident neutrons. In particular, when 14 MeV neutrons are used, this probability is up by almost a factor of 100. The valley in the curve tends to fill and can almost disappear for still higher energy neutrons - see Figure 8.8. With 90 MeV neutrons, only one peak is observed suggesting that symmetric fission occurs at these energies, A similar behaviour is observed for ^{233}U and ^{239}Pu

8.3.2 Energy Distribution

Fission fragments carry away nearly 80% of the energy released in fission. To understand how this energy is distributed in these two groups of fragments, let us assume that the fission of a nucleus occurs when it is stationary so that the net momentum of the particles produced must be zero. Since the two fragments are very much heavier than all other particles produced in fission, they carry most of the momentum and will fly off in opposite directions with equal moments, i.e. $M_1v_1=M_2v_2$, where M_1 and M_2-are the masses of the two fragments and v_1 and v_2 are their respective velocities. Hence, the kinetic energies of the two fragments will be in the ratio

$$\frac{E_2}{E_1} = \frac{\frac{1}{2}M_2v_2^2}{\frac{1}{2}M_2v_2^2} = \frac{M_1}{M_2}$$

i.e. the kinetic energy of a fragment is inversely proportional to its mass. Hence for the nuclides at the peaks of the fission yield curve, we have

$$\frac{E_2}{E_1} = \frac{95}{140}$$

The energy distribution of fission fragments therefore exhibits two peaks. For thermal fission of

^{233}U, ^{235}U and ^{239}Pu, this is shown in Figure 8.9 . The higher energy peak around 95 MeV corresponds to the lighter group of fragments while the lower energy peak near 65 MeV corresponds to the heavier group. The energy distribution of fragments in case of fission induced by 14 MeV neutrons in ^{235}U also exhibits similar two peaks. A similar behaviour is observed for fission of ^{233}U and ^{239}Pu.

It may be remarked here that the measured energy distribution of fragments can be used to obtain their mass distribution and vice versa.

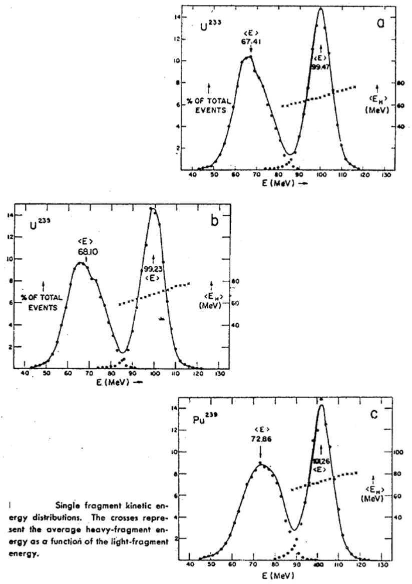

Single fragment kinetic energy distributions. The crosses represent the average heavy-fragment energy as a function of the light-fragment energy.

Figure 8.9 Energy distribution curves for thermal fission

8.3.3 B-**decay chains: secondary fission fragments**

We have learnt that primary fission fragments cluster around (Z = 35, N = 55) and (Z = 55, N = 85). These regions lie above the line of stability. These nuclei contain a much larger number of neutrons than the corresponding stable isotopes. As discussed in earlier, if a nucleus departs from the line of stability, it becomes unstable and undergoes radioactive decay. These neutron rich nuclei, in some cases, get rid of their excess neutrons by direct neutron emission, but the dominant process is successiveβ- emission. This chain of β-decays, which must terminate in a stable nucleus, is called the 'fission decay chain'. A decay chain of particular interest is

$${}^{140}_{54}Xe \xrightarrow[16s]{\beta^-} {}^{140}_{55}Cs \xrightarrow[66s]{\beta^-} {}^{140}_{56}Ba \xrightarrow[12.8d]{\beta^-} {}^{140}_{57}La \xrightarrow[40h]{\beta^-} {}^{140}_{58}Ce$$

because it contains two nuclides ^{140}Ba and ^{140}La whose identification led to the discovery of fission. Two β-decay chains which influence the operation of reactors are :

$${}^{135}_{52}Te \xrightarrow[18s]{\beta^-} {}^{135}_{53}I \xrightarrow[6.75h]{\beta^-} {}^{135}_{54}Xe \xrightarrow[9.21h]{\beta^-} {}^{135}_{55}Cs \xrightarrow[2.6\times10^6 a]{\beta^-} {}^{135}_{56}Ba$$

and

$${}^{149}_{60}Nd \xrightarrow[1.7h]{\beta^-} {}^{149}_{61}Pm \xrightarrow[54h]{\beta^-} {}^{149}_{62}Sm$$

Figure 8.10 Visualization of ^{144}Ba β^- decay

In these chains occur the isotopes of xenon and samarium which are strong neutron absorbers and work as 'poisons' in nuclear reactors. In all, about 80 different characteristic β-decay chains and more than 200 different radio-nuclides have been observed in fissions of uranium. Nuclei resulting from the decay of primary fission fragments are called 'secondary fission fragments'. For example, ^{140}Xe, ^{135}Te, ^{149}Nd are primary fission fragments, whereas ^{140}Cs, ^{140}Ce, ^{135}I, ... ,^{135}Ba , ^{149}Pm and ^{149}Sm are all secondary fission fragments. It may be pointed out here that most of the secondary fragments are formed in an excited state and therefore emit γ-rays. (It is these β- and γ-rays which are a grave radiation hazard to scientists and other personnel working around a reactor.)

8.3.4 Fission neutrons

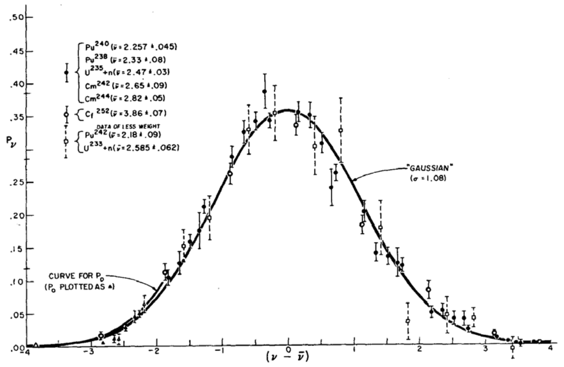

Figure 8.11 Statistical variation of number of neutrons produced per fission - ν

The number of neutrons emitted in fission depends upon the particular mode of fission. For thermal fission of ^{235}U, this number can be two or three; the statistical average being 2.44. The average number of neutrons released per fission is denoted by ν and is statistically varying as shown on Figure 7.10 . It depends both on the fission isotope and the energy of the incident neutron. For ^{233}U, ^{235}U, ^{239}Pu we have plotted in Figure 8.12, ν(E) as a function of energy and note that ν increases as the energy of the incident neutron increases. In fact, for every 6 to 7 MeV increase in energy, one additional neutron is emitted.

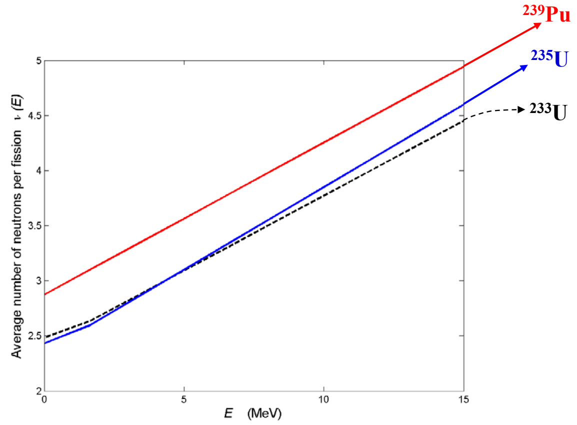

Figure 8.12 Energy variation of the average number of neutron produced per fission.

8.3.5 Prompt neutrons

As mentioned earlier, nearly 99.3% of the neutrons emitted in fission appear instantaneously (within about 10^{-14} s) with the fission event. These neutrons have an energy distribution ranging from 10 MeV down to very low energies. The fraction of prompt neutrons emitted in fission with energies in the range E to E+ dE is called the fission spectrum and is denoted by N(E)dE. For ^{235}U, the measured spectrum of prompt neutrons emitted in thermal fission is shown in Figure 8.13 . These measurements can be fitted to a Maxwellian, i.e.

$$N(E) = \frac{2}{\sqrt{\pi}}\sqrt{\frac{E}{T^3}}e^{-\frac{E}{T}}$$

where neutron energy E is in MeV and T (= 1.29 MeV) is an effective temperature. (It is two-third of the average energy.) The observed spectrum can also be represented in the energy range from 0.1-10 MeV by the following semi-empirical expression:

$$N(E) == .453e^{-1.036E}\sinh\sqrt{2.29E} \tag{8.3}$$

Since the function N(E) is a probability density, it is normalized to unity $\left(\int_0^\infty N(E)dE = 1\right)$

The average energy E of the prompt neutrons defined as

$$\overline{E} = \int_0^\infty EN(E)dE = 1$$

comes out to be 1.94 ± 0.05 MeV when averaged over the Maxwellian and 1.98 MeV when the expression given in Eq. (8.3) is used. The most probable energy E_p (i.e. energy corresponding to the peak of N(E) vs E curve) is slightly below 1 MeV.

Like other fission parameters, the prompt fission spectrum also depends upon the nucleus undergoing fission and on the incident neutron energy. For instance, the measured spectrum for thermal fission of ^{239}Pu can be fitted to a Maxwellian with T = 1.33 MeV (corresponding to E = 2.00 ± 0.05 MeV). It is interesting to note that the average energy of fission neutrons is related to the average number of neutrons emitted in fission by the semi- empirical relation:

$$\overline{E}=0.74+0.65\sqrt{\nu+1}$$

We may mention here that neutrons are emitted almost isotropically in fission.

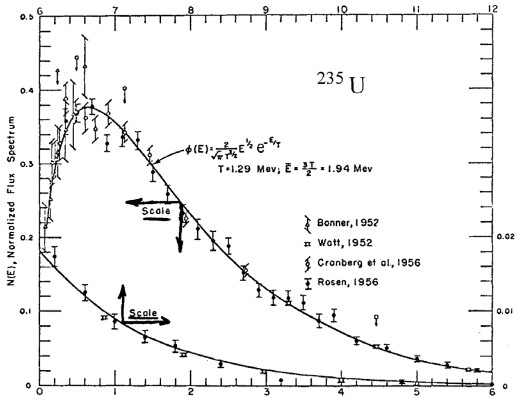

Figure 8.13 Prompt neutron spectrum for thermal fission of ^{235}U

8.3.6 Delayed neutrons

As stated earlier, nearly 0.7% of the total number of neutrons emitted during fission are given off appreciably after the actual event. These neutrons originate from the highly unstable primary, and sometimes secondary, fission fragments. The best known example of this is the ${}^{87}_{35}$Br decay scheme shown inFigure 8.14. If the β^-particle emitted by ${}^{87}_{35}$Br carries away a large fraction of the excitation energy, and ${}^{87}_{36}$Kr is formed in a low excitation state it decays further through a β^- - emission to ${}^{87}_{37}$Rb . This in turn undergoes another β- decay to form ${}^{87}_{38}$Sr as the stable end product. However, when ${}^{87}_{35}$Br undergoes decay and the energy carried away by the β^--particle is small, the resulting nucleus ${}^{87}_{36}$Kr is formed in a highly excited state. This can decay with the emission of a neutron of energy nearly 0.3 MeV. ${}^{87}_{36}$Kr then attains the ground state by the emission of γ-rays. The neutron is emitted as soon as ${}^{87}_{36}$Kr is formed so that the effective delay time of this process is controlled by the half-life for β^-decay of the parent nucleus, ${}^{87}_{35}$Br, which is 54. 7 s. The fission fragments such as ${}^{87}_{35}$Br, whose β^-decay yields a nucleus which subsequently emits neutrons, are referred to as 'delayed neutron precursors'. A large number (> 65) of such delayed neutron precursors are believed to exist, and some of these are listed in Table II.

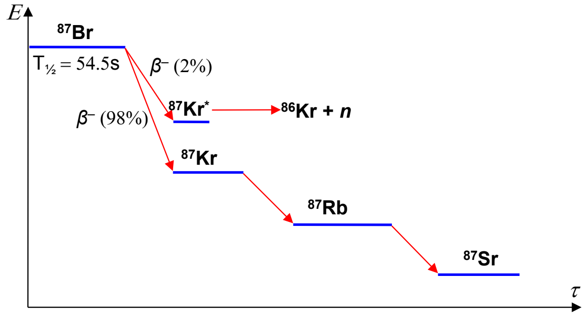

Figure 8.14 Mechanism of delay neutron emission: decay scheme of ^{87}Br.

A detailed study shows that delayed neutron precursors can be classified into six well-defined groups, each with its own characteristic half life. Each precursor group usually contains more than one isotope. Figure 8.15 shows delayed neutron emission scheme for another precursor - ^{137}I. For thermal fission of ^{235}U , we have given in Table II the values of half-lives, decay constants and mean energies for these six groups. Also included in the table are the delayed neutron fraction bi, defined as the ratio of delayed neutrons in the ith group to the total number of neutrons released in fission, and the relative yield fraction β_i/β where $\beta=\sum\beta_i$. From the Table II we observe that the average energy of delayed neutrons is different for different groups, and in all cases it is much lower than that of prompt neutrons.

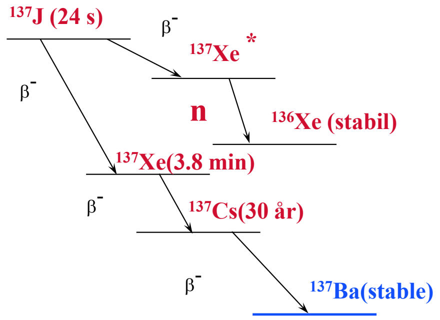

Figure 8.15 Decay scheme for ^{137}I delayed neutrons precursor

Unlike other fission parameters, the delayed neutron fractions β_i and hence also β (and the corresponding half-life $T½_i$ for the ith group) vary only with the fissile isotope but are almost independent of the incident neutron energy below 4 MeV. The fractions of delayed neutrons in cases of ^{233}U and ^{239}Pu are 0.00298 and 0.00225 respectively. (The total delayed yield being 0.0074 ± 0.0004, 0.01668 ± 0.00070 and 0.00645±0.00040 neutron per fission for ^{233}U, ^{235}U and ^{239}Pu, respectively.) We may mention here that for these two nuclid.es also, the delayed neutrons are classified into six groups. The half-life (and the decay constant) for each group is only slightly different from that of the corresponding group in ^{235}U. This is because each group is composed of a few delayed neutron precursors and their decay constants are averaged quantities. Moreover, the fission fragments in cases of ^{233}U or ^{239}Pu may not necessarily be identical with those of ^{235}U.

Table II. Delayed neutron data for thermal and fast (in red) fission of ^{235}U.

Gr	$T_{½}$ [s]	β_i / β	E_n [MeV]	Possible precursors
1	55.90 (54.58)	0.033 (0.038)	0.25	^{87}Br
2	22.73 (21.87)	0.219 (0.213)	0.46	^{88}Br, ^{137}I, ^{136}Te, ^{134}Sb, ^{141}Cs
3	6.24 (6.03)	0.196 (0.188)	0.40	^{89}Br, ^{138}I, ^{92,93}Rb, ^{147}La, ^{87}Se, ^{84}As
4	2.30 (2.23)	0.395 (0.407)	0.45	^{85}As, ^{90}Br, ^{135}Sb, ^{94}Rb,^{139}I, ^{98,99}Y, ^{142}Cs, ^{80}Ga
5	0.61 (0.50)	0.115 (0.128)	0.42	^{86,87}As, ^{136}Sb, ^{147,148}Ba, ^{81,82}Ga, ^{140,141}I, ^{91}Br, ^{134}Sn, ^{145}Cs, ^{89}Se
6	0.23 (0.18)	0.042 (0.026)	÷	^{83}Ga, ^{146,147}Cs, ^{95,96,97,98,99}Rb, ^{92}Br, ^{91}Se

The measured delayed neutron spectrum for thermal fission of ^{235}U is given in Figure 8.16. The presence of delayed neutrons, though they form only a very small fraction of the total number, is vital for safe reactor operation.

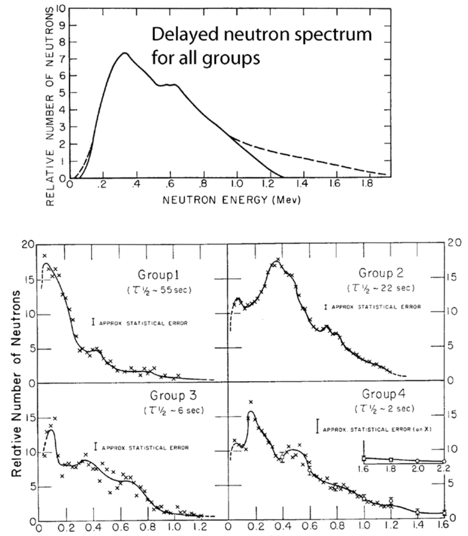

Figure 8.16 Delayed neutron spectrum for thermal fission of^{235}U

8.3.7 γ-Rays, β^-- particles and neutrinos

In addition to fission fragments and neutrons, in a fission event γ-rays, β^--particles and neutrinos are also produced. The γ-rays may arise

- at the time of fission,
- during the decay of primary fragments, and

- from the recapture of some of the fission neutrons.

Like neutrons they are also classified as prompt and delayed. The prompt γ-rays are defined, somewhat arbitrarily, as those produced within 1 ms of the fission event. (Obviously, they will consist of the γ-rays released at the time of fission and partly of γ-rays from the decay of short-lived primary fragments.) On the other hand, delayed γ-rays are those which are given off appreciably after the actual fission event by the primary fragments with half-lives greater than 1 ms. The measured spectrum of prompt gamma rays for thermal fission of ^{235}U is shown in Figure 8.17 . We note that the spectrum is approximately exponential. The average energy per prompt γ-ray is nearly 1 MeV.

As mentioned earlier, β^--particles are emitted by the unstable primary fragments undergoing radioactive decay. This is invariably accompanied by neutrino emission.

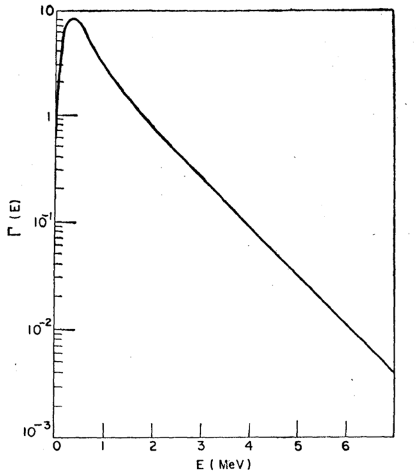

Figure 8.17 Prompt gamma ray spectrum for thermal fission of ^{235}U.

8.3.8 Energy released in fission

The energy released in fission appears as the kinetic energy of the various fission products and γ-rays. On an average the total energy released in one event varies from 190-210 MeV and its distribution among various products for thermal fission of ^{235}U and ^{239}Pu is given in Table III. This energy is dissipated into the surrounding environment as heat.

Table III. Energy release in thermal fission of ^{235}U and ^{239}Pu

Fission products	Realesed Energy (MeV)		Range (m)
	^{235}U	^{239}Pu	
Lighter fragments	99.8 ± 1.0	101.8 ±1.0	< 1·10^{-4}
Heavier fragments	68.4 ± 0.7	73.2 ± 0.7	< 1 · 10^{-4}
Prompt neutrons	4.8	5.8	*
Prompt γ(t< 1 ms)	7.5	7.0	1
Decay products:			
β^--particles	7.8	8.0	
γ	6.8	6.2	< 1
Neutrinos	12.0	12.0	Extremely large

Fission fragments interact with nuclei of the medium via Coulomb force and slow down within a distance of a few microns. Fission neutrons slow down due to elastic as well as inelastic collisions with the nuclei of the medium. γ-rays of energy less than or nearly equal to 3 MeV lose energy via photoelectric effect. If their energy lies in the range from 0.3 to 10 MeV, Compton scattering becomes important and for γ-ray energies greater than 10 MeV, pair production is the dominant mode of energy transfer.

From the Table III we note that for ^{235}U, on an average, fission fragments share nearly 168 MeV of energy (80% of the total) released in fission. The uncertainty in this value may be about 2 MeV. The average energy carried away by prompt neutrons and γ-rays is nearly 4.8 MeV and 7.5 MeV, respectively. The energy carried away by all other radiations (β^--particles, delayed γ -rays and neutrinos) coming from the decay of primary fission fragments, is 27 ± 3 MeV. Of this, nearly 12 MeV is carried away by neutrinos. In a nuclear reactor this energy is lost from the system. However, some of the neutrons produced during fission are subsequently absorbed by materials present there. This leads to the production of γ-rays. Depending on the materials involved, 3-12 MeV of energy can be released per fission. This partially compensates for the energy carried away by neutrinos. Thus, for all practical purposes we can take the effective value of energy released per fission to be 200 MeV with an uncertainty of 5-10 MeV.

Theoretically one can see this in a number of ways. One can calculate this energy from the binding energy curve. This gives an energy of about 212 MeV. If we regard the fission process purely as a Coulomb repulsion after the critical stage (Figure 8.3 e) has been reached, we get a figure of about 240 MeV for symmetric fission and 218 MeV for most probable fragments with A = 95 and 140. However, to make a better estimation one must calculate the difference in mass between the initial nucleus and that of the final products. For ^{235}U, this leads to a value of about 208 MeV for the specific case when the final stable product nuclei are and. It may, however, be pointed out here that the exact value of energy released per fission will depend upon the mode of fission and one usually takes the mean value as 200 ± 10 MeV for ^{235}U.

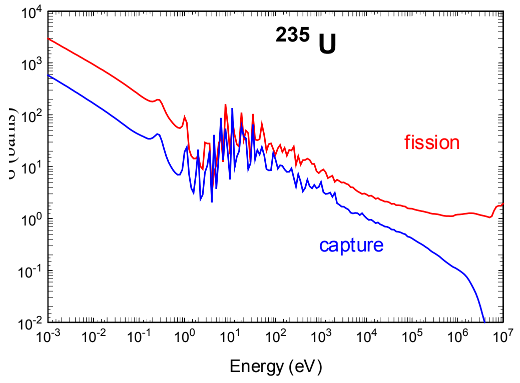

Figure 8.18 Energy variation of fission and capture cross sections of ^{235}U.

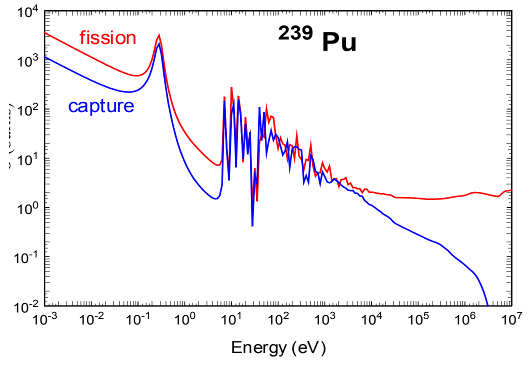

Figure 8.19 Energy variation of fission and capture cross sections of ^{239}Pu.

8.3.9 Fission cross sections

Nuclear fission reaction proceeds via compound nucleus formation and one expects the fission cross section, σ_f, to exhibit a resonance behaviour. This indeed is true, as may be seen from Figure 8.18, where we have plotted the energy variation of fission cross section for ^{235}U. We find that in the thermal energy region varies as 1/v and is very large. At E= 0.025 eV, the value of sf for ^{235}U is about 582 b, suggesting that low energy neutrons are very effective in causing ^{235}U nuclei to fission. This behaviour of ^{235}U fission cross section makes possible the design of thermal nuclear reactors using natural uranium. For ^{239}Pu, the value of σ_f for thermal neutrons is still larger; being about 742 b - see Figure 8.19.

Above the thermal energy region (E > 1 eV), σ_f exhibits a jumble of closely packed large resonances. These resonances become wider and lower as energy increases. At still higher energies (E > 10 keV), sf approaches an asymptotic value of a few barns.

In Fig. , the fission cross sections for ^{232}Th, ^{238}U and ^{240}Pu, as a function of energy are shown. As will be noted, the energy variation of fission cross section for these isotopes is quite different from that of ^{235}U. This is because ^{232}Th and other fertile nuclides fission only with fast neutrons

(E > 1-2 MeV) and exhibit a fission threshold, which occurs just above the resonance region. Below the fission threshold, sf is zero. Above this it rises rapidly and varies relatively smoothly at higher energies. Around 10 MeV, sf attains its maximum value of a few barns; the actual value depending upon the nuclide.

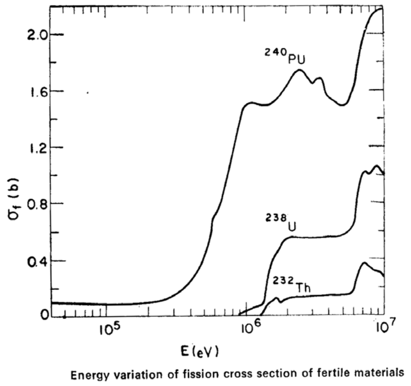

Figure 8.20 Energy variation of fission cross section of fertile isotopes

When a neutron is absorbed by a fissile isotope, it does not always lead to fission. Sometimes the compound nucleus decays to its ground state by emitting a gamma ray. The ratio of the cross section for radiative capture to fission cross section is called the 'fission to capture ratio' and is denoted by α:

$$\alpha = \frac{\sigma_f}{\sigma_c}$$

It is different for different nuclei and is dependent upon neutron energy. Figure 8.21 shows variation of a for ^{235}U. Another quantity of interest is the average number of fast neutrons produced per thermal neutron absorbed by a nuclide. It is denoted by η and for materials composed of a single species, it is equal to ν multiplied by the relative probability that absorption of a thermal neutron leads to fission, i.e.

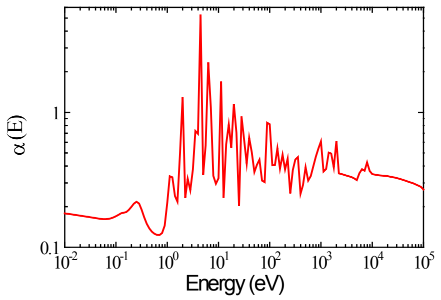

Figure 8.21 Variation of α for ^{235}U.

$$\eta = \nu\frac{\sigma_f}{\sigma_a} = \nu\frac{\sigma_f}{\sigma_c + \sigma_f} = \frac{\nu}{1+\alpha}$$

For materials like natural uranium, which are composed of different isotopes, we define η in terms of macroscopic (fission and absorption) cross sections characterizing each isotope:

$$\eta = \frac{\sum_i \nu_i \Sigma_{f_i}}{\sum_i \Sigma_{a_i}}$$

where $\nu_i, \Sigma_{f_i}\, and\, \Sigma_{a_i}$ are respectively the average number of neutrons produced per fission, macroscopic fission cross section and macroscopic absorption cross section for the ith isotope. It is important to emphasize here that all the quantities in the last equation should be evaluated at the energy of the neutron inducing fission.

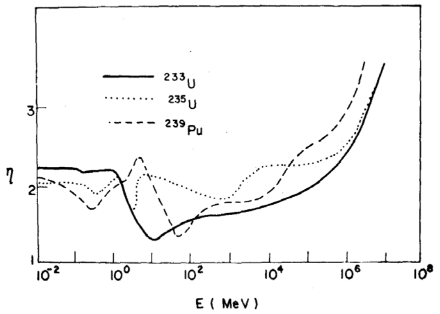

Figure 8.22 Energy variation of η for different isotopes.

Since η is defined in terms of ν and α, which depend on neutron energy, η will also be a function of energy. The energy variation of h for fissile isotopes is shown in Figure 8.22 As will be noted, h is generally of the order of 2 for low energy neutrons and increases with energy above 0.1 MeV. This high value of η makes it possible to 'breed' more fissile isotope than what is consumed. For this reason, this parameter is probably the most important physical constant concerning fissile isotopes.

Chapter 9

The Chain Reaction and Multiplication of Neutrons

9.1 Introduction

In this chapter we shall consider the necessary requirements for a chain reaction, and also some other topics that are of im portance in the development of nuclear energy for peaceful purposes.

The achievement of a system in which a controlled, self-sustaining fission chain reaction takes place is the first requirement, as this is the way in which the energy of fission can be released, also in a controlled way, and put to good use. The system in which the chain reaction takes place is called a nuclear reactor, and there are many possible types of reactor, depending on the materials of construction and the energy of the neutrons which cause fission. In this lecture we will consider qualitatively the conditions necessary for a chain reaction and will identify a number of different possible reactor types. Some types of reactor require enriched uranium to achieve a chain reaction, and the processes for enrichment are briefly described.

The complete utilization of the world's resources of uranium to provide energy is an important aspect of nuclear power, and the discussion of this topic leads to a description of the types of reactor and the fuel cycles that will enable not only uranium, but also thorium to be used as a long-term source of energy. Finally, the role which nuclear power can play in supplying a world in which energy demands are increasing and resources are being rapidly depleted will be discussed.

9.2 The chain reaction

The condition that is necessary for a stable, self-sustaining chain reaction is that exactly one of the neutrons produced in one fission event proceeds to cause a second fission from which one neutron goes on to cause a third fission, and soon. In such a reaction the neutron density and fission rate remain constant. This condition can be expressed by means of a multiplication factor, k, which is defined as the ratio of the number of neutrons in one generation to the number of neutrons in the preceding generation. When this factor is exactly one the condition for a stable chain reaction is satisfied and the reactor is said to be critical. If this factor is greater than one the reactor is supercritical and a divergent chain reaction exists in which the neutron density and fission rate increase, possibly at an explosive rate as in an atomic bomb. If the multiplication factor is less than one the reactor is subcritical and the chain reaction decreases and eventually dies out.

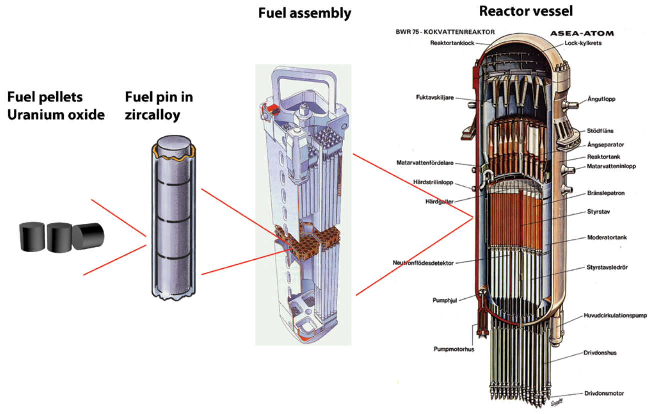

Figure 9.1 Main components of the nuclear reactor - Light Water Boiling Reactor - BWR

A nuclear reactor is an assembly of many components - see Figure 9.1 - of which at this stage we need mention a few of the most important. The most important component of any reactor is the fuel in which fission takes place and energy, in the form of heat, is released. At the present time uranium is the most widely used nuclear fuel, although the isotope ^{239}Pu is becoming increasingly important. In many reactors a light element is included for the specific purpose of slowing down neutrons from fission to thermal energy at which they are most effective for causing further fission. This material is called the moderator and we shall discuss moderators and their characteristics later in this chapter. Finally cladding materials are required to contain and support the fuel and prevent the release of radioactive fission products, and in the case of all reactors, except those operating at very low power, a coolant is required which is circulated through the core to transport the energy released in the fuel by fission to external heat exchangers.

Returning to the conditions for a critical reactor we can say that the rate at which neutrons are used up or lost in a reactor must be exactly equal to the rate at which they are produced by fission. Neutrons are used up or lost in two ways, either they leak out of the reactor or they are absorbed within the reactor. Absorption within the reactor includes fission and capture in the fuel and capture in the other materials of the reactor such as the moderator, coolant, cladding and control rods. The relative rates at which these processes take place depend on the size and composition of the reactor. It is the purpose of reactor theory to analyse the various processes in a reactor, determine their rates and calculate for a given composition and size of core the value of the multiplication factor. Alternatively the calculation may be directed towards finding the critical size or composition of a reactor for a given value of the multiplication factor.

As an introduction to this type of problem let us consider the possibility of a chain reaction in an infinitely large system of pure natural uranium which consists of 99.285 per cent ^{238}U and 0,715 per cent ^{235}U. (The ratio of ^{238}U atoms to ^{235}U atoms is approximately 139 to 1.) The purpose of considering an infinite system is to avoid for the present time the question of neutron leakage as neutrons cannot leak out of an infinite system.

Neutrons produced by fission in the uranium have an average energy of 2 MeV and at this energy the significant cross-sections are:^{238}U; σ_i = 2. 87 barns, σ_f = 0.6 barns; ^{235}U; σ_i = 2.3 barns, σ_f = 1.3 barns. (The values of the other cross-sections are negligibly small) Bearing in mind the greater amount of ^{238}U, it is evident that inelastic scattering in ^{238}U will be the dominant process for 2 MeV neutrons, which will rapidly lose energy and fall below the threshold for fission in ^{238}U (see Figure 9.2). There may be some fission in ^{238}U caused by neutrons of energy greater than 1 MeV, but it will not be sufficient to establish a chain reaction. At about 0 3 MeV the significant cross-sections are: ^{238}U; σ_i, = 0.5 barns; ^{235}U; σ_i= 0.7 barns, σ_f=1.3 barns. Bearing in mind the ^{238}U to ^{235}U ratio, it is evident that inelastic scattering in ^{238}U continues to be the most probable type of interaction and the neutron energy falls to about 1000 eV, the upper limit of the resonance region of ^{238}U (see Figure 9.3). Below this energy the capture cross- section of 238U rises to isolated values or resonances which are much higher than the scattering cross-section. The fission cross-section of ^{235}U (Figure 9.2) has similar resonances between 100 eV and 1 0 eV, but they are not so high as the ^{238}U resonances. In this energy range, therefore, neutron capture in ^{238}U becomes the dominant process to such an extent that practically all neutrons are captured in ^{238}U resonances and negligibly few cause fission in ^{235}U. A chain reaction is thus impossible in pure natural uranium.

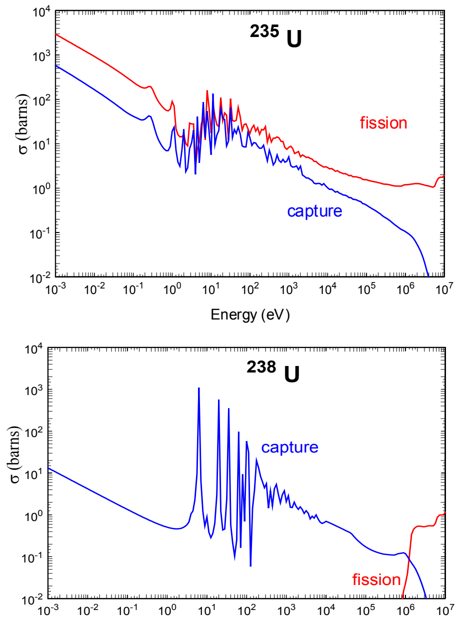

Figure 9.2 Fission and capture cross sections for ^{235}U and ^{238}U.

Let us now consider the possibility of a chain reaction in an infinite system of enriched uranium with 50 per cent ^{235}U and 50 per cent ^{238}U. Neutrons with an energy of 2 MeV have, referring to the cross- section values already quoted, about a 27 per-cent chance of causing fission and a 73 per cent chance of being inelastically scattered. This is not sufficient to establish a chain reaction at 2 MeV. At lower energies the values of σ_i, for both ^{235}U and ^{238}U decrease and the value of σ_f for ^{235}U increases so that at 0.3 MeV, using the previous figures, fission occurs in just about 50 per cent of interactions and a chain reaction is possible. The conclusion to be drawn from this very qualitative argument is that in a system of 50 per cent ^{235}U and 50 per cent ^{238}U a chain reaction can be established by neutrons in the energy range 0.3 to 2 MeV. This is the basis of a fast reactor, the word fast indicating that the fission causing neutrons have high energy.

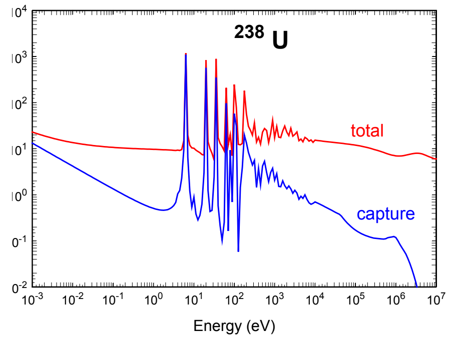

Figure 9.3 Total and capture cross section of ^{238}U

Turning our attention again to an infinite system of natural uranium the question arises as to whether there is any neutron energy at which fission in ^{235}U would be a sufficiently probable reaction to establish a chain reaction. Considering thermal neutrons whose energy is taken as 0.025 eV, the values of the relevant cross-sections are: ^{238}U; σ_c = 2.72 barns; ^{235}U σ_c= 101 barns, σ_f= 579 barns. (Scattering need not be considered as the scattering of thermal neutrons does not, on average, affect their energy.) Using these figures the fraction of thermal neutrons absorbed in natural uranium which cause fission is:

$$\frac{579}{579+101+2.72\times 139}=0.547$$

If 2.42 neutrons are produced per fission and 54.7 per cent of these cause fission then the multiplication factor is 2.42 * 0.547 = 1.32, and a chain reaction is established. This is of course a highly simplified argument and has ignored several important aspects such as neutron capture in other components of the reactor and neutron leakage in a reactor of finite size, however the fact remains that there is a possibility of establishing a chain reaction in natural uranium with thermal neutrons.

The problem now arises as to how to slow down fission neutrons to thermal energy and at the same time ensure that as few as possible are captured in the ^{238}U resonances during the process. This is achieved by combining the uranium fuel with a material, called the moderator, which is effective at slowing down neutrons. The moderator should be an element of low mass number (or a compound containing such an element), it should have a high scattering cross-section if possible, and in order that it does not capture neutrons (which would reduce the possibility of a chain reaction) it should have a low capture cross-section. Furthermore, in order that scattering should be the dominant process at all energies, including the ^{238}U resonance region, the quantity of moderator should be much greater than the quantity of fuel. A reactor in which fission is caused predominantly by thermal neutrons is called a thermal reactor.

The choice of the moderator for a thermal reactor is governed by the considerations mentioned in previous lectures, and there are three materials which are suitable and widely used, namely water, heavy water and carbon in the form of graphite. Beryllium, beryllium oxide and certain hydrocarbon compounds might also be suitable, but they each have certain disadvantages which have prevented their large scale use as moderators. The important properties of some of these materials are listed in Table I.

Table I. Moderating properties of some important moderators and uranium.

Moderator	σ_a	σ_s	ξ	N	$\xi\sigma_s$	$\xi\sigma_s/\sigma_a$
H_2O	0.66	~50	0.927	19.7	46	62
D_2O	0.001	10.6	0.510	36	5.4	5400
Be	0.0092	6.1	0.209	87	1.27	139
C	0.0045	6.1	0.158	115	0.74	165
U-nat	3.4	8.3	.0084	2170	0.07	0.02

Each of the moderators listed in Table I has certain advantages and disadvantages which makes the choice of one of them as the best possible moderator more or less impossible. Water is cheap and has excellent slowing-down properties and a high scattering cross-section, however its capture cross-section is rather high and enriched uranium is required as fuel in a water-moderated reactor. Heavy water has good slowing down properties and a very low capture cross-section. It is, however, very expensive to separate heavy water from ordinary light water, and this economic factor is a disadvantage in the use of heavy water as the moderator in large reactors. Graphite is fairly cheap and has a low capture cross-section, but its mass number is rather too high for it to be regarded as an ideal moderator; it is nevertheless extensively used, particularly in British power reactors. Beryllium is rather expensive and toxic and has not been used as a moderator on a large scale.

9.3 The neutron cycle in a thermal reactor

Accurate calculations of the multiplication factor for any reactor must take full account of all the processes involving neutrons between the time when they are produced by fission and the time when they eventually disappear either by absorption or by leakage from the reactor. The procedure is simplified if we consider various parts of the neutrons' lifetime separately, and we will apply this method to a thermal reactor of finite size fuelled with natural or enriched uranium. The neutron cycle for such a reactor is illustrated in Figure 9.4.

Consider **n** neutrons at an average energy of 2 MeV produced by thermal fission in ^{235}U. Before these neutrons slow down below 1 MeV there is a possibility that a few cause fission, referred to as fast fission, in ^{238}U. The fast fission factor, **ε** is defined as:

The number of neutrons slowing down below 1 MeV per neutron produced by thermal fission.

Now **nε** neutrons are slowing down below 1 MeV and continue to slow down as a result principally of elastic scattering collisions with the moderator. During the slowing down process some neutrons leak out of the reactor, and some neutrons are captured in the ^{238}U resonances. The resonance escape probability, **p**, is defined as:

The fraction of neutrons which escape capture in the ^{238}U resonances during slowing down in the reactor.

The fast non-leakage probability, $\mathbf{P_{NLf}}$ is defined as:

The fraction of neutrons which do not leak out of the reactor during slowing down.

The number of neutrons which slow down and become thermal is $\mathbf{n\varepsilon pP_{NLf}}$.

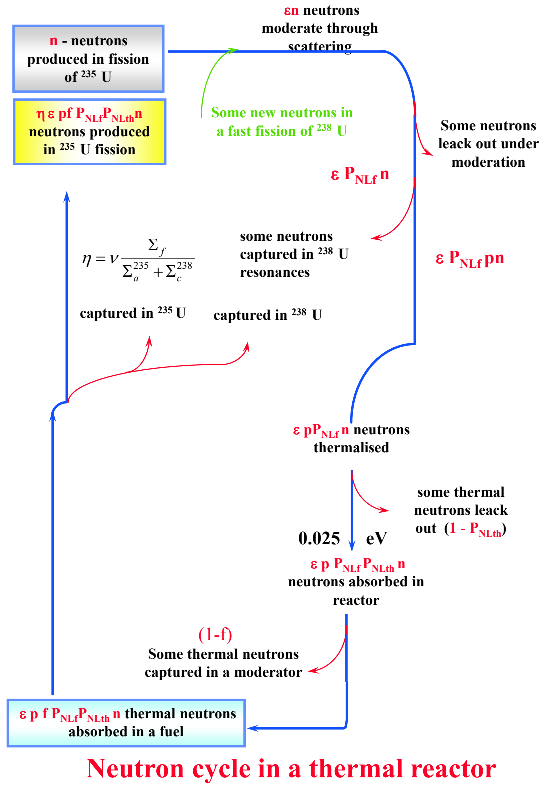

Figure 9.4 The neutron life-cycle in the thermal reactor

Once the slowing down process is complete and neutrons are thermalized they will continue to diffuse in the reactor until they are absorbed or leak out. Only a fraction of the absorption of neutrons is in the fuel, and some neutrons are captured in the moderator, coolant or structural materials of the core. The thermal non-leakage probability, $\mathbf{P_{NLth}}$, is defined as:

The fraction of thermal neutrons which do not leak out of the reactor.

The thermal utilization factor, **f**, is defined as:

The fraction of thermal neutrons absorbed in the reactor which are absorbed in the fuel.

It is evident that the number of neutrons which is absorbed in the fuel, is $\mathbf{n\varepsilon pfP_{NLf}P_{NLth}}$. Not all these neutrons cause fission, in fact in natural uranium our earlier calculation indicates that about 55 per cent of thermal neutrons absorbed in the fuel cause fission, and that the number of neutrons produced is about 1.33 per neutron absorbed in the fuel. This quantity, the average number of fission neutrons produced per neutron absorbed in the fuel, has the symbol **η** and is usually just called eta.

Finally, therefore, at the beginning of the second generation $\mathbf{n\varepsilon pf\eta P_{NLf}P_{NLth}}$ fission neutrons are produced from n fission neutrons at the beginning of the first generation. From our definition of the multiplication factor, which is called more explicitly for a finite reactor the effective multiplication factor, $\mathbf{k_{eff}}$, we can write:

$$k_{eff} = \varepsilon pf\eta P_{NLf}P_{th} \tag{9.1}$$

It is often convenient to consider an infinitely large reactor, as this enables us to neglect neutron

diffusion and leakage, and $P_{NLf}=P_{NLth} = 1$. The multiplication factor is then referred to as the infinite multiplication factor, k_∞, and is expressed by the important Four Factor Formula:

$$k_\infty = \varepsilon pf\eta \tag{9.2}$$

The relationship between the two multiplication factors is:

$$k_{eff} = k_\infty P_{NLf}P_{th} \tag{9.3}$$

The calculation of keff, or k_∞ can be carried out by calculating separately the factors on the right-hand side of equation (9.1) or (9.2), and some of the elementary theory underlying these calculations will be dealt with in the next chapter.

It was pointed out earlier that for certain types of reactor enriched uranium is necessary to achieve criticality. The most important examples are the boiling water reactor and the pressurized water reactor which require uranium enriched with 2 to 4 per cent of ^{235}U. Uranium fuelled fast reactors (of which very few have been built - see lecture Reactor Types) require highly enriched uranium with 25 to 50 per cent of ^{235}U. See Figure 9.6 and Figure 9.7 for a simplified neutron economy assessment.

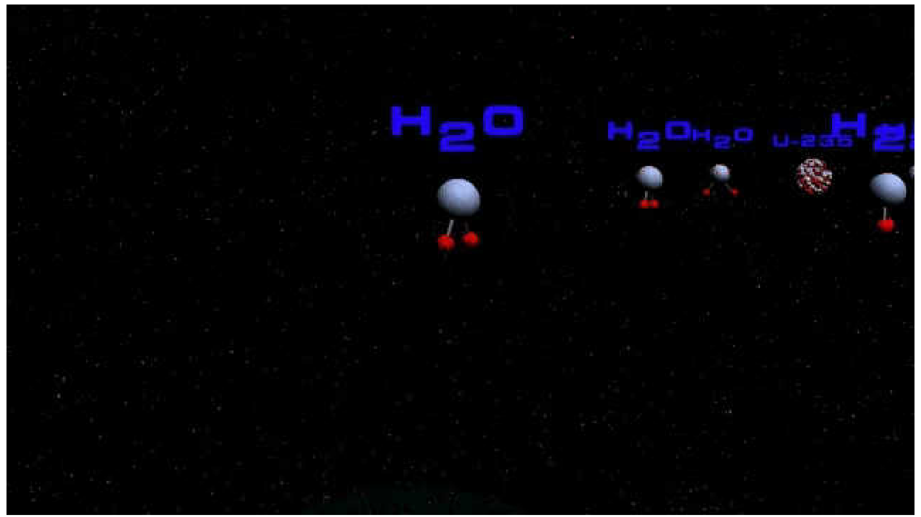

Figure 9.5 A simplified model of a thermal neutron induced fission. Click to watch.

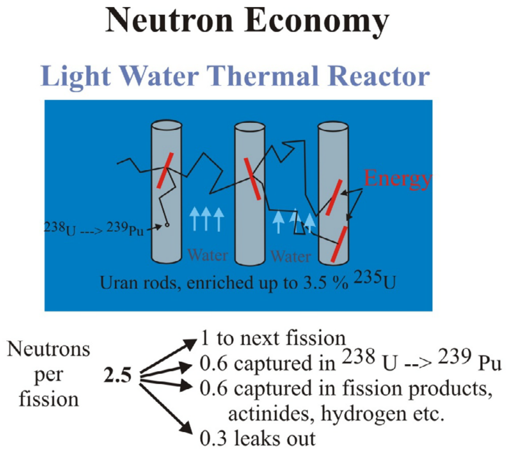

Figure 9.6 Neutron economy balance in Light Water Reactors

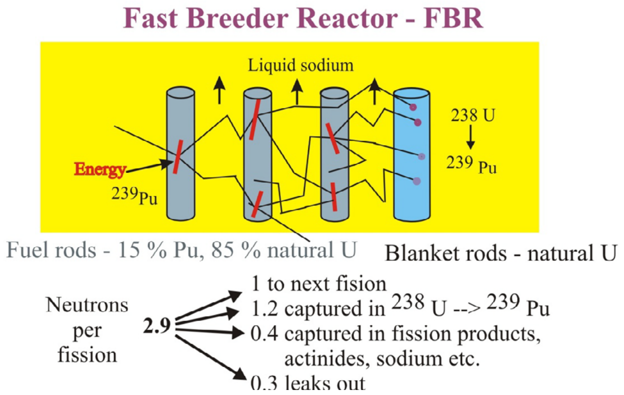

Figure 9.7 Neutron economy balance in Fast Breeder Reactor

9.4 Conversion and breeding

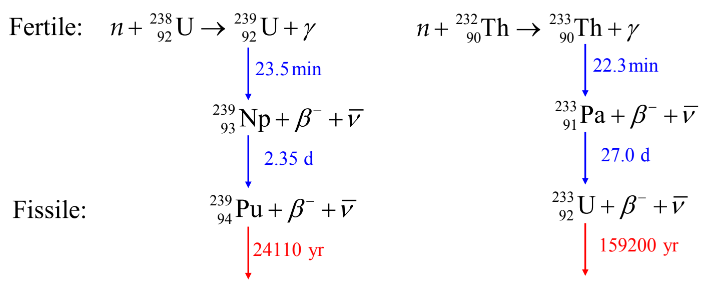

$$B\equiv\frac{\text{Number of new fissile nuclides produced}}{\text{Number of fissile nuclides consumed}}$$

Figure 9.8 Schematic picture of breeding processes from fertile isotopes of ^{238}U and ^{232}Th

One important point to emerge from earlier sections of this chapter is that in thermal reactors fuelled with uranium, either natural or enriched, practically all the fission occurs in ^{235}U. In fast reactors, which contain no moderator and in which neutron energies are much higher than in thermal reactors, ^{238}U fission occurs to a small extent, but even in this type of reactor it is ^{235}U fission which predominates and sustains the chain reaction. It is nearly correct to say, therefore, that only the ^{235}U in natural uranium contributes energy directly from its own fission.

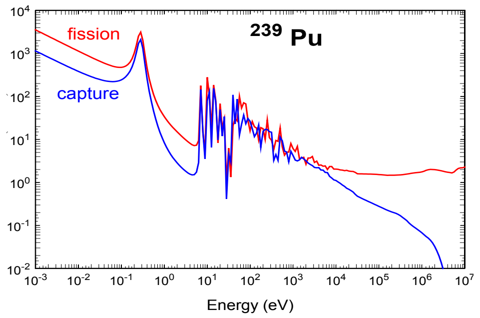

Figure 9.9 Fission and capture cross section of ^{239}Pu

Although ^{238}U cannot itself be used as the fuel in a nuclear reactor, it does have a vital role to play as an isotope from which new fissile fuel can be created. In a uranium fuelled reactor a significant fraction of the neutrons produced by fission, possibly 30-40 per cent, are captured in ^{238}U and produce ^{239}U by an (n,γ) reaction. ^{239}U is the start of a radioactive decay chain which produces neptunium 239 - ^{239}Np, also radioactive and plutonium 239 - ^{239}Pu, which has a very long half-life and can almost be regarded - in reactor context - as a stable isotope. See conversion path from ^{238}U to ^{239}Pu at Figure 9.8. ^{239}Pu, as already pointed out and as can be seen from Figure 9.9 presenting fission and capture cross-sections of ^{239}Pu, is fissile, its characteristics as far as fission is concerned are similar to those of ^{235}U, and it can be used as the nuclear fuel in both fast and thermal reactors.

Another isotope which has characteristics similar to ^{238}U is ^{232}Th, the only naturally occurring isotope of the element thorium. This isotope can only undergo fission with neutrons of energy greater than about 1-4 MeV - see Figure 9.10 , so it cannot sustain a chain reaction and be used directly as a nuclear fuel. However, as a result of neutron capture in ^{232}Th the processes presented on the above picture take place.

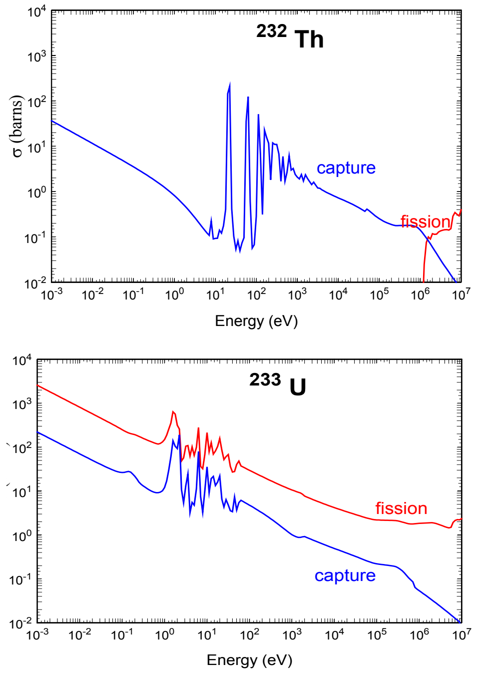

Figure 9.10 Fission and capture cross sections of ^{232}Th and ^{233}U

^{233}U is fissile with neutrons of all energies and like ^{235}U and ^{239}Pu it can be used as the fuel for nuclear reactors - see Figure 9.10.

The importance of ^{233}U and ^{232}Th lies in their ability to act as fertile materials from which, as a result of neutron capture in nuclear reactors, the fissile isotopes ^{239}Pu and ^{233}U are produced. This process is known as breeding or conversion, and it provides the method whereby ^{238}U and ^{232}Th can be used as sources of energy through fission. Breeding processes make nuclear energy sustainable in a very, very long time scale.

An important characteristic of a nuclear reactor, particularly one which is designed to produce new fissile material by one of the processes just described as well as power, is the ratio of the rate at which new fissile atoms are produced to the rate at which existing fissile atoms are used up. This ratio is the breeding ratio B and is defined as:

$$B\equiv\frac{\text{Number of new fissile nuclides produced}}{\text{Number of fissile nuclides consumed}}$$

in other words: *The number of new fissile atoms produced in a reactor per atom of existing fissile fuel consumed by fission and neutron capture.*

If the breeding ratio is exactly 1 then the quantity of fissile fuel re- mains constant, if it is greater than 1 the quantity of fissile fuel increases, and if it is less than 1 the quantity of fissile fuel decreases. In order to utilize all the world's resources of ^{238}U and ^{232}Th it is essential that some, though not necessarily all, of the world's reactors are designed so that their breeding ratios are greater than l.

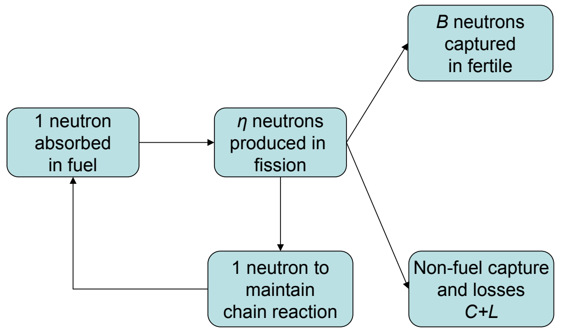

Figure 9.11 Neutron cycle illustrating breeding

The following simplified argument illustrates this point. Consider a reactor (or a number of reactors) whose breeding ratio is B, fuelled with natural uranium, the total mass of ^{235}U being M tonnes. If all the ^{235}U is used up, the quantity of ^{238}U converted to ^{239}Pu is approximately BM tonnes - see Figure 9.11. If this plutonium is used to provide the second charge of fuel for the reactors, and if the value of B is the same for a plutonium fuelled reactor as for a uranium fuelled reactor (which is not strictly true as we shall see), then the use of BM tonnes of ^{239}Pu results in another B2M tonnes of ^{238}U being converted to ^{239}Pu, and so on. The total amount of uranium used up would be M + BM + B^2M +.... If B 1, then this is equal to M/(1–B). If this result were exact, which it is not, the value of B necessary to use up all the natural uranium originally in the reactors would be about 0.993, or for all practical purposes l. In fact it is necessary that the value of B should be slightly greater than 1 as the foregoing argument neglects the inevitable losses of plutonium and uranium during chemical processing, separation of fission products and manufacture of fuel elements.

If the value of B is much less than 1 then only a fraction of the available uranium is used up, for example if B = 0.75, then theoretically 2.86 per cent of the natural uranium can be used, still a very small fraction which in practice would be even smaller. The dependence of the breeding ratio on other reactor parameters can be deduced from the following argument. When a neutron is absorbed in an atom of fissile fuel, that atom is consumed (in the sense used in the definition of the breeding ratio) and ηf, neutrons are produced, where ηf is the average number of neutrons produced per neutron absorbed in the fissile fuel. For a steady chain reaction in a reactor one of these neutrons must be absorbed in another atom of fissile fuel to keep the reaction going, and according to the definition of the breeding ratio, B neutrons must be captured in the fertile material. Some neutrons will inevitably be captured in non-fuel materials, and some will leak out of the reactor. The sum of these two processes is represented by (C + L) neutrons per neutron absorbed in the fissile fuel. These processes are shown in Figure 9.11. It is clear that in order to maintain a steady chain reaction:

$$\eta = 1 + B + (C + L) \quad \text{or} \quad B = \eta - 1 - (C + L) \tag{9.4}$$

Clearly if B is to be greater than 1, η, must exceed 2 by an amount that allows for the term (C + L), whose value is likely to be about 0.2. Values of η for the three fissile isotopes for fission caused by thermal and high energy neutrons are given in Table II.

It will be seen from Table II that, allowing for reasonable non-fuel neutron capture and leakage, only a ^{233}U fuelled thermal reactor can achieve a breeding ratio greater than l. In fast reactors there is a considerable improvements, and reactors of this type are capable of giving breeding ratios greater than 1. The value of B in a fast reactor is actually greater than that given by equation due to the effect of fast fission in ^{238}U or ^{232}Th, which is very slight in a thermal reactor but may be considerable in a fast reactor in which as much as 20 per cent of the fission may be in the ^{238}U (less in ^{232}Th).

Table II. η

ISOTOPE (100%)	Fast neutrons (>0.5 MeV)	Thermal neutrons (0.025 eV)
^{235}U	2.35	2.07
^{239}Pu	2.90	2.15
^{233}U	2.40	2.29

9.5 Fuel cycles and breeder reactors

In view of what has been said about breeding and the characteristics of the fissile isotopes in thermal and fast reactors, it is possible to visualize certain types of reactor and their associated fuel cycles.

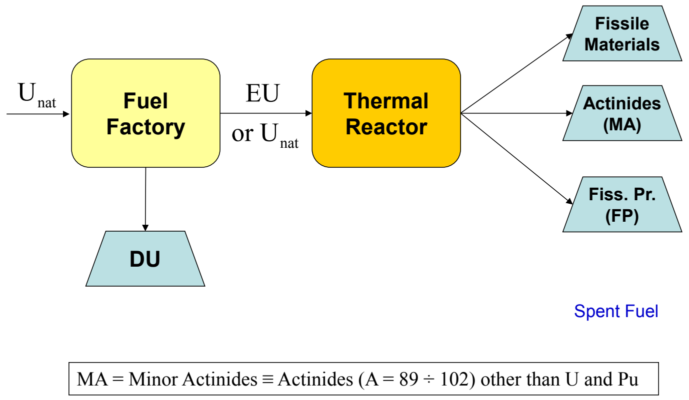

MA = Minor Actinides ≡ Actinides (A = 89 ÷ 102) other than U and Pu

Figure 9.12 Thermal reactor fuelled with uranium

Figure 9.12 shows a thermal reactor fuelled initially with natural or enriched uranium; it is typical of the vast majority of reactors built up to the present. The breeding ratio of such a reactor is less than 1 so the amount of ^{239}Pu produced is less than the amount of ^{235}U used. When the reactor is refuelled, although the ^{239}Pu might be recycled with the depleted uranium (which contains much less than 0.715 per cent of ^{235}U), some additional fissile fuel is needed to make up the deficit. Up to 1980 practically all the plutonium produced in this way has been stockpiled for nuclear weapons and future reactors, so that up to the present nearly all nuclear reactors have been fuelled with natural or enriched uranium and stocks of plutonium and depleted uranium have been steadily accumulating in several countries.

Typically about one percent of the spent fuel discharged from a reactor is plutonium, and some two thirds of the plutonium is ^{239}Pu. Worldwide, almost 100 tonnes of plutonium in spent fuel arises each year. A single recycling of plutonium increases the energy derived from the original uranium by some 12%, and if the ^{235}U is also recycled by re-enrichment, this becomes about 20%.With additional recycling the percentage of fissile (usually meaning odd-neutron number nuclides) in the mix decreases and even-neutron number, neutron-absorbing nuclide increase, requiring the total plutonium and/or enriched uranium percentage to be increased. Today in thermal reactors plutonium is only recycled once as MOX (Mixed OXides) fuel, and spent MOX fuel, with a high proportion of minor actinides and even plutonium isotopes, is stored as waste.

Today about 30 thermal reactors in Europe (Belgium, Switzerland, Germany and France) are using MOX and a further 20 (including in Sweden) have been licensed to do so. Most reactors use it as about **one third** of their core, but some will accept up to 50% MOX assemblies. In France, the nuclear operator (EdF) aims to have all its 900 MWe series of reactors running with at least one-third MOX. Of the total nuclear fuel used today, MOX provides only 2%. About 30% of the plutonium originally loaded into MOX fuel is consumed by use in a thermal reactor. If one third of the core fuel load is MOX and two-thirds uranium fuel, there is zero net gain of plutonium in the spent fuel. As plutonium isotopes absorb more neutrons than uranium fuels, reactor control systems need modifications. Moreover, fission gas release in MOX fuel assemblies may limit the maximum burn-up time of MOX fuel.

Future reactors will probably be fuelled with ^{239}Pu and depleted uranium, which can be regarded as pure ^{238}U, and in such reactors ^{238}U will be converted to ^{239}Pu, but only in fast reactors will the breeding ratio be greater than 1 and in such reactors more ^{239}Pu will be produced than is destroyed.

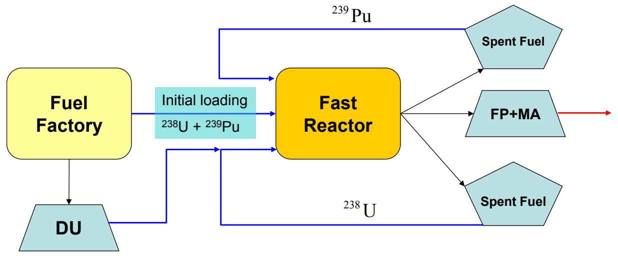

Figure 9.13 Fuel cycle for a fast reactor fuelled with ^{239}Pu and ^{238}U

Figure 9.13 shows the fuel cycle of a fast reactor fuelled with ^{239}Pu and ^{238}U in which the breeding ratio is greater than l.

When the first fuel charge is unloaded from the reactor it contains more ^{239}Pu and less ^{238}U than it did when new, and it is contaminated with fission products which must be removed during reprocessing. Some ^{239}Pu is available for other uses such as fuelling thermal reactors, while the rest is recycled. The ^{238}U is recycled but there is less of this isotope than in the original charge, so an additional supply ^{238}U is required for the second and subsequent fuel loadings. The important point about this fuel cycle is that the reactor is kept going by fresh supplies of non-fissile 238U, and in this way ^{238}U can be completely converted to ^{239}Pu and used as a source of energy.

If the reactor of Figure 9.13 had been a thermal reactor in which the breeding ratio is less than 1, it would require a continuous supply of ^{239}Pu as well as ^{238}U to keep it going. It is obvious that in a planned long-term nuclear power programme a combination of fast and thermal reactors will be able to utilize all the world's resources of uranium.

Similar ideas apply to reactors making use of the ^{232}Th – ^{233}U breeding process. A reactor fuelled initially with either ^{235}U or ^{239}Pu as the fissile material, and ^{232}Th as the fertile material will produce ^{233}U. When sufficient ^{233}U is produced it can be used as the fuel charge in either a fast or thermal reactor with ^{232}Th, and in such a reactor a breeding ratio greater than 1 is possible. In such a reactor the ^{233}U can be recycled, and the only fuel requirement is ^{232}Th, which can thus be completely used for the production of energy.

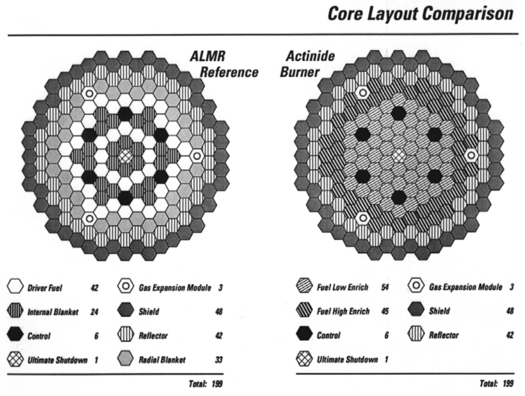

Figure 9.14 Core layout of the Advanced Liquid Metal Reactor (ALMR) for a reference case (left side) and for the actinide burner mode of operation

In reactors which are designed for breeding as well as power production the core may be subdivided into two regions as shown on Figure 9.14 presenting the core layout of the Advanced Liquid Metal Reactor - ALMR. In this type of reactor the inner region, called the core, contains nearly all the fissile material (^{239}Pu), and it is in this part of the reactor that most of the energy is released by fission. The outer region is called the blanket and contains the fertile material (^{238}U). At the start of the reactor's life there is very little fission in the blanket. However neutrons produced by fission in the core may diffuse into the blanket and be captured in ^{238}U to produce ^{239}Pu . As the operation of this reactor proceeds, fissile material builds up in the blanket and provision must be made to remove the energy released by fission from the blanket as well as from the core.

Another point worthy of mention is that in any reactor designed for breeding, neutron capture in the moderator, structural materials, etc., and neutron leakage from the core should be reduced to a minimum. This capture and leakage is the term (C + L) in equation (9.4), and it is clear from this equation that any increase of the term (C + L) reduces the possible value of the breeding ratio. As an example of this, it is generally true to say that the breeding ratio in a water-moderated reactor is less than in a graphite or heavy water-moderated reactor due to the rather high capture cross-section of water. In a reactor with a reasonably high value of the breeding ratio (say between 0.8 and 1.0) new fissile fuel is being produced almost as fast as it is being consumed, and the fuel in such a reactor can be used to a very high burnup, thus prolonging the periods between refuelling and reducing fuel costs.

In an expanding programme of nuclear power using breeder reactors to produce new fuel for later reactors, an important parameter is the doubling time, T_d, which is defined as the time required for the quantity of fissile fuel in a breeder reactor to double itself. Clearly, it can be interpreted as the time required for a breeder reactor to produce enough new fuel to provide the first fuel charge for another identical reactor, and this time will control the rate at which a breeder reactor programme can be expanded.

Figure 9.15 Mechanism of delay neutron emission: decay scheme of ^{87}Br.

An expression for the doubling time can be derived as follows:

If the rating of a reactor is given by:

$$R = N_F \sigma_f \phi E \ watts / gram \qquad (9.5)$$

where N_F is the number of atoms per gram of fissile fuel and E is the energy released per fission, Joules.

If the mass of fissile fuel in the reactor is M_F grams, then the rate of consumption of fissile fuel is $M_f N_f \sigma_a \Phi$ atoms/second, and the rate of production of new fissile fuel is $BM_f N_f \sigma_a \Phi$ atoms/second. The net rate of production of new fissile fuel, i.e. the rate at which production exceeds consumption = $(B-1)M_f N_f \sigma_a \Phi$ atoms/second. This rate multiplied by the doubling time must by definition be equal to the original number of atoms of fissile fuel $M_F N_{F.}$ Thus:

$$T_d (B-1) M_F N_F \sigma_a \phi = M_F N_F \qquad (9.6)$$

Substituting for Φ from equation (9.5) and rearranging, we get:0

$$T_d = \frac{N_F \sigma_f E}{(B-1) R \sigma_a} \qquad (9.7)$$

Since $N_{f,} \sigma_a$, σ_f are all constant for any particular fissile isotope, equation (9.7) can be interpreted as stating that the doubling time is inversely proportional to both (B – 1) and the reactor rating R. In order to reduce the doubling time it is therefore desirable to design a breeder reactor with as high a value of B as possible, and to operate the reactor at as high a rating as possible.

Doubling times are measured in years, rather than weeks or months. For example, if the following values for a ^{239}Pu fueled fast breeder reactor are used, namely NF= 2.52×10^{21} atoms/gram, E = 3.36×10^{-11} joules/fission, σ_f= 1.8 barns and σ_a = 2.15 barns, and if the breeding ratio is assumed to be 1.2 and the rating 500 MW/tonne of ^{239}Pu, then the doubling time can be calculated to be about 22 years.

The operation of fast breeder reactors at high ratings is also dictated by the fact that the mass of fuel in these reactors is much smaller than in thermal reactors, and if these reactors are to produce large quantities of energy for, say, electricity generation, then they must operate at high ratings. The high ratings characteristic of fast breeder reactors lead to certain engineering features which will be described in a other lectures.

9.5.1 Conversion factor for a thermal reactor

If B<1 it is called usually C - a conversion factor. Let us estimate number of created ^{239}Pu nuclei per a neutron absorbed in a reactor core.

$$\frac{\Sigma_c^{238}}{\Sigma_a^{235} + \Sigma_c^{238}} + \eta_{nat.U} \varepsilon (1-p) P_{NLf} P_{NLth} \qquad (9.8)$$

The first term of expression (9.8) describes thermal neutrons absorbed in ^{238}U, the second term - the neutrons absorbed during slow-down process.

Consequently the number of utilized nuclei of ^{235}U per absorbed neutron becomes:

$$\frac{\Sigma_f^{235}}{\Sigma_a^{235} + \Sigma_c^{238}} \qquad (9.9)$$

Dividing expressions (9.8) and (9.9) - C can be derived as:

(9.10)

Remembering that:

$$\eta_{nat.U} = \frac{\Sigma_f^{235}}{\Sigma_a^{235} + \Sigma_c^{238}}\nu$$

Examples

Estimate conversion factor C for heavy water (or graphite) moderated reactor with natural uranium fuel.

Data:

^{238}U - 99.285%
^{235}U - 0.715%
σ_{c238} - 2.72 b
σ_{c235} - 101 b
σ_{f235} - 579 b
ν - 2.42
η_{235}- 2.07

Putting above data into Eq. (9.10) we get

$$\mathbf{C = \underset{\displaystyle\downarrow \atop \displaystyle 0.556}{\frac{2.72}{680} \cdot 140} + \underset{\displaystyle\downarrow \atop \displaystyle 0.10}{2.07 \cdot 1.03 \cdot 0.05 \cdot 0.95} \approx 0.65}$$

Table III. Conversion factor for different reactor types

Reactor type	Initial fuel	Conversion cycle	Conversion factor
BWR	^{235}U (2-4%)	^{238}U → ^{239}Pu	0.6
PWR	^{235}U (2-4%)	^{238}U → ^{239}Pu	0.6
PHWR (CANDU)	Unat	^{238}U → ^{239}Pu	0.8
HTGR	^{235}U (5%)	^{232}Th → ^{233}U	0.8
LMFBR	^{239}Pu (10-20%)	^{238}U → ^{239}Pu	1.0 – 1.6

Is a chain reaction possible in natural uranium?

Thermal utilization factor for pure natural uranium is f:

$$f = \frac{579}{579 + 101 + 2.72 \cdot 139} = 0.574$$

and consequently number of fission neutrons produced per one absorbed neutron in natural uranium is η_{nat}:

$$\eta_{natU} = \nu \cdot f > 1$$

and is bigger than 1 - ***chain reaction is theoretically possible using natural uranium***. Heavy water and graphite moderated reactors take advantage of this due to very low absorption of neutrons in heavy water and graphite.

9.6 Nature of multiplication constant

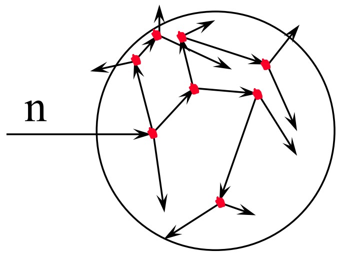

Let's consider sphere of fissile material e.g. ^{235}U or ^{239}Pu. Per 1 neutron absorbed η are new created. If P = probability that particle stays in sphere so after one generation of neutrons we have :

After one generation —- ηP neutrons

So

$$\frac{\eta P}{1} = k \rightarrow \text{multiplication constant}$$

Generally:

$N_2 = k N_1$
$N_3 = k N_2 = k^2 N_1$
.
.
$N_n = k^{n-1} N_1$

If time between two neutron generations = τ or in other words if the life time of neutron generation = t so number of neutrons after time t:

$$N(t) = N_1 k^{\frac{t}{\tau}} \tag{9.11}$$

to make this equation easier for analytical solutions we can logarithm and derived equation (9.11) getting:

$$\frac{1}{N}\frac{dN}{N} = \frac{\ln k}{\tau} \approx \frac{k-1}{\tau} \tag{9.12}$$

Solution of this equation is:

$$N(t) = N_1 e^{(k-1)\frac{t}{\tau}} \tag{9.13}$$

Equation (9.13) describes the relation between the neutron density, multiplication factor and life time of neutron generation in the system for the "violent" chain reaction.

To investigate the importance of this equation we can analyze closely the chain reaction in the uranium sphere described above.

Example on magnitudes in a chain reaction governed by prompt fission neutrons in ^{235}U

data for ^{235}U:

$\rho=19$ g/cm^3, $\sigma_f=1.2$ b, $\sigma_t=6$ b.

From equation (9.13) we get:

$$N(t)=N_1e^{(k-1)\frac{t}{\tau}}=N_0e^{\frac{t}{T}}\ if\ T=\frac{\tau}{k-1} \tag{9.14}$$

where T is called a ***PERIOD*** of this fissile system.

Remebering that neutron velocity for energy 2 MeV — $V_{2MeV}=2\times10^9$ cm/s we estimate the ration between fission and total cross-section for ^{235}U

$$\frac{\sigma_f}{\sigma_f+\sigma_c+\sigma_s}=\frac{\sigma_f}{\sigma_T}\cong\frac{1.2}{6}=\frac{1}{5} \tag{9.15}$$

and corresponding macroscopic total cross-section and neutron mean free-path:

$$\Sigma_T=\frac{6\cdot10^{23}\cdot19\cdot6\cdot10^{-24}}{235}=0.29\,cm^{-1}$$
$$\tau_T=\frac{1}{\Sigma_T}=3.4\,cm \tag{9.16}$$

Time elapsed during 1 neutron mean free-path (1 neutron transport step) is:

$$\tau=\frac{\lambda_T}{V}=\frac{3.4}{2\cdot10^9}1.7\cdot10^{-9}\,s \tag{9.17}$$

From equation “(9.15)” on page 206can be seen that there are needed 5 steps (5 mean free-paths) for fission to occur. These steps take 8.5×10^{-9} s. Assuming k-1=0.85 (a reasonable value or our ^{235}U sphere) w can calculate the period T:

$$T=\frac{8.5\cdot10^{-9}}{0.85}=10^{-8}\,s \tag{9.18}$$

Now we try to estimate how long time it takes to get $3\cdot10^{24}$ neutrons (enough to fission 1 kg ^{235}U)

$$\frac{N(t)}{N_1}=3\cdot10^{24}\cdot e^{\frac{t}{10^{-8}}}\approx5.6\cdot10^{-7}\,s$$

$$1\,gatom=6\cdot10^{23}\ \ atoms\,of\ {}^{235}_{92}U=235g$$

$$3\cdot10^{24}\ \ neutrons\ \ can\,theoretically\ \ fission:$$

$$\frac{3\cdot10^{24}}{6\cdot10^{23}}\cdot235=1175\,g\ {}^{235}_{92}U$$

If c:a 10 % of neutrons leak out so result becomes c:a 1 kg ^{235}U is fissioned by $3\cdot10_{24}$ neutrons. Fission of 1g ^{235}U releases energy 1 MWd (= 1 megawattday) = 24·3600 MJ = $8.6\cdot10^4$MJ. This corresponds an explosive power of 20 ton TNT (1 W = $3.1\cdot10^{10}$ fissions/s). So fission of 1 kg 235U corresponds 20 kiloton TNT.

In the case described here this energy is released in the extremely short time of ~$6\cdot10^{-7}$s (as it is done in a nuclear bomb explosion). In the reactor case - like Forsmark reactors - 1 kg of ^{235}U is fissioned in 8 hours ($2.9\cdot10^4$ seconds) giving the power of 3 000 MW$_{th}$. So the power of the bomb compare to the reactor is:

$$300\cdot\frac{2.9\cdot10^4}{6\cdot10^{-7}}MW\approx1.5\cdot10^{14}\,MW \tag{9.19}$$

Reactors FORSMARK 3 and OSKARSHAMN 3 operate with a thermal effect of c:a 3000 MW. They deliver energy of 3000MWd, which corresponds to fission of 3 kg ^{235}U per day or to three (3) atom bombs (as this one dropped on Nagasaki) a day!

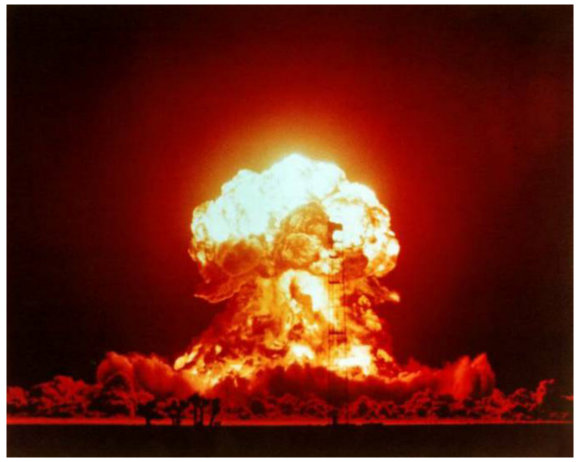

Figure 9.16 Badger atomic bomb test.18 April 1953 - Nevada Test Site 23 kilotons

Figure 9.17 Forsmark 3 reactor - 3157 MW thermal power

Figure 9.18 Nuclear weapon and nuclear power are not “two sides of the same coin”. They have different purpose, different physics and very different time scales.

Chapter 10

Slowing Down of Neutrons - Thermalisation of Neutrons

10.1 Introduction

Neutrons are produced by fission at an average energy of about 2 MeV, and that in the case of ^{235}U, ^{239}Pu and ^{233}U low energy neutrons are the most effective for causing fission, as the value of σ_f, rises at low energy. Anticipating some of the subject matter of the next chapter, we may conclude that if neutrons are produced by fission at high energy and are most effective in causing fission at low energy, then an important process in a reactor is the slowing down of neutrons in which, as a result of successive scattering collisions, their energy is progressively reduced.

With intermediate and heavy nuclei inelastic scattering is the most effective process for slowing down neutrons provided their energy is high enough, however the analysis of this process is beyond the scope of this book, and we will confine our attention to elastic scattering, which is the only possible type of scattering between neutrons produced by fission and light nuclei.

As it was shown in the lecture *"Neutron interactions with matter"*, the energy of a neutron after an elastic scattering collision is related to its energy before collision, the mass of the scattering nucleus and the angle of scattering in the C-System. In a reactor in which billions of neutrons are being scattered each second, we are interested not so much in the loss of energy of each neutron as the average loss of energy per scattering. In the C system this distribution is given by the empirical scattering law saying:

Elastic scattering is isotropic in the C system.

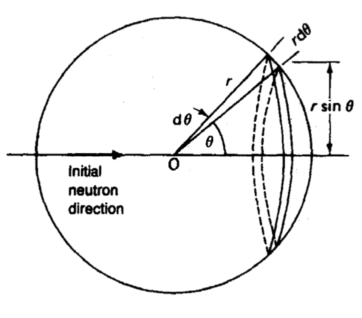

Figure 10.1 Scattering law for the C-system

In other words there is no preferential direction of scattering in the C system. If we imagine a large number of neutrons, all moving initially along the same path and being scattered at point 0, the centre of a sphere, then the number of neutrons emerging through any unit area on the surface of the sphere is independent of the position of the unit area. We can deduce a scattering law in terms of q, the angle of scattering in the C system. Referring to Figure 10.1 the fraction of neutrons whose angle of scattering in the C system is between θ and θ + dθ is given by the distribution function p(θ) dθ:

$$p(\Theta)d\Theta = \frac{The\,area\,of\,the\,ring\,rd\Theta}{Total\,surface\,area\,of\,the\,sphere}$$

$$= \frac{2\pi r\sin\Theta rd\Theta}{4\pi r^2} = \frac{1}{2}\sin\Theta d\Theta$$

It is more useful to have a distribution function in terms of the post-collision energy. If P(E) dE is the fraction of post-collision neutrons with energies in the range E to E + dE, then p(q) dq and P(E) dE are related by:

$$P(E)dE = -p(\theta)d(\theta)$$

$$= -p(\theta)\frac{d(\theta)}{dE}dE$$

Remembering the equation for neutron energy after an elastic collision (see lecture "Neutron interactions with matter")

$$E_2 = E_1\left\{\frac{1 + A^2 + 2A\cos\Theta}{(1+A)^2}\right\}$$

and replacing the post-collision energy E2 by E, we get

$$dE = -\frac{2AE_1}{(1+A)^2}\sin\Theta d\Theta$$

and consequently

$$P(E)dE = \frac{(A+1)^2}{4AE_1}dE$$

$$= \frac{dE}{(1-\alpha)E_1}$$

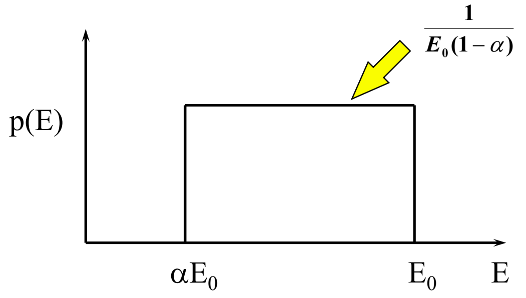

Figure 10.2 Probability of neutron energy after elastic collision in C- system

The quantity (1-α)E1 is the range of possible post-collision energies, and equation above indicates that after scattering collisions neutrons are uniformly distributed throughout this range - see Figure 10.2. Alternatively, neutron scattering may be said to be isotropic in post-collision energy in the range E1 to aE1. The average energy of neutrons after collision is 1/2(1 + α)E1, and the average loss of energy is 1/2(1- α)E1 .

Two important points emerge from these results. Firstly, the average loss of energy increases as a decreases, or as the mass number, A, of the scattering nucleus decreases, from which we conclude that light elements are more effective than heavy elements as far as neutron slowing down is concerned. Secondly, the average loss of energy is proportional to the pre-collision energy, and therefore decreases as neutrons lose energy. In order to have a quantity which characterizes the average loss of energy per collision and is at the same time independent of energy we will introduce the average decrease of (log energy) per scattering collision, $\overline{\log E_1 - \log E_2}$ which is given the symbol ξ(xi), and may be expressed as follows:

$$\xi = \overline{\ln\frac{E_1}{E}} = \frac{\int_{\alpha E_1}^{E_1} \ln\frac{E_1}{E}\, p(E)dE}{\int_{\alpha E_1}^{E_1} p(E)dE}$$

$$= \frac{1}{(1-\alpha)E_1}\int_{\alpha E_1}^{E_1} \ln\frac{E_1}{E}dE$$

By making the substitution ξ= E/E1 we get:

$$\xi = \frac{1}{(1-\alpha)}\int_{1}^{\alpha_1} \ln x dx$$

$$= 1 + \frac{\alpha}{1-\alpha}\ln\alpha = 1 + \frac{(A-1)^2}{2A}\ln\frac{A-1}{A+1}$$

$$\Rightarrow 1 \; for \; A = 1$$

$$for \; A > 10 \; can \; be \; approximated \; by$$

$$\Rightarrow \frac{2}{A+\frac{2}{3}} \; for \; A > 10$$

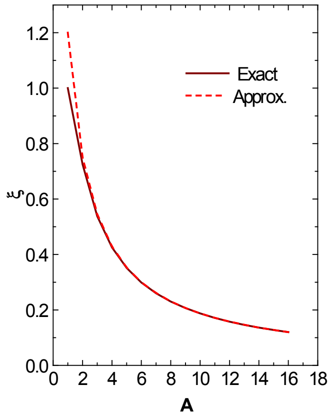

Figure 10.3 Comparison between the exact form for ξ and the approximated form

The quantity ξ, often called the logarithmic energy decrement, characterizes the slowing down power of an element for neutrons of any energy, and in the form given by equation above it is seen quite clearly that the most effective elements for slowing down neutrons are those of low mass number. Frequently, slowing down takes place in a mixture of elements or a compound, and in this case the average value of the logarithmic energy decrement $\overline{\xi}$ for such a mixture is found as the weighted average of the values of (for each of the constituents of the mixture. The weighting factors are, logically, the probabilities of scattering in each of the constituents, which are proportional to the numbers of atoms of each constituent per cm³ of mixture multiplied by their scattering cross-sections. Thus $\overline{\xi}$ is calculated from the equation:

$$\overline{\xi} = \frac{\sum_i N_i(\sigma_s)_i\xi_i}{\sum_i N_i(\sigma_s)_i}$$

Where N_i , is the number of atoms per unit volume of the mixture of each element i whose microscopic scattering cross-section is σ_{si} and logarithmic energy decrement is ξ_i. The summation is carried out for all the constituents of the mixture.

In the case which is very common in nuclear engineering in which a heavy element such as uranium is mixed with a light element whose function is to slow down neutrons, the slowing down effect of the heavy element can often be neglected (provided the neutron energy is below the inelastic scattering threshold of that element), and for such a mixture the value of $\overline{\xi}$ is nearly the same as ξ for the light element.

In concluding we may mention that although neutron scattering in the C system is isotropic, and the average angle of scattering, θ, in the C system is 90°, neutron scattering is not isotropic in the L system. It can be shown that the average value of cos ψ, where ψ is the angle of scattering in the L system, is given by:

$$\overline{\cos\Psi} = \frac{2}{3A}$$

where A is the mass number of the scattering nucleus. The inference from this result is that neutron scattering in the L system is preferentially in the forward direction since cos ψ as given by equation above is always positive. As the mass of the scattering nucleus increases, $\overline{\cos\psi}$ approaches zero and the average angle of scattering approaches 90°. Thus for heavy elements it may be said that neutron scattering is nearly isotropic in the L system.

Table I. Average cosine of scattering angle in the LAB-system

Material	A	α	μ_0
^{1}H	1	0	0.667
^{2}D	2	0.111	0.333
^{4}He	4	0.360	0.167
^{6}Li	6	0.510	0.095
^{9}Be	9	0.640	0.074
^{10}B	10	0.669	0.061
^{12}C	12	0.716	0.056
^{238}U	238	0.938	0.003
H_2O	*	*	0.037
D_2O	*	*	0.033

Table II. Slowing-down features of some moderators

Moderator	ξ	N	$\xi\Sigma_s$	$\xi\Sigma_s/\Sigma_a$
H_2O	0.927	19.7	1.36	62
D_2O	0.510	36	0.180	5860
Be	0.209	87	0.153	138
C	0.158	115	0.060	166
U	.0084	2170	.0040	0.011

10.2 Thermal neutrons

In analysing elastic scattering collisions we have assumed that the nuclei of the medium are at rest since their speeds are much less than that of the neutrons. As the neutrons slow down their energies are reduced to values comparable with the energies of the nuclei, and a point is reached when scattering collisions no longer progressively reduce neutron energies. At this point neutrons have reached thermal equilibrium with the medium in which they are being scattered, and are known as thermal neutrons. The scattering of thermal neutrons has on the average no effect on their energy, although individual neutrons are at different energies and as a result of individual scatteriqg collisions they may suffer either a slight increase or decrease of energy. The important point is that their average energy remains constant.

The situation is analogous to gas molecules in a rigid container at a constant temperature. The molecules are moving to and from colliding with each other and the walls of the container and gaining and losing energy, but the total energy (or average energy) of all the molecules remains constant. The distribution in terms of speed (or energy) of gas molecules is given by the Maxwell-Boltzmann distribution, and this function can be applied to thermal neutrons provided that their rate of absorption is small compared with their rate of scattering, that is provided $\sigma_a << \sigma_s$.

The Maxwell – Boltzmann distribution in terms of neutron speed, v, is:

$$n(v)dv = n_0 \frac{4\pi v^2}{\left(2\pi \frac{k_B T}{m}\right)^{\frac{3}{2}}} e^{-\frac{mv^2}{2k_B T}} dv \tag{10.1}$$

where n(v) dv is the number of neutrons per unit volume whose speeds are in the range v to v + dv; N is the total number of neutrons per unit volume; m is the neutron mass, kg; T is the absolute temperature of the scattering medium, K; and kB is the Boltzmann constant, 1.381×10^{-23} J/K = 8.617×10^{-5} eV/K. The upper curve of Figure 10.4 shows the shape of the Maxwell- Boltzmann distribution for neutrons in a medium at 20°C.

The most probable neutron speed, corresponding to the maximum point on this curve in Figure 10.4, is obtained by differentiating the distribution function - Equation (10.1) - with respect to v and equating to zero. The result is

$$v_{MP} = v_0 = \sqrt{\frac{2k_B T}{m}}$$

and the corresponding energy is

$$E_0 = \frac{mv_0^2}{2} = k_B T$$

Example: Calculate the most probable speed and the corresponding energy of thermal neutrons at 20°C.

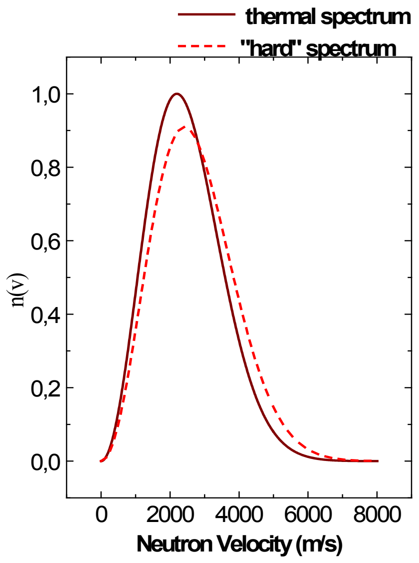

Figure 10.4 The Maxwell-Boltzman distribution for thermal neutrons

$$v_{MP} = \sqrt{\frac{2\times1.38\times10^{-23}\times293}{1\times1.66\times10^{-27}}} = 2299\,m/s$$

$$E = \frac{1.38\times10^{-23}\times293}{1.602\times10^{-19}} = 0.0253\,eV = 25.3\,meV$$

These values of the speed and kinetic energy are taken to characterize thermal neutrons in a medium at 20°C. The average speed of thermal neutrons is determined from the distribution function by the standard statistical method:

$$\bar{v} = \frac{\int_0^\infty vn(v)dv}{\int_0^\infty n(v)dv} = \frac{2}{\sqrt{\pi}}v_0 = 1.128v_0$$

$$\overline{v^2} = \frac{3}{2}v_0^2$$

$$\frac{m\overline{v^2}}{2} = \frac{3}{2}k_B T$$

The integration is carried out from zero to infinity to include all neutron speeds, although negligibly few neutrons have speeds greater than three or four times the most probable speed.

Maxwell-Boltzman distribution for the neutron flux is expressed by

$$\Phi(v)dv = n_0 \frac{4v^3}{v_0^3\sqrt{\pi}} e^{-\left(\frac{v}{v_0}\right)^2} dv =$$

$$= n_0 v_0 \frac{4v^3}{v_0^4\sqrt{\pi}} e^{-\left(\frac{v}{v_0}\right)^2} dv =$$

$$= \Phi_0 \frac{4v^3}{v_0^4\sqrt{\pi}} e^{-\left(\frac{v}{v_0}\right)^2} dv$$

Having in mind that

$$E = \frac{mv^2}{2}$$

$$dE = mvdv$$

Neutron flux distribution as a function of neutron energy can be expressed by

$$\Phi(E) = M(E) = \frac{E}{(k_B T)^2} e^{-\frac{E}{k_B T}}$$

$$E_0 = k_B T$$

$$\overline{E} = 2k_B T$$

See Figure 10.5 for the Maxwell-Boltzman distribution of thermal neutrons.

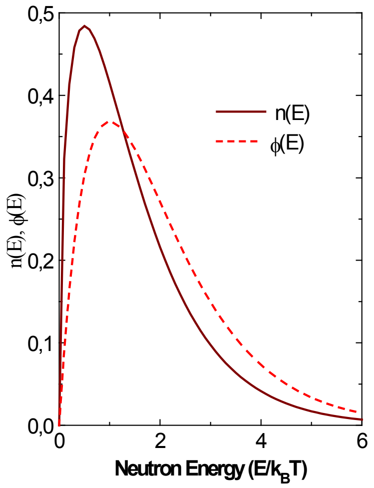

Figure 10.5 Thermal neutron density (Maxwell-Boltzman distribution) -n(E)- and thermal neutron flux -Φ(E)- as functions of neutron energy

Chapter 11

Diffusion in Homogeneous Thermal Reactors

11.1 Introduction

Nuclear reactor theory is concerned with the analysis of all the processes which take place in the core of a reactor, and in particular with the slowing down, diffusion and absorption of neutrons. Only by analysing these processes in detail can accurate calculations be made to determine the multiplication factor, critical mass of fuel or size of a reactor. The complete analysis of these processes is extremely difficult and complicated, and it is necessary to simplify the theory of nuclear reactors and develop approximate models for their analysis.

In this lecture we will describe some of the models in use for thermal reactors, and apply them to the analysis of homogeneous reactors. Infinite reactors will be considered first in order to simplify the problem by neglecting neutron leakage. Subsequently neutron diffusion and slowing down will be studied and applied to finite reactors to calculate critical size and mass. It should be emphasized that calculations based on the approximate models that we will use cannot be expected to give exact answers, but they are at least of first order accuracy. More exact and elaborate reactor theories require computers for the solution of numerical problems, and is presented in the separate lectures.

11.2 Homogeneous and quasi-homogeneous reactors

The core of a homogeneous reactor, as the name implies, is a uniform mixture of fuel, moderator and possibly other materials. For example, the core of the homogeneous aqueous reactor consists of a solution of uranyl sulphate, UO_2SO_4 in water. Reactors of this type are rather uncommon, and the vast majority of thermal reactors built up to 1987 have solid fuel elements arranged in a lattice within the moderator, which may be either solid or liquid. These reactors are clearly not homogeneous in the true sense, but if the characteristic dimensions of the fuel and its lattice (for example, the diameter of the fuel rods and the spacing between them) are smaller than the neutron mean free paths in the fuel and moderator, then the reactor is effectively homogeneous as far as neutrons are concerned. Reactors of this type are referred to as quasi-homogeneous, and can be analysed as if they are homogeneous. On the other hand, if the fuel or lattice dimensions are greater than the neutron mean free paths, the reactor must be treated as heterogeneous, and this type of reactor will be discussed in the next chapter. The theory of homogeneous reactors which is developed in this lecture can be applied to quasi-homogeneous reactors, and is therefore of more general application than might appear at first sight.

11.3 Reactor models

As we have already seen, the lifetime of a neutron in a reactor consists firstly of a period during which it is being slowed down by a number of scattering collisions. The neutron's energy is reduced at each scattering collision, and remains constant between collisions. When the neutron is the analyzed it continues to diffuse in the reactor and its energy, on average, remains constant until eventually it is absorbed or leaks out of the reactor. Neutrons may also be absorbed or leak out of the reactor before they have a chance to become thermalized. The complete analysis of the slowing down and diffusion processes is very complex, and the following models have been developed to simplify matters:

1. **The continuous slowing-down model.** The principal assumptions of this model are that all neutrons lose exactly ξ units of (log energy) at each scattering collision, and that the neutron density is a continuous function of energy. The first assumption implies that all neutrons behave as ”average” neutrons as far as their energy loss per scattering collision is concerned. In a reactor in which neutrons are produced with a spectrum of energies by fission, and slow down by many scattering collisions in a moderator such as graphite, these assumptions are more or less correct. In a hydrogenous moderator, however, in which neutrons may be thermalized after a few collisions, the departure from these assumptions may be considerable, and the continuous slowing down model is not reliable for water moderated reactors.

2. **The one-group model**. In this model it is assumed that all neutrons are produced at thermal energy and remain at this energy throughout their lifetime, and the slowing down process is ignored. Clearly this model has serious limitations and is unlikely to give accurate solutions to reactor problems; its main advantage lies in its simplicity. It is possible, however, to make modifications to the one-group model to enable the capture and leakage of fast neutrons to be taken into account, and thereby improve the accuracy of the model.

3. **The two-group model.** In this model it is assumed that all neutrons above thermal energy can be treated as a single group, called the fast group, having a common energy. All thermal neutrons are taken as being in the second group. Suitable cross-sections for the fast group enable the rate of capture of neutrons in that group, and the rate of scattering from the fast group to the thermal group to be determined. Two-group theory represents a considerable improvement over one-group theory for reactor calculations.

4. **Multi-group models.** In these models the neutrons in the reactor are divided into a number of groups, each representing a particular energy range. In a thermal reactor one or more of these groups would include the thermal neutrons. As in two-group theory suitable cross- sections determine the rates at which neutrons are captured in each group, and are scattered from one group to another. The mathematical complexity of these models increases as the number of groups increases, and computers are required for the solution of problems.

11.3.1 The infinite homogeneous reactor

The infinite multiplication factor,**k_∞**, was defined in the last chapter, and we will now develop expressions for calculating the four factors of k_∞.

η

describes average number of fission neutrons produced per neutron absorbed in the fuel, its value for thermal neutron fission in natural uranium is about 1.32. A general expression for this factor for thermal fission in natural or enriched uranium is:

$$\eta = \frac{\Sigma_f^{235}}{\Sigma_a^{235} + \Sigma_c^{238}}\bar{\nu} = \frac{N(^{235}U)\overline{\sigma_f^{235}}}{N(^{235}U)\overline{\sigma_a^{235}} + N(^{238}U)\overline{\sigma_c^{238}}}\bar{\nu} \tag{11.1}$$

N(^{235}U) and N(^{238}U) are the numbers of atoms of ^{235}U and ^{238}U, and the cross-sections are average values for thermal neutrons. Natural uranium contains 99.285 per cent of ^{238}U, and the value of η(nat U) is 1.32. The variation of η(U) with enrichment is shown in Figure 11.1, from which it can be seen that it increases with enrichment and reaches the value 2-07 for pure ^{235}U.

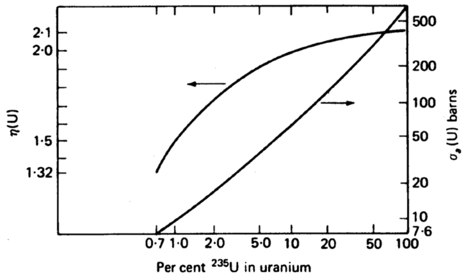

Figure 11.1 Eta (η) and the microscopic absorption cross-section of enriched uranium

The thermal utilization factor - f

The thermal utilization is defined as:

$$f = \frac{\text{The number of neutrons absorbed in the fuel}}{\text{Total number of thermal neutrons absorbed in the reactor}}$$

thus

$$f = \frac{N_F \overline{\sigma}_{aF} \phi_{thF}}{N_F \overline{\sigma}_{aF} \phi_{thF} + N_M \overline{\sigma}_{cM} \phi_{thM} + N_i \overline{\sigma}_i \phi_{thi}} \tag{11.2}$$

where N_F, N_M and N_i, are the numbers of atoms of fuel, moderator and other materials per cm^3 of the reactor. In a homogeneous reactor, in which all elements in the core are completely mixed, $f_{thF} = f_{thM} = f_{thi}$. If it is assumed that all materials have non-(1/v) factors equal to 1, the expression (11.2)for f becomes:

$$f = \frac{N_F \overline{\sigma}_{aF}}{N_F \overline{\sigma}_{aF} + N_M \overline{\sigma}_{cM} + N_i \overline{\sigma}_i} \tag{11.3}$$

where the cross-sections are tabulated (2200 m/s) values.

Recalling the definition of macroscopic cross-sections, $N_F\sigma_{aF}$ is Σ_{aF} , the macroscopic absorption cross-section of the fuel component of the reactor, and the denominator in equation (11.3) is the macroscopic absorption cross-section of the mixture of all the materials in the core of the reactor, which may be given the symbol Σ_{ac} . Thus the thermal utilization factor may be expressed in terms of macroscopic cross-sections as:

$$f = \frac{\Sigma_{aF}}{\Sigma_{ac}} \tag{11.4}$$

The value of σ_{aF} in equation (11.3) for natural uranium is 7.6 barns. A general expression for σ_a(U) for natural and enriched uranium is:

$$\sigma_a(U) = \frac{N(^{235}U)\sigma_a(^{235}U) + N(^{238}U)\sigma_c(^{238}U)}{N(^{235}U) + N(^{238}U)} \tag{11.5}$$

The value of σ_a(U) increases with enrichment as shown in Fig. , reaching the value of 680 barns for pure ^{235}U. This increase in the value of σ_a(U) has the effect of increasing the thermal utilization factor, provided the fuel-moderator ratio and the amounts of other materials remain constant.

In a water moderated reactor, or a reactor containing significant quantities of structural materials such as stainless steel which like water has rather a high capture cross-section, the use of enriched uranium is necessary to maintain a sufficiently high value of the thermal utilization factor to make criticality possible.

The variation of thermal utilization factor with moderator to fuel ratio for a natural uranium, graphite moderated reactor is shown in Figure 11.3 .

According to the one-group model, in which the existence of fast neutrons and slowing down are neglected, the resonance escape probability and the fast fission factor are both equal to 1, and therefore:

$$k_\infty = f\eta \tag{11.6}$$

This result is fairly accurate for reactors fuelled with highly enriched uranium or pure ^{235}U, in which the fast fission and resonance capture effects are negligible. It is certainly not accurate for reactors fuelled with natural or slightly enriched uranium in which the amount ^{238}U is large compared with the ^{235}U, and the fast fission and (to a greater extent) the resonance capture effects are significant. One method of calculating the resonance escape probability makes use of the continuous slowing-down model.

11.3.1.1 The continuous slowing-down model and resonance escape probability

At the outset we will define a quantity known as the neutron slowing- down density, q(E), as the rate at which neutrons slow down past energy E per unit volume.

According to our analysis of elastic scattering in the lecture about neutron interactions the average decrease of (log energy) per collision, ξ, is constant. The continuous slowing-down model assumes that all neutrons behave in the average fashion and that for all neutrons the decrease of (log energy) per collision is exactly ξ at all energies. Consider an interval of (log energy), d(log E), at which the slowing-down density is q(E). The fraction of neutrons which, while slowing down, is scattered into the interval d(log E) is d(log E)/ξ, which is equal to dE/ξE. The total number of neutrons scattered into the interval dE at E is therefore:

$$\frac{q(E)\,dE}{\xi E} \quad \text{neutrons}/\text{cm}^3\text{s} \tag{11.7}$$

In a purely scattering medium, in which $\sigma_c = 0$, the number of neutrons scattered into dE per second is equal to the number of neutrons scattered out of dE per second. If $\phi(E)$ dE is the flux of neutrons whose energy is in the range E to E + dE, the rate of scattering out of dE is $\Sigma_s\phi(E)$ dE.

We now have

$$\frac{q(E)\,dE}{\xi E} = \Sigma_s\phi(E)\,dE$$

or

$$\phi(E) = \frac{q(E)}{\xi\Sigma_s E} \tag{11.8}$$

In a pure scattering medium in which no neutrons are captured, the slowing-down density in a steady-state situation is constant at all energies. If Σ_s is assumed to be constant, and noting that ξ is independent of energy, it follows that the neutron flux per unit energy at energy E is inversely proportional to E:

$$\phi(E) \propto \frac{1}{E} \tag{11.9}$$

This result is only true for an infinite scattering medium, however in a thermal reactor the scattering cross-section of the fuel-moderator mixture is much greater than the capture cross-section. (If this were not so, neutrons would not be thermalized and a chain reaction would be impossible.) Equation (11.9) represents quite accurately, therefore, the variation of neutron flux with energy in a thermal reactor down to the upper end of the thermal neutron spectrum.

In a scattering and absorbing medium the number of neutrons scattered into the energy interval dE at E is still [q(E) dE]/ξE, although the slowing-down density is no longer constant at all energies, but decreases as the neutron energy decreases due to capture during slowing down. The rate at which neutrons are scattered into the energy interval dE is equal to the rate at which neutrons are captured in this interval plus the rate at which they are scattered out to lower energies:

$$\frac{q(E)\,dE}{\xi E} = (\Sigma_s + \Sigma_a)\phi(E)\,dE \tag{11.10}$$

The rate at which neutrons are captured in dE is a measure of the decrease in the slowing-down density, dq(E):

$$dq(E) = \Sigma_a(E)\phi(E)\,dE$$

$$\frac{dq(E)}{q(E)} = \frac{1}{\xi}\frac{\Sigma_a(E)}{\Sigma_s + \Sigma_a(E)}\frac{dE}{E} \tag{11.11}$$

(Note that Σ_a, is dependent on energy while Σ_s is assumed to be constant, and that ξ refers to the mixture of fuel and moderator in a reactor.) Dividing equation (11.11) by (11.10), and rearranging:

Integrating:

$$\ln\frac{q(E_2)}{q(E_1)} = \frac{1}{\xi}\int_{E_2}^{E_1}\frac{\Sigma_a(E)}{\Sigma_s + \Sigma_a(E)}\frac{dE}{E}$$

or

$$\frac{q(E_2)}{q(E_1)} = \exp\left[-\frac{1}{\xi}\int_{E_2}^{E_1}\frac{\Sigma_a(E)}{\Sigma_s + \Sigma_a(E)}\frac{dE}{E}\right] \tag{11.12}$$

If E_1 and E_2 are the upper and lower limits of the resonance range, then $q(E_2)/q(E_1)$ is the fraction of neutrons which, while slowing down, escape capture in the resonance absorber, that is the resonance escape probability. To include neutron capture at all energies from fission to thermal, E_1 should be taken as fission energy and E_2 as thermal energy.

Now:

$$p = \exp\left[-\frac{1}{\xi}\int_{E_2}^{E_1}\frac{\Sigma_a(E)}{\Sigma_s + \Sigma_a(E)}\frac{dE}{E}\right] \tag{11.13}$$

This expression for the resonance escape probability is the starting point for several different methods of calculation. The problem in using it lies in evaluating the integral, particularly in view of the fact that the capture cross-section of ^{238}U varies widely in the resonance range, and it is quite impossible to represent this variation by any relationship between Σ_a, and E.

One method of evaluating the integral in equation (11.13) which relies on experimental measurements of the cross-sections of ^{238}U (or ^{232}Th, the other possible resonance absorber) will be outlined. If it is assumed that in the fuel-moderator mixture ^{238}U is the only significant absorber of resonance neutrons, then $\Sigma_a(E) = N(^{238}U)\sigma_c(^{238}U)$ where $N(^{238}U)$ is the number of atoms of ^{238}U/cm^3 of the mixture. Equation (11.13) can be written as:

$$p = \exp\left[-\frac{N(^{238}U)}{\xi}\int_{E_2}^{E_1}\frac{\sigma_c(E)}{1 + \frac{N(^{238}U)\sigma_c(^{238}U)}{\Sigma_s}}\frac{dE}{E}\right] \tag{11.14}$$

The only variable in this equation for the resonance escape probability is N(^{238}U)/Ss or its reciprocal $\Sigma_s/N(^{238}U)$ which is the total scattering cross-section of the fuel-moderator mixture per atom of ^{238}U, regardless of the identity of the moderator. The integral of equation (11.14) is known as the effective resonance integral, I:

$$I = \left[\int_{E_2}^{E_1}\frac{\sigma_c(E)}{1 + \frac{N(^{238}U)\sigma_c(^{238}U)}{\Sigma_s}}\frac{dE}{E}\right] \tag{11.15}$$

For pure ^{238}U:

$$I=\left[\int_{E_2}^{E_1}\frac{\sigma_c(\mathrm{E})}{1+\dfrac{\sigma_c(^{238}U)}{\sigma_s(^{238}U)}}\frac{\mathrm{dE}}{\mathrm{E}}\right] \tag{11.16}$$

which has been experimentally determined to be about 9 barns, and $\Sigma_s/N(^{238}U)=\sigma_s(^{238}U)$ which is 8.3 barns.

For very large values of the moderator to fuel ratio, $\Sigma_s/N(^{238}U)$ becomes very large, and in the limit as $\Sigma_s/N(^{238}U)\rightarrow\infty$, the effective resonance integral becomes:

$$\mathrm{I}=\left[\int_{E_2}^{E_1}\sigma_c(^{238}\mathrm{U})\frac{\mathrm{dE}}{\mathrm{E}}\right] \tag{11.17}$$

which has been experimentally determined to be about 280 barns.

The available data for the variation of I with $\Sigma_s/N(^{238}U)$ for values of $\Sigma_s/N(238U)$ up to about 10 000 barns is best represented by the empirical equation:

$$\mathrm{I}=2.73\left\{\frac{\Sigma_s}{N(^{238}\mathrm{U})}\right\}^{0.486}\ \text{barns} \tag{11.18}$$

This variation is shown inFigure 11.2 .

Inserting the expression for the effective resonance integral, Equation (11.18), into the expression for the resonance escape probability, Equation (11.14), one gets:

$$\mathrm{p}=\exp\left[-\frac{2.73}{\bar{\xi}}\left\{\frac{\Sigma_s}{N(^{238}\mathrm{U})}\right\}^{-0.514}\right] \tag{11.19}$$

This equation can be used for computational purposes for homogeneous systems of natural or slightly enriched uranium with any moderator. The value of should be an average value for the fuel- moderator mixture, but the difference between this average value and the value for the pure moderator is likely to be very small and is usually negligible. The variation of resonance escape probability with moderator to fuel ratio for a homogeneous mixture of natural uranium and graphite is shown in Figure 11.3.

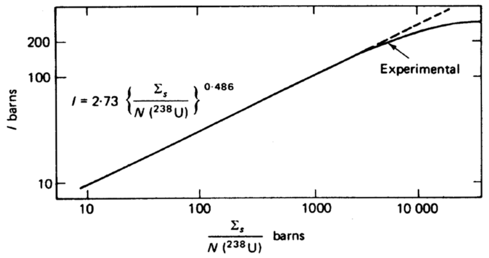

Figure 11.2 The variation of effective resonance integral with total scattering cross-section for ^{238}U

11.3.1.2 The fast fission factor - ε

For dilute mixtures of fuel and moderator (in which the ratio of moderator atoms or molecules to fuel atoms is greater than, say, 50 to 1), the fast fission factor, e, may be taken as equal to 1 without the need for detailed calculation. The reason for this is that when fission neutrons are emitted at an average energy of 2 MeV in a medium containing a small quantity of fuel and a large quantity of moderator the most probable type of interaction is elastic scattering in the moderator. There may be a little inelastic scattering in the fuel, but negligibly few neutrons will cause fission in the fuel. As a result the neutrons' energy is reduced below 1 MeV, the fission threshold in ^{238}U, without any appreciable increase in the number of neutrons due to fast fission.

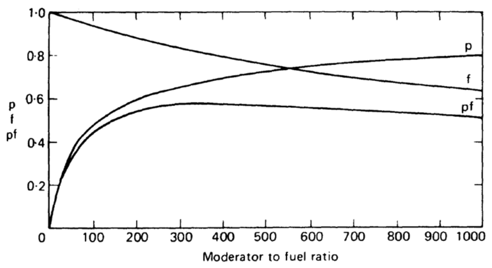

Figure 11.3 Variation of resonance escape probability and thermal utilizatio factor of a natural uranium and graphite mixture

In the case of certain water moderated reactors which use enriched uranium as the fuel, the moderator-fuel ratio may be less than the figure quoted above, and the fast fission factor may be significant. Calculations for this type of reactor have given the following formula

$$\varepsilon=\frac{1+0.690\dfrac{\mathrm{N}(^{238}\mathrm{U})}{\mathrm{N}(\mathrm{H_2O})}}{1+0.583\dfrac{\mathrm{N}(^{238}\mathrm{U})}{\mathrm{N}(\mathrm{H_2O})}} \tag{11.20}$$

where $N(^{238}U)/N(H_2O)$ is the ratio of the number of atoms of ^{238}U to the number of molecules of water.

11.3.1.3 The infinite multiplication factor

The infinite multiplication factor can now be calculated for a given fuel-moderator mixture using the equation:

$$k_\infty=\varepsilon pf\eta \tag{11.21}$$

and the expressions for ε, p, f and η that we have developed. The following example illustrates the procedure.

Example: Calculate the infinite multiplication factor for a solution of uranyl sulphate in heavy water, the composition being 1 molecule of UO_2SO_4, to 1000 molecules of D_2O. The UO_2SO_4 contains natural Uranium

In this example we can base our calculation on any quantity of fuel- moderator mixture that is convenient, and in this case the simplest quantity is one molecule of fuel and 1000 molecules of moderator. The average value of the logarithmic energy decrement for D_2O is found using equation :

$$\bar{\xi}=\frac{\sum_i N_i\sigma_{si}\xi_i}{\sum_i N_i\sigma_{si}} \tag{11.22}$$

then

$$\overline{\xi}(D_2O) = \frac{N(D)\sigma_s(D)\xi(D) + N(O)\sigma_s(O)\xi(O)}{N(D)\sigma_s(D) + N(O)\sigma_s(O)} =$$

$$= \frac{2\times 3.4\times 0.725 + 1\times 3.8\times 0.120}{2\times 3.4 + 1\times 3.8} = 0.509$$

The calculation may be carried out in tabular form as follows:

Sub-stance	**Atomic Weight**	**N**	**σ_a**	**σ_s**	**$N\sigma_a$**	**$N\sigma_s$**	**ξ**	**$N\sigma_s\xi$**
U	238	1	7.6	8.3	7.56	8.3	0.0084	0.0697
O	16	6	0	3.6	0	22.8	0.1209	2.755
S	32	1	0.52	1.1	0.52	1.1	0.0616	0.0678
D2O	-	1000	0.001	10.6	100	10600	0.509	5395.4
					$\Sigma N\sigma_a$	$\Sigma N\sigma_s$		$\Sigma N\sigma_s\xi$
					9.08	**10632**		**5398.3**

From equation (11.4):

$$f = \frac{N(U)\sigma_a(U)}{\Sigma N\sigma_a} = \frac{7.56}{9.08} = 0.833$$

From equation (11.22) :

$$\overline{\xi} = \frac{\sum_i N_i\sigma_{si}\xi_i}{\sum_i N_i\sigma_{si}} = \frac{5398.3}{10632} = 0.508$$

This result illustrates the point mentioned earlier that the value of ξ for a dilute fuel-moderator mixture is very nearly the same as for pure moderator. From the values in the table above:

$$\frac{\Sigma_s}{N(^{238}U)} = \frac{10632}{0.99285} = 10710 \text{ barns per atom of } {}^{238}U$$

From Equation (11.19):

$$p = \exp\left[\frac{2.73\times 10710^{-0.514}}{0.508}\right] = \exp(-0.04625) = 0.955$$

Combining these results:

$$k_\infty = 1\times 0.955\times 0.833\times 1.32 = 1.05$$

This result indicates that a chain reaction is possible with an infinite system of natural uranium (as UO_2SO_4) in heavy water for the moderator to fuel ratio chosen. In the case of graphite or light

water as moderator, similar calculations show that in an infinite homogeneous system with natural uranium as fuel, criticality is impossible for any moderator to fuel ratio.

For a given fuel, an increase in the moderator to fuel ratio has the effect of decreasing **f** and increasing **p**, while leaving the values of ε and η unchanged. This situation is shown inFigure 11.3 for a natural uranium and graphite mixture. The variation of the product **pf** is also shown and it can be seen that this quantity, and hence k_∞ has a maximum value corresponding to an optimum moderator to fuel ratio. Figure 11.3 also illustrates the point just mentioned that a chain reaction in a natural uranium-graphite system is impossible, even at the optimum moderator to fuel ratio. The maximum value of the product **pf** for this system is (referring to Figure 11.3) just less than 0 6, and the maximum value of k is less than 0.75.

11.3.2 One-group neutron diffusion theory

The calculation of neutron leakage from a reactor core depends on a knowledge of the way in which neutrons move about or diffuse in the reactor both during slowing down and while they are thermal. The simplest theory of neutron diffusion is the one-group theory, in which it is assumed that all neutrons in the reactor are at thermal energy. The effect of scattering collisions on these neutrons is to alter their direction of motion, but not their speed.

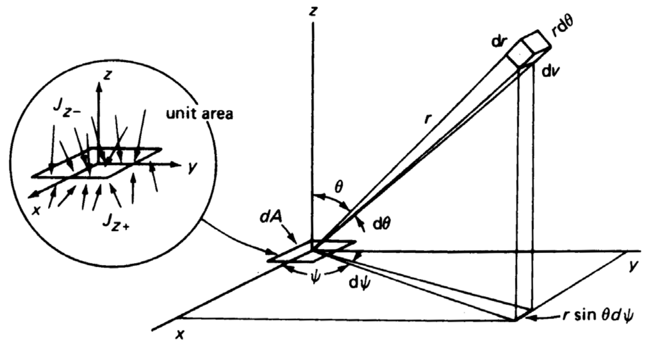

Figure 11.4 Model of neutron diffusion - neutron scattering and current

In connection with neutron motion we define a quantity called the neutron current density, ***J***, as follows:

In a Cartesian coordinate system (see Figure 11.4) the partial neutron current density in the positive z-direction, J_{z+}, is the number of neutrons per second which pass upwards through a unit area parallel to the x-y plane. The partial neutron current density in the negative z-direction, J_{z-}, is the number of neutrons per second which pass downwards through a unit area parallel to the x-y plane. The neutron current density in the z-direction, J_z , is given by:

$$\overline{J}_Z = \overline{J}_{Z^+} - \overline{J}_{Z^-} \qquad (11.23)$$

In order to derive an expression for the neutron current density in terms of the neutron flux we will make the following assumptions:

1. The medium in which neutrons are diffusing is homogeneous and isotropic, and neutron scattering is isotropic in the L system. This implies that neutrons scattered at any point emerge isotropically from that point. A correction can be made to the result of this analysis to take account of non-isotropic scattering in the L system.
2. The scattering cross-section of the medium is much larger than the absorption cross-section.
3. The neutron flux is a slowly varying function of position. This will be the case if $\Sigma_a << \Sigma_s$ and at points a few mean free paths away from the boundary of the medium, and neutron sources.

One-group diffusion theory, which is based on these assumptions, provides a simple and fairly accurate method for analysing neutron diffusion, and in practice it is not necessary to impose too strictly the restrictions implied by these assumptions. Consider an infinite medium in which neutrons are diffusing and being scattered, with an element of volume d V whose position is defined by the vector r, and an element of area dA lying in the x-y plane at the origin of the coordinate system, Figure 11.4

If the neutron flux at position **r** is ϕ(**r**), the rate of scattering in dV per second is . Σ_s ϕ(**r**)dv

The fraction of neutrons which are scattered in dV into the direction towards dA is $\frac{dA\cos\theta}{4\pi r^2}$, **r** being the distance from dV to dA.

The fraction of neutrons which, having been scattered in dV towards dA, reach and pass through dA without further interaction is $e^{-\Sigma_t r}$. Since the validity of diffusion theory depends, as stated above, on Σ_a, being much less than Σ_s this term can be written as $e^{-\Sigma_s r}$.

Combining these three quantities, the number of neutrons which are scattered in dV and then pass through dA per second is:

$$\frac{\sum_s \phi(r) e^{-\sum_s r} \cos\theta}{4\pi\ r^2} d\,Ad\ V \tag{11.24}$$

The element of volume d V may be expressed in spherical coordinates as:

$$dV = r^2 \sin\theta\, d\theta\, dr\, d\,\psi \tag{11.25}$$

The total number of neutrons which pass through drf per second from above to below, that is in the negative z-direction, is obtained by integrating the expression:

$$\frac{\sum_s dA}{4\pi}\phi(r)e^{-\sum_s r}\ \cos\theta\sin\theta\, d\theta\, d\,\psi \tag{11.26}$$

over the whole of space above the x-y plane. In fact only the region within about four or five mean free paths of the origin contributes to the integral because of the term $e^{-\Sigma_s r}$. The expression we derive for neutron current by considering an infinite medium can therefore be applied to a finite medium at all points more than a few mean free paths from its boundary. This condition was noted in assumption 3 above.

To evaluate the integral of the preceding expression, ϕ(**r**) must be expressed in terms of ϕ_0 the flux at the origin where the neutron current is being evaluated. Expressing ϕ(**r**) in terms of ϕ_0, and its derivatives by means of a Taylor series, and bearing in mind that f is assumed to be a slowly varying function, we have:

$$\phi = \phi_0 + x\left(\frac{\partial\phi}{\partial x}\right)_0 + y\left(\frac{\partial\phi}{\partial y}\right)_0 + z\left(\frac{\partial\phi}{\partial z}\right)_0 + \ldots \tag{11.27}$$

in polar coordinates:

$$x = r\sin\theta\cos\psi;\ y = r\sin\theta\sin\psi;\ z = r\cos\theta \tag{11.28}$$

When this expression for ϕ(**r**) is inserted in the integral the terms involving y become zero as the integration with respect to y is carried out from 0 to 2π. The partial neutron current in the negative z-direction can be determined by dividing the total number of neutrons passing through dA from above by dA, giving:

$$\begin{aligned} J_- &= \frac{\sum_s}{4\pi}\int_{\Psi=0}^{2\pi}\int_{\theta=0}^{\frac{\pi}{2}}\int_{\theta=0}^{\infty}\phi(r)\cos\theta\, e^{-\sum_s r}\sin\theta\, d\,\theta\, d\,r\, d\,\psi \\ J_- &= \frac{\sum_s}{4\pi}\int_{\Psi=0}^{2\pi}\int_{\theta=0}^{\frac{\pi}{2}}\int_{\theta=0}^{\infty}\left\{\phi_0 + r\cos\theta\left(\frac{\partial\phi}{\partial z}\right)_0\right\}e^{-\sum_s r}\sin\theta\, d\,\theta\, d\,r\, d\,\psi \end{aligned} \tag{11.29}$$

The solution of this integral - Equation (11.29) - gives:

$$J_{z-} = \frac{\phi_0}{4} + \frac{1}{6\sum_s}\left(\frac{\partial\phi}{\partial z}\right)_0 \tag{11.30}$$

The expression for J_{z+} is obtained by the same method, with θ varying from π/2 to π, and is:

$$J_{z+} = \frac{\phi_0}{4} - \frac{1}{6\sum_s}\left(\frac{\partial\phi}{\partial z}\right)_0 \tag{11.31}$$

The neutron current density in the z-direction is obtained by subtracting equation (11.30) from (11.31).

$$J_z = J_{z+} - J_{z-} = \frac{1}{3\sum_s}\left(\frac{\partial\phi}{\partial z}\right)_0 \tag{11.32}$$

The neutron current density in the x and y directions are given by similar expressions, namely:

$$J_x = -\frac{1}{3\sum_s}\left(\frac{\partial\phi}{\partial x}\right) \quad and \quad J_y = -\frac{1}{3\sum_s}\left(\frac{\partial\phi}{\partial y}\right)$$

In general:

$$J = -\frac{1}{3\Sigma_S}\nabla\phi \tag{11.33}$$

where:

$$\nabla\phi = grad\phi = i\frac{\partial\phi}{\partial x} + j\frac{\partial\phi}{\partial y} + k\frac{\partial\phi}{\partial z} \tag{11.34}$$

The neutron current is proportional to the gradient of the flux, and the flow of neutrons is in the direction of decreasing flux. The constant of proportionality in equation (11.33) is called the diffusion coefficient, D, and this equation may be written as:

$$J = -D\nabla\phi \tag{11.35}$$

where:

$$D = \frac{1}{3\Sigma_S} = \frac{\lambda_s}{3} \qquad (11.36)$$

One of the assumptions upon which these results are based is that of isotropic scattering in the L system which we know to be incorrect, especially for scattering with light elements such as hydrogen. If scattering is isotropic in the C system, but anisotropic in the L system, it is possible by the methods of transport theory to show (in the ease where Σ_s, is much larger than Σ_a) that the diffusion coefficient is given by:

$$D = \frac{1}{3(1-\overline{\mu})\Sigma_S} = \frac{\lambda_r}{3} \qquad (11.37)$$

Σ_{tr} and λ_{tr} are called the transport cross-section and the transport mean free path respectively, and:

$$\Sigma_{tr} = \Sigma_S(1-\overline{\mu}) \qquad (11.38)$$

where $\overline{\mu}$ is the average cosine of the scattering angle in the L system. Equation (11.37) is preferred to (11.36) for expressing the diffusion coefficient in terms of the scattering cross-section.

We can now use the equation for neutron current density to determine the neutron leakage out of unit volume in a diffusing medium. Considering an element of volume in a Cartesian coordinate system (see Figure 11.5) we can use the result of the preceding section as follows:

The flow of neutrons into the element of volume through the lower face parallel to the x-y plane = $-D(\partial\phi/\partial z)_z dxdy$. The flow of neutrons out of the element of volume through the upper face parallel to the x – y plane = $-D(\partial\phi/\partial z)_{z+dz} dxdy$ $(\partial\phi/\partial z)$ at coordinate z + dz can be expressed in terms of $(\partial\phi/\partial z)$ at z by the first two terms of a Taylor series as:

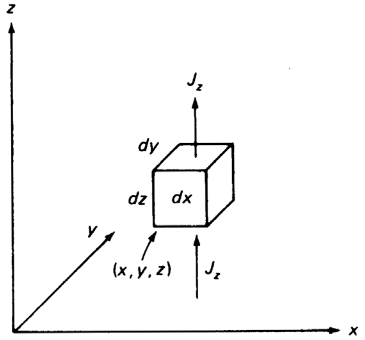

Figure 11.5 Neutron leakage from an element volume.

$$(J_{z+d} - J_z)dxdy = -D\left[\left(\frac{\partial\phi}{\partial z}\right)_{z+d} - \left(\frac{\partial\phi}{\partial z}\right)\right]dxdy \qquad (11.39)$$

Using this equation, the net flow of neutrons out of the element of volume through the faces parallel to the x-y plane is:

$$-D\frac{\partial^2\phi}{\partial z^2}dxdydz = -D\frac{\partial^2\phi}{\partial z^2}dV \qquad (11.40)$$

Noting that dx dy dz is the volume of the element, and that similar expressions will give the rate of leakage through the other faces of the element of volume, the total leakage of neutrons per second out of a unit volume in a Cartesian coordinate system is:

$$Leakage = -D\left(\frac{\partial^2}{\partial x^2}+\frac{\partial^2}{\partial y^2}+\frac{\partial^2}{\partial z^2}\right) = -D\ div\ grad\phi = -D\Delta\phi \quad \frac{n}{cm^3\cdot s} \qquad (11.41)$$

$$Laplace\quad operator\quad \Delta = \nabla^2$$

Equation (11.41) is a general equation for the rate of neutron leakage from unit volume in any coordinate system. In a cylindrical coordinate system the corresponding expression for $\nabla^2\phi$ is:

$$\Delta\phi = \nabla^2\phi = \left(\frac{1}{r}\frac{\partial}{\partial r}r\frac{\partial\phi}{\partial r}+\frac{1}{r^2}\frac{\partial^2\phi}{\partial\theta^2}+\frac{\partial^2\phi}{\partial z^2}\right) \qquad (11.42)$$

and in a spherical coordinate system, whose coordinates are the same as those used in Figure 11.4 , the corresponding expression for $\nabla^2\phi$ is:

$$\Delta\phi = \nabla^2\phi = \left(\frac{1}{r^2}\frac{\partial}{\partial r}r^2\frac{\partial\phi}{\partial r}+\frac{1}{r^2\sin\theta}\frac{\partial}{\partial\theta}\sin\theta\frac{\partial\phi}{\partial\theta}+\frac{1}{r^2\sin^2\theta}\frac{\partial^2\phi}{\partial\psi^2}\right) \qquad (11.43)$$

In practice these expressions can usually be simplified as in most cases of interest the neutron flux is independent of angular coordinate.

Simplified expressions for $\nabla^2\phi$ can be used for three special cases, (a) rectangular geometry with flux variation in one direction only, (b) cylindrical geometry with flux variation in the radial direction only (i.e. no angular or axial variation), and (c) spherical geometry with flux variation in the radial direction only (i.e. no angular variation) as follows:

$$\Delta\phi = \nabla^2\phi = \left(\frac{1}{r}\frac{\partial}{\partial r}r\frac{\partial\phi}{\partial r}+\frac{1}{r^2}\frac{\partial^2\phi}{\partial\theta^2}+\frac{\partial^2\phi}{\partial z^2}\right) \qquad (11.44)$$

where n = 0 for rectangular geometry, n = 1 for cylindrical geometry, and n = 2 for spherical geometry.

11.4 The neutron diffusion equation

We can now develop a neutron balance equation for unit volume of a medium in which neutrons are being produced, absorbed and are diffusing at constant energy, The rate of change of the neutron density is equal to the rate at which neutrons are produced per unit volume in the medium minus the sum of the rates of neutron leakage and absorption per unit volume in the medium. The neutron diffusion equation

$$D\Delta\phi - \Sigma_a\phi + S = \frac{1}{v}\frac{\partial\phi}{\partial t} \qquad (11.45)$$

where S is the source of neutrons per unit volume.

In a reactor operating at steady-state the neutron density is independent of time and equation (11.45) becomes:

$$D\Delta\phi - \Sigma_a\phi + S = 0$$

$$\Delta\phi - \frac{1}{L^2}\phi + \frac{1}{D}\phi = 0 \qquad (11.46)$$

This is the steady-state diffusion equation. It is the starting point for the solution of neutron diffusion problems both in multiplying media such as reactors, and in non-multiplying media in which neutrons are not being produced by fission.

The solution of the diffusion equation must satisfy certain boundary and other conditions. These are summarized below.

1. *The neutron flux must be finite and non-negative at all points where the diffusion equation applies. The condition of finite flux does not necessarily apply at points where localized neutron sources exist as the diffusion equation itself is not valid at such points.*
2. *In a system which has a plane, line or point of symmetry, the neutron flux is symmetrical about such a plane, line or point.*
3. *At an interface between two different media the neutron current density normal to the interface and the neutron flux are both continuous across the interface.*
4. *At the free surface of a medium the neutron flux varies in such a way that if it is extrapolated beyond the free surface it becomes zero at a fixed distance, known as the extrapolation distance.*

Conditions 1 and 2 are mathematically self-evident.

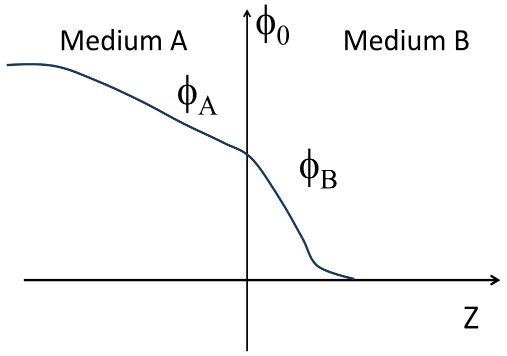

Figure 11.6 Interface between 2 media A and B in a diffusion process

If the interface between two media, A and B - see Figure 11.6, referred to in condition 3 is parallel to the y-z plane at x = 0, then:

$$J_{z-} = \frac{\phi_0}{4} + \frac{1}{6\Sigma_s}\left(\frac{\partial\phi}{\partial z}\right)_0 \qquad J_{z+} = \frac{\phi_0}{4} - \frac{1}{6\Sigma_s}\left(\frac{\partial\phi}{\partial z}\right)_0 \tag{11.47}$$

(If these equations were not correct, then there would be an accumulation or loss of neutrons at the interface which is physically impossible.) The preceding equations may be written, referring to equations (11.30) and (11.31):

$$\frac{\phi_A}{4} - \frac{\lambda_{trA}}{6}\frac{\partial\phi_A}{\partial z} = \frac{\phi_B}{4} - \frac{\lambda_{trB}}{6}\frac{\partial\phi_B}{\partial z} \tag{11.48}$$

and

$$\frac{\phi_A}{4} + \frac{\lambda_{trA}}{6}\frac{\partial\phi_A}{\partial z} = \frac{\phi_B}{4} + \frac{\lambda_{trB}}{6}\frac{\partial\phi_B}{\partial z} \tag{11.49}$$

Adding these two equations we get:

$$\phi_A = \phi_B \ at\ x = 0\ and\ D_A\frac{\partial\phi_A}{\partial z} = D_B\frac{\partial\phi_B}{\partial z} \tag{11.50}$$

and subtracting the first equation from the second we get:

$$J_{xA} = J_{xB}\ at\ x = 0 \tag{11.51}$$

The conditions of continuity of neutron flux and current at the interface between A and B are thus demonstrated.

If a neutron diffusing medium is bounded by a plane surface beyond which is a space of very low density, such as air (which from the point of view of neutron scattering js for all practical purposes a vacuum), then neutrons escaping from the medium through its surface into the surrounding space are not scattered and none return across the surface. The neutron current at this free surface is therefore entirely in the outward direction, or (referring to Figure 11.7 in which the free surface is normal to the x-axis) the positive x direction. Recalling equation (11.32), this implies that the flux gradient at the free surface is negative.

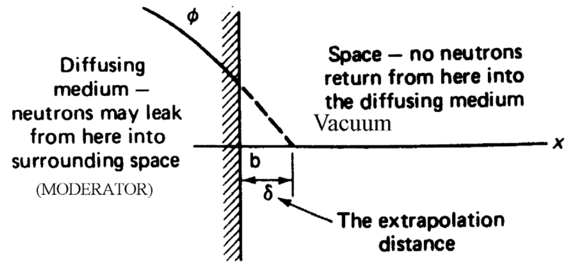

Figure 11.7 The free surface boundary condition

The neutron flux in the diffusing medium at the free surface can be assumed to vary in such a way as to satisfy the equation:

$$\frac{1}{\phi_b}\left(\frac{\partial\phi}{\partial x}\right)_b = -\frac{1}{\delta} \tag{11.52}$$

where b is the coordinate of the free surface, and d is the distance beyond the free surface at which the flux, if extrapolated linearly beyond the free surface, becomes zero. d is called the extrapolation distance, and b + δ the extrapolated boundary.

Referring to Figure 11.7 at the boundary of the diffusing medium, where x = b, the partial neutron current density in the negative x direction, J_{x-}, is zero, and the net neutron current density J_x is equal to the partial neutron current density in the positive x direction, J_{x+}. This condition may be expressed, using equations (11.31) and (11.32) as:

$$-\frac{1}{3\Sigma_s}\left(\frac{\partial\phi}{\partial x}\right)_b = \frac{\phi_b}{4} - \frac{1}{6\Sigma_s}\left(\frac{\partial\phi}{\partial x}\right)_b \tag{11.53}$$

which, using equation(11.36), gives:

$$\frac{1}{\phi_b}\left(\frac{\partial\phi}{\partial x}\right)_b = -\frac{1}{2D} \tag{11.54}$$

Comparing equations (11.52) and (11.54), it can be seen that the assumption implied in equation (11.52) is justified by diffusion theory, and the extrapolation distance d is related to the diffusion coefficient D by the equation:

$$\delta = 2D \tag{11.55}$$

According to transport theory it can be shown that better agreement between equation (11.52) and the actual flux distribution at the free surface is given by:

$$\delta = 2.13D \tag{11.56}$$

A simpler form of boundary condition 4 which mathematically is more convenient to use, although it is not physically correct, is:

$$\delta = 0.71\ \lambda_{tr} \tag{11.57}$$

The neutron flux becomes zero at the extrapolated boundary of the medium, i.e. $\phi = 0$ at x = b + δ.

For most media the diffusion coefficient is about 1 cm, and the extrapolation distance is about 2 cm. Many reactors, particularly power reactors, are a few meters in size, and the extrapolation distance can be neglected by comparison with this size. In such cases the flux may be assumed to be zero at the actual surface of the reactor.

11.4.3 The diffusion length

Returning to the diffusion equation (11.46), we will consider the case of a diffusing medium in which there are localized neutron sources only. In such a medium, at all points where there are no sources, the steady- state diffusion equation is written as:

$$
\begin{aligned}
&D\Delta\phi - \Sigma_a\phi + S = 0 \\
&\Delta\phi - \frac{1}{L^2}\phi + \frac{1}{D}\phi = 0
\end{aligned}
\qquad (11.58)
$$

where $L = \sqrt{\frac{D}{\Sigma_a}}$ and is called the diffusion length.

The diffusion length is a very important parameter in nuclear engineering and it is useful at this stage to obtain some idea of its significance. Let us consider a point source emitting S neutrons per second isotropically in an infinite medium. At all points, except in the vicinity of the neutron source, the flux is found from the solution of equation (11.58) , which in terms of spherical coordinates with angular symmetry may be written as:

$$\frac{d^2\phi}{dr^2} + \frac{2}{r}\frac{d\phi}{dr} - \frac{1}{L^2}\phi = 0 \qquad (11.59)$$

Making the substitution x =ϕr, this equation becomes:

$$\frac{d^2x}{dr^2} - \frac{1}{L^2}x = 0 \qquad (11.60)$$

The solution of this equation is:

$$x = Ae^{-\frac{r}{L}} + Ce^{\frac{r}{L}} \qquad (11.61)$$

or

$$\phi = \frac{A}{r}e^{-\frac{r}{L}} + \frac{C}{r}e^{\frac{r}{L}} \qquad (11.62)$$

As **r→∞** the second term of this solution becomes infinite, and therefore C must be zero to satisfy boundary condition 1. The equation for the flux is, therefore:

$$\phi = \frac{A}{r}e^{-\frac{r}{L}} \qquad (11.63)$$

The value of the constant A may be found in terms of the source strength, S, by noting that at steady state the rate of production of neutrons is equal to the total rate of absorption of neutrons in the entire infinite medium. This condition can be expressed by the equation:

$$S = \int_0^\infty \Sigma_a\phi(r)4\pi r^2 dr \qquad (11.64)$$

or

$$S = 4\pi\Sigma_a A\int_0^\infty e^{-\frac{r}{L}} r dr \qquad (11.65)$$

The value of the integral is L², and consequently:

$$A = \frac{S}{4\pi D} \qquad (11.66)$$

and the flux is given by:

$$\phi(r) = \frac{S}{4\pi Dr}e^{-r/L} \qquad (11.67)$$

The mean square crow-flight distance, $\overline{r}^2$, travelled by neutrons from their source to their point of absorption may be expressed by the equation:

$$
\begin{aligned}
\overline{r^2} &= \frac{1}{S}\sum_{\substack{all \\ neutrons}} \left\{\begin{matrix} The\ number\ of\ neutrons\ absorbed\ per\ second \\ in\ the\ distance\ r \to r + dr\ from\ the\ source \end{matrix}\right\} \times r^2 \\
&= \frac{1}{S}\int_0^\infty \Sigma_a\phi(r)4\pi r^2 dr \\
&= \frac{1}{r^2}\int_0^\infty e^{-r/L} r^3 dr
\end{aligned}
\qquad (11.68)
$$

The integral is equal to 6L², consequently:

$$
\begin{aligned}
&\overline{r^2} = 6L^2 \\
&or \\
&L^2 = \frac{1}{6}\overline{r^2}
\end{aligned}
\qquad (11.69)
$$

The diffusion length squared is one sixth of the mean square crow- flight distance travelled by neutrons which are diffusing with constant energy from their source up to their point of absorption.

The significance of L² as being proportional to the mean square crowflight distance travelled by neutrons in a material is important, as will be seen in later. At this stage it is sufficient to emphasize that the larger the value of L², the further neutrons travel (on average) from their source to the point where they are absorbed.

For thermal neutrons, L² is one-sixth or the mean square crow-flight distance travelled from the point at which neutrons become thermalized at the end of the slowing down process, to the point where they are absorbed.

11.5 Neutron diffusion in multiplying media – the reactor equation

The most important use of the one-group neutron diffusion equation is in the solution of problems associated with thermal reactors, in particular the determination of the critical size of the core and the spatial variation of the neutron flux in the core. One-group theory for thermal reactors assumes that all neutrons in the core are thermal neutrons, and the monoenergetic diffusion equation (11.45) , can be used for the analysis of thermal reactors by integrating this equation over the thermal neutron spectrum, and using appropriate values of the diffusion coefficient and the absorption cross-section.

Integrating equation (11.45) over the thermal neutron energy range we get the following equation:

$$\int_{th}\frac{\partial n(\boldsymbol{r},E,t)}{\partial t}dE=\int_{th}D_c(E)\Delta\phi(\boldsymbol{r},E,t)dE-\int_{th}\Sigma_{ac}(E)\phi(\boldsymbol{r},E,t)dE+\int_{th}S(\boldsymbol{r},E,t)dE \qquad (11.70)$$

If it is assumed that the neutron flux and density can be considered as separable functions of position, energy and time, for example if:

$$\phi(\boldsymbol{r},E,t)=F(\boldsymbol{r})G(E)T(t) \qquad (11.71)$$

then the integration of equation (11.70) over thermal energies can be carried out using:

$$\int_{th}\phi(E)dE=\phi_{th}$$

$$\int_{th}n(E)dE=\frac{\phi_{th}}{v_{av}} \qquad (11.72)$$

$$\int_{th}\Sigma_{ac}(E)\phi(E)dE=\overline{\Sigma_{ac}}\phi_{th}$$

The average diffusion coefficient for thermal neutrons is defined as:

$$\overline{D_c}=\frac{\int_{th}D_c(E)\phi(E)dE}{\phi_{th}} \qquad (11.73)$$

Now equation (11.70) becomes:

$$\frac{1}{v_{av}}\frac{\partial\phi_{th}(\boldsymbol{r},t)}{\partial t}=D_c\Delta\phi_{th}(\boldsymbol{r},t)-\Sigma_{ac}\phi_{th}(\boldsymbol{r},t)+S_{th}(\boldsymbol{r},t) \qquad (11.74)$$

The average absorption cross-section $\overline{\Sigma}_{ac}$ and the average diffusion coefficient D_c, refer to the mixture of materials in the core of the reactor, as the suffix c is intended to emphasise. The absorption cross-section depends strongly on the fuel and its concentration in the reactor. On the other hand, particularly for dilute fuel-moderator mixtures, the diffusion coefficient (which is determined principally by the scattering cross-section) depends almost entirely on the moderator, and its value can be taken as nearly equal to the value for pure moderator.

The source of thermal neutrons per unit volume, $S_{th}(\mathbf{r})$, in a reactor is from fission. The rate of thermal fission is $\overline{\Sigma}_f\,\phi_{th}(\mathbf{r})$ the total number of fission neutrons produced from both thermal and fast fission is $\varepsilon\nu\overline{\Sigma}_f\,\phi_{th}(\mathbf{r})$, and the number of neutrons which survive slowing down and become thermalized is $p\varepsilon\nu\overline{\Sigma}_f\,\phi_{th}(\mathbf{r})$. (The leakage of neutrons while slowing down is neglected in this expression, but the capture of neutrons is taken into account by the factor p.)

The infinite reproduction constant may be expressed as:

$$k_\infty=\frac{Rate\ of\ \ neutron\ production\ \ in\ \ reactor\ core}{Rate\ of\ \ neutron\ absorption\ \ in\ \ reactor\ core}=$$
$$=\frac{\int_{core}p\varepsilon\nu\overline{\Sigma_f}\phi_{th}(\boldsymbol{r})dV}{\int_{core}\overline{\Sigma_{ac}}\phi_{th}(\boldsymbol{r})dV} \qquad (11.75)$$

Since p,ε, ν, and the cross-sections are independent of position in a homogeneous reactor, it follows from this equation that:

$$k_\infty\overline{\Sigma_{ac}}=\varepsilon p\nu\overline{\Sigma_f}$$
$$and \qquad (11.76)$$
$$S_{th}(\boldsymbol{r})=k_\infty\overline{\Sigma_{ac}}\phi_{th}(\boldsymbol{r})$$

Using this result, equation (11.74) becomes:

$$\frac{1}{v_{av}}\frac{\partial\phi_{th}(\boldsymbol{r},t)}{\partial t}=\overline{D_c}\Delta\phi_{th}(\boldsymbol{r},t)-\overline{\Sigma_{ac}}\phi_{th}(\boldsymbol{r},t)+k_\infty\overline{\Sigma_{ac}}\phi_{th}(\boldsymbol{r},t)$$
$$or \qquad (11.77)$$
$$\frac{1}{\overline{D_c}v_{av}}\frac{\partial\phi_{th}(\boldsymbol{r},t)}{\partial t}=\Delta\phi_{th}(\boldsymbol{r},t)+\frac{k_\infty-1}{L_c^2}\phi_{th}(\boldsymbol{r},t)$$

where

$$L_c^2=\frac{\overline{D_c}}{\overline{\Sigma_{ac}}} \qquad (11.78)$$

L_c^2 is the diffusion length squared of thermal neutrons in the fuel – moderator mixture that constitutes the core of the reactor.

At this point we define the material buckling B_m^2 of a reactor by the equation:

$$B_m^2=\frac{k_\infty-1}{L_c^2}$$

and equation (11.77) becomes:

$$\frac{1}{\overline{D_c}v_{av}}\frac{\partial\phi_{th}(\boldsymbol{r},t)}{\partial t}=\Delta\phi_{th}(\boldsymbol{r},t)+B_m^2\phi_{th}(\boldsymbol{r},t) \qquad (11.79)$$

If the thermal neutron flux $\phi_{th}(\mathbf{r},t)=F(\mathbf{r})T(t)$ is now expressed as the product of two functions, one of position r and one of time t, thus:

$$\frac{1}{\overline{D_c}v_{av}T}\frac{DT}{dt}=\frac{\nabla^2F}{F}+B_m^2 \qquad (11.80)$$

The material buckling B_m^2 is constant, therefore:

$$\frac{\nabla^2 F}{F} \quad \text{and} \quad \frac{1}{T}\frac{dT}{dt}$$

are independently equal to constants. Let:

$$\frac{\nabla^2 F}{F} = -B_g^2$$

$$\text{or} \qquad (11.81)$$

$$\nabla^2 F + B_g^2 F = 0$$

Equation (11.81) expresses the spatial variation of the flux in a reactor. Its solution subject to appropriate boundary conditions enables B_g^2 to be expressed in terms of the dimensions of a reactor, and the value of B_g^2 corresponding to the fundamental solution of this equation (which is the only solution of interest to us), is called the geometric buckling. (The name arises because B_g^2 is a measure of the curvature of the flux, or the extent to which it buckles.)

In a critical reactor, that is one in which $\partial\phi/\partial t$ (or dT/dt) is zero, it is clear, comparing equations (11.80) and (11.81), that:

$$B_m^2 = B_g^2 \qquad (11.82)$$

In a non-critical reactor B_m^2 is not equal to B_g^2, and if the reactor is supercritical, $\partial\phi/\partial t$ (or dT/dt) > 0, and $B_m^2 > B_g^2$. On the other hand if the reactor is subcritical, $\partial\phi/\partial t$ (or dT/dt) < 0 and $B_m^2 < B_g^2$..

In this lecture we are concerned only with critical reactors, so B_m^2 and B_g^2 can be regarded as always equal to each other and will be denoted simply by B^2, the buckling. For a critical reactor, equation (11.59) becomes:

$$B^2 = \frac{k_\infty - 1}{L_c^2} \qquad (11.83)$$

and this is the one-group critical equation. The reactor flux equation

$$\nabla^2\phi + B^2\phi = 0 \qquad (11.84)$$

(Henceforth in this chapter ϕ_{th} will be written simply as ϕ) The fundamental solution of this equation together with equation (11.83) provides the necessary relationship between the materials of the core, (k_∞ and L_c^2)and its critical size, in which the buckling can be regarded as the link.

11.6 Diffusion length and slowing-down length

In the calculation of L_c^2 for a reactor the value of the average diffusion coefficient can, as already stated, usually be taken as being the same as the value for pure moderator. This is certainly the case for dilute fuel-moderator mixtures. The average absorption cross-section for the reactor is :

$$\overline{\Sigma_{ac}} = 0.8862\sum_i N_i\sigma_i \qquad (11.85)$$

where N_i is the number of atoms/cm^3 of the reactor of each constituent i whose 2200 m/s absorption cross-section is σ_{ai}. These constituents will include the fuel and moderator, and possibly also coolant, cladding and structural materials.

If the core of the reactor can be regarded as consisting only of fuel and moderator, then, recalling equation (11.4):

$$f = \frac{\overline{\Sigma_{aF}}}{\overline{\Sigma_{ac}}} = \frac{\overline{\Sigma_{aF}}}{\overline{\Sigma_{aF}} + \overline{\Sigma_{aM}}} \qquad (11.86)$$

and

$$1 - f = \frac{\overline{\Sigma_{aM}}}{\overline{\Sigma_{ac}}} \qquad (11.87)$$

where $\overline{\Sigma}_{aM}$ is the average absorption cross-section of the moderator component of the reactor, $N_M\overline{\sigma}_{cM}$($N_M$ being the number of atoms of moderator/cm3 of the reactor). If the fuel-moderator mixture is dilute, then the volume occupied by fuel in the core is very small, and (in terms of volume) the core is nearly all moderator. Thus $\overline{\Sigma}_{aM}$ is very nearly equal to $\overline{\Sigma}_a$ for pure moderator and:

$$\overline{\Sigma_{ac}} = \frac{\overline{\Sigma_a}\ \textit{for pure moderator}}{1-f} \qquad (11.88)$$

Combining this result with the earlier statement regarding the average diffusion coefficient, we conclude that:

$$L_c^2 = (1-f)\times L^2\ \textit{for pure moderator} \qquad (11.89)$$

Thus the diffusion length for the reactor can be expressed in terms of the diffusion length of its moderator and the thermal utilization factor. Values of L^2 for the principal moderators are shown in Table II. From these values it can be seen that L^2 for water is very much less than for heavy water and graphite, and thus the average crow flight distance travelled by thermal neutrons in a water moderated reactor is much less than in heavy water or graphite moderated reactors. This in turn means that water moderated reactors can be designed with much smaller cores than other reactor types. (The values of L^2 for graphite and heavy water depend on the purity of these materials, and the values given are for reactor grade materials).

Hitherto the distance travelled by neutrons during slowing down has been neglected; however, by analogy with the diffusion length squared, L^2 (which can be thought of as the product of the diffusion coefficient and the mean free path of thermal neutrons up to their point of absorption), the slowing-down length squared, $L_s^2(\tau_0)$ is the diffusion coefficient multiplied by the mean total distance travelled by fission neutrons during slowing down to the point where they become thermalized. Thus:

$$L_s^2 = D\times\lambda_s\times\left(\begin{array}{c}\textit{The average number of collision}\\ \textit{to thermalize fission neutrons}\end{array}\right) \qquad (11.90)$$

$$= \frac{D}{\xi\Sigma_s}\ln\frac{E_f}{E_{th}}$$

Using the same arguments that have been applied to D and Σ_s it may be said that the value of L_s^2 for a dilute fuel-moderator mixture is very nearly equal to the value of L_s^2 for the pure moderator. These values are shown in Table III for the principal moderators.

Table III. Diffusion and slowing-down parameters for different moderators.

Moderator	ρ, g/cm^3	λ_{tr} cm	L cm	t_{th} ms	ξ	t_s µs	τ_0 cm^2
H_2O	1.0	0.43	2.7	0.21	0.92	1	27
D_2O (pure)	1.1	2.5	165	130	0.51	8	131
D_2O (normal)	1.1	2.5	100	50	0.51	8	115
Be	1.8	1.5	22	3.8	0.21	10	102
BeO	2.96	1.4	31	8.1	0.17	12	100
C (pure graphite)	1.6	2.6	59	17	0.158	24	368
C (normal. graphite)	1.6	2.6	50	12	0.158	24	368

It is possible to show that $L_s^2$is equal to one-sixth of the mean square crow-flight distance travelled by neutrons during slowing down from fission to thermal energy, i.e.:

$$L_s^2 = \frac{\overline{r_{term}^2}}{6} \tag{11.91}$$

where r, denotes the crow-flight distance travelled by a neutron during slowing down. The similarity between this result and the result expressed by equation (11.69) for the diffusion length squared should be noted. L_s^2 has the same significance for the slowing down process as L^2 has for the diffusion of thermal neutrons.

Looking at the values of $L_s^2(\tau_0)$ in Table III, it is seen that water has the smallest value, which is not surprising as from the point of view of slowing neutrons down by scattering collisions, water has already been seen to be the most effective moderator. Thus water is seen to have the advantage over other moderators that both during slowing down and during thermal diffusion neutrons travel shorter distances than in other moderators, and the probability of neutron leakage from water moderated cores is less than from other cores of the same size.

11.7 Migration length and the modified one-group equation

The migration length squared M^2 for a reactor is defined as:

$$M^2 = L_c^2 + L_s^2 \tag{11.92}$$

and its significance can be interpreted by reference to Figure 11.8 which shows the zig-zag track of a single neutron slowing down from fission to thermal energy and diffusing at this energy until it is absorbed.

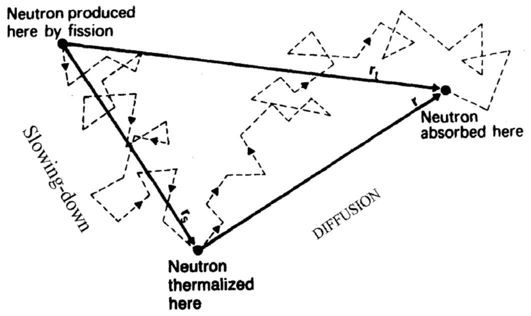

Figure 11.8 Microscopic model of neutron slowing down and diffusion.

The crow-flight distance travelled during slowing down is represented by the vector $\mathbf{r}_s$ and the crow-flight distance travelled during thermal diffusion is represented by the vector **r**. The total crow-flight distance travelled by the neutron from production to absorption is represented by the vector $\mathbf{r}_t$,. If the angle between the vectors $\mathbf{r}_s$, and **r** is 90^0, then $r_t^2 = r_s^2 + r^2$. Now thinking in terms of a large number of neutrons, if scattering is assumed to be isotropic then the average angle between the vectors $\mathbf{r}_s$, and **r** is 90^0, and the average values of are related by:

$$\overline{r_t^2} = \overline{r_s^2} + \overline{r^2} \tag{11.93}$$

Comparing this equation with (11.93), and recalling also equations (11.69) and (11.91), it follows that M^2 can be interpreted as one-sixth of the mean square crow-flight distance travelled by neutrons from the point where they are produced by fission to the point where they are ultimately absorbed after thermalization. Thus M^2 has the same significance for the total crow-flight distance travelled by neutrons as L^2 has for the crow-flight distance travelled after they become thermalized.

In order to take account of the diffusion of neutrons during slowing down, which was ignored in the analysis leading to the one-group equation, L_c^2 in the one-group critical equation (11.83) can be replaced by M^2 to give the modified one-group critical equation:

$$B^2 = \frac{k_\infty - 1}{M^2} \tag{11.94}$$

This equation has the advantages of being much more accurate than the one-group equation, while at the same time being no more difficult to use. Its use is therefore preferred to the one-group equation.

11.8 Solution of the reactor equation

The reactor equation(11.84), will now be solved for a bare cylindrical reactor core, the most common shape. The corresponding results for the other possible core shapes are tabulated at the end of this section. Boundary condition 4 can be applied at the surface of a bare core as it is assumed that no neutrons which leak from the core can return to it.

Figure 11.9 shows a bare cylindrical core whose dimensions are height L and radius R. If the extrapolation distance is $0.71\lambda_{tr}$, the extrapolated dimensions of the core are given by the equations:

$$L' = L + 1.42\lambda_{tr}$$
$$R' = R + 0.71\lambda_{tr} \qquad (11.95)$$

In cylindrical coordinates with angular symmetry the reactor equation is:

$$\frac{\partial^2 \phi}{\partial r^2} + \frac{1}{r}\frac{\partial \phi}{\partial r} + \frac{\partial^2 \phi}{\partial z^2} + B^2\,\phi = 0 \qquad (11.96)$$

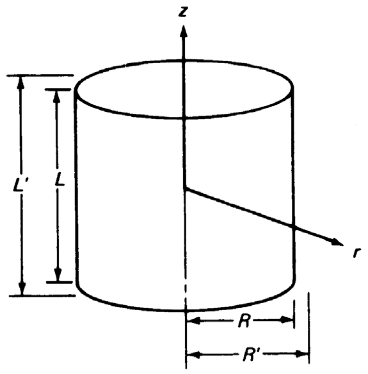

Figure 11.9 Bare cylinder reactor core

It is assumed that the flux ϕ(r, z) can be expressed as the product of two functions, one of r only and the other of z only, thus:

$$\phi(r,z) = F(r)G(z) \qquad (11.97)$$

Equation (11.97)can now be written as:

$$\frac{1}{F}\frac{d^2F}{dr^2} + \frac{1}{Fr}\frac{dF}{dr} + \frac{1}{G}\frac{d^2G}{dz^2} + B^2 = 0 \qquad (11.98)$$

$\left\{\frac{1}{F}\frac{d^2F}{dr^2} + \frac{1}{Fr}\frac{dF}{dr}\right\} and \frac{1}{G}\frac{d^2G}{dz^2}$ are independent of each other, and each is equal to some constant. Let:

$$\frac{1}{F}\frac{d^2F}{dr^2} + \frac{1}{Fr}\frac{dF}{dr} = \alpha^2$$
$$and \qquad (11.99)$$
$$\frac{1}{G}\frac{d^2G}{dz^2} = -\beta^2$$

from equations (11.98) and (11.99) we see that:

$$\alpha^2 + \beta^2 = B^2 \qquad (11.100)$$

The solution of equation (11.98) is:

$$G(z) = A\sin(\beta z) + C\cos(\beta z) \qquad (11.101)$$

The solution must be symmetrical above and below the centre plane of the core, z = 0, therefore A = 0. The flux must be zero at the extrapolated boundaries of the core, namely at z = ± L'/2. This condition is satisfied if **β=nπ/L'**, where n = 1, 3, 5, etc.

Only the fundamental solution, n = 1, is of interest, thus the solution of equation (11.99) is:

$$\phi(r,z) = \phi_{max}\cos\left(\frac{\pi z}{L'}\right)J_0\left(\frac{2.405\,r}{R'}\right) \qquad (11.102)$$

and defining x=αr we get from equation (11.99)

$$x^2\frac{d^2F}{dx^2} + x\frac{dF}{dx} + x^2F = 0 \qquad (11.103)$$

This is Bessel's ordinary equation of zero order, of which the solution is:

$$F(x) = DJ_0(x) + EY_0(x)$$
$$or$$
$$F(r) = DJ_0(\alpha r) + EY_0(\alpha r) \qquad (11.104)$$

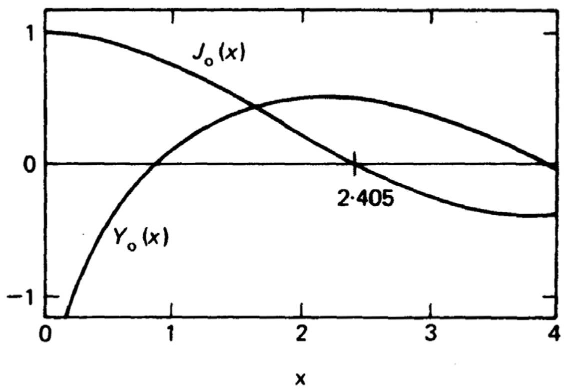

Figure 11.10 Ordinary Bessel functions of zero order.

where J_0, and Y_0, are ordinary Bessel functions of zero order. These functions are shown in Figure 11.10 .

As αr → 0, Y_0(αr)→∞, which would give a physically impossible solution, therefore E = 0. The flux must be zero at the extrapolated radius of the core, R', and considering the fundamental solution of the equation F(r) = DJ_0(αr), the result for α is α = 2.405/R' since the first zero of the J_0, function is at 2.405. The solution of equation (11.98) is therefore:

$$F(r) = DJ_0\left(\frac{2.405r}{R'}\right)$$
$$while \qquad (11.105)$$
$$\alpha = \frac{2.405}{R'}$$

Combining equations (11.102) and (11.105), the complete solution for the flux in a cylindrical reactor core is:

$$\phi(r,z) = A'\cos\left(\frac{\pi z}{L'}\right)J_0\left(\frac{2.405\,r}{R'}\right) \qquad (11.106)$$
$$A' = C\cdot D \rightarrow \phi_{max}$$

This is the maximum value of the flux, and the preceding equation may be written:

$$\phi(r,z) = \phi_{max}\cos\left(\frac{\pi z}{L'}\right)J_0\left(\frac{2.405\,r}{R'}\right) \qquad (11.107)$$

This equation expresses the flux variation in the core, and the buckling B^2 is related to the dimensions of the core giving from equations (11.102) and (11.105):

$$B^2 = \left(\frac{\pi}{L'}\right)^2 + \left(\frac{2.405}{R'}\right)^2 \qquad (11.108)$$

The buckling is also related to the materials of the core by the one- group equation, (11.83), or the modified one-group equation, (11.94). The use of equation(11.108) with either (11.83) or (11.94) enables the dimensions of a critical reactor to be expressed in terms of the materials of the core, or vice versa.

It should be remembered that the extrapolated dimensions, L' and R', differ from the actual dimensions of the core by $1.42\lambda_{tr}$ and $0.71\lambda_{tr}$ respectively, which for most moderators is only a few centimeters. If the actual dimensions of the core are large by comparison then it is possible without serious loss of accuracy to use the actual dimensions L and R instead of the extrapolated dimensions L' and R' in the pre- ceding equations. The critical size of the core is determined by the values of L and R which satisfy equation (11.108) for a value of B^2 which is determined by the materials of the reactor. The solution of the reactor equation for the other core shapes follows the same procedure as outlined above for a cylindrical core, and the results are summarized in Table IV.

Table IV. The solution of the reactor equation for the principal geometries.

Shape	Extrapolated dimensions	Flux	Buckling B^2
Rectangular parallelepiped	$a' \times b' \times c'$	$\phi = \phi_{max} \cos\left(\frac{\pi x}{a'}\right) \cos\left(\frac{\pi y}{b'}\right) \cos\left(\frac{\pi z}{c'}\right)$	$\left(\frac{\pi}{a'}\right)^2 + \left(\frac{\pi}{b'}\right)^2 + \left(\frac{\pi}{c'}\right)^2$
Cylinder	$L' \times R'$	$\phi = \phi_{max} \cos\left(\frac{\pi z}{L'}\right) J_0\left(\frac{2{\cdot}405 r}{R'}\right)$	$\left(\frac{\pi}{L'}\right)^2 + \left(\frac{2{\cdot}405}{R'}\right)^2$
Sphere	R'	$\phi = \phi_{max} \frac{R'}{\pi r} \sin\left(\frac{\pi r}{R'}\right)$	$\left(\frac{\pi}{R'}\right)^2$

The question arises in the case of rectangular parallelepiped and cylindrical reactors as to the values of the dimensions which, for a fixed composition and value of B^2, give the minimum critical volume, and hence the minimum mass of fuel in the core. The problem can be solved easily for a cylindrical core, neglecting the difference between the actual and the extrapolated dimensions. The conditions are:

$$B^2 = \left(\frac{\pi}{L}\right)^2 + \left(\frac{2.405}{R}\right)^2 \tag{11.109}$$

is constant, and the volume, $\pi R^2 L$ is to be minimized. The volume can be expressed as:

$$V = \pi R^2 L = \frac{\pi L (2.405)^2}{B^2 - \left(\frac{\pi}{L}\right)^2} \tag{11.110}$$

and is a minimum when dV/dL is zero, which gives the result:

$$L = \frac{\pi\sqrt{3}}{B} \tag{11.111}$$

From this it follows that:

$$R = \frac{2.405}{B}\sqrt{\frac{3}{2}} \qquad V_{\min} = \frac{148}{B^3} \tag{11.112}$$

The ratio of the radius to the height is given by:

$$\frac{R}{L} = \frac{2.405}{\sqrt{2}\pi} = 0.54 \tag{11.113}$$

Thus the minimum volume of a cylindrical core of fixed buckling is obtained when the diameter is approximately equal to the height. Figure 11.11 shows the variation of R with L for a cylindrical core of fixed buckling, and also the variation of the critical mass with L. The latter curve shows a minimum point which corresponds to the optimum dimensions just derived.

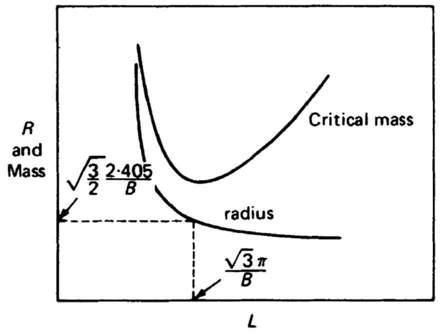

Figure 11.11 Optimum dimension and critical mass of cylindrical core

In the case of a rectangular parallelepiped it can be shown that the minimum volume, as might be expected, occurs when the three sides are equal and the shape of the core is a cube. Table V shows the optimum dimensions and the corresponding volume of the three core shapes in terms of the buckling. The minimum volume is obtained with a spherical core, which is to be expected as of the three core shapes the sphere has, for a given volume, the minimum surface area. Since neutron leakage is a surface effect, the leakage per unit volume of core is least for a sphere, and this is therefore from a purely physical point of view the best core shape. From the practical point of view, however, it has disadvantages and is rarely used.

Table V. Optimum core dimensions and minimum volumes

Core shape	Optimum dimensions	Minimum volume
Cube	$a = b = c = \frac{\sqrt{3}\pi}{B}$	$\frac{161}{B^3}$
Cylinder	$L = \frac{\sqrt{3}\pi}{B}, R = \frac{2{\cdot}405}{B}\sqrt{\frac{3}{2}}$	$\frac{148}{B^3}$
Sphere	$R = \frac{\pi}{B}$	$\frac{130}{B^3}$

Example: *Calculate the dimensions of the cylindrical core and the minimum critical mass of uranium for a homogeneous reactor consisting of a mixture of enriched uranium (2 per cent ^{235}U) and graphite in the ratio 1 to 300 by atoms.*

The modified one-group equation is used in the form:

$$\varepsilon = 1.0 \quad p = 0.659\; f = 0.923\; \eta = 1.722$$

$$\Rightarrow k_\infty = 1.048$$

$$L_{MOD}^{2\ \ Grafit} = 2650\ cm^2 \quad L_s^{2\ \ Grafit} = 368\ cm^2$$

$$L_c^2 = L_{MOD}^2(1 - f) = 2650 \cdot 0.077 = 204\ (cm^2)$$

$$f = \frac{\Sigma_{ac}}{\Sigma_{ac} + \Sigma_{aM}} \rightarrow 1 - f = \frac{\Sigma_{aM}}{\Sigma_{ac}} = \frac{L_c^2}{L_{MOD}^2}$$

$$M^2 = L_c^2 + L_s^2$$

$$\Rightarrow M^2 = 204 + 368 = 572\ \ (cm^2)$$

$$B^2 = \frac{k_\infty - 1}{M^2} = \frac{0.048}{572} = 0.839 \cdot 10^{-4} \quad cm^2$$
$$B = 0.00916\, cm^{-1}$$

The minimum core volume, and hence minimum critical mass of uranium is obtained with a radius to height ratio of 0.54. From Table V, neglecting extrapolation distances, the dimensions of the core are L = 5.94 m, R = 3.22 m, and the volume V= 193 m^3. The mass of uranium is calculated by neglecting the fractional volume of fuel in the core and calculating first the number of atoms of graphite per cm^3 of the core.

$$N(C) = \frac{1620 \times 6.023 \times 10^{23}}{12} = 8.13 \times 10^{28} atoms\, /\, m^3$$

where the density of graphite has been taken as 1620 kg/m^3, and its atomic mass is 12.

The number of atoms of uranium per m^3 of the core:

$$N(U) = \frac{8.13 \times 10^{28}}{300} = 2.71 \times 10^{26}\ atoms\, /\, m^3$$

The mass of uranium per m^3 of the core:

$$M(U) = \frac{2.71 \times 10^{26} \times 238}{6.023 \times 10^{26}} = 107 kg\, /\, m^3$$

The mass of uranium in the reactor = 107 × 193 ×10^{-3} =20.7 tonnes.

The error involved by neglecting the extrapolation distances may be estimated. The extrapolation distance for a graphite moderated reactor is about 2 cm, and the error involved in the length and radius of the core by neglecting it is about 0.7 per cent. The error in the volume of the core and the critical mass of uranium is therefore about 2 per cent.

11.9 Neutron leakage

In earlier lectures the non-leakage probabilities for fast and thermal neutrons, P_{NLf} and PN_{Lth}, were defined. The fraction of all fission produced neutrons which do not leak out of the core, P_{NL} is related to these two non-leakage probabilities by:

$$P_{NL} = P_{NLth} \times P_{NLf} \tag{11.114}$$

and the fraction of all fission produced neutrons which do leak out of the core, P_L, is given by:

$$P_L = 1 - P_{NL} = 1 - (P_{NLth} \times P_{NLf}) \tag{11.115}$$

In a critical finite reactor in which the value of k_{eff}= 1, k_∞ and P_L are related by:

$$P_L = 1 - \frac{1}{k_\infty} \tag{11.116}$$

According to one-group theory in which all neutrons are assumed to be thermal neutrons, the leakage of fast neutrons is neglected and therefore $P_L = P_{Lth}$. Using equation (11.83) in the form $k=1 + B^2L_c^2$ with equation (11.116) it can be shown that the leakage of thermal neutrons is:

$$P_{Lth} = \frac{B^2 L_c^2}{1 + B^2 L_c^2} \tag{11.117}$$

According to modified one-group theory, equation (11.94) in the form $k\infty = 1 + B^2M^2$ can be combined with equation (11.116) to show that the leakage fraction of all neutrons, fast and thermal, is given by:

$$P_L = \frac{B^2 M^2}{1 + B^2 M^2} \tag{11.118}$$

11.10 Form factors

It is important to know the relationship between the maximum rate of energy release and the average rate of energy release in the reactor core. These quantities are in turn proportional to the maximum and average thermal neutron fluxes in the core.

The rate of energy release per unit volume at any point in a reactor core is given by:

$$H(\boldsymbol{r}) = 3.2 \times 10^{-11} \overline{\Sigma_f} \phi_{th}(\boldsymbol{r})\ W\, /\, cm^3 \tag{11.119}$$

The thermal output of the whole reactor, Q_r is:

$$Q_r = 3.2 \times 10^{-11} \int_{core} \overline{\Sigma_f} \phi_{th}(\boldsymbol{r}) dV\ Watts \tag{11.120}$$

or alternatively

$$Q_r = 3.2 \times 10^{-11} \times \overline{\Sigma_f} \times Volume\ of\ core \times \phi_{av} \tag{11.121}$$

where ϕ_{av} is the spatially averaged thermal neutron flux in the core

In a cylindrical reactor core the relationship between the average and maximum fluxes can be derived from equation (11.107) as:

$$\phi_{av} = \frac{1}{\pi R^2 L} \int_0^R \int_{-L/2}^{L/2} \phi_{\max} \cos\left(\frac{\pi z}{L'}\right) J_0\left(\frac{2.405 r}{R'}\right) 2\pi r dr dz \tag{11.122}$$

It is convenient to define axial (α_z) and radial (α_r) form factors for a cylindrical reactor as follows:

$$\alpha_z = \frac{The\ flux\ at\ the\ centre\ of\ the\ reactor}{The\ average\ flux\ along\ the\ central\ axis\ of\ the\ core}$$

$$= \frac{\phi_{\max}}{1/L \int_{-L/2}^{L/2} \phi_{\max} \cos\left(\frac{\pi z}{L'}\right) dz} \tag{11.123}$$

$$= \frac{\pi L / 2L'}{\sin(\pi L / 2L')}$$

$$\alpha_z = \pi / 2 = 1.57$$

If L = L′, that is if the extrapolation distance is neglected, then:

$$\alpha_r = \frac{\text{The flux at the centre of the reactor}}{\text{The average flux along the central plane of the core at } z = 0} \tag{11.124}$$

$$= \frac{\phi_{\max}}{\frac{1}{\pi R^2}\int_0^R \phi_{\max} J_0\left(\frac{2.405r}{R'}\right) 2\pi r dr}$$

$\int rJ_0(\beta r)dr = \frac{1}{\beta} rJ_1(\beta r)$. and the values of $J_1(\beta r)\, at\, \beta r = 0$ and 2.405 are 0 and 0.52 respectively. The expression for α_r becomes:

$$\alpha_r = \frac{1.2R/R'}{J_1(2.405R/R')} \tag{11.125}$$

and if the extrapolation distances are neglected, i.e. if R = R':

$$\alpha_r = 2.31 \tag{11.126}$$

The overall form factor α_0 is the product of the axial and radial form factors, and using the preceding equations for α_z, and α_r it is seen that the overall form factor is the ratio of the maximum to average Thus in the core:

$$\alpha_0 = \alpha_z \times \alpha_r = \frac{\phi_{\max}}{\phi_{av}} \tag{11.127}$$

If extrapolation distances are neglected, α_0=3.63.

11.11 Conclusion

The accuracy of any calculations based on the theory outlined in this chapter depends on two factors – the accuracy of the theory itself, and the accuracy with which data such as cross-sections and the value of ν are known. The limitations of one-group theory have already been mentioned, and it should be pointed out that cross-sections and other nuclear data, which must be determined experimentally, are not known with complete accuracy. Consequently calculations alone are not sufficient for the design of reactors and the exact prediction of criticality, and experimental results also have to be used. One example of the use of experimental data is in the empirical formula for the effective resonance integral which was introduced earlier in this chapter,and two further examples will be mentioned. Both these examples depend on the fact that if in a sub-critical assembly (one that is either too small or has too low a concentration of fuel) a source of neutrons is present, a steady-state flux is established in the system, and this flux may be measured.

In the exponential experiment an assembly of fuel and moderator is built of a size considerably less than the critical size, and a source of neutrons is located at one side of the assembly. Measurements of the flux distribution in the assembly enable the value of k_∞ to be determined. In the "approach to critical" experiment the reactor core is constructed with a neutron source, and the fuel is loaded progressively, one fuel element at a time, into the core. The variation of the neutron flux as the fuel is loaded enables the critical mass of fuel to be very accurately predicted before it is actually loaded into the core and the reactor becomes critical.

Finally, it should be pointed out that it is not sufficient to design a reactor whose initial value of k_{eff} is exactly l. If this were done, it would not be possible, without a neutron source, to start up the reactor, and once the reactor is started up it would soon become subcritical and shut down as some fissile material is used up and other changes occur. A reactor is always designed so that the initial value of k_{eff} is slightly greater than 1 . The excess reactivity δk, which is defined as $k_{eff} - 1$, may be in the range 0.01 to 0.25 or more depending on the type of reactor, and it is offset at the start of the reactor's life by inserting into the core rods of neutron absorbing material known as control rods. These rods are progressively withdrawn to keep the value of k_{eff} equal to 1 and enable the reactor to operate at steady power for long periods of time. This subject will be dealt with in more detail in a later chapter, however the point to note at this stage is that the method developed in this chapter may be modified slightly to determine the composition or size of a reactor with a certain amount of excess reactivity.

For example, if it is desired to find the size of a reactor of given composition and a given excess reactivity, δk, the value of k_∞ for the reactor is calculated in the normal way by the four factor formula, and L_c^2 and L_s^2 are obtained. Equation (11.94) is then used in the modified form

$$B^2 = \frac{(k_\infty - \delta k) - 1}{M^2} \tag{11.128}$$

to determine B^2, and hence the dimensions of the core. This is equivalent to using a fictitious value of the infinite multiplication factor which is equal to the actual value minus the excess reactivity.

Two-Group and Continuous Slowing Down Model

Of the various reactor models only the one-group model was developed fully, although the continuous slowing down model was used to study resonance capture. In this lecture we will study very briefly the two-group model, and use the continuous slowing-down model to analyse the combined slowing down and diffusion of neutrons. These two models yield slightly different forms of the critical equation for bare reactors, which can be compared with the one-group and modified one-group equations. The theory of homogeneous reactors is to some extent limited in its application, and although many reactors can be regarded as quasi-homogeneous there are also many that can not, and these must be analysed by methods that take account of their heterogeneous structure. Furthermore few reactors are bare, and there are obvious advantages to be gained by surrounding the core by some material which scatters neutrons, some of which return into the core, thereby reducing leakage and the critical mass of fuel. Such a material is called a reflector, and the reactor is described as a reflected reactor. The theories of heterogeneous reactors and reflected reactors are much more complicated than the theory of bare homogeneous reactors. For this reason only some qualitative descriptions and very simple models to point out the principal physical differences between these reactors are presented.

Two-group theory for bare reactors

For accurate design work it is not sufficient to consider all neutrons in one energy group as in one-group theory, and in multi-group models neutrons are subdivided according to their energy into several groups, each one representing a particular energy range. Diffusion equations for each group are set up using appropriate constants, and the simultaneous solution of these equations provides the condition for criticality of the reactor.

The method will be demonstrated by considering the two-group model, which has the advantages that it is considerably more accurate than the one-group model, and at the same time is the simplest of the multi-group models and the only one that does not require a computer for the numerical solution of problems.

In the two-group model all thermal neutrons are considered to be in one group, the thermal group, and all neutrons slowing down from fission to thermal energy are considered to be in the other group, called the fast group. Neutrons in the fast group remain in that group until they are captured, leak out of the core, or undergo a sufficient number of scattering collisions to become thermalized and enter the thermal group.

For fission neutrons to be scattered from the fast to the thermal group, they must each suffer on the average $\left[\ln(E_f / E_{th})\right] / \xi$ elastic scattering collisions. The effective cross-section Σ_1, for the removal of neutrons from the fast group is therefore given, in the absence of resonance capture, by:

$$\Sigma_1 = \frac{\Sigma_s \xi}{\ln(E_f / E_{th})} \tag{1}$$

where Σ_s, is the scattering cross-section for fast neutrons. From the definition of the slowing-down length given in the last chapter it is evident that:

$$\Sigma_1 = \frac{D_1}{L_s^2} \tag{2}$$

where D_1 is the diffusion coefficient of fast neutrons. The steady-state diffusion equations for the two groups of neutrons are written as:

$$\begin{aligned} &\textit{Fast group} && D_1\nabla^2\phi_1 - \Sigma_1\phi_1 + \varepsilon\nu\Sigma_{f2}\phi_2 = 0 \\ &\textit{Thermal group} && D_2\nabla^2\phi_1 - \Sigma_{a2}\phi_2 + p\Sigma_1\phi_1 = 0 \end{aligned} \tag{3}$$

(Suffix 1 refers to the fast group, and suffix 2 refers to the thermal group.) Note that the source of neutrons in the fast group (from thermal and fast fission) is given by $\varepsilon\nu\Sigma_{f2}\phi_2$ and that resonance capture has been taken into account by expressing the rate at which fast neutrons enter the thermal group as $p\Sigma_1\phi_1$.

The homogeneous parts of equations (3) are similar to the one-group equation $\nabla^2\phi + B^2\phi = 0$ so we assume solutions of the same form, i.e.

$$\begin{aligned} \nabla^2\phi_1 &= -B_1^2\phi_1 \\ \nabla^2\phi_2 &= -B_2^2\phi_2 \end{aligned} \tag{4}$$

If these expressions for $\nabla^2\phi_1$ *and* $\nabla^2\phi_2$ are substituted into equations (3) it can be shown that $\phi_1 = \phi_2 \times constant$ determined by the material properties of the core. From this it follows that $\nabla^2\phi_1 = \nabla^2\phi_2 \times the\,same\;constant$, therefore:

$$\frac{\nabla^2\phi_1}{\phi_1} = \frac{\nabla^2\phi_2}{\phi_2} \qquad (5)$$

$$B_1^2 = B_2^2$$

In other words the solutions B_1^2 *and* B_2^2 assumed above are the same, and will be denoted by B^2, the buckling of both fast and thermal fluxes in the core. Replacing $\nabla^2\phi_1\,and\,\nabla^2\phi_2\;by - B^2\phi_1\;and\; - B^2\phi_2$, and noting that:

$$k_\infty = \frac{\varepsilon\nu p\Sigma_{f2}}{\Sigma_{a2}} \qquad (6)$$

Equations (3) become

$$\begin{aligned}(1 + B^2L_s^2)\phi_1 - \frac{k_\infty\Sigma_{a2}}{p\Sigma_1}\phi_2 &= 0\\ (1 + B^2L_c^2)\phi_2 - \frac{p\Sigma_1}{\Sigma_{a2}}\phi_1 &= 0\end{aligned} \qquad (7)$$

Where L_c^2 is the diffusion length squared of thermal neutrons in the core of the reactor. The solution of these (5)

$$\begin{vmatrix} (+B^2L_s^2) & -\frac{k_\infty\Sigma_{a2}}{p\Sigma_1} \\ -\frac{p\Sigma_1}{\Sigma_{a2}} & (1 + B^2L_c^2 \end{vmatrix}$$

or

$$k_\infty = (1+B^2L_s^2)(1+B^2L_c^2) \tag{8}$$

This is the critical equation of a bare reactor according to two-group theory, and it should be compared with the one-group and modified one-group equations (see lecture ***Neutron diffusion theory***). The similarity between these equations is obvious; in particular, if the right-hand side of equation (8) is expanded and the term involving B^4 is neglected (it will be very small for a large core), this equation becomes identical with the modified one-group equation. Equation (8) is a quadratic in B^2; however, of the two values of B^2 which satisfy it, one is negative and does not contribute to the solution for a bare core. The positive value of B^2 is given by:

$$B^2 = \frac{1}{2L_s^2L_c^2}\left[-(L_s^2+L_c^2)+\sqrt{(L_s^2+L_c^2)^2}+4(k_\infty-1)L_s^2L_c^2\right] \tag{9}$$

A simpler approximate form is:

$$B^2 \approx \frac{k_\infty - 1}{L_s^2+L_c^2} \tag{10}$$

and the resemblance to the modified one-group equation is again evident.

The leakage probabilities for fast (P_{LF}) and thermal (P_{Lth}) neutrons can be inferred from equations $k_{eff} = k_\infty P_{NLf} P_{NLth}$ and (8) as:

$$\begin{aligned} P_{Lf} &= \frac{B^2L_s^2}{1+B^2L_s^2} \\ P_{Lth} &= \frac{B^2L_c^2}{1+B^2L_c^2} \end{aligned} \tag{11}$$

Fermi Age Theory

Another modification to one-group theory can be made to take into account the diffusion of fast neutrons while slowing down. This modification involves the use of the continuous slowing-down model, which was introduced in the previous chapter, and is known as Fermi Age theory.

A new variable called the neutron age, τ, will first be introduced. It may be defined as follows :

The age, τ , corresponding to energy *E,* is:

$$\tau(\mathrm{E}) = \int_{E}^{E_1} \frac{D(E)}{\xi\Sigma_t(E)} \frac{dE}{E} \tag{12}$$

where *E,* is the source energy of the neutrons (2 MeV in the case of fission produced neutrons). From equation (12) it is clear that the age of fission neutrons is zero, and that the age increases as neutrons lose energy.

In a medium in which fission neutrons are slowing down and being thermalized, i.e. a medium in which $\Sigma_s >> \Sigma_a, \Sigma_s \approx \Sigma_t$ the age of thermal neutrons can be shown, using equation (12) and assuming that D, Σ_s and ξ are independent of energy, to be given by :

$$\tau_{th} = \frac{D}{\Sigma_s} \frac{\ln E_f - \ln E_{th}}{\xi} \tag{13}$$

This equation may be interpreted as :

$$\begin{aligned}\tau_{th} &= D \times (The\, scattering\, mean\, free\, path) \times (The\, average\, number\, of\, collisions\\ &\quad required\, to\, thermalize\,\, fission\, neutrons)\\ &= D \times (The\, mean\, total\, distance\, travelled\, by\, fission\, neutrons\, during\, slowing\\ &\quad down\, to\, the\, point\, where\, they\, become\, thermalized)\end{aligned}$$

Evidently τ_{th} is the same quantity as L_s^2 which was introduced to characterize the distance travelled by neutrons during slowing down. The names ”age” and ”slowing-down length squared” can both be used for this quantity. Despite its name, τ has the dimensions of length squared, and it can be shown by considering neutron slowing down in a non-absorbing medium that :

$$\tau_{th} = \frac{1}{6}\overline{r_s^2} \tag{14}$$

where r_s, is the crow-flight distance travelled by fission neutrons from their source to the point where they become thermalized. When this result is compared with equation

$$\overline{r^2} = 6L^2 \tag{15}$$

the similarity between τ_{th} and L^2 for fast and thermal neutrons respectively is emphasized.

The combined diffusion and slowing down of neutrons in the energy range E to E+dE, ($E_f > E > E_{th}$), is expressed by the steady-state diffusion equation in the form:

$$D(E)\nabla^2\phi(r,E)\ dE - \Sigma_a(E)\phi(r,E)dE + S(r,E)dE = 0 \tag{16}$$

The source of neutrons in the energy interval dE at E is due to the difference in the rates at which neutrons slow down into and out of this interval :

$$S(r,E)dE = q(r,E+dE) - q(r,E) \tag{17}$$

Expressing $q(r,E+dE)$ in terms of $q(r,E)$ by means of the first two terms of a Taylor series we get :

$$S(r,E)dE = \frac{\partial q}{\partial E}(r,E)dE, \tag{18}$$

and using this result in equation (16) we get:

$$D(E)\nabla^2\phi(r,E)\ dE - \Sigma_a(E)\phi(r,E)dE + \frac{\partial q}{\partial E}(r,E)dE = 0 \tag{19}$$

Recalling a result of the continuous slowing-down model, namely:

$$\phi(E)dE = \frac{q(E)dE}{\xi\Sigma_t(E)dE} \tag{20}$$

and assuming that the spatial variation of the slowing-down density is the same as the spatial variation of the neutron flux, i.e. $\nabla^2 q = \nabla^2\phi$ at all energies, equation (20) becomes:

$$\frac{D(E)}{\xi\Sigma_t(E)}\nabla^2 q(r,E) - \frac{\Sigma_a(E)}{\xi\Sigma_t(E)}q(r,E) + E\frac{\partial q}{\partial E}(r,E) = 0 \tag{21}$$

This equation is solved by assuming that the slowing-down density *q,* which is a function of position and energy, can be treated as the product of two functions, one of position only, and the other of energy only, thus:

$$q(r,E) = F(r)\times G(E)$$

Making use of this, equation (21) becomes, dividing throughout by $\frac{D(E)FG}{\xi\Sigma_t(E)}$:

$$\frac{\nabla^2 F(r)}{F(r)} - \frac{\Sigma_a(E)}{D(E)} + \frac{\xi\Sigma_t(E)E}{D(E)G(E)}\frac{dG(E)}{dE} = 0 \tag{22}$$

The first term on the left-hand side, $\frac{\nabla^2 F}{F}$, is a function of position only, and the other two terms are functions of energy only. It follows that:

$$\frac{\nabla^2 F}{F} = \frac{\Sigma_a(E)}{D(E)} - \frac{\xi\Sigma_t(E)}{D(E)G(E)}\frac{dG(E)}{dE} = a\ constant \tag{23}$$

The spatial variation of *F* is, as already noted, the same as the spatial variation of ϕ, and the variation of ϕ is given by the equation, familiar from one-group theory:

$$\nabla^2\phi = -B^2\phi \quad or \quad \frac{\nabla^2\phi}{\phi} = -B^2 \tag{24}$$

It follows that:

$$\frac{\nabla^2 F}{F} = -B^2 \tag{25}$$

where B^2 is the buckling already encountered in one-group theory. The energy dependent part of equation (22) can now be written as:

$$\frac{dG(E)}{G(E)} = \frac{\Sigma_a(E)}{\xi\Sigma_t(E)}\frac{dE}{E} + \frac{B^2 D(E)}{\xi\Sigma_t(E)}\frac{dE}{E} = 0 \tag{26}$$

Integrating from fission to thermal energy, reversing the sign and taking antilogarithms we get

$$\frac{G_{E_{th}}}{G_f} = \exp\left[-\int_{E_{th}}^{E_f}\frac{\Sigma_a(E)dE}{\xi\Sigma_t(E)E}\right]\times\exp\left[-B^2\int_{E_{th}}^{E_f}\frac{D(E)dE}{\xi\Sigma_t(E)dE}\right] \tag{27}$$

The first term on the right-hand side is recognized as the resonance escape probability, and the second term may be simplified by using the definition of τ_{th}. Equation (27) becomes:

$$\frac{G_{E_{th}}}{G_{E_f}} = p\exp\left(-B^2\tau_{th}\right)$$

$$\textit{from which} \qquad (28)$$

$$\frac{q_{E_{th}}}{q_{E_f}} = p\exp\left(-B^2\tau_{th}\right)$$

$q_{E_{th}}$ is the slowing-down density at thermal energy which is the number of neutrons becoming thermal per cm^3 per second, and q_{E_f}, is the slowing-down density at fission energy which is the number of neutrons per cm^3 per second which are produced by fission. The ratio $\frac{q_{E_{th}}}{q_{E_f}}$, is, by definition, the product of the resonance escape probability and the fast non-leakage probability. The term $\exp\left(-B^2\tau_{th}\right)$ can therefore be identified as the fast non-leakage probability. Integrating equation (20) over the thermal neutron spectrum we get:

$$\overline{D}\nabla^2\phi_{th}(r) - \overline{\Sigma_a}\phi_{th}(r) + q_{E_{th}}(r) = 0 \qquad (29)$$

This corresponds to a steady-state version of equation

$$\frac{1}{v_{av}}\frac{\partial\phi_{th}(\boldsymbol{r},t)}{\partial t} = \overline{D}_c\nabla^2\phi_{th}(\boldsymbol{r},t) - \overline{\Sigma}_{ac}\phi_{th}(\boldsymbol{r},t) + S_{th}(\boldsymbol{r},t) \qquad (30)$$

since, according to Fermi Age theory, the source of thermal neutrons is the slowing-down density of neutrons reaching thermal energy, $q_{E_{th}}$.

The slowing-down density of neutrons at fission energy is simply the total number of neutrons produced by fission:

$$q_{E_f}(r) = \varepsilon\nu\overline{\Sigma_f}\phi_{th}(r) \qquad (31)$$

and consequently :

$$q_{E_f}(r) = \varepsilon p \nu \exp\left(-B^2\tau_{th}\right)\overline{\Sigma_f}\phi_{th}(r)$$

$$= k_\infty \exp(-B^2\tau_{th})\overline{\Sigma_a}\phi_{th}(r) \qquad (32)$$

$$since$$

$$k_\infty\overline{\Sigma_a} = \varepsilon p \nu \overline{\Sigma_f}$$

If equation (32) for $q_{E_{th}}(r)$ is substituted into equation (31), $\nabla^2\phi_{th}(r)$ is replaced by $-B^2\phi_{th}(r)$, and the resulting equation is divided throughout by $\Sigma_a\phi_{th}(r)$, we get :

$$B^2L_c^2 + 1 = k_\infty \exp(-B^2\tau_{th})$$

$$or \qquad (33)$$

$$k_\infty = (1 + B^2L_c^2)\exp(B^2\tau_{th})$$

This is the Fermi Age critical equation, and may be compared with the two-group and modified one-group critical equations, (8) and $B^2 = \frac{k_\infty - 1}{M^2}$. In particular it should be noted that if the size of the reactor is large, B^2 is very small and $\exp(B^2\tau_{th}) \approx 1 + B^2\tau_{th}$. In this case the Fermi Age equation becomes :

$$k_\infty = (1 + B^2L_c^2)(1 + B^2\tau_{th}) \qquad (34)$$

which is identical with the two-group equation, and very nearly the same as the modified one-group equation. All these equations are similar in that they relate the materials of a reactor, as expressed by $k_\infty, L_c^2 \; and \; L_s^2 \; (or \; \tau_{th})$, to the dimensions of the reactor as expressed by B^2, whose values for different core shapes are given in Table III in the lecture ***The theory of nuclear reactors – homogeneous thermal reactors*** .

Equation (33) is transcendental in B^2, and if B^2 **is** unknown it must be found by an iterative procedure. A good first approximation for B^2 **is** the value given by modified one-group theory, namely:

$$\frac{k_\infty - 1}{L_c^2 + L_s^2} \tag{35}$$

The leakage probabilities for fast and thermal neutrons are given by Fermi Age theory as:

$$P_{Lf} = 1 - \exp\left(-B^2 \tau_{th}\right)$$

$$\text{and} \tag{36}$$

$$P_{Lth} = \frac{B^2 L_c^2}{1 + B^2 L_c^2}$$

as in one-group theory.

Heterogeneous reactors

There are several reasons why a heterogeneous system of fuel and moderator is preferable to a homogeneous one. In a power reactor with solid fuel (as distinct from a liquid or slurry fuel) the rate of energy release by fission is high and it is essential to circulate the coolant in dose contact with the fuel. It is also important from time to time during the operating life of a reactor to be able to remove fuel from the core as it is burned up, and replace it with fresh fuel. Both these requirements dictate that the fuel should be in the form of individual elements, or bundles of elements, arranged in a regular lattice within the moderator.

There are also good reasons from the reactor physics point of view for preferring a heterogeneous reactor, as was realized in the early years of the development of the first nuclear reactors in the United States of America. At that time natural uranium was the only available nuclear fuel, and water and graphite were the only available moderators. A critical system, even of infinite size, is not possible with natural uranium and either graphite or water. It was realized, however, that the resonance capture of neutrons in ^{238}U can be greatly reduced if the fuel is concentrated in lumps or elements which are dispersed throughout the moderator. In this way some neutrons may slow down in the moderator without ever entering the fuel, and those neutrons which do enter the fuel elements at energies corresponding to the ^{238}U resonances are captured near the surface of the fuel with the result that the ^{238}U in the interior of a fuel element is shielded from these neutrons. This effect results in a considerable increase in the value of the resonance escape probability as compared with the value for the equivalent homogeneous system with the same fuel-moderator ratio, and makes possible a critical system with natural uranium and graphite.

In many ways the analysis of a heterogeneous reactor is similar to that of a homogeneous reactor. The reproduction constant is defined in the same way, and the four factors of k_∞ have essentially the same meaning in both types of reactor; however, in a heterogeneous reactor these factors cannot be calculated by the expressions developed in the lecture ***The theory of nuclear reactors – homogeneous thermal reactors*** for homogeneous reactors. Once the four factors and the value of k_∞ are known, the determination of the critical size follows the method of the lecture ***The theory of nuclear reactors – homogeneous thermal reactors*** using equation $B^2 = \frac{k_\infty - 1}{M^2}$ and appropriate values of L_s^2 *and* L_c^2, which may also have to take account of the heterogeneous structure of the core.

Eta - η

The factor η depends on the composition of the fuel and not the moderator, so it might be expected that its value in a heterogeneous system is the same as in a homogeneous system with the same fuel. This is not strictly true because of hardening of the neutron spectrum in the fuel of a heterogeneous reactor and the non-(1/v) variation of the fuel cross-section. In practice the value of η used in a heterogeneous reactor calculation may be an empirical value chosen to make calculated values of ε, p and *f* agree with a value of k_∞ determined from an exponential experiment. The empirical value can be used in further calculations in which the fuel and moderator are the same, but the lattice dimensions are altered.

Thermal utilization factor - f

The thermal utilization factor is affected by a change from a homogeneous to **a** heterogeneous system. This change can be explained by noting that thermal neutrons are produced in the moderator as **a** result of slowing down, but are nearly all absorbed in the fuel due to **its** much greater absorption cross-section. There is therefore **a** net flow or current of thermal neutrons from the moderator into the fuel. Since, as was shown in the last chapter, the direction of neutron current is also the direction of decreasing neutron flux, it follows that the average thermal neutron flux in the fuel is less than in the moderator.

The variation of the flux in the fuel and moderator can be deter- mined approximately by applying one-group diffusion theory to an equivalent lattice cell consisting of **a** fuel element and its associated moderator, see Figure 1(a). If the number of fuel elements in the core is large, a single cell can be regarded as representative of the core as a whole. A typical flux variation is shown in Figure 1(b), which shows the depression of the flux from the moderator into the fuel, and also a slight depression in the fuel itself.

The expression for the thermal utilization factor of a heterogeneous reactor is:

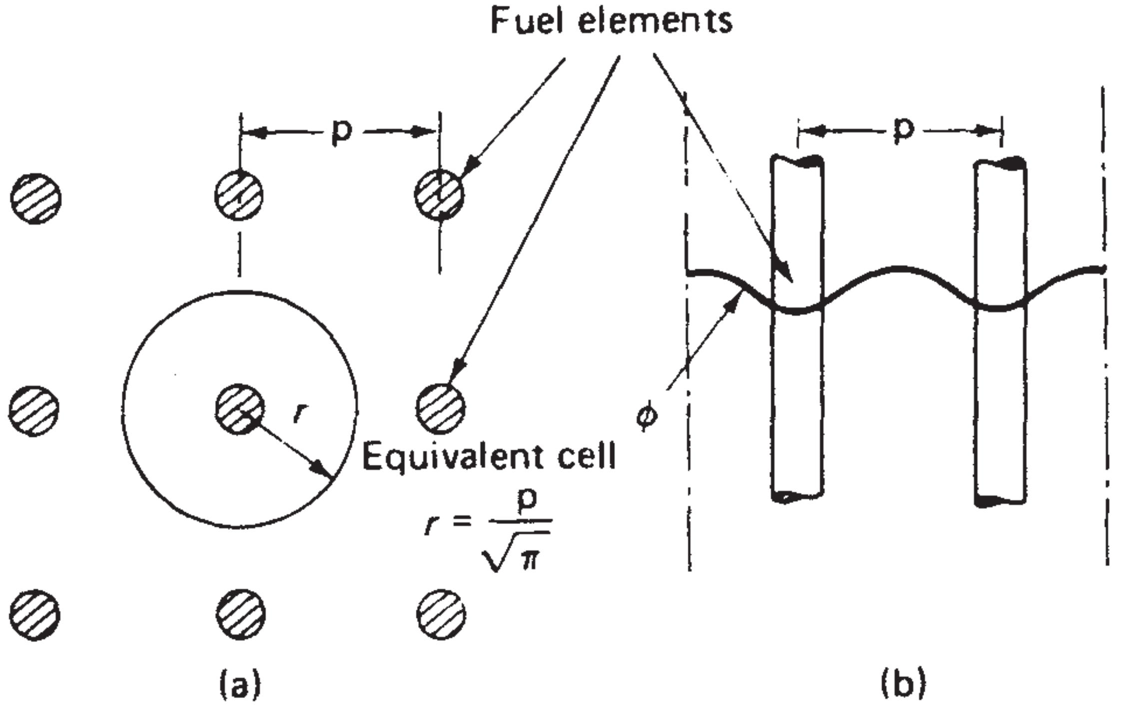

Fig. 1 Thermal neutron flux variation in a heterogeneous reactor

$$f = \frac{V_F \Sigma_{aF} \bar{\phi}_F}{V_F \Sigma_{aF} \bar{\phi}_F + V_M \Sigma_{aM} \bar{\phi}_M} \tag{39}$$

where V_F and V_M are the volumes of fuel and moderator, Σ_{aF} and Σ_{aM} are their macroscopic cross-sections, and $\bar{\phi}_F$ and $\bar{\phi}_M$ are the average thermal neutron fluxes in the fuel and moderator. An alternative expression for f is:

$$f = \frac{V_F \Sigma_{aF}}{V_F \Sigma_{aF} + V_M \Sigma_{aM} \left(\bar{\phi}_M / \bar{\phi}_F \right)} \tag{39a}$$

The ratio $\bar{\phi}_M / \bar{\phi}_F$ is known as the disadvantage factor and is greater than 1, consequently the value of f is less than the value for the equivalent homogeneous system in which $\bar{\phi}_M = \bar{\phi}_F$. The decrease is about 5 per cent in the case of a natural uranium, graphite-moderated reactor with 2 5 cm diameter fuel elements in a 20 cm square lattice.

In a large reactor the fine structure flux illustrated in Figure 1(b) is the same in all lattice cells, and is superimposed on the overall flux shape in the core which was derived in the last chapter for the principal core geometries.

Resonance escape probability - p

The increase in the resonance escape probability referred to earlier in this chapter is due to two effects. In the first place neutrons whose energy corresponds to one of the resonances of ^{238}U and which diffuse from the moderator into the fuel are captured very close to the surface of the fuel. For example, neutrons of energy 6.7 eV (corresponding to the lowest energy resonance of ^{238}U whose value is about 7000 barns) have a mean free path of about 0.003 cm in natural uranium, so it is obvious that very few of these neutrons penetrate more than a fraction of a millimeter into the fuel. This is an extreme case, however the important point is that resonance energy neutrons are captured near the surface of the fuel, and the interior of the fuel is shielded from these neutrons. Stated in another way, it may be said that the flux of resonance neutrons is very much depressed in the interior of fuel elements, with a consequent reduction in the capture of these neutrons.

The production of neutrons by fission takes place throughout the fuel, consequently the fraction of these that are captured in ^{238}U resonances can be minimized by reducing the surface to volume (or mass) ratio of the fuel. For cylindrical fuel elements the surface to volume ratio is inversely proportional to the radius, so that increasing the fuel element size for a given moderator-fuel ratio has the effect of increasing the resonance escape probability. The calculation of the resonance escape probability for a heterogeneous core uses the equivalent cell concept introduced in the last section, and an effective resonance integral which includes a surface to mass term to take account of the surface capture effect. One form of this effective resonance integral for natural uranium rods is:

$$I(nat\,U) = 9.25 + 24.7\frac{S}{M}barns \qquad (40)$$

where the surface to mass ratio, *S/M,* is in cm^2/g. The resonance escape probability is given by an equation of the form:

$$p = \exp - \left(\frac{N_F V_F I}{\xi_M V_M \Sigma_{sM}} \right) \tag{41}$$

which is similar to the corresponding expression for p in a homogeneous core.

The second effect of a homogeneous system on resonance capture **is** purely geometrical. If the fuel elements are widely spaced in the moderator, some neutrons may slow down in the moderator without entering the fuel and being liable to resonance capture. This effect is not as important as the one already described.

The overall result of changing from a homogeneous to a heterogeneous system of the same composition is to increase the resonance escape probability by possibly as much as 50 per cent. It is this effect which makes possible a critical system with natural uranium and graphite.

Fast fission factor ε

A heterogeneous arrangement also has an effect on the fast fission factor. In a homogeneous system a fission neutron emitted from the point of fission travels through a medium consisting almost entirely of moderator, with fuel atoms thinly dispersed in it, and the probability of ^{238}U fission in such a medium before the neutron's energy falls below 1 MeV is negligibly small. In a heterogeneous system, however, a fission neutron travels for a short distance through pure fuel before it passes into the moderator. During its passage through the fuel the neutron may interact, the probability depending on the neutron's track length in the fuel which in turn depends on the size of the fuel element. If an interaction does occur in a natural uranium fuel element there is about a 1 in 6 chance that it is fission in ^{238}U. Consequently the probability of fast fission is slightly greater in a heterogeneous reactor than in a homogeneous reactor, the magnitude of the effect depending on the size of the fuel elements. For 2.5 cm diameter natural uranium fuel elements the value of the fast fission factor is about 1.03.

Diffusion length and slowing-down length

If neutron absorption in the cladding, coolant and structural materials is negligible, and if the volume of fuel is small compared with the volume of moderator, the diffusion length squared for the core may be determined by :

$$L_c^2 = (1 - f)L_M^2 \tag{42}$$

where L_M is the diffusion length of pure moderator. This expression may have to be modified if gas-filled coolant channels (which are for all practical purposes voids as far as neutrons are concerned) permit neutron streaming and increased leakage in the direction of the channels.

The slowing-down length squared (or age) may also have to be modified in heterogeneous assemblies. Although heavy fuel atoms are ineffective at slowing down neutrons by elastic scattering, they are very effective at slowing down high energy neutrons by inelastic scattering. The age of fuel-moderator assemblies can be calculated by methods which take into account both elastic and inelastic scattering, but these methods are beyond the scope of this,book. The results of such calculations for uranium-water mixtures, however, have shown that the age of the mixture is nearly the same as the age of pure water, presumably because inelastic scattering of high energy neutrons by the uranium is nearly as effective as elastic scattering by water.

In conclusion it must be emphasized that the approximate nature of some of the theory of heterogeneous reactors makes it necessary to obtain further data from experiments such as the exponential and ”approach to critical” experiments. In this way calculated results can be verified, and empirical quantities such as η can be determined.

Reflected reactors

Hitherto we have considered bare reactors, which implies that neutrons leaking from the core cannot be scattered back into it. A bare core is impracticable in a power reactor as there must be some structural material and shielding surrounding it, and from the point of view of neutron economy it is clearly desirable that some neutrons leaking from the core should be scattered and return to it. In this way neutron leakage is reduced, and the critical size and mass of fuel can also be reduced.

It is usual, therefore, for a reactor to be built with its core surrounded by a reflector. The primary function of the reflector is to scatter neutrons back into the core, it should therefore be a material of high scattering cross-section and low capture cross-section. Furthermore, if the reflector is an element (or contains an element) of low mass number, then fast neutrons leaking into the reflector may not only be scattered back into the core, but slowed down in the process, which is an advantage in a thermal reactor. From these points it is obvious that a good moderator is also a good reflector, and in many thermal reactors the moderator and the reflector are of the same material. A further advantage is that the thermal neutron flux in the core of a reflected reactor is more uniform than in a bare core, and consequently the flux form factors are closer to unity. This has the advantages in a power reactor that the rate of burnup of the fuel and the outlet temperature of the coolant are more nearly uniform across the core.

One-group theory of reflected reactors

The simplest theory for the analysis of reflected reactors is one-group theory. The method used for bare reactor analysis by separation of variables is limited because.of the difficulty of satisfying the boundary conditions at the core-reflector interface. (This is because the reflector is more effective at the corners of the core than at other points on its surface.) It is possible to analyse a reflected spherical reactor as this involves only one coordinate, and the results can be applied to cylindrical and rectangular cores.

Consider a spherical reactor core of radius R_c surrounded by a reflector of outer radius R_R(extrapolated radius R^+), see Figure 2(a). The core of the reactor has material properties defined by its infinite multiplication constant k_∞ , diffusion coefficient D_C, and diffusion length L_C. The diffusion coefficient and diffusion length of the reflector are D_R and L_R. Following the method used in the last chapter for the analysis of bare reactors, the one-group diffusion equation for the core is written using spherical coordinates and assuming angular symmetry as:

$$\frac{d^2\Phi_c}{dr^2} + \frac{2}{r}\frac{d\Phi_c}{dr} + B_c^2\Phi_c = 0$$

where

$$B_c^2 = \frac{k_\infty - 1}{L_c^2} \tag{42}$$

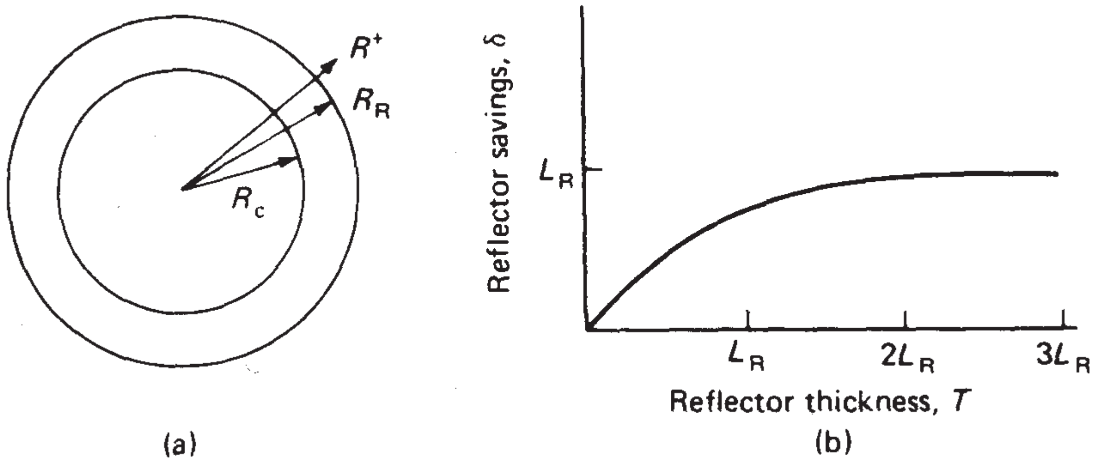

Fig. 2 Reflected spherical reactor and reflector savings

The one-group equation for the reflector is:

$$\frac{d^2\Phi_R}{dr^2}+\frac{2}{r}\frac{d\Phi_R}{dr}+\kappa_R^2\Phi_R=0$$

$$\textbf{\textit{where}} \tag{43}$$

$$\kappa_R=\frac{1}{L_R}$$

The solution of equation (43) is:

$$\Phi_c=\frac{A\sin(B_c r)}{r}+\frac{C\cos(B_c r)}{r} \tag{44}$$

and the constant $C = 0$, otherwise ϕ_c, would become infinite as $r \to \infty$, therefore:

$$\Phi_c = \frac{A\,sin(b_c r)}{r};\ C = 0 \ \text{ för } \lim_{r \to 0} \frac{cos(B_c r)}{r} = \infty \tag{45}$$

The solution of equation (43) is:

$$\Phi_R = \frac{A'\,sinh(\kappa_R r)}{r} + \frac{C'\,cos(\kappa_R r)}{r} \tag{46}$$

To satisfy the boundary condition at the outer surface of the reflector, namely $\phi_R(R^+) = 0$, we get:

$$C' = -A' \tanh \kappa_R R^+ \tag{47}$$

The conditions of continuity of neutron flux and current at the interface between the core and the reflector yield the equations:

$$A\,sin(B_c R_c) = A'[sinh(\kappa_R R_c) - tanh(\kappa_R R^+) \times cosh(\kappa_R R_c)]$$

and

$$\begin{aligned} &D_c A[B_c R_c\, cos(B_c R_c) - sin(B_c R_c)] = \\ &= D_R A'\{\kappa_R R_c\, cosh(\kappa_R R_c) - sinh(\kappa_R R_c) \\ &- tanh(\kappa_R R^+)[\kappa_R R_c\, sinh(\kappa_R R_c) - cosh(\kappa_R R_c)]\} \end{aligned} \tag{48}$$

Dividing equation (47) by (48) we get:

$$D_c[B_c R_c\, cot(B_c R_c) - 1] = -D_\rho\{\kappa_R R_c\, coth[\kappa_R(R^+ - R_c) + 1]\}$$

or, if the extrapolation distance is neglected (implying that $R^+ = R_R$):

$$D_c[B_cR_c\cot(B_cR_c)-1]=-D_R[\kappa_RR_c\coth(\kappa_RT)+1] \tag{49}$$

Equation (49) gives the relationship between the buckling, core size and reflector thickness for a spherical reactor, and may be compared with the corresponding equation for the bare spherical core which is $B=\pi/R'$, where R' is the extrapolated radius of the bare core. Equation (49) is an eigenvalue equation, and it is the funda- mental solution of this equation, that is the one giving the lowest value of B_C, R_C that determines the critical condition. The equation may be used to determine the core size of a reflected reactor whose composition $(B_C, D_C, \kappa_R, D_R)$ and reflector thickness (T) are known, in which case the equation is solved for R_C. Alternatively if the unknown quantity is the composition of the core and the core size and reflector thickness are known, equation (49) is solved for B_C, and the composition determined using equation $B^2=\dfrac{k_\infty-1}{L_c^2}$.

While the one-group method is not particularly accurate in some respects, it does predict quite accurately the reduction in the core size that results from using a reflector. The term reflector savings is used to denote this reduction in core size. For a spherical core

$$\begin{aligned}\textit{Reflector savings} &= \textit{Radius of bare core}\\ &\quad - \textit{Radius of reflected core of the same composition.}\end{aligned}$$

Neglecting the extrapolation distance, the radius of a bare spherical core of buckling B_C, is equal to π/B_c.

The reflrector savings is:

$$\delta=\frac{\pi}{B_c}-R_c$$

therefore:

$$B_cR_c=\pi-B_c\delta$$

Substituting this expression for B_C, R_C into equation (49), and making the simplifying assumption that the moderator and the reflector are the same material, which is quite usual in practice and means that $D_C = D_R$, we get:

$$B_c \cot(\pi - B_c\delta) = -\kappa_R \coth \kappa_R T$$

from which

$$B_c \cot(B_c\delta) = \kappa_R \coth \kappa_R T$$

Bearing in mind that B_C, is small for a large core:

$$\cot(B_c\delta) \approx \frac{1}{B_c\delta}$$

and the preceding equation becomes:

$$\delta \approx L_R \tanh \frac{T}{L_R}$$

If $T < L_R$, then:

$$\tanh \frac{T}{L_R} \approx \frac{T}{L_R} \; and \; \delta \approx T$$

In other words if the reflector thickness is small compared with the diffusion length of the reflector, then the reflector savings is approximately equal to the reflenor thickness.

On the other hand, if $T > L_R$:

$$\tanh \frac{T}{L_R} \to 1 \; and \; \delta \to L_R$$

This implies that as the reflector thickness increases, the reflector savings reaches a limiting value equal to the diffusion length of the reflector. In fact this limiting value is nearly reached when the reflector thickness is twice the diffusion length since tanh 2 = 0.964, so there is no point in making the reflector thickness greater than about twice the diffusion length of the reflector material. Figure 2(b) shows the variation of reflector savings with reflector thickness.

This conclusion regarding the reflector savings for a spherical reactor can be applied to other reactor shapes provided the size of the reactor is large enough to make $B_C\delta$ small. Furthermore the result is quite accurate and agrees well with more rigorous calculations. The usefulness of the reflector savings concept is that it can be used with bare reactor calculations to determine the size of a reflected reactor. The bare reactor calculations may be performed using modified one- group theory (which will give a more accurate result than one-group theory), and the size of the reflected reactor may be obtained by subtracting from the bare core size the reflector savings corresponding to the chosen reflector thickness.

It can be seen by comparing the flux equation for a reflected spherical core, (45), with the corresponding equation for a bare spherical core in Table III (the lecture ***The theory of nuclear reactors – homogeneous thermal reactors***) that the flux shape is the same in both provided their values of B^2 are the same. This applies also to other core shapes. The size of the reflected core is less than the bare core, and the extrapolation distance for the reflected core is effectively increased by an amount equal to the reflector savings.

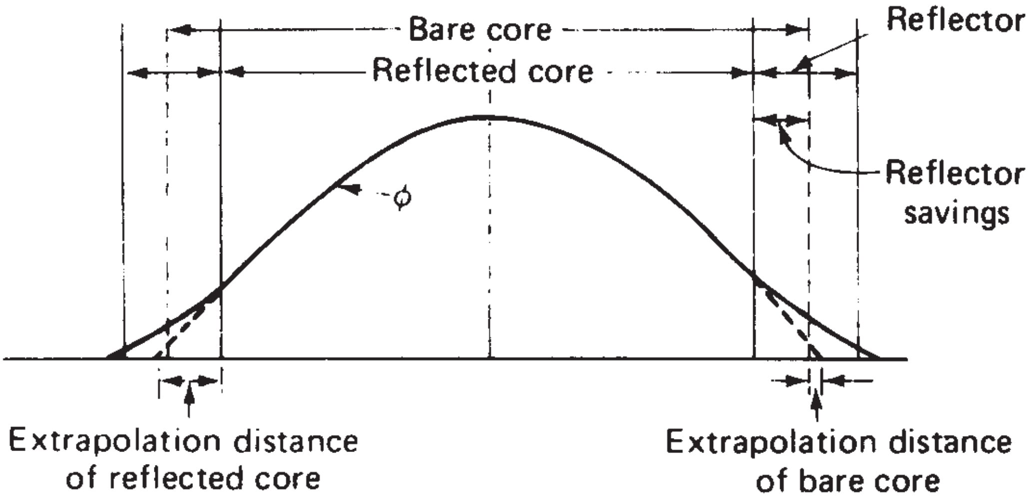

Fig. 3 Comparison between one-group fluxes in bare and reflected cores of equal buckling.

The comparison between the fluxes in a bare and a reflected core is shown in Figure 3, in which the solid line shows the flux variation in the core and the reflector, and the dotted line shows the variation of the flux near the edge of the equivalent bare core. It is evident that the flux in the reflected core is more nearly uniform, and that as a result the form factor is more nearly equal to one than in the equivalent bare core.

Reactor kinetics

Introduction

Hitherto we have been concerned with reactors which are operating at steady state, in which the effective multiplication factor is exactly one and the neutron flux, power and temperatures are constant. These are the conditions under which power reactors operate for long periods, and for which they are designed.

It is necessary, however, to consider several other aspects of reactor operation. In the first place we will study the way in which the neutron flux varies when a reactor is non-critical. This is the state that exists when a reactor is starting up or undergoing a power increase (in which case it is supercritical), or when a reactor is shutting down or decreasing power (in which case it is subcritical). Secondly, we will study the changes which take place during prolonged operation of a reactor which have an effect on its criticality. These changes result from the burnup of fissile fuel, the production of new fissile fuel from fertile isotopes, and the buildup in a reactor of fission products with high capture cross- sections. Thirdly, we will discuss qualitatively the effects of changes of temperature within a reactor as these changes can affect the reproduction constant and introduce a feedback effect during power changes.

At all stages during the operation of a reactor a control system is essential, not only to effect startup, shutdown and power changes, but also to compensate for the changes in the reactor itself which occur during operation.

Reactor kinetics

The study of the response of a reactor to a change in the multiplication factor from a value of one (at which the reactor is operating at steady state) to either slightly more or less than 1 is known as reactor kinetics. It is convenient at this point to define some terms of importance in reactor kinetics.

The excess reactivity δk id defined as:

$$\delta k = k_{eff} - 1 \tag{1}$$

The reactivity ρ is defined in a slightly different way as:

$$\rho = \frac{k_{eff} - 1}{k_{eff}} \tag{2}$$

or for an infinite reactor:

$$\rho = \frac{k_{\inf} - 1}{k_{\inf}} \tag{3}$$

Clearly at all conditions under which reactors operate, $\rho \approx \delta k$.

Another important parameter in the study of reactor kinetics is the prompt neutron lifetime, l_p. In an infinite reactor the prompt neutron lifetime is the average time between the birth of prompt neutrons by fission and their final absorption in the reactor. In a thermal reactor this time is the sum of the average neutron slowing-down time (during which neutrons are slowing down from fission to thermal energy), and the average diffusion time (during which neutrons are diffusing at thermal energy up to their point of absorption). In all thermal reactors the diffusion time is much greater than the slowing-down time, typical values being about 10^{-3} seconds and 10^{-5} seconds respectively, so that the prompt neutron lifetime is very nearly equal to the diffusion time. The average diffusion time t_d for thermal neutrons in a reactor is:

$$\begin{aligned} t_d &= \frac{Absorption\ mean\ free\ path\ of\ thermal\ neutrons\ in\ the\ reactor}{Average\ speed\ of\ thermal\ neutrons} \\ &= \frac{\lambda_a}{v_{av}} \ or \ \frac{1}{\overline{\Sigma}_{ac} v_{av}} \end{aligned} \tag{4}$$

where $\overline{\Sigma}_{ac}$ is the average macroscopic absorption cross-section of the fuel- moderator mixture in the core of the reactor, and v_{av} is the average speed of thermal neutrons.

The diffusion time can be expressed in terms of the absorption cross-section of the moderator $\overline{\Sigma}_{aM}$ (se lecture **Multiplication factor and chain reaction**):

$$\overline{\Sigma}_{aM} = (1 - f)\overline{\Sigma}_{ac}$$

From this it follows that:

$$t_d = \frac{(1-f)}{\overline{\Sigma}_{aM} v_{av}}$$

For a *1/v* absorbing medium:

$$\overline{\Sigma}_a v_{av} = \Sigma_{a0} v_{MP}$$

Using this result with the preceding equation, it follows that:

$$t_d = \frac{(1-f)}{\Sigma_{a0} v_{MP}} \tag{5}$$

where Σ_{a0M} is the tabulated (2200 m/s) absorption cross-section of the moderator, and $v_{MP} = 2200$ m/s. For example, the diffusion time (and also the prompt neutron lifetime) for a graphite moderated reactor in which the thermal utilization factor is 0.9 is:

$$t_d = l_p = \frac{0.1}{0.000385 \times 2.2 \times 10^5} = 1.18 \times 10^{-3}\, seconds$$

This value, namely about 0.001 seconds, is typical of graphite-moderated reactors. Water-moderated, enriched uranium reactors have typical prompt neutron lifetimes of about 0.0001 seconds, and fast reactors, in which neutrons do not become thermalized, have prompt neutron lifetimes of about 10^{-7} seconds.

Not all neutrons produced by fission are emitted promptly at the instant of fission - see lecture about **Fission**. A very few neutrons, less than 1 per cent, are emitted during the radioactive decay of certain fission products, and these are called the delayed neutrons. Their properties will be described presently, however to emphasize their importance in reactor kinetics we will consider first the response of a thermal reactor to an instantaneous or step change of reactivity on the incorrect supposition that all fission neutrons are prompt. The problem may be simplified without any serious loss of accuracy by considering an infinite reactor and no neutron leakage.

The one-group diffusion equation for this problem may be written as:

$$
\begin{aligned}
\frac{dn}{dt} &= (k_\infty - 1)\overline{\Sigma}_{ac}\phi_{th} \\
&= (k_\infty - 1)\overline{\Sigma}_{ac} n v_{av} \\
&= \frac{(k_\infty - 1)}{l_p} n
\end{aligned}
\tag{6}
$$

The solution of this equation for a step change of reactivity at time t =0 is:

$$
n = n_0 e^{\left[\frac{(k_\infty - 1)t}{l_p}\right]} \tag{7}
$$

where *n,* is the steady-state neutron density before the reactivity change. Equation (7) shows that the neutron density, and hence the reactor power, vary exponentially, and the rate of this change (which is an increase or decrease depending on whether the step change of reactivity is positive or negative) is characterized by the period *T,* which is the time for the power to change by a factor *e.* In terms of the period, equation (7) may be written as:

$$
n = n_0 e^{\frac{t}{T}} \tag{8}
$$

The period is given by:

$$
T = \frac{l_p}{k_\infty - 1} \tag{9}
$$

As an illustration of this result, consider an infinite thermal reactor in which the prompt neutron lifetime is 0.001 seconds, and k_∞ is changed from 1 to 1.001 to give an excess reactivity of 0.001. From equation (9) the resulting reactor period is 1 second, and in 10 seconds the reactor power increases by a factor of e^{10} or about 22 000. This is a very rapid rate of power increase which would be difficult to control. In a fast reactor a similar change in k_∞ would lead to a period of about 10^{-4} seconds, and control would be impossible. In the event of a negative step change of reactivity (for instance at shutdown), the reactor power would decrease exponentially at a rapid rate.

These results, although they have been derived for an infinite reactor, are also valid for a finite reactor, and k_∞ in the preceding equations may be replaced by k_{eff}. The effective prompt neutron lifetime in a finite reactor is however slightly less than in an infinite reactor due to neutron leakage. The reason for this is that neutrons which leak from the core have shorter than average lives. The conclusion from the preceding discussion is that, in the absence of delayed neutrons, reactor power levels would change very rapidly as a result of reactivity changes, and control during startup would be very difficult and, in the case of fast reactors, impossible.

Delayed neutrons

The delayed neutrons are produced as a result of the decay of certain radioactive fission products, mainly isotopes of bromine and iodine. Figure 1 shows the decay scheme of one such isotope ^{87}Br. The average time by which the emission of each group of neutrons **is** delayed is equal to the mean life of the corresponding delayed neutron precursor, which is about 80 seconds in the case of ^{87}Br. These precursors can be conveniently divided into six groups according to their half-lives, and the delayed neutron data for thermal fission in ^{235}U is shown in Table I.

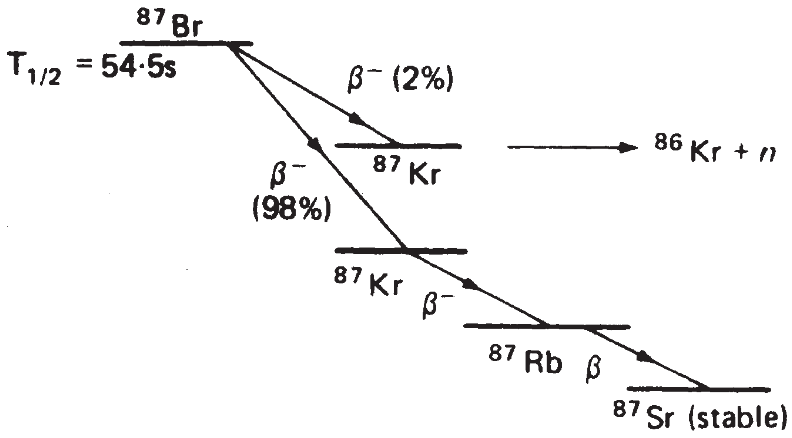

Figure 1. Bromine-87 decay as a source of delayed neutrons.

The total fraction of neutrons which are delayed β is:

$$\beta = \sum_{i=1}^{6} \beta_i \tag{10}$$

Table I.. Delayed neutron data for thermal fission in ^{235}U.

Group	**Half-life $T_{1/2}$(s)**	**Mean life, τ (s)**	**Decay constant,λ_i (s^{-1})**	**Fraction of total fission neutrons, β_i**
1	55.7	80.2	.0124	.000215
2	22.7	32.7	.0305	.001424
3	6.2	8.9	.111	.001274
4	2.3	3.3	.301	.002568
5	.61	.88	1.14	.000748
6	.23	.33	3.01	.000273

and its value for. thermal fission in ^{235}U is 0.0065.

The average mean life τ_μ of all the delayed neutron precursors is given by the equation:

$$\bar{\tau}_m = \frac{1}{\beta}\sum_{i=1}^{6}\beta_i\tau_{mi} \tag{11}$$

The values of $\bar{\tau}_m \, and \, \beta\bar{\tau}_m$ for ^{235}U are about 12.5 seconds and 0.08 seconds respectively. The mean lifetime l of all neutrons, both prompt and delayed is:

$$\begin{aligned} l &= (1-\beta)l_p + \beta(\bar{\tau}_m + l_p) \\ &= l_p + \beta\bar{\tau}_m \end{aligned} \tag{12}$$

Since $\beta\bar{\tau}_m >> l_p, l \approx \beta\bar{\tau}_m$ which is 0.08 seconds. Returning to the earlier example and assuming that equation (7) can be used with a mean life- time calculated by equation (12), a 0.1 per cent change of k_∞ will now result in a period of 80 seconds. This implies a very much slower rate of power rise which can be easily controlled. Unfortunately, this method does not correctly predict the response of a reactor to a step change of reactivity, and the period calculated by this method is only correct for reactivities less than about 0.0005.

Reactor kinetics with delayed neutrons

In order to correctly predict the response of a reactor to a change of reactivity it is necessary to consider the prompt neutrons, and also the production and decay of the delayed neutron precursors which produce delayed neutrons. Once again we will consider an infinite thermal reactor, using one-group theory and diffusion equation (equation 40 in **Diffusion lecture**) in a modified form. The equation for the rate of change of neutron density is:

$$\begin{aligned}\begin{pmatrix}\textit{The rate of change}\\ \textit{of neutron density}\end{pmatrix} &= \begin{pmatrix}\textit{The rate of production}\\ \textit{of prompt neutrons}\end{pmatrix}\\ &+\begin{pmatrix}\textit{The rate of decay of all}\\ \textit{delayed neutron precursors}\end{pmatrix}\\ &-\begin{pmatrix}\textit{The rate of}\\ \textit{absorption of neutrons}\end{pmatrix}\end{aligned} \tag{13}$$

$$\frac{dn}{dt} = k_\infty(1-\beta)\overline{\Sigma}_a\phi_{th} + \sum_{i=1}^{6}\lambda_i C_i - \overline{\Sigma}_a\phi_{th}$$

On the right-hand side of this equation the first term takes account of the fact that a fraction (1 – β) of all fission neutrons are prompt. The second term is in fact six terms, one for each group of delayed neutron precursors, the symbol C_i, being the concentration of the ith group of delayed neutron precursors. $\lambda_i C_i$ is the rate of decay of the ith precursor and the rate of production of delayed neutrons from this particular source. Equation (13) can be rewritten as:

$$\frac{dn}{dt} = \frac{k_\infty(\rho-\beta)}{l_p}n + \sum_{i=1}^{6}\lambda_i C_i \tag{14}$$

There are six equations for the concentrations of the six groups of delayed neutron precursors, each one of the form:

$$\begin{pmatrix} \text{The rate of change of the} \\ \text{concentration of the } i-th \text{ group} \\ \text{of delayed neutron precursors} \end{pmatrix} = \begin{pmatrix} \text{The rate of formation of} \\ \text{the } i-th \text{ group of precursors} \end{pmatrix}$$

$$- \begin{pmatrix} \text{The rate of decay of the} \\ i-th \text{ group of precursors} \end{pmatrix}$$

$$\begin{aligned} \frac{dC_i}{dt} &= k_\infty \beta_i \overline{\Sigma}_a n v_{av} - \lambda_i C_i \\ &= \frac{k_\infty \beta_i n}{l_p} - \lambda_i C_i \quad (i = 1 \text{ to } 6) \end{aligned} \tag{15}$$

The response of a reactor to a step change of reactivity is determined by solving the seven simultaneous linear differential equations (14) and (15). The solution is laborious and the result can most easily be obtained by solving the equations on an analogue or digital computer.

The essential features of the solution can be seen by simplifying the problem and replacing the six groups of delayed neutron precursors by a single group. The value of β for the single group of delayed neutrons is given by equation (10), and the value of the decay constant λ of the single group of delayed neutron precursors is given by:

$$\lambda = \frac{1}{\overline{\tau}_m}$$

where $\overline{\tau}_m$ is given by equation (11). The value of λ for a ^{235}U fueled reactor is about 0.08 second^{-1}. The seven equations (14) and (15) can now be reduced to two equations:

$$\frac{dn}{dt} = \frac{k_\infty(\rho - \beta)}{l_p} n + \lambda C \tag{16}$$

and:

$$\frac{dC}{dt} = \frac{k_\infty \beta}{l_p} - \lambda C \tag{17}$$

where C is now the concentration of all the delayed neutron precursors. By inspecting equation (16) it is possible to get a qualitative idea of the response of a reactor to a positive step change of reactivity. If ρ is positive and less than β, the first term on the right-hand side of equation (16) is negative, and the increase of the neutron density is governed by the term λC, the rate at which the delayed neutron pre- cursors decay, which as we have seen is quite slow. If ρ = β, then dn/dt = λC, the reactor is critical on prompt neutrons alone and the rate of increase of the neutron density is equal to the rate of production of delayed neutrons. In this condition the reactor is referred to as being prompt critical. If ρ is greater than β, then both terms on the right-hand side of equation (16) are positive and the first term produces an exponential increase with a short period because of the small value of l_p. This is a similar situation to that which existed in the case in which delayed neutrons were neglected. The conclusion to be drawn from this argument is that provided ρ is less than β, the rate of power increase following a positive step change of reactivity is fairly slow and can be controlled. On the other hand if ρ is greater than β the rate of power increase is rapid and difficult (if not impossible) to control. The criterion for safe operation during startup and power increase is that the reactor must not be allowed to become prompt critical.

Equations (16) and (17) may be solved by standard methods. If solutions of the form:

are assumed, and these are substituted into equations (16) and (17), and the approximation $k_\infty = 1$ is made, the following quadratic equation for w is obtained:

$$n(t) = \sum A e^{\omega t} \quad and \quad C(t) = \sum B e^{\omega t}$$

$$\omega^2 l_p + \omega(\beta - \rho + l_p \lambda) - \lambda\rho = 0$$

If $(\beta - \rho + l_p\lambda)^2$ is much greater than $|2 l_p \lambda \rho|$, and if $l_p\lambda$ is much less than $(\beta - \rho)$, the two values of ω satisfying the above equation are approximately:

$$\omega_1 \approx \frac{\lambda\rho}{(\beta-\rho)} \; and \; \omega_2 \approx \frac{-(\beta-\rho)}{l_p}$$

The validity of these approximations depends on the value of ρ being less than about β/2 , as can be verified by substituting the following values into the above expressions:

$\beta = 0.0065,\ \rho = 0.003, \lambda = 0.08 s^{-1}, l_p = 0.001 s$

The complete solution for *n* has two terms:

$$n = A_1 e^{\omega_1 t} + A_2 e^{\omega_2 t}$$

The values of A_1 and A_2 can be found to be given approximately by:

$$A_1 \approx \frac{\beta}{\beta - \rho} n_0 \ and\ A_2 \approx \frac{-\rho}{\beta - \rho} n_0$$

where *n* is the steady-state neutron density prior to the step change of reactivity. The complete solution for *n* is:

$$n = n_0 \left\{ \frac{\beta}{\beta - \rho} \exp\left(\frac{\lambda\rho}{\beta - \rho} t \right) - \frac{\rho}{\beta - \rho} \exp\left(-\frac{\beta - \rho}{l_p} t \right) \right\} \tag{18}$$

This equation is valid, as already noted, if ρ is less than about β*/2.* If ρ is positive the solution consists of a positive term with a positive exponent whose period is $\frac{(\beta - \rho)}{\lambda\rho}$, and a negative term with a negative exponent which decays rapidly as its period is $\frac{l_p}{(\beta - \rho)}$. The complete solution for a ^{235}U fueled thermal reactor with a prompt neutron lifetime of 0.001 second following a step change of reactivity of +0.002 is shown in Figure 2.

From Fig. 2 it can be seen that after an initial rapid rise which causes the neutron density and reactor power to increase by a factor $\frac{\beta}{\beta - \rho}$ in about 1 second, the rate

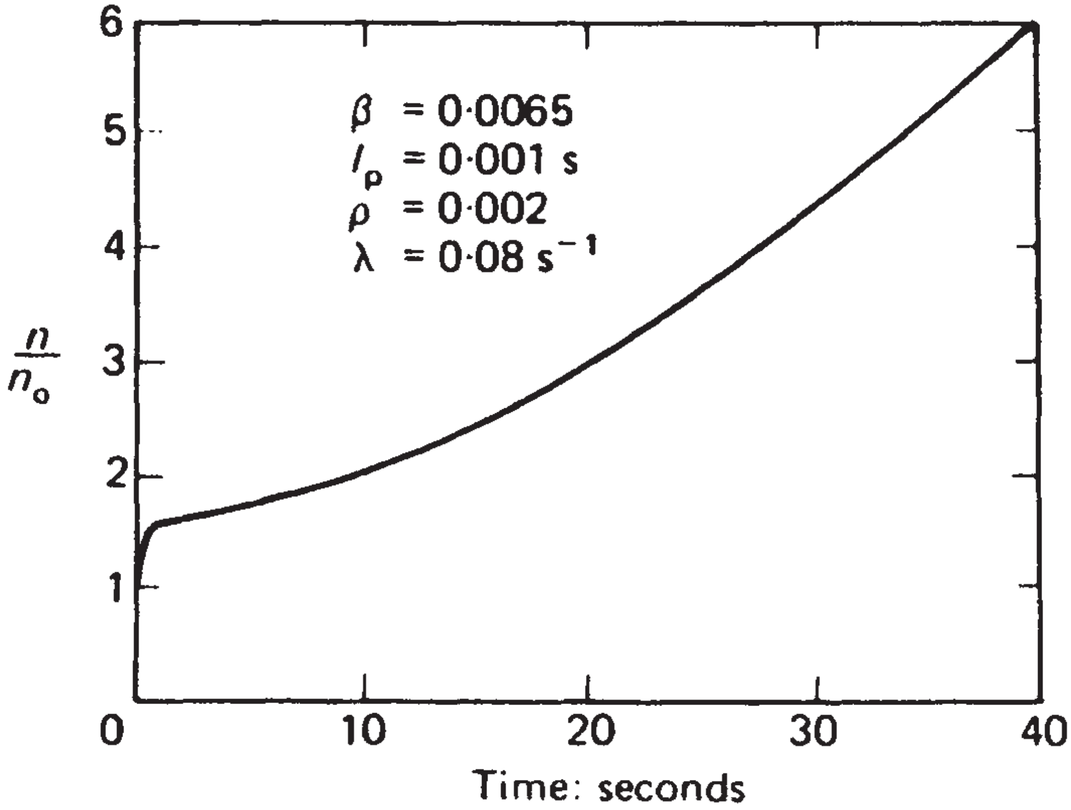

Figure 2. The response of a reactor to a step change of reactivity.

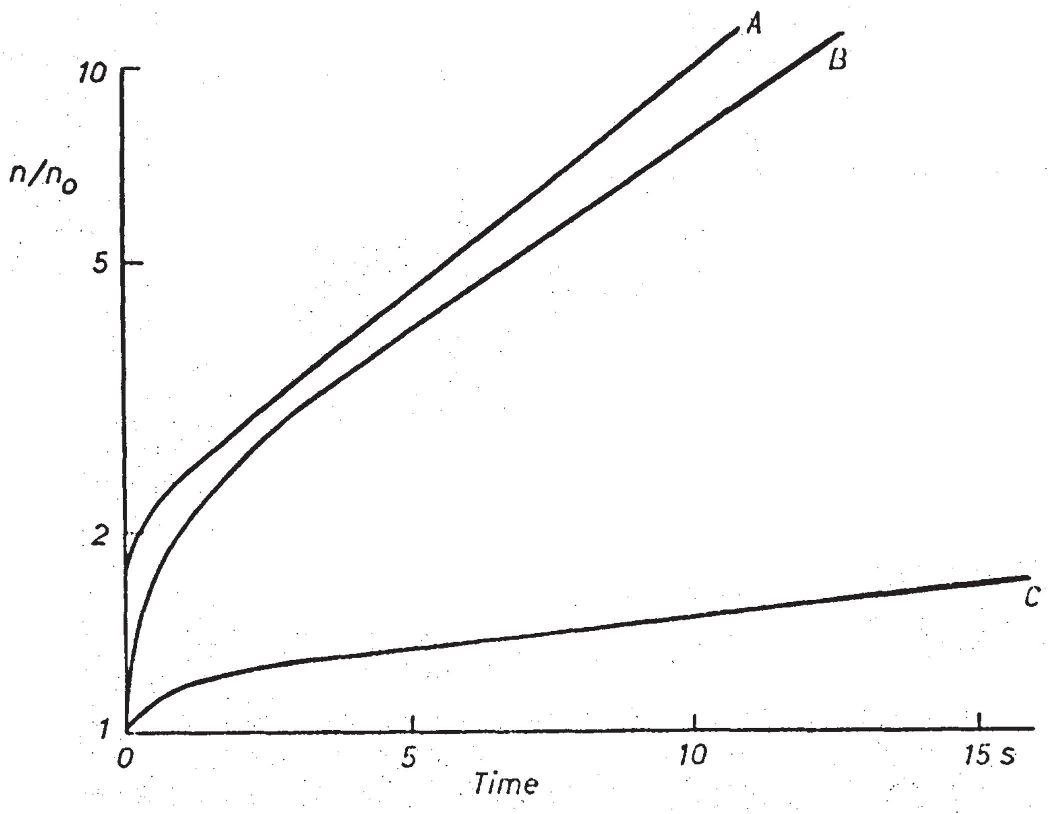

Figure 3. Relative neutron density as a function of time far various step reactivity inputs and neutron life-times. The fuel is ^{235}U. A: ρ=0.3‰, τ=60μs;, B: ρ=0.3‰, τ=1ms; C: ρ=0.1‰, τ=1ms

of increase is slowed down and the neutron density increases exponentially with a stable period.

$$T = \frac{\beta - \rho}{\lambda \rho} \tag{19}$$

For example, a positive step change of reactivity of 0.002 causes the power to increase promptly by a factor 1 44, and thereafter to increase exponentially with a stable period of about 28.1 seconds, which makes the reactor easily controllable. Smaller reactivities result in a smaller prompt increase and a longer stable period.

While these figures are not exact due to the inherent inaccuracy of the “one group of delayed neutrons” approximation, they do give a qualitatively correct idea of the way in which a reactor responds to an increase of reactivity, and for small reactivities (ρ less than about 0.1β) the results are quite accurate. Fig. 3 presents the changes of the neutron density as a function of time for different reactivity changes and different prompt neutron life-times (i.e. different reactor types).

The response of a reactor to a negative step change of reactivity, as would occur at shutdown, can also be deduced from equation (18). In this case ρ is negative and both parts of the solution for n have positive coefficients and negative exponents. The term

$$\frac{\rho}{\beta - \rho} \exp\left(-\frac{\beta - \rho}{l_p} t \right)$$

has a very short period and therefore contributes a rapid drop in the neutron density. The term

$$\frac{\beta}{\beta - \rho} \exp\left(-\frac{\lambda \rho}{\beta - \rho} t \right)$$

has a longer period, and contributes a more slowly decaying component to the neutron density. This slowly decaying density is due to the fact that after shutdown delayed neutrons continue to be produced by the decay of their precursors, which were in the reactor before the shut- down. For large negative reactivities, possibly resulting from the insertion of all control rods during a rapid shutdown,

$\beta - \rho \approx \rho$, and after the prompt drop the neutron density decays with a period of about $1/\lambda$, the average mean life of the delayed neutron precursors. This is shown in Fig. 4 for a negative reactivity of 0.05.

The "one group of delayed neutron"s approximation does not accurately predict the final rate of decrease of the neutron density after shutdown. According tn the approximate solution the period is $1/\lambda$, which is about 12 seconds for a ^{235}U fuelled reactor. Ia fact the neutron density finally decays with a period equal to the mean life of the longest lived delayed neutron precursor, which is about 80 seconds. This means that it is impossible to shut down a reactor completely in a matter of seconds, and many minutes may elapse before the power of a reactor operating at several megawatts drops to a few watts. This effect is even more pronounced in reactors containing large amounts of deuterium (in heavy water) or beryllium. Gamma radiation from radioactive fission products induces (γ,n) reactions in these elements and produces neutrons long after shutdown. Consequently, the time for the reactor power to fall to a very low level is prolonged. A similar effect occurs as a result of the heat released by the decay of radioactive fission products. Figure 5 shows the solution of point neutron kinetic equation for the negative reactivity input - 0.5, -5 and -10 % - together with decay heat evolution curve.

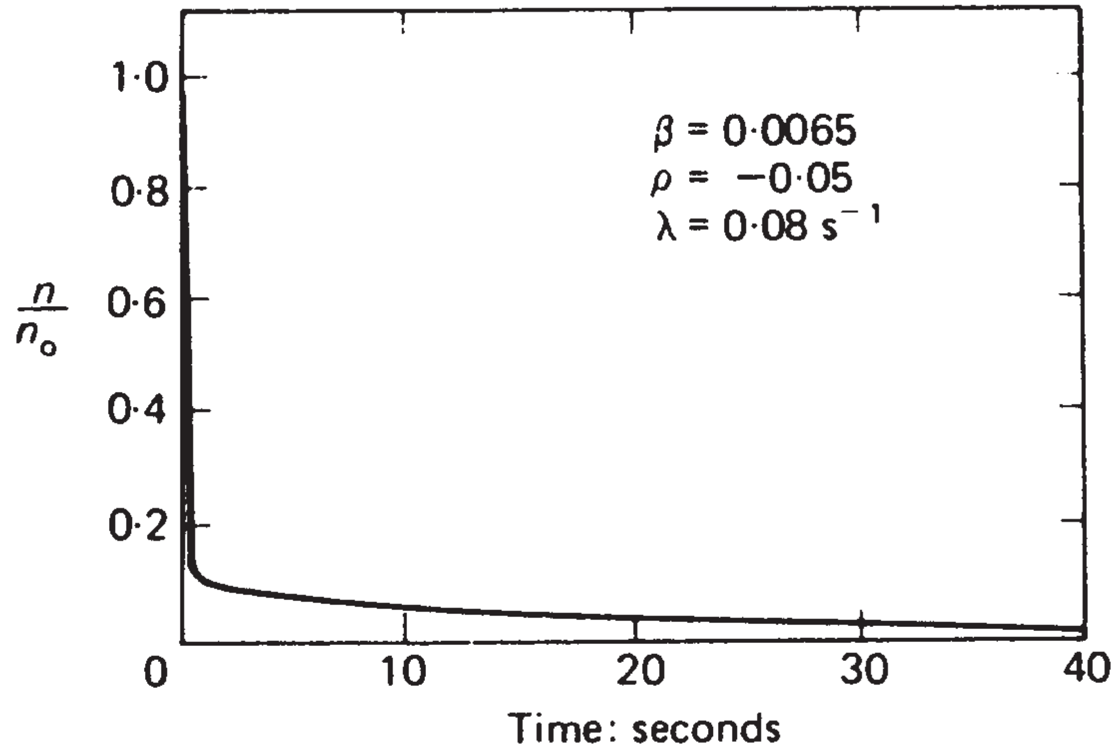

Figure 4. The response of a reactor to a negative step change of reactivity

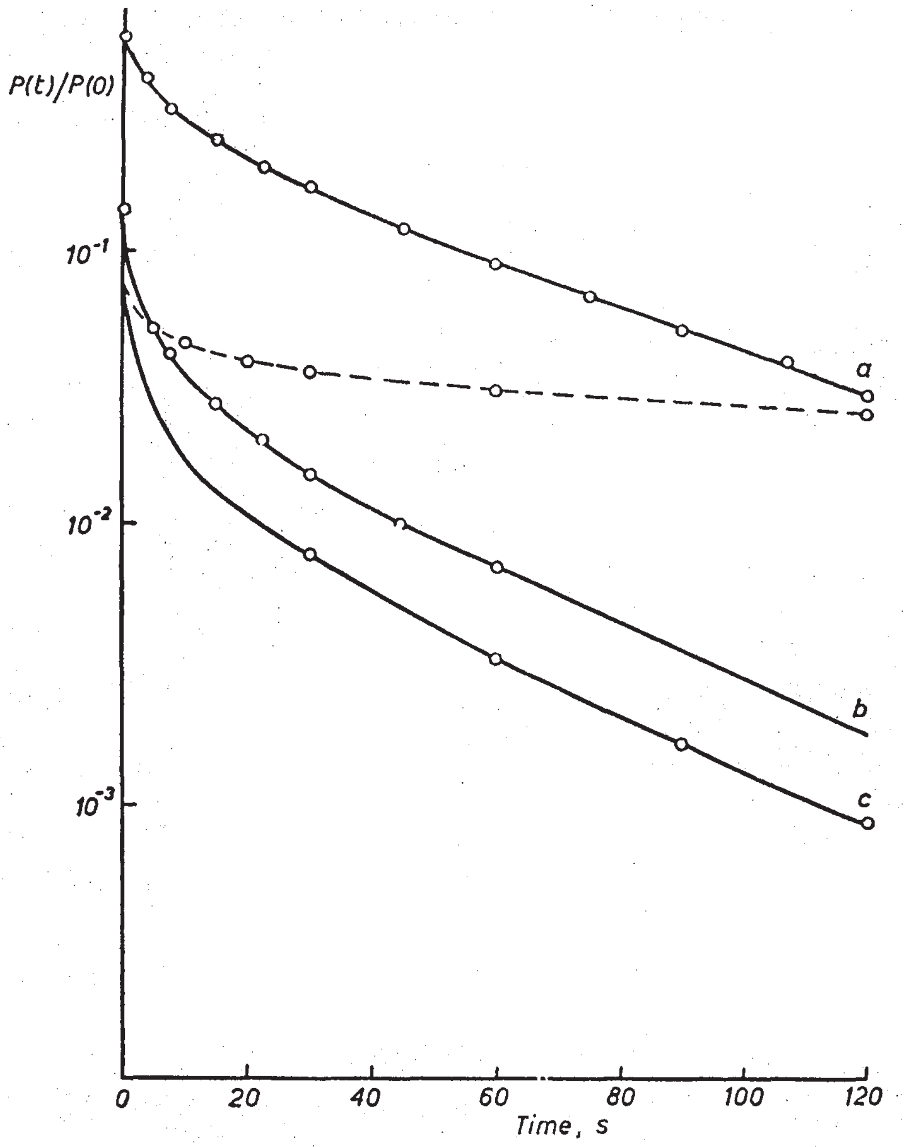

Figure 5. Relative neutron power due to a negative step reactivity input. The effects of any neutron sources are neglected. Curve (a): ρ=-0.5%; curve (b): ρ=-5.%; curve (c):ρ=–10%. Stretched line ----- decay heat (fission product power).

Inhour equation

Equations (15) can be solved using Laplace transform which gives us the relation,

$$(\omega+\lambda_i)C_i = \beta_i k_\infty \overline{\Sigma}_{ac}\phi_{th} \tag{20}$$

then we can eliminate C_i from Laplace transformed equation (14) :

$$\omega n = \frac{k_\infty(\rho-\beta)}{l_p} n + k_\infty \Sigma_a \sum_{i=1}^{6} \frac{\beta_i\lambda_i}{\omega+\lambda_i}\phi_{th}$$

which gives us

$$\left(\omega - \frac{k_\infty(\rho-\beta)}{l_p}\right) n = k_\infty \overline{\Sigma}_{ac} n v_{av} \sum_{i=1}^{6} \frac{\beta_i\lambda_i}{\omega+\lambda_i} \tag{21}$$

After canceling *n* from both sides of equation (21) and after some transformation we are getting for the finite reactor

$$\frac{\omega l_p}{k} = -\omega \sum_{i=1}^{6} \frac{\beta_i}{\omega+\lambda_i} \tag{22}$$

leading to a relation

$$\rho = \frac{\omega l_p}{k} + \omega \sum_{i=1}^{6} \frac{\beta_i}{\omega+\lambda_i} \tag{23}$$

Without a detailed analysis we can concentrate only on so called stable frequency (or ground tone solution) of the reactor - ω_0, giving a reactor period $T = \frac{1}{\omega_0}$. If we substitute ω=1/T in equation (23),

$$\rho = \frac{l_p}{kT} + \sum_{i=1}^{6} \frac{\beta_i}{1+\lambda_i T}$$

or (24)

$$\rho = \frac{l_p}{kT} + \sum_{i=1}^{6} \frac{\beta_i \tau_i}{\tau_i + T}, \quad \tau_i = \frac{1}{\lambda_i}$$

a relation generally called the ***inhour equation*** (This nomenclature is derived from the observation that in the early days of reactor development, values ω_i were quoted *inverse hours*). The inhour is the unit of reactivity ρ for which the stable period T is equal 1 h.

Let's analyse some special cases of the *inhour equation*.

1) $\rho > \beta$; **T<<τ_i**

$$\therefore \rho \cong \frac{l_p}{T} + \sum \beta_i = \frac{l_p}{T} + \beta$$

$$\therefore T = \frac{l_p}{\rho - \beta} \quad \textit{prompt critical reactor}$$

2) $\rho < \beta$; **T>>τ_i**

$$\rho = \frac{l_p + \sum \beta_i \tau_i}{T}$$

$$T = \frac{0.083}{\rho}$$

It a normal reactor operation.

T = 1hour corresponds to $\rho = 0.083/3600 \sim 2.3 \cdot 10^{-5}$ = 1 inhour

UNITS AND VALUES ρ

1.

$$\rho = \frac{0.083}{3600\ T_{hours}} = \frac{2.3 \cdot 10^{-5}}{T_{hours}}$$

$$\therefore \rho = 2.3 \cdot 10^{-5} \quad \text{gives} \quad T = 1\ \text{hour}$$

$$\rho = 2.3 \cdot 10^{-5} \quad = \quad 1\ \text{inhour}$$

2.

$$\rho = \beta = 0.0064 = 1\ \text{dollar}$$

$$\therefore 1 \quad \text{cent} \quad = 0.000064 = 6.4 \cdot 10^{-5} =$$

$$= 2.78\ \text{inhour} \quad (T = \frac{1}{2.78}\ h)$$

3.

$$\rho = 10^{-5} = pcm \quad (\text{pro centimille})$$

$$(T = 2.3\ \text{hour})$$

REMEMBER !!

Because the life-time of the prompt neutrons $10^{-8} < l_p < 10^{-3}$ s in different existing reactors it implies that k-1 must be kept very small if reactor control is to possible.

Formula $T = \dfrac{l_p}{k-1}$ **represents an asymptotic case.**

The delayed neutron fraction 0.0064 is a BALANCE POINT!

1) If k>1.0064 $T = \dfrac{l_p}{k-1}$ **- CATASTROPHE!**

2) If k<.0064 so T=0.083/(k-1) - normal operation!

REACTOR DYNAMICS

Reactor dynamics - reactor performance due to the reactivity changes influenced by:

- **Temperature variation of the core**
- **Poisoning of the core**
- **Burn-up of the fissile material**

Temperature effects on reactivity

Changes in the temperature of a reactor which result from a change of power can cause changes in reactivity which in turn affect the power. Thus a feedback process is established whose characteristics have an important bearing on the safety of the reactor. For instance, if an increase in power followed by an increase in the temperature of parts of a reactor causes an increase in reactivity, this will lead to a further increase in power and an unstable situation will exist which, if it is not controlled, could lead to an accident. On the other hand if an increase in power and temperature leads to a decrease in reactivity, the original power rise will be retarded or reversed and a stable situation will exist in which the reactor tends to control itself. This is obviously desirable from the point of view of safety (see Fig. 1).

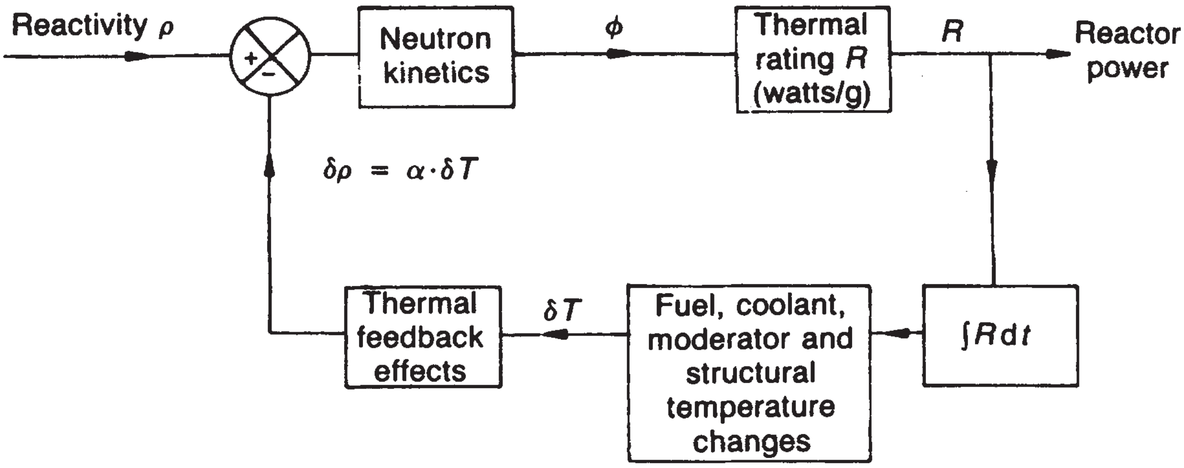

Figure 1. Thermal feedback in nuclear reactors

The term temperature coefficient of reactivity is used to express the effects of temperature changes on reactivity, and the temperature coefficient, α, is defined as the change of reactivity per degree change in the temperature of some component of a reactor:

$$\alpha = \frac{d\rho}{dT} \tag{1}$$

A positive temperature coefficient implies an increase in reactivity as a result of an increase in temperature, and thus an unstable effect in a reactor. On the other hand, a negative temperature coefficient, which implies a decrease of reactivity as a result of an increase of temperature, provides a stabilizing effect.

When a reactor undergoes a power increase, the resulting temperature changes in different components of the reactor occur at different rates. The fuel temperature will rise at nearly the same rate as the power with little or no lag. The coolant temperature will rise more slowly because of the time lag in the transfer of heat from the fuel to the coolant. Finally (in the case of a large graphite-moderated reactor), the moderator temperature will rise much more slowly due to its large mass and thermal capacity. The temperature coefficients of the fuel, coolant and moderator must be considered separately, and it must be borne in mind that they act at different rates.

It is particularly important that the fuel temperature coefficient, which acts with little or no delay in a power rise, should be negative for safe operation. All existing types of power reactors do have negative fuel temperature coefficients due to the phenomenon known as “Doppler broadening of the resonances”. This effect is due to the fact that as the temperature of the fuel rises, the thermal vibration of the fuel nuclei also increases. Consequently the range of neutron energies which corresponds to the increased thermal vibration of the fuel nuclei also increases, and the resonance peaks in the absorption cross-sections of the fuel nuclei are broadened. See Fig. 2 for an illustration of this effect. Overall, the increase in temperature and broadening of the resonances leads to increased resonance neutron absorption in the fuel, and in a reactor in which the most abundant fuel isotope is ^{238}U (and this applies to all existing types) the increased neutron capture in ^{238}U is the most important effect. Thus the Doppler coefficient of reactivity is negative in all existing types of reactor. Its value is typically of the order of -10^{-5} $\delta k/k$

This effect is of fundamental importance because the ^{238}U, which is responsible for the Doppler effect, is an integral part of the reactor fuel, being mixed with the

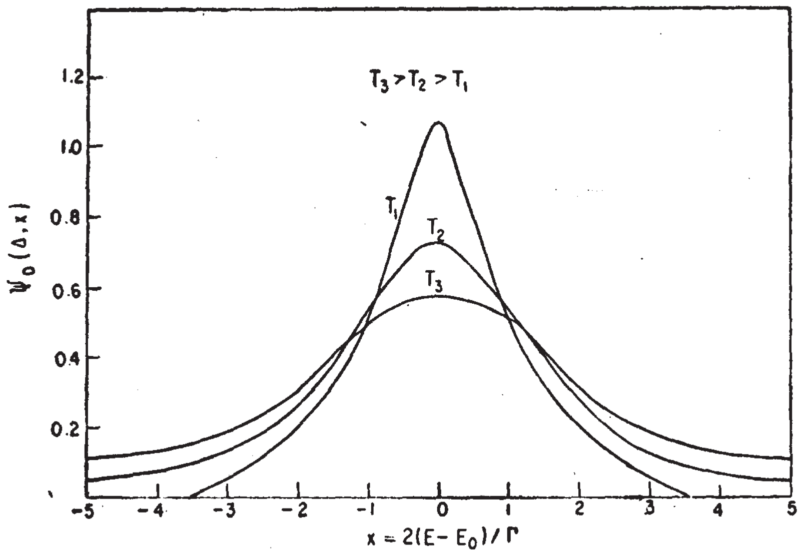

Figure 2. Energy variation of the Doppler broadened resonance cross-section (e.g. in ^{238}*U). One may observe that broadening of the resonance half-width at half is proportional to* $\sqrt{T}$.

^{238}U or (in the case of fast reactors) the ^{239}Pu in which energy is being released by fission. Any rise in the fuel temperature due to an increased fission rate causes a decrease of reactivity due to the Doppler effect with no time delay at all.

In light water-cooled and moderated reactors, the coolant temperature affects the reactivity primarily as a result of any nucleate or bulk boiling that may occur. The production of steam bubbles or voids by boiling reduces the average density of the water in the core and also reduces the moderator to fuel ratio. This may affect the reactivity in the following ways:

1. Reduction of the average density of the moderator (e.g. due to void effect in BWRs- see Fig. 3) causes neutron mean free paths in the core to be increased, thus increasing neutron leakage. This is a negative reactivity effect.

2. Reduction in the moderator to fuel ratio increases the fraction of neutrons captured in ^{238}U resonances during slowing down. This is also a negative reactivity effect.

3. Reduction in the moderator to fuel ratio reduces the fraction of thermal neutrons captured in the moderator and the thermal utilization factor increases. This is a positive reactivity effect.

4. Hardening of the thermal neutron spectrum due to decreased moderation of neutrons increases the average energy of the thermal neutrons. At this slightly higher energy the fraction of neutrons absorbed in ^{235}U decreases due to the decrease in the value of $\sigma_a(^{235}\mathrm{U})$ relative to $\sigma_c(^{238}\mathrm{U})$. This is a negative reactivity effect.

The overall void coefficient of reactivity is the sum of these effects, and in general depends upon whether the reactor is designed to be over- or under-moderated. Figure 4 shows the typical variation of the critical mass of fuel in a thermal reactor with the moderator to fuel (M/F) ratio, showing the existence of a minimum critical mass at one particular value of this ratio. If the design M/F ratio exceeds this value, then the reactor is said to be over-moderated, and if the design M/F ratio is less, then the reactor is under-moderated.

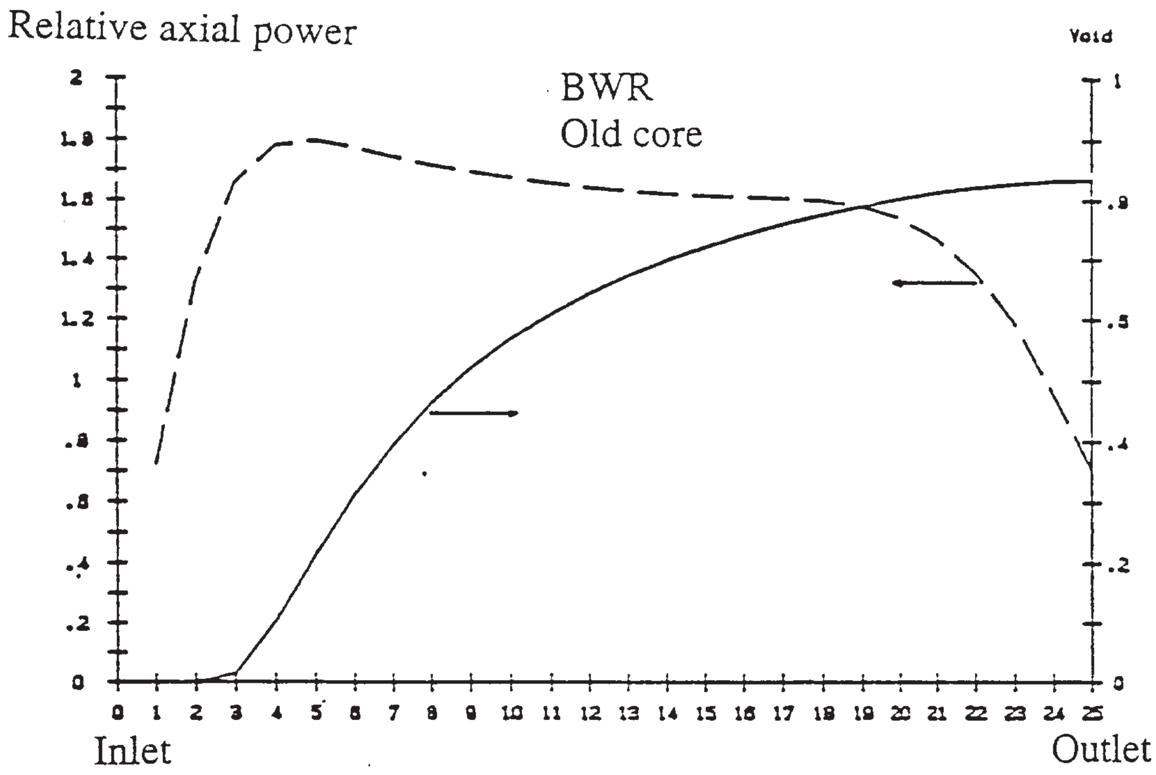

Figure 3. The axial void and power distribution in a BWR "old core".

The effect of voidage as pointed out above is to reduce the M/F ratio and the actual value moves to the left of the design value on Fig. 4. If this happens in a critical reactor which is over-moderated, the reactor becomes supercritical (A) and this is a positive reactivity effect. If it happens in an under-moderated reactor, the latter becomes subcritical (B) and this is a negative reactivity effect. Since the formation of voids by boiling is likely to occur very quickly following an increase in reactor power, a negative void coefficient is desirable from the viewpoint of reactor safety. Look into the lecture about **Chernobyl accident.**

In reactors other than PWRs and BWRs the functions of the moderator and coolant are carried out by different substances. For example an AGR has graphite moderator and carbon dioxide coolant. Even in the CANDU design, in which

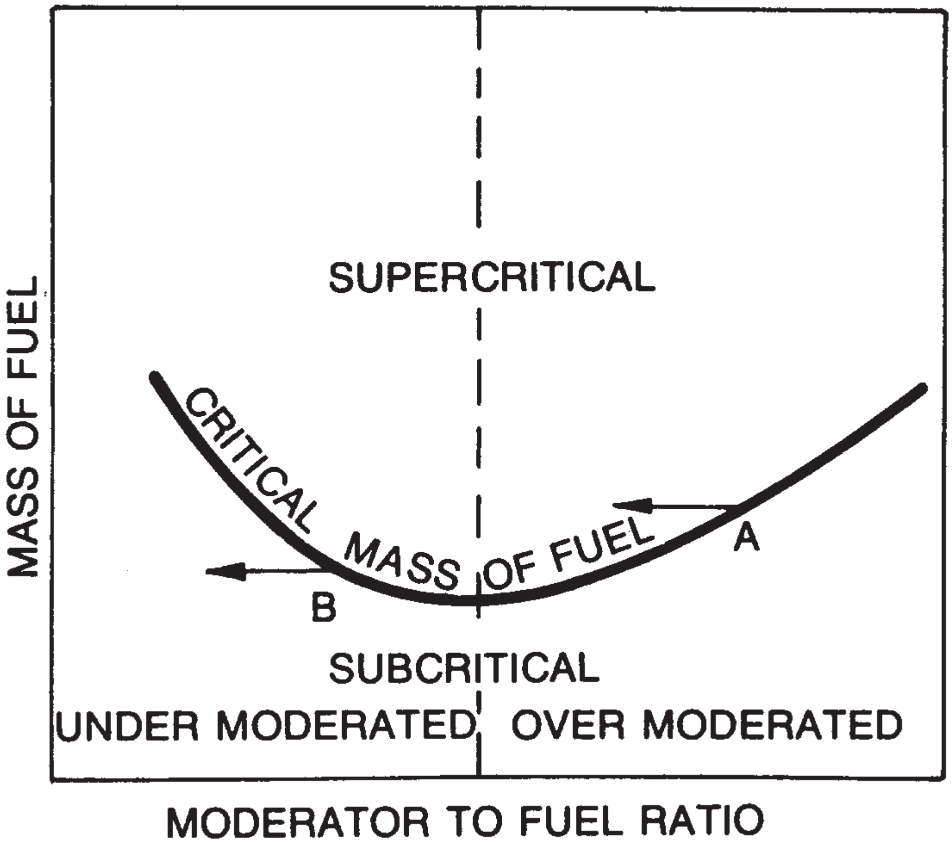

Figure 4. The variation of critical fuel mass with moderator to fuel ratio, showing the effect of voidage on reactivity.

both cooling and moderation are done by heavy water, the D_2O coolant is physically separated from the D_2O moderator, and they are at different temperatures during reactor operation. Thus in such reactors it is necessary to consider the moderator temperature coefficient as distinct from the coolant temperature (or void) coefficient.

As the moderator temperature rises, the average energy of the thermal neutrons (which are in energy equilibrium with the moderator) also rises. The fission cross-section of ^{235}U generally decreases with increasing neutron energy in the energy range 0.01 to 0.1 eV, the upper part of the thermal neutron spectrum, so a rise in moderator temperature leads to a reduction in fission in ^{235}U relative to capture in ^{238}U, thus reducing the factor eta (η) and the reactivity ρ. In this respect the moderator temperature coefficient is negative.

The moderator temperature coefficient can become positive if the fuel has been in the reactor for a long time and a significant amount of ^{239}Pu has been produced by neutron capture in ^{238}U. This isotope has a pronounced resonance in its absorption cross-section at 0.3 eV, and an increase in the moderator temperature, increasing the average energy of thermal neutrons towards this resonance, results in an increase in the rate of fission in ^{239}Pu. This is a positive reactivity effect which is particularly evident in natural uranium fuelled reactors, e.g. Magnox and CANDU designs. However, in these two reactor types the moderator has a large mass and is physically separated from the coolant, so the temperature of the moderator rises quite slowly in any power increase, no matter how rapid the latter is. Thus the time constant for the moderator temperature coefficient is long, and even if the coefficient is positive, it is readily controllable.

Finally, a rise in temperature of the reactor structure causes thermal expansion of the structure. This expansion implies that the mean interatomic distance in the reactor structure has increased. Hence the mean free path of neutrons is increased, and the probability of a neutron leaking out of the core (instead of being reflected back into the core) is increased. Similarly thermal expansion of the control rods means that a larger portion of the rods are in the core, and thus that neutron capture within them (a form of leakage) is more likely. Hence the reactivity coefficient due to structural temperature is normally negative in well-designed reactors. This effect, like the moderator temperature coefficient, is normally much slower to act than the fuel temperature or void coefficients.

To quantify the temperature effects we shall analyze the temperature changes of the reactivity starting from equation (1):

where: σ - cross section, d - density (to be different from the reactivity symbol ρ), B^2 - buckling.

$$\alpha(\rho) = \frac{d\rho}{dT} = \frac{1}{k^2}\frac{dk}{dT}$$

$$\text{for k close 1 (reactor operation)}$$

$$\alpha = \frac{d\rho}{dT} = \frac{1}{k}\frac{dk}{dT} = \frac{d}{dT}(\ln k) \tag{2}$$

$$= \left(\frac{\partial\rho}{\partial T}\right)_{B^2,d} + \left(\frac{\partial\rho}{\partial T}\right)_{B^2,\sigma} + \left(\frac{\partial\rho}{\partial T}\right)_{d,\sigma}$$

$$\begin{array}{lll} \sigma & d & B^2 \\ \text{varies} & \text{varies} & \text{varies} \end{array}$$

Considering first volume and dimension changes, we join together two parts of the equation above :

The a volume expansion coefficient - α_T - can be expressed as:

$$\left(\frac{\partial\rho}{\partial T}\right)_{B^2,\sigma} + \left(\frac{\partial\rho}{\partial T}\right)_{d,\sigma}$$

$$\alpha_T = \frac{1}{V}\frac{dV}{dT}$$

Atom density is inversely proportional to volume - , $N \propto \frac{1}{V}$ so we can write

$$\therefore \frac{1}{N}\frac{dN}{dT} = -\alpha_T$$

and remembering the way we defined the multiplication factor

$$k_{eff} = \eta\varepsilon p f P_{NLf} P_{NLth} = k_\infty P_{NLf} P_{NLth}$$

we get:

$$\frac{d\rho}{dT} = \frac{1}{k}\frac{dk}{dT} = \frac{d}{dT}(\ln k) = \frac{1}{k_\infty}\frac{dk_\infty}{dT} + \frac{1}{P_{NLf}}\frac{dP_{NLf}}{dT} + \frac{1}{P_{NLth}}\frac{dP_{NLth}}{dT} \qquad (3)$$

In principle k_∞ varies weaker with T (mainly due to the Doppler effects) than neutron leakage. So we shall analyze first the temperature effects on neutron leakage.

As it was shown before (see **Diffusion** lecture), leakage of neutrons are described by two terms, so called non-leakage probabilities:

$$P_{NLf} = e^{-B^2\tau} \quad and \quad P_{NLth} = \frac{1}{1+B^2L^2} \qquad (4)$$

Temperature dependence of P_{NLf} can be described as a temperature derivative of P_{NLf}:

$$\left(\frac{1}{P_{NLf}}\frac{dP_{NLf}}{dT}\right)_{\sigma} = -\left(\tau\frac{d(B^2)}{dT} + B^2\frac{d\tau}{dT}\right) \tag{5}$$

Remembering that

$$B^2 = \frac{c_1}{V^{\frac{2}{3}}} \; and \; \tau = \frac{c_2}{N^2} = c_3V^2$$

$$\frac{d(B^2)}{dT} = -\frac{2}{3}\alpha_T B^2 \, and \; \frac{d\tau}{dT} = 2\alpha\lambda \tag{6}$$

which leads to the final equation for the temperature dependence of P_{NLf} (assuming constant σ)

$$\left(\frac{1}{P_{NLf}}\frac{dP_{NLf}}{dT}\right)_{\sigma} = -\frac{4}{3}B^2\tau\alpha_T \tag{7}$$

Performing the same operation on P_{NLth} we get:

$$\left(\frac{1}{P_{NLth}}\frac{dP_{NLth}}{dT}\right) = -\frac{1}{1+B^2L^2}\left(B^2\frac{d(L^2)}{dT} + L^2\frac{d(B^2)}{dT}\right) \tag{8}$$

But

$$\begin{gathered} L^2 = \frac{c_4}{N^2\sigma_a\sigma_s} = c_5V^2 \; giving \\ \frac{d(L^2)}{dT} = 2L^2\alpha_T \end{gathered} \tag{9}$$

Putting equation (9) into (8):

$$\left(\frac{1}{P_{NLth}}\frac{dP_{NLth}}{dT}\right)_{\sigma} = -\frac{4}{3}\alpha_T \frac{B^2L^2}{1+B^2L^2} \tag{10}$$

Summing-up equation (7) and (10) we get the contribution of the neutron leakage terms to reactivity temperature dependence:

$$\left(\frac{d\rho}{dT}\right)_{\sigma} = \frac{1}{P_{NLf}}\frac{dP_{NLf}}{dT} + \frac{1}{P_{NLth}}\frac{dP_{NLth}}{dT} = -\frac{4}{3}\alpha_T\left(B^2\tau + \frac{B^2L^2}{1+B^2L^2}\right) \tag{11}$$

The temperature dependence of the microscopic cross-sections - σ_a, σ_f and σ_s in thermal reactors.

Variation of the capture and fission cross-sections in the Maxwell spectrum of thermal neutrons can be described as:

$$\sigma_a(\bar{v}) = \frac{\sigma_0 v_0}{\bar{v}} \tag{12}$$

where σ_0 and v_0 are cross section and neutron velocity for the reference temperature T_0.

Neutron velocity is proportional to the $\sqrt{T}$, i.e.

$$\bar{v} \propto \sqrt{T} \tag{13}$$

Relation (13) can be written as:

$$\sigma_a(T) = \frac{c}{\sqrt{T}}$$

and the temperature dependence can be presented as:

$$\frac{1}{\sigma_a}\frac{d\sigma_a}{dT} = -\frac{1}{2}\frac{1}{T} \tag{14}$$

For the moderator the most important is the temperature dependence of the scattering cross-section. Without going into details we can assume that for H_2O - see Fig. 5 - the temperature dependence of the scattering cross section can be written as:

$$\sigma_s \propto \frac{1}{E^n} \quad where \;\; n = 0.225 \tag{15}$$

which gives us:

$$\frac{1}{\sigma_s}\frac{d\sigma_s}{dT} = -\frac{n}{T} \; as\ long\ as\ (E \propto T) \tag{16}$$

Cross section variation affects L^{2} and consequently P_{NLth} on the following way:

$$L^2 = \frac{c}{\sigma_a \sigma_s}$$

$$\left(\frac{1}{L^2}\frac{dL^2}{dT}\right)_{B^2,d} = -\frac{1}{\sigma_a}\frac{d\sigma_a}{dT} - \frac{1}{\sigma_s}\frac{d\sigma_s}{dT}$$

It can be seen from equation (4) that temperature variation of L^2 leads to variation of P_{NLth}

$$\left(\frac{1}{P_{NLth}}\frac{dP_{NLth}}{dT}\right)_{B^2,d} = -\frac{1}{1+B^2L^2}B^2\frac{d(L^2)}{dT} = \\ -\frac{B^2L^2}{1+B^2L^2}\frac{\frac{1}{2}+n}{T} \tag{17}$$

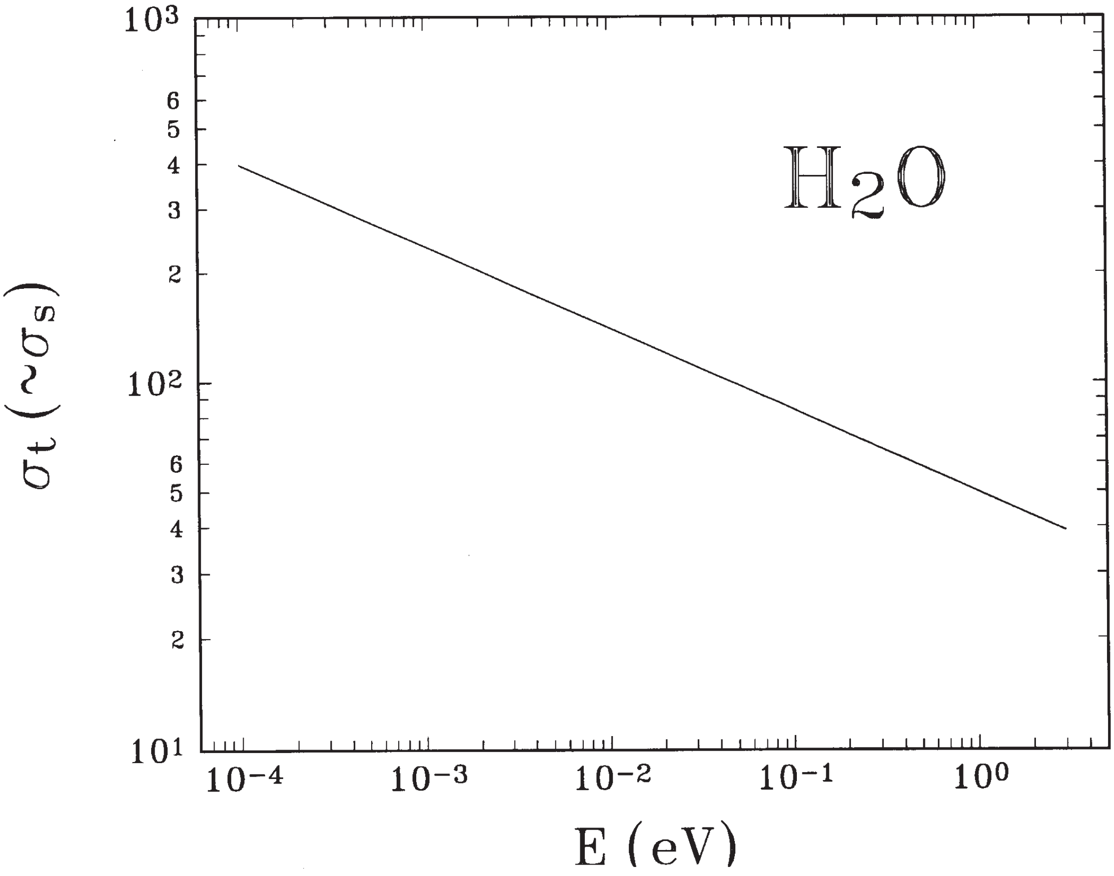

Figure 5. Neutron energy dependence of the capture microscopic cross section for H_2O*.*

As mentioned before it is mainly P_{NLth} which is affected by a thermal cross-section variation. k_∞ and P_{NLf} are weakly dependent thermal cross-section variation. **However, the thermal utilization factor *f* in formula for k_∞ can be severely affected in a case of loss of absorber (term in denominator): *f* can increase in this case. E.g. result of water boiling (void buildup) in the Chernobyl reactor!**

The dependence of k_∞ on Doppler effect is showed on Fig. 6.

The summary of the temperature effects on reactor reactivity is presented in Fig. 7.

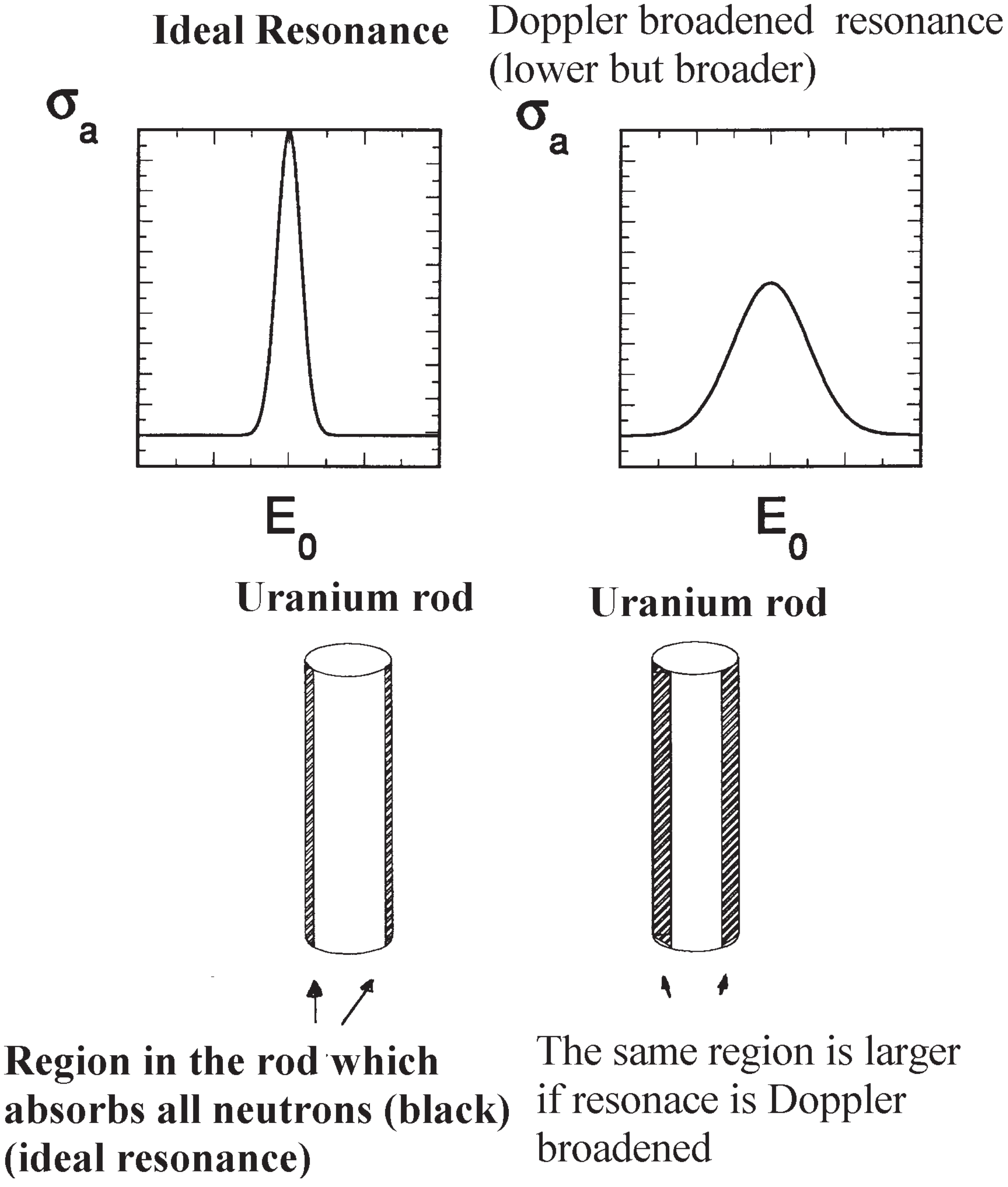

Figure 6. The simple illustration of Doppler broadening effect on k_∞. *The Doppler-broadened resonance integral* $[I_{res}]_{Doppler\ broadened} > [I_{res}]_{ideal}$ *leading to relation that resonance passage* $p_{Doppler\ broadened} < p_{ideal}$.

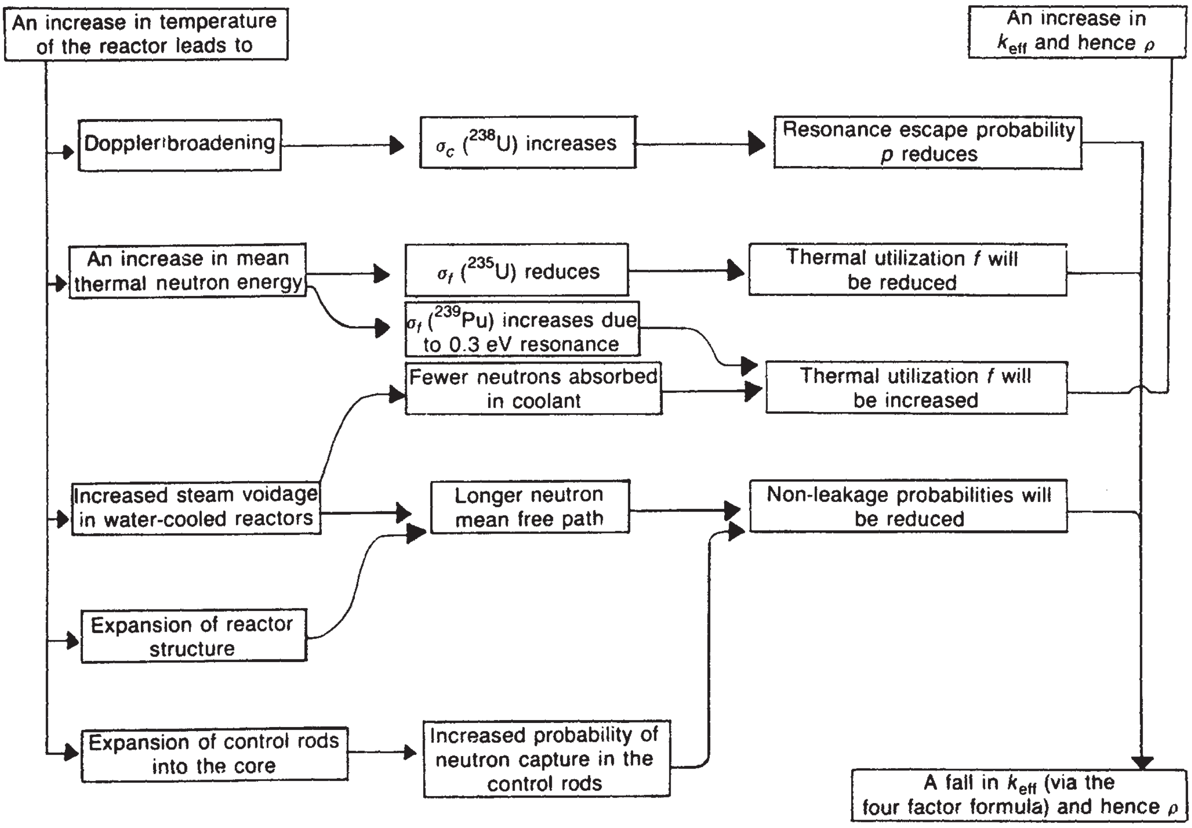

Figure 7. The ways in which temperature affects reactivity in a thermal reactor.

Example:

Estimate the temperature reactivity effect for the H_2O - moderated reactor working at 20^O C. (R2 Studsvik reactor - type).

Data:

$$\tau = 33\,\text{cm}^2$$

$$L^2 = (2.81)^2\,\text{cm}^2 = 7.7\,\text{cm}^2$$

$$k_\infty = 1.5$$

$$B^2 = 0.0113\,\text{cm}^2$$

$$\alpha_{T(H_2O,20^\circ\,C)} = 2.07\cdot 10^{-4}\,/^\circ\,C$$

From equation (11) we get the reactivity variation due to the leakage variation for constant σ and from equation (17) - affect of the variation H_2O scattering cross section :

$$\left(\frac{d\rho}{dT}\right)_{\sigma} = -\frac{4}{3}\cdot 2.07\cdot 10^{-4}(\underset{\substack{\textit{leakage of}\\ \textit{fast}\\ \textit{neutrons}}}{0.373} + \underset{\substack{\textit{leakage of}\\ \textit{thermal}\\ \textit{neutrons}}}{0.085}) = -12.6\,\frac{pcm}{{}^{o}C}$$

$$\left(\frac{d\rho}{dT}\right)_{B^2,d} = -0.085\cdot\frac{0.725}{293} = -21\,\frac{pcm}{{}^{o}C}$$

$$\left(\frac{d\rho}{dT}\right)_{total} \approx -33.6\,\frac{pcm}{{}^{o}C}$$

As a result we get that 300^{O} C increase of the reactor temperature corresponds 10000 pcm = 10%.

Reactor poisons

Of the many isotopes that are formed as fission products in a reactor, two are of particular importance because they have very high absorption cross-sections, and their presence in the reactor has a considerable effect on reactivity. These two isotopes are xenon 135 and samarium 149, and they are known as reactor poisons. Fig. 8 presents the energy variation of absorption cross-sections for ^{135}Xe, ^{149}Sm and ^{156}Gd. Attention should be paid into extremely high absorption cross section of ^{135}Xe exceeding 10^6 barns. ^{156}Gd is not a fission product poison, it is a burnable poison used in a modern reactor fuel in order to limit the excess of reactivity in a fresh fuel.

Xenon poisoning

Xenon-135 is the most important fission product poison. Its average thermal neutron absorption cross-section at 20°C is 2.75×10^6 barns, and it is formed directly as a fission product and also in the decay chain of the fission product tellurium 135. The tellurium decay chain is as shown on Fig. 9. The fission yield of ^{135}Te from ^{235}U fission is 0.061 atoms per fission. The half-life of ^{135}Te is so short, however, that ^{135}I may be considered the primary fission product as presented on Fig.

10. ^{135}Xe is also produced as a primary fission product to the extent of 0.003 atoms per fission. The effect of ^{135}Xe on the reactivity of a reactor depends on its concentration during steady power operation and after shutdown. The equation for the concentration N(I) of ^{135}I from which it is formed can be written as:

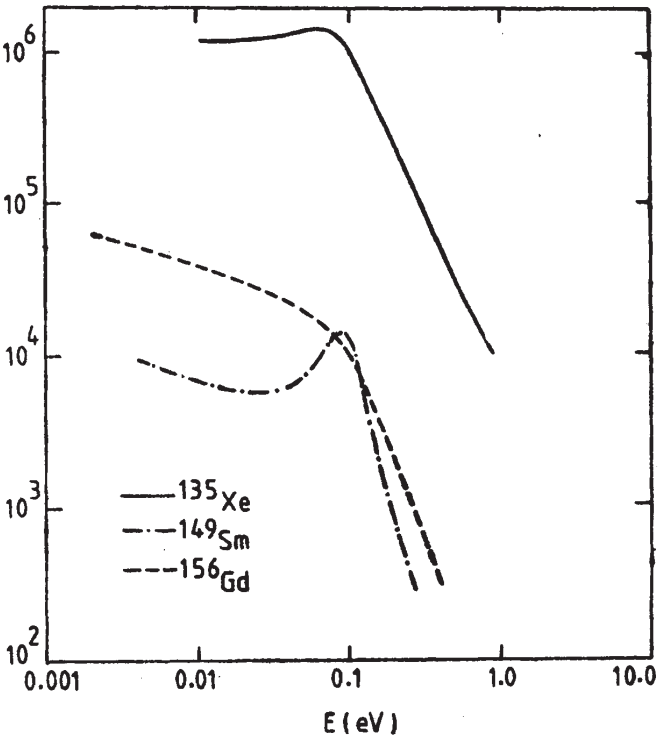

Figure 8. The energy variation of the absorption cross sections of ^{135}Xe, ^{149}Sm and ^{156}Gd.

$$\left(\begin{array}{c}\text{The rate of change}\\ \text{of } ^{135}I \text{ concentration}\end{array}\right)=\left(\begin{array}{c}\text{The rate of}\\ \text{formation of } ^{135}I\end{array}\right)-\left(\begin{array}{c}\text{The rate of}\\ \text{decay of } ^{135}I\end{array}\right)$$

$$\frac{dN(I)}{dt}=\gamma(I)\overline{\Sigma}_f\phi_{th}-\lambda(I)N(I) \tag{18}$$

where γ(I) is the fission yield of ^{135}I. The solution of this equation is:

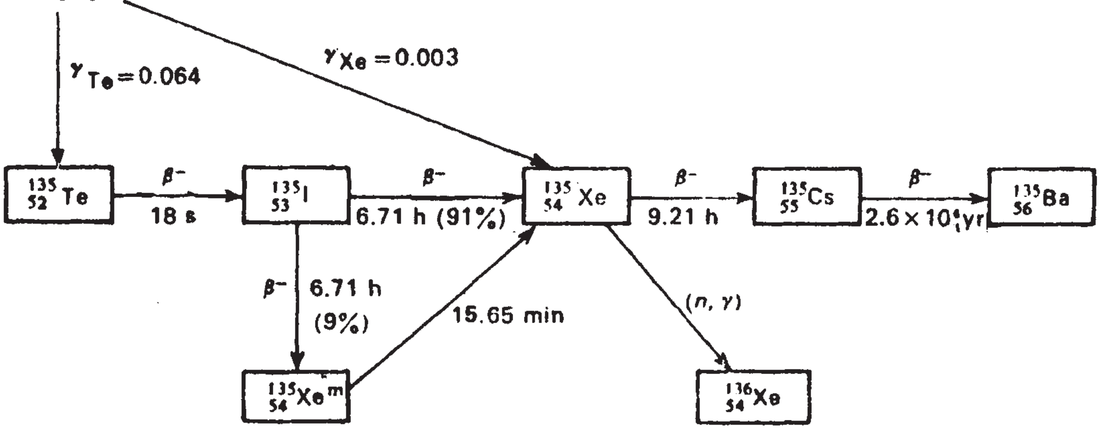

Figure 9. Decay chain of fission products involving ^{135}Xe.

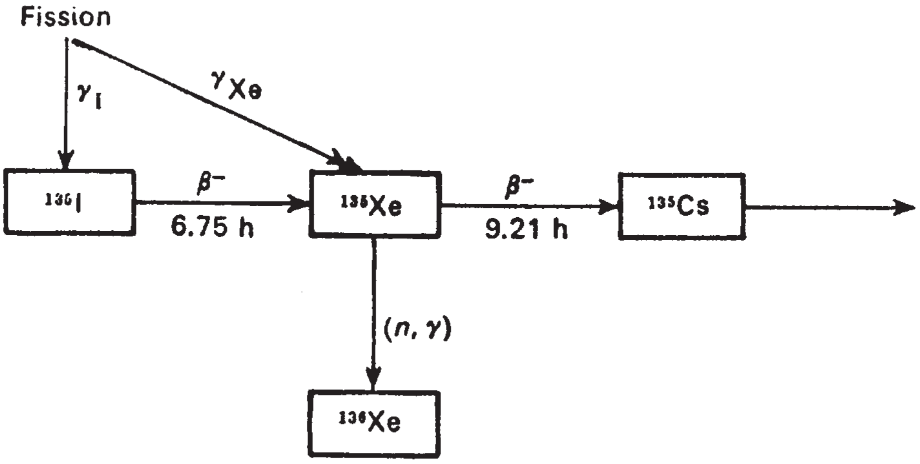

Figure 10. A simplified decay chain of fission products involving ^{135}Xe.

$$N(I) = \frac{\gamma(I)\overline{\Sigma}_f \phi_{th}}{\lambda(I)}\left(1 - e^{-\lambda(I)t}\right) \tag{19}$$

where *t* is the time after startup of an initially clean reactor (i.e. no fission products). The ^{135}I concentration reaches equilibrium after about 30 hours operation, the value being:

$$N(I)_{eq} = \frac{\gamma(I)\overline{\Sigma}_f \phi_{th}}{\lambda(I)} \tag{20}$$

The equation for the ^{135}Xe concentration N(Xe) is:

$$\begin{aligned}\begin{pmatrix}\text{The rate of change of}\\ {}^{135}\text{Xe concentration}\end{pmatrix} &= \begin{pmatrix}\text{The rate of production}\\ \text{of } {}^{135}\text{Xe by decay of } {}^{135}\text{I}\end{pmatrix}\\ &+ \begin{pmatrix}\text{The rate of production of}\\ {}^{135}\text{Xe as a fission product}\end{pmatrix}\\ &- \begin{pmatrix}\text{The rate of}\\ \text{decay of } {}^{135}\text{Xe}\end{pmatrix}\\ &- \begin{pmatrix}\text{The rate of neutron}\\ \text{capture in } {}^{135}\text{Xe}\end{pmatrix}\end{aligned}$$

$$\frac{dN(Xe)}{dt} = \lambda(I)N(I) + \gamma(Xe)\overline{\Sigma}_f\phi_{th} - \lambda(Xe)N(Xe) - \overline{\sigma}_c(Xe)N(Xe)\phi_{th} \tag{21}$$

where γ(Xe) is the fission yield of ^{135}Xe. Like the ^{135}I, the ^{135}Xe reaches an equilibrium concentration after about two days' operation, the value being found from equations (20) and (21) to be:

$$N(Xe)_{eq} = \frac{\{\gamma(I)+\gamma(Xe)\}\bar{\Sigma}_f \phi_{th}}{\gamma(Xe)+\bar{\sigma}_c(Xe)\phi_{th}} \tag{22}$$

The effect of this equilibrium concentration of ^{135}Xe on the reactivity of a reactor can be determined. An infinite homogeneous re- actor will be considered, and it will be assumed that the presence of ^{135}Xe affects only the value of the thermal utilization factor. The change of reactivity may be written as

$$\rho(Xe) = \frac{k_{\infty}^{'} - k_{\infty}}{k_{\infty}^{'}} = \frac{f'-f}{f'} = f\left(\frac{1}{f}-\frac{1}{f'}\right) \tag{23}$$

where k'_{∞} and f' refer to the poisoned reactor. Expressions for f' and f are:

$$f' = \frac{\bar{\Sigma}_{aF}}{\bar{\Sigma}_{aF}+\bar{\Sigma}_{cM}+\bar{\Sigma}_c(Xe)}$$

and

$$f = \frac{\bar{\Sigma}_{aF}}{\bar{\Sigma}_{aF}+\bar{\Sigma}_{cM}}$$

Consequently

$$\frac{1}{f}-\frac{1}{f} = -\frac{\bar{\Sigma}_c(Xe)}{\bar{\Sigma}_{aF}} = -\frac{N(Xe)\bar{\sigma}_c(Xe)}{\bar{\Sigma}_{aF}}$$

and

$$\rho(Xe) = -f\,\frac{N(Xe)\bar{\sigma}_c(Xe)}{\bar{\Sigma}_{aF}}$$

Using equation (22) for $N(Xe)_{eq}$, and noting that $\bar{\Sigma}_f \,/\, \bar{\Sigma}_{aF} = \eta \,/\, \nu$,

$$\rho(Xe) = -\frac{f\eta}{\nu}\,\frac{\left\{\gamma(I)+\gamma(Xe)\right\}}{\left(\dfrac{\lambda(Xe)}{\bar{\sigma}_c(Xe)\phi_{th}}+1\right)} \tag{24}$$

Evidently ρ(Xe) increases as ϕ_{th} increases, and reaches a limiting value when $\phi_{th} >> \lambda(Xe) \,/\, \bar{\sigma}_c(Xe)$. The value of this ratio is about 0.75×10^{13} $cm^{-2}\ s^{-1}$, so when ϕ_{th} is 10^{14} neutrons/cm^2 s, a typical value for a power reactor, this limiting value is nearly reached. It is:

$$\rho(Xe)_{maximum} = -\frac{f\eta\left\{\gamma(\mathrm{I})+\gamma(Xe)\right\}}{\nu} \tag{25}$$

Consider a natural uranium fuelled reactor in which η = 1.32, ν = 2.42 and $\left\{\gamma(I)+\gamma(Xe)\right\}$. If we assume that $f = 0.9$, then the maximum value of ρ(Xe) is – 3.1 per cent. This figure represents the amount of excess reactivity which must be built into the reactor to enable the maximum possible effect of ^{135}Xe poisoning to be overcome during steady-state operation. The dependence of the ^{135}Xe poisoning on the neutron flux is shown on Fig. 11.

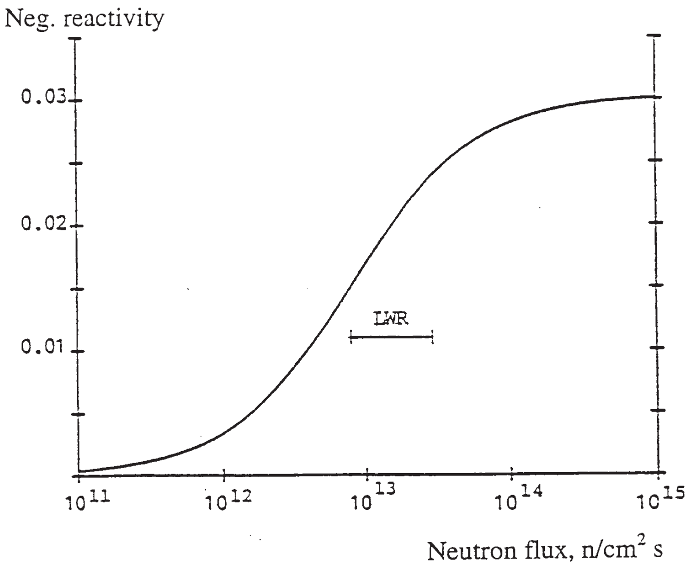

Figure 11. The dependence of ^{135}Xe poisoning on the neutron flux in the thermal reactors.

It is also important to consider the way in which the ^{135}Xe concentration varies after a rapid reactor shutdown. (The ^{135}Xe may be assumed to be at its equilibrium concentration before shutdown.) Immediately after shutdown the rate of production of ^{135}Xe decreases to a fraction $\gamma(I)/\{\gamma(I)+\gamma(Xe)\}$ of the pre-shutdown value, while the rate of elimination decreases to a fraction $\lambda(Xe)/\left[\lambda(Xe)+\overline{\sigma}_c(Xe)\phi_{th}\right]$ of the pre-shutdown value. In a power reactor, whose average thermal neutron flux is 10^{12} neutrons/cm^2 s or more, the second fraction is smaller than the first, and the ^{135}Xe concentration rises after shutdown. The rate of rise depends on the pre-shutdown flux, and increases as this flux increases. In due course, as the ^{135}I decays, the ^{135}Xe concentration reaches a peak (which also increases as the pre- shutdown flux increases) and thereafter decays. This behaviour is shown in Fig. 12.

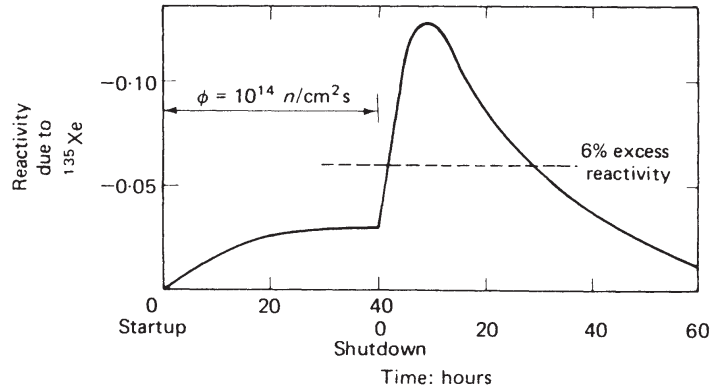

Figure 12. ^{135}Xe concentration in a reactor during operation and after shutdown.

The important point concerning the peak ^{135}Xe concentration after shutdown is that unless sufficient excess reactivity is built into the reactor to overcome the increased poisoning effect, it may not be possible to restart the reactor until many hours have elapsed. To override the maximum xenon poisoning in a reactor operating at 10^{14} n/cm^{2}s an excess reactivity of about 13 per cent is required. If less reactivity is available, for example 6 per cent *(see* Fig. 12) then after shutdown about 2 hours are available to restart the reactor before the ^{135}Xe builds up, and failing this it is necessary to wait for about 28 hours until the ^{135}Xe has passed its maximum and decayed sufficiently.

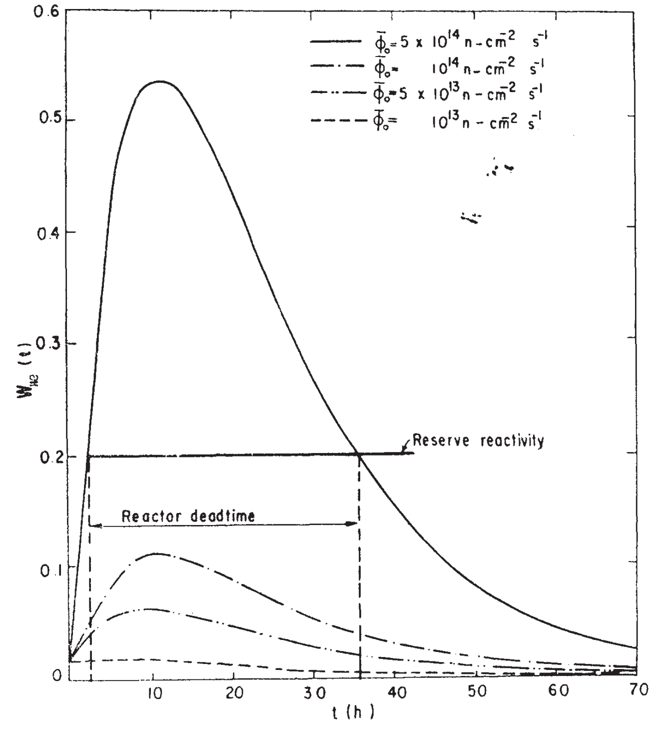

Figure 13. ^{135}Xe poisoning after the reactor shut-down from different neutron flux levels.

As mentioned above the ^{135}Xe poisoning depends on the neutron flux. The time dependence of the ^{135}Xe poisoning after shut-down from different neutron flux levels is shown on Fig. 13.

Samarium poisoning

Samarium 149 is formed from the fission product neodymium 149 by the decay chain as shown on Fig. 14.

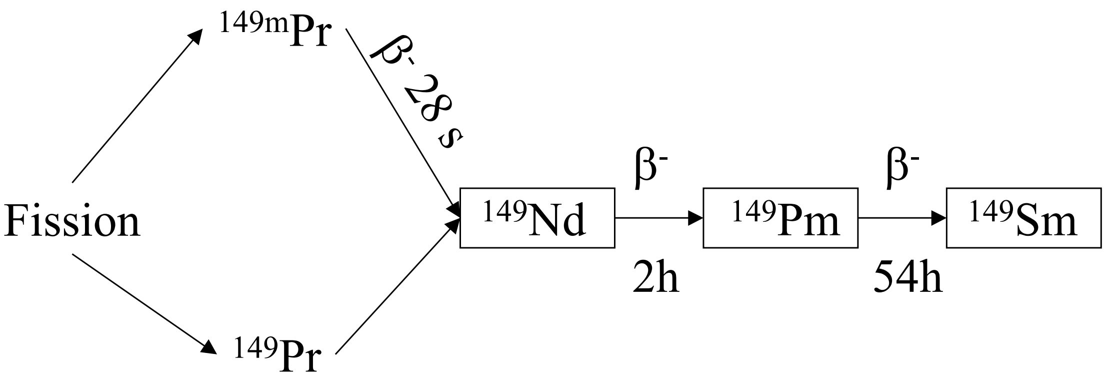

Pr - Praseodymium, Nd- Neodymium, Pm-Promethium
Sm - Samarium

Figure 14. The fission product decay chain involving ^{149}Sm.

The half-life of ^{149}Nd is short compared with that of the intermediate product promethium 149, and the latter may be considered as the primary fission product. The fission yield of ^{149}Pm, $\gamma(Pm)$ is 0.0113 atoms per fission, and the average thermal neutron capture cross-section of ^{149}Sm is 5.8×10^4 barns. The concentration of ^{149}Sm may be found from the equations:

$$\frac{dN(Pm)}{dt} = \gamma(Pm)\overline{\Sigma}_f\phi_{th} - \lambda(Pm)N(Pm) \qquad (26)$$

and

$$\frac{dN(Sm)}{dt} = \lambda(Pm)N(Pm) - N(Sm)\overline{\sigma}_c(Sm)\phi_{th} \qquad (27)$$

where N(Pm) and N(Sm) are the concentrations of ^{149}Pm and ^{149}Sm respectively. The equilibrium concentration of ^{149}Sm, which is reached after several days operation, is:

$$N(Sm)_{eq} = \frac{\gamma(Pm)\overline{\Sigma}_f}{\overline{\sigma}_c(Sm)} \tag{28}$$

This concentration is independent of the reactor flux or power, and its effect on the reactivity is:

$$\rho(Sm) = -\frac{f\eta\gamma(Pm)}{\nu} \tag{29}$$

From the figures used previously for a natural uranium fuelled reactor, the value of ρ(Sm) is – 0.55 per cent.

After shutdown the ^{149}Sm in the reactor, being stable, remains, while the ^{149}Pm in the reactor decays to produce more ^{149}Sm, whose concentration therefore rises to a higher level. The post-shutdown equilibrium concentration is:

$$N(Sm)_{eq\ \ post\ shutdown} = \frac{\gamma(Pm)\overline{\Sigma}_f}{\overline{\sigma}_c(Sm)}\left(1 + \frac{\overline{\sigma}_c(Sm)\phi_{th}}{\lambda(Pm)}\right) \tag{30}$$

The variation of ^{149}Sm in an operating reactor is shown in Fig. 15. In a reactor operating at a thermal neutron flux of 10^{14} n/cm^2 s the reactivity effect of ^{149}Sm after shutdown rises to a constant value of – 1.45 per cent. and there must be sufficient excess reactivity available in the reactor to overcome this. It is obvious, however, from the figures that have been calculated for ^{135}Xe and ^{149}Sm that the former is much more important as a reactor poison.

Figure 16 presents the samarium negative reactivity worth as a function of time for a ^{235}U fuelled reactor for different neutron flux levels prior to shutdown. Higher the flux level prior to shutdown, higher will be the equilibrium samarium level. We note that unlike in the case of xenon, samarium poisoning gradually approaches a constant maximum value.

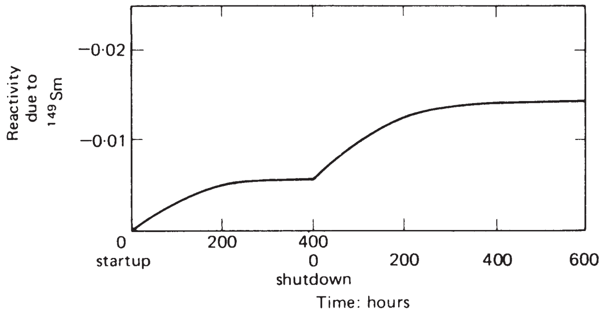

Figure 15. ^{149}Sm concentration in a reactor during operation and after shutdown.

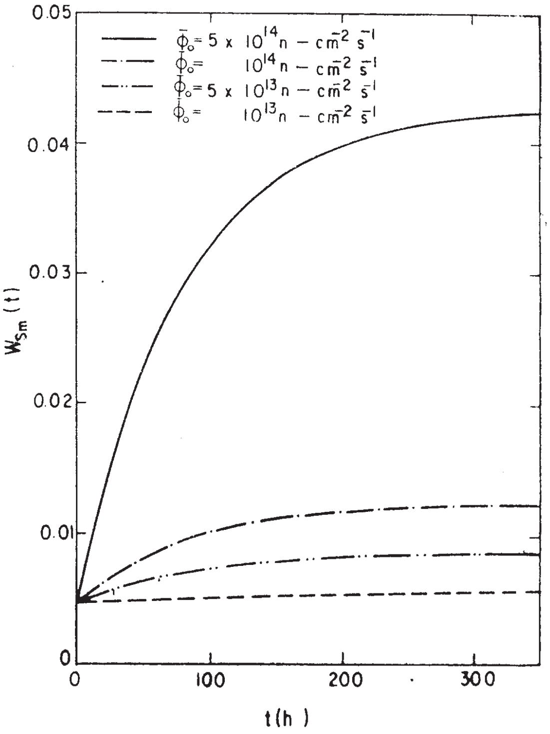

Figure 16. Time variation of the post-shutdown samarium reactivity worth in a ^{235}U fuelled reactor for four flux levels just before shutdown.

In our discussion we have considered only two fission products - xenon and samarium - since these make the major contribution to fission product poisoning and make their presence felt soon after a reactor is put in operation. There are, of course, many other fission product poisons, which either because of their low cross-section or because of their low yield, or both, do not produce an immediate observable effect. Nevertheless, they go on accumulating and tend to decrease reactivity. The method for calculating reactivity worth of each nuclide is the same as described for iodine and xenon. Since there are nearly 300 or more different species it is very difficult to calculate the overall effect.

Burnup of fuel

During reactor operation, fissile material is being consumed or burned up at a rate proportional to the power of the reactor. In a reactor containing fertile material, new fissile material is also being created by one of the breeding processes. It is necessary in the design of a reactor to be able to estimate the fuel concentration as a function of time to ensure that the reactor has sufficient fuel to enable it to re- main critical for a specified time, possibly a year or two. The accurate prediction of the fuel concentration in a reactor over a prolonged period is difficult, and we will restrict ourselves to a qualitative discussion.

It is important to note that burn-up processes involve many different nuclei and the specific isotopes depend on the type of fuel used. For reactors fuelled with natural uranium, the build-up and decay chains of interest are shown on Fig. 17. Heavy nuclides like ^{239}Np, (neptunium), ^{239}Pu (plutonium), ^{241}Am (americium),..., ^{244}Cm (curium), which were not present initially are created. Some of these nuclei are fissile while others act as poisons (or fertile materials). Poisons affects the multiplication factor adversely due to their large neutron capture cross-sections. Also, due to their large β^- -decay half-lives, poisons do not decay rapidly. For example ^{239}Np is an important connecting isotope in the formation of ^{239}Pu from ^{238}U. As is well known, ^{239}Np is a good thermal neutron absorber and can be fissioned only by fast neutrons. Therefore it will lead to neutron loss. However, a far more important effect is the reduction in the production rate of ^{239}Pu, a thermally fissile isotope. Similarly, the neutron capture chain starting from ^{239}Pu results in ^{241}Pu whose β^- decay product, ^{241}Am will act as poison. (this nuclide causes more ham in systems using plutonium or MOX(mixed-oxide)- fuel.

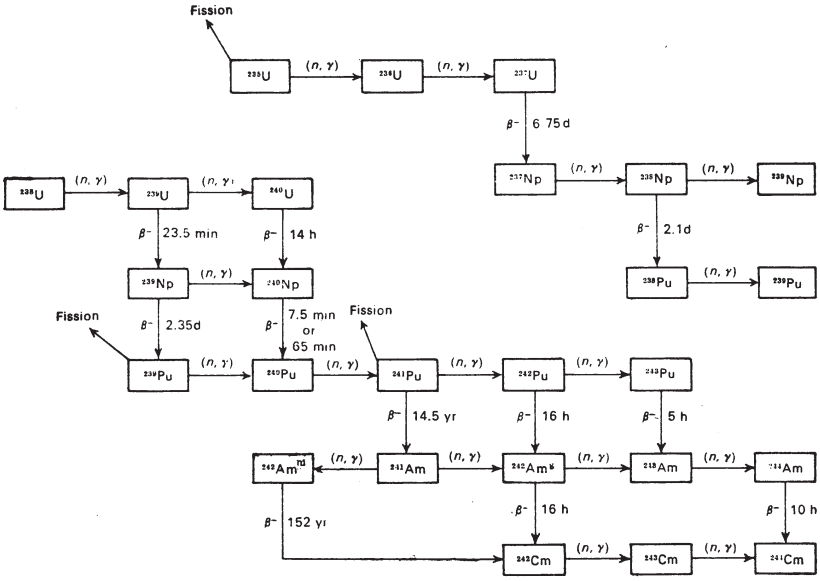

Figure 17. The build-up and decay chains of isotopes in a reactor fuelled with natural uranium.

The build-up and decay chains of interest in a thorium fuelled reactor core are shown in Fig.18. Like ^{239}Np and ^{241}Am, here ^{233}Pa (protactinium) influences th neutron multiplication factor by increasing neutron loss and affecting the production rate of ^{233}U. Moreover, the β^- decay half-life of ^{233}Pa (27 days) is much greater than the β^- decay half-life of ^{239}Np.

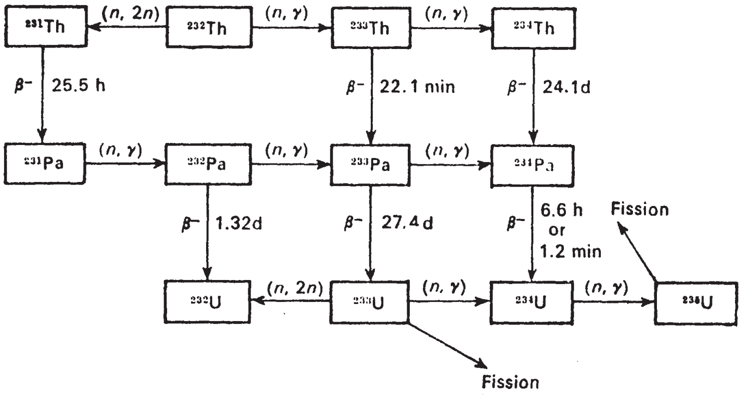

Figure 18. The build-up and decay chains of isotopes in a reactor fuelled with thorium.

In an infinite reactor fuelled with pure ^{235}U, operating at constant power, the rate of fission and hence the rate of burnup is constant and uniform throughout the reactor, and the ^{235}U concentration decreases linearly with time and uniformly throughout the reactor. In a finite reactor fuelled with ^{235}U, the rate of burnup is greatest at the centre of the core where the flux is greatest, thus the composition of the reactor varies non-uniformly, the flux shape changes, and the problem becomes more complicated.

The important feature of a reactor fuelled with highly enriched uranium or pure ^{235}U is that the fuel concentration, and hence the excess reactivity of the reactor, decrease continuously as operation proceeds.

In a reactor containing a large amount of fertile material, for example a natural or slightly enriched uranium reactor, the burnup of the original fissile isotope is offset to some extent by the production of new fissile material. In the case of a uranium fuelled reactor the important processes are as presented on Fig. 19.

$$^{235}U + n \rightarrow \begin{cases} ^{236}U \\ fission \end{cases}$$

$$^{238}U + n \rightarrow {}^{239}U \rightarrow {}^{239}Np \rightarrow {}^{239}Pu$$

$$^{239}Pu + n \rightarrow \begin{cases} ^{240}Pu \\ fission \end{cases}$$

$$^{240}Pu + n \rightarrow {}^{241}Pu$$

$$^{241}Pu + n \rightarrow \begin{cases} ^{242}Pu \\ fission \end{cases}$$

Figure 19. Important processes induced by neutron absorption in a uranium fuelled

The creation of fissile ^{239}Pu is important during the early stages of reactor operation when burnup is low; however, ^{241}Pu becomes significant at high burnup. The equations for the concentrations of ^{235}U, ^{238}U and ^{239}Pu are:

$$^{235}_{92}U: \qquad \frac{dN\left(^{235}_{92}U\right)}{dt} = -\Phi\sigma_a\left(^{235}_{92}U\right)N\left(^{235}_{92}U\right)$$

$$^{238}_{92}U: \qquad \frac{dN\left(^{238}_{92}U\right)}{dt} = -\Phi\sigma_a\left(^{238}_{92}U\right)N\left(^{238}_{92}U\right)$$

$$^{239}_{94}Pu: \qquad \frac{dN\left(^{239}_{94}Pu\right)}{dt} = \Phi\sigma_a\left(^{238}_{92}U\right)N\left(^{238}_{92}U\right) - \Phi\sigma_a\left(^{239}_{94}Pu\right)N\left(^{239}_{94}Pu\right)$$

(In these equations the terms on the right-hand sides represent total rates of neutron absorption at all neutron energies, and include resonance capture in ^{238}U.)

To simplify the solution, which would otherwise be rather complicated, we will consider an infinite reactor operating at constant flux, and assume that the concentration of ^{238}U is constant. (The value of $\phi\sigma_c(^{238}U)$ is much less than either $\phi\sigma_a(^{235}U)$ or $\phi\sigma_a(^{239}Pu)$.)

The solutions of the above equations for N(^{235}U) and N(^{239}Pu) are:

$$N\left(^{235}_{92}U\right) = N_0\left(^{235}_{92}U\right)e^{-\Phi\sigma_a\left(^{235}_{92}U\right)t}$$

where N$_0$(^{235}U) is the initial concentration of ^{235}U, and:

$$N\left(^{239}_{94}Pu\right) = N_0\left(^{238}_{92}U\right)\frac{\Phi\sigma_c\left(^{238}_{92}U\right)}{\Phi\sigma_a\left(^{239}_{94}Pu\right)}\left\{1-e^{-\Phi\sigma_a\left(^{239}_{94}Pu\right)t}\right\}$$

where $N_0(^{238}U)$ is the initial concentration of ^{238}U.

Figure 20 shows approximately the variation of the ^{235}U and ^{239} Pu concentrations in a natural uranium fuelled reactor operating at constant flux. In the early stages of operation the production of ^{239}Pu more than offsets the burnup of ^{235}U, and there is an increase of reactivity. In due course this trend is reversed, the concentration of ^{239}Pu tends to become constant while the concentration of ^{235}U continues to decrease. Consequently the reactivity decreases and after some time the reactor will become subcritical and require refuelling.

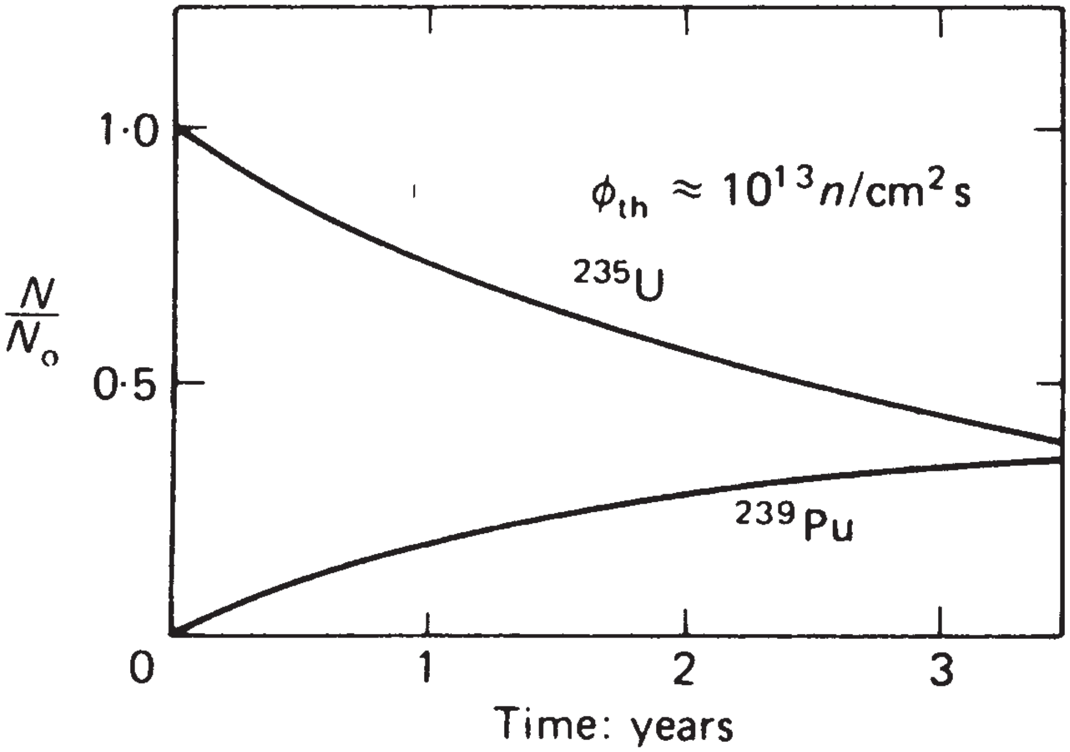

Figure 20. The concentration of ^{235}U *and* ^{239}Pu *in an operating reactor.*

Control systems in reactors

The control system of a reactor is required to perform three functions, namely:

1.Bring about the small changes nf reactivity necessary to start up the reactor, change its power level as desired, and shut down the reactor.
2.Absorb the built-in excess reactivity, and compensate for the spontaneous reactivity changes due to fuel burnup, fission product poisoning and temperature effects.
3. Provide a means of shutting down the reactor rapidly in an emergency by inserting a large amount of negative reactivity.

In many reactors two or three control systems may be used, one for each of these functions; however, different reactor types employ different systems. Two more considerations are that the control system should not absorb neutrons wastefully, and it should not distort the flux in the reactor more than necessary.

The most common control system for thermal reactors consists of rods containing a neutron-absorbing material such as boron, cadmium or hafnium. These rods are moved into and out of the core by drive mechanisms which can be precisely controlled. This system is good for startup, power changes and shutdown, but is less suitable for absorbing all the reactor’s built-in reactivity. This is because at the start of the reactor’s life some or all the control rods would be partially in the core for a long period, neutrons would be wastefully absorbed and the flux in the core distorted with the result that fuel temperatures would differ from, and in some cases be greater than, the values calculated.

Control rods of this type are suitable for emergency shutdown. The rods, usually known as safety rods, are held permanently out of the reactor during normal operation by electromagnetic clutches. In an emergency the clutches are released and the rods drop into the core, or may be driven in hydraulically.

Another, complementary means of reactivity control is to use burnable poisons. Burnable poisons are materials that have high neutron cross- sections, and which on capturing neutrons produce low capture cross-section materials. Boron 10 (which forms 18.8 per cent of naturally occurring boron) is such a material, and the ^{10}B(n,α) ^{7}Li reaction produces isotopes with very low capture cross-sections. In the burnable poison method of control a boron compound such as boric acid is mixed with the moderator to absorb the excess reactivity of a new reactor. As operation proceeds, the ^{10}B is ’burned out’ by neutron capture and its negative reactivity effect is reduced, thus compensating for fuel burnup. The concentration of boron in the moderator can be controlled either by injecting more boron or by circulating the moderator through an ion exchange column to remove boron. This method has the advantage that the flux is not perturbed by the presence of boric acid throughout the core, however it cannot be used for con- trolling startup, power variation and xenon fluctuations so control rods are still necessary. Burnable poisons are used in water-cooled reactors which have off-load refuelling, since they enable longer periods of power generation (in between refuelling shutdowns) to be achieved.

Burnable poisons are also used in Swedish reactors in form gadolinium oxide (Gd_2O_3,) poison, ^{157}Gd has a very large neutron capture cross-section (254 000 barns - look Fig. 8), but ^{158}Gd – the product of the ^{157}Gd(n,γ) ^{158}Gd reaction – has a much lower cross-section (2.5 barns); hence gadolinium oxide acts as a burnable poison.

Taking a reactor critical

Taking a reactor critical is a routine operation which has to be carried out after each shutdown. Nevertheless the operation has to be performed with some care since, at low powers, the effects of thermal feedback will be at their minimum. Hence the possibility of a power overshoot (as opposed to a gentle power rise) exists. Reactors are designed to protect themselves against this possibility by means of their shutdown systems but nevertheless a 'critical approach' is always undertaken with some care.

The primary objective of a critical approach is thus to take the reactor up to power in a smooth, controlled manner. A secondary objective (particularly following a refuelling shutdown) is to confirm that the 'critical balance height' – the height of the control rods to give k_{eff} exactly equal to unity – is in agreement with that predicted by computer calculations. This then provides a cross-check that any new fuel has been correctly located in the core. In PWRs, for example, it is common to use fuel of different enrichments to help flatten the flux distribution. If a new fuel sub-assembly of 3 per cent enrichment, which would normally be placed at the edge of the core, was wrongly located at the centre of the core where the enrichment is usually about 2.5 per cent, then the critical balance height would be lower than anticipated. This should alert the operators that a mistake had been made. If no action were taken, such fuel would operate at a higher than normal temperature, and perhaps suffer some damage as a result.

If we consider a subcritical reactor with a neutron source producing S fissions per second and with a multiplication factor k_{eff} (k_{eff}<1.0) then we may say that:

S fissions/sec are produced by the source

Sk_{eff} fissions/sec are produced from the previous fission generation and Sk^2_{eff} fissions/sec are produced from the generation previous to that.

Hence the total number of fissions per second ***is:***

$$S + Sk_{eff} + S^2_{eff} + \ldots\ldots\ldots = \frac{S}{1 - k_{eff}}, \quad for \quad k_{eff} < 1$$

and therefore the subcritical power is (P_s / ($1 - k_{eff}$)) watts, where $P,$ is the power due to source S. Also, we can write that:

$$\rho = \frac{k_{eff} - 1}{k_{eff}} = k_{eff} - 1$$

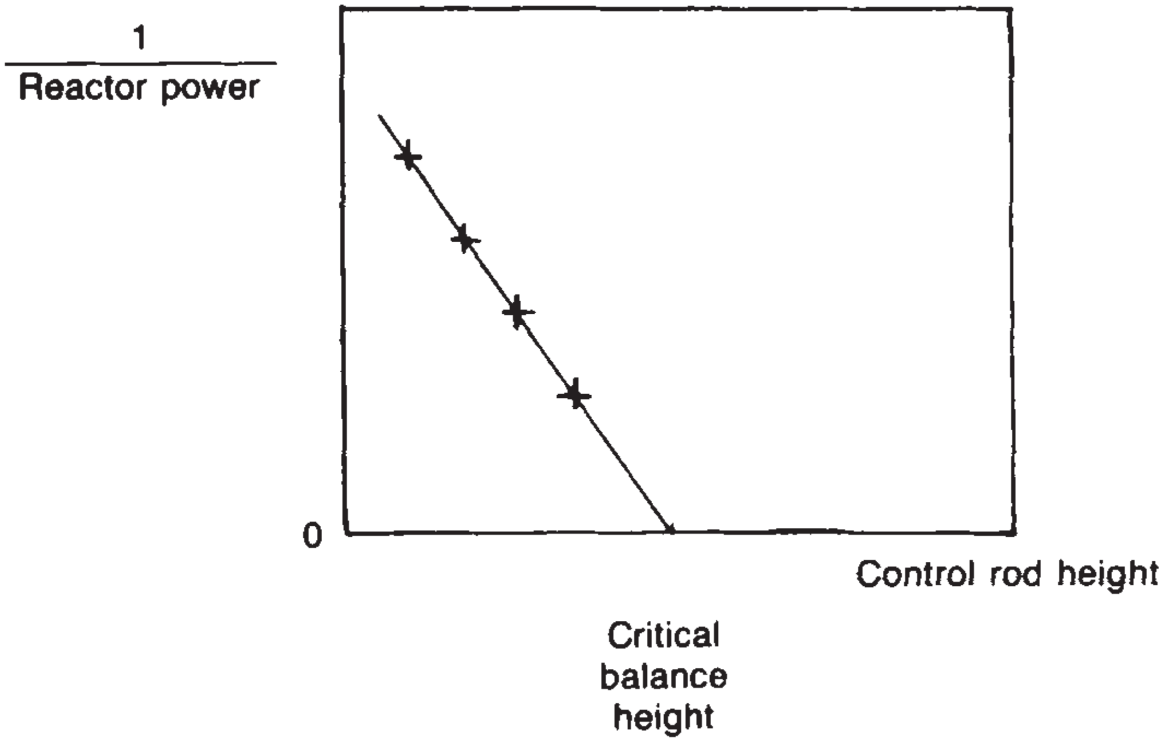

Figure 21. The determination of critical balance height during a critical approach .

if the reactor is just subcritical. So, for such a reactor:

$$Reactor\ power = -\frac{P_s}{\rho}$$

For a typical reactor, the shutdown ('neutron') power P_s is of the order of 50 mW or so.

During a critical approach, the reactivity ρ is increased by raising the control rods. However when $\rho = 0$ (i.e. the reactor is just critical) equation (look equation above) becomes meaningless. The control rod height to give a reactivity of exactly zero – the critical balance height – may therefore be determined by extrapolating a line of points plotted on a graph of (1/power) versus (control rod height) as shown in Fig. 21. Values for reactor power may be obtained from the reactor nucleonic instrumentation.

MC

Introduction to Monte Carlo Methods

1 Introduction to Monte Carlo Methods

Numerical methods that are known as Monte Carlo methods can be loosely described as statistical simulation methods, where statistical simulation is defined in quite general terms to be any method that utilizes sequences of random numbers to perform the simulation. Monte Carlo methods have been used for centuries, but only in the past several decades has the technique gained the status of a full-fledged numerical method capable of addressing the most complex applications. The name "Monte Carlo" was coined by Metropolis (inspired by Ulam's interest in poker) during the Manhattan Project of World War II, because of the similarity of statistical simulation to games of chance, and because the capital of Monaco was a center for gambling and similar pursuits. Monte Carlo is now used routinely in many diverse fields, from the simulation of complex physical phenomena such as radiation transport in the earth's atmosphere and the simulation of the esoteric subnuclear processes in high energy physics experiments, to the mundane, such as the simulation of a Bingo game or the outcome of Monty Hall's vexing offer to the contestant in "Let's Make a Deal." The analogy of Monte Carlo methods to games of chance is a good one, but the "game" is a physical system, and the outcome of the game is not a pot of money or stack of chips (unless simulated) but rather a solution to some problem. The "winner" is the scientist, who judges the value of his results on their intrinsic worth, rather than the extrinsic worth of his holdings.

Statistical simulation methods may be contrasted to conventional numerical discretization methods, which typically are applied to ordinary or partial differential equations that describe some underlying physical or mathematical system. In many applications of Monte Carlo, the physical process is simulated directly, and there is no need to even write down the differential equations that describe the behavior of the system. The only requirement is that the physical (or mathematical) system be described by probability density functions (pdf's), which will be discussed in more detail later in this chapter. For now, we will assume that the behavior of a system can be described by pdf's. Once the pdf's are known, the Monte Carlo simulation can proceed by random sampling from the pdf's. Many simulations are then performed (multiple "trials" or "histories") and the desired result is taken as an average over the number of observations (which may be a single observation or perhaps millions of observations). In many practical applications, one can predict the statistical error (the "variance") in this average result, and hence an estimate of the number of Monte Carlo trials that are needed to achieve a given error.

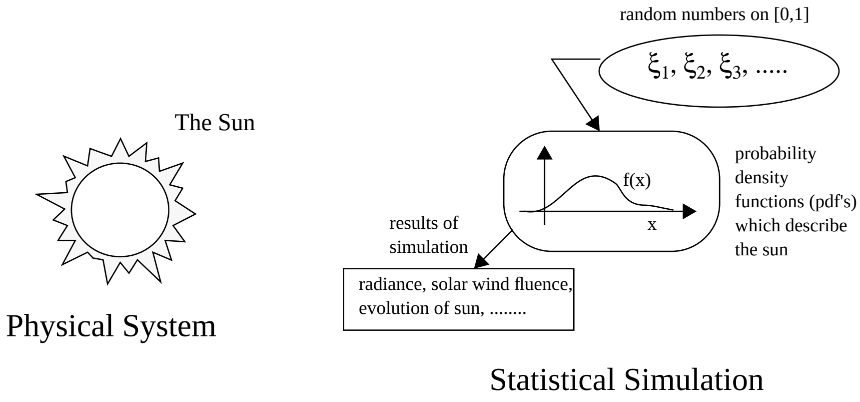

Figure 1: Monte Carlo Simulation of Physical System

Figure 1 illustrates the idea of Monte Carlo, or statistical, simulation as applied to an arbitrary physical system. Assuming that the evolution of the physical system can be described by probability density functions (pdf's), then the Monte Carlo simulation can proceed by sampling from these pdf's, which necessitates a fast and effective way to generate random numbers uniformly distributed on the interval [0,1]. The outcomes of these random samplings, or trials, must be accumulated or tallied in an appropriate manner to produce the desired result, but the essential characteristic of Monte Carlo is the use of random sampling techniques (and perhaps other algebra to manipulate the outcomes) to arrive at a solution of the physical problem. In contrast, a conventional numerical solution approach would start with the mathematical model of the physical system, discretizing the differential equations and then solving a set of algebraic equations for the unknown state of the system.

It should be kept in mind though that this general description of Monte Carlo methods may not directly apply to some applications. It is natural to think that Monte Carlo methods are used to simulate random, or stochastic, processes, since these can be described by pdf's. However, this coupling is actually too restrictive because many Monte Carlo applications have no apparent stochastic content, such as the evaluation of a definite integral or the inversion of a system of linear equations. However, in these cases and others, one can pose the desired solution in terms of pdf's, and while this transformation may seem artificial, this step allows the system to be *treated* as a stochastic process for the purpose of simulation and hence Monte Carlo methods can be applied to simulate the system. Therefore, we take a broad view of the definition of Monte Carlo methods and include in the Monte Carlo rubric all methods that involve statistical simulation of some underlying system, whether or not the system represents a real physical process.

To illustrate the diversity of Monte Carlo methods, Figure 2 lists applications that have been addressed with statistical simulation techniques. As can be seen, the range of applications is enormous, from the simulation of galactic formation to quantum chromodynamics

Nuclear reactor design
Quantum chromodynamics
Radiation cancer therapy
Traffic flow
Stellar evolution
Econometrics
Dow-Jones forecasting
Oil well exploration
VLSI design

Figure 2: Monte Carlo Applications

to the solution of systems of linear equations.

This wide diversity of methods is the reason that "Monte Carlo is not Monte Carlo is not Monte Carlo."

1.1 Major Components of a Monte Carlo Algorithm

Given our definition of Monte Carlo, let us now describe briefly the major components of a Monte Carlo method. These components comprise the foundation of most Monte Carlo applications, and the following sections will explore them in more detail. An understanding of these major components will provide a sound foundation for the reader to construct his or her own Monte Carlo method, although of course the physics and mathematics of the specific application are well beyond the scope of this chapter. The primary components of a Monte Carlo simulation method include the following:

- *Probability distribution functions (pdf's)* — the physical (or mathematical) system must be described by a set of pdf's.

- *Random number generator* — a source of random numbers uniformly distributed on the unit interval must be available.

- *Sampling rule* — a prescription for sampling from the specified pdf's, assuming the availability of random numbers on the unit interval, must be given.

- *Scoring (or tallying)* — the outcomes must be accumulated into overall tallies or scores for the quantities of interest.

- *Error estimation* — an estimate of the statistical error (variance) as a function of the number of trials and other quantities must be determined.

- *Variance reduction techniques* — methods for reducing the variance in the estimated solution to reduce the computational time for Monte Carlo simulation
- *Parallelization and vectorization* — algorithms to allow Monte Carlo methods to be implemented efficiently on advanced computer architectures.

The remainder of this chapter will treat each of these topics in some detail. Later chapters will describe specific applications of the Monte Carlo method, relying on material in this chapter for the generic aspects common to most, if not all, such methods. But before we actually delve into the subject of Monte Carlo methods, let us look backwards and review some of their history.

1.2 History of Monte Carlo

Continue with Pat Burns contributions here.

2 An Introduction to Probability and Statistics

An essential component of a Monte Carlo simulation is the modeling of the physical process by one or more probability density functions (pdf's). By describing the process as a *pdf*, which may have its origins in experimental data or in a theoretical model describing the physics of the process, one can sample an "outcome" from the pdf, thus simulating the actual physical process. For example, the simulation of the transport of 2 MeV neutrons in a tank of water will necessitate sampling from a pdf that will yield the distance the neutron travels in the water before suffering a collision with a water molecule. This pdf is the well-known exponential distribution and is an example of a continuous pdf because the outcomes (distances to collision) are described by real numbers. The exponential distribution will be described in more detail later in this chapter. On the other hand, the simulation of roulette will require sampling from a discrete pdf that describes the probability of obtaining one of the 37 (36 outside the U.S.) numbers on a roulette wheel.

2.1 Sample Spaces, Outcomes, and Events

Let us now be more precise about our terminology and define some additional terms that lead to the concept of a pdf. Consistent with standard textbooks (e.g., [Hamming] or [DeGroot]), we will refer to the physical or mathematical process as an *experiment*, and this experiment has a number (possibly infinite) of *outcomes*, to which we will assign probabilities. The *sample space* S of the experiment is the collection of all possible outcomes s. Thus if the experiment is carried out, its outcome is assured to be in the sample space S. We will also describe one realization of the experiment as a *trial*, and by definition a trial will have an outcome s in the sample space S. The experiment may result in the occurrence of a specific *event* E_k. An event may be viewed as a consequence of the outcome (or outcomes) of the experiment. Let us now illustrate these concepts with a simple example.

Example 1

An illustration of an experiment and the terminology used in the experiment.

The experiment consists of one roll of a normal die (with faces labeled 1, 2, 3, 4, 5, and 6) and observing the top face of the die. The outcomes s_i are the six faces, and the sample space S consists of these six outcomes, since every realization of the experiment (i.e., each trial) results in one of these faces being the top face. (We will assume that the die will not balance on an edge or corner.) Events can then be defined in terms of the possible outcomes. Possible events that may be defined in terms of the six unique outcomes are:

- E_1: top face is an even number
- E_2: top face is larger than 4
- E_3: top face is equal to 2 (hence the event is one of the outcomes)

Disjoint events are events that cannot happen at the same time. In the above example, events E_2 and E_3 are disjoint, because a single roll of the die (as the experiment was defined) cannot lead to both events occurring. On the other hand, events E_1 and E_3 can occur at the same time, as can events E_1 and E_2.

2.2 Probability

Since this chapter is not intended to be a complete and rigorous treatment of probability, we will avoid the formal theory of probability and instead present a functional description. This should be sufficient preparation to understand the concept of a pdf, which is the goal of this section. The reader who is interested in delving deeper into the subject is encouraged to read the standard textbooks on the subject, a couple of which were named above.

To an event E_k we will assign a probability p_k, which is also denoted $P(E_k)$, or "probability of event E_k". The quantity p_k must satisfy the properties given in Figure 3 to be a legitimate probability.

2.2.1 Joint, marginal, and conditional probabilities

We now consider an experiment that consists of two parts, and each part leads to the occurrence of specified events. Let us define events arising from the first part of the experiment by F_i with probability f_i and events from the second part by G_j with probability g_j. The combination of events F_i and G_j may be called a *composite* event, denoted by the ordered pair $E_{ij} = (F_i, G_j)$. We wish to generalize the definition of probability to apply to the composite event E_{ij}. The *joint* probability p_{ij} is defined to be the probability that the first part

Figure 3: Properties of a Valid Probability p_k

- $0 \leq p_k \leq 1$
- If E_k is certain to occur, $p_k = 1$.
  If E_k is certain not to occur, $p_k = 0$.
- If events E_i and E_j are mutually exclusive, then
  $P(E_i \text{ and } E_j) = 0$
  $P(E_i \text{ or } E_j) = p_i + p_j$
- If events E_i, $i = 1, 2, \ldots, N$, are mutually exclusive and exhaustive (one of the N events E_i is assured to occur), then

$$\textstyle\sum_{i=1}^{N} p_i = 1$$

of the experiment led to event F_i and the second part of the experiment led to event G_j. Thus, the joint probability p_{ij} is the probability that the composite event E_{ij} occurred (i.e., the probability that both events F_i and G_j occur).

Any joint probability can be factored into the product of a marginal probability and a conditional probability:

$$p_{ij} = p(i)\, p(j|i) \tag{1}$$

where p_{ij} is the joint probability, $p(i)$ is the *marginal* probability (the probability that event F_i occurs *regardless* of event G_j), and $p(j|i)$ is the *conditional* probability (the probability that event G_j occurs *given that event F_i occurs*). Note that the marginal probability for event F_i to occur is simply the probability that the event F_i occurs, or $p(i) = f_i$. Let us now assume that there are J mutually-exclusive events G_j, $j = 1, \ldots, J$ and the following identity is evident:

$$p(i) = \sum_{k=1}^{J} p_{ik} \tag{2}$$

Using Eq. (2), we easily manipulate Eq. (1) to obtain the following expression for the joint probability

$$p_{ij} = p_{ij} \left(\frac{\sum\limits_{k=1}^{J} p_{ik}}{\sum\limits_{k=1}^{J} p_{ik}} \right) = p(i) \left(\frac{p_{ij}}{\sum\limits_{k=1}^{J} p_{ik}} \right) \tag{3}$$

Using Eq. (1), Eq. (3) leads to the following expression for the conditional probability:

$$p(j|i) = \frac{p_{ij}}{\sum\limits_{k=1}^{J} p_{ik}} \tag{4}$$

It is important to note that the joint probability p_{ij}, the marginal probability $p(i)$, and the conditional probability $p(j|i)$ are all legitimate probabilities, hence they satisfy the properties given in the box above. Finally, it is straightforward to generalize these definitions to treat a three-part experiment that has a composite event consisting of three events, or in general an n-part experiment with n events occurring.

If events F_i and G_j are *independent*, then the probability of one occurring does not affect the probability of the other occurring, therefore:

$$p_{ij} = f_i g_j \tag{5}$$

Using Eq. (4), Eq. (5) leads immediately to

$$p(j|i) = g_j \tag{6}$$

for independent events F_i and G_j. This last equation reflects the fact that the probability of event G_j occurring is independent of whether event F_i has occurred, *if events F_i and G_j are independent.*

2.2.2 Random variables

We now define the concept of a random variable, a key definition in probability and statistics and for statistical simulation in general. We define a random variable as a real number x_i that is assigned to an event E_i. It is random because the event E_i is random, and it is variable because the assignment of the value may vary over the real axis. We will use "r.v." as an abbreviation for "random variable".

Example 2

Assign the number $10n$ to each face n of a die. When face n appears, the r.v. is $10n$.

Random variables are useful because they allow the quantification of random processes, and they facilitate numerical manipulations, such as the definition of mean and standard deviation, to be introduced below. For example, if one were drawing balls of different colors from a bowl, it would be difficult to envision an "average" color, although if numbers were assigned to the different colored balls, then an average could be computed. On the other hand, in many cases of real interest, there is no reasonable way to assign a real number to the outcome of the random process, such as the outcome of the interaction between a 1 eV neutron and a uranium-235 nucleus, which might lead to fission, capture, or scatter. In this case, defining an "average" interaction makes no sense, and assigning a real number to the random process does not assist us in that regard. Nevertheless, in the following discussion, we have tacitly assumed a real number x_i has been assigned to the event E_i that we know occurs with probability p_i. Thus, one can in essence say that the r.v. x_i occurs with probability p_i.

2.2.3 Expectation value, variance, functions of r.v.'s

Now that we have assigned a number to the outcome of an event, we can define an "average" value for the r.v. over the possible events. This average value is called the *expectation value* for the random variable x, and has the following definition:

$$\text{expectation value (or mean)} \equiv E(x) = \bar{x} - \sum_i p_i x_i \tag{7}$$

One can define a unique, real-valued function of a r.v., which will also be a r.v. That is, given a r.v. x, then the real-valued function $g(x)$ is also a r.v. and we can define the expectation value of $g(x)$:

$$E[g(x)] = \bar{g} = \sum_i p_i \, g(x_i) \tag{8}$$

The expectation value of a linear combination of r.v.'s is simply the linear combination of their respective expectation values;

$$E[ag(x) + bh(x)] = aE[g(x)] + bE[h(x)] \tag{9}$$

The expectation value is simply the "first moment" of the r.v., meaning that one is finding the average of the r.v. itself, rather than its square or cube or square root. Thus the mean is the average value of the first moment of the r.v., and one might ask whether or not averages of the higher moments have any significance. In fact, the average of the square of the r.v. does lead to an important quantity, the *variance*, and we will now define the higher moments of a r.v. x as follows:

$$E(x^n) = \overline{x^n} \tag{10}$$

We also define "central" moments that express the variation of a r.v. about its mean, hence "corrected for the mean":

$$n^{\text{th}} \text{ central moment } = \overline{(x - \bar{x})^n} \tag{11}$$

The first central moment is zero. The second central moment is the *variance:*

$$\text{variance } \equiv \text{var}(x) \equiv \sigma^2(x) = \overline{(x - \bar{x})^2} = \sum_i p_i (x_i - \bar{x})^2 \tag{12}$$

It is straightforward to show the following important identity:

$$\sigma^2 = \overline{x^2} - \bar{x}^2 \tag{13}$$

We will also find useful the square root of the variance, which is the *standard deviation*,

$$\text{standard deviation } = \sigma(x) = [\text{var}(x)]^{1/2} \tag{14}$$

2.2.4 Variance of linear combination

The mean of a linear combination of r.v.'s is the linear combination of the means, as shown in Eq. (9), because the mean is a linear statistic, as is clear from Eq. (7). On the other hand, the variance is clearly not a linear statistic, since the r.v. is squared. However, we will find it necessary to consider the variance of a linear combination of r.v.'s, and it is straightforward to show the following:

$$\sigma^2(ag+bh) = a^2\sigma^2(g) + b^2\sigma^2(h) + 2ab[\overline{gh} - \bar{g}\bar{h}] \tag{15}$$

Let us consider the average value of the product of two r.v.'s:

$$E(xy) = \sum_{i,j} p_{ij}\, x_i\, y_j \tag{16}$$

Now if x and y are independent r.v.'s, then

$$p_{ij} = p_i q_j, \tag{17}$$

where q_j is the probability for the r.v. y_j to occur. But if Eq. (17) is inserted into Eq. (16), we find

$$\begin{aligned} E(xy) &= \sum_{i,j} p_{ij}\, x_i\, y_j = \sum_{i,j} p_i\, q_j\, x_i\, y_j \\ &= \sum_i p_i x_i \sum_j q_j y_j = E(x)E(y) \end{aligned} \tag{18}$$

Thus, if two r.v.'s are independent, the expectation value of their product is the product of their expectation values. Now consider the case of the variance of a linear combination of r.v.'s given in Eq. (15), and note that if the r.v.'s g and h are independent, Eq. (18) when inserted into Eq. (15) yields the following expression, *valid only when* $g(x)$ *and* $h(x)$ *are independent r.v.'s:*

$$\sigma^2[ag(x) + bh(x)] = a^2\sigma^2(g) + b^2\sigma^2(h) \tag{19}$$

2.2.5 Covariance and correlation coefficient

The cancellation of the last term in Eq. (15) for independent r.v.'s motivates the concept of the *covariance.*

$$\text{covariance } = \text{cov}(x,y) = \overline{xy} - \bar{x}\bar{y} \tag{20}$$

If x and y are independent, then $\text{cov}(x,y) = 0$. However, it is possible to have $\text{cov}(x,y) = 0$ even if x and y are not independent. It should be noted that the covariance can be negative. A related quantity that arises often in statistical analysis is the *correlation coefficient*, which is a convenient measure of the degree to which two r.v.'s are correlated (or anti-correlated).

$$\text{correlation coefficient } = \rho(x,y) = \text{cov}(x,y)/[\sigma^2(x)\sigma^2(y)]^{1/2} \tag{21}$$

It is easily shown that $-1 \le \rho(x,y) \le 1$.

2.3 Continuous Random Variables

So far we have considered only discrete r.v.'s, that is, a specific number x_i is assigned to the event E_i, but what if the events cannot be enumerated by integers, such as the angle of scattering for an electron scattering off a gold nucleus or the time to failure for a computer chip? The above definitions for discrete r.v.'s can be easily generalized to the continuous case.

First of all, if there is a continuous range of values, such as an angle between 0 and 2π, then the probability of getting exactly a specific angle is zero, because there are an infinite number of angles to choose from, and it would be impossible to choose exactly the correct angle. For example, the probability of choosing the angle $\theta = 1.34$ radians must be zero, since there are an infinite number of alternative angles. In fact, there are an infinite number of angles between 1.33 and 1.35 radians or between 1.335 and 1.345 radians, hence the probability of a given angle must be zero. However, we can talk about the probability of a r.v. taking on a value *within* a given interval, e.g., an angle θ between 1.33 and 1.35 radians. To do this, we define a probability density function, or *pdf.*

2.3.1 Probability density function (pdf)

The significance of the pdf $f(x)$ is that $f(x)\,dx$ is the probability that the r.v. is in the interval $(x, x + dx)$, written as:

$$\text{prob}(x \le x' \le x + dx) \equiv P(x \le x' \le x + dx) = f(x)\,dx \tag{22}$$

This is an operational definition of $f(x)$. Since $f(x)\,dx$ is unitless (it is a probability), then $f(x)$ has units of inverse r.v. units, e.g., 1/cm or 1/s or 1/cm^2, depending on the units of x. Figure 4 shows a typical pdf $f(x)$ and illustrates the interpretation of the probability of finding the r.v. in $(x, x + dx)$ with the area under the curve $f(x)$ from x to $x + dx$.

We can also determine the probability of finding the r.v. somewhere in the finite interval $[a, b]$:

$$\text{prob}(a \le x \le b) \equiv P(a \le x \le b) = \int_a^b f(x')\,dx' \tag{23}$$

which, of course, is the area under the curve $f(x)$ from $x = a$ to $x = b$.

As with the definition of discrete probability distributions, there are some restrictions on the pdf. Since $f(x)$ is a probability density, it must be positive for all values of the r.v. x. Furthermore, the probability of finding the r.v. *somewhere* on the real axis must be unity. As it turns out, these two conditions are the only necessary conditions for $f(x)$ to be a legitimate pdf, and are summarized below.

$$f(x) \ge 0, \quad -\infty < x < \infty \tag{24}$$

$$\int_{-\infty}^{\infty} f(x')\,dx' = 1 \tag{25}$$

Note that these restrictions are not very stringent, and in fact allow one to apply Monte Carlo methods to solve problems that have no apparent stochasticity or randomness. By

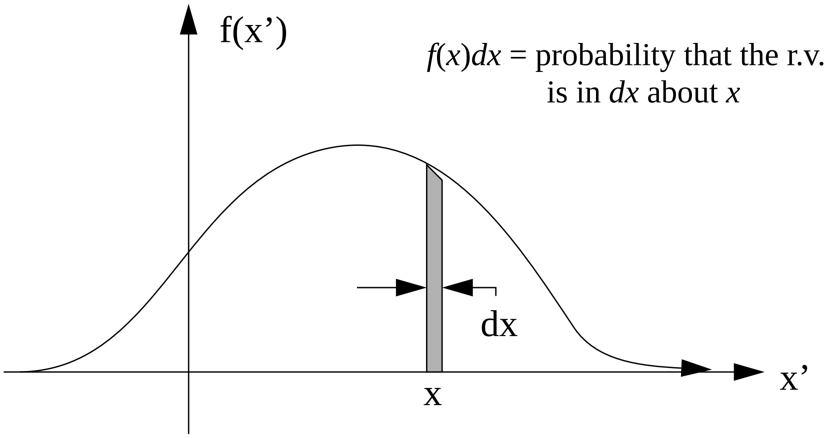

Figure 4: Typical Probability Distribution Function (pdf)

posing a particular application in terms of functions that obey these relatively mild conditions, one can treat them as pdf's and perhaps employ the powerful techniques of Monte Carlo simulation to solve the original application. We now define an important quantity, intimately related to the pdf, that is known as the cumulative distribution function, or *cdf.*

2.3.2 Cumulative distribution function (cdf)

The cumulative distribution function gives the probability that the r.v. x' is less than or equal to x:

$$\begin{aligned} \mathrm{CDF} &\equiv \mathrm{prob}(x' \leq x) \equiv F(x) \\ &= \int_{-\infty}^{x} f(x')\,dx' \end{aligned} \tag{26}$$

Note that since $f(x) \geq 0$, and the integral of $f(x)$ is normalized to unity, $F(x)$ obeys the following conditions:

- $F(x)$ is monotone increasing
- $F(-\infty) = 0$
- $F(+\infty) = 1$

Figure 5 illustrates a representative cdf. Note the dependence of $F(x)$ as $x \to \pm\infty$. Since $F(x)$ is the indefinite integral of $f(x)$, $f(x) = F'(x)$. The cdf can also be defined for a discrete pdf; however, this will be deferred until we discuss the subject of sampling from a discrete distribution.

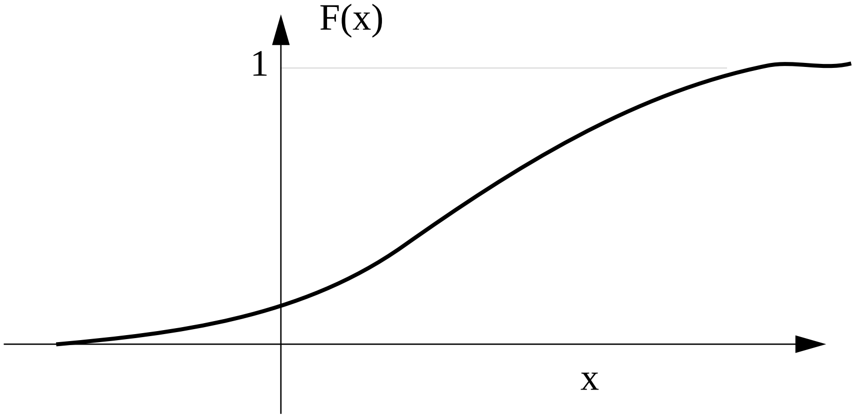

Figure 5: Representative Cumulative Distribution Function (cdf)

2.3.3 Expectation value and variance for continuous pdf's

We can define the expectation value and variance for a continuous pdf, consistent with our earlier definitions for a discrete pdf:

$$E(x) \equiv \mu \equiv \bar{x} = \int_{-\infty}^{\infty} f(x')\, x'\, dx' \tag{27}$$

$$\mathrm{var}(x) \equiv \sigma^2 = \int_{-\infty}^{\infty} f(x')\,(x' - \mu)^2\, dx' \tag{28}$$

Similarly, if we define a real-valued function $g(x)$ of the r.v. x, we readily obtain the following expressions for the mean and variance of g for a continuous pdf:

$$E(g) \equiv \bar{g} = \int_{-\infty}^{\infty} f(x')\, g(x')\, dx' \tag{29}$$

$$\mathrm{var}(g) \equiv \sigma^2(g) = \int_{-\infty}^{\infty} f(x')\,[g(x') - \bar{g}]^2\, dx' \tag{30}$$

It is important to keep in mind that the quantities $\bar{x}$ and $\bar{g}$ are *true* means, *properties* of the pdf $f(x)$ and the function $g(x)$. In many cases of practical interest the true mean is not known, and the purpose of the Monte Carlo simulation will be to *estimate* the true mean. These estimates will be denoted by a caret or hat, e.g., $\hat{x}$ and $\hat{g}$. Thus the result of a Monte Carlo simulation might be $\hat{g}$, and the hope is that this is a good approximation to the true (but unknown) quantity $\bar{g}$. This notation will be adhered to throughout this chapter on Monte Carlo methods.

2.3.4 Relationship of discrete and continuous pdf's

Compare these definitions for a continuous pdf with the previous definitions for the mean and variance for a discrete pdf, given in Eq. (7) and Eq. (12), respectively, and reproduced below for convenience (where the subscript "d" corresponds to "discrete"):

$$E_{\mathrm{d}}(x) = \sum_{i=1}^{N} p_i x_i$$

$$\mathrm{var}_{\mathrm{d}}(x) = \sum_{i=1}^{N} p_i (x_i - \mu)^2$$

Now take the limit $N \to \infty$ to pass from the discrete to the continuous versions for these quantities:

$$\begin{aligned} \lim_{N\to\infty} E_{\mathrm{d}}(x) &= \lim_{N\to\infty} \sum_{i=1}^{N} x_i p_i = \lim_{N\to\infty} \sum_{i=1}^{N} x_i \frac{p_i}{\Delta x_i} \Delta x_i \\ &= \lim_{N\to\infty} \sum_{i=1}^{N} x_i\, f_i\, \Delta x_i = \int_{-\infty}^{\infty} f(x')\, x'\, dx' \\ &= E(x) \end{aligned} \tag{31}$$

$$\begin{aligned} \lim_{N\to\infty} \mathrm{var}_{\mathrm{d}}(x) &= \lim_{N\to\infty} \sum_{i=1}^{N} (x_i - \mu^2)\, p_i = \lim_{N\to\infty} \sum_{i=1}^{N} (x_i - \mu^2) \frac{p_i}{\Delta x_i} \Delta x_i \\ &= \lim_{N\to\infty} \sum_{i=1}^{N} (x_i - \mu^2)\, f_i\, \Delta x_i = \int_{-\infty}^{\infty} f(x')\, (x' - \mu^2)\, dx' \\ &= \mathrm{var}(x) \end{aligned} \tag{32}$$

2.4 Examples: Continuous pdf's

2.4.1 Exponential distribution

$$f(x) = \lambda e^{-\lambda x}, \quad x \geq 0, \ \ \lambda > 0 \tag{33}$$

This distribution can describe a number of physical phenomena, such as the time t for a radioactive nucleus to decay, or the time x for a component to fail, or the distance z a photon travels in the atmosphere before suffering a collision with a water molecule. The exponential distribution is characterized by the single parameter λ, and one can easily show that the mean and variance for the exponential distribution are given by:

$$\mu = \frac{1}{\lambda} \tag{34}$$

$$\sigma^2 = \left(\frac{1}{\lambda}\right)^2 \tag{35}$$

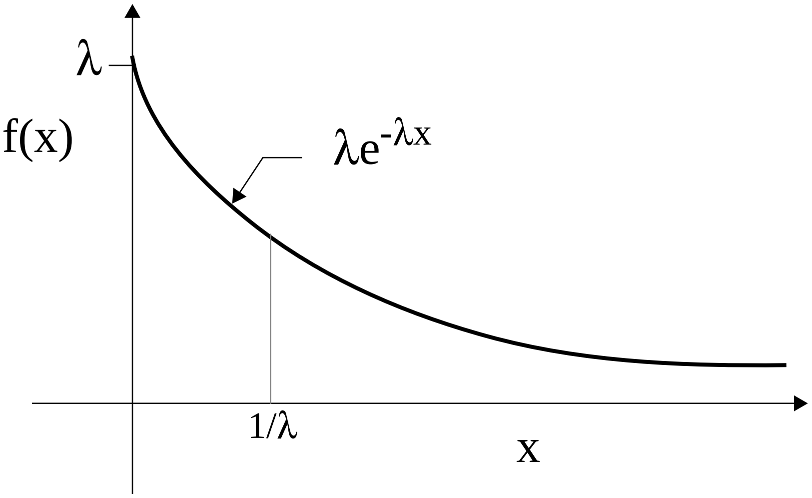

Figure 6: Exponential pdf

Figure 6 illustrates the exponential distribution. Note that the standard deviation of the exponential distribution is

$$\sigma = \frac{1}{\lambda} \tag{36}$$

Later we will learn that we can associate the standard deviation with a sort of expected deviation from the mean, meaning that for the exponential distribution, one would expect most samples x to fall within $1/\lambda$ of μ, even though the actual range of samples x is infinite. One can see this by computing the probability that a sample from the exponential distribution falls within $\sigma/2$ of the mean μ :

$$\text{prob}\left(\mu - \frac{\sigma}{2} \leq x \leq \mu + \frac{\sigma}{2}\right) = \int_{\frac{1}{2\lambda}}^{\frac{3}{2\lambda}} \lambda e^{-\lambda x}\, dx = 0.83$$

hence 83% of the samples from the exponential distribution can be expected to fall within a half of a standard deviation of the mean, although some of the samples will be far from the mean, since $0 \leq x < \infty$.

The second example is perhaps the most important pdf in probability and statistics, the *Gaussian*, or *normal*, distribution.

2.4.2 Gaussian (normal) distribution:

$$f(x) = \frac{1}{(2\pi\sigma)^{1/2}} e^{-\frac{(x-\mu)^2}{2\sigma^2}}, \quad -\infty < x < \infty \tag{37}$$

This is a two-parameter (σ and μ) distribution, and it can be shown that μ is the mean of the distribution and σ^2 is the variance. Figure 7 illustrates the Gaussian pdf.

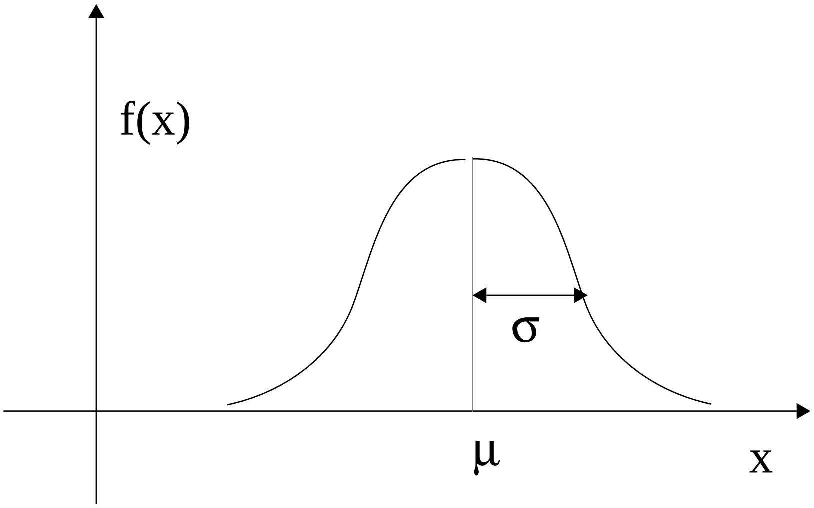

Figure 7: Gaussian (Normal) Probability Distribution Function

Let us calculate the probability that a sample from the Gaussian distribution will fall within a single standard deviation σ of the mean μ:

$$P(\mu - \sigma \leq x \leq \mu + \sigma) = .6826 \tag{38}$$

Similarly, the probability that the sample is within two standard deviations (within "2σ") of the mean is

$$P(\mu - 2\sigma \leq x \leq \mu + 2\sigma) = .9544 \tag{39}$$

hence 68% of the samples will, on average, fall within one σ, and over 95% of the samples will fall within two σ of the mean μ.

The Gaussian distribution will be encountered frequently in this course, not only because it is a fundamental pdf for many physical and mathematical applications, but also because it plays a central role in the estimation of errors with Monte Carlo simulation.

2.4.3 Cauchy distribution

$$f(x) = \frac{a}{a^2 + x^2}, \quad -\infty < x < \infty \tag{40}$$

This is an interesting pdf, because strictly speaking, its mean does not exist and its variance is infinite. Given our definition of mean,

$$\mu = \int_{-\infty}^{\infty} x \, \frac{a}{a^2 + x^2} \, dx \tag{41}$$

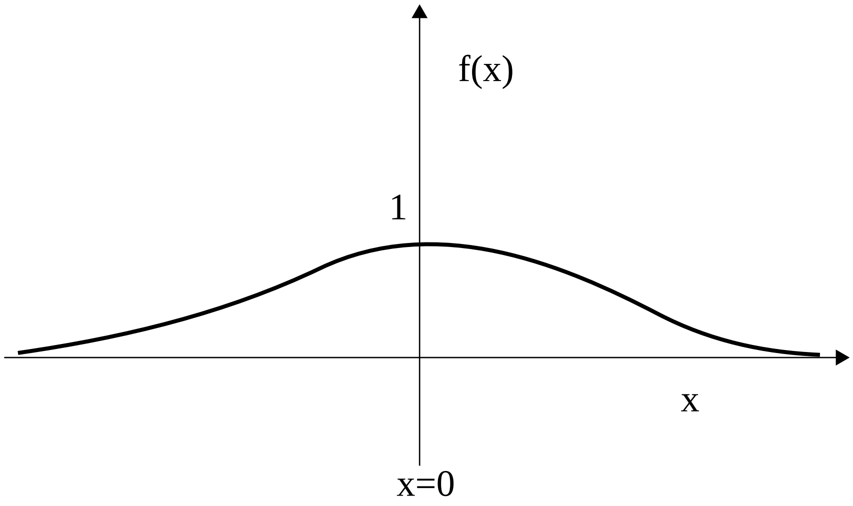

Figure 8: Cauchy Probability Distribution Function

we find that this integral does not exist because the separate integrals for $x > 0$ and $x < 0$ do not exist. However, if we allow a "principal value" integration, where the limits are taken simultaneously, we see that the integral for $x < 0$ will cancel the integral for $x > 0$ and the mean is zero, consistent with a graphical interpretation of this pdf, as depicted in Figure 8. However, if we try to compute the variance, we find:

$$\sigma^2 = \int_{-\infty}^{\infty} (x - \mu)^2 \, \frac{a}{a^2 + x^2} \, dx \tag{42}$$

which is an unbounded integral. Thus if we sample from the Cauchy distribution and we attempt to predict the extent to which samples will fall "close" to the mean, we will fail. Note that the Cauchy distribution is a legitimate pdf, because it satisfies the properties of a pdf given in Eq. (24) and Eq. (25), namely,

$$\int_{-\infty}^{\infty} f(x) \, dx = \int_{-\infty}^{\infty} \frac{a}{a^2 + x^2} \, dx = 1$$

$$f(x) = \frac{a}{a^2 + x^2} \geq 0, \quad \text{all } x$$

but its variance is infinite and its mean necessitates a more general definition of integration.

These have been examples of single random variable, or univariate, pdf's. Let us now consider bivariate pdf's, which generalize readily to multivariate pdf's (the important conceptual step is in going from one to two random variables). Bivariate distributions are needed for a number of important topics in Monte Carlo, including sampling from multidimensional pdf's and the analysis of rejection sampling.

2.4.4 Bivariate Probability Distributions

We now consider two r.v.'s x' and y', where $-\infty < x' < \infty$ and $-\infty < y' < \infty$. We ask what is the probability that the first r.v. x' falls within $[x, x+dx]$ and the second r.v. y' falls within $[y, y+dy]$, which defines the bivariate pdf $f(x,y)$:

$$f(x,y)\,dx\,dy = \text{prob}[(x \leq x' \leq x + dx) \text{ and } (y \leq y' \leq y + dy)] \tag{43}$$

Using this operational definition of $f(x,y)$, let us multiply and divide by the quantity $m(x)$, where we assume $m(x) \neq 0$,

$$m(x) = \int_{-\infty}^{\infty} f(x,y')\,dy' \tag{44}$$

It is readily shown that $m(x)$ satisfies the properties for a legitimate pdf given in Eq. (24) and Eq. (25), and we can interpret $m(x)$ as follows:

$$m(x)\,dx = \text{probability that } x' \text{ is in } dx \text{ about } x, \textit{ irrespective} \text{ of } y'. \tag{45}$$

The quantity $m(x)$ is known as the *marginal* probability distribution function. Now define the quantity $c(y|x)$,

$$c(y|x) = \frac{f(x,y)}{m(x)} \tag{46}$$

As with $m(x)$, it can be shown that $c(y|x)$ is a legitimate pdf and can be interpreted as follows:

$$c(y|x)\,dy = \text{probability that } y' \text{ is in } dy \text{ about } y, \textit{ assuming } x' = x. \tag{47}$$

The quantity $c(y|x)$ is called the *conditional* pdf. The constraint that $m(x) \neq 0$ simply means that the r.v.'s x' and y' are *not mutually exclusive*, meaning there is some probability that both x' and y' will occur together. Note that if x and y are independent r.v.'s, then $m(x)$ and $c(y|x)$ reduce to the univariate pdf's for x and y:

$$m(x) = f(x) \tag{48}$$

$$c(y|x) = g(y) \tag{49}$$

and therefore for independent pdf's we find that the bivariate pdf is simply the product of the two univariate pdf's:

$$f(x,y) = f(x)g(y) \tag{50}$$

2.4.5 Bivariate cdf

The cumulative distribution function for a bivariate pdf is defined in an analogous way to the univariate case:

$$\begin{aligned} F(x,y) &= \text{prob}[x' \leq x \text{ and } y' \leq y] \\ &= \int_{-\infty}^{x} dx' \int_{-\infty}^{y} dy'\, f(x',y') \end{aligned} \tag{51}$$

and we can express the probability that the random doublet (x', y') falls within a finite region of the x–y plane in terms of this pdf:

$$\text{prob}[a \leq x \leq b \text{ and } c \leq y \leq d] = \int_a^b dx' \int_c^d dy' \, f(x', y') \tag{52}$$

2.4.6 Sums of random variables

Now let us draw N samples $x_1, x_2, x_3, \ldots, x_N$ from the pdf $f(x)$ and define the following linear combination of the samples:

$$G = \sum_{n=1}^{N} \lambda_n g_n(x_n) \tag{53}$$

where the parameters λ_n are real constants and the $g_n(x)$ are real-valued functions. Since the x_n are r.v.'s, and G is a linear combination of functions of the r.v.'s, G is also a r.v. We now examine the properties of G, in particular its expectation value and variance. Referring to our earlier discussion of the mean and variance of a linear combination, expressed as Eq. (9) and Eq. (15), respectively, we find

$$E[G] \equiv \overline{G} = E\left[\sum_{n=1}^{N} \lambda_n g_n(x_n)\right] = \sum_{n=1}^{N} \lambda_n E[g_n] = \sum_{n=1}^{N} \lambda_n \overline{g_n} \tag{54}$$

$$\text{var}[G] = \text{var}\left[\sum_{n=1}^{N} \lambda_n g_n(x_n)\right] = \sum_{n=1}^{N} \lambda_n^2 \, \text{var}[g_n] \tag{55}$$

Now consider the special case where $g_n(x) = g(x)$ and $\lambda_n = 1/N$:

$$G = \frac{1}{N} \sum_{n=1}^{N} g(x_n) \tag{56}$$

Note that G is simply the *average* value of the N sampled r.v.'s. Now consider the expectation value for G, using Eq. (56):

$$\overline{G} = \frac{1}{N} E\left[\sum_{n=1}^{N} g(x_n)\right] = \frac{1}{N} \sum_{n=1}^{N} \bar{g} = \bar{g} \tag{57}$$

In other words, the *expectation value* for the average (*not* the average itself!) of N observations of the r.v. $g(x)$ is simply the expectation value for $g(x)$. This statement is not as trivial as it may seem, because we may not know $E[g]$ in general, because $E[g]$ is a property of $g(x)$ and the pdf $f(x)$. However, Eq. (57) assures us that an average of N observations of $g(x)$ will be a reasonable estimate of $E[g]$. Later, we will introduce the concept of an unbiased estimator, and suffice to say for now, that Eq. (57) proves that the simple average is an unbiased estimator for the mean. Now let us consider the variance in G, in particular its dependence on the sample size.

Considering again the case where $g_n(x) = g(x)$ and $\lambda_n = 1/N$, and using Eq. (55), the variance in the linear combination G is given by:

$$\mathrm{var}(G) = \left(\frac{1}{N}\right)^2 \sum_{n=1}^{N} \mathrm{var}[g(x_n)] = \left(\frac{1}{N}\right)^2 \sum_{n=1}^{N} \mathrm{var}(g) = \frac{1}{N}\mathrm{var}(g) \tag{58}$$

hence the variance in the average value of N samples of $g(x)$ is a factor of N smaller than the variance in the original r.v. $g(x)$. Note that we have yet to say anything about how to estimate var(G), only that its value decreases as $1/N$.

This point deserves further elaboration. The quantities $E(g)$ and var(g) are *properties* of the pdf $f(x)$ and the real function $g(x)$. As mentioned earlier, they are known as the *true mean* and *true variance*, respectively, because they are known *a priori*, given the pdf $f(x)$ and the function $g(x)$. Then if we consider a simple average of N samples of $g(x)$, denoted G, Eq. (57) tells us that the true mean for G is equal to the true mean for $g(x)$. On the other hand, Eq. (58) tells us that the *true variance for G is $1/N$ smaller than the true variance for $g(x)$*, an important consequence for estimating errors.

Later we will show how to estimate var(G), an important task since in general we don't know the true mean and variance, and these terms will have to be estimated. Let us now apply this discussion to an important application of Monte Carlo methods, the evaluation of definite integrals.

2.4.7 Monte Carlo Integration (our first application of Monte Carlo)

We would like to evaluate the following definite integral,

$$I = \int_a^b g(x)\,dx \tag{59}$$

where we assume that $g(x)$ is real-valued on $(-\infty, \infty)$. Figure 9 depicts a typical integral to be evaluated.

The idea is to manipulate the definite integral into a form that can be solved by Monte Carlo. To do this, we define the following function on $[a, b]$,

$$f(x) = \begin{cases} 1/(b-a), & a \le x \le b \\ 0, & \text{otherwise} \end{cases} \tag{60}$$

and insert into Eq. (59) to obtain the following expression for the integral I:

$$I = \frac{1}{b-a}\int_a^b g(x)\,f(x)\,dx \tag{61}$$

Note that $f(x)$ can be viewed as a uniform pdf on the interval $[a, b]$, as depicted in Figure 9. Given that $f(x)$ is a pdf, we observe that the integral on the right hand side of Eq. (61) is simply the expectation value for $g(x)$:

$$I = \frac{1}{b-a}\int_a^b g(x)\,f(x)\,dx = \frac{1}{b-a}\bar{g} \tag{62}$$

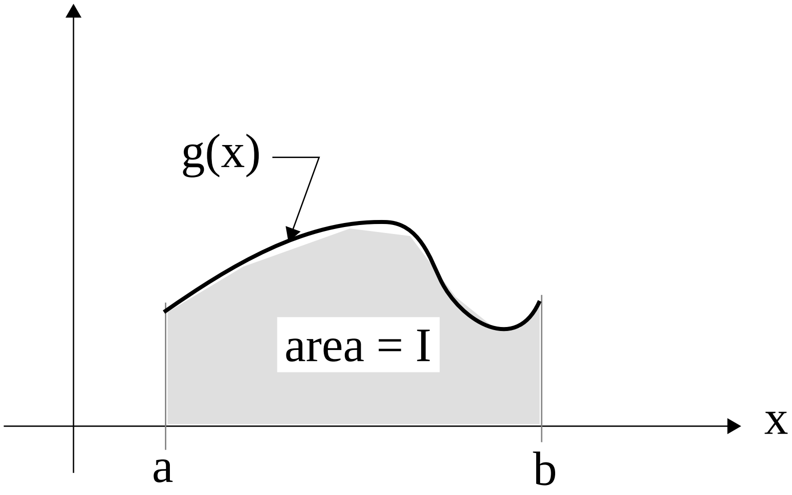

Figure 9: Monte Carlo Integration

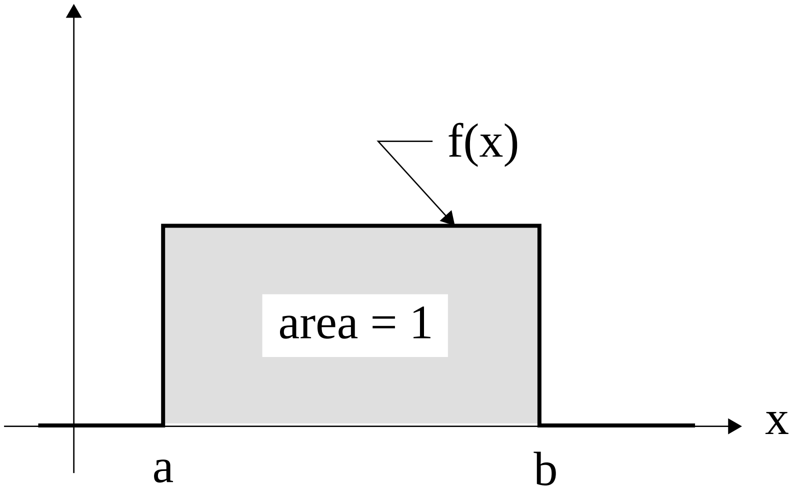

Figure 10: Uniform pdf on [a,b]

We now draw samples x_n from the pdf $f(x)$, and for each x_n we will evaluate $g(x_n)$ and form the average G,

$$G = \frac{1}{N} \sum_{n=1}^{N} g(x_n) \tag{63}$$

But Eq. (57) states the expectation value for the average of N samples is the expectation value for $g(x)$, $\overline{G} = \bar{g}$, hence

$$I = \frac{1}{b-a} \overline{G} \approx \frac{1}{b-a} G = \frac{1}{b-a} \left(\frac{1}{N} \sum_{i=1}^{N} g(x_n) \right) \tag{64}$$

Thus we can *estimate* the true value of the integral I on $[a,b]$ by taking the average of N observations of the integrand, with the r.v. x sampled uniformly over the interval $[a,b]$. For now, this implies that the interval $[a,b]$ is finite, since an infinite interval cannot have a uniform pdf. We will see later that infinite ranges of integration can be accommodated with more sophisticated techniques.

Recall that Eq. (58) related the true variance in the average G to the true variance in g,

$$\mathrm{var}(G) = \frac{1}{N} \mathrm{var}(g) \tag{65}$$

Although we do not know $\mathrm{var}(g)$, since it is a property of the pdf $f(x)$ and the real function $g(x)$, it is a constant. Furthermore, if we associate the error in our estimate of the integral I with the standard deviation, then we might expect the error in the estimate of I to decrease by the factor $N^{-1/2}$. This will be shown more rigorously later when we consider the Central Limit Theorem, but now we are arguing on the basis of the functional form of $\mathrm{var}(G)$ and a hazy correspondence of standard deviation with "error". What we are missing is a way to estimate $\mathrm{var}(g)$, as we were able to estimate $E(g)$ with G.

3 Sampling from Probability Distribution Functions

As described earlier, a Monte Carlo simulation consists of some physical or mathematical system that can be described in terms of probability distribution functions, or pdf's. These pdf's, supplemented perhaps by additional computations, describe the evolution of the overall system, whether in space, or energy, or time, or even some higher dimensional phase space. The goal of the Monte Carlo method is to simulate the physical system by random sampling from these pdf's and by performing the necessary supplementary computations needed to describe the system evolution. In essence, the physics and mathematics are replaced by random sampling of possible states from pdf's that describe the system. We now turn our attention to how one actually obtains random samples from arbitrary pdf's.

This chapter will consider sampling from both continuous and discrete pdf's, and the following chart summarizes the important properties of both types of pdf's:

Property	**Continuous:** $f(x)$	**Discrete:** $\{p_i\}$
Positivity	$f(x) \geq 0$, all x	$p_i > 0$, all i
Normalization	$\int_{-\infty}^{\infty} f(x')\,dx' = 1$	$\sum_{j=1}^{N} p_j = 1$
Interpretation	$f(x)\,dx$ $\text{prob}(x \leq x' \leq x + dx)$	$p_i = \text{prob}(i) =$ $\text{prob}(x_j = x_i)$
Mean	$\bar{x} = \int_{-\infty}^{\infty} x f(x)\,dx$	$\bar{x} = \sum_{j=1}^{N} x_j p_j$
Variance	$\sigma^2 = \int_{-\infty}^{\infty} (x - \bar{x})^2 f(x)\,dx$	$\sigma^2 = \sum_{j=1}^{N} (x_j - \bar{x})^2 p_j$

We will now discuss how to obtain a random sample x from either a continuous pdf $f(x)$ or a discrete pdf $\{p_i\}$.

3.1 Equivalent continuous pdf's

It will be convenient to express a discrete pdf as a continuous pdf using "delta functions". This will make the ensuing discussion easier to follow and simplifies many of the manipulations for discrete pdf's. Given a discrete pdf $\{p_i\}$, let us associate event i with the discrete r.v. x_i, and then define an equivalent "continuous" pdf as follows:

$$f(x) = \sum_{i=1}^{N} p_i\,\delta(x - x_i) \tag{66}$$

Here $\delta(x - x_i)$ is the "delta" function and it satisfies the following properties:

$$\int_{-\infty}^{\infty} \delta(x - x_i)\,dx = 1 \tag{67}$$

$$\int_{-\infty}^{\infty} f(x)\,\delta(x - x_i)\,dx = f(x_i) \tag{68}$$

Using these properties, it is straightforward to show that the mean and variance of the equivalent continuous pdf, as defined in Eq. (66), are identical to the mean and variance of the original discrete pdf. Begin with the definition of the mean of the equivalent continuous pdf:

$$\bar{x} = \int_{-\infty}^{\infty} x\,f(x)\,dx = \int_{-\infty}^{\infty} x \left[\sum_{i=1}^{N} p_i\,\delta(x - x_i)\right] dx \tag{69}$$

Now take the summation outside the integral and use Eq. (68),

$$\bar{x} = \sum_{i=1}^{N} \int_{-\infty}^{\infty} x p_i\,\delta(x - x_i)\,dx = \sum_{i=1}^{N} x_i\,p_i \tag{70}$$

which is the true mean for the discrete pdf. It is left as an exercise to show that this also holds for the variance, and in general for any moment of the distribution.

Much of the material that follows holds for both discrete and continuous pdf's, and this equivalence will be useful in this discussion.

3.2 Transformation of pdf's

In order to have a complete discussion of sampling, we need to explain transformation rules for pdf's. That is, given a pdf $f(x)$, one defines a new variable $y = y(x)$, and the goal is to find the pdf $g(y)$ that describes the probability that the r.v. y occurs. For example, given the pdf $f(E)$ for the energy of the scattered neutron in an elastic scattering reaction from a nucleus of mass A, what is the pdf $g(v)$ for the speed v, where $E = \frac{1}{2}mv^2$?

First of all, we need to restrict the transformation $y = y(x)$ to be a unique transformation, because there must be a 1-to-1 relationship between x and y in order to be able to state that a given value of x corresponds unambiguously to a value of y. Given that $y(x)$ is 1-to-1, then it must either be monotone increasing or monotone decreasing, since any other behavior would result in a multiple-valued function $y(x)$.

Let us first assume that the transformation $y(x)$ is monotone increasing, which results in $dy/dx > 0$ for all x. Physically, the mathematical transformation must conserve probability, i.e., the probability of the r.v. x' occurring in dx about x must be the same as the probability of the r.v. y' occurring in dy about y, since if x occurs, the 1-to-1 relationship between x and y necessitates that y appears. But by definition of the pdf's $f(x)$ and $g(y)$,

$$\begin{aligned} f(x)\,dx &= \text{prob}(x \le x' \le x + dx) \\ g(y)\,dy &= \text{prob}(y \le y' \le y + dy) \end{aligned}$$

The physical transformation implies that these probabilities must be equal. Figure 11 illustrates this for an example transformation $y = y(x)$.

Equality of these differential probabilities yields

$$f(x)\,dx = g(y)\,dy \tag{71}$$

and one can then solve for $g(y)$:

$$g(y) = f(x)/[dy/dx] \tag{72}$$

This holds for the monotone increasing function $y(x)$. It is easy to show that for a monotone decreasing function $y(x)$, where $dy/dx < 0$ for all x, the fact that $g(y)$ must be positive (by definition of probability) leads to the following expression for $g(y)$:

$$g(y) = f(x)/[-dy/dx] \tag{73}$$

Combining the two cases leads to the following simple rule for transforming pdf's:

$$g(y) = f(x)/|dy/dx| \tag{74}$$

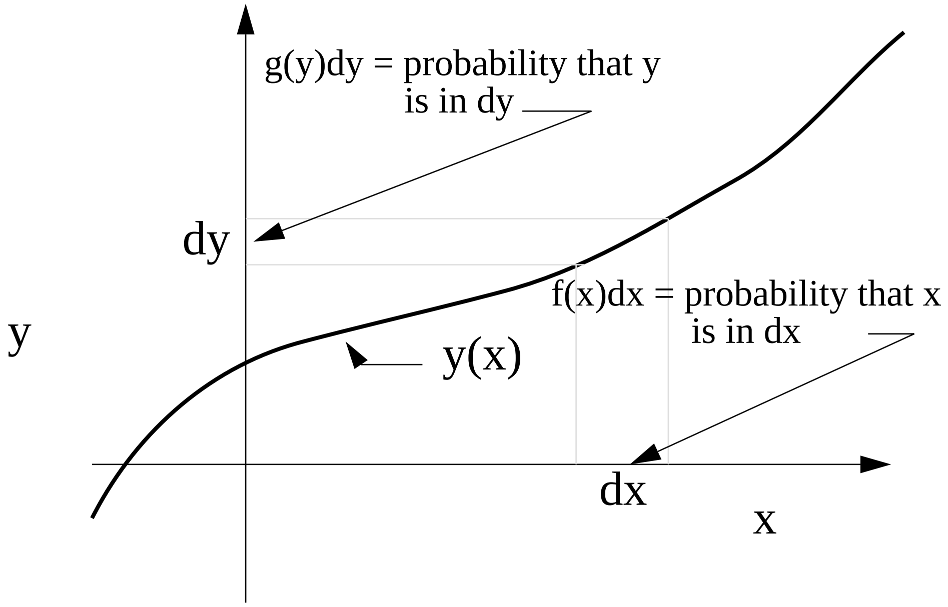

Figure 11: Transformation of pdf's

For multidimensional pdf's, the derivative $|dy/dx|$ is replaced by the Jacobian of the transformation, which will be described later when we discuss sampling from the Gaussian pdf.

Example 3

An illustration of neutron elastic scattering.

Consider the elastic scattering of neutrons of energy E_0 from a nucleus of mass A (measured in neutron masses) at rest. Define $f(E)\,dE$ as the probability that the final energy of the scattered neutron is in the energy interval dE about E, given that its initial energy was E_0. The pdf $f(E)$ is given by:

$$f(E) = \begin{cases} \dfrac{1}{(1-\alpha)E_0}, & \alpha E_0 \le E \le E_0 \\ 0, & \text{otherwise} \end{cases} \tag{75}$$

We now ask: what is the probability $g(v)\,dv$ that the neutron scatters in the speed interval dv about v, where $E = \frac{1}{2}mv^2$? Using Eq. (74), one readily finds the following expression for the pdf $g(v)$:

$$g(v) = \begin{cases} \dfrac{2v^2}{(1-\alpha)v_0}, & \sqrt{\alpha}v_0 \le v \le v_0 \\ 0, & \text{otherwise} \end{cases} \tag{76}$$

It is easy to show that $g(v)$ is a properly normalized pdf in accordance with Eq. (24).

Example 4

An illustration of the cumulative distributtion function, or cdf.

Perhaps the most important transformation occurs when $y(x)$ is the cumulative distribution function, or cdf:

$$y(x) = F(x) \equiv \int_{-\infty}^{\infty} f(x')\,dx' \tag{77}$$

In this case, we have $dy/dx = f(x)$, and one finds the important result that the pdf for the transformation is given by:

$$g(y) = 1, \quad 0 \le y \le 1 \tag{78}$$

In other words, **the cdf is always uniformly distributed on [0,1]**, independent of the pdf $f(x)$! *Any value for the cdf is equally likely on the interval [0,1].* As will be seen next, this result has important ramifications for sampling from an arbitrary pdf.

3.2.1 Sampling via inversion of the cdf

Since the r.v. x and the cdf $F(x)$ are 1-to-1, one can sample x by first sampling $y = F(x)$ and then solving for x by inverting $F(x)$, or $x = F^{-1}(y)$. But Eq. (78) tells us that the cdf is uniformly distributed on [0,1], which is denoted $U[0,1]$. Therefore, we simply use a random number generator (RNG) that generates $U[0,1]$ numbers, to generate a sample ξ from the cdf $F(x)$. Then the value of x is determined by inversion, $x = F^{-1}(\xi)$. This is depicted graphically in Figure 12. The inversion is not always possible, but in many important cases the inverse is readily obtained.

This simple yet elegant sampling rule was first suggested by von Neumann in a letter to Ulam in 1947 [Los Alamos Science, p. 135, June 1987]. It is sometimes called the "Golden Rule for Sampling". Since so much use will be made of this result throughout this chapter, we summarize below the steps for sampling by inversion of the cdf:

Step 1. Sample a random number ξ from $U[0,1]$

Step 2. Equate ξ with the cdf: $F(x) = \xi$

Step 3. Invert the cdf and solve for x: $x = F^{-1}(\xi)$

Example 5

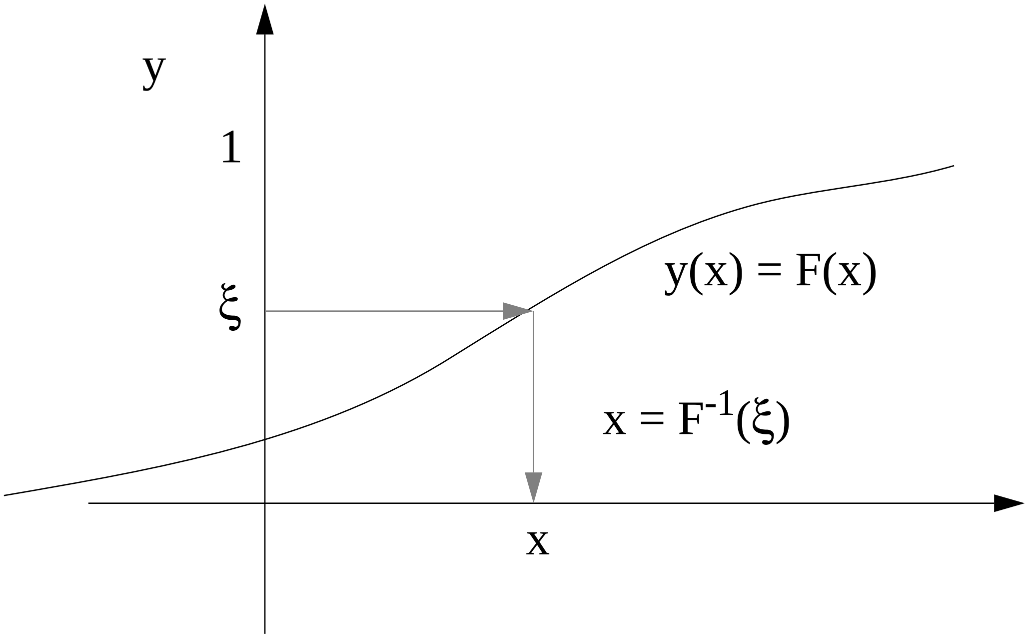

Figure 12: Sampling Using the Inverse of the cdf

An illustration of a uniform distribution.

Let the r.v. x be uniformly distributed between a and b. In this case, $f(x)$ is given by: **what is it?** and the cdf $F(x)$ is easily found:

$$F(x) = (x - a)/(b - a) \tag{79}$$

Now sample a random number ξ from $U[0,1]$, set it equal to $F(x)$, and solve for x:

$$x = a + (b - a)\xi \tag{80}$$

which yields a sampled point x that is uniformly distributed on the interval $[a, b]$.

Example 6

An illustration of exponential distribution.

Consider the penetration of neutrons in a shield, where the pdf for the distance x to collision is described by the exponential distribution,

$$f(x) = \lambda e^{-\lambda x}, \quad x \geq 0, \;\; \lambda > 0$$

The cdf is easily seen to be: **what is it?** A distance x to collision is then determined by first sampling a value for the cdf from $U[0,1]$ and solving for x.

One does not need to subtract the random number from unity, because ξ and $1-\xi$ are both uniformly distributed on [0,1], and statistically the results will be identical. So the actual sampled value of x is usually taken to be: **what is it?**

3.2.2 Remainder of Chapter 3 (Sampling):

Example—Gaussian distribution (Box–Muller)
  Discrete probability distribution functions
  Composition techniques
  Sum of 2 r.v.'s
  $(\text{r.v.})^n$
  Sum of several pdf's
  Rejection sampling

4 Estimation of Mean and Variance

True mean, true variance
  Unbiased estimators
  Sample mean and variance
  Canonical tallies - implementation
  Example - Monte Carlo integration

5 Error Estimates

Law of large numbers
  Chebychev inequality
  Central Limit Theorem (CLT)
  Application of CLT to Monte Carlo experiments - scoring
  Standard deviation, relative standard error
  "One sigma" and "two sigma" error estimates

6 Variance Reduction

Zero variance (or single history) Monte Carlo
  Importance sampling
  Application - Monte Carlo integration (variational derivation)

7 Case Study: Monte Carlo Particle Transport

The analysis of particle transport problems motivated the development of the Monte Carlo method, as we noted in our earlier chapter on the history of the Monte Carlo method. While Monte Carlo methods are used in virtually all branches of science and engineering, it is still the case that the most prevalent application of Monte Carlo is for the solution of complex problems that are encountered in particle transport applications. For example, the analysis of electron transport for electron beam cancer therapy, or the analysis of photon transport in a cloudy atmosphere, or the attenuation of neutrons in a biological shield. These problems are typically characterized by the following features:

- Complex 3-D and non-Cartesian geometry (e.g., nuclear reactor plant; human body)
- Complex material configurations (e.g., semiconductor chips)
- Complicated physical phenomena due to interaction of radiation (neutrons, photons, . . .) with medium
- Some known source of radiation incident on (or emitted within) the geometry
- Required output is the amount of radiation, its deposition, or its effect in arbitrary regions
- It is desirable to estimate the uncertainties in the simulation
- The computational effort to carry out the simulation should be reasonable

These rather general characteristics of a typical particle transport Monte Carlo code are represented in one or more of the following modules that appear in most production Monte Carlo codes used for radiation transport analysis:

- Source module
- Boundary crossing and geometry module
- Distance to collision module
- Collision analysis module
- Scoring (tallying) module
- Estimate of variance, confidence intervals
- Variance reduction techniques

Let us now consider each of these modules in more detail.

7.1 Source module

A specified source of radiation may either be given as (1) a *specified incident distribution* in space, energy, angle, and time or (2) as a *known source of radiation* that is emitting a specified amount of radiation as a function of time, space, energy, and angle. Although it is possible to show that these are mathematically equivalent [CdHP], the actual implementation of these "sources" into a Monte Carlo code will depend on which type of source is being examined.

Specified incident distribution

In order to specify an incident flux of particles on a surface, one needs to determine the following quantities:

- position $\mathbf{r}_{\mathrm{s}} = (x_{\mathrm{s}}, y_{\mathrm{s}}, z_{\mathrm{s}})$,
- the energy E,
- the angle $\Omega = (\Omega_x, \Omega_y, \Omega_z)$ that the incident particle is traveling, and
- the time t that the particle is incident on the surface.

For simplicity, let us assume that the incident radiation is monoenergetic at energy E_0, and it is monodirectional, traveling down the z-axis. Let us assume that the surface that is being irradiated is in the x–y plane, ranging over $x : [0, a]$ and $y : [0, b]$.

In this case, one typically knows the number of particles incident on the boundary per unit area of boundary, as a function of time, position on the boundary, energy, and angle. For example, consider a beam of monoenergetic particles incident normally and uniformly on the negative "y" surface of a "brick" of edges a, b, and c, corresponding to the three coordinate axes x, y, and z.

In this case, there are I_0 particles incident per unit area per unit time on the slab, and they are all travelling perpendicular to the surface of the slab. To start a particle in a Monte Carlo simulation, the source module would sample a position on the incoming surface of the brick at $y = 0$, or **what goes here?**

Nuclear engineers working in reactor physics and radiation shielding areas generally employ the concept of neutron "flux" to describe the amount of radiation, while other disciplines employ a "density" or "intensity" to describe what is in essence a very similar quantity. However, since the Monte Carlo simulation is a direct analog of the physical application, how these terms relate to a real application will be apparent after a few examples.

7.2 Remainder of Chapter 4: (will actually be separate section, it is out of order in this draft)

Boundary crossing and geometry module

Distance to collision module

Collision analysis module

Scoring (tallying) module

Estimate of variance, confidence intervals
Variance reduction techniques (for particle transport applications)

Monte Carlo Methods
for Accelerator-Driven Systems

Waclaw Gudowski
Royal Institute of Technology
Stockholm, Sweden

Motto:
Sir,
In your otherwise beautiful poem (The vision of Sin) there is a verse which reads:
"Every moment dies a man
every moment one is born"
Obviously, this cannot be true and I suggest that in the next edition you have it read
"Every moment dies a man
every moment 1 and 1/16 is born"
Even this value is slightly in error but should be sufficiently accurate for poetry.
....Olga C. in a letter to Lord Tennyson

Program

- Introduction
- History of Monte Carlo
- Basics of Monte-Carlo
- Random Number Generators
- High-Energy Transport Modelling
- Neutron Transport
  - Neutron Cross Section Data
  - Estimators
- Expected results

Introduction: Monte Carlo

The Monte Carlo method has been used for almost 60 years to solve radiation transport problems in high energy physics, nuclear reactor analysis, radiation shielding, medical imaging, oil well-logging, etc. Individual particle histories are simulated using random numbers, highly accurate representations of particle interaction probabilities, and exact models of 3D problem geometry. Monte Carlo methods are sometimes the only viable methods for analyzing complex, demanding particle transport problems.

Modern applications of Monte Carlo

- Nuclear reactor design
- Quantum chromodynamics
- Radiation cancer therapy
- Traffic flow
- Stellar evolution
- Econometrics
- Dow-Jones forecasting
- Oil well exploration
- VLSI design

History of Monte Carlo

John Von Neumann invented scientific computing in the 1940’s

- stored programs, “software”
- algorithms & flowcharts
- assisted with hardware design as well “ordinary” computers are called “Von Neumann machines”

John Von Neumann invented Monte Carlo particle transport in the 1940’s

- Highly accurate - no essential approximations
- Expensive -typically “method of last resort”
- Monte Carlo codes for particle transport have been proven to work effectively on all computers
- Vector, parallel, supercomputers, workstations, clusters of workstations, ...

John von Neumann, 1903-57, American mathematician, b. Hungary, Ph.D. Univ. of Budapest, 1926

He came to the United States in 1930 and was naturalized in 1937. He taught (1930-33) at Princeton and after 1933 was associated with the Institute for Advanced Study. In 1954 he was appointed a member of the Atomic Energy Commission. A founder of the mathematical theory of games, he also made fundamental contributions to quantum theory and to the development of the atomic bomb (Stan Ulam was another great mathematician in this environment). He was a leader in the design and development of high-speed electronic computers; his development of maniac-an acronym for mathematical analyzer, numerical integrator, and computer-enabled the United States to produce and test (1952) the world's first hydrogen bomb. With Oskar Morgernstern he wrote Theory of Games and Economic Behavior). Von Neumann's other writings include Mathematical Foundations of Quantum Mechanics (1926), Computer and the Brain (1958), and Theory of Self-reproducing Automata (1966).

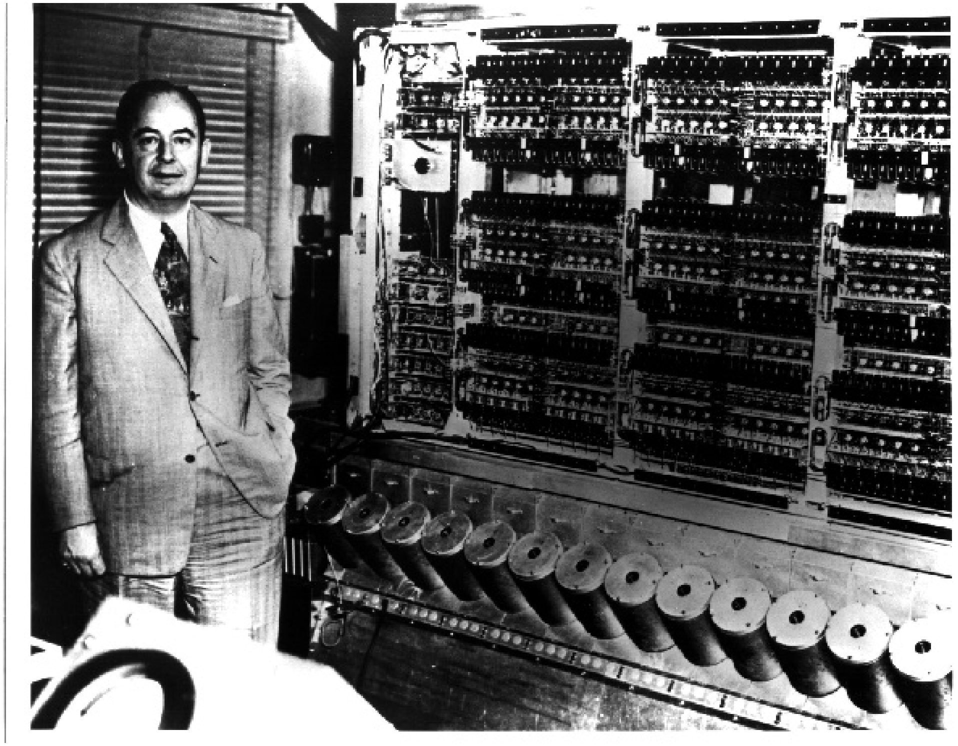

”Parties and nightlife held a special appeal for von Neumann. While teaching in Germany, von Neumann had been a denizen of the Cabaret-era Berlin nightlife circuit. ”

Basics of M-C

Two basic ways to approach the use of Monte Carlo methods for solving the transport equation:

→

- **mathematical technique for numerical integration**
- **computer simulation of a physical process**

Each is "correct"

mathematical approach useful for:

- importance sampling, convergence, variance reduction, random sampling techniques, . ..*.

simulation approach useful for:

collision physics, tracking, tallying, ...

- **For Monte Carlo approach, consider the integral form of the Boltzmann equation.**
- **Most theory on Monte Carlo deals with fixed-source problems.**
- **Eigenvalue problems are needed for reactor physics calculations**

SCIENCE AND ART THE ROYAL INSTITUTE OF TECHNOLOGY

Major Components of a Monte Carlo Algorithm

The primary components of a Monte Carlo simulation method:

- **Probability distribution functions** (pdf's) - the physical (or mathematical) system must be described by a set of pdf's.
- **Random number generator** - a source of random numbers uniformly distributed on the unit interval must be available.
- **Sampling rule** - a prescription for sampling from the specified pdf's, assuming the availability of random numbers on the unit interval, must be given.
- **Scoring (or tallying)** - the outcomes must be accumulated into overall tallies or scores for the quantities of interest.
- **Error estimation** - an estimate of the statistical error (variance) as a function of the number of trials and other quantities must be determined.
- **Variance reduction techniques** - methods for reducing the variance in the estimated solution to reduce the computational time for Monte Carlo simulation
- **Parallelization and vectorization** - algorithms to allow Monte Carlo methods to be implemented efficiently on advanced computer architectures.

The Essence of Monte Carlo

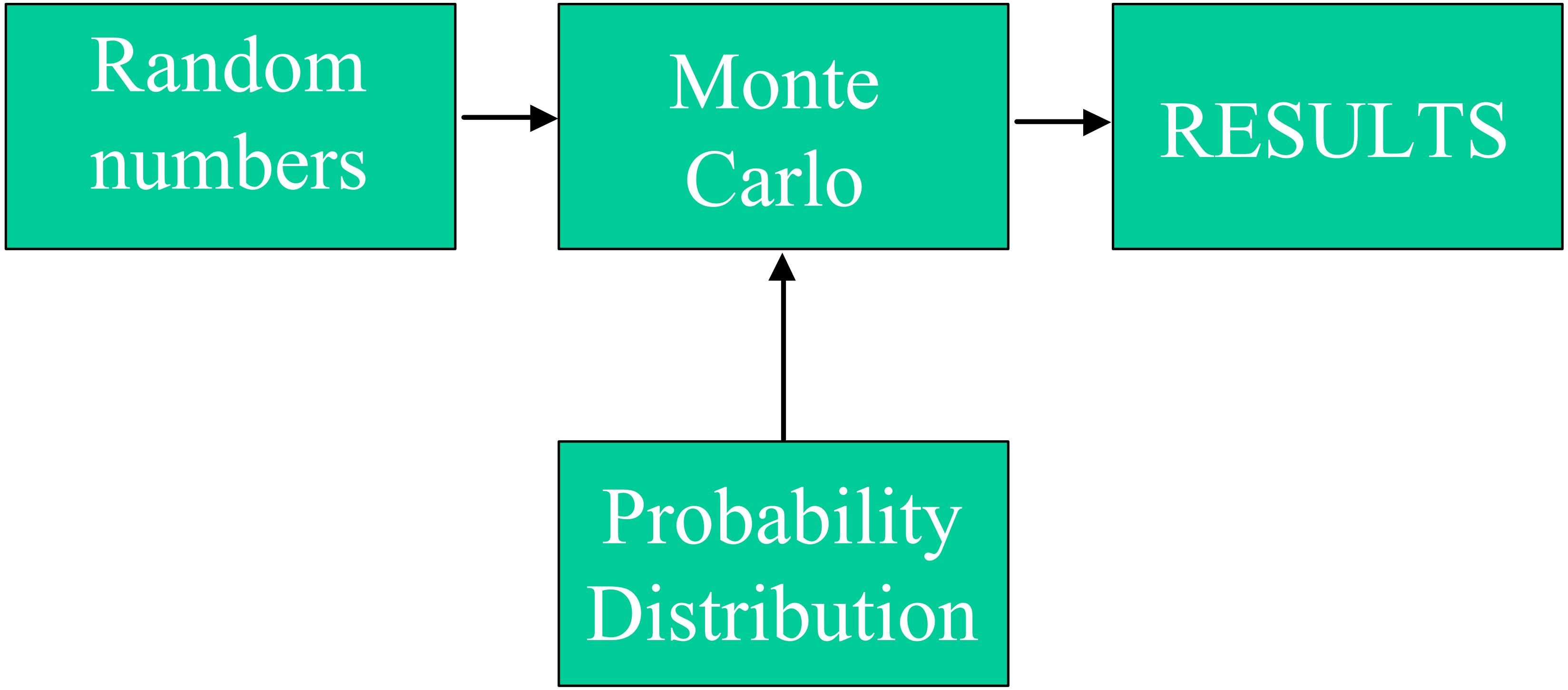

Random numbers

Monte Carlo

RESULTS

Probability Distribution

The Essence of Monte Carlo

Monte Carlo

Sampling
Scoring (tallying)
Error estimations
Variance reduction techniques
Vectorization and parallerization

Simple Monte Carlo Example:

$$\text{Evaluate } G = \int_0^1 g(x)dx \text{ with } g(x) = \sqrt{1 - x^2}$$

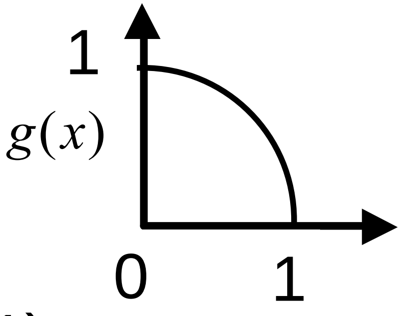

Mathematical approach:

For k = 1, ... N: choose $\hat{x}_k$ randomly in (0,1)

G = (1-O) •[average value of g(x)] $= \frac{1}{N}\sum_{k=1}^{N} g(\hat{x}_k) = \frac{1}{N}\sum_{k=1}^{N}\sqrt{1-\hat{x}_k{}^2}$

Simulation approach:

“darts game”

For k = 1, ... N: choose $\hat{x}_k$ *and* $\hat{y}_k$ *randomly in* (0,1)

$$If\ x_k{}^2 + y_k{}^2 \leq 1,\ tally\,(register)\ a\ "hit"$$

Simulation approach:

“darts game”

For k = 1, ... N: choose $\hat{x}_k$ *and* $\hat{y}_k$ *randomly in* $(0,1)$

$$If\ \ x_k^{\ 2} + y_k^{\ 2} \le 1,\ tally\,(register)\ \ a\,"\,hit"$$ ●

● miss

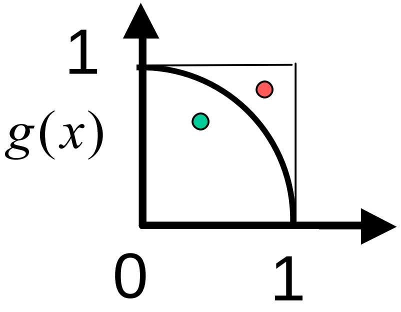

G = [area under curve] $\approx (1\cdot 1)\cdot \dfrac{number\ of\ hits}{N},\ \ N - a\, total\ number\ of\ shots$

M-C as integration tool

Monte Carlo is often the method-of-choice for applications with integration over many dimensions:

Examples: high-energy physics, particle transport (ADS)

$$\text{Evaluate}: \quad G = \int_{a_1}^{b_1}\int_{a_2}^{b_2}\int_{a_3}^{b_3} \ldots\ldots \int_{a_M}^{b_M} g(r_1, r_2 \ldots\ldots r_M)\, dr_1 dr_2 \ldots dr_M$$

where $r_1, r_2 \ldots\ldots r_M$ are all indendent variables

For $\mathrm{k} = 1, \ldots\ldots \mathrm{N}$:

$$\textit{For } m = 1, \ldots\ldots M: \ \textit{chose } R_m^{(k)} \textit{ randomly in } (a_m, b_m)$$

$$G \approx (b_1 - a_1) \cdot \ldots\ldots \cdot (b_M - a_M) \cdot \frac{1}{N} \sum_{k\_1}^{N} g\left(R_1^{(k)}, R_2^{(k)} \ldots\ldots R_M^{(k)}\right)$$

THE ROYAL INSTITUTE OF TECHNOLOGY

Probability Density Functions:

Continuous Probability Density

$f(x)$

$0 \leq f(x)$

$$\text{Probability } \{a \leq x \leq b\} = \int_a^b f(x)\,dx$$

$$\text{Normalization} \quad \int_0^{+\infty} f(x)\,dx = 1$$

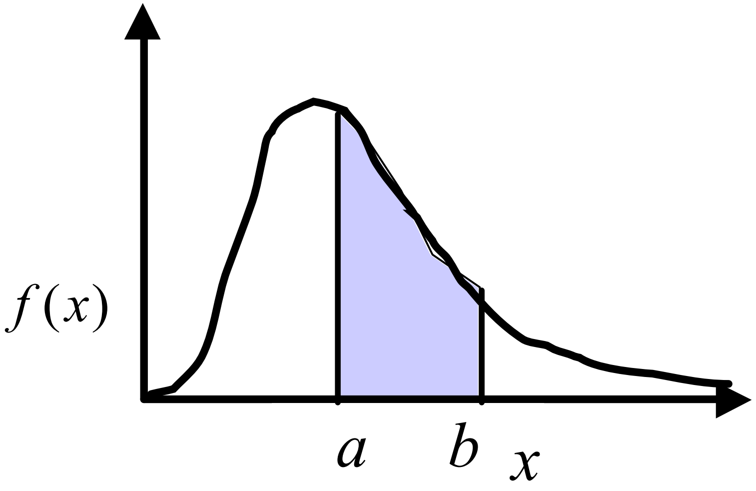

Discrete Probability Density

$$\{\mathrm{f_k}\}\ \mathrm{k} = 1, \ldots\ldots, \mathrm{N} \quad \text{where } \mathrm{f_k} = f(x_k)$$

$0 \leq \mathrm{f_k}$

$$\text{Probability}\{\mathrm{x} = \mathrm{x_k}\} = \mathrm{f_k}$$

$$\text{Normalization} \quad \sum_{k=1}^{N} \mathrm{f_k} = 1$$

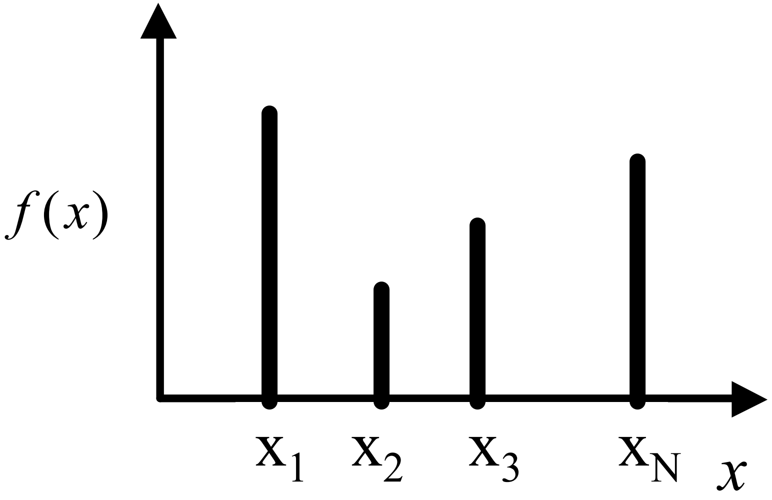

THE ROYAL INSTITUTE OF TECHNOLOGY

Basic parameters

Mean, Average, Expected Value (1st statistical moment)

$$\overline{x} = m = \langle x \rangle = E\,[x]$$

$$m = \int_{-\infty}^{+\infty} x f(x)\,dx \;\; - for\ continuous\ probablity$$

$$m = \sum_{k=1}^{N} x_k f_k \quad - for\ discrete$$

Variance (2nd statistical moment), standard deviation

$$\operatorname{var}(x) = \overline{(x-m)^2} = s^2 = \left\langle (x-m)^2 \right\rangle = E\left[(x-m)^2\right]$$

$$s^2 = \int_{-\infty}^{+\infty} (x-m)^2 f(x)dx \qquad s^2 = \sum_{k=1}^{N} (x_k - m)^2 f_k$$

standard deviation $s = \sqrt{s^2}$

THE ROYAL
INSTITUTE OF
TECHNOLOGY

Basic functions

Function of Random Variable

Consider $g(x)$, where x is a random variable *with density* $f(x)$

$$E[g(x)] = \int_{-\infty}^{\infty} g(x) f(x) dx \qquad E[g(x)] = \sum_{k=1}^{N} g_k f_k$$

The key of MC methods is the notion of RANDOM sampling

The problem can be stated this way:

Given a probability density, ***f(x)*,** produce a sequence of $\hat{x}'s$
The $\hat{x}'s$ should be distributed in the same manner as **f(x).**

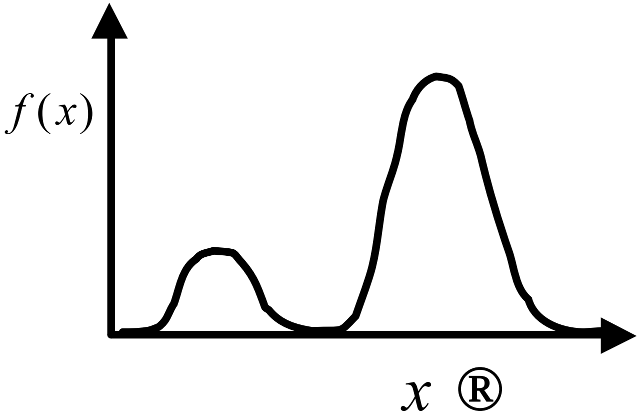

The use of random sampling distinguishes Monte Carlo from all other methods
When Monte Carlo is used to solve the integral Boltzmann transport equation:

- Random sampling models the outcome of physical events (e.g., neutron collisions, fission process, source, ...)
- Computational geometry models the arrangement of materials

Monte Carlo and Transport Equation

Boltzman Transport Equation - Time-independent, Linear
A general integral form:

$$\Psi(r,v) = \int \left[\Psi(r',v') C(v' \to v, r') dv' + Q(r',v) \right] T(r' \to r, v) dr'$$

where

$\Psi(r,v) \quad = \quad$ particle density

$Q(r',v) \quad = \quad$ source term

$C(v' \to v, r') =$ collision kernel, change velocity at fixed position

$T(r' \to r, v) \; =$ transport kernel

$$\textit{Angular flux} \quad \Psi(r,v) = \frac{\Psi(r,v)}{\Sigma(r,v)}$$

$$\textit{Scalar flux} \qquad \Phi(r,v) = \int_{\vec{\Omega}} \frac{\Psi(r,v)}{\Sigma(r,v)} d\vec{\Omega} \qquad v = |v| \vec{\Omega}$$

THE ROYAL
INSTITUTE OF
TECHNOLOGY

Monte Carlo and Transport Equation

Source term for the Boltzmann equation

$$Q(r,v)=\begin{cases} S(r,v) & \Leftrightarrow \textit{Fixed Source} \\ S(r,v)+\int\Psi(r,v')F(v'\to v,r)dv' & \Leftrightarrow \textit{Fixed Source}+\textit{Fission} \\ \frac{1}{k}\int\Psi(r,v')F(v'\to v,r)dv' & \Leftrightarrow \textit{Eigenvalue} \end{cases}$$

$$S(r,v) = \textit{fixed source}$$

$$F(v'\to v,r) = \textit{creation operator (due to fission)}$$

$$k = \textit{eigenvalue}$$

Transport Equation

$$\Psi(r,v)=\int\left[\int\Psi(r',v')C(v'\rightarrow v,r')dv'+Q(r',v)\right]T(r'\rightarrow r,v)dr'$$

Assumptions

- static homogeneous medium
- time-independent
- Markovian - next event depends only on current (r,v) not on previous events
- particles do not interact with each other
- neglect relativistic effects
- no long-range forces (particles fly in straight lines between events)
- material properties are not affected by particle reactions
- etc., etc.

$\Rightarrow$ can use superposition principle

Basis for Monte Carlo Solution Method

$$Let \quad p=(r,v) \quad and \quad R(p'\rightarrow p)=C(v'\rightarrow v,r')T(r'\rightarrow r,v)$$

$$Expand \ \Psi \ \mathrm{into} \ components \ having \ 0,1,2,.....k \ collisions$$

$$\Psi(p)=\sum_{k=0}^{\infty}\Psi_k(p), \ with \ \Psi_0(p)=\int Q(r',v)T(r'\rightarrow r,v)dr'$$

by definition

$$\Psi_k(p)=\int \Psi_{k-1}(p')R(p'\rightarrow p)dp'$$

Note that collision **k** depends only on the results of collision **k-l,** and not on any prior collisions **k-2, k-3, . . .**

Statistical approach to determining Ψ_k

$$\Psi_k(p) = \int \Psi_{k-1}(p')R(p' \to p)dp'$$

interpret terms in the following manner:

$$\Psi_{k-1}(p') = \textit{probability density for occurence of } (k-1)^{st} \textit{ collisions at } p'$$

$$R(p' \to p) = \textit{conditional probablity that a } (k-1)^{st} \textit{ collision at } p' \textit{ will}$$

$$\textit{result in a } (k)^{th} \textit{ collision at } p.$$

Monte Carlo method:

1. Randomly sample p’ from Ψ_{k-1}(p’)
2. Given p’, randomly sample p from R (p’→p)
3. If p lies within dp_i at p_i, tally 1 in bin i

⇒ Repeat steps 1,2,3 N times,

then $\hat{\Psi}(p_i)dp_i \approx \{counts\ per\ bin\ i\}/N$

Histories (trajectories)

After repeated substitution for Ψ_k

$$\Psi_k(p) = \int \Psi_{k-1}(p')R(p' \to p)dp$$
$$= \int .....\int \Psi_0(p_0)R(p_0 \to p_1)R(p_1 \to p_2)......R(p_{k-1} \to p)dp_0 dp_1 ...dp_{k-1}$$

A "history" (trajectory) is a sequence of states (p_0,p_1,p_2,p_3...)

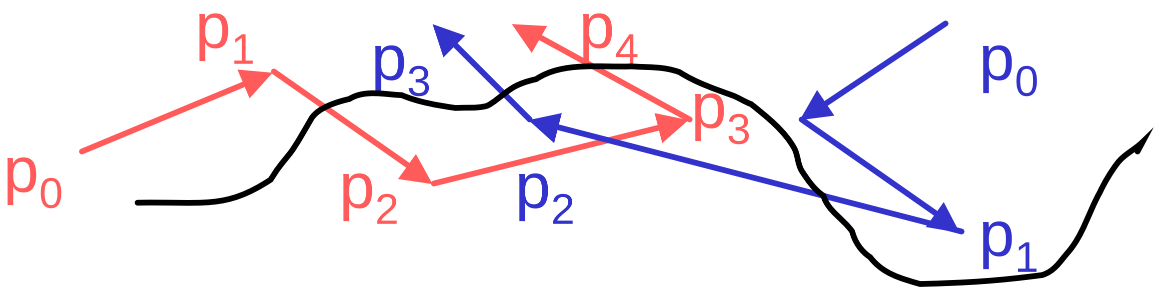

For estimates in a given region, tally the occurrences for **each collision** of **each "history"** within a region

Transport Equation

$$\Psi_k(p) = \int .....\int \Psi_0(p_0) R(p_0 \to p_1) R(p_1 \to p_2) ...... R(p_{k-1} \to p)\, dp_0\, dp_1 ... dp_{k-1}$$

Monte Carlo approach:

Generate a sequence of **States,** (p_0, p_1, ... p_k), [i.e., a **history by:**

- Randomly sample from PDF for source: $\Psi_0(p_0)$
- Randomly sample from PDF for kth transition: R ($p_{k-1} \to p_k$)

Generate estimates of results, by averaging over M histories:

$$A = \int A(p)\Psi(p)\,dp \approx \frac{1}{M}\sum_{m=1}^{M}\left(\sum_{k=1}^{\infty} A(p_{k,m})\right)$$

Simulations

Simulation approach to particle transport

Faithfully simulate the history of a single particle from birth to death

During the particle history,

- model collisions using physics equations & cross-section data
- model free-flight using computational geometry
  - tally the occurrences of events in each region

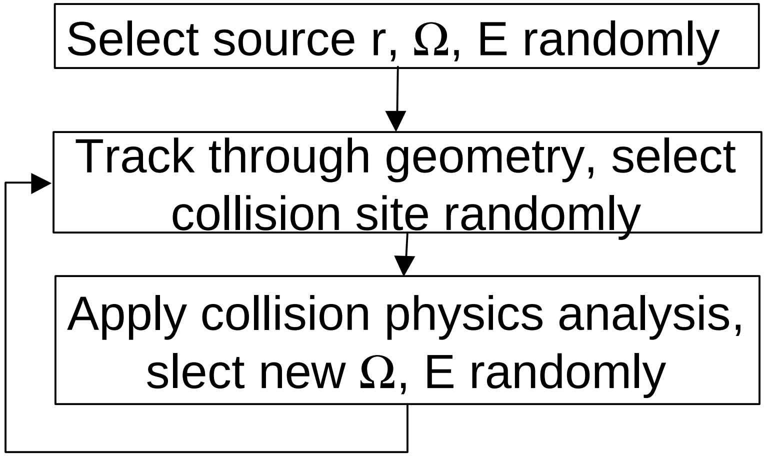

Select source r, Ω, E randomly

Track through geometry, select collision site randomly

Apply collision physics analysis, slect new Ω, E randomly

Repeat the simulation for many histories, accumulating the tallies

Fundamental rule:

Think like a neutron or other projectile (proton)

MC rules for simulations

Source

- Random sampling
  - E, Ω -analytic, discrete, or piecewise-tabulated PDF’s
- Computational geometry
  - **r** -sample from region in 3-D space, or from discrete PDF

Tracking

- Random sampling
  - $d_{collide}$-distance to collision, from mfp or exponential PDF
- Computational geometry
  - d_{geom} - distance-to-boundary, ray-tracing, next-region, ...

Collisions

- Random sampling
  - E', Ω' - analytic, discrete, or piecewise-tabulated PDF’s
- Physics
  - Σ, $f(\mu)$ - cross-section data, angular PDFs, kinematics, ...

Tallies

- Statistics

Variance Reduction

- Random sampling

MC rules for simulations

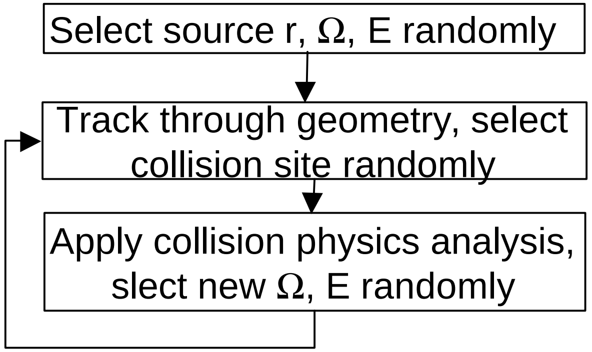
Select source r, Ω, E randomly

Track through geometry, select collision site randomly

Apply collision physics analysis, slect new Ω, E randomly

Single particle

- random-walk for particle history
- simulate events, from birth to death
- tally events of interest

Batch of histories (”generation”)

- random-walk for many particle histories
- tally the aggregate behavior

Overall

timesteps

- geometry changes
- material changes
    - fuel depletion
    - burnable absorbers
    - control rods

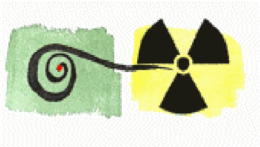

Random number generators

- **Truly random** - is defined as exhibiting ”true" randomness, such as the time between ”tics" from a Geiger counter exposed to a radioactive element
- **Pseudorandom** - is defined as having the appearance of randomness, but nevertheless exhibiting a specific, repeatable pattern.
- **Quasi-random** - is defined as filling the solution space sequentially (in fact, these sequences are not at all random - they are just comprehensive at a preset level of granularity). For example, consider the integer space [0, 100]. One quasi-random sequence which fills that space is 0, 1, 2,...,99, 100. Another is 100, 99, 98,...,2, 1, 0. Yet a third is 23, 24, 25,..., 99, 100, 0, 1,..., 21, 22. Pseudorandom sequences which would fill the space are pseudorandom permutations of this set (they contain the same numbers, but in a different, ”random" order).

Random number generators

Desirable Properties

Random numbers are used to determine:

(1) attributes (such as outgoing direction, energy, etc.) for launched particles,
(2) Interactions of particles with the medium.

Physically, the following properties are desirable:

- **The attributes of particles should not be correlated.** The attributes of each particle should be independent of those attributes of any other particle.
- **The attributes of particles should be able to fill the entire attribute space** in a manner which is consistent with the physics. E.g. if we are launching particles into a hemispherical space above a surface, then we should be able to approach completely filling the hemisphere with outgoing directions, as we approach an infinite number of particles launched. At the very least, ”holes" or sparseness in the outgoing directions should not affect the answers significantly. Also, if we are sampling from an energy distribution, with an increasing number of particles, we should be able to duplicate the energy distribution better and better, until our simulated distribution is ”good enough."

Random number generators

Desirable properties

Mathematically, the sequence of random numbers used to effect a Monte Carlo model should possess the following properties:

- **Uncorrelated Sequences** - The sequences of random numbers should be serially uncorrelated. Any subsequence of random numbers should not be correlated with any other subsequence of random numbers. Most especially, n-tuples of random numbers should be independent of one another. For example, if we are using the random number generator to generate outgoing directions so as to fill the hemispherical space above a point (or area), we should generate no unacceptable geometrical patterns in the distribution of outgoing directions
- **Long Period** - The generator should be of long period (ideally, the generator should not repeat; practically, the repetition should occur only after the generation of a very large set of random numbers).

- **Uniformity** - The sequence of random numbers should be uniform, and unbiased. That is, equal fractions of random numbers should fall into equal ”areas" in space. For example, if random numbers on [0,1) are to be generated, it would be poor practice were more than half to fall into [0, 0.1), presuming the sample size is sufficiently large. Often, when there is a lack of uniformity, there are n-tuples of random numbers which are correlated. In this case, the space might be filled in a definite, easily observable pattern. Thus, the properties of uniformity and uncorrelated sequences are loosely related.
- **Efficiency** - The generator should be efficient. In particular, the generator used on vector machines should be vectorizable, with low overhead. On massively parallel architectures, the processors should not have to communicate among themselves, except perhaps during initialization. This is not generally a signiffcant issue. With minimal effort, random number generators can be implemented in a high level language such as C or FORTRAN, and be observed to consume well less than 1% of overall CPU time over a large suite of applications.

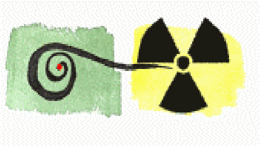

Multiplicative, Linear, Congruential Generators - the one most commonly used for generating random integers.

$$x_i = (Ax_{i-1} + B)\ modulo\ M$$

or

$$x_i = mod(Ax_i + B, M)$$

$$x_o - a\ "seed"$$

in practice

$$x_i = mod(M x_{i-1}, 2^{48})$$

$$M = 5^{19}$$

from integer to real

$$x_i = \frac{x_i}{float(M)}$$

Thinking like a ”proton”

- Charged particle transport:
  - Transport in electron/atomic nucleus media:
    - interactions with electrons are dominant
      - energy transfer inverse proportional to the target mass thus negligible except for the lightest target
      - collision with atomic nuclei result in negligible energy losses but the angular deflection is roughly proportional to Z^2
      - can be treated calssically (see next slide)
  - Ineractions with nuclei
    - INC
    - Fast processes
    - Compound nuclei
    - Inter Nuclear cascade
    - Low energy inelastic reactions

Transport in electron/atomic nucleus media: Proton and ”heavy” particle dE/dx

- Classical treatment

$$\frac{dE}{dx} = \frac{2p\ n_e r_e^2 m_e c^2 z^2}{b^2}\left[\ln\left(\frac{2m_e c^2 b^2 T_{\max}}{I^2(1-b^2)}\right) - 2b^2 - 2\frac{C}{Z} - d\right]$$

$where$

$r_e - classical\ electron\ radius$

$n_e - number\ of\ electrons\ per\ cm^3\ in\ the\ medium,\ n_e = \frac{N_A Z r}{A}$

$N_A - Avogadro's\ number$

$d - density\ correction$

$C - shell\ correction\ (accounts'\ for\ difference\ between\ free\ and\ bound\ electron\ targets$

$I - average\ ionization\ potential$

$T_{\max} - maximum\ energy\ transfer\ to\ the\ electron,\ T_{\max} = \frac{2m_e c^2 b^2 g^2}{1 + 2g\frac{m_e}{M} + \left(\frac{m_e}{M}\right)^2}$

IntraNuclear Cascade -INC

- Hydron-nucleus non-elastic interactions
- Two approaches:
  1. ”cross-section approach) - develop sophisticated models (not necessarily M-C) to produce comprhensive tabulations of energy-angle spectra of all emitted particles for a fine mesh of energies of possible projectilies.

     Drawbacks – extensive memory requirements, lost correlations!

IntraNuclear Cascade -INC

2. M-C method simulating at run time every interaction

   Drawbacks – may be slow, at the moment not very good at energies 20- 150 MeV.

INC – Basic assumptions

1. Hydrons propagate like free particles in the nuclear media, with interaction probablity per unit length given by free space cross sections, properly averaged over the Fermi motion of the target nucleons, times the local density
2. The particle motion is formulated in a classical way (average nuclear mean potential added to the free particle kinetic energy when tracking through the nucleus. The radial and energy dependence of such field are model and particle dependent.
3. The effect of the nuclear mean field on the particle motion can either be null or can produce curved trajectories in a semiclassical approach, according to energy and momentum conservation (called refraction or reflection effects)

INC – Basic assumptions

4. Interactions occur like in free space in the Centre of Mass System of two colliding hadrons
5. Interactions occur in a completely incoherent and uncorrelated way. No coherence diffractive effect is included. No multibody or cluster process is included.
6. Quantum effects are limited mainly to Pauli blocking (except for QMD models)
7. Secondaries are treated exactly like primary particles, with the only difference that they start their trajectories alrfeady inside the nucleus.

SCIENCE AND ART
THE ROYAL INSTITUTE OF TECHNOLOGY

INC – Basic assumptions

The requirement is that teh wavelength associated to hydron motion must be much shorter than the hydron mean free path inside the target nucleus, and much shorter than the average distance among two neighboring nucleons:

$$l_h = \frac{2p\hbar}{p} << \frac{1}{s_h N r}$$

$$l_h = \frac{2p\hbar}{p} << \left(\frac{3}{4p r} \right)^{1/3}$$

With the nucleon density at the centre of nuclei - ρ=0.17fm^{-3} one gets that INC works only above 200 MeV.... (Pauli blocking and lower peripheral densities help)

Steps of an INC simulation

1. Target nucleus description, typically realised through a few concentric sphere of different density and Fermi energy
2. Geometrical cross sections corresponding to the nuclear or to the maximum posible impact parameter
3. Impact parameter selection with a constant probability over the geometrical cross section area. More than one selection can be required if the particle crosses the nucleus without inetracting
4. Interaction point selection and projectile tracking through nucleus, according to Fermi motion averaged hadron-nucleon cross sections and possibly to the nuclear mean field, including Coulomb field

Steps of an INC simulation

5. Target-nucleon selection according to σ_{hp} , σ_{hn} and local Fermi energy
6. Interaction simulation according to free hN interactions, local Fermi energy and Pauli blocking
7. Secondary tracking into the nucleus, until interaction, escape, or energy cut-off
8. Pre-equilibrium stage, whenever all excited nucleons are below a given energy treshold (typically a few tens of MeV)
9. Evaporation stage whenever the preequilibrium stage is finished, or all particles are below a given treshold (of the order of the binding energy), and the system can be assumed to be equilibrated
10. Final de-excitation stage when the excitation energy is below the treshold for particle emission and it is spent through photon emission

Advantages and Limitations of INC models

- Advantages:
  - No other model avaialble for energies above the pion treshold (290 MeV)
  - No other model for projectiles other than nucleons
  - Easily available for on-line integration into transport codes
  - Every target-projectile combination, without any extra information
  - Particle-to-particle correlations preserved
  - Equally valid on very light as well on very heavy nuclei (with problems for evaporation)
  - Capability of computing reaction cross-sections where unknown

Advantages and Limitations of INC models

- Limitations:
  - May be slow in complex calculations (not a big deal with processor&computer rapid development)
  - Not well validated for projectiles heavier than α particles)
  - Low projectile energies (20<E<150 MeV) are badly modelled
  - For energies < 100 MeV reactions (p,xn), (n,xp) spectra of emitted particles are particularly badly modelled
  - Faulty cross section simulations when no potential effects are included for E< 100MeV (HETC, INC)
  - Quasielastic peaks above 100 MeV are usually too sharp compared to experiments
  - Composite particle emission (d,t, ^{3}He,α) badly modelled in the evaporation stage.
  - Problems with residual nuclei

Modelling Hadron-Nucleon Interactions

- First step: elastic-nonelastic interaction
  - – Elastic interactions
    - Below pion production – just elastic scaterring
    - Pion-Nucleon elastic and charge exchange interactions at intermediate energies
    - Elastic nuclear interactions (optical model, diffraction pattern of the differential elastic cross-section)
  - – Inelastic processes
    - Pion production at intermediate energies
    - Hydron-nucleon high energy inelastic and diffractive interactions (above 2-3 GeV)
    - Nonelastic nuclear interactions
      - – eg. pre-equilibrium emission
      - – evaporation/fragmentation
      - – residual nucleus deexcitation

What data do we need from HET:

Neutron yield
Neutron spectrum
(+coordinates)
Spallation residuals
Energy depostion

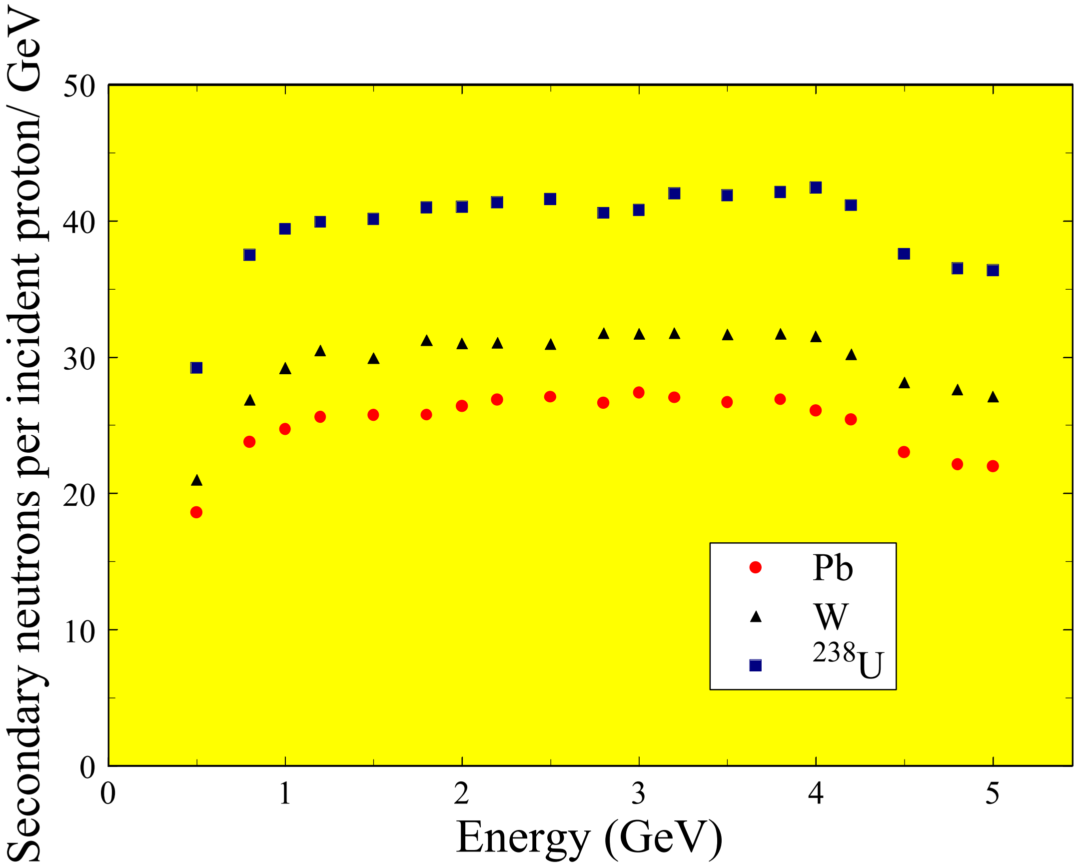

Fluka calculations

Pb/Bi cylindrical target

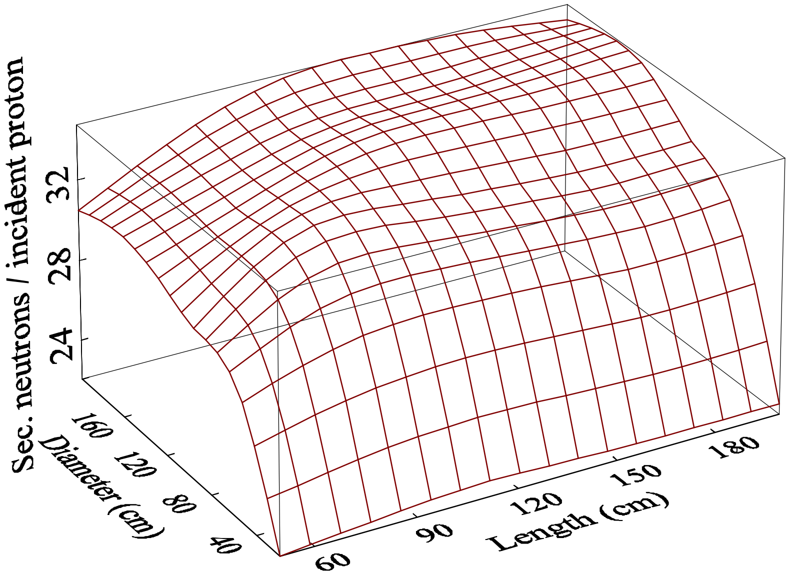

1 GeV protons

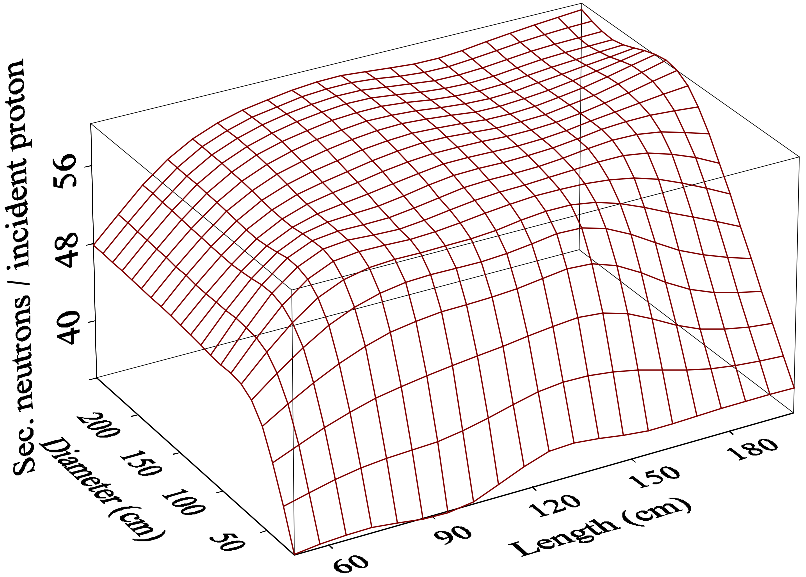

1.6 GeV protons

Spectrum of spallation neutrons

Pb/Bi target120x150 cm^2, 1,6 GeV

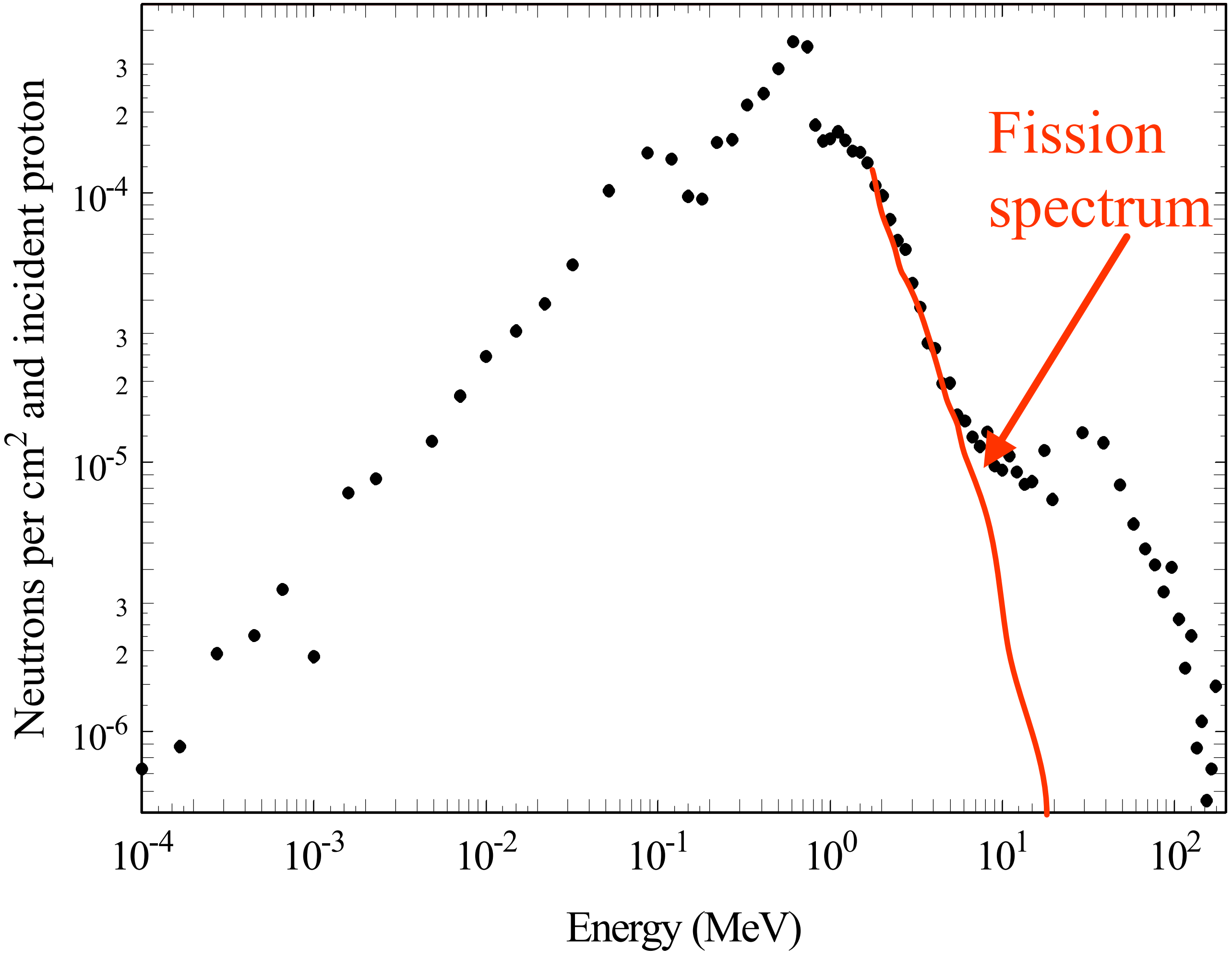

THE ROYAL INSTITUTE OF TECHNOLOGY

Hadron codes availabilty

Code	Availability		
	Free	**Limited (bin.)**	**Restricted/comm**
FLUKA		X	
HERMES	X		
MARS	X		
MCNP - (X)	X		
EA-MC			X
NMTC/JAERI-JAM	?	?	?
DPMJET-III	X		
TIERCE			X (very restricted)

THE HEART OF THE MONTE CARLO FOR NEUTRON/PHOTON TRANSPORT

sampling of mean free path

probability of passing distance $x+dx$

$$p(x)\,dx = \Sigma e^{-\Sigma x}\,dx$$

cumulative probability for passing distances up to z

$$x = \int_0^z \Sigma e^{-\Sigma x}\,dx$$

$$x = -e^{-\Sigma x}\Big|_0^z$$

$$x = 1 - e^{-\Sigma z}$$

thus $-\Sigma z = \ln(1-x)$

thus $z = -\frac{1}{\Sigma}\ln x'$

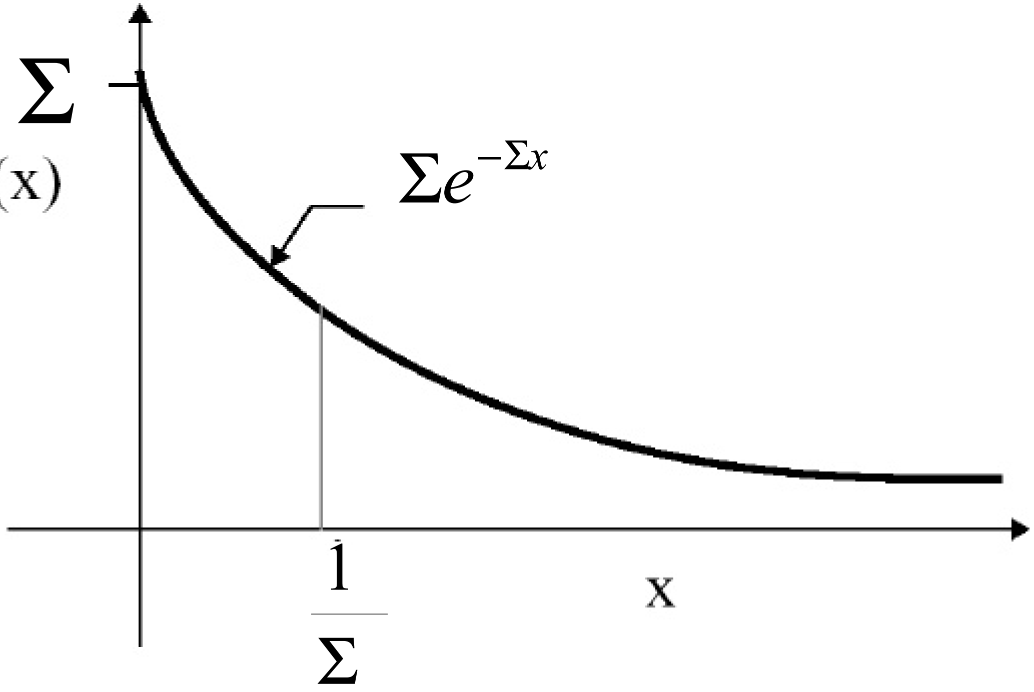

x, x' - random numbers

THE ROYAL INSTITUTE OF TECHNOLOGY

Thinking like a neutron:

$$w(x, y, z, v_x, v_y, v_z, t)$$

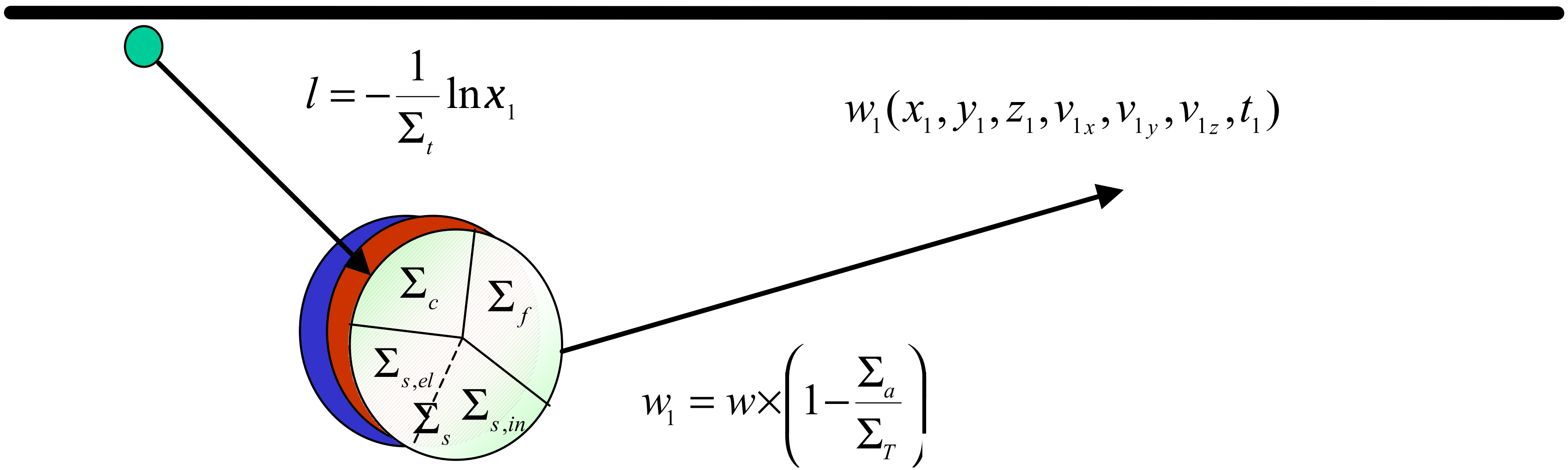

$$l = -\frac{1}{\Sigma_t} \ln x_1$$

$$w_1(x_1, y_1, z_1, v_{1x}, v_{1y}, v_{1z}, t_1)$$

$$w_1 = w \times \left(1 - \frac{\Sigma_a}{\Sigma_T}\right)$$

$$x_2 - choice\ of\ \ the\ nucleus\,(isotope/\,material)$$

$$x_3 - choice\ of\ \ interaction$$

$$x_4 - choice\ \ of\ \ angle$$

Cross sections – probability distribution functions!

$$x_i - random\ numbers$$

$$medium\ \ \ with\ \Sigma_t$$

Interactions of neutrons with the matter

1. Potential (elastic) scattering
   Kinetic energy conserves
2. Formation of a compound nucleus

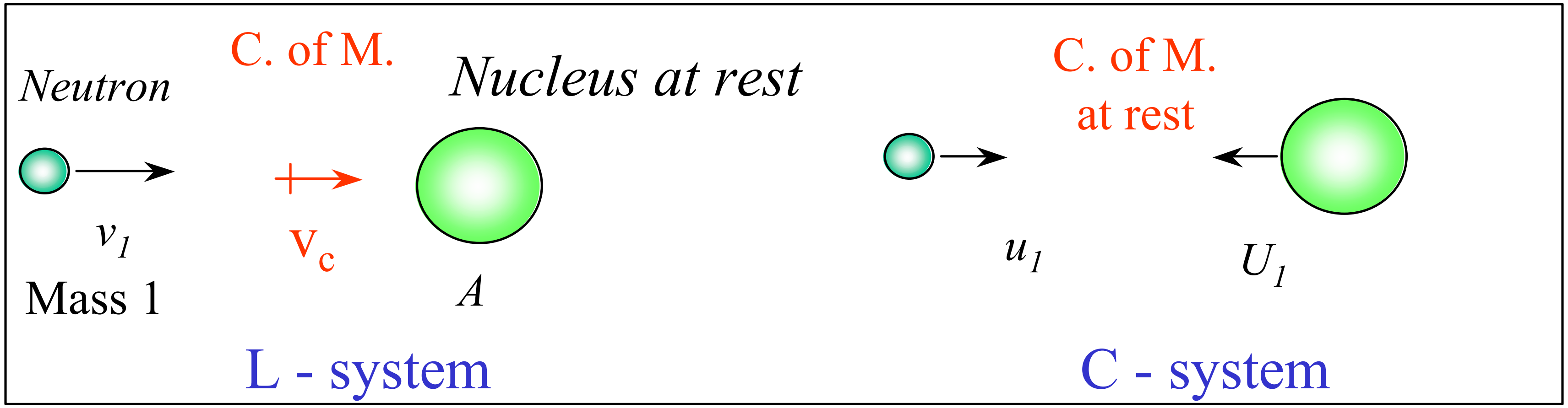

Collision in a LAB-SYSTEM

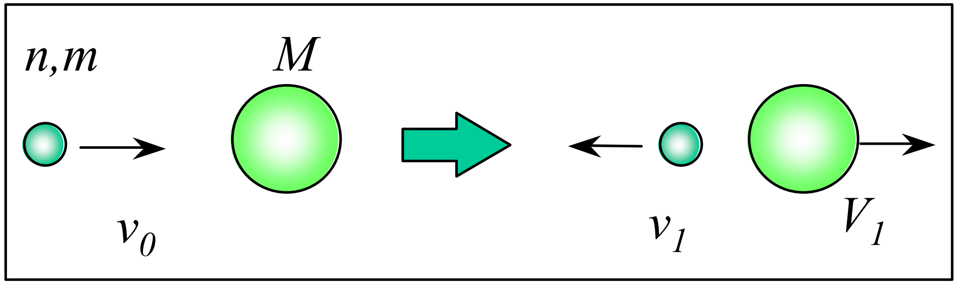

Collision in a C.M.-SYSTEM

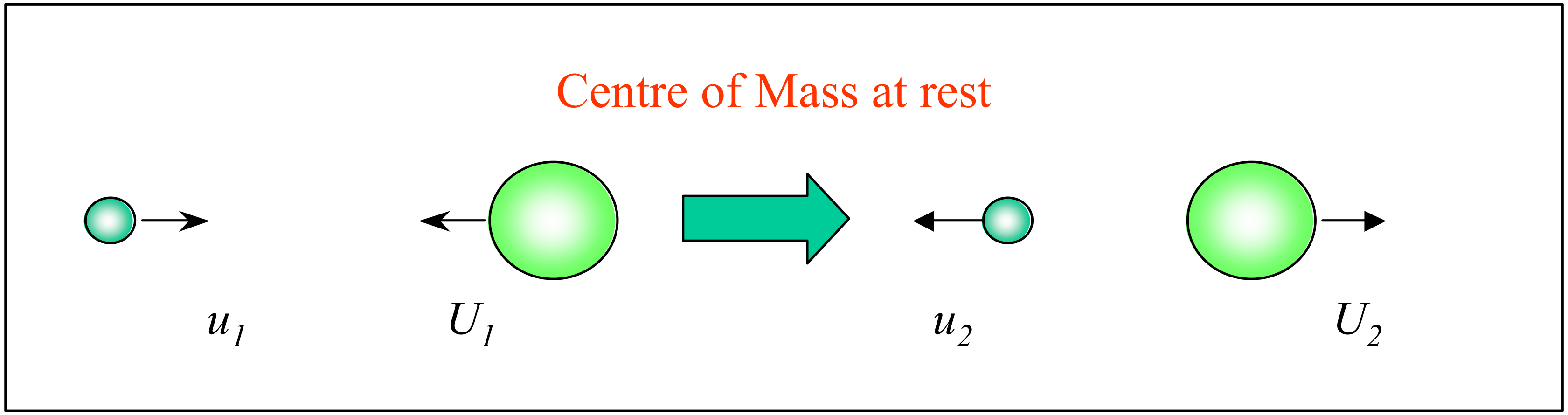

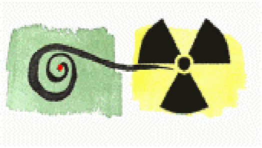

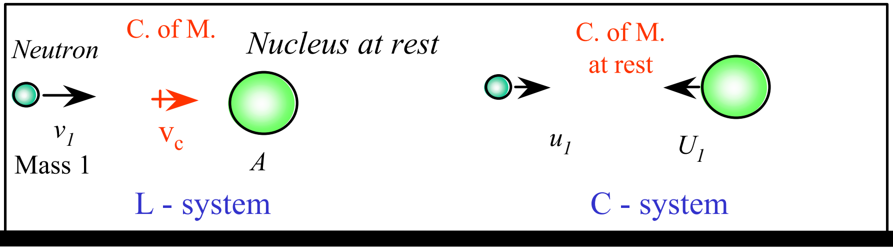

$$\hat{v}_c = \frac{m}{M+m}\hat{v}_1$$

$$\hat{u}_1 = \frac{M}{M+m}\hat{v}_1$$

$$\hat{U}_1 = -\frac{m}{M+m}\hat{v}_1$$

$$m\hat{u}_1 + M\hat{U}_1 = 0$$

$$m\hat{u}_2 + M\hat{U}_2 = 0$$

$$\frac{1}{2}mu_1^2 + \frac{1}{2}MU_1^2 = \frac{1}{2}mu_2^2 + \frac{1}{2}MU_2^2$$

$$U_1 = U_2$$

$$u_1 = u_2$$

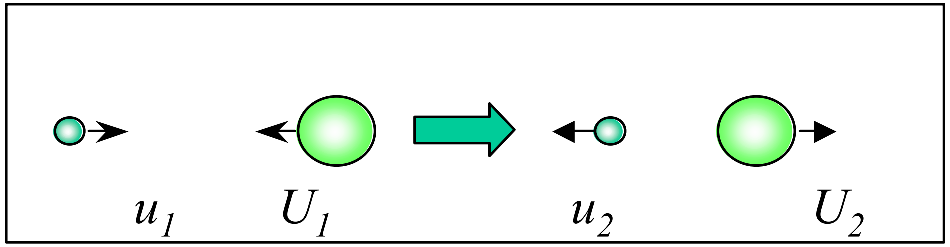

$$E_c = \frac{1}{2}mu_1^2 + \frac{1}{2}MU_1^2 = \frac{1}{2}\frac{mM^2}{(m+M)^2}v_1^2 + \frac{1}{2}\frac{Mm^2}{(m+M)^2}v_1^2$$

$$= \frac{1}{2}\frac{mM}{(m+M)}v_1^2$$

$$= \frac{M}{m+M}E_1$$

A≈M; m=1

$$\hat{v}_c = \frac{1}{A+1}\hat{v}_1 \qquad \hat{u}_1 = \frac{A}{A+1}\hat{v}_1 \qquad \hat{U}_1 = -\frac{1}{A+1}\hat{v}_1 \qquad E_c = \frac{A}{A+1}E_1$$

Collision in CM-system - vector analysis

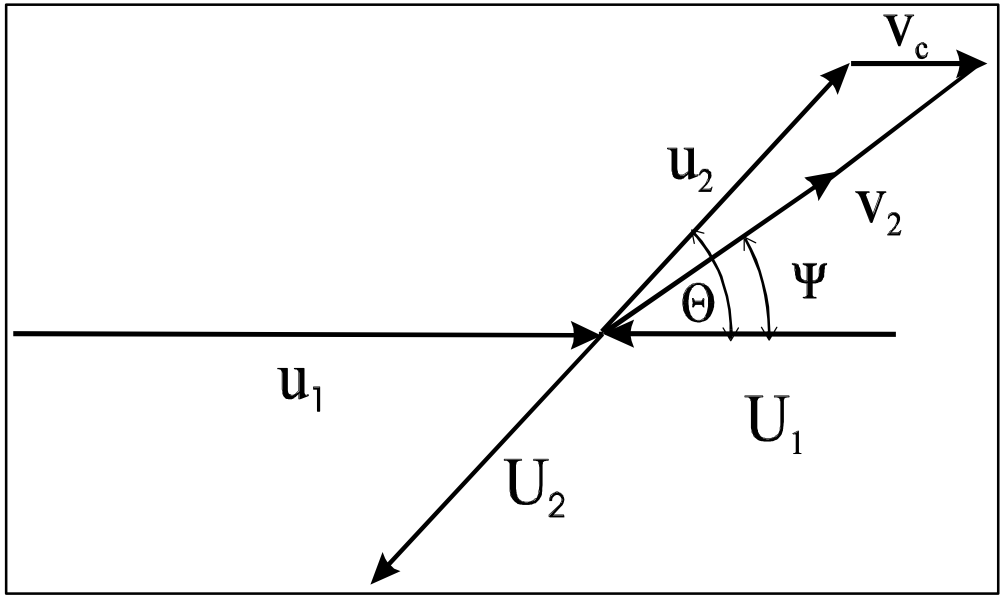

$$v_2^2 = u_2^2 + v_c^2 + 2u_2 v_c \cos Q$$

$$v_2^2 = v_1^2 \left\{ \frac{A^2 + 1 + 2A\cos Q}{(A+1)^2} \right\}$$

$$E_2 = E_1 \left\{ \frac{A^2 + 1 + 2A\cos Q}{(A+1)^2} \right\}$$

<u>For Θ = 180</u> ^{0}

$$E_2 = E_1 \left(\frac{A-1}{A+1} \right)^2$$

$$a = \left(\frac{A-1}{A+1} \right)^2$$

$$\frac{E_1 - E_2}{E_1} = (1-a)$$

Formation of a compound nucleus

$$ {}^{A}_{Z}X + {}^{1}_{0}n \rightarrow \left[{}^{A+1}_{Z}X \right]^{*} \rightarrow Y + b $$

Examples of different reactions (reaction channels):

- Neutron capture (n,γ)
- Emission of α-particle (n,α)
- Emission of proton (n,p)
- Inelastic scattering (n,n')
- Neutron "multiplication" through (n,2n), (n,3n)
- FISSION (n,f)

Neutron capture (n,g)

$$^{23}_{11}Na + ^{1}_{0}n \rightarrow ^{24}_{11}Na^{*} + g$$

$$or \quad ^{23}Na(n,g)\,^{24}Na$$

$$^{238}_{92}U + ^{1}_{0}n \rightarrow ^{239}_{92}U^{*} \rightarrow ^{239}_{92}U + g$$

$$or \quad ^{238}U(n,g)\,^{239}U$$

Emission of a-particle (n,a)

$$^{10}_{5}B+^{1}_{0}n \rightarrow \left(^{11}_{5}B\right)^{*} \rightarrow ^{7}_{3}Li+^{4}_{2}He$$

$$or\ ^{10}_{5}B(n,a)\,^{7}Li$$

$$^{6}_{3}Li+^{1}_{0}n \rightarrow ^{4}_{2}He+^{3}_{1}H$$

$$or\ ^{6}_{3}Li\ (n,a)\ ^{3}_{1}H$$

$$^{3}_{2}He+\ ^{1}_{0}n \rightarrow ^{1}_{1}H+^{3}_{1}H$$

$$or\ ^{3}_{2}He(n,p)\,^{3}_{1}H$$

(n,p) reactions $^{14}_{7}N+^{1}_{0}n \rightarrow ^{14}_{6}C+^{1}_{1}H$ (^{14}C–production in the atmosphere)

$$^{31}_{15}P+^{1}_{0}n \rightarrow ^{31}_{14}Si+^{1}_{1}H$$

(n,2n) reactions

$$^{63}_{29}Cu(n,2n)\ ^{62}_{29}Cu$$

$$^{65}_{29}Cu(n,2n)\ ^{64}_{29}Cu$$

FISSION

Otto Hahn and Fritz Strassman, 1938 - Berlin
Otto Frisch and Lisa Meitner explanation, 1939

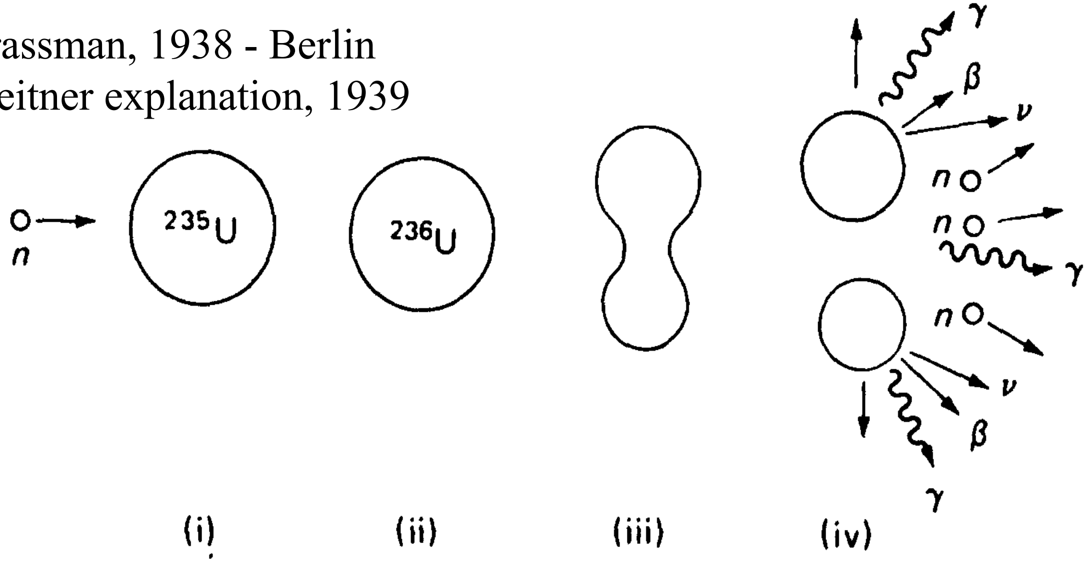

Four stages in the fission process

$$ {}^{235}_{92}U + n \rightarrow \left({}^{235}_{92}U \right)^{*} \rightarrow X + Y + neutrons $$

$$ {}^{235}_{92}U + n \rightarrow \left({}^{235}_{92}U \right)^{*} \rightarrow {}^{144}_{56}Ba + {}^{89}_{36}Kr + 3\,{}^{1}_{0}n $$

$$ {}^{235}_{92}U + n \rightarrow \left({}^{235}_{92}U \right)^{*} \rightarrow {}^{140}_{54}Xe + {}^{94}_{38}Sr + 2\,{}^{1}_{0}n $$

Energy dependent fission product yield – it is still a problem

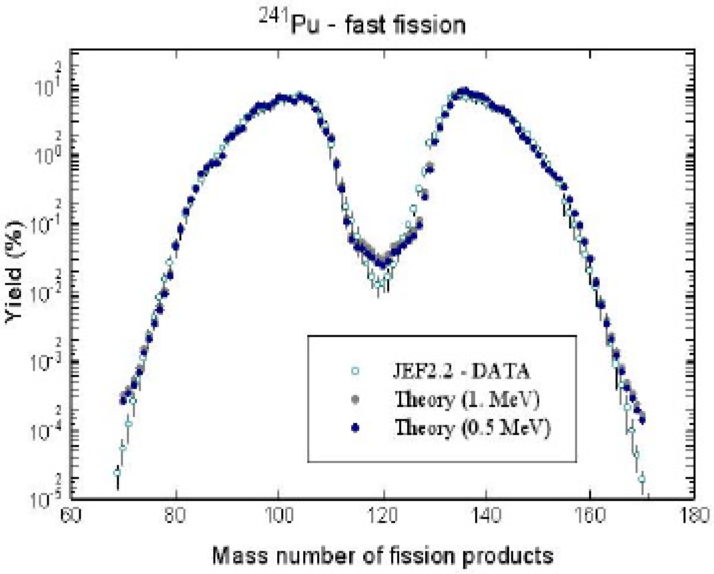
^{241}Pu - fast fission

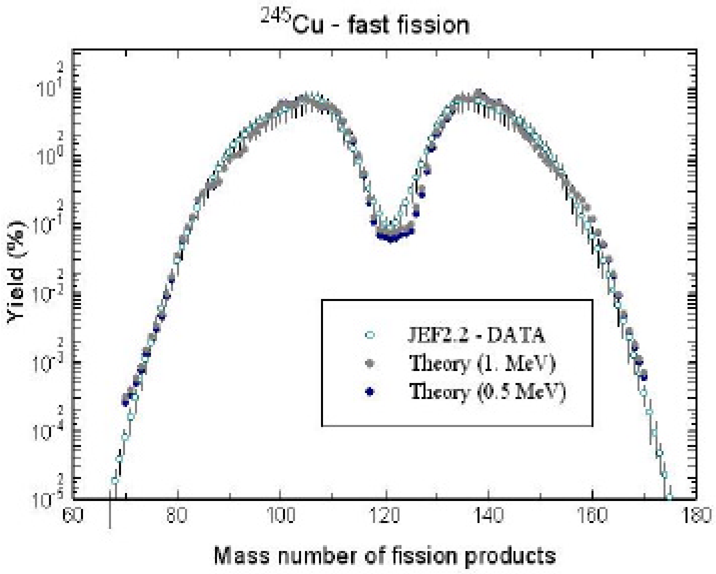
^{245}Cu - fast fission

Neutron flux, neutron cross section for a reaction, reaction rate

n - neutron density - number of neutrons per cm^3 (n/cm^3)

v - neutron velocity (cm/s)

Φ - neutron flux ($n/(cm^2\ s)$)

$$dF = ndv$$

$$F = \int_{all\ v} n(v)dv$$

for monoenergetic neutrons

$$F = nv$$

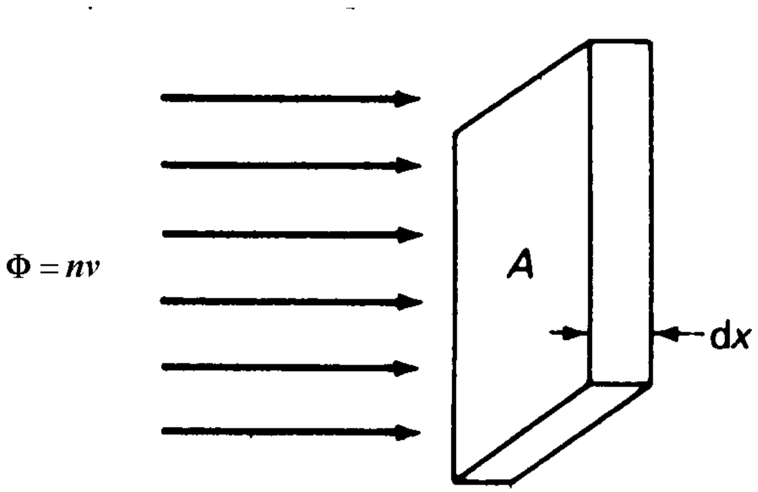

F - reaction rate, number of the reactions per second

$$F \propto F\ N\ V$$

s – **constant of proportionality:**

$$F = s\ F\ N\ V$$

σ - probability for a reaction between neutron and nucleus is called a microscopic cross-section (X-section).

$$1 \text{ barn} = 10^{-24} \text{ cm}^2$$

Σ - macroscopic cross section - $\Sigma = N\times\sigma$ (cm^{-1})

Reaction rate:

$$\mathbf{F{=}Y = S\,F\,V}$$

Interaction probability for a neutron i dx:

$$\frac{\textbf{Number of neutrons interacting per second in a target of thickness dx}}{\textbf{Number of neutrons per second incident on the target}} = \frac{s\,F\,N\,A\,dx}{F\,A} = s\ N\,dx = S\ dx$$

Mean free path

Since Σ is the probability of interaction per unit distance, the probability of a neutron interaction within a distance dx beyond x is:

$$p(x)dx = e^{-\Sigma_t x}\Sigma_t dx$$

the mean free path is then defined as

$$l_t = \frac{\int_0^\infty x\, p(x)dx}{\int_0^\infty p(x)dx} = \frac{\int_0^\infty x\,\Sigma_t\, e^{-\Sigma_t x}dx}{\int_0^\infty \Sigma_t\, e^{-\Sigma_t x}dx} = \frac{1}{\Sigma_t}$$

Partial Cross-Sections

- Scattering X-section, σ_s. Probability that neutron re-emitts from the compound nucleus or that neutron potentially scatters on the nucleus surface: $\sigma_s = \sigma_{n,n} + \sigma_{n,n'} = \sigma_s + \sigma_i$
- Absorption X-section, σ_a. Probability that neutron is captured by the nucelus. Absorption can lead to fission, pure capture and other reactions like (n,p), (n,α) etc : $\sigma_a = \sigma_f + \sigma_c$
  - Fission X- section, σ_f . Probablity that nucleus fission in result of neutron absorption.
  - Capture X-section, σ_c. Probability that neutron is captured and remains in the excited absorbing nucleus. The nucleus can de-excite thruogh e.g. emission of γ-quanta ($\sigma_{n,\gamma}$)
- Total X-section, $\sigma_t = \sigma_s + \sigma_i + \sigma_f + \sigma_c$

THE ROYAL INSTITUTE OF TECHNOLOGY

Scattering-free mean free path:

$$l_s = \frac{1}{S_s}$$

Absortption-free mean free path:

$$l_a = \frac{1}{S_a} =$$

Mean free path:

$$\frac{1}{l_t} = \frac{1}{l_s} + \frac{1}{l_a}$$

σ(E) - Energy Variation of Neutron Cross Section

$$s_a = c_1\left(\frac{1}{E_n}\right)^{0.5}$$

$$E_n = \frac{mv^2}{2}$$

$$s_a \sim \frac{1}{v}$$

$$s_f \sim \frac{1}{v}$$

$$s_c \sim \frac{1}{v}$$

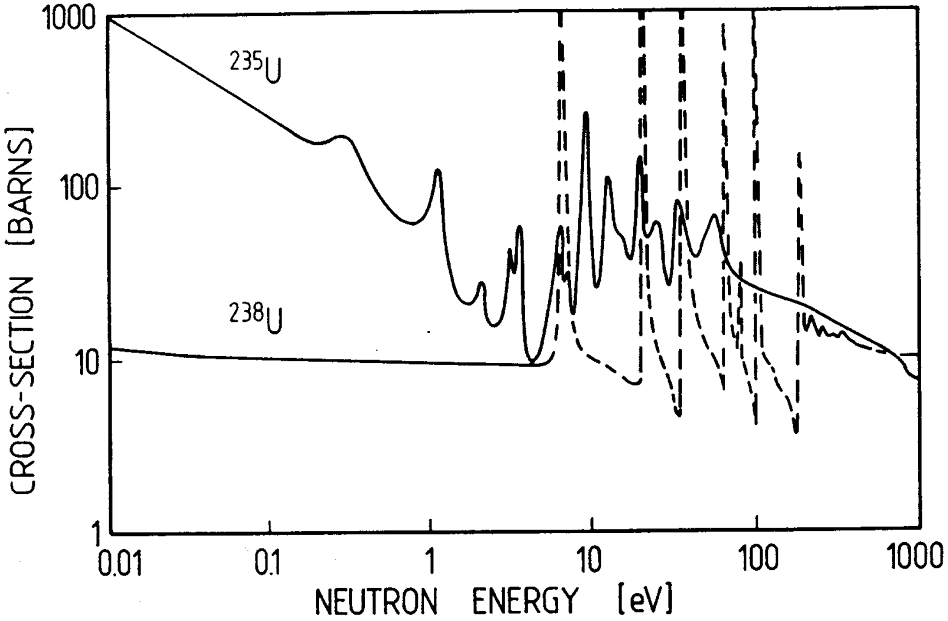

Examples of cross-sections

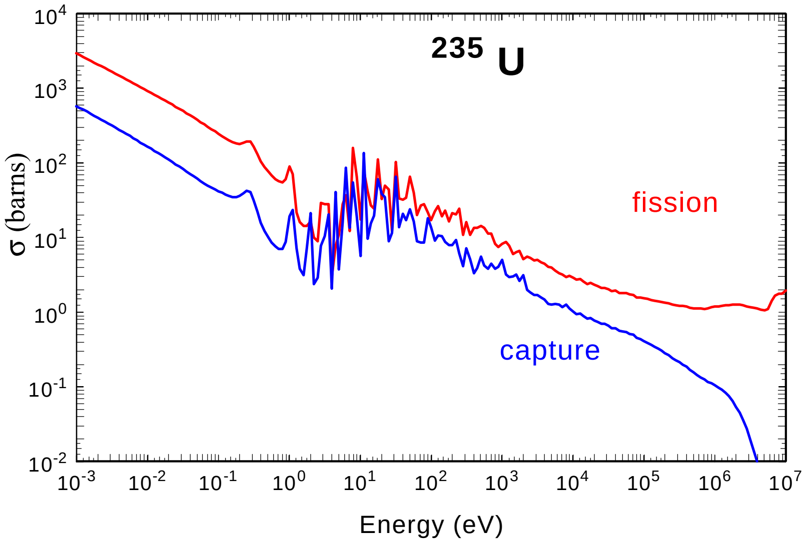

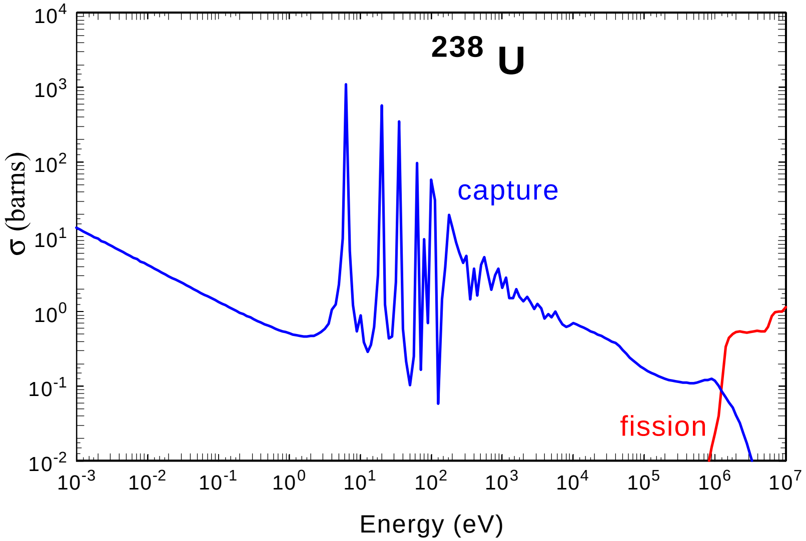

Examples of cross-sections

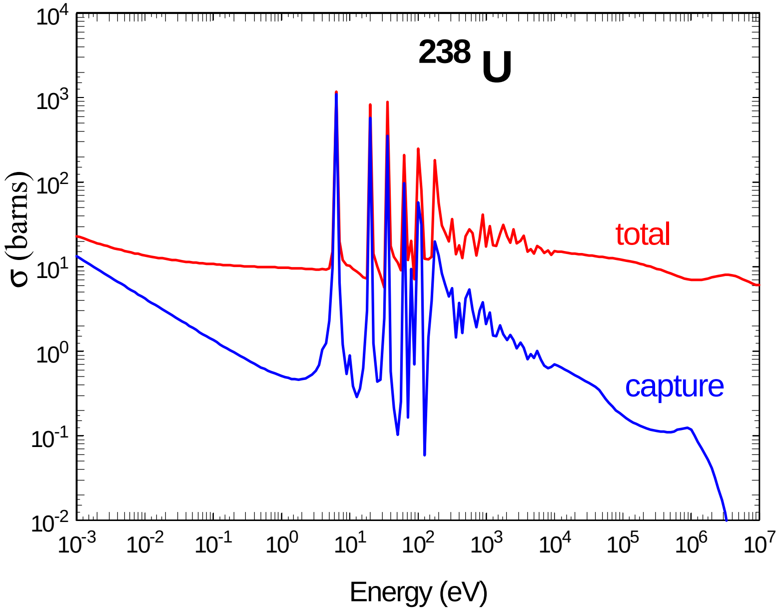

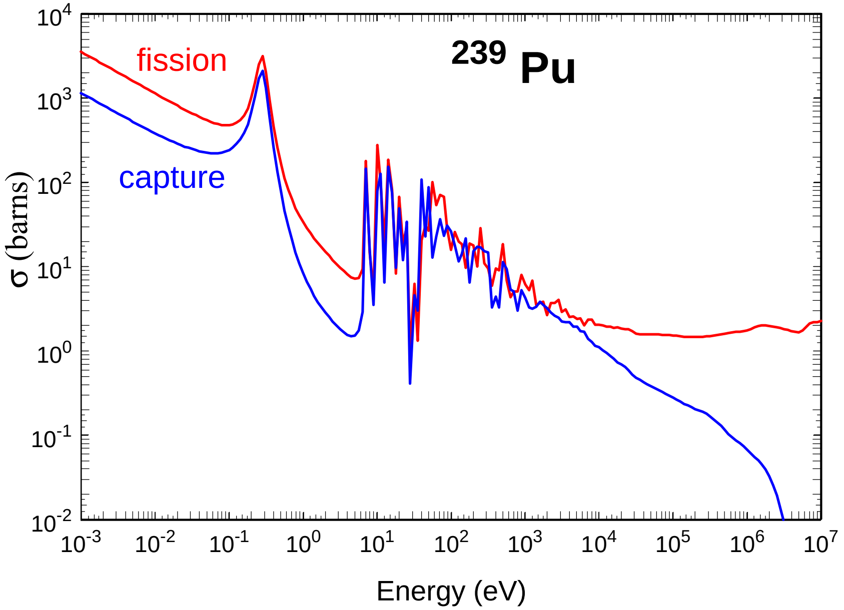

Examples of cross-sections

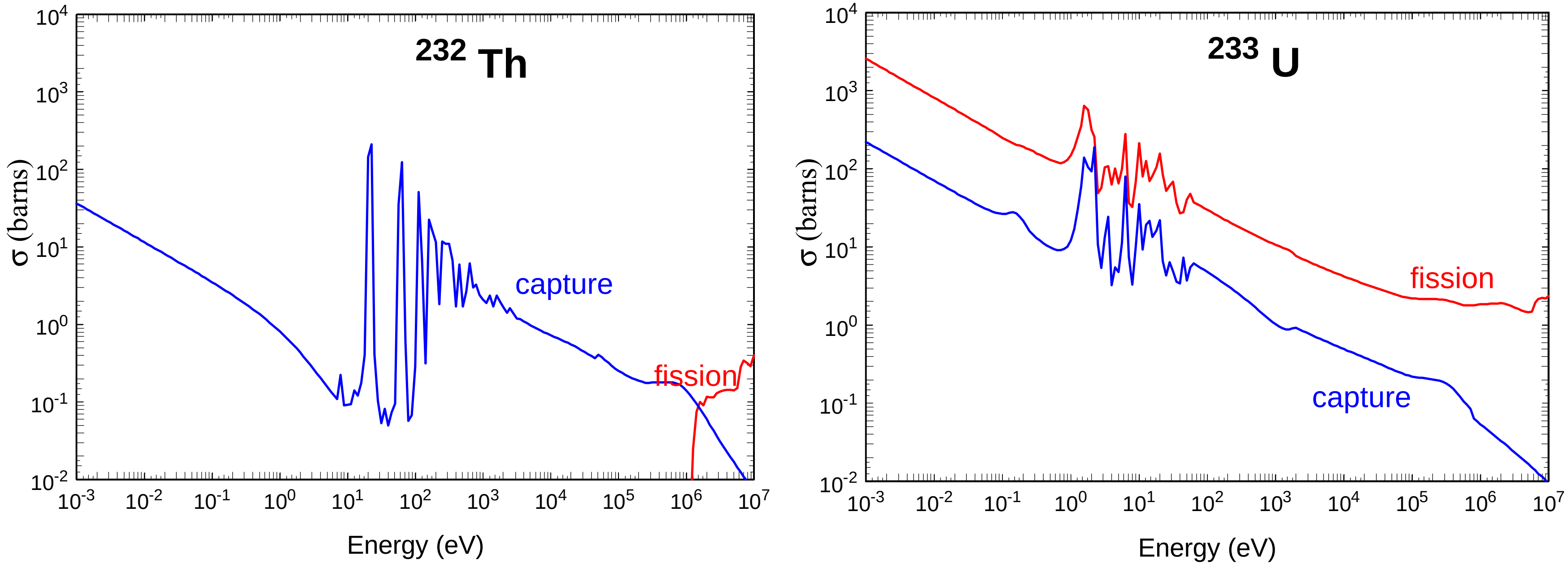

THE ROYAL INSTITUTE OF TECHNOLOGY

RESONANCES

Γ- resonance width --> peak width at half maximum, a measure of compound nucleus probability for decay

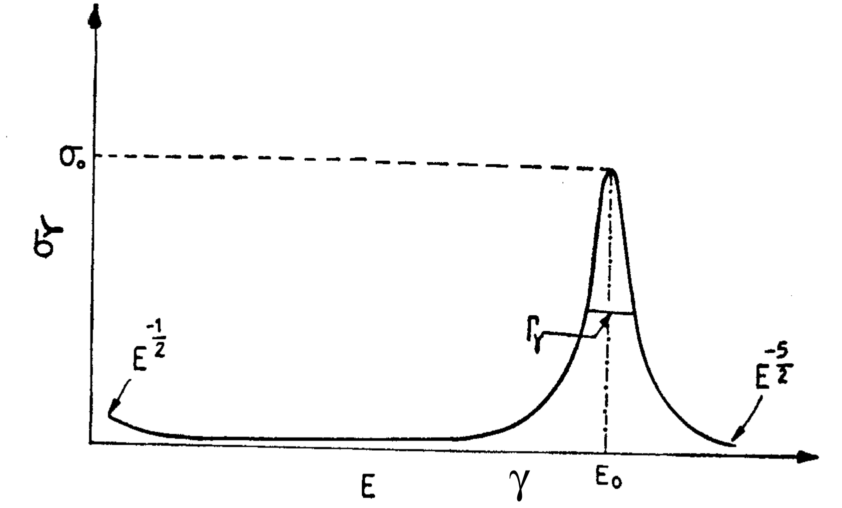

Energy variation of radiative capture cross section around resonance energy

Breit-Wigner formula:

X-section for scattering ⇨

$$s_s(E) = \frac{s_{s\Gamma}\Gamma^2}{4(E-E_\Gamma)^2+\Gamma}$$

X-section for other interactions ⇨

$$s_x(E) = \frac{s_{x\Gamma}\Gamma^2}{4(E-E_\Gamma)^2+\Gamma} \cdot \sqrt{\frac{E_r}{E}}$$

$$\sigma_s(E)=\frac{\sigma_{s\Gamma}\Gamma^2}{4(E-E_\Gamma)^2+\Gamma}$$

$$\sigma_x(E)=\frac{\sigma_{x\Gamma}\Gamma^2}{4(E-E_\Gamma)^2+\Gamma}\cdot\sqrt{\frac{E_r}{E}}$$

- E - neutron kinetic energy (in CM-system),
- E_Γ- neutron energy at resonance,
- σ_{sr}- scattering X-section at resonance,
- σ_{xr}- X-section for process ‘x’ at resonance

- For light nuclei resonance levels are scarce with distance of ab. 100 keV or more. For the heavy nuclei distance between the levels is of the order of few eV
- Density of levels increase with energy Pronounced effect of EVEN - UNEVEN nuclei. When neutrons interact with nuclei with EVEN mass number resonances are at larger distances than for UNEVEN mass numbers..
- Shell structure of the nuclei clearly visible. E.g. Bi and Pb have unusual large distance between the levels because Pb has a “magic” number of protons (82) and Bi - neutrons (126).

^{209}Bi and ^{nat}Pb

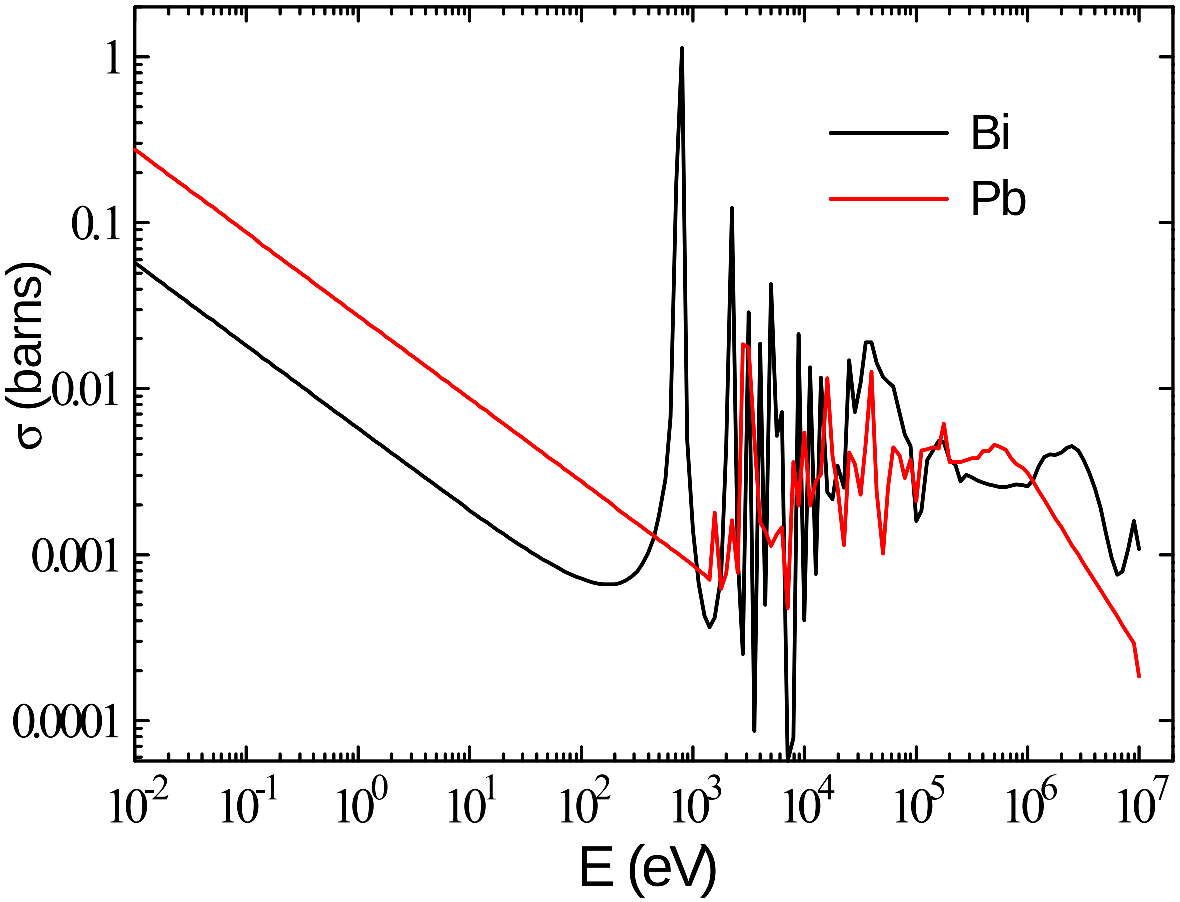

DATA LIBRARIES FOR MC ARE OF TWO FORMS

- **Pointwise**
    - Cross sections are specified at a sufficient number of energy points to faithfully reproduce the evaluated cross section
    - Used with:
        - Continuous energy Monte Carlo codes
- **Multigroup**
    - All data are collapsed and averaged into energy groups
    - Used with:
        - Multigroup Monte Carlo codes and of course
            - Diffusion codes
            - Discrete ordinate codes

CROSS-SECTION LIBRARIES

- Pointwise
  - User does not have to worry about:
    - Group structure
    - Flux spectrum
    - Self-shielding
  - Small amount of work in processing code
  - Large amount of work in transport code
- Multigroup
  - User needs to worry about everything
  - Large amount of work in processing code
  - Small amount of work in transport code

^{235}U - fission cross sections in resonanse region Pointwise and multigroup JEF2 data

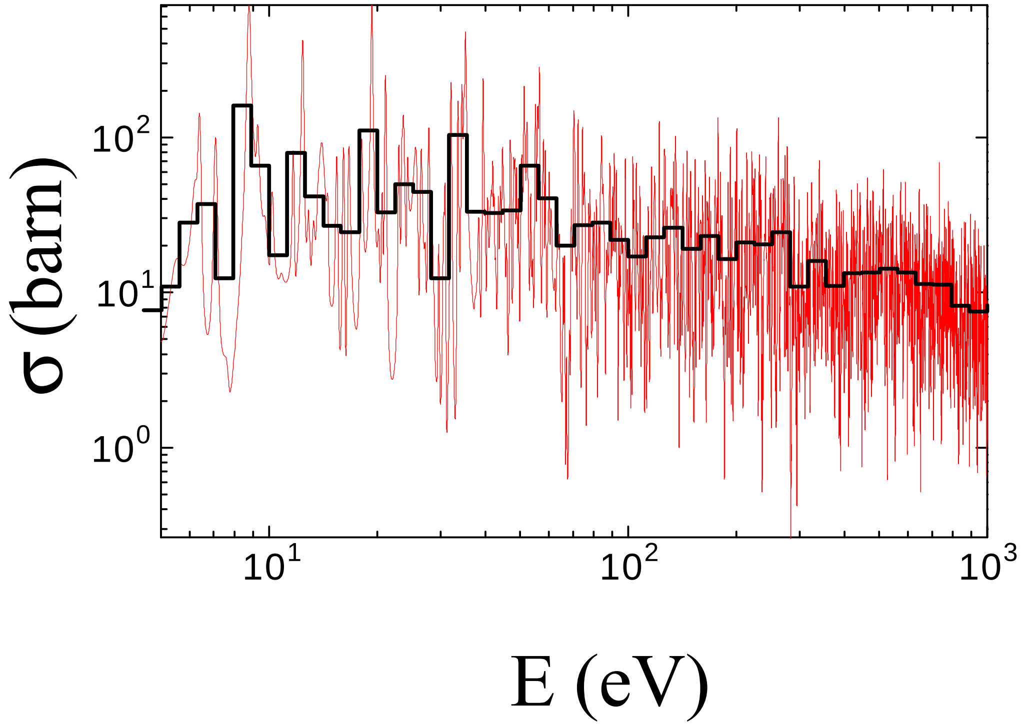

THE ROYAL INSTITUTE OF TECHNOLOGY

^{235}U - fission and capture cross sections JEF2

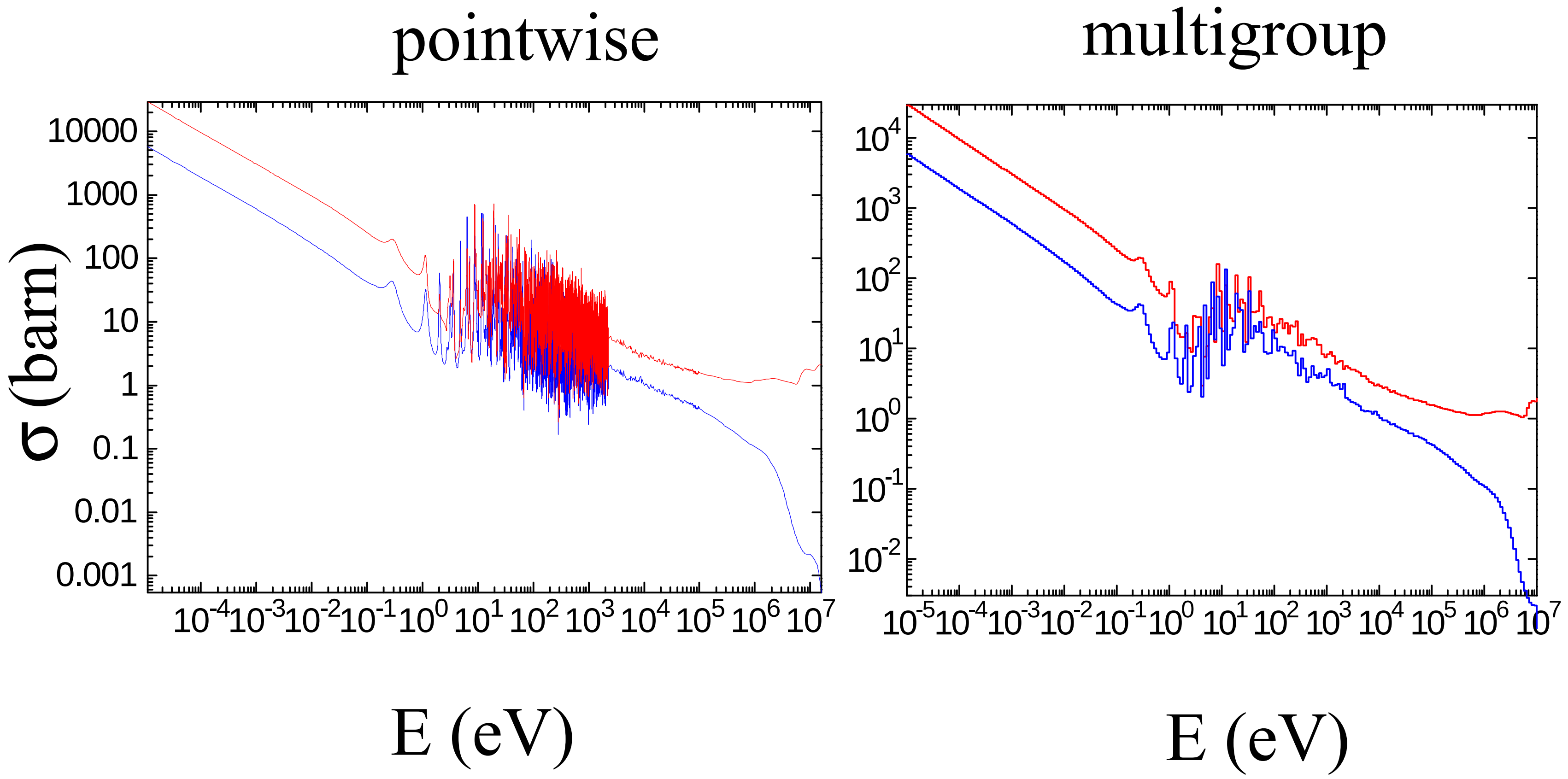

THE ROYAL INSTITUTE OF TECHNOLOGY

Neutron cross section data contain

- Cross sections for reactions:
  - elastic scattering, (n,2n), (n,3n), (n,n’,p)
  - inelastic scattering (n,n’) continuum, (n,γ), (n,p) and (n,α)
  - total, absorption, proton prod. and α production
- Angular distrubutions for different reactions
- Energy distrubution for some reactions
- Heating numbers and Q-values
- Photon production cross sections, angular distributions for (n,γ), (n,n’), (n,2n) and n,3n)
- GOOD NEWS – DELAYED NEUTRON SPECTRA

Existing nuclear data libraries:

Transport libraries (about 340 isotopes):

- ENDFB6.6
- JEF2.2 (3)
- JENDL3.3
- CENDL
- BROND
- FENDL (50 MeV)
- JEFF (50 MeV)
- JAR + more

- Good news: 150 MeV libraries (50 isotopes) – included in ENDFB6.6

Existing nuclear data libraries:

Activation, dosimetry, decay:

- EAF 3.1
- TOI 8.3
- etc.

THE ROYAL
INSTITUTE OF
TECHNOLOGY

150 MeV for ^{232}Th and ^{239}Pu

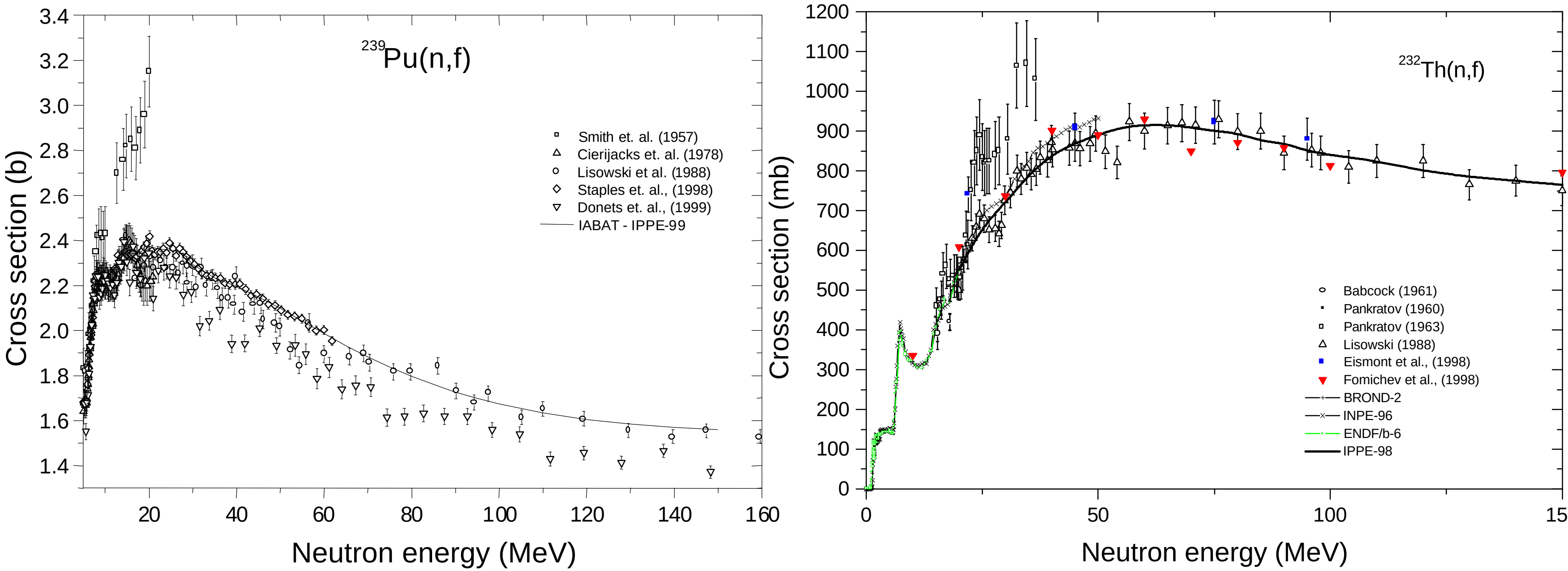

Extensive processing of nuclear data

- There is a long way from measurements to evaluated libraries and finally to Monte-Carlo:

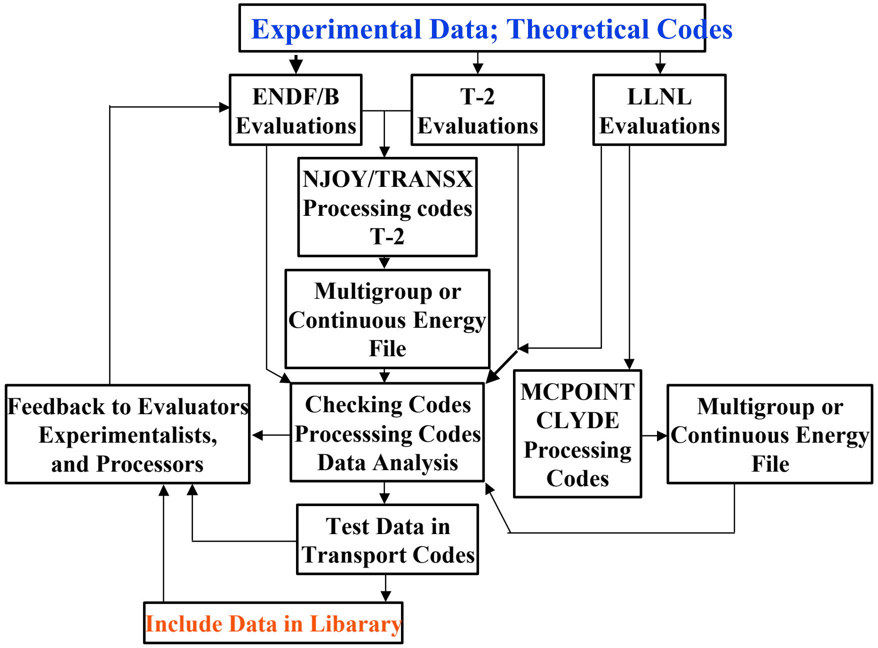

Experimental Data; Theoretical Codes

ENDF/B Evaluations

T-2 Evaluations

LLNL Evaluations

NJOY/TRANSX Processing codes T-2

Multigroup or Continuous Energy File

Feedback to Evaluators Experimentalists, and Processors

Checking Codes Processsing Codes Data Analysis

MCPOINT CLYDE Processing Codes

Multigroup or Continuous Energy File

Test Data in Transport Codes

Include Data in Libarary

Approximations in generating data

- Evaluation Assumptions:
  - choice of experiments
  - choice of representations, i.e., discrete lines for continuous distributions
  - interpolation (model codes)
  - bin sizes
  - tresholds, Q-values, particularly for elements
- Processing Assumptions:
  - representation of angular distributions as equiprobable bins
  - resonance parameter treatment

Things to consider when choosing neutron cross-section data

- Differences in evaluator’s philosophy
- Neutron energy spectrum
- Temperature at which set was processed
- Availability of photon-production data
- Sensitivity of results to different evaluations
- Use the best data that you can afford

Major Neutron Physics Approximations

- (n,xn) sampled independently
- (n,f),(n,xn) happen instantly
- unresolved resonances treated as average cross section
- no delayed gamma production

THERMAL EFFECTS

- Target motion (gas liquid, solid) --> incident neutron “sees” targets with various velocities, i.e., many different relative velocities
  - $s = f(V_{relative})$;so average cross section is changed
  - kinematics are different
    - neutron upscattering
    - Doppler broadening

THERMAL EFFECTS (cont.)

- Lattice structure (solid)

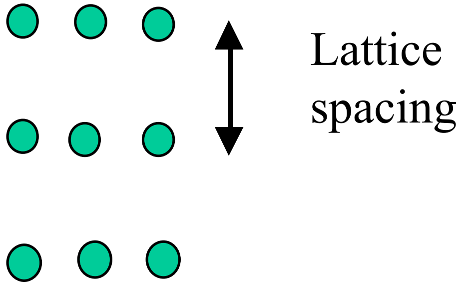

At high energy - wavelength of neutron << lattice spacing

At low energy - wavelength of neutron ≅ lattice spacing

  - Cross sections show very jagged behaviour, each peak corresponds to a particular set of crystal planes
  - Coherent scattering (interference of scattered waves) add constructively in some directions and add destructively in others
    - ==>Angular distribution changed
      - Bragg scattering

THERMAL EFFECTS (cont.)

- Molecular energy levels (liquid, solid)

  vibrational and rotational levels

  ~0.1 eV spacing below a few eV

  Neutron loses or gains energy in discrete amounts

  ==> modify DOUBLE-DIFFERENTIAL

  thermal inelastic scattering $s(E \rightarrow E', \Theta')$

Pay attention to some cross section in thermal region!!

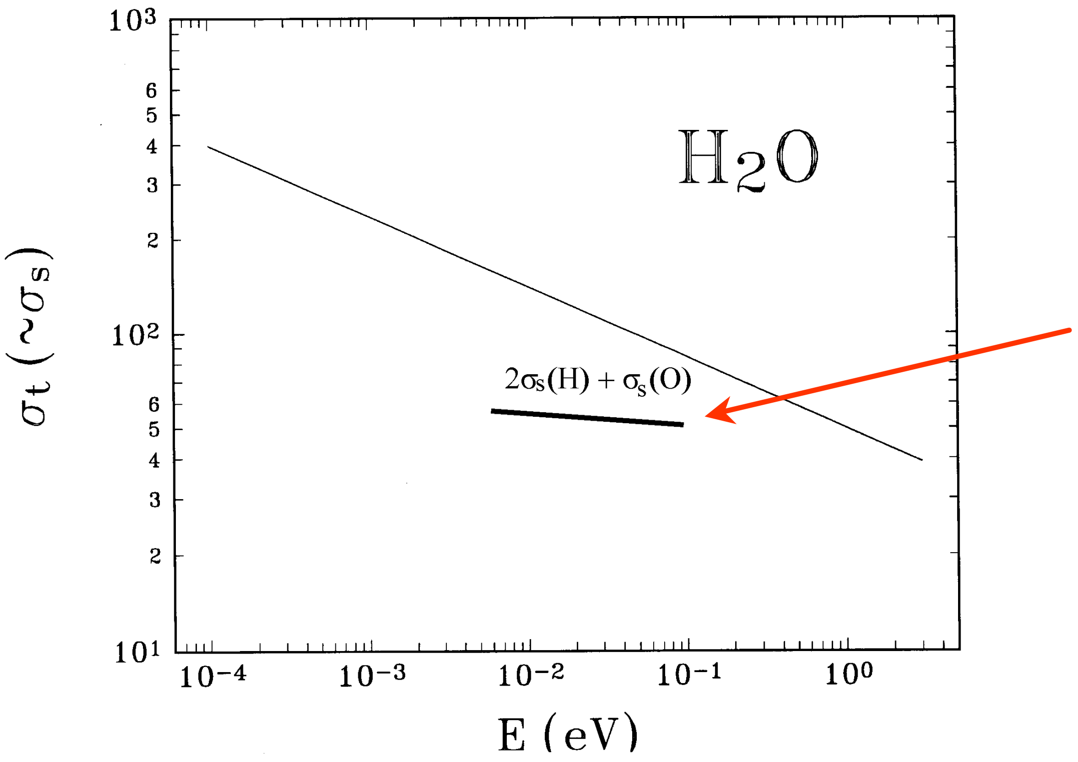

Cross-section for water molecule is not equal to sum of the partial cross-sections

THE ROYAL INSTITUTE OF TECHNOLOGY

Photon Physics

- Coherent (Thomson) Scattering + Form Factors
- Inhorenet (Compton) Scattering + Form Factors
- Pair Production
- Photoelectric Absorption and Fluorescence
- Thick-Target Bremsstrahlung
- GOOD NEWS – PHOTONUCLEAR REACTIONS AVAILABLE

Photon Physics Approximations

Only K,L edges treated for photoelectric absorption

Distance to collision sampled, not distance to scatter

Thick/thin-target bremsstrahlung

No distinction between pair and triplet production

No anomalous scattering factors

Reminder:

f(x) = probability density function (PDF)

= history score distribution

$$If \int_{-\infty}^{\infty} f(x)dx = 1 \text{ then}$$

$$\text{mean: } m = \overline{x} = \int_{-\infty}^{\infty} x f(x) dx \quad \text{- 1st moment}$$

$$\text{variance: } s^2 = \int_{-\infty}^{\infty} (x - \overline{x})^2 f(x) dx \quad \text{- 2nd moment}$$

$$\text{vov (variance of variance): } \int_{-\infty}^{\infty} (x - \overline{x})^4 f(x) dx \quad \text{- 4th moment}$$

Key of Symbols in Monte Carlo

W - particle weight, **W_s** - source weight

E- particle energy (MeV); **E_D** - energy deposited (MeV)

m- cosine of angle between surface normal and trajectory

A- surface area (cm^2); **V** - cell volume (cm^3)

l - track length (cm)

p(μ) - probability density function: m - cosine of angle between particle
trajectory and detector

s - total mean free path to the detector

R- distance to the detector

s_T**(E)**- microscopic cross section (barns), s_f**(E)** - fission x-section

H(E) - heating number (MeV/collision)

Q - fission heating Q-value (MeV)

r_a - atom density (atoms/barn-cm), **m** - cell mass (g)

ESTIMATORS

- Definitions:
  - – Particle speed - v(cm/s)
  - – Particle density - n (particles/cm3), a function of position, energy, angle, and time
  - – Flux (particles/cm^2·s) $\phi\left(\bar{\boldsymbol{r}},\boldsymbol{E},\hat{\Omega},\boldsymbol{t}\right) \equiv \boldsymbol{v}\cdot\boldsymbol{n}\left(\bar{\boldsymbol{r}},\boldsymbol{E},\hat{\Omega},\boldsymbol{t}\right)$
  - – Fluence (particles/cm^2)

$$\Phi\left(\bar{\boldsymbol{r}},\boldsymbol{E},\hat{\Omega}\right) \equiv \int_0^\infty \phi\left(\bar{\boldsymbol{r}},\boldsymbol{E},\hat{\Omega},\boldsymbol{t}\right)\boldsymbol{dt} = \int_0^\infty \boldsymbol{v}\cdot\boldsymbol{n}\left(\bar{\boldsymbol{r}},\boldsymbol{E},\hat{\Omega},\boldsymbol{t}\right)\boldsymbol{dt}$$

Estimators

Cell fluence estimator (track length)

$$\sum \frac{\boldsymbol{W}}{\boldsymbol{V}} \cdot \boldsymbol{v}\Delta \boldsymbol{t} = \sum \frac{\boldsymbol{W}}{\boldsymbol{V}} \cdot \lambda$$

- Surface flux estimator:

$$\boldsymbol{\Phi}_s = \sum_{\delta \to 0} \frac{\boldsymbol{W}\delta / |\mu|}{\delta \boldsymbol{A}} = \sum \frac{\boldsymbol{W}}{\boldsymbol{A}|\mu|}$$

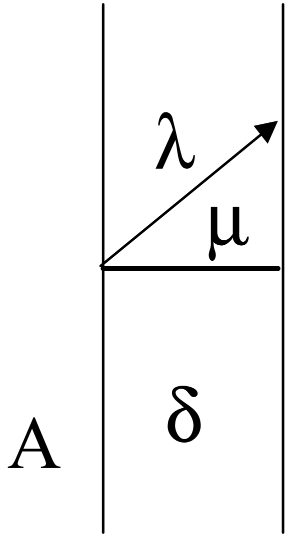

Estimators

- **Total heating:** $$F_{TH} = \frac{r_a}{r_g} \text{ò} f\, s_T HdE$$
- **Fission Heating** $$F_{fH} = \frac{r_a}{r_g} \text{ò} f\, s_f QdE$$
- **k_{eff}** $$k_{eff} = V r_a \text{ò} f\, n\, s_f dE$$

Results we get from MC (relevant for ADS)

- k_{eff}, k_{src}
- Neutron fluxes in every cell
- Reactions rates (important for burnup!!)
- Heating rates
- and other data we wish: like photon fluxes, detector responses, electron transport results
- ERRORS BARS!!

Deterministic

- solves the transport equation (integro-differential) for the average particle behaviour
- gives fairly complete information (e.g. flux) throughout the phase space of the problem

Monte-Carlo

- simulates individual particles and records some aspects of their behaviour
- supplies information only about the specific “sampled” distribution (“tally”)
- No transport equation need to be written to solve a transport problem by Monte Carlo - but - equation of the probability density of particles = integral transport equation

Deterministic

- the discrete ordinates method visualises the phase space to be divided into many small boxes, the particles move from one box to another. Boxes get progressively smaller, particles moving from box to box take differential amount of time to move and differential distance in space ----> approaches the integro differential tarnsport

Monte-Carlo

- Monte-Carlo transports particle between events (e.g. collisions) that are separated in space and time. Neither differntial space nor time are inherent parameters of Monte-Carlo. The integral equation ***does not have*** time or space derivatives

MC codes and availabilty

Code	Availability		
	Free	Limited (bin.)	Restricted/comm.
MCBEND/MONK			X
TRIPOLI-3	X		
MVP	?	?	?
A3MCNP			X
MCU	?	?	?
MCB (MC burnup)	X		
SCALE V	X		